National Research Council Canada

Conseil national de recherches Canada

NRC · CNRC

Canadian Journal of Fisheries and Aquatic Sciences

Journal canadien des sciences halieutiques et aquatiques

http://cjfas.nrc.ca

http://jcsha.cnrc.ca

ISSN 0706-652X / CJFSDX 62(5) 961–1199 (2005)

The *Canadian Journal of Fisheries and Aquatic Sciences*, previously published as *Contributions to Canadian Biology* 1901–1925, *Contributions to Canadian Biology and Fisheries* 1926–1934, *Journal of the Biological Board of Canada* 1934–1937, and *Journal of the Fisheries Research Board of Canada* 1938–1979, is issued monthly to form annual volumes of 12 numbers plus supplements.

Editorial policy. The Journal publishes original research articles, perspectives (syntheses, critiques, re-evaluations), discussions (comment and reply), and rapid communications. Manuscripts may concern cells, organisms, populations, communities, ecosystems, or processes that affect aquatic systems. They may cover a range of disciplines including biology and ecology of marine and freshwater organisms, limnology, oceanography, physiology, toxicology, genetics, economics, disease, and management. Preference will be given to manuscripts that emphasize understanding of observed phenomena and interpretation of experimental results. The Journal encourages papers that lead from clearly stated purpose or rationale and from testable hypotheses, concepts, or questions to identifiable conclusions or syntheses. Such papers may amplify, modify, question, or redirect accumulated knowledge embodied in contemporary perceptions of a particular state of aquatic sciences. The Journal discourages papers that are essentially descriptive, except in emerging disciplines; have only site-specific or local applications (a certain year, place, taxon, chemical compound, etc.); only confirm previously established principles; or apply standard techniques without breaking new methodological ground.

Manuscripts for publication should be submitted to the Senior Editor, *Canadian Journal of Fisheries and Aquatic Sciences*, Department of Integrative Biology, Building #006, Room 118, University of Guelph, Guelph, ON N1G 2W1, Canada (519-824-4120 ext. 52646; fax: 519-767-9798; e-mail: cjfas@uoguelph.ca).

Submissions in either English or French are acceptable. The information must be original, that is, not copyrighted, published, or submitted elsewhere except in abstract form or unless by written consent of the Editor.

Correspondence concerning accepted manuscripts and corrected proofs should be sent to NRC Research Press, National Research Council of Canada, Ottawa, ON K1A 0R6, Canada (fax: 613-952-7656; e-mail: pubs@nrc-cnrc.gc.ca).

Instructions to Authors are published once a year in the first issue of each volume. Copies are available from NRC Research Press or at http://cjfas.nrc.ca. The **Publication Policy** of NRC Research Press is available at http://pubs.nrc-cnrc.gc.ca.

Microfilm. Issues from 1934 through the current volume can be purchased on 16- or 35-mm microfilm. Photocopies of individual articles or issues can be purchased from University Microfilms International, 330 North Zeeb Road, Ann Arbor, MI 48106, USA.

US periodical postage paid at Champlain, NY 12919, USA, and at additional mailing offices. Attention US POSTMASTER: Send address changes to **Canadian Journal of Fisheries and Aquatic Sciences**, c/o USACAN Media Distribution Center, P.O. Box 2688, Plattsburgh, NY 12901, USA.

Publié sans interruption depuis 1901, le *Journal canadien des sciences halieutiques et aquatiques* a paru sous plusieurs titres : *Contributions to Canadian Biology* 1901–1925, *Contributions to Canadian Biology and Fisheries* 1926–1934, *Journal of the Biological Board of Canada* 1934–1937, et *Journal of the Fisheries Research Board of Canada* 1938–1979. Le Journal paraît tous les mois, formant ainsi un volume de 12 numéros, et offre en plus jusqu'à deux suppléments par année.

Politique éditoriale. On publie, dans le Journal, des articles rendant compte de recherche originale, des perspectives (synthèses, critiques et réévaluations), des discussions (commentaires et réponses) et des communications rapides. Les documents peuvent porter sur les cellules, organismes, populations, communautés, écosystèmes ou processus qui affectent les systèmes aquatiques. Ils peuvent relever de divers domaines y compris la biologie et l'écologie des organismes marins et d'eau douce, la limnologie, l'océanographie, la physiologie, la toxicologie, la génétique, l'économie, la pathologie et la gestion. On accorde la préséance aux articles qui contribuent à la compréhension de phénomènes observés et à l'interprétation de résultats expérimentaux. On invite les auteurs à soumettre des articles ayant des objectifs précis ou relevant d'hypothèses, de concepts ou de questions vérifiables et se terminant par de solides conclusions ou d'utiles synthèses. Ces articles enrichissent, changent, mettent en question ou réorientent les connaissances acquises sur divers aspects des sciences aquatiques. On décourage toutefois la soumission d'articles simplement descriptifs (à moins qu'il ne s'agisse de nouvelles disciplines), d'application très limitée (applicables à une seule année, une seule région ou un seul taxon, portant sur un unique composé chimique, etc.); d'articles qui ne font que reprendre les principes énoncés dans des articles précédents; et d'articles rendant compte de l'application de normes sans gain de méthodologie.

Les auteurs voudront adresser leurs **manuscrits** à la directrice scientifique principale, *Journal canadien des sciences halieutiques et aquatiques*, Département de biologie intégrative, édifice 006, bureau 118, University of Guelph, Guelph, ON N1G 2W1, Canada (519-824-4120 poste 52646; télécopieur : 519-767-9798; courriel : cjfas@uoguelph.ca).

Les contributions peuvent être en anglais ou en français. Elles doivent être originales, c.-à.-d. qu'elles ne doivent pas avoir fait l'objet d'un copyright, avoir été publiées ou soumises ailleurs, sauf sous forme abrégée ou avec le consentement du rédacteur. Le CNRC ne se tient en aucune façon responsable des opinions exprimées par un collaborateur ou des déclarations qui pourrait faire ce dernier.

La correspondance ayant trait aux manuscrits acceptés et les **épreuves corrigés** doivent être envoyées aux Presses scientifiques du CNRC, Conseil national de recherches du Canada, Ottawa, ON K1A 0R6, Canada (télécopieur : 613-952-7656; courriel : pubs@nrc-cnrc.gc.ca).

Les Recommandations aux auteurs sont publiées une fois par année dans le premier numéro de chaque volume. Des copies sont disponibles auprès du Bureau de la rédaction aux Presses scientifiques du CNRC ou au http://jcsha.cnrc.ca. **La Politique de publication** est disponible auprès des Presses scientifiques du CNRC ou au http://pubs.nrc-cnrc.gc.ca.

Microfilms. On peut acheter sur microfilms de 16 ou 35 mm tous les numéros depuis 1934. Des photocopies d'articles ou de numéros individuels sont aussi en vente auprès de University Microfilms International, 330 North Zeeb Road, Ann Arbor, MI 48106, É.-U.

This Journal is indexed or abstracted in / Cette revue est signalée ou résumée dans
ABSEARCH, Applied Science and Technology Index and Abstracts, Aquatic Sciences and Fisheries Abstracts, Biological Abstracts, Biological and Agricultural Abstracts, CAB Abstracts, Chemical Abstracts, Current Contents, Elsevier BIOBASE, Environmental Abstracts, ETDE Energy Database, General Science Index and Abstracts, GEOBASE, GeoRef, Life Sciences Collection, Meteorological and Geoastrophysical Abstracts, Oceanic Abstracts, PASCAL Database, and Science Citation Index.

Volume 62, Number 5, May 2005

Canadian Journal of Fisheries and Aquatic Sciences

Published by the National Research Council of Canada

Volume 62, numéro 5, mai 2005

Journal canadien des sciences halieutiques et aquatiques

Publié par le Conseil national de recherches du Canada

Senior Editor / Directrice scientifique principale **Moira M. Ferguson**

Editors / Directeurs

Jeffrey A. Hutchings, *Dalhousie University, Halifax*

Pierre Pepin, *Northwest Atlantic Fisheries Centre, DFO/MPO, St. John's, Newfoundland*

W. Gary Sprules, *University of Toronto at Mississauga*

Assistant to the Editors / Adjointe aux directeurs scientifiques **Holly Foster**

Associate Editors / Directeurs scientifiques associés

D. Boisclair, *Université de Montréal*
U. Borgmann, *Environment Canada, Burlington*
M.J. Bradford, *DFO/MPO and Simon Fraser University*
S.E. Campana, *DFO/MPO, Dartmouth*
R. Carignan, *Université de Montréal*
G.T. Evans, *DFO/MPO, St. John's, Newfoundland*
K.T. Frank, *DFO/MPO, Dartmouth*
J.W.A. Grant, *Concordia University*
M.M. Hansen, *Danish Institute for Fisheries Research, Silkeborg, Denmark*
R. Hilborn, *University of Washington*
D.F. Houlihan, *University of Aberdeen*
F.A. Huntingford, *University of Glasgow*
J.M. Jech, *NFSC/NOAA, Woods Hole, Mass.*
B. Jonsson, *Norwegian Institute for Nature Research, Oslo, Norway*
K.A. Kidd, *University of New Brunswick*
D.L. MacLatchy, *University of New Brunswick, Saint John*
P. Magnan, *Université du Québec à Trois Rivières*
C.T. Marshall, *University of Aberdeen*
R.B. Millar, *University of Auckland, New Zealand*
W.P. Patterson, *University of Saskatchewan*
Y.T. Prairie, *Université du Québec à Montréal*
T.J. Quinn II, *University of Alaska–Fairbanks, Juneau, Alaska*
T.P. Quinn, *University of Washington*
C.W. Ramcharan, *Laurentian University*
J.S. Richardson, *The University of British Columbia*
B. Sainte-Marie, *DFO/MPO, Mont-Joli*
R.E.H. Smith, *University of Waterloo*
S.J. Smith, *DFO/MPO, Dartmouth*
E.B. Taylor, *The University of British Columbia*
W.F. Vincent, *Université Laval*
R.D. Vinebrooke, *University of Alberta*
C.J. Walters, *The University of British Columbia*
B. de Young, *Memorial University of Newfoundland*

NRC Research Press / Presses scientifiques du CNRC

Editor-in-Chief / Directeur scientifique en chef **Bruce P. Dancik**

Assistant Editor-in-Chief / Adjoint au directeur scientifique en chef **Iain E.P. Taylor**

Journals Program / Programme des revues

Fax / Télécopieur : 613-952-7656; e-mail / courriel : pubs@nrc-cnrc.gc.ca; URL / URL : pubs.nrc-cnrc.gc.ca

Director / Directeur **Cameron D. Macdonald**

Business Manager / Gestionnaire des affaires **Jason Charron**

Manager, Journals Program / Gestionnaire, Programme des revues **Carolyn Brown**

Managing Editor / Rédactrice administrative **Cecily M. Pearson** (613-993-9099)

Publication Officers / Agents de publication **Jennifer McColl, Thad Costigan**

Advertising and reprints / Annonces publicitaires et tirés à part **Roxanne Landriault** (613-990-2254)

Subscriptions / Abonnements **Eileen Evans-Nantais** (613-990-7873)

The National Research Council of Canada accepts no responsibility for statements or opinions expressed by a contributor. Acceptance of an advertisement, announcement, or other material does not imply endorsement by either the Journal's Senior Editor or the National Research Council.

© National Research Council of Canada 2005. All rights reserved.

No part of this publication may be reproduced, stored, or transmitted in any form or by any means, without the written permission of the publisher, except as stated below.

The National Research Council of Canada grants **permission*** to individuals to make single copies of articles for personal use. Any person may reproduce short excerpts from articles in the journal for any purpose that respects the moral rights of authors, provided that the source is fully acknowledged. As a courtesy, the consent of authors of such material should be obtained directly from the author.

Authorization to reproduce items for other than personal use, as stated above, is granted by the National Research Council of Canada provided that the copyright fee of $7.00 per copy is paid directly to CANCOPY, One Yonge Street, Suite 1900, Toronto, ON M5E 1E5, Canada.

*The above permission does not extend to other kinds of copying, such as copying for general distribution, for advertising, or promotional purposes, for creating new collective works, or for resale. For such copying, arrangements must be made with the publisher, National Research Council of Canada, Ottawa, ON K1A 0R6, Canada.

Subscription information

The *Canadian Journal of Fisheries and Aquatic Sciences* (ISSN 0706-652X) is published monthly by the National Research Council of Canada. The 2005 annual subscription rates (second class postage) for Canada are $892CAN institutional and $276CAN personal, for US & foreign $892US institutional and $276US personal. For air mail add $175US to foreign rate. Canadian customers please include 7% GST (business no. 12149 1807 RT 0275). Subscriptions are entered for the calendar year. Remittances should be made payable to the Receiver General for Canada, credit NRC. Price for regular single issues: institutional, $110.00; personal, $35.00. Supplements will be priced separately. Special rates apply to members of Canadian scientific and engineering societies if they subscribe through their respective societies.

There are no refunds on cancelled subscriptions once delivery has begun. Claims for missing issues should be made within four months (N. America) or six months (outside N. America) following the date of publication. The publisher expects to supply missing issues only when losses have occurred in transit and when the reserve stock will permit. For change of address and subscription enquiries: Subscription Office, NRC Research Press, National Research Council of Canada, Ottawa, ON K1A 0R6, Canada; tel.: 613-993-9084; fax: 613-952-7656; e-mail: pubs@nrc-cnrc.gc.ca.

Microform backfiles are available from UMI, P.O. Box 1346, Ann Arbor, MI 48106-1346, USA, and Micromedia Ltd., 20 Victoria St., Toronto, ON M5C 2N8, Canada.

All issues of the *Canadian Journal of Fisheries and Aquatic Sciences* since 1996 are available on the Web. Pricing information can be found at http://pubs.nrc-cnrc.gc.ca.

Le Conseil national de recherches du Canada ne se tient en aucune façon responsable des opinions exprimées par un collaborateur ou des déclarations que pourrait faire ce dernier. La publication d'annonces publicitaires, d'avis et autres n'implique pas l'endossement de leur contenu par la directrice principale de la Revue ou le CNRC.

© Conseil national de recherches du Canada 2005. Tous droits réservés.

Il est interdit de reproduire, de sauvegarder ou de transmettre quelque partie de la présente publication dans quelque format ou de quelque façon sans le consentement écrit de l'éditeur, à l'exception des conditions suivantes.

Le Conseil national de recherches du Canada accorde aux particuliers le droit de faire des copies individuelles pour leur usage personnel. Toute personne peut reproduire de courts extraits des articles de la Revue pour autant que les droits moraux de l'auteur soient respectés et que la mention de provenance soit clairement indiquée. Il est de convenance de demander le consentement de l'auteur avant de faire mention de son travail.

On obtiendra l'autorisation de reproduire des articles à d'autres fins que l'usage personnel (tel qu'on l'a décrit ci-dessus) auprès du Conseil national de recherches du Canada pour autant que des redevances de droits d'auteurs de 7,00 $/copie soient versées au CANCOPY, 1, rue Yonge, bureau 1900, Toronto, ON M5E 1E5, Canada.

*La permission ci-dessus ne s'applique pas à la reproduction à grande échelle, telle que la reproduction aux fins de distribution générale, publicitaire ou promotionnelle, de compilation de nouveaux ouvrages collectifs ou de revente. Dans de tels cas, il faudra ratifier une entente particulière avec l'éditeur, le Conseil national de recherches du Canada, Ottawa, ON K1A 0R6, Canada.

Renseignements sur l'abonnement

Journal canadien des sciences halieutiques et aquatiques (ISSN 0706-652X) est une publication mensuelle du Conseil national de recherches du Canada. Le prix de l'abonnement annuel en 2005 au Canada (courrier de deuxième classe) est de 892 $CAN pour les organismes et de 276 $CAN pour les particuliers. À l'étranger (y compris les É.-U.), le prix de l'abonnement est de 892 $US pour les organismes et de 276 $US pour les particuliers. L'expédition par avion exige des frais de 175 $US en sus du prix d'abonnement à l'étranger. Les clients du Canada doivent ajouter la TPS de 7 % (numéro d'entreprise 12149 1807 RT 0275). Les abonnements sont pour l'année civile. Tout paiement doit être adressé au Receveur général du Canada, crédit du CNRC. Le prix par numéro est de 110 $ pour les organismes et de 35 $ pour les particuliers. Le prix des hors-série varie. Les membres des sociétés canadiennes de sciences et de génie bénéficient de taux préférentiels en s'abonnant via leurs sociétés respectives.

Aucun remboursement ne sera accordé ni aucune annulation acceptée une fois que les livraisons auront commencé. Les réclamations de numéros manquants devront être soumises dans les quatre mois (Amérique du Nord) ou dans les six mois (à l'extérieur de l'Amérique du Nord) suivant la date de publication. L'éditeur ne fournira de numéros manquants que si le document a été perdu pendant l'expédition et que si le stock le permet. Adressez tout changement d'adresse ou toute question quant à l'abonnement au : Bureau des abonnements, Presses scientifiques du CNRC, Conseil national de recherches Canada, Ottawa, ON K1A 0R6, Canada; téléphone : 613-993-9084; télécopieur : 613-952-7656; courriel : pubs@nrc-cnrc.gc.ca.

On peut obtenir les fichiers rétrospectifs sur **microforme** auprès de UMI, P.O. Box 1346, Ann Arbor, MI 48106-1346, É.-U., et auprès de Micromedia Ltée, 20, rue Victoria, Toronto, ON M5C 2N8, Canada.

À partir de 1996, tous les numéros de *Journal canadien des sciences halieutiques et aquatiques* sont accessibles sur le Web. On trouvera des renseignements sur les tarifs à http://pubs.nrc-cnrc.gc.ca.

RAPID COMMUNICATION / COMMUNICATION RAPIDE

A new perspective on the importance of marine-derived nutrients to threatened stocks of Pacific salmon (*Oncorhynchus* spp.)

Mark D. Scheuerell, Phillip S. Levin, Richard W. Zabel, John G. Williams, and Beth L. Sanderson

Abstract: Considerable research has highlighted the important role of anadromous salmon in importing marine-derived nutrients to freshwater and riparian ecosystems. These subsidies are thought to support diverse food webs and increase the growth and survival of juvenile salmon during their freshwater residency. Quite recently, however, salmon smolts have been identified as important exporters of nutrients from freshwater ecosystems. Using a mass-balance approach, we examined the phosphorus-transport dynamics by spring/summer Chinook salmon (*Oncorhynchus tshawytscha*) in the Snake River basin and estimated that net phosphorus transport into the basin over the past 40 years was <2% of historical levels. Furthermore, a nonlinear relationship existed between nutrient import by adults and subsequent export by smolts, such that smolts exported proportionally more phosphorus as spawner abundance decreased. In 12% of years, smolts exported more than adults imported, resulting in a net loss of phosphorus from the ecosystem. This loss of marine subsidies may have caused a state shift in the productivity of the freshwater ecosystem, resulting in strong density-dependent survival observed in juvenile salmon. These results suggest that conserving this threatened stock of salmon requires the need to explicitly address the important role of marine-derived nutrients and energy in sustaining salmon populations.

Résumé : De nombreux travaux ont démontré le rôle significatif des saumons anadromes dans le transport des nutriments d'origine marine vers les écosystèmes d'eau douce et les écosystèmes de rivage. On croit que ces apports alimentent divers réseaux trophiques et favorisent la croissance et la survie des jeunes saumons durant leur séjour en eau douce. Tout à fait récemment, cependant, il a été démontré que les saumoneaux exportent d'importantes quantités de nutriments hors des écosystèmes d'eau douce. L'établissement de bilans massiques nous a permis d'étudier la dynamique du transport du phosphore par les saumons quinnat (*Oncorhynchus tshawytscha*) de printemps et d'été dans le bassin versant de la rivière Snake; le transport net de phosphore vers le bassin au cours des 40 dernières années est <2 % des quantités du passé. De plus, il existe une relation non linéaire entre l'importation des nutriments par les adultes et l'exportation subséquente par les saumoneaux : les saumoneaux exportent en proportion plus de phosphore à mesure que l'abondance des reproducteurs diminue. Dans 12 % des années, les saumoneaux exportent plus que les adultes n'importent, ce qui entraîne une perte nette de phosphore dans l'écosystème. Cette perte des apports marins peut avoir causé une modification du niveau de productivité de l'écosystème d'eau douce, ce qui explique que la survie observée chez les jeunes saumons est fortement reliée à la densité. Nos résultats indiquent qu'il faut tenir compte de façon particulière du rôle significatif des nutriments et de l'énergie d'origine marine dans le maintien des populations de saumons, si l'on veut conserver ce stock menacé de saumons.

[Traduit par la Rédaction]

Introduction

The century-long decline of Pacific salmon in the Columbia River Basin is well documented, and because of the enormous economic, social, and ecological value that society places on salmon, the "salmon problem" now represents one of the United States' most contentious environmental issues (Ruckelshaus et al. 2002). In the Snake River, the larg-

Received 15 April 2005. Accepted 20 April 2005. Published on the NRC Research Press Web site at http://cjfas.nrc.ca on 13 May 2005.
J18655

M.D. Scheuerell,[1] P.S. Levin, R.W. Zabel, J.G. Williams, and B.L. Sanderson. National Marine Fisheries Service, Northwest Fisheries Science Center, 2725 Montlake Boulevard East, Seattle, WA 98112, USA.

[1]Corresponding author (e-mail: mark.scheuerell@noaa.gov).

 doi: 10.1139/F05-113 © 2005 NRC Canada

est tributary to the Columbia River, wild populations of spring/summer Chinook salmon (*Oncorhynchus tshawytscha*) fell dramatically from the 1960s through the 1990s, resulting in their listing under the US Endangered Species Act. Habitat degradation, overharvest, hydroelectric dams, hatchery production, interactions with exotic species, and shifts in ocean-climate conditions have all contributed to their demise (Ruckelshaus et al. 2002). No matter what the ultimate cause of their downfall, another more subtle problem emerges from this large drop in salmon abundance: freshwater spawning and rearing habitat has experienced a massive decrease in marine-derived nutrients (Gresh et al. 2000).

Anadromous salmon play an integral role on their return to freshwater ecosystems because they accumulate >95% of their biomass in the ocean, which results in the import of substantial marine-derived nutrients into the relatively nutrient-poor streams and lakes (Schindler et al. 2003). Nutrient enrichment from decomposing carcasses leads to increased production of benthic algae and macroinvertebrates, which indirectly enhances salmon food resources (Wipfli et al. 2003). Salmon eggs and carcasses also serve as a direct food source for macroinvertebrates and fishes, and juvenile salmonids show increased growth in streams with additional salmon resources (Bilby et al. 1998; Wipfli et al. 2003). This implies a positive feedback loop, such that increasing numbers of returning adult salmon contribute more marine-derived nutrients to freshwater systems, thereby leading to better juvenile growth and survival and subsequently larger population sizes (Wipfli et al. 2003).

Recent investigations aimed at understanding the causes and consequences of juvenile mortality in wild Snake River spring/summer Chinook salmon suggest that the large decline in marine-derived nutrients over the past century limits the survival of juveniles (Achord et al. 2003; Zabel et al. 2005). While the import of nutrients by adult salmon has potentially large value to freshwater ecosystems, recent work by Moore and Schindler (2004) on Alaska sockeye salmon (*O. nerka*) stocks highlighted the importance of nutrient export by salmon smolts as they migrate to sea. They hypothesized that depending on the strength of density dependence, at low spawning densities smolts could theoretically export more nutrients than their parents import to freshwater ecosystems. Here we estimated changes in net transport of marine-derived nutrients into the Snake River basin over the last 40 years compared with historical periods to determine how they might have influenced the threatened wild stock of Snake River spring/summer Chinook salmon. We hypothesized that a large reduction in marine-derived nutrients could have caused the strong density-dependent survival observed among juveniles and resulted in a state shift in the productivity of the freshwater ecosystem.

Methods

Following Moore and Schindler (2004), the annual import (I) of phosphorus by adult salmon into freshwater in year t is

$$I_t = A_t \cdot m_A \cdot p_A$$

while the annual export (E) of phosphorus by salmon smolts to the ocean in year t is

$$E_t = S_t \cdot m_S \cdot p_S$$

where A_t is the total number of adult spawners in year t, S_t is the total number of smolts going to sea in year t, m represents the mean mass of an individual adult (m_A) or smolt (m_S), and p represents the proportion of phosphorus in the body of adults (p_A) or smolts (p_S). Our spawner data from 1962–1999 came from Petrosky et al. (2001) and included an average 9.2% of hatchery adults that were released to spawn in the wild. For 2000–2004 we used spawner estimates from Scheuerell and Williams (2005), which did not include any additional hatchery adults. We used the number of wild smolts recorded at the uppermost dam on the Snake River from brood years 1962–1984 and 1990–2002 (for details see Scheuerell and Williams 2005). We did not include any hatchery smolts in our calculations because their food comes from outside the basin, making their nutrient export irrelevant for our purposes. We used 5.5 kg as the mean mass of adult Chinook salmon from the Snake River basin (Peery et al. 2003) and 12 g for the mean mass of smolts (Doug Marsh, Northwest Fisheries Science Center, National Marine Fisheries Service, 2725 Montlake Boulevard East, Seattle, WA 98112, USA, unpublished data). Following Moore and Schindler (2004), we assumed that the mass-specific concentrations of phosphorus were 0.38% and 0.43% for adults and smolts, respectively. These concentrations may vary somewhat but are assumed to be broadly applicable (Moore and Schindler 2004) and would only influence our results slightly. We concentrated on phosphorus because of its importance in limiting primary productivity in freshwater ecosystems, but similar results could be shown for nitrogen by applying the respective nitrogen-to-phosphorus ratios from the literature (sensu Moore and Schindler 2004).

We fit a Beverton-Holt stock–recruit relationship to the phosphorus imported by the adults (stock) in year t and those exported by their smolts (recruits) 2 years later. This relationship takes the form

$$E_{t+2} = \frac{a \cdot I_t}{b + I_t}$$

where the export (E) of phosphorus by smolts is a nonlinear function of the nutrients imported (I) by their parents. We fit the parameters by minimizing the negative log-likelihood of the model and assuming log-normally distributed errors. We also calculated the percentage of imported adult phosphorus that smolts export for the same brood years (E_{t+2}/I_t).

The mass-balance approach that we used to estimate net imports of marine-derived nutrients delivered to the Snake River basin was based on calendar years. We used this basis rather than brood years because of the strong seasonal dynamics in biogeochemical cycles driven by abiotic factors such as temperature, precipitation, and irradiance. The annual net flow (F) of phosphorus into freshwater in year t simply becomes

$$F_t = I_t - E_t$$

where I_t and E_t are the import and export of phosphorus, respectively, as described above. When F_t is positive, there is a net import of nutrients into the freshwater ecosystem in a given year, but when F_t is negative, smolts actually export

© 2005 NRC Canada

Fig. 1. (*a*) Nutrient import–export (stock–recruit) relationship of phosphorus transport by spring/summer Chinook salmon (*Oncorhynchus tshawytscha*) based on brood years 1962–1982 and 1990–2002 and (*b*) the percent of the adult nutrients that smolts export for the same brood years. Similar relationships exist for nitrogen but vary by a factor of 7.9 for adults and 5.7 for smolts, their respective N:P ratios (for details see Moore and Schindler 2004).

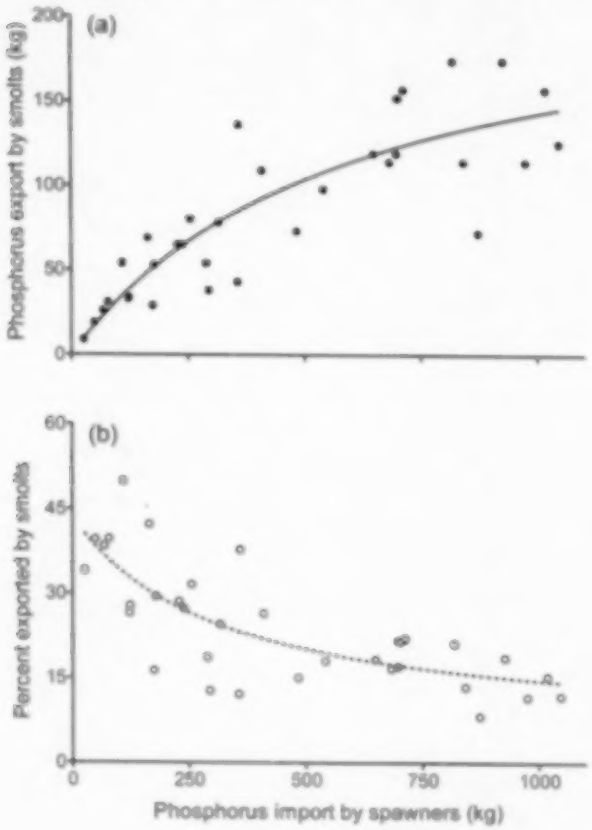

more nutrients than adults bring back. For these calculations, we also included adult return data from 2003 and 2004.

Results and discussion

We found a strong relationship between the amount of phosphorus imported by adult Chinook salmon and that exported by their offspring (R^2 = 0.74, a = 207, b = 537; Fig. 1*a*). Across the entire data set examined, adult Chinook salmon imported 456 ± 322 kg phosphorus·year^{-1} (mean ± 1 standard deviation, SD), whereas smolts exported 86 ± 49 kg phosphorus·year^{-1}. Using a historical estimate of 1.1 × 10^5 spawners (Peery et al. 2003) at an average weight of 8 kg (Gresh et al. 2000), adult Chinook would have imported 33 440 kg phosphorus·year^{-1} into the Snake River basin, more than 70 times the current estimate. In addition, if we assume a historical smolt-to-adult survival rate of 4.6% (the maximum over the past 40 years) and a individual mass of 18 g (1.5 times the current mass), smolts would have exported 1851 kg phosphorus·year^{-1}, more than 20 times the amount of phosphorous currently exported by smolts.

Fig. 2. Net phosphorus transport by spring/summer Chinook salmon (*Oncorhynchus tshawytscha*) over time. In years when net transport is negative, smolts export more phosphorus to the ocean than adults import to the freshwater ecosystem.

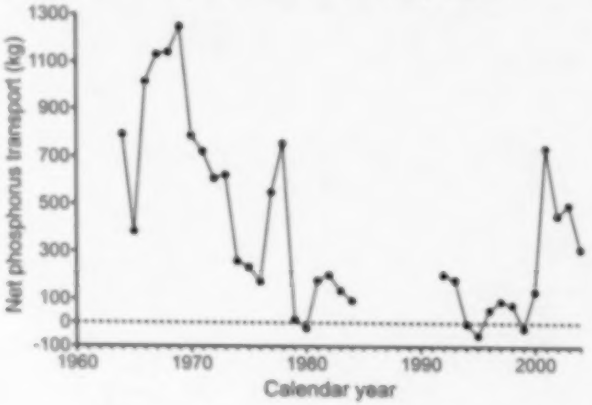

As the number of spawners decreased, smolts subsequently exported a greater percentage of the phosphorus that their parents imported into basin (Fig. 1*b*). On average, smolts exported 24 ± 10% of the phosphorus imported by adults since the early 1960s. This was significantly higher than our historical estimate of 5.5% based on the calculations above (t = 10.4, df = 33, P < 0.0001) or the overall average 16% for Bristol Bay sockeye salmon (t = 4.52, df = 33, P < 0.0001) reported by Moore and Schindler (2004). Furthermore, if we adjust their estimates to account for the 67% average harvest rate on adults, average phosphorus export by Bristol Bay smolts would also drop to near 5%.

We found a sharp decline in net transport of phosphorus from the early 1960s to the early 1980s (Fig. 2) corresponding to the large reduction in the size of adult salmon runs during that time. This downturn in phosphorous transport was followed by low and relatively constant transport through the 1990s, until an upswing began around 2000. Importantly, our calculations reveal that in 1980, 1994, 1995, and 1999, Chinook smolts actually exported more phosphorus than adults imported in those years (Fig. 2), resulting in a net export of nutrients from the system. Earlier research indicated that a major reduction in marine-derived nutrients delivered to the freshwater and surrounding riparian ecosystems coincided with dramatic declines in returns of adult salmon to the Columbia River basin over the last century (Gresh et al. 2000), but our findings based on the mass-balance approach of Moore and Schindler (2004) suggest that the situation is worse than previously thought for the Snake River basin — in some years, the input of nutrients was reduced to the point that nutrient exports actually exceeded imports.

Two lines of evidence suggest that marine-derived nutrients are important for supporting productive freshwater ecosystems in this region. First, Achord et al. (2003) found compensatory mortality in Chinook juveniles even though populations were far below historic levels, and they hypothesized that the large loss of marine-derived nutrients in the Snake River basin had lowered carrying capacity. As the

© 2005 NRC Canada

number of returning adults declined during the 1980s and 1990s, the percent of marine-derived nutrients exported by smolts increased (Fig. 1), with a subsequent decrease in the overall transport of phosphorus to fresh waters (Fig. 2), possibly creating the negative feedback loop postulated by Achord et al. (2003). Second, following a shift toward improved ocean conditions in 1999, the number of spawning adults destined for the Snake River basin increased (Scheuerell and Williams 2005), with a subsequent increase in the net transport of marine-derived nutrients (Fig. 2). However, the number of smolts per spawner produced in the 2001 and 2002 brood years was 33 and 55, respectively (John G. Williams, unpublished data), significantly lower than the average 69 ± 24 smolts per spawner produced during the previous period (1962–1977) of good ocean conditions and relatively high nutrient transport (2001, $t = 6.05$, df = 15, $P < 0.0001$; 2002, $t = 2.32$, df = 15, $P < 0.05$). This raises the possibility that the freshwater ecosystem has shifted to a less productive state (sensu Scheffer and Carpenter 2003).

Our results clearly have important implications for the recovery of threatened Snake River Chinook salmon. Recent population viability analyses of Snake River spring/summer Chinook salmon found that increasing juvenile productivity could lead to large increases in overall population size and that overall declines in marine-derived nutrients almost certainly contributed to the currently low productivity (Zabel et al. 2005). While the direct impacts of habitat degradation, harvest, hydroelectric dams, and hatchery production all contributed to the observed declines in salmon populations throughout this region, their indirect effects on the amount of marine-derived nutrients and energy delivered to these ecosystems also exacerbated the problem (Ruckelshaus et al. 2002). Can the recent high returns of adults to the basin restore the century-long depletion of marine-derived nutrients and increase overall productivity of the freshwater ecosystem? Certainly shifts in ocean-climate conditions and their subsequent impacts on salmon survival occur over time, and we cannot predict how long the currently favorable ocean conditions will last (Scheuerell and Williams (2005) and references therein). Therefore, it remains to be seen how the ecosystem will respond before the Northeast Pacific switches once again to a less productive regime for Columbia River salmon.

Much of the discussion related to habitat restoration for threatened and endangered salmon concentrates on the small-scale physical aspects of habitat (e.g., adequate streamflow, spawning gravel, large woody debris) or the large-scale processes (e.g., agricultural land use, road density) that alter those habitat features (Ruckelshaus et al. 2002). Nevertheless, carrying capacity for Pacific salmon depends fundamentally on properly functioning biogeochemical cycles and diverse food webs that are strongly influenced by marine-derived nutrients and energy (Schindler et al. 2003). Thus, while the amount and quality of habitat may limit population size, our results indicate that levels and dynamics of nutrients may also be crucial. This means that an ecosystem approach to management requires "ecologically defensible recovery goals" (sensu Peery et al. 2003) that take into consideration the important role of anadromous salmon in maintaining healthy freshwater and riparian ecosystems.

Acknowledgements

Comments by Jon Moore, Daniel Schindler, Jim Helfield, and an anonymous reviewer helped to improve the manuscript. We also thank the numerous personnel who assisted with data collection over the past 43 years. The views expressed herein are those of the authors and do not necessarily reflect those of the National Oceanic and Atmospheric Administration or its agencies.

References

Achord, S., Levin, P.S., and Zabel, R.W. 2003. Density-dependent mortality in Pacific salmon: the ghost of impacts past? Ecol. Lett. **6**: 335–342.

Bilby, R.E., Fransen, B.R., Bisson, P.A., and Walter, J.K. 1998. Response of juvenile coho salmon (*Oncorhynchus kisutch*) and steelhead (*Oncorhynchus mykiss*) to the addition of salmon carcasses to two streams in southwestern Washington, U.S.A. Can. J. Fish. Aquat. Sci. **55**: 1909–1918.

Gresh, T., Lichatowich, J., and Schoonmaker, P. 2000. An estimation of historic and current levels of salmon production in the Northeast Pacific ecosystem: evidence of a nutrient deficit in the freshwater systems of the Pacific Northwest. Fisheries, **25**: 15–21.

Moore, J.W., and Schindler, D.E. 2004. Nutrient export from freshwater ecosystems by anadromous sockeye salmon (*Oncorhynchus nerka*). Can. J. Fish. Aquat. Sci. **61**: 1582–1589.

Peery, C.A., Kavanagh, K.L., and Scott, J.M. 2003. Pacific salmon: setting ecologically defensible recovery goals. BioScience, **53**: 622–623.

Petrosky, C.E., Schaller, H.A., and Budy, P. 2001. Productivity and survival rate trends in the freshwater spawning and rearing stage of Snake River chinook salmon (*Oncorhynchus tshawytscha*). Can. J. Fish. Aquat. Sci. **58**: 1196–1207.

Ruckelshaus, M.H., Levin, P., Johnson, J.B., and Kareiva, P.M. 2002. The Pacific salmon wars: what science brings to the challenge of recovering species. Annu. Rev. Ecol. Syst. **33**: 665–706.

Scheffer, M., and Carpenter, S.R. 2003. Catastrophic regime shifts in ecosystems: linking theory to observation. Trends Ecol. Evol. **18**: 648–656.

Scheuerell, M.D., and Williams, J.G. 2005. Forecasting climate-induced changes in the survival of Snake River spring/summer Chinook salmon. Fish. Oceanogr. **14**. In press.

Schindler, D.E., Scheuerell, M.D., Moore, J.W., Gende, S.M., Francis, T.B., and Palen, W.J. 2003. Pacific salmon and the ecology of coastal ecosystems. Front. Ecol. Environ. **1**: 31–37.

Wipfli, M.S., Hudson, J.P., Caouette, J.P., and Chaloner, D.T. 2003. Marine subsidies in freshwater ecosystems: salmon carcasses increase the growth rates of stream-resident salmonids. Trans. Am. Fish. Soc. **132**: 371–381.

Zabel, R.W., Scheuerell, M.D., McClure, M.M., and Williams, J.G. 2005. The interplay between climate variability and density dependence in the population viability of Chinook salmon. Conserv. Biol. **19**. In press.

© 2005 NRC Canada

Fishing methods to reduce sea turtle mortality associated with pelagic longlines

John W. Watson, Sheryan P. Epperly, Arvind K. Shah, and Daniel G. Foster

Abstract: Changes in hook design and bait type were investigated as measures to reduce the bycatch of sea turtles on pelagic longlines in the western North Atlantic Ocean. Specifically, the effectiveness of 18/0 circle hooks and mackerel (*Scomber scombrus*) bait was evaluated with respect to reducing sea turtle interactions and maintaining swordfish (*Xiphias gladius*) and tuna (*Thunnus* spp.) catch rates. Individually, circle hooks and mackerel bait significantly reduced both loggerhead (*Caretta caretta*) and leatherback (*Dermochelys coriacea*) sea turtle bycatch. Circle hooks also significantly reduced the rate of hook ingestion by the loggerheads, potentially reducing postrelease mortality. The combination of circle hooks and mackerel bait was even more effective for loggerhead turtles and had no negative effect on swordfish catch. These modifications in fishing methods, in conjunction with tools developed to remove hooks and line from the turtles, significantly reduced the capture rate of sea turtles and potentially the post-hooking mortality of those that were caught and did not negatively impact the primary target species catch rate. In addition, these mitigation measures have the potential to reduce mortality of sea turtles and other bycatch species worldwide.

Résumé : Nous avons évalué les changements de forme des hameçons et de type d'appât sur les palangres pélagiques comme moyens de réduire les prises accessoires de tortues de mer dans la partie occidentale de l'Atlantique nord. Nous avons, en fait, évalué l'efficacité des hameçons autoferrants 18/0 et des appâts de maquereau (*Scomber scombrus*) pour restreindre les interactions avec les tortues de mer, tout en maintenant les taux de capture d'espadons (*Xiphias gladius*) et de thons (*Thunnus* spp.). Les hameçons autoferrants et les appâts de maquereau réduisent significativement, tous les deux, les prises accessoires des tortues de mer, tant des caouannes (*Caretta caretta*) que des tortues luth (*Dermochelys coriacea*). Les hameçons autoferrants réduisent aussi significativement le taux d'ingestion des hameçons chez les caouannes, ce qui diminue potentiellement la mortalité après la libération. L'utilisation combinée d'hameçons autoferrants et d'appâts de maquereau est encore plus efficace chez les caouannes, sans effet négatif sur la capture des espadons. Ces modifications des techniques de pêche et la mise au point d'outils pour retirer les hameçons et les lignes des tortues réduisent significativement le taux de capture des tortues de mer et diminuent potentiellement la mortalité d'après ferrage des tortues qui sont capturées, sans effet négatif sur le taux de capture des espèces principales ciblées. De plus, ces mesures de mitigation peuvent potentiellement réduire la mortalité des tortues de mer et des autres espèces dans les prises accessoires à l'échelle globale.

[Traduit par la Rédaction]

Introduction

Six of the seven extant species of sea turtles living in the world's oceans are listed as either critically endangered or endangered (IUCN 2003), and international trade of these species is prohibited (CITES 2003); the seventh species is listed as data deficient. They also are protected by the United States Endangered Species Act and similar laws of other nations. The failure worldwide of most sea turtle populations to recover is attributed, in part, to their incidental capture in fisheries (Hillestad et al. 1995; Lutcavage et al. 1996). Trawls (Magnuson et al. 1990; Poiner and Harris 1996), gill nets (De Metrio and Megalofonu 1988; Julian and Beeson 1998), and longlines (Camiñas 1997; Witzell 1999; Lewison et al. 2004) are gears known to interact with turtles worldwide. Bycatch (unintended and discarded catch) in trawls, identified as the most important source of human-associated mortality (Magnuson et al. 1990), is being addressed with turtle excluder devices (Epperly 2003). This paper focuses on pelagic longlines, which primarily target tuna (*Thunnus* spp.), swordfish (*Xiphias gladius*), and sharks (Squaliformes) worldwide, and on methods to significantly reduce the incidental bycatch of sea turtles in these fisheries.

Estimates of turtle takes in the Atlantic pelagic longline fisheries have raised concern that the pelagic longline fishery may be impacting the potential recovery of loggerhead (*Caretta caretta*) and leatherback (*Dermochelys coriacea*) sea turtle populations. From 1992 to 1999, the United States Atlantic pelagic longline fleet incidentally caught an estimated 7891 loggerhead and 6363 leatherback sea turtles (Yeung 2001); the United States fleet represents less than

Received 26 July 2004. Accepted 17 December 2004. Published on the NRC Research Press Web site at http://cjfas.nrc.ca on 13 May 2005.
J18234

J.W. Watson[1] and D.G. Foster. National Oceanic and Atmospheric Administration (NOAA), National Marine Fisheries Service, Mississippi Laboratories, 3209 Frederic Street, Pascagoula, MS 39568, USA.
S.P. Epperly. National Oceanic and Atmospheric Administration (NOAA), National Marine Fisheries Service, 75 Virginia Beach Drive, Miami, FL 33149, USA.
A.K. Shah. Merck Research Laboratories, RY34-B370, P.O. Box 2000, Rahway, NJ 07065-0900, USA.

[1]Corresponding author (e-mail: john.watson@noaa.gov).

 doi: 10.1139/F05-004 © 2005 NRC Canada

Fig. 1. The Northeast Distant Waters (NED) was closed to fishing 2001–2003 because of high sea turtle bycatch rates and was the study area for the bycatch experiments.

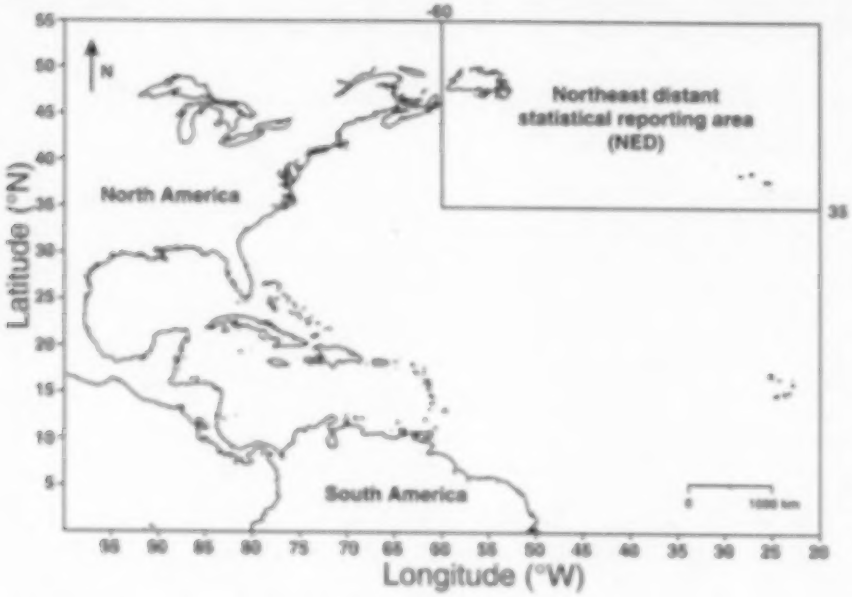

10% of the pelagic longline fishing effort in the North Atlantic Ocean (Witzell et al. 2001). Recent management actions by the United States were designed to reduce the impact of the United States pelagic longline fisheries on sea turtles in both the Pacific Ocean and Atlantic Ocean basins. Prime fishing grounds, including international waters of both the Pacific and Atlantic, have been closed to United States fishermen in an attempt to reduce incidental fishing mortality of sea turtles in the longline fishery (US Department of Commerce 1999, 2000). These actions have been legally contentious (Blue Water Fishermen's Association vs. National Marine Fisheries Service, 226 F. Supp. 2d 330 (D. Mass. 2002); Hawaii Longline Association vs. National Marine Fisheries Service, 281 F. Supp. 2d 1 (D.D.C. 2003)), and the outcomes are being scrutinized by the international fishing community, nongovernmental organizations, and foreign governments.

The Northeast Distant (NED) statistical reporting area in the Western North Atlantic (Fig. 1), including the productive Grand Banks, was closed to the United States fleet, partly in 2000 and completely during 2001–2003, as a result of interactions with threatened and endangered loggerhead and leatherback sea turtles (US Department of Commerce 2000, 2001*a*, 2001*b*). Our research focused first on eliminating or reducing interactions between the swordfish fishery and sea turtles. Second, for those interactions that could not be avoided, we strove to reduce the likelihood of sea turtles being injured or killed during or as a result of the interaction. There are many possible avenues for research to reduce sea turtle bycatch and mortality. Some may focus on the behavior of bycatch species, while others involve efforts to physically limit capture. We focused on the latter course of study and investigated the effects of hook style and bait.

The predominant hook type used historically in the United States Western Atlantic pelagic longline fishery for swordfish is the 9/0 J hook with 20°–25° offset (Fig. 2), and the predominant bait is squid (*Illex* spp.) (Hoey and Moore 1999). Offset hooks are hooks with the point bent sideways (usually 18°–20°) in relation to the shank. Offset hooks are believed to be more effective in hooking and retaining fish than a straight (0° offset) hook and are easier to bait. Recent studies have shown that circle style hooks with no offset or minor offset (about 4°) cause less physical damage to fish than J style hooks because of the tendency of circle hooks to engage fish in the mouth rather than in the pharynx, esophagus, or stomach and also because circle hooks minimize foul hooking (externally hooked) and bleeding (Prince et al. 2002; Skomal et al. 2002). Circle hook use in pelagic longline fisheries may increase the catch per unit effort (CPUE) of yellowfin tuna (*Thunnus albacares*) and improve the survival of incidental fish bycatch (Hoey 1996; Falterman and Graves 2002). With respect to sea turtles, a study conducted in the Azores found that 0° offset 16/0 circle hooks significantly decreased the proportion of swallowed hooks in loggerhead turtles but did not reduce the rate of turtle interaction (Bolten et al. 2002). Loggerhead turtle interactions observed include swallowed hooks, mouth hooked, hooked externally, and entangled. In 2001, leatherback turtle interactions in the Canadian longline fishery (Canadian Atlantic waters and NED) were higher with J hooks than with 10° offset 16/0 circle hooks (Javitech 2002). In this same study, interaction rates were lower for both leatherback and loggerhead turtles with mackerel (*Scomber scombrus*) bait versus squid bait (Javitech 2002).

In 2001 and 2002, we conducted research in the NED to evaluate the effects of pelagic longline fishing gear modifications. In 2002, we focused the research on hook style and bait. The goal of the research was to investigate methods to reduce turtle captures and turtle mortalities, while retaining viable fishing performance by the longline fleet. We also

© 2005 NRC Canada

Fig. 2. Control (9/0 J hook with 25° offset) and experimental (18/0 circle hook with 0° offset and 18/0 circle hook with 10° offset) hook designs.

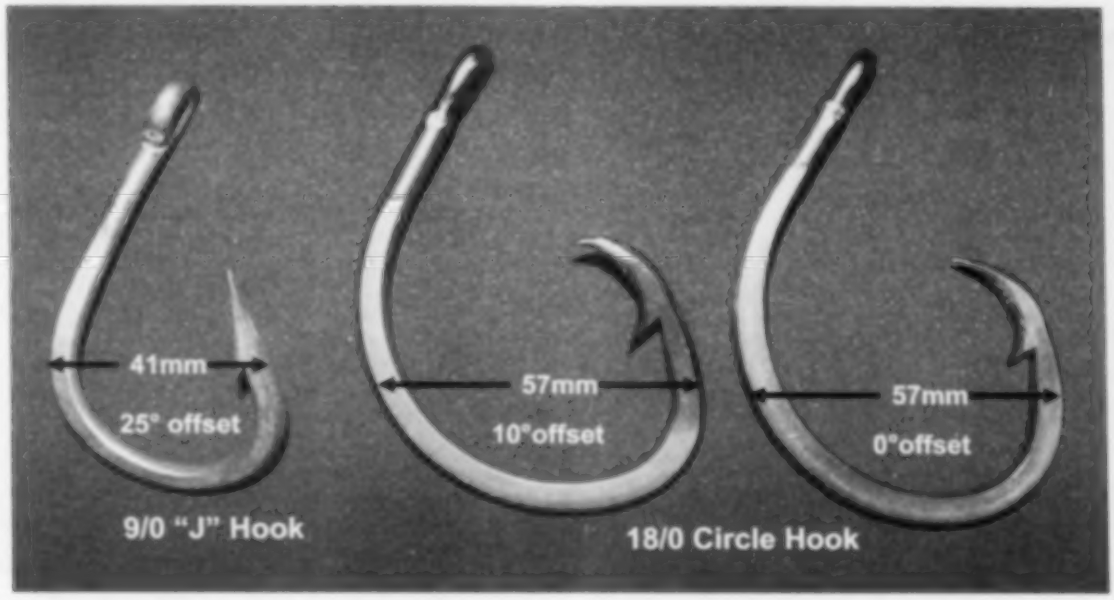

evaluated the effects of these modifications on the bycatch species most frequently discarded by the United States fleet, blue shark (*Prionace glauca*), which is a target species in some fisheries around the world.

Materials and methods

Experimental design

We evaluated the effectiveness of circle hooks (C) versus J hooks (J) and mackerel (M: *Scomber scombrus*) bait versus squid (S: *Illex* spp.) bait in reducing the sea turtle interaction rate and injury associated with pelagic longline gear. The control treatment was the industry standard 20°–25° offset J hooks with squid bait (JS). Four experimental treatments were tested: (*i*) 0° offset 18/0 circle hooks with squid bait (C_1S), (*ii*) 10° offset 18/0 circle hooks with squid bait (C_2S), (*iii*) 20°–25° offset 9/0 J hooks with mackerel bait (JM), and (*iv*) 10° offset 18/0 circle hooks with mackerel bait (C_2M). Offset hooks were included among the treatments because it is difficult to bait the 0° offset 18/0 circle hooks with mackerel. The experimental treatments hooks were from a single manufacturer, Lindgren-Pitman Inc. (Pompano Beach, Florida) (LP).

Control and experimental hooks were alternated on each longline section (length of mainline between highflyer buoys) along the entire set. Only one bait type was used within a set to avoid possible interaction effect of bait types. Vessels alternated among the three experimental set configurations. On every set, vessels deployed the gear with three hooks fished between each set of floats: one placed directly adjacent to each float, and the other two placed between the floats at an equal distance from each other.

Fishing gear was standardized among the vessels to reduce gear-induced variability. Hook spacing was consistent within a trip, and a hook was fished adjacent to each float. Buoy lines, leader lengths and size, mainline, buoy line, and leader color were consistent within a trip. Green light sticks and leaded swivels were used on every leader, and placement was consistent. Bait used was 150–300 g squid bait or 200–500 g mackerel bait, and baiting technique was consistent within a trip. Control hooks were Mustad 9/0 #7698 RD, Mustad 9/0 #76801 (O. Mustad & Son, A.S., Gjövik, Norway), Eagle Claw 9/0 #9016 (Eagle Claw Fishing Tackle Co. Denver, Colorado), or LP-SW 9/0.

Setting time was restricted to no earlier than sunset, and captains attempted to have the gear hauled between 1000 and 1300 Eastern Standard Time. Other than the experimental design requirements, captains were allowed to fish normally and chose the location of fishing, length of trips, total number of hooks fished, etc. Fishing locations, length of trips, number of hooks fished, and catch rates were similar to those of observed trips prior to closure of the NED area to United States fishing vessels in 2000 (Hoey and Moore 1999; Beerkircher et al. 2002).

We conducted a power analysis to estimate the experimental fishing effort required to detect a fishing method that has different degrees of effectiveness in reducing bycatch of turtles in comparison with the control fishing method (Appendix A). The number of hooks required to detect a 25% and 50% reduction in loggerhead CPUE was 54 054 and 9012 hooks per treatment, respectively. Comparative efforts required for leatherback turtles were 163 548 and 26 828 hooks per treatment, respectively.

Data collection

All vessels participating in the experiment carried observers, and both the observers and the captains were well versed on the experimental design. Each observer was trained in safety; fish, mammal, and seabird identifications; data collection, and the operation of a pelagic longline fishing ves-

© 2005 NRC Canada

sel; many had prior experience. Observers also received extensive training on sea turtles: safe handling, collection of biological data, gear removal, tagging, etc.

Observers collected fishery data as described by the Southeast Fisheries Science Center (SEFSC) Pelagic Longline Observer Program (Beerkircher et al. 2002), with minor modifications to accommodate the experiment. Details on the Pelagic Observer Program are available online at http://www.sefsc.noaa.gov/pop.jsp. The time and location of each section of gear was recorded as it was deployed and retrieved, as was the sea surface temperature. These data were obtained from the vessel's existing wheelhouse equipment and were reported in nonmetric units. The section number, treatment (hook type and style), time on deck, and species were recorded for each animal captured. If boated, length was measured in centimetres. Length was estimated for marine mammals, which were not boated. A carcass tag applied to each fish was used to match the dressed weight (carcass with head and fins removed and animal eviscerated) of the fish during unloading at the dock to the particular data collected on that animal at sea.

For sea turtles, the type of interaction (hooked, entangled, or hooked and entangled), the exact location of the hook in the turtle, and the hook style was recorded. The protocols for collecting sea turtle capture data are available online at http://www.sefsc.noaa.gov/seaturtlefisheriesobservers.jsp. In addition, time, sea surface temperature, location, and the position of turtle (section and hook position relative to a buoy) within the set were noted. Carapace lengths of turtles not boated (leatherbacks) were estimated. Observers and crew attempted to remove fishing gear using long-handled dehookers and line cutters. When possible, turtles (loggerheads) were boated with a large dip net. Observers attempted to remove all gear immediately. They were instructed to remove all external hooks and those in the mouth, as well as hooks in the esophagus when the insertion point of the barb could be seen. Boated turtles were measured to the nearest 0.1 cm and tagged. Details about any gear remaining on the animal at time of release were noted, in addition to the turtle's condition, the time, location, and sea surface temperature.

Statistical methods

The relationship between the catch rate (or catch probability) and the explanatory variables (hook type, sea surface temperature, daylight soak time, and total soak time) was investigated using generalized linear models (Agresti 1996; Draper and Smith 1998; Hosmer and Lemeshow 1989). In particular, logistic regression analysis (with maximum likelihood estimation procedure) for binary response (turtle and blue shark) count data and traditional regression analysis (with least squares estimation procedure) for continuous response weight data was used. (Swordfish and bigeye tuna (*Thunnus obesus*) were retained for sale.) There were some animals caught for which a treatment (hook type) could not be determined; these included animals that were hooked with both control and treatment hooks and animals that were entangled (not hooked). These data were excluded from the analysis. Section sea surface temperatures and hook soak time measurements were averaged for each set. Total soak time and daylight soak time values were estimated by averaging the soak times for the beginning and end of each section. Sunrise and sunset values were obtained for centralized locations within the fishing area using software provided by the Astronomical Applications Department of the US Naval Observatory. Sunrise and sunset estimates are within 20 min of actual times. The effect of hook depth was not examined, since swordfishers set fish hooks at approximately the same depth.

The modeling results presented used set as the experimental unit. A test of coincidence of the models was performed, and the treatments were combined where appropriate. The confidence intervals (CIs) on appropriate model coefficients (or its functions) were constructed to arrive at the CIs on reduction rate for each of the treatments. All analyses utilized the original units of measurements (e.g., dressed weight and sea surface temperature).

Since the probability of a turtle catch (per hook) for the hook types being compared is fairly small, the catch probability ratio for the two hook types was approximated from the odds ratio (corresponding to hook types) estimated from the fitted logistic regression models. Thus, subtracting the odds ratio (and confidence limits) from 1 provides an estimate of reduction rate (and related confidence limits) due to experimental hook. Approximation of relative risk for other factors also utilized odds ratio owing to low magnitude of catch probability. For swordfish and bigeye tuna, where catch weight per hook is modeled through traditional regression techniques, a CI on absolute weight reduction (per hook) was constructed. The limits of this CI were then divided by average catch per control hook to estimate CIs for reduction rate. The ratio is a natural scale for multiplicative models, while the difference is a natural scale for additive models. Thus, ratio of odds (of turtle capture for control and experimental hooks) is a natural scale for the logistic models, while the difference in the means (of catch per hook for the control and experimental hooks) is a natural scale for the traditional regression model for continuous response variable. Chi-square tests were used to compare hook locations in sea turtles among hook types and bait types.

Results

During July–October 2002, 13 commercial longline vessels made 489 research sets in the NED, fishing a total of 427 382 hooks: approximately 142 000 for the control (J hooks with squid bait) and about 71 000 hooks for each treatment. Vessels fished an average of 874 hooks per set; the minimum number of hooks fished in a set was 210 hooks, and the maximum was 1173 hooks. The average number of sections per set was eight and the range was 2–11. The spatial and temporal distribution of the sets by hook and bait type and the mean sea surface temperature among treatments were the same (Figs. 3 and 4). The combined length of float lines and gangions was between 11.0 and 23.8 m, which represents the approximate depth of the hooks, excluding curvature of mainline. Soak times ranged from 524 to 1556 min, with an average of 761 min and standard deviation of 99 min, while temperature ranged from 12 to 23 °C, with an average of 17 °C and standard deviation of 1.7 °C. The vessels caught 34 taxa of fish (Table 1). The target species, swordfish and bigeye tuna, along with blue

© 2005 NRC Canada

Fig. 3. Geographical effort distribution by bait type. Circles represent sets using mackerel (*Scomber scombrus*) bait; triangles represent sets using squid (*Illex* spp.) bait. Grayscale represents depth contours.

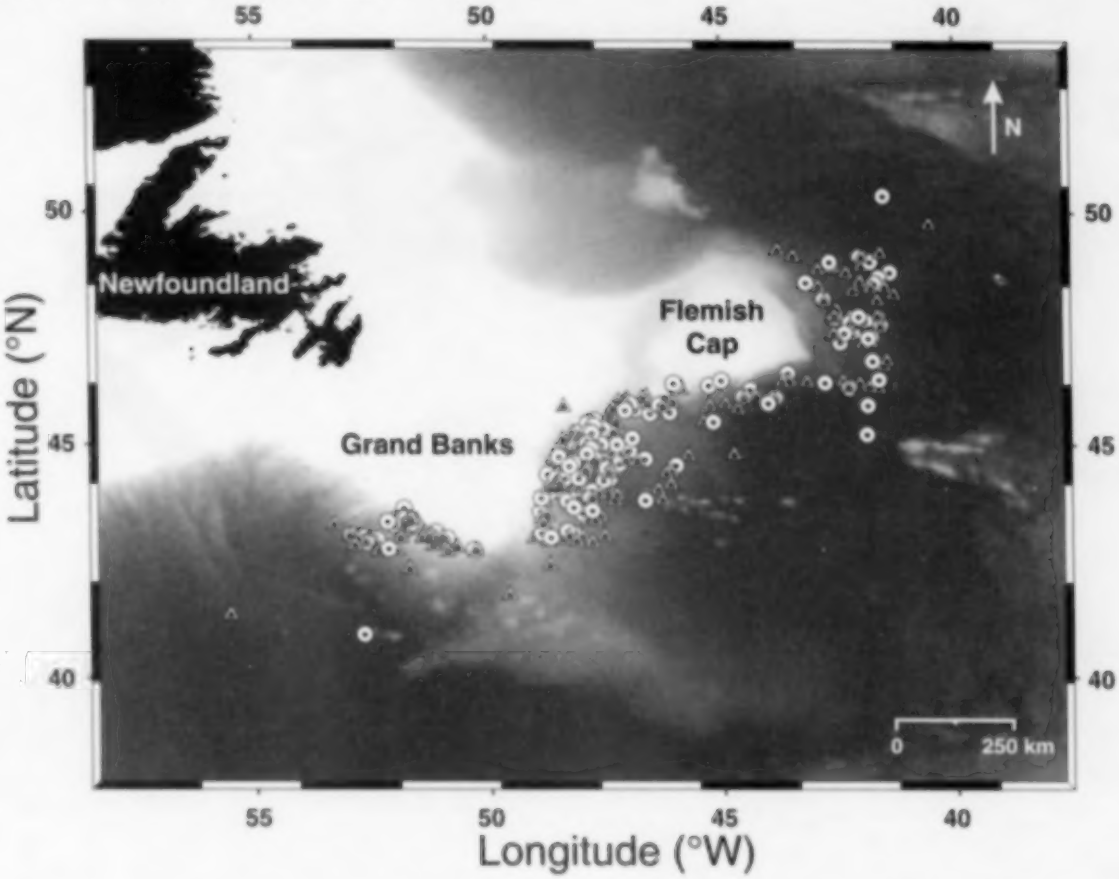

Fig. 4. Sea surface temperature distribution (mean section temperature) by bait type. Solid line represents temperatures at which mackerel (*Scomber scombrus*) bait were fished; broken line represents temperatures at which squid (*Illex* spp.) bait were fished.

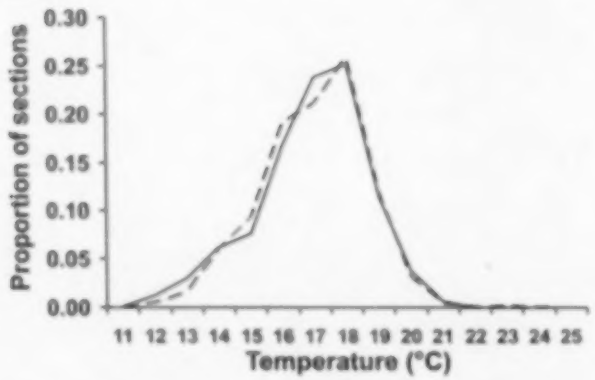

shark, were the species most often caught. The vessels kept for sale 7925 swordfish (total dressed weight of 399.2 tonnes (t)) and 864 bigeye tuna (total dressed weight of 30.8 t). Blue shark was the species most frequently captured, but few (n = 8, total dressed weight = 0.2 t) were kept. During the course of the experiment, 96 loggerhead and 148 leatherback turtles were captured and released alive (original data shown in National Research Council Data Depository (NRC-DD) Table S1[2]). The vessels also captured 12 seabirds and nine marine mammals: five unidentified seabirds (one estimated at 120 cm in length), three greater shearwaters (*Puffinus gravis*, 60–75 cm), three *Puffinus* spp.(one 65 cm in length), one northern gannet (*Sula bassanus*), four Risso's dolphins (*Grampus griseus*, 1.5–2.4 m), two *Stenella* spp. (1.5–1.7 m), one common dolphin (*Delphinus delphis*, 2.1 m), one pilot whale (*Globicephala* spp., 1.8 m), and one unidentified marine mammal (6 m). All mammals were released alive, as were the northern gannet, one *Puffinus* spp., and three unidentified seabirds.

[2] Supplementary data for this article are available on the Web site or may be purchased from the Depository of Unpublished Data, Document Delivery, CISTI, National Research Council Canada, Ottawa, ON K1A 0S2, Canada. DUD 3659. For more information on obtaining material refer to http://cisti-icist.nrc-cnrc.gc.ca/irm/unpub_e.shtml.

© 2005 NRC Canada

Table 1. Fish and sharks caught on experimental pelagic longline sets.

Scientific name	Common name	Discarded	Kept
Prionace glauca	Blue shark	12 747	8
Xiphias gladius	Swordfish	1 338	7 925
Thunnus obesus	Bigeye tuna	60	864
Thunnus alalunga	Aalbacore	180	233
Isurus oxyrinchus	Shortfin mako	144	191
Lamna nasus	Porbeagle	257	16
Thunnus thynnus	Bluefin tuna	76	30
Alepisaurus spp.	Lancetfishes	98	1
Rajiformes	Skates, rays, sawfishes, and guitarfishes	91	
Coryphaena spp.	Dolphins	37	7
Unknown	—	42	
Mola spp.	Molas	20	
Ruvettus pretiosus	Oilfish	19	1
Squaliformes	Dogfish and angel sharks	16	
Lepidocybium flavobrunneum	Escolar	13	1
Tetrapturus albidus	White marlin	8	
Trichiuridae	Snake mackerels	8	
Thunnus albacares	Yellowfin tuna	1	2
Thunnus spp.	Tunas and albacore	3	
Isurus paucus	Longfin mako	2	
Makaira nigricans	Blue marlin	2	
Polyprion americanus	Wreckfish	2	
Somniosus microcephalus	Greenland shark	2	
Tetrapturus georgei	Roundscale spearfish	2	
Tetrapturus spp.	Marlins and spearfish	2	
Acanthocybium solandri	Wahoo		1
Alopias spp.	Thresher sharks	1	
Alopias superciliosus	Bigeye thresher	1	
Bruma spp.	Pomfrets	1	
Cetorhinus maximus	Basking shark	1	
Isurus spp.	Mako sharks	1	
Katsuwonus pelamis	Skipjack tuna	1	
Lophius americanus	Goosefish	1	
Tetrapturus pfluegeri	Longbill spearfish	1	

Treatment effects

Loggerhead sea turtles

Loggerheads ranged in size from 32.4 to 68.0 cm standard straight line carapace length (SCL_{-nt}) and averaged 56.8 cm ($n = 93$) (Fig. 5*a*). No loggerheads had been tagged previously. The highest reduction rates for loggerhead turtle interaction with pelagic longline gear, when compared with the traditional *J* hook and squid bait used in this fishery, was achieved with 18/0 circle hooks with mackerel bait. Circle hooks used in combination with mackerel bait reduced loggerhead catch by 90% (CI = 70%–97%, $p < 0.0001$). Circle hooks with squid bait reduced loggerhead catch by 86% (CI = 73%–93%, $p < 0.0001$) and mackerel bait with *J* hooks by 71% (CI = 42%–86%, $p = 0.0005$) (Fig. 6*a*). The odds ratio ranged from 0.10 to 0.29 in these models, suggesting the loggerhead turtle catch on the control hook and bait was between 3.4 and 10 times (increase of 240%–900%) that of the experimental hooks and bait (Table 2).

The sea surface temperature effect for loggerhead turtles also was highly significant ($p < 0.0001$). The loggerhead turtle catch rate increased by a multiplicative factor of 25%–35% with 0.6 °C increase in sea surface temperature. Thus, the loggerhead catch rate increased 200%–350% with every 2.8 °C increase in sea surface temperature. Extrapolations of effects of sea surface temperature outside the range observed were not appropriate.

The effect of total soak time on loggerhead turtle catch was highly significant ($p \leq 0.0003$) as well, suggesting an increase in the loggerhead turtle catch rate by a multiplicative factor of 0.6%–0.8%, with a unit increase (min) in total soak time. The effect of daylight soak time (a portion of the total soak time) was varied and inconclusive (p values ranging from 0.0008 to 0.5822). We suspect that there was a confounding effect between total soak time and daylight soak time. Swordfish sets were made at sunset and retrieved early in the morning, which means any increase in total soak time was an increase in daylight soak time. The odds ratios ranged between 0.987 and 0.999.

Circle hooks also resulted in a significant change in hooking location ($p < 0.01$). Loggerheads most often were hooked internally, although foul hooking sometimes occurred. The majority (68.8%, $n = 55$) of the 80 loggerheads caught on *J* hooks swallowed the hooks (Fig. 7*a*), which probably is the most lethal form of hooking interaction. In contrast, only 27.3% ($n = 3$) of the 11 loggerheads caught on

© 2005 NRC Canada

Fig. 5. Carapace lengths of (*a*) loggerhead turtles (*Caretta caretta*; $n = 93$) and (*b*) leatherback turtles (*Dermochelys coriacea*; $n = 147$).

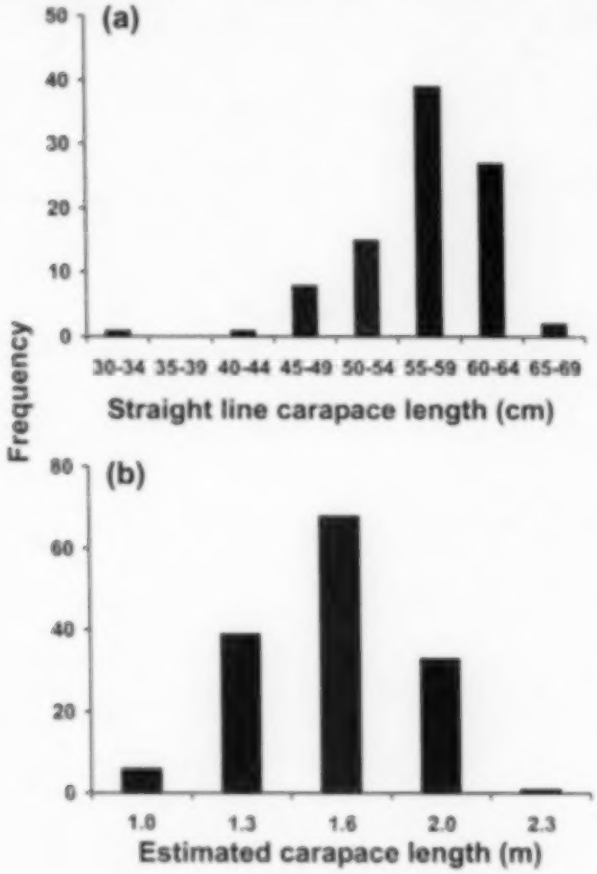

Fig. 6. Catch per unit effort for (*a*) loggerhead turtles (*Caretta caretta*) and (*b*) leatherback turtles (*Dermochelys coriacea*) caught on (*i*) 25° offset 9/0 J hooks using squid bait ($n = 142\,701$) (JS), (*ii*) 0° and 10° offset 18/0 circle hooks combined using squid bait ($n = 142\,701$) (CS), (*iii*) 25° offset 9/0 J hooks using mackerel bait ($n = 70\,990$) (JM), and (*iv*) 10° offset 18/0 circle hooks using mackerel bait ($n = 70\,990$) (C_2M).

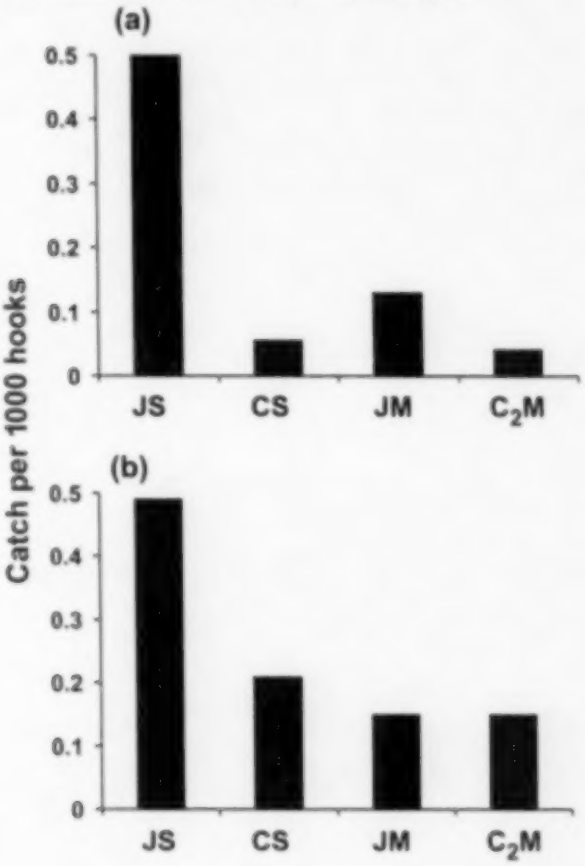

circle hooks swallowed the hooks; most were hooked in the mouth, where the hooks could be removed more safely (Fig. 7*a*). There was no significant difference in hooking location of loggerheads between hooks baited with mackerel and hooks baited with squid ($p > 0.5$). Sample size was too small to statistically evaluate the effects of hook offset or the interaction of bait and hook type on the hooking location.

Leatherback sea turtles

The estimated carapace lengths of leatherbacks ranged from 1.0 to 2.3 m, with a mode of 1.6 m ($n = 147$) (Fig. 5*b*). The largest reduction in leatherback turtle catch rate was achieved with mackerel bait. The J hooks with mackerel bait reduced leatherback catch by 66% (CI = 37%–81%, $p = 0.0006$), and circle hooks with mackerel bait reduced leatherback catch by 65% (CI = 36%–81%, $p = 0.0007$) (Fig. 6*b*). Circle hooks with squid bait reduced leatherback turtle catch by 57% (CI = 34%–72%, $p < 0.0001$) (Table 3). The leatherback turtle catch rate on the control hook and bait was 2.0–2.9 times (increase of 100%–190%) that of the experimental hooks and bait (the odds ratios ranged from 0.34 to 0.50).

The sea surface temperature effect for leatherback turtles was also highly significant ($p \leq 0.0095$). The leatherback catch rate increased by a multiplicative factor of 14%–22%, with a 0.6 °C increase in sea surface temperature. Neither total soak time nor daylight soak time had a significant effect on leatherback catch rates ($p \geq 0.1761$ and $p \geq 0.6421$, respectively). This difference compared with loggerhead turtles may indicate a difference in time of interaction between these two species.

In contrast with loggerheads, the change in hooking location with treatments was not as pronounced. Leatherbacks most often were hooked externally or were entangled in the lines (Fig. 7*b*); often they were both hooked and entangled ($n = 23$). They mostly were hooked in the shoulder, armpit, or front flipper ($n = 107$); rarely was the hook internal ($n = 8$). The comparison of hook locations between the two bait types was not significant ($p > 0.10$). However, there was a significant difference in hooking location between hook types ($p < 0.0001$; Fig. 7*b*). With circle hooks, a signifi-

© 2005 NRC Canada

Table 2. Odds ratio estimates from the models for loggerhead (*Caretta caretta*) turtles.

Effect	Odds ratio	95% Wald confidence limits		*p*
Treatment C_1S (0° offset 18/0 circle hook with squid bait)				
Hook type	0.125	0.044	0.352	<0.0001
Sea surface temperature	1.348	1.253	1.449	<0.0001
Total soak time	1.007	1.003	1.011	0.0003
Daylight soak time	0.987	0.979	0.995	0.0008
Treatment C_2S (10° offset 18/0 circle hook with squid bait)				
Hook type	0.15	0.064	0.353	<0.0001
Sea surface temperature	1.245	1.134	1.367	<0.0001
Total soak time	1.008	1.004	1.011	0.0001
Daylight soak time	0.999	0.993	1.004	0.5822
Treatment CS (C_1S and C_2S combined)				
Hook type	0.139	0.072	0.269	<0.0001
Sea surface temperature	1.287	1.216	1.362	<0.0001
Total soak time	1.006	1.004	1.008	<0.0001
Daylight soak time	0.994	0.990	0.998	0.0051
Treatment JM (25° offset J hook with mackerel bait)				
Hook type	0.291	0.145	0.585	0.0005
Sea surface temperature	1.276	1.204	1.353	<0.0001
Total soak time	1.006	1.004	1.009	<0.0001
Daylight soak time	0.993	0.988	0.997	0.001
Treatment C_2M (10° offset 18/0 circle hook with mackerel bait)				
Hook type	0.096	0.030	0.305	<0.0001
Sea surface temperature	1.276	1.201	1.355	<0.0001
Total soak time	1.006	1.004	1.008	<0.0001
Daylight soak time	0.993	0.993	0.998	0.0024

Note: Sea surface temperature data were modeled in degrees Fahrenheit; soak times were were modeled in minutes.

cantly larger proportion (of a smaller number) were not hooked externally and instead were getting the bait into their mouth (Fig. 7*d*); seven of eight leatherbacks hooked in the mouth were taken on circle hooks (six of seven on the circle hook with a 10° offset), and seven of the eight were taken on squid. Sample size was too small to statistically evaluate the effects of hook offset or the interaction of bait and hook type on the hooking location.

Swordfish

Swordfish is the primary target species in the NED fishery studied. Swordfish caught averaged 164 cm in length (range 57–283 cm), and the mean weight of swordfish retained was 50.1 kg (range 10.9–245.5 kg). Swordfish catch rate was increased 30% (CI = 14%–46%, $p = 0.0002$) by circle hooks with mackerel bait and 63% (CI = 46%–81%, $p < 0.0001$) by J hooks with mackerel bait. The catch rate of swordfish was reduced 33% (CI = 19%–46%, $p < 0.0001$) by 0° offset circle hooks with squid bait (C_1S) and 29% (CI = 14%–44%, $p = 0.0002$) by 10° offset circle hooks with squid bait (C_2S) (Fig. 8*a*). The models for treatments C_1S and C_2S could not be combined for swordfish because of a significant difference between the two models ($p = 0.0005$). Both circle hook types (C_1 and C_2) and mackerel bait significantly ($p = 0.0002$) affected swordfish catch (Table 4).

The sea surface temperature effect for swordfish was found to be significant only in the models for the circle hooks baited with squid treatments (C_1S, $p = 0.0413$; C_2S, $p = 0.0441$). The respective regression coefficients of 0.046 and 0.060 indicate an increase of between 20.9 and 27.2 kg of swordfish catch per 1000 hooks per 0.6 °C increase in sea surface temperature. The effect of total soak time on swordfish catch was not significant ($p \geq 0.0629$). However, the effect of daylight soak time was positive and significant ($p \leq 0.0279$). The positive relationship between daylight soak time and swordfish catch is most likely spurious, because swordfish are caught on longline gear at night (Hoey and Moore 1999). A probable explanation of this positive relationship is that daylight soak time is related to haul time, which increases as nighttime swordfish catch increases because of the increased time required for handling and processing the catch.

The mouth was the most frequent location of hooks in swordfish caught in the control and each treatment. However, hooking location proportions did vary among the treatments. Differences among treatments were mainly due to a shift between gut and mouth hooking. Both circle hooks, baited with squid and with mackerel (11%–18%) and mackerel alone (24%), resulted in less gut hooking than J hooks baited with squid (30%) ($p < 0.0001$) (original data shown in NRC-DD Table S2[2]). Gut hooking was more frequent with the 10° offset circle hook (18%) than with the 0° offset circle hook (12%) when baited with squid ($p < 0.0001$), but still was less than with J hooks. The observed reduction in swordfish catch with circle hooks is believed to be due to the increased percentage of mouth-hooked fish and the tendency

© 2005 NRC Canada

Fig. 7. Location of hooks in (*a*) loggerhead turtles (*Caretta caretta*) caught on J hooks (solid bars) (n = 80) and 18/0 circle hooks (hatched bars) (n = 11) and (*b*) leatherback turtles (*Dermochelys coriacea*) caught on J hooks (n = 82) and 18/0 circle hooks (n = 40). Note that the totals reported are fewer than the total number of animals captured (loggerheads n = 96 and leatherbacks n = 148) because some animals were not hooked or hook type was unknown or they were caught with more than one hook.

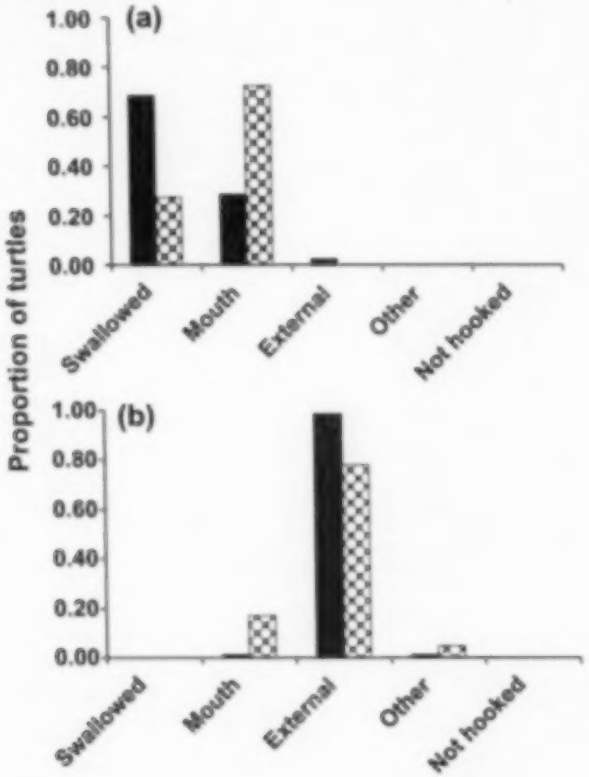

of hooks to pull out of the relatively weak jaw structure of swordfish. Fishers have also reported that a larger percentage of swordfish are alive and active when using circle hooks, as compared with J hooks, and that the fish quality is better.

Bigeye tuna

Bigeye tuna are a secondary target catch in the fishery and are retained for sale. Bigeye tuna caught averaged 130 cm in length (range 70–181 cm) and the mean weight of retained fish was 35.3 kg (range 11.8–87.7 kg). Circle hooks baited with squid increased the catch rate of bigeye tuna (26%), but the increase was not significant (p = 0.1463). Mackerel bait significantly reduced the catch rate of bigeye tuna on both 18/0 circle hooks (81%, CI = 49%–100%, $p < 0.0001$) and J hooks (90%, CI = 58%–100%, $p < 0.0001$) (Fig. 8*b*).

The sea surface temperature effect for bigeye tuna was highly significant ($p < 0.0001$) (Table 5). Bigeye tuna catch rates increased between 10.9 and 18.1 kg per 1000 hooks for every 0.6 °C increase in sea surface temperature (the regression coefficients for temperature varied between 0.024 (for treatments JM and C_2M) and 0.040 (for treatments C_1S, C_2S, and CS)). The effect of total soak time on bigeye tuna catch was significant ($p \leq 0.0176$), but the effect of daylight soak time was not ($p \geq 0.1101$), which may again be related to the confounding effects of total soak time and daylight soak time.

The majority of bigeye tuna were hooked in the mouth (91%–100%) regardless of hook type or bait type (orginal data shown in NRC-DD Table S3[2]), but there was significantly more gut hooking (8%) ($p < 0.005$) with J hooks baited with squid than with circle hooks (2%). There was no significant effect on hook location by mackerel or by circle hook offset ($p > 0.05$).

Blue shark

Blue shark is primarily a bycatch species in the United States Atlantic longline fishery, but is a target species in some other fisheries (Hazin et al. 2002). The catch rate of blue sharks was increased 8% (CI = 2%–14%, $p < 0.0073$) by 0° offset circle hooks (C_1S) with squid bait and 9% (CI = 3%–16%, p = 0.0030) by 10° offset circle hooks (C_2S) with squid bait (Fig. 8*c*). The models for treatments C_1S and C_2S could not be combined for blue sharks because of a major difference between the two. Mackerel bait reduced the catch of blue sharks on both 18/0 circle hooks (31%, CI = 27%–35%, $p < 0.0001$) and J hooks (40%, CI = 36%–43%, $p < 0.0001$) (Fig. 8*c*).

The sea surface temperature effect for blue shark was highly significant ($p < 0.0001$) (Table 6). The blue shark catch rate decreased by a multiplicative factor of 9.7%–11.4% with 0.6 °C increase in sea surface temperature (odds ratio varied from 0.886 to 0.903), depending on the treatment comparison.

The effect of total soak time of the hooks on blue shark catch was statistically significant ($p < 0.002$), but the effect was too small to be of practical importance. The odds ratio was very close to 1.000 (ranged between 0.999 and approximately 1.000). We suspect that there was a confounding effect between total soak time and daylight soak time. The effect of daylight soak time was highly significant ($p < 0.0001$) and fairly consistent in the four models fitted. In each model, the odds ratio was 1.005. Thus, the blue shark catch rate increased by a multiplicative factor of 0.5% with a unit increase (min) in daylight soak time. This means that blue shark catch rate increased by 16% with every 30 min increase in daylight soak time.

Hooking location in blue sharks varied by hook type, and for J hooks, by bait; circle hook offset also was significant. Blue sharks were hooked more frequently in the gut with 9/0 J hooks (25%–32%) compared with 18/0 circle hooks (10%–12%; $p < 0.0001$; original data shown in NRC-DD Table S4[2]). Mackerel increased the gut hooking with J hooks (35% vs. 25%) ($p < 0.0001$), but not with circle hooks ($p > 0.25$). Circle hook offset also resulted in a greater gut hooking ($p < 0.0001$), but still was less than that with J hooks.

Removal of gear

Hooks and line were removed from many of the sea turtles with the tools provided to the vessels; these same tools were also used to remove gear from marine mammals and sometimes from other bycatch species, such as *Mola* spp., and blue shark. Detailed information on the amount of gear

© 2005 NRC Canada

Table 3. Odds ratio estimates from the models for leatherback (*Dermochelys coriacea*) turtles.

Effect	Odds ratio	95% Wald confidence limits		*p*
Treatment C_1S (0° offset 18/0 circle hook with squid bait)				
Hook type	0.361	0.191	0.681	0.0016
Sea surface temperature	1.201	1.102	1.309	<0.0001
Total soak time	1.001	0.998	1.004	0.4332
Daylight soak time	1.001	0.996	1.005	0.7772
Treatment C_2S (10° offset 18/0 circle hook with squid bait)				
Hook type	0.5	0.284	0.880	0.0163
Sea surface temperature	1.144	1.033	1.266	0.0095
Total soak time	0.998	0.994	1.002	0.3049
Daylight soak time	1.001	0.996	1.006	0.7618
Treatment CS (C_1S and C_2S combined)				
Hook type	0.43	0.282	0.656	<0.0001
Sea surface temperature	1.178	1.102	1.259	<0.0001
Total soak time	1	0.998	1.002	0.9324
Daylight soak time	1.001	0.997	1.004	0.6421
Treatment JM (25° offset J hook with mackerel bait)				
Hook type	0.344	0.187	0.634	0.0006
Sea surface temperature	1.184	1.096	1.280	<0.0001
Total soak time	0.998	0.995	1.001	0.1761
Daylight soak time	1	0.996	1.005	0.8257
Treatment C_2M (10° offset 18/0 circle hook with mackerel bait)				
Hook type	0.346	0.187	0.637	0.0007
Sea surface temperature	1.219	1.130	1.314	<0.0001
Total soak time	0.999	0.996	1.002	0.366
Daylight soak time	1	0.996	1.004	0.8863

Note: Sea surface temperature data were modeled in degrees Fahrenheit; soak times were were modeled in minutes.

remaining at release was recorded only for sea turtles and marine mammals. All gear was removed from three of the marine mammals; the fishers attempted to remove gear from the other animals, but they were released with the hook and some line still attached. For loggerheads, 7 of the 58 swallowed hooks were removed, along with all other hooks located in the mouth or externally, except for one lodged in the glottis (Table 7). A small amount of line was left on some hooks that had been swallowed ($n = 31$); usually the line remaining was <3 cm. Hooks were also retrieved from captured leatherbacks, which, except on two occasions, were not boated. One hundred thirty leatherbacks were hooked or possibly hooked. The hooks were recovered from 61 of these animals (information was not recorded for an additional five). This included six of eight hooks in the mouth (Table 7). All line was removed from 90 leatherbacks, and the line remaining on the rest usually (>50%) was less than 0.3 m.

Discussion

Loggerheads and leatherbacks, like all sea turtles, hatch from eggs laid on ocean beaches. Their life histories are very different in other respects, however, and pelagic longlines impact these species differently. Loggerheads have a distinct juvenile life stage that lives in the oceanic environment leading a pelagic existence (Carr 1987). After about 8–15 years, the young juveniles move to the neritic environment and become demersal (Bjorndal et al. 2000; Snover 2002), reaching maturity after nearly 20 years in that stage–environment (Snover 2002). There is some movement between the two habitats, at least during the period when the juveniles are transitioning to the neritic environment (Witzell 2002; Bolten 2003). Loggerheads captured on pelagic longlines in the NED are young, oceanic, pelagic animals or are those in transition and are the largest loggerheads in that environment (Bjorndal et al. 2003; S. Epperly, unpublished data). They may be either about to leave the oceanic environment or are transients, and this may explain why we did not recapture any turtles that were tagged during our experiments. In contrast, leatherbacks are pelagic animals living mostly in the oceanic environment (Pritchard and Trebbau 1984). Leatherbacks across a large range of sizes are captured on the longlines, including big animals comparable in size to nesting females of the Western North Atlantic (Boulon et al. 1996).

Pelagic longlines have been implicated as a major source of anthropogenic mortality for loggerhead and leatherback sea turtles (Lewison et al. 2004). The present study demonstrates that loggerhead and leatherback sea turtle interactions associated with the Western Atlantic pelagic swordfish longline fishery can be significantly reduced by employing 18/0 circle hooks or by using mackerel bait in place of squid bait. Importantly, when the two treatments are used in com-

© 2005 NRC Canada

Fig. 8. Catch per unit effort for (*a*) swordfish (*Xiphias gladius*), (*b*) bigeye tuna (*Thunnus obesus*), and (*c*) blue sharks (*Prionace glauca*) caught on (*i*) 25° offset 9/0 J hooks using squid (*Illex* spp.) bait (n = 142 701) (JS), (*ii*) 0° and 10° offset 18/0 circle hooks combined using squid bait (n = 142 701) (CS), (*iii*) 0° offset 18/0 circle hooks using squid bait (n = 71 931) (C_1S), (*iv*) 10° offset 18/0 circle hooks using squid bait (n = 70 700) (C_2S), (*v*) 25° offset 9/0 J hooks using mackerel (*Scomber scombrus*) bait (n = 70 990) (JM), and (*vi*) 10° offset 18/0 circle hooks using mackerel bait (n = 70 990) (C_2M).

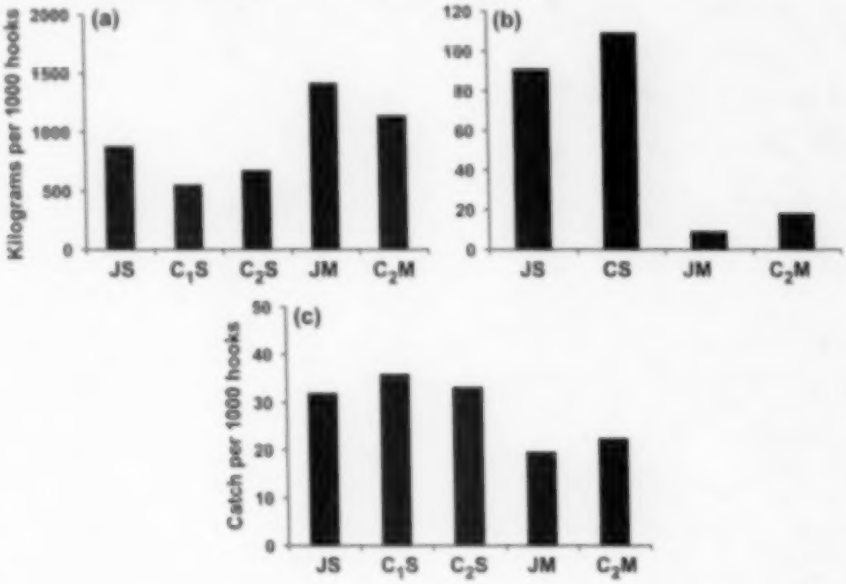

Table 4. Odds ratio estimates from the models for swordfish (*Xiphias gladius*).

Effect	Odds ratio	95% Wald confidence limits		p
Treatment C_1S (0° offset 18/0 circle hook with squid bait)				
Hook type	–0.592	–0.842	–0.341	<0.0001
Sea surface temperature	0.046	0.002	0.090	0.0413
Total soak time	–0.001	–0.002	0.001	0.2221
Daylight soak time	0.002	0.0002	0.004	0.0279
Treatment C_2S (10° offset 18/0 circle hook with squid bait)				
Hook type	–0.596	–0.912	–0.279	0.0002
Sea surface temperature	0.06	0.002	0.119	0.0441
Total soak time	0.002	–0.0001	0.004	0.0629
Daylight soak time	0.005	0.002	0.008	0.0007
Treatment JM (25° offset J hooks with mackerel bait)				
Hook type	1.235	0.894	1.576	<0.0001
Sea surface temperature	0.032	–0.027	0.090	0.2857
Total soak time	0.0004	–0.002	0.002	0.689
Daylight soak time	0.005	0.002	0.008	0.0005
Treatment C_2M (10° offset 18/0 circle hooks with mackerel bait)				
Hook type	0.589	0.276	0.902	0.0002
Sea surface temperature	0.034	–0.020	0.087	0.2148
Total soak time	0.0004	–0.001	0.002	0.669
Daylight soak time	0.005	0.003	0.008	0.0001

Note: Sea surface temperature data were modeled in degrees Fahrenheit; soak times were were modeled in minutes.

bination, the resulting reduction in turtle interactions — 90% for loggerheads and 65% for leatherbacks — can be obtained without negatively impacting swordfish catch on the Grand Banks.

The post-hooking survival of sea turtles is unknown, but a pilot study employing pop-off archival satellite tags was initiated during these experiments and is ongoing (Epperly et al. 2002, 2003). Harm from gear left in place may include

© 2005 NRC Canada

Table 5. Odds ratio estimates from the models for bigeye tuna (*Thunnus obesus*).

Effect	Odds ratio	95% Wald confidence limits		*p*
Treatment C_1S (0° offset 18/0 circle hook with squid bait)				
Hook type	0.063	−0.042	0.169	0.2403
Sea surface temp.	0.04	0.021	0.059	<0.0001
Total soak time	0.001	0.000	0.001	0.0176
Daylight soak time	0	−0.001	0.001	0.9086
Treatment C_2S (10° offset 18/0 circle hook with squid bait)				
Hook type	0.043	−0.054	0.140	0.3863
Sea surface temp.	0.038	0.020	0.056	<0.0001
Total soak time	0.002	0.001	0.002	<0.0001
Daylight soak time	−0.001	−0.002	0.000	0.1101
Treatment CS (C_1S and C_2S combined)				
Hook type	0.053	−0.019	0.125	0.1463
Sea surface temp.	0.038	0.025	0.051	<0.0001
Total soak time	0.001	0.001	0.002	<0.0001
Daylight soak time	0	−0.001	0.000	0.257
Treatment JM (25° offset J hooks with mackerel bait)				
Hook type	−0.184	−0.250	−0.118	<0.0001
Sea surface temp	0.024	0.012	0.035	<0.0001
Total soak time	0.001	0.000	0.001	<0.0001
Daylight soak time	0	−0.001	0.000	0.4019
Treatment C_2M (10° offset 18/0 circle hooks with mackerel bait)				
Hook type	−0.166	−0.232	−0.099	<0.0001
Sea surface temp.	0.025	0.014	0.036	<0.0001
Total soak time	0.001	0.001	0.001	<0.0001
Daylight soak time	0	−0.001	0.000	0.2144

Note: Sea surface temperature data were modeled in degrees Fahrenheit; soak times were were modeled in minutes.

tissue damage, infection, and digestive track blockage. Hooks may perforate internal organs or vessels; in some cases, hooks become encapsulated or are expelled. Trailing line can encircle a limb, restrict circulation, and cut deeply into the tissue, and eventually cause loss of function. Ingested line may irritate the lining of the gastrointestinal tract and cause death by torsion (involution) or intussusception (telescoping of the gut tube, cutting off its circulation). A panel of experts was convened by the US National Marine Fisheries Service on the topic of post-hooking mortality in January 2004. Although no hard data exist, based on the panel's input the agency prepared draft criteria that indicate the relative degree of impact on survival as a function of hook location and amount of gear remaining at release. Gut hooking, releasing entangled turtles, and resuscitation of drowned turtles are associated with the highest mortality rates. These criteria are being used by the agency to evaluate the impact of hook-and-line fishing activities on sea turtle survival (Epperly and Boggs 2004).

Circle hooks can reduce the mortality associated with fishing interactions for both fish and sea turtles. In a review of studies evaluating fish mortality associated with circle hooks compared with other types of hooks, Cooke and Suski (2004) concluded that overall the mortality rates were consistently lower for circle hooks than for J hooks. They found that circle hooks were more frequently hooked in the jaw and less frequently hooked in the gut. We found that also to be the case for swordfish, tuna, and blue shark caught with circle hooks on pelagic longlines. In addition, we found that not only can 18/0 circle hooks and mackerel bait significantly reduce both loggerhead and leatherback catch rates, but also significantly reduce the rate of gut hooking by loggerhead turtles. Because circle hooks are more likely to lodge in the jaw of a loggerhead rather than in the gut, hooks and line can be removed more easily. Dehookers and line cutters were used successfully by fishers to remove line and hooks from the turtles, including the leatherbacks, which most often were hooked externally and rarely were boated. The observed reduction in leatherback interactions with mackerel bait is believed to be the result of the fish bait masking the hook point.

In virtually all cases, loggerhead turtle interaction with pelagic longline gear appears to be a result of feeding behavior resulting in the apprehension and (or) ingestion of the bait, and data indicate that the interaction occurs primarily during daylight hours. The behavior leading to leatherback interactions with pelagic longline gear is not so apparent. While the majority of leatherback captures results from foul hooking, mostly in the shoulder, armpit, and front flipper area, some do ingest the bait. It is not known whether the interaction is a result of attraction to (*i*) bait upon which they are attempting to feed, (*ii*) light sticks used on the branchlines (light trapping or simple phototaxis), (*iii*) mainline, floats, buoys, branchlines, or hardware — structures in an otherwise featureless environment, or (*iv*) their mainstay prey, jellyfish, impinged upon the gear. Unlike loggerhead

© 2005 NRC Canada

Table 6. Odds ratio estimates from the models for blue sharks (*Prionace glauca*).

Effect	Odds ratio	95% Wald confidence limits		*p*
Treatment C_1S (0° offset 18/0 circle hook with squid bait)				
Hook type	1.081	1.021	1.144	0.0073
Sea surface temp.	0.886	0.877	0.895	<0.0001
Total soak time	1	0.999	1.000	0.0018
Daylight soak time	1.005	1.005	1.006	<0.0001
Treatment C_2S (10° offset 18/0 circle hook with squid bait)				
Hook type	1.094	1.031	1.162	0.003
Sea surface temp.	0.903	0.892	0.913	<0.0001
Total soak time	0.999	0.998	0.999	<0.0001
Daylight soak time	1.005	1.004	1.005	<0.0001
Treatment JM (25° offset J hooks with mackerel bait)				
Hook type	0.601	0.566	0.639	<0.0001
Sea surface temp	0.9	0.891	0.909	<0.0001
Total soak time	0.999	0.999	0.999	<0.0001
Daylight soak time	1.005	1.004	1.005	<0.0001
Treatment C_2M (10° offset 18/0 circle hooks with mackerel bait)				
Hook type	0.691	0.652	0.733	<0.0001
Sea surface temp.	0.889	0.880	0.897	<0.0001
Total soak time	0.999	0.999	0.999	<0.0001
Daylight soak time	1.005	1.004	1.005	<0.0001

Note: Sea surface temperature data were modeled in degrees Fahrenheit; soak times were were modeled in minutes.

turtles, leatherbacks do not have the ability to maneuver backwards (Davenport 1987; J. Wyneken, Florida Atlantic University, 777 Glades Road, Boca Raton, FL 33431-0991, USA, personal communication) away from the lines and hooks and thus could become foul hooked even if attempting to ingest the bait. Research is needed to determine the nature of leatherback interactions to facilitate the development of more effective mitigation measures. Because leatherbacks over a large size range were foul hooked, these experimental results are applicable to leatherback turtles in other geographic areas. Furthermore, it is likely that the use of smaller circle hooks, with smaller gaps between the barb and shank, will be at least as effective in reducing foul hooking as the 18/0 circle hook tested. For loggerheads, however, these experimental results are applicable only for the sizes we encountered in the NED and for the sizes of the hooks we compared. There is evidence that the ability of a loggerhead to ingest a hook is a function of both the hook size and the animal's size (e.g., mouth gape) (Watson et al. 2003; S. Epperly, unpublished data). Bolten et al. (2002) found that although smaller circle hooks (16/0) significantly decreased the proportion of swallowed hooks by loggerheads of a size range comparable to the animals in the NED, when compared with 9/0 J hooks they did not reduce the rate of turtle interaction. Similarly, an 18/0 circle hook may not reduce the catch rates of a larger size class of loggerheads hypothetically found in other areas. Thus, we urge caution in extending these conclusions to geographic areas where loggerhead turtle size distributions may vary from those encountered during the experiments described herein.

The effect of sea surface temperature on turtle catch rates and swordfish catch rates with mackerel bait suggests that fishing cooler water (using real-time sea surface imaging technology) could reduce turtle interactions while sustaining swordfish catch. Fishing cooler water also would reduce the bycatch of blue shark, but it would negatively impact bigeye tuna catch.

Table 7. Hooks removed from loggerhead (*Caretta caretta*) and leatherback (*Dermochelys coriacea*) turtles.

	Hook removed				
Hook Location	No	Yes	Unknown	NA*	Total
Loggerhead					
Swallowed	51	7	0	0	58
Mouth	1	30	0	0	31
External	0	2	0	0	2
Not known if hooked	0	0	0	1	1
Not hooked	0	0	0	4	4
Total	52	40	0	4	96
Leatherback					
Swallowed	0	0	0	0	0
Mouth	2	6	0	0	8
External	61	53	1	0	115
Not known if hooked	0	2	4	0	6
Not hooked	0	0	0	18	18
Unknown	1	0	0	0	1
Total	64	61	5	18	148

*Not applicable.

Previous studies have indicated a small degree of offset (≤4°) does not increase the rate of gut hooking, but an offset of 15° or larger does result in gut hooking comparable to that of a J hook (Malchoff et al. 2002; Prince et al. 2002;

© 2005 NRC Canada

Skomal et al. 2002); hook size may be a factor in the effect of offset. Our experimental design did not directly compare the two circle hooks, but rather each was compared with the J hooks. However, we found no significant differences in sea turtle and bigeye tuna catch rates of 10° offset and 0° offset 18/0 circle hooks baited with squid, but the two hooks were significantly different for swordfish and blue shark and did result in significantly more gut hooking in those two species. There were insufficient data to compare hooking locations in sea turtles as a function of offset. However, Canadian observer data (Javitech 2002) and experiments in the Azores (Bolten et al. 2002) do not indicate that 10° offset 16/0 circle hooks result in greater gut hooking of loggerhead turtles than 0° offset 16/0 hooks. For turtle species, swordfish, bigeye tuna, and blue sharks, the catch rates and proportion of gut hooking with the circle hooks were significantly different from those with J hooks. More research is needed to determine the effect on bycatch and target species of offset for different sizes of circle hooks.

The 18/0 circle hooks maintained catch efficiency for bigeye tuna when baited with squid and for swordfish when baited with mackerel. Circle hooks also significantly reduced gut hooking in these two species as well as in blue shark; presumably post-hooking survival of animals discarded also was increased. Circle hooks retained more sharks, but may not actually have caught more sharks than J hooks. The results presented on blue shark catch are likely confounded because sharks that are gut hooked are more likely to bite off monofilament leaders and thus escape detection at haulback. The benefit of using circle hooks for the target species is that undersized fish to be discarded likely have a higher probability of surviving the interaction, and those retained are more likely to be alive on the line at haulback, resulting in a higher quality product for the market.

Because sea turtles are migratory, cross international boundaries, and often are outside the boundaries of any national jurisdiction, successful methods adopted by one nation's vessels may not be sufficient to ensure species recovery, unless they also are adopted by the vessels of other nations. The sea turtle mitigation techniques described in this paper can be exported to other fisheries and countries for evaluation, but more research is needed on pelagic longline gear modifications to develop effective bycatch mitigation techniques for longline fisheries worldwide. Circle hooks (18/0) and mackerel bait were found to be highly effective in reducing turtle interactions with pelagic longline gear and were effective in maintaining the primary target catch in the Western Atlantic swordfish fishery, but may not be as effective in other areas and for other target species or size classes of swordfish or loggerheads. The majority of worldwide pelagic longline fishing effort targets tuna, and research is needed to determine if large circle hooks are effective in catching species other than bigeye tuna. Mackerel bait also was found to be effective in reducing sea turtle interactions compared with squid bait, but mackerel bait was ineffective in catching bigeye tuna. Most tuna fisheries use fish species for bait that are smaller than the mackerel evaluated in this study. Observer data from the Gulf of Mexico indicate that loggerhead interactions in a fishery predominately targeting yellowfin tuna may be reduced by using small fish bait (sardines and herring) in combination with 16/0 circle hooks (Garrison 2003). More research is needed on the effect of hook size and hook design to maximize hook efficiency in reducing sea turtle interactions and maintaining target catch.

As the world population continues to grow and the demand for fisheries resources increases, bycatch has become a serious concern in the effort to wisely manage the world's fisheries resources (Alverson et al. 1994). The development of selective fishing technologies and strategies can be effective in reducing the ecological impact of fishing practices by reducing bycatch and discards. To be effective, these measures must be efficient in harvesting target species, or they will likely be resisted by users (Witherall 2004). We have demonstrated that selective fishing techniques can be developed that are capable of reducing the unintended ecological impact of pelagic longline fishing while maintaining effective harvesting efficiency. We have outlined an experimental design that is effective in evaluating gear modification treatment effects on bycatch and target species catch. The results of this study indicate that it is possible to mitigate turtle interactions with the longline fishery by manipulating hook style and bait type while still maintaining catch of targeted fish species. Furthermore, implementation of the techniques developed as a result of our research made it possible to reopen both the Hawaii-based pelagic longline fishery and the NED to United States longline fishermen, effective 3 May 2004 and 6 July 2004, respectively (US Department of Commerce 2004*a*, 2004*b*). We encourage international evaluation of the techniques described here, as well as research to develop more effective and selective fishing technologies.

Acknowledgments

We gratefully acknowledge the efforts of the owners, managers, captains, and crews of the F/Vs *Beth Anne*, *Bjorn II*, *Deesie*, *Destiny*, *Eagle Eye*, *Eagle Eye II*, *Eyelander*, *Hannah Lee*, *Karen L*, *Monica*, *Sea Hawk*, *Seneca*, and *Whitewater*; Blue Water Fishermen's Association; NOAA Fisheries observers Patrick Bellew, Jeff Bernia, Ryan Brown, Thomas Droz, Georg Hinteregger, Nick Hopkins, Daniel Lawson, Mathew Maiello, Benjamin Rhame, Patrick Rice, Jimmy Rollo, Joshua Sheldon, Jeff Trew, C. Jain Vaughn, and C.R. Wurster; NOAA Fisheries personnel and contractors Dennis Lee, Cheryl Brown, Charlie Bergmann, Myrto Argyropoulou, Lesley Stokes, Lisa Belskis, Ron Rinaldo, Lionel Laforce, Lawrence Beerkircher, Chris Orphanides, David Bernhart, Terri Jordan, Ben Higgins, Larisa Avens, and Joanne Braun McNeill; and colleagues Jeanette Wyneken, George Burgess, and Craig Harms. A very special thanks to Bill Hogarth (NOAA Fisheries Assistant Administrator for Fisheries), Aquatic Release Corporation, and Lindgren-Pitman Inc. We also express our sincere appreciation to Alex Chester, Eric Prince, Chris Boggs, Scott Nichols, Larisa Avens, Kenneth Frank, Graeme Hays, Stephen Smith, and anonymous reviewers for providing critical review of this manuscript. We were issued an United States Endangered Species Act Section 10 Permit (#1324) to capture sea turtles and a Magnuson Act Exempted Fishing Per-

© 2005 NRC Canada

mit (#HMS-ERF-02-006) to fish in the closed NED area. The National Marine Fisheries Service (NMFS) does not approve, recommend, or endorse any proprietary product or material mentioned in this publication. No reference shall be made to NMFS or to this publication in any advertising or sales promotion that would imply that NMFS approves, recommends, or endorses any proprietary product or proprietary material herein or which has as its purpose any intent to cause directly or indirectly the advertised produce to be used or purchased because of NMFS publication.

References

Agresti, A. 1996. An introduction to categorical data analysis. Wiley, New York.

Alverson, D.L., Murawski, S.A., and Pope, J.G. 1994. A global assessment of fisheries bycatch and discards. FAO Fish. Tech. Pap. **339** pp. 1–233.

Beerkircher, L.R., Brown, C.J., and Lee, D.W. 2002. SEFSC pelagic observer program data summary for 1992–2000. NOAA Tech. Memo. NMFS-SEFSC-486: 1–23. Available from http://www.sefsc.noaa.gov/observerresearch.jsp [accessed July 2004; updated April 2005].

Bjorndal, K.A., Bolten, A.B., and Martins, H.R. 2000. Somatic growth model of juvenile loggerhead sea turtles *Caretta caretta*: duration of pelagic stage. Mar. Ecol. Prog. Ser. **202**: 265–272.

Bjorndal, K.A., Bolten, A.B., and Martins, H.R. 2003. Estimates of survival probabilities for oceanic-stage loggerhead sea turtles (*Caretta caretta*) in the North Atlantic. Fish. Bull. **101**: 732–736.

Bolten, A.B., Martins, H., Isidro, E., Ferreira, R., Santos, M., Bettencourt, E., Giga, A., Cruz, A., Riewald, B., and Bjorndal, K. 2002. Preliminary results of experiments to evaluate effects of hook type on sea turtle bycatch in the swordfish longline fishery in the Azores. University of Florida contract report to NOAA, National Marine Fisheries Service, Office of Protected Resources, Silver Spring, Md., USA. Available from http://www.sefsc.noaa.gov/seaturtlecontractreports.jsp [accessed July 2004; updated April 2005].

Bolten, A.B. 2003. Active swimmers – passive drifters: the oceanic juvenile stage of loggerheads in the Atlantic system. *In* Loggerhead sea turtles. *Edited by* A.B. Bolten and B.E. Witherington. Smithsonian Institute Press, Washington, D.C. pp. 63–78.

Boulon, R.H., Dutton, P.H., and McDonald, D.L. 1996. Leatherback turtles (*Dermochelys coriacea*) on St. Croix, U.S. Virgin Islands: fifteen years of conservation. Chelonian Conserv. Biol. **2**: 141–147.

Camiñas, J.A. 1997. Capturas accidentales de tortuga boba (*Caretta caretta*, L. 1758) en el Mediterráneo occidental en la pesquería de palangre de superficie de pez espada (*Xiphias gladius* L.) Int. Comm. Conserv. Atl. Tunas Collect. Vol. Sci. Pap. **46**: 446–455.

Carr, A. 1987. New perspectives on the pelagic stage of sea turtle development. Conserv. Biol. **1**: 103–121.

Cooke, S.J., and Suski, C.D. 2004. Are circle hooks an effective tool for conserving marine and freshwater recreational catch-and-release fisheries? Aquatic Conserv: Mar. Freshw. Ecosyst. **14**: 299–326.

Convention on International Trade in Endangered Species of Wild Fauna and Flora (CITES). 2003. Appendices I, II, and III. Geneva, Switzerland. Available from http://www.cites.org/eng/app/appendices.shtml [accessed July 2003; updated April 2005].

Davenport, J. 1987. Locomotion in hatchling leatherback turtles *Dermochelys coriacea*. J. Zool. (Lond.), **212**: 85–101.

De Metrio, G., and Megalofonu, P. 1988. Mortality of marine turtles (*Caretta caretta* L., and *Dermochelys coriacea* L.) consequent to accidental capture in the Gulf of Taranto. Rapp. P.-V. Reun. Comm. Int. Explor. Sci. Mer Mediterr. Monaco, **31**: 285.

Draper, N.R., and Smith, H. 1998. Applied regression analysis. Wiley, New York.

Epperly, S.P. 2003. Fisheries-related mortality and turtle excluder devices (TEDs). *In* The biology of sea turtles. Vol. II. *Edited by* P.J. Lutz, J.A. Musick, and J. Wyneken. CRC Press, Boca Raton, Fla. pp. 339–353.

Epperly, S.P., and Boggs, C. 2004. Post-hooking mortality in pelagic longline fisheries using "J" hooks and circle hooks. Application of new draft criteria to data from the Northeast Distant Experiments in the Atlantic. Contribution # PRD-03/04-04 of NOAA, National Marine Fisheries Service, Miami, Fla., USA. Available from http://www.sefsc.noaa.gov/seaturtleunpublishedreports. jsp [accessed February 2004; updated April 2005].

Epperly, S.P., Bolten, A., and Prince, E. 2002. Development of an experimental design and research plan to estimate post-hooking survival of sea turtles captured in pelagic longline fisheries. *In* Experiments in the western Atlantic Northeast Distant Waters to evaluate sea turtle mitigation measures in the pelagic longline fishery. Report on experiments conducted in 2001. *Compiled by* J.W. Watson, D.G. Foster, S. Epperly, and A. Shah. ESA permit #1324 annual report to NOAA, National Marine Fisheries Service, Office of Protected Resources, Silver Spring, Md., USA. Available from http://www.sefsc.noaa.gov/seaturtleunpublishedreports.jsp [accessed July 2004; updated April 2005]. pp. 67–135.

Epperly, S.P., Bolten, A., Prince, E., Sasso, C., and Rivero, C. 2003. Post-hooking survival pilot study. *In* Experiments in the western Atlantic Northeast Distant Waters to evaluate sea turtle mitigation measure in the pelagic longline fishery. Report on experiments conduced in 2001 and 2002. *Compiled by* J.W. Watson, D.G. Foster, S. Epperly, and A. Shah. ESA permit #1324 final report to NOAA, National Marine Fisheries Service, Office of Protected Resources, Silver Spring, Md., USA. Available from http://www.sefsc.noaa.gov/seaturtleunpublishedreports.jsp [accessed July 2004; updated April 2005]. pp. 53–75.

Falterman, B., and Graves, J.E. 2002. A preliminary comparison of the relative mortality and hooking efficiency of circle and straight shank ("J") hooks used in the pelagic longline industry. Am. Fish. Soc. Symp. **30**: 80–87.

Garrison, L.P. 2003. Summary of target species and protected resource catch rates by hook and bait type in the pelagic longline fishery in the Gulf of Mexico 1992–2002. Contribution # PRD-02/03-08 of NOAA, National Marine Fisheries Service, Miami, Fla., USA. Available from http://www.sefsc.noaa.gov/seaturtleunpublishedreports.jsp [accessed July 2004; updated April 2005].

Hazin, F.H.V., Broadhurst, M.K., Hazin, H.G., and Travassos, P. 2002. Historic trends in catches of the Brazilian longline fishery in the southwestern equatorial Atlantic Ocean. Shark News, **14**: The IUCN/SSC Shark Specialist Group, March 2002. Available from http://www.flmnh.ufl.edu/fish/organizations/ssg/sharknews/sn14/shark14news13.htm. [accessed November 2004; updated April 2005].

Hillestad, H.O., Richardson, J.I., McVea, C., Jr., and Watson, J.M., Jr. 1995. Worldwide incidental capture of sea turtles. *In* Biology and conservation of sea turtles. Revised edition. *Edited by* K.A. Bjorndal. Smithsonian Institute Press, Washington, D.C. pp. 489–495.

© 2005 NRC Canada

Hoey, J.J. 1996. Bycatch in western Atlantic pelagic longline fisheries. Solving bycatch: considerations for today and tomorrow. University of Alaska, Fairbanks. Alaska Sea Grant Prog. Rep. No. 96-03. pp. 193–203.

Hoey, J.J., and Moore, N. 1999. Captain's report: multi-species characteristics for the U.S. Atlantic pelagic longline fishery. National Fisheries Institute Report to NOAA, National Marine Fisheries Service, Silver Spring, Md., USA. Available from http://www.sefsc.noaa.gov/seaturtlecontractreports.jsp [accessed July 2004; updated April 2005].

Hosmer, D.W., and Lemeshow, S. 1989. Applied logistic regression. Wiley, New York.

International Union for Conservation of Nature and Natural Resources (IUCN). 2004. IUCN redlist of threatened species. Cambridge, UK. Available from http://www.redlist.org/ [accessed April 2005; updated April 2005].

Javitech Limited. 2002. Report on sea turtle interactions in the 2001 pelagic longline fishery. Report submitted to Nova Scotia Swordfish Association & Habitat Stewardship Program, Canadian Wildlife Service, Environment Canada. Javitech, Dartmouth, N.S.

Julian, F., and Beeson, M. 1998. Estimates of marine mammal, turtle, and seabird mortality for two California gillnet fisheries: 1990–1995. Fish. Bull. **96**: 271–284.

Lewison, R.L., Freeman, S.A., and Crowder, L.B. 2004. Quantifying the effects of fisheries on threatened species: the impact of pelagic longlines on loggerhead and leatherback sea turtles. Ecology, **7**: 221–231.

Lutcavage, M.E., Plotkin, P., Witherington, B., and Lutz, P. 1996. Human impacts on sea turtle survival. *In* The biology of sea turtles. *Edited by* P.L. Lutz and J.A. Musick. CRC Press, New York. pp. 387–409.

Magnuson, J.J., Bjorndal, K.A., Dupaul, W.A., Graham, G.L., Owens, F.W., Peterson, C.H., Pritchard, P.C.H., Richardson, J.I., Saul, G.E., and West, C.W. 1990. Decline of the sea turtles: causes and prevention. National Academy Press, Washington, D.C.

Malchoff, M.H., Gearhart, J., Lucy, J., and Sullivan, P.J. 2002. The influence of hook type, hook wound location, and other variables associated with post catch and release mortality in the U.S. summer flounder recreational fishery. Am. Fish. Soc. Symp. **30**: 101–105.

Poiner, I.R., and Harris, A.N.M. 1996. Incidental capture, direct mortality and delayed mortality of sea turtles in Australia's northern prawn fishery. Mar. Biol. **125**: 813–825.

Prince, E.D., Ortiz, M., and Venizelos, A. 2002. A comparison of circle and "J" hook performance in recreational catch and release fisheries for billfish. Am. Fish. Soc. Symp. **30**: 66–79.

Pritchard, P.C.H., and Trebbau, P. 1984. The turtles of Venezuela. Contrib. Herpetol. **2**: 1–414.

Skomal, G.B., Chase, B.C., and Prince, E.D. 2002. A comparison of circle and straight hooks relative to hooking location, damage, and success while catch and release fishing for Atlantic bluefin tuna. Am. Fish. Soc. Symp. **30**: 57–65.

Snover, M.L. 2002. Growth and ontogeny of sea turtles using skeletochronology: methods, validation and application to conservation. Ph.D. thesis, Duke University, Durham, N.C. Available from http://www.sefsc.noaa.gov/seaturtledissertations.jsp [accessed July 2004; updated April 2005].

US Department of Commerce. 1999. Western Pacific pelagic fisheries; Hawaii-based pelagic longline area closure. Fed. Regist. **64**: 72290–72291.

US Department of Commerce. 2000. Atlantic highly migratory species: pelagic longline fishery; sea turtle protection measures. Fed. Regist. **65**: 60889–60892.

US Department of Commerce. 2001*a*. Atlantic highly migratory species: pelagic longline fishery; sea turtle protection measures. Fed. Regist. **66**: 36711–36714.

US Department of Commerce. 2001*b*. Atlantic highly migratory species: pelagic longline fishery; sea turtle protection measures. Fed. Regist. **66**: 64378–64379.

US Department of Commerce. 2004*a*. Fisheries off west coast states and in the Western Pacific; Western Pacific pelagic fisheries; pelagic longline fishing restrictions, seasonal area closure, limit on swordfish fishing effort, gear restrictions, and other sea turtle take mitigation measures. Fed. Regist. **69**: 17329–17354.

US Department of Commerce. 2004*b*. Atlantic highly migratory species (HMS); pelagic longline fishery. Fed. Regist. **69**: 40734–40758.

Watson, J.W., Hataway, B.D., and Bergmann, C.E. 2003. Effect of hook size on ingestion of hooks by loggerhead sea turtles. Report of NOAA National Marine Fisheries Service, Pascagoula, Miss., USA. Available from http://www.sefsc.noaa.gov/seaturtleunpublishedreports.jsp [accessed July 2004; updated April 2005].

Witherall, D. (*Editor*). 2004. Managing our nations fisheries: past, present, and future. Proceedings of a Conference on Fisheries Management in the United States, Washington, D.C., November 2003. Report of National Oceanic and Atmospheric Association (NOAA), National Marine Fisheries Service, Silver Spring, Md., USA. Available from http://www.managingfisheries.org/proceedings.htm [accessed July 2004; updated April 2005].

Witzell, W.N. 1999. Distribution and relative abundance of sea turtles caught incidentally by U.S. longline fleet in the western North Atlantic Ocean, 1992–1995. Fish. Bull. **97**: 200–211.

Witzell, W.N. 2002. Immature Atlantic loggerhead turtles (*Caretta caretta*): suggested changes to the life history model. Herpetol. Rev. **33**: 266–269.

Witzell, W.N., Epperly, S.P., and Csuzdi, L.A. 2001. Description of the Atlantic Ocean and Mediterranean Sea pelagic longline fisheries. NOAA Tech. Memo. NMFS-SEFSC-455: 108–119. Availble from http://www.sefsc.noaa.gov/seaturtletechmemos.jsp [accessed July 2004; updated April 2005].

Yeung, C. 2001. Analysis of marine turtle bycatch by the U.S. Atlantic pelagic longline fleet. NOAA Tech. Memo. NMFS-SEFSC-455: 120–142. Available from http://www.sefsc.noaa.gov/seaturtletechmemos.jsp [accessed July 2004; updated April 2005].

Appendix A

Power analysis

The null hypothesis for the experiment was constructed so that the burden of proof is on the treatment to be proven; that is, we initially assumed that the treatment is not effective unless there was enough (statistical) evidence otherwise for its effectiveness. The factors affecting the required level of effort were the actual sea turtle catch rates and variability, the effectiveness of a measure being tested (i.e., the difference in catch rate between the experimental and control treatments), and acceptable risk levels for type I and type II errors. We projected the expected sea turtle catch rates based on the average catch rate observed in the Grand Banks fishery over 1991–1999 (Yeung 2001). For the expected effectiveness of the treatments, we looked at 50% and 25% bycatch reduction. We chose 25% as the minimum accept-

© 2005 NRC Canada

able reduction rate useful to sea turtle management and conservation. The detection of reduction rates below 25% would also require a very large increase in the effort. We set α (probability of rejecting true null hypothesis) and β (probability of accepting false null hypothesis) levels at 10% and 20%, respectively, which are typical levels of statistical risk for this type of gear evaluation experiment. The number of hooks required to detect a 25% and 50% reduction in loggerhead catch per unit effort (CPUE) was 54 054 and 9012 hooks per treatment, respectively. Comparative efforts for leatherback turtles were 163 548 and 26 828 hooks per treatment, respectively. The number of hooks fished in our experiment was at least 70 700 per treatment, giving us the power of a least 80% to detect a 25% reduction in loggerhead catch and 50% reduction in leatherback catch.

© 2005 NRC Canada

Disruption of the hypothalamo-pituitary-interrenal axis in 1+ yellow perch (*Perca flavescens*) chronically exposed to metals in the environment

A. Gravel, P.G.C. Campbell, and A. Hontela

Abstract: Although it has been reported that adult yellow perch (*Perca flavescens*) chronically exposed to metals in the environment exhibit endocrine impairment characterized by blunted cortisol secretion, little is known about the vulnerability of early life stages. Young-of-the-year (YOY) and 1+ yellow perch were captured, subjected to a standardized stress test or adrenocorticotropic-hormone stimulation in lakes situated along a contamination gradient of Cd, Cu, and Zn in the mining region of Abitibi, Quebec. For the first time, whole-body cortisol concentrations were measured. The 1+ fish with elevated whole-body Cd, Cu, and Zn concentrations had an impaired capacity to respond to an acute stress challenge. Although YOY perch had similar whole-body Cd concentrations to 1+ perch, no effects on physiological status were detected in relation to body burdens of metals. Metal contamination did not affect whole-body thyroid-hormone concentrations, condition factor, or hepatosomatic index in 1+ or YOY perch. These results indicate that effects of Cd, Cu, and Zn on the functional integrity of the hypothalamo-pituitary-interrenal axis in yellow perch are detectable after only 1 year of environmental exposure.

Résumé : Bien qu'on ait signalé que les perchaudes adultes exposées de façon chronique aux métaux dans leur environnement subissent une déficience endocrinienne, caractérisée par une sécrétion inadéquate de cortisol, on connaît mal la vulnérabilité des jeunes stades. Nous avons capturé des jeunes de l'année (YOY) et d'âge 1+ de la perchaude (*Perca flavescens*) et les avons soumis à une épreuve de stress standardisée ou à une stimulation à l'ACTH (l'hormone adrénocorticotrope) dans des lacs situés le long d'un gradient de contamination au Cd, au Cu et au Zn dans la région minière de l'Abitibi, Québec. Nous avons mesuré pour la première fois les concentrations corporelles globales de cortisol. Les poissons (1+) ayant des concentrations corporelles élevées de Cd, de Cu et de Zn ont une capacité réduite de réagir à une épreuve aiguë de stress. Bien que les perchaudes YOY aient des concentrations corporelles de Cd semblables à celles des perchaudes 1+, nous n'avons pas mesuré d'effet sur l'état physiologique en fonction des charges corporelles de métaux. La contamination par les métaux chez les perchaudes YOY et 1+ n'affecte pas les concentrations corporelles d'hormone thyroïdienne, ni le coefficient de condition, ni l'indice hépatosomatique (HSI). Ces résultats indiquent que les effets d'expositions au Cd, au Cu et au Zn dans le milieu sur l'intégrité fonctionnelle de l'axe hypothalamo-hypophyso-interrénal (HPI) ne sont décelables chez la perchaude qu'après une année d'exposition.

[Traduit par la Rédaction]

Introduction

Metals are ubiquitous pollutants detected in the aquatic environment, where they can accumulate at different trophic levels (Per-Arne et al. 1997; Mason et al. 2000). In fish, metals are absorbed by the digestive tract and gills (Verbost et al. 1989) and can accumulate in different organs such as kidney, liver, and interrenal tissue (Laflamme et al. 2000; Lévesque et al. 2002, 2003). Although some metals (Zn, Cu, Co, Fe, Mn, Mg, Mo, Se, Ni) are essential for normal physiological processes, Cd, Hg, Pb, and As (nonessential metals) do not have a known biological function in animals. In excess concentrations, all metals have toxic effects, ranging from histological lesions (Forlin et al. 1986; Lévesque et al. 2003) to disruption of metabolic and endocrine functions (Lévesque et al. 2002, 2003; Campbell et al. 2003).

Impairment of the hypothalamo-pituitary-interrenal (HPI) axis, characterized by lower plasma cortisol levels in response to acute stress or adrenocorticotropic-hormone (ACTH) stimulation in vivo has been reported in adults of

Received 9 January 2004. Accepted 29 September 2004. Published on the NRC Research Press Web site at http://cjfas.nrc.ca on 16 May 2005.
J17911

A. Gravel and A. Hontela.[1,2] Département des sciences biologiques, Centre de recherche en toxicologie de l'environnement (TOXEN), Université du Québec à Montréal, C.P. 8888, succursale Centre-ville, Montréal, QC H3C 3P8, Canada.
P.G.C. Campbell. Centre Eau, Terre & Environnement, Institut national de la recherche scientifique (INRS-ETE), Université du Québec, C.P. 7500, Sainte-Foy, QC G1V 4C7, Canada.

[1]Corresponding author (e-mail: alice.hontela@uleth.ca).
[2]Present address: Department of Biological Sciences, Water Institute for Semi-arid Ecosystems, University of Lethbridge, Lethbridge, AB T1K 3M4, Canada.

 doi: 10.1139/F05-011 © 2005 NRC Canada

several species of fish sampled from metal-contaminated sites (Lockhart et al. 1972; Hontela et al. 1995; Lévesque et al. 2003). Since cortisol plays an important role in osmoregulation (Laurent and Perry 1990), immune defence (Wendelaar Bonga 1997), reproduction (Pankhurst and Van Der Kraak 2000), and metabolism (Vijayan and Moon 1992; Vijayan et al. 1997; Mommsen et al. 1999), it is important to understand the mechanisms and physiological consequences of pollutant-induced disruption of the HPI axis.

Cortisol interacts with other hormones such as thyroid hormones and growth hormone through permissive actions (Young and Lin 1988; De Jesus et al. 1990). It has been shown that cortisol-impaired adult yellow perch (*Perca flavescens*) from metal-contaminated lakes had lower plasma triiodothyronine (T_3) and thyroxine (T_4) levels (Lévesque et al. 2003), a lower condition factor (Laflamme et al. 2000; Sherwood et al. 2000; Eastwood and Couture 2002), and reduced growth efficiency (Sherwood et al. 2002), i.e., the capacity to convert consumed food to body mass.

Cortisol and T_4 have synergistic effects during larval development of fish, promoting growth and larval differentiation and modulating metabolism (Plisetskaya et al. 1983; De Jesus et al. 1990). Although eggs, larvae, and early juveniles are the stages in the life cycle of a fish that are the most vulnerable to pollutants, and also the most vulnerable in populations according to some authors (McKim 1977; von Westernhagen 1988; Sorensen 1991), few studies have investigated the effects of metals on the metabolic and endocrine functions of young fish exposed in the field. Moreover, the minimum duration of field exposure to metals that is necessary to cause physiological anomalies has not so far been determined.

The objectives of the present study were, therefore, to assess the physiological status and metal concentrations in young-of-the-year (YOY) and 1+ yellow perch (*Perca flavescens*) in metal-contaminated lakes situated along a contamination gradient in a mining region. To evaluate the functional integrity of the HPI axis in young fish sampled in the field and too small to blood-sample, cortisol and thyroid-hormone levels following capture of YOY or following a confinement-stress test or an ACTH injection for 1+ fish, and concentrations of metals accumulated in the fish, were measured in the whole body.

Materials and methods

Study sites

Fish were sampled in six lakes in the mining area of Rouyn-Noranda, northwestern Quebec, Canada (48°00′N, 79°00′W), in June of 1999, 2000, and 2001. Lakes in the area are affected primarily by their proximity to the Horne smelter and atmospheric deposition brought by dominant winds, and also by mining operations and abandoned mine sites in the area. Previous studies (Laflamme et al. 2000; Perceval et al. 2002; Lévesque et al. 2003) provided data on metal concentrations in water, sediments, and yellow perch tissues that enabled us to make a preliminary ranking of the lakes based on contamination levels (Fig. 1). Lakes Osisko and Dufault, subjected to point-source and atmospheric metal inputs, are classified as high-contamination lakes; Lakes Vaudray and Bousquet, affected by metals via atmospheric transport, are classified as intermediate-contamination lakes; and Lakes Dasserat and Opasatica, upwind from the smelter, are classified as reference lakes. Limnological characteristics of the lakes are detailed in Sherwood et al. (2002) and Perceval et al. (2002).

Capture of the fish

The yellow perch was chosen for this study because of its relative sedentariness (Aalto and Newsome 1990), tissue metal levels that reflect the contamination of the sites where it is sampled, and its abundance in North American lakes. Age 1+ yellow perch (average body mass 2.5 g) were captured by seine or small gill net. They were placed in floating enclosures (1 m × 1 m × 0.5 m depth) made of nylon net subdivided into four individual compartments (15 fish per compartment) near shore for at least 16 h to allow recovery from the stress of capture, as demonstrated previously (Brodeur et al. 1997; Girard et al. 1998). YOY perch (body mass 0.006–0.12 g) were captured at night with a mysis net and immediately frozen at –20 °C.

Stress test and ACTH-challenge test for 1+ fish

The day after capture, 1+ fish were removed from the enclosures and subjected to a standardized confinement and net stress test. Each group of 15 fish was held in a small aquarium net and taken in and out of the water for 90 s. Fish were then placed back in the compartment for 15, 30, 45, 60, or 120 min and euthanized with 150 $mg \cdot L^{-1}$ tricaine methanesulfonate (MS 222). One group of 15 fish was removed from the compartment and euthanized directly in the MS 222 solution, without the confinement-stress test. These fish are referred to as the basal group.

The last two groups of fish that did not undergo the net stress were subjected to the ACTH-challenge test (Girard et al. 1998) modified for use with young fish. Following light anaesthesia in MS 222, one group (ACTH group) received an intraperitoneal injection of 4 IU ACTH·100 g body $mass^{-1} \cdot 100$ µL saline $(0.7\% \ NaCl)^{-1}$ and the control group (saline group) received an intraperitoneal injection of 100 µL saline·100 g body $mass^{-1}$. After injection, fish were put back in their compartments to recover from the anaesthesia, which occurred within a few minutes. These two groups were euthanized in MS 222 after 120 min.

All fish were treated during the same period of the day to avoid diel effects on hormone secretion (Audet and Claireaux 1992), and after treatment they were frozen whole at –20 °C for later analysis in the laboratory.

Sample preparation

In the laboratory, body mass and length of thawed fish were recorded for calculating the condition factor, $(g \cdot cm^{-3}) \times 100$. Livers of 1+ fish were dissected out for glycogen analysis and calculation of the hepatosomatic index (HSI), $(g \cdot g^{-1}) \times 100$, and opercular bones were removed for age determination. Identification of YOY was confirmed in the laboratory using identification keys (Norden 1961; Auer 1982).

Because of the small body mass of these fish and difficulty with blood sampling in the field, an alternative method of hormone assessment was required. The whole body of each fish (without the liver in 1+ perch) was homogenized in three volumes (mL) of phosphate buffer (0.168 g KH_2PO_4

© 2005 NRC Canada

Fig. 1. Map showing the study area with the six lakes sampled in the Rouyn-Noranda region in Quebec, Canada, and the location (★) of the Horne smelter. The reference lakes are Dasserat (DS) and Opasatica (OP); the intermediate-contamination lakes are Bousquet (BO) and Vaudray (VD); and the high-contamination lakes are Osisko (OS) and Dufault (DF). The direction of dominant winds is west to east.

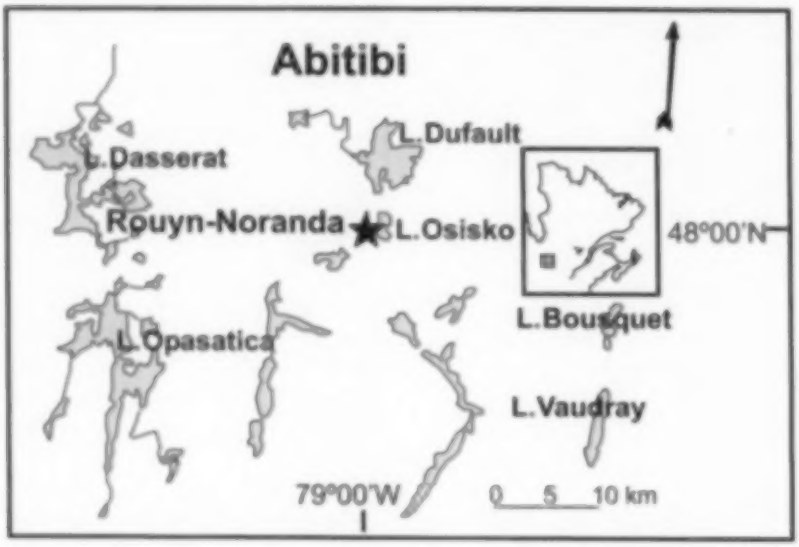

and 1.26 g Na_2HPO_4 in 1 L of deionized water), 0.01 mol·L^{-1} at pH 7.5. Homogenates of YOY perch were made up from pools of fish to obtain a final weight of about 2.0 g. One aliquot of the homogenate was used for metal analysis by inductively coupled plasma atomic emission spectrophotometry (ICP-AES), and a second aliquot of the homogenate was centrifuged (13 000*g*) three times for 10 min each time and the supernatant was frozen (–20 °C) for hormone analyses.

Biochemical analyses

Total body cortisol, T_4, and T_3 were assayed with a radioimmunoassay (ICN Biochemicals No. 07-221102; ICN No. 06B263676; ICN No. 06B254221) according to the manufacturer's protocol. The characteristics of the assays were described previously (Hontela et al. 1995). Liver glycogen was measured by a method described previously (Lévesque et al. 2002).

Statistical analysis

Differences among groups were tested using one-way analysis of variance followed by a Tukey–Kramer test to compare more than two groups, or a Student's *t* test. Data were transformed when necessary to obtain normality. A statistical significance level of $\alpha = 0.05$ was used. Relationships between plasma cortisol and total body cortisol levels in the homogenates were evaluated with Pearson's correlation coefficient.

Results

Whole-body metal concentrations

Whole-body concentrations of Cd in YOY (Fig. 2*a*) and 1+ yellow perch (Fig. 2*b*) increased along a contamination gradient among lakes. Differences in total body concentrations of Ni or Pb in YOY and 1+ fish either did not vary significantly among lakes or did not follow a consistent gradient, while Zn and Cu concentrations were higher in fish sampled in Osisko and Dufault, the most contaminated lakes (Table 1).

Stress response

The stress test and the use of whole-body cortisol levels were initially validated in a pilot field study with 1+ yellow perch (Fig. 3*a*) from a reference site near Montreal (Île Perrot) and in a laboratory study with 1+ rainbow trout (*Oncorhynchus mykiss*). A significant ($P < 0.006$) linear correlation ($r^2 = 0.38$) was established between plasma and body cortisol concentrations in the laboratory test with rainbow trout (data not shown). The pilot field study with 1+ yellow perch (Fig. 3*a*) demonstrated that body cortisol concentrations increased significantly with time following a net-stress test lasting 90 s and reached a maximum value (4× the resting basal value) after 45 min, maintained for up to 2 h. Homogenates of whole fish were either extracted as described in De Jesus et al. (1991) or simply centrifuged prior to radioimmunoassay. The pattern of the stress response was similar with both assay methods but whole-body cortisol concentrations after extraction were about 25% of the concentrations in homogenates that were only centrifuged. Based on the results from the pilot study, the maximal time allocated for hormone secretion post stressor exposure was 120 min and the assay method chosen for hormone analysis of the whole body of small fish for the present project was homogenization without extraction.

The sampling was repeated in a reference lake in the Rouyn-Noranda region (Fig. 3*b*). Whole-body cortisol concentrations in 1+ yellow perch increased significantly 30 min following a net and confinement stress test in a reference lake, and the maximal value (twice the resting value)

© 2005 NRC Canada

Table 1. Whole-body concentrations of Cu, Zn, Pb, and Ni (mean ± standard error of the mean; $\mu g \cdot g^{-1}$ dry weight) in young-of-the-year (YOY) and 1+ yellow perch, *Perca flavescens*, in six lakes in the Rouyn-Noranda region.

	YOY yellow perch						1+ yellow perch					
Lake	Year	*n*	[Cu]	[Zn]	[Pb]	[Ni]	Year	*n*	[Cu]	[Zn]	[Pb]	[Ni]
OP	2001	8	7.6±0.3c	97.6±0.8a	1.25±0.04a	2.0±0.2a	1999	22	5.8±0.5b	153.7±4.9b	1.4±0.1de	18.1±3.4cd
							2000	10	5.7±0.3bc	132.0±4.7ab	0.6±0.02ab	20.0±2.3d
DS	2000	6	5.5±0.3ab	126.7±1.2b	1.07±0.02a	24.0±3.6a	1999	15	5.1±0.3ab	144.4±9.1b	0.7±0.02b	53.6±26.7d
	2001	13	5.4±0.3a	145.0±2.7c	1.05±0.04a	2.2±0.2a						
BO	2001	16	6.6±0.3b	119.3±0.9b	1.01±0.03a	5.1±0.6b	1999	21	4.8±0.3ab	124.9±4.7ab	1.1±0.03d	14.6±3.7cd
VD							1999	14	5.2±0.4ab	145.5±2.9ab	0.8±0.04bcd	12.7±5.9bc
OS	2000	6	14.1±0.5c	142.1±1.0c	1.10±0.04a	29.5±5.2c	1999	15	3.8±0.2a	114.9±2.2a	0.6±0.1a	10.1±1.0cd
							2000	10	4.2±0.4ab	124.4±3.2ab	0.7±0.03ab	0.4±0.07a
DF	2001	12	11.8±0.5d	149.7±1.4c	1.94±0.22b	3.2±0.5ab	1999	23	4.5±0.4ab	175.8±6.5c	1.6±0.1ef	4.2±1.2b
							2000	10	9.3±1.9c	176.7±13.0c	2.4±0.4f	13.5±2.8cd

Note: Values followed by a different letter are significantly different (Tukey–Kramer test, $P < 0.05$) from those for the other lakes; *n* is the number of 1+ fish or the number of pools of YOY. Opasatica (OP) and Dasserat (DS) are reference lakes, Bousquet (BO) and Vaudray (VD) are intermediate-contamination lakes, and Osisko (OS) and Dufault (DF) are high-contamination lakes.

Fig. 2. Whole-body Cd concentrations (mean ± standard error of the mean) in young-of-the-year (YOY) (*a*) and 1+ yellow perch, *Perca flavescens* (*b*), from metal-contaminated lakes sampled in 1999 (open bars), 2000 (solid bars), or 2001 (shaded bars) in the Rouyn-Noranda region. Opasatica (OP) and Dasserat (DS) were the reference lakes, Bousquet (BO) and Vaudray (VD) were intermediate-contamination lakes, and Osisko (OS) and Dufault (DF) were the most contaminated lakes. The samples consisted of 6–16 pools of YOY and 10–23 individual 1+ fish. A different letter above the bar indicates a significant difference (Tukey–Kramer test, $P < 0.05$) from the other lakes.

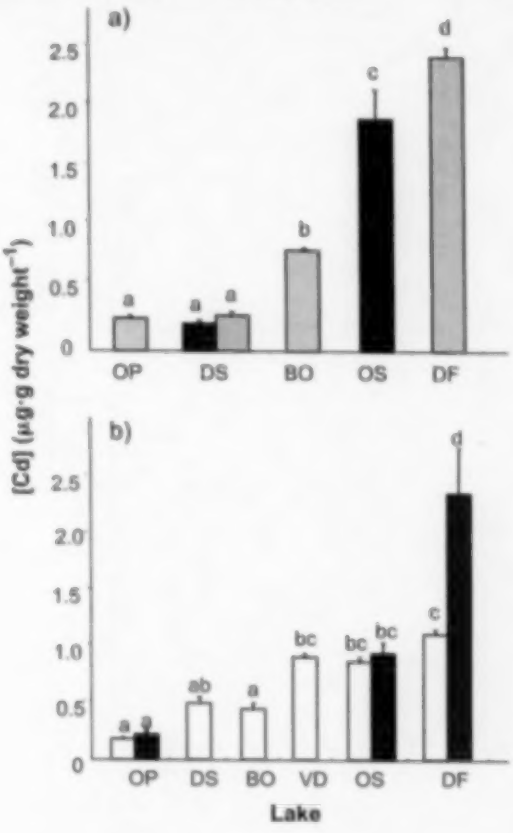

was reached 2 h post stressor exposure. Cortisol concentrations attained in fish from the reference site in Île Perrot (not situated in a mining region) were significantly higher than those in fish from the reference lake in the Rouyn-Noranda mining region. Whole-body cortisol concentrations in the two Rouyn-Noranda reference lakes (Opasatica and Dasserat) increased significantly above basal levels in response to the net stress at 30 min, increasing still further after 120 min in fish from Lake Opasatica, the cleanest lake (Fig. 4). Although cortisol levels after exposure to the stress test were elevated in fish from the intermediate-contamination lakes (Bousquet and Vaudray), no detectable increase in body cortisol concentrations following the stress test was detected in the most contaminated fish, those from Lake Dufault.

© 2005 NRC Canada

Fig. 3. Validation of the standardized stress test and the whole-body cortisol assay. Whole-body cortisol concentrations (mean ± standard error of the mean) before (basal) and after a stress test in 1+ yellow perch from a reference lake in a pilot study (*a*) at Île Perrot and (*b*) in the Rouyn-Noranda region. Cortisol was measured in the homogenate after extraction (open bars) or centrifugation only (solid and shaded bars). Number of fish sampled was 9–10 each for Île Perrot and 12–15 in the Rouyn-Noranda region. A different letter above the bar indicates a significant difference (Tukey–Kramer test, $P < 0.05$) from the other groups. An asterisk indicates a significant difference (Student's *t* test, $P < 0.05$) from the no-stressor group (basal).

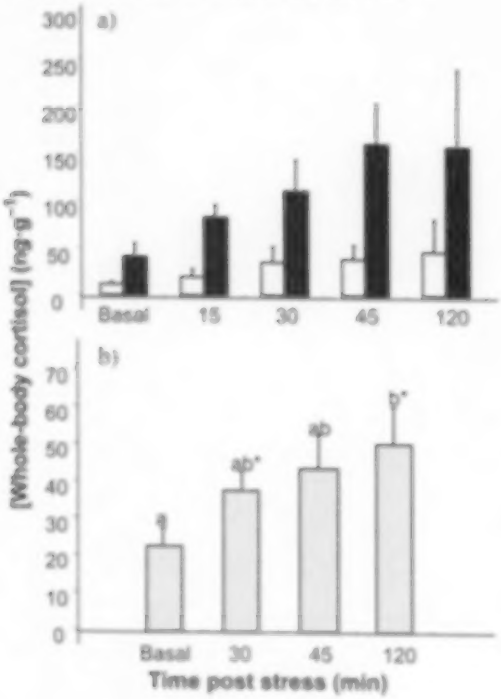

Fig. 4. Whole-body cortisol concentrations (mean ± standard error of the mean) in 1+ yellow perch from metal-contaminated lakes in the Rouyn-Noranda region, sampled without a stress test (open bars), 30 min after a stress test (shaded bars), or 120 min after a stress test (solid bars). The number of fish sampled was 10–15 each time. A different letter above the bar indicates a significant difference (Tukey–Kramer test, $P < 0.05$) from the other lakes. An asterisk indicates a significant difference (Student's *t* test, $P < 0.05$) from the basal level; # denotes a significant difference (Student's *t* test, $P < 0.05$) from the value after 30 min.

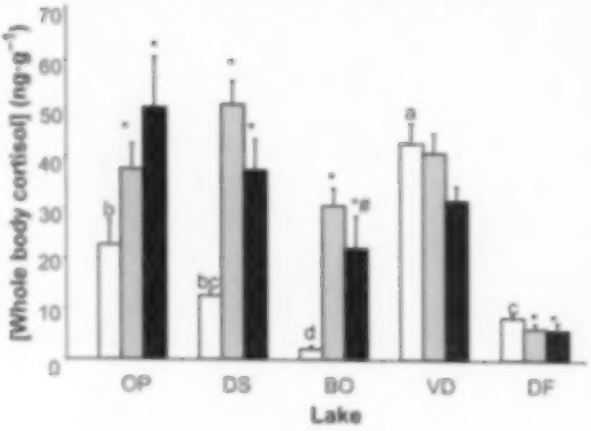

An in-vivo injection of ACTH increased whole-body cortisol concentrations in 1+ fish from a reference lake (Opasatica) or intermediate-contamination lake (Vaudray) but not in fish from the most contaminated lake (Dufault) sampled in 1999 (Fig. 5*a*). A similar trend was also observed in 2000 (Fig. 5*b*). The cortisol levels reached after injection were higher in 1999 (first study with ACTH in young fish) than in 2000 (second ACTH study), when the handling of the fish was better standardized.

Whole-body concentrations of cortisol in YOY and thyroid hormones in YOY and 1+ perch (Table 2) varied among lakes, independently of the metal-contamination gradient.

Condition factor and HSI

Condition factor and HSI values in YOY and 1+ fish varied among lakes independently of the contamination gradient (data not shown). Mean values for each group are given in Table 2.

Glycogen

Hepatic glycogen reserves before stress (basal) in 1+ yellow perch varied among lakes, independently of contamination levels (Table 3). However, 120 min following the stress test, the decrease of glycogen concentration in the liver was significant in fish from the two reference lakes (Opasatica and Dasserat) but not in intermediate- (Bousquet and Vaudray) or high-contamination (Osisko and Dufault) lakes.

Discussion

Characterization of exposure is an integral part of all ecotoxicological studies and, given the lack of field data on young fish, it was particularly important in evaluating the sensitivity of young perch to metals. A gradient in whole-body Cd concentrations — consistent with the gradient of Cd concentrations within the lakes from which the fish were sampled (Laflamme et al. 2000; Perceval et al. 2002) — was evident in 1+ and YOY fish. Metal concentrations in the whole-body homogenates were similar from one year to another, except for those of 1+ perch from the most contaminated lake (Dufault), which had, for unknown reasons, a more than twofold increase of Cd in 2000 compared with 1999. The pattern of Cd accumulation in the body of young fish followed the same pattern as that reported for liver, kidney, and interrenal tissue of adult yellow perch from the same study sites (Brodeur et al. 1997; Laflamme et al. 2000; Lévesque et al. 2003). Metal concentrations in the whole-body homogenates (without liver) of young perch were, however, a small fraction of the concentrations in tissues of adult fish. Other studies have shown that Cd, Cu, and Zn accumulate in internal organs, with Cd tending to accumulate

© 2005 NRC Canada

Fig. 5. Whole-body cortisol concentrations (mean ± standard error of the mean) after an intraperitoneal injection of saline (open bars) or adrenocorticotropic hormone (ACTH; solid bars) in 1+ yellow perch sampled from metal-contaminated lakes in the Rouyn-Noranda region in (*a*) 1999 and (*b*) 2000. The number of fish sampled (each bar) was 9–15. A different letter above the bar indicates a significant difference (Tukey–Kramer test, $P < 0.05$) from the other lakes. An asterisk indicates a significant difference (Student's *t* test, $P < 0.05$) from the saline-injected fish in the same lake.

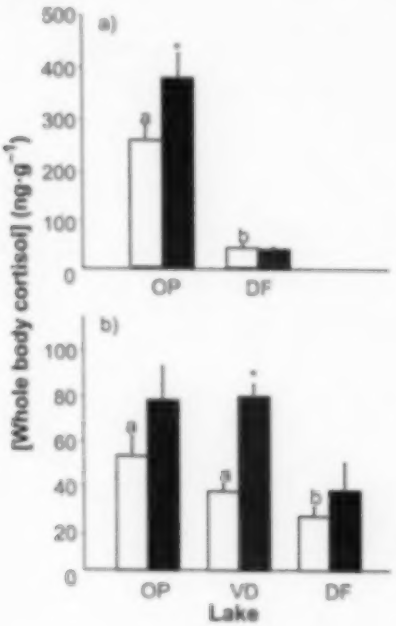

in kidney and Cu in liver (McGeer et al. 2000; Lévesque et al. 2003). Since liver was not included in the homogenates of 1+ perch, the gradient of whole-body Cd concentrations could be attributed, in large part, to accumulation in the kidney. Metal accumulation increases with time of exposure (McGeer et al. 2000), and in the present study, higher concentrations of metals were expected after 1 year of exposure (1+ perch) than after a few weeks (YOY). However, Cd and also Cu concentrations expressed per gram of body mass of YOY from the two highly contaminated lakes tended to be higher than those of 1+ perch. The higher whole-body concentrations of metals in the YOY than in the 1+ perch, both chronically exposed to nonlethal metal concentrations in the present study, could be related to a change in the accumulation rate of Cd with age and in ambient metal concentrations, as was seen before in a study on early life stages of *Cyprinus carpio* exposed to Cd (Suresh et al. 1993). Our results with young perch could also be explained by the way metal accumulation is expressed, either as a body burden ($\mu g \cdot fish^{-1}$) or as a concentration ($\mu g \cdot g^{-1}$). The hypothesis, proposed by others (Spehar 1976; Arnac and Lassus 1985), that fish grow at a faster rate than they accumulate contaminants is another possible explanation for the lower Cd accumulation in 1+ than in YOY perch homogenates.

Similar to metal concentrations in adult perch kidney (Lévesque et al. 2002), Cu, Zn, Ni, and Pb concentrations in young perch did not follow the contamination gradient among lakes, in contrast to Cd concentrations. However, 1+ and YOY fish from Lake Dufault were, in general, the most contaminated according to whole-body metal concentrations, despite the fact that livers were removed from the 1+ perch for glycogen analyses and that the liver is an important organ for accumulation of some metals, particularly Cu (Laflamme et al. 2000; McGeer et al. 2000). Unlike Cd, a nonessential metal, Zn and Cu are trace metals required for the metabolic activity of fish, and their intake and elimination are regulated (Arnac and Lassus 1985; Collvin 1985). The ability of fish to reestablish homeostasis rapidly after exposure to Cu (Laurén and McDonald 1987*a*, 1987*b*) and Zn (Alsop et al. 1999) was demonstrated in laboratory studies. Exposure to higher concentrations or for a longer period would likely saturate these mechanisms of regulation of Cu and Zn and eventually lead to the tissue accumulation patterns reflecting the gradient of ambient contamination that were observed with adult fish exposed for several years (Lévesque et al. 2002). The pattern of response to Cd, however, is suggestive of a process that is not metabolically regulated. McGeer et al. (2000) suggested that Cd detoxification would be more passive, involving storage, particularly in the kidney, rather than active regulation and elimination, resulting in continuous metal accumulation over an extended time course.

To test the link between exposure of young life stages of perch and the capacity to generate the normal stress response, changes in cortisol levels in response to an acute stressor were measured. In adult fish, plasma cortisol concentrations increase with time, following exposure to diverse types of acute stressors (Barton and Iwama 1991). To characterize the stress response in young fish, too small to blood-sample in the field, it was necessary to validate the use of measured whole-body cortisol levels. Changes in whole-body cortisol levels of fish larvae following extraction of whole-body homogenates using diethylether were reported previously (Feist et al. 1990; De Jesus et al. 1991; Barry et al. 1995). However, in view of the important loss of corticosteroid hormones caused by the extraction, as shown in the pilot study, and the technical difficulties of working with ether, we chose homogenization without extraction for the present project. A significant positive linear correlation was demonstrated between plasma cortisol and whole-body cortisol concentrations, providing further support for the use of a whole-body homogenate as an alternative to plasma. In the pilot study the standardized confinement-stress test led to a normal and detectable stress response characterized by a significant increase in cortisol concentration with time in 1+ perch from reference sites. Whole-body cortisol concentrations in 1+ perch from reference lakes in Abitibi also increased with time following confinement, compared with basal levels. It should be noted that the increase in cortisol levels in fish from the reference site in the mining region was less than that in fish from the reference site near Montreal, providing further evidence for metal-induced impairment of the cortisol stress response. Although Lakes Opasatica and Dasserat were used as reference lakes in the Rouyn-Noranda region, metal concentrations in these lakes

© 2005 NRC Canada

Table 2. Gross morphology and hormone levels (mean ± standard error of the mean) for young-of-the-year (YOY) and 1+ yellow perch sampled in six lakes in the Rouyn-Noranda region.

	YOY yellow perch	1+ yellow perch
Body length (cm)	1.8±0.08 (n = 34)	6.6±0.04 (n = 300)
Body mass (g)	0.07±0.04 (n = 34)	2.49±0.06 (n = 300)
Condition factor (%)	1.19±0.07 (n = 34)	0.84±0.01 (n = 300)
Hepatosomatic index (%)	nd[a]	1.52±0.09 (n = 300)
[T_3] (ng·g^{-1})	1.39±0.06[b] (n = 48)	0.32±0.03 (n = 84)
[T_4] (ng·g^{-1})	9.6±1.2[b] (n = 48)	3.0±0.2 (n = 84)
[Cortisol] (ng·g^{-1})	10.50±2.51[b] (n = 48)	—[c]

[a]Not determined.
[b]Hormone concentrations in YOY are expressed in nanograms per gram of body mass of pooled fish sampled after capture.
[c]See data in the Stress response section of Results.

were higher than in reference lakes near Montreal (Hontela et al. 1995).

Whole-body cortisol concentrations demonstrated, for the first time, that 1+ yellow perch from metal-contaminated lakes have a reduced capacity to increase their cortisol secretion following an acute stress test or ACTH stimulation. In contrast, YOY perch were not impaired, despite similar or even higher whole-body Cd concentrations. Further studies are required to confirm this finding, since eggs and larvae are normally considered the most sensitive life stages (Spehar 1976; McKim 1977; Sorensen 1991). However, a certain period of time may be required before the endocrine impairment becomes detectable.

Although impairment of the HPI axis in 1+ perch exposed to metals was revealed, no other physiological anomalies linked to metal exposure were detected. Thyroid-hormone levels in young perch, measured in whole-body homogenates, were not affected by 1 year of exposure to metals even though thyroid-hormone and cortisol levels often follow a similar pattern because of paracrine regulation (Young and Lin 1988), and adult perch from the same metal-contaminated sites had lower plasma T_3 and T_4 levels than perch from the reference lakes (Lévesque et al. 2003). Our data suggest that an impaired cortisol stress response and impaired thyroid function do not necessarily occur together.

Condition factor and HSI were measured to assess whether metal exposure and HPI impairment led to altered somatic growth. Again, similar to plasma thyroid-hormone levels, although the condition factor of adult perch in the metal-contaminated lakes sampled in this study was lower (Sherwood et al. 2000), no differences in condition were detected in YOY or 1+ perch. There was no effect of metal exposure on HSI in young or adult fish (Laflamme et al. 2000; Sherwood et al. 2000; Lévesque et al. 2002), suggesting that HSI is not sensitive to pollutant-induced stress.

Liver glycogen reserves were assessed to evaluate whether the metal-induced disruption of the HPI axis had an effect on the metabolic status of fish. In the two reference lakes, there was a significant decrease of glycogen stores in the liver following the stress challenge. These findings are consistent with the mobilization of glycogen and the increase in plasma glucose that coincides with an elevation in plasma cortisol concentrations after exposure to a stressor in rainbow trout and adult yellow perch (Haux and Larsson 1984; Vijayan and Moon 1992; Lévesque et al. 2002). Acute laboratory exposures to Cd also led to a decrease in liver glycogen accompanied by increased plasma glucose (Haux and Larsson 1984; Lowe-Jinde and Niimi 1984; Pratap and Wendelaar Bonga 1990). In the present study, stress-related glycogen mobilization was significant in the reference lakes, while in the intermediate- and high-contamination lakes, only a trend toward lower liver glycogen levels after exposure to the stress test was observed. This trend toward reduced mobilization of glycogen could be the first sign of an alteration in metabolic functions of young perch exposed to Cd. Field studies on adult perch have shown that fish from contaminated sites maintained liver glycogen stores after exposure to the stress test but plasma glucose was depleted (Hontela 1998; Lévesque et al. 2002). Moreover, the seasonal cycling of glycogen reserves was altered in metal-contaminated adult perch (Lévesque et al. 2002). Surprisingly, the highest liver glycogen levels were recorded in young perch from the most contaminated lake. Whether this reflects a seriously impaired ability to mobilize energy reserves in these fish remains to be demonstrated.

Table 3. Liver glycogen concentrations (mean ± standard error of the mean) before and after a confinement-stress test of 1+ yellow perch sampled in six lakes in the Rouyn-Noranda region.

	Glycogen concentration (mg·g^{-1})	
Lake	Before stress (basal)	After stress
Opasatica	5.09±0.26ab	3.36±0.22*
Dasserat	10.30±1.74bc	4.13±1.66*
Bousquet	6.91±1.20ab	4.85±0.49
Vaudray	7.56±1.35ab	4.99±0.54
Osisko	3.60±0.60a	2.61±0.36
Dufault	13.83±2.12c	9.65±1.24

Note: The number of fish sampled in each group was 14. Values followed by a different letter are significantly different (Tukey–Kramer test, $P < 0.05$).
*Significantly different from basal levels in fish sampled in the same lake (Student's t test, $P < 0.05$).

Our study demonstrated that effects of environmental exposure to metals on the HPI axis in yellow perch are detectable after only 1 year of exposure. This chronic exposure caused an increase in Cd body burdens of YOY and 1+ yellow perch. Cd accumulation was linked to an impaired stress

© 2005 NRC Canada

response characterized by an inability to increase whole-body cortisol concentrations and reduced mobilization of glycogen reserves in response to an acute stressor. Our study characterized for the first time the physiological status of young life stages of yellow perch exposed to metals in the field. The disruption of cortisol secretion seems to be one of the first physiological alterations detectable in young fish exposed to metals in the environment. The stress response of 1+ fish could be used as an early biomarker of toxicity in fish chronically exposed to contaminants.

Acknowledgements

We thank J. Doire, G. Sherwood, M.-C. Tardif, A. Lacroix, and H. Lévesque for field assistance, V. Leblond for help in the laboratory, and S. Prémont (INRS-ETE, Université du Québec) for metal analyses. This study was funded by the Metals in the Environment Research Network), a grant from the Natural Sciences and Engineering Research Council of Canada to A.H., and a scholarship from the Fonds pour la formation des chercheurs et l'aide à la recherche (Québec) to A.G.

References

Aalto, S.K., and Newsom, G.E. 1990. Additional evidence supporting demic behaviour of a yellow perch (*Perca flavescens*) population. Can. J. Fish. Aquat. Sci. **47**: 1959–1962.

Alsop, D.H., McGeer, J.C., McDonald, D.G., and Wood, C.M. 1999. Assessing the costs and consequences of chronic waterborne zinc exposure to juvenile rainbow trout in hard and soft water. Environ. Toxicol. Chem. **18**: 1014–1025.

Arnac, M., and Lassus, C. 1985. Heavy metal accumulation (Cd, Cu, Pb, and Zn) by smelt (*Osmerus mordax*) from the north shore of the St. Lawrence estuary. Water Res. **19**(6): 725–734.

Audet, S.K., and Claireaux, G. 1992. Diel and seasonal changes in resting levels of various blood parameters in brook trout (*Salvelinus fontinalis*). Can. J. Fish Aquat. Sci. **49**: 870–877.

Auer, N.A. 1982. Identification of larval fishes of the Great Lakes basin with emphasis on the Lake Michigan drainage. Great Lakes Fish. Comm. Spec. Publ. No. 82-3.

Barry, T.P., Malison, J.A., Held, J.A., and Parrish, J.J. 1995. Ontogeny of the cortisol stress response in larval rainbow trout. Gen. Comp. Endocrinol. **97**: 57–65.

Barton, B.A., and Iwama, G.K. 1991. Physiological changes in fish from stress in aquaculture with emphasis on the response and effects of corticosteroids. Annu. Rev. Fish Dis. **1**: 3–26.

Brodeur, J.C., Sherwood, G., Rasmussen, J.B., and Hontela, A. 1997. Impaired cortisol secretion in yellow perch (*Perca flavescens*) from lakes contaminated by heavy metals: *in vivo* and *in vitro* assessment. Can. J. Fish. Aquat. Sci. **54**: 2752–2758.

Campbell, P.G.C., Hontela, A., Rasmussen, J.B., Giguère, A., Gravel, A., Kraemer, L., et al. 2003. Differentiating between direct (physiological) and food-chain mediated (bioenergetic) effects on fish in metal-impacted lakes. Hum. Ecol. Risk Assess. **9**(4): 847–866.

Collvin, L. 1985. The effect of copper on growth food consumption and food conversion of perch *Perca fluviatilis* offered maximal food rations. Aquat.Toxicol. **6**(2): 105–114.

De Jesus, E.G., Inui, Y., and Hirano, T. 1990. Cortisol enhances the stimulating action of thyroid and steroid hormones on dorsal fin-ray resorption of flounder larvae *in vitro*. Gen. Comp. Endocrinol. **79**: 167–173.

De Jesus, E.G., Hirano, T., and Inui, Y. 1991. Changes in cortisol and thyroid hormone concentration during early development and metamorphosis in the Japanese flounder, *Paralichthys olivaceus*. Gen. Comp. Endocrinol. **82**: 369–376.

Eastwood, S., and Couture, P. 2002. Seasonal variations in condition and liver metal concentrations of yellow perch (*Perca flavescens*) from a metal-contaminated environment. Aquat. Toxicol. **58**: 43–56.

Feist, G., Schreck, C.B., Fitzpatrick, M.S., and Redding, J.M. 1990. Sex steroid profiles of coho salmon *Oncorhynchus kisutch* during early development and sexual differentiation. Gen. Comp. Endocrinol. **80**(2): 299–313.

Forlin, L., Haux, C., Karlsson-Norrgren, L., Runn, P., and Larsson, A. 1986. Biotransformation enzyme activities and histopathology in rainbow trout, *Salmo gairdneri*, treated with cadmium. Aquat. Toxicol. **8**: 51–59.

Girard, C., Brodeur, J.C., and Hontela, A. 1998. Responsiveness of the interrenal tissue of yellow perch (*Perca flavescens*) from contaminated sites to an ACTH challenge test *in vivo*. Can. J. Fish. Aquat. Sci. **55**: 438–450.

Haux, C., and Larsson, A. 1984. Long-term sub-lethal physiological effects on rainbow trout, *Salmo gairdneri*, during exposure to cadmium and after subsequent recovery. Aquat. Toxicol. **5**: 129.

Hontela, A. 1998. Interrenal dysfunction in fish from contaminated sites: *in vivo* and *in vitro* assessment. Annual review. Environ. Toxicol. Chem. **17**: 44–48.

Hontela, A., Dumont, P., Duclos, D., and Fortin, R. 1995. Endocrine and metabolic dysfunction in yellow perch, *Perca flavescens*, exposed to organic contaminants and heavy metals in the St. Lawrence River. Environ. Toxicol. Chem. **14**: 725–731.

Laflamme, J.-S., Couillard, Y., Campbell, P.G.C., and Hontela, A. 2000. Interrenal metallothionein and cortisol secretion in relation to Cd, Cu and Zn exposure in yellow perch, *Perca flavescens*, from Abitibi lakes. Can. J. Fish. Aquat. Sci. **57**: 1692–1700.

Laurén, D.J., and McDonald, D.G. 1987*a*. Acclimatation to copper by rainbow trout, *Salmo gairdneri*: physiology. Can. J. Fish. Aquat. Sci. **44**: 99–104.

Laurén, D.J., and McDonald, D.G. 1987*b*. Acclimatation to copper by rainbow trout, *Salmo gairdneri*: biochemistry. Can. J. Fish. Aquat. Sci. **44**: 105–111.

Laurent, P., and Perry, S.F. 1990. Effects of cortisol on gill chloride cell morphology and ionic uptake in the freshwater trout, *Salmo gairdneri*. Cell. Tissue Res. **259**: 429–442.

Lévesque, H., Moon, T.W., Campbell, P.G.C., and Hontela, A. 2002. Seasonal variation in carbohydrate and lipid metabolism of cortisol-impaired metal-exposed yellow perch (*Perca flavescens*). Aquat. Toxicol. **60**: 257–267.

Lévesque, H., Dorval, J., Van Der Kraak, G., Campbell, P.G.C., and Hontela, A. 2003. Hormonal, morphological and physiological responses of yellow perch (*Perca flavescens*) to chronic environmental metal exposures. J. Toxicol. Environ. Health A, **66**: 657–676.

Lockhart, W.L., Uthe, J.F., Kinney, A.R., and Mehrle, P.M. 1972. Methylmercury in northern pike (*Esox lucius*): distribution, elimination and some biochemical characteristics of contaminated fish. J. Fish. Res. Board Can. **29**: 1519–1523.

Lowe-Jinde, L., and Niimi, A.J. 1984. Short-term and long-term effects of cadmium on glycogen reserves and liver size in rainbow trout (*Salmo gairdneri* Richardson). Arch. Environ. Contam. Toxicol. **13**: 759–764.

© 2005 NRC Canada

Mason, R.P., Laporte, J.-M., and Andres, S. 2000. Factors controlling the bioaccumulation of mercury, methylmercury, arsenic, selenium, and cadmium by freshwater invertebrates and fish. Arch. Environ. Contam. Toxicol. **38**: 283–297.

McGeer, J.C., Szebedinszky, C., McDonald, G.D., and Wood, C.M. 2000. Effects of chronic sublethal exposure to waterborne Cu, Cd or Zn in rainbow trout 2: tissue specific metal accumulation. Aquat. Toxicol. **50**: 245–256.

McKim, J.M. 1977. Evaluation of tests with early life stages of fish for predicting long-term toxicity. J. Fish. Res. Board Can. **34**: 1148.

Mommsen, T.P., Vijayan, M.M., and Moon, T.W. 1999. Cortisol in teleosts: dynamics, mechanisms of action, and metabolic regulation. Rev. Fish Biol. Fish. **9**(3): 211–268.

Norden, C.R. 1961. The identification of larval yellow perch, *Perca flavescens* and walleye, *Stizostedion vitreum*. Copeia, 3: 282–288.

Pankhurst, N.W., and Van Der Kraak, G. 2000. Evidence that acute stress inhibits ovarian steroidogenesis in rainbow trout *in vivo*, through the action of cortisol. Gen. Comp. Endocrinol. **117**: 225–237.

Per-Arne, A., Staldvik, F.J., Lukin, A.A., Kashuli, N.A., Popova, O.A., and Reshetnikov, Y.S. 1997. Heavy metal contamination in freshwater fish from the border region between Norway and Russia. Sci. Total Environ. **201**: 211–224.

Perceval, O., Pinel-Alloul, B., Methot, G., Couillard, Y., Giguère, A., and Campbell, P.G.C. 2002. Cadmium accumulation and metallothionein synthesis in freshwater bivalves (*Pyganodon grandis*): elative influence of the metal exposure gradient versus limnological variability. Environ. Pollut. **118**(1): 5–17.

Plisetskaya, E., Woo, N.Y.S., and Murat, J.-C. 1983. Thyroid hormones in cyclostomes and fish and their role in regulation of intermediary metabolism. Comp. Biochem. Physiol. A, **74**: 179–187.

Pratap, H.B., and Wendelaar Bonga, S.E. 1990. Effects of waterborne cadmium on plasma cortisol and glucose in the cichlid fish *Oreochromis mossambicus*. Comp. Biochem. Physiol. C, **95**: 313–317.

Sherwood, G.D., Rasmussen, J.B., Rowan, D.J., Brodeur, J., and Hontela, A. 2000. Bioenergetic costs of heavy metal exposure in yellow perch (*Perca flavescens*): *in situ* estimates with a radiotracer (^{137}Cs) technique. Can. J. Fish Aquat. Sci. **57**: 441–450.

Sherwood, G.D., Kovecses, J., Hontela, A., and Rasmussen, J.B. 2002. Simplified food webs lead to energetic bottlenecks in polluted lakes. Can. J. Fish Aquat. Sci. **59**: 1–5.

Sorensen, E.M. 1991. Metal poisoning in fish. CRC Press, Boston.

Spehar, R.L. 1976. Cadmium and zinc toxicity to flagfish, *Jordanella floridae*. J. Fish. Res. Board Can. **33**: 1939–1945.

Suresh, A., Sivaramakrishna, B., and Radhakrishnaiah, K. 1993. Patterns of cadmium accumulation in the organs of fry and fingerlings of freshwater fish *Cyprinus carpio* following cadmium exposure. Chemosphere, **26**(5): 945–953.

Verbost, P.M., Van Rooij, J., Flick, G., Lock, R.A.C., and Wendelaar Bonga, S.E. 1989. The movement of cadmium through freshwater trout branchial epithelium and its interference with calcium transport. J. Exp. Biol. **145**: 185–197.

Vijayan, M.M., and Moon, T.W. 1992. Acute handling stress alters hepatic glycogen metabolism in food-deprived rainbow trout (*Oncorhynchus mykiss*). Can. J. Fish Aquat. Sci. **49**: 2260–2266.

Vijayan, M.M., Pereira, C., Grau, E.G., and Iwama, G.K. 1997. Metabolic responses associated with confinement stress in tilapia: the role of cortisol. Comp. Biochem. Physiol. C, **116**: 89–95.

Wendelaar Bonga, S.E. 1997. The stress response in fish. Physiol. Rev. **77**: 591–625.

Westernhagen Von, H. 1988. Sublethal effects of pollutants on fish eggs and larvae. *In* The physiology of developing fish, eggs and larvae. *Edited by* W.S. Hoar and D.J. Randall. Academic Press, New York. pp. 253–346.

Young, G., and Lin, R.J. 1988. Response on the interrenal to adrenocorticotropic hormone after short term thyroxine treatment of coho salmon (*Oncorhynchus kisutch*). J. Exp. Zool. **245**: 53–58.

© 2005 NRC Canada

Divergent impacts of experimental lake-level drawdown on planktonic and benthic plant communities in a boreal forest lake

Michael A. Turner, David B. Huebert, David L. Findlay, Leonard L. Hendzel, Wolfgang A. Jansen, R.A. (Drew) Bodaly, Llwellyn M. Armstrong, and Susan E.M. Kasian

Abstract: Water-surface elevation in lake 226 (L226) of the Experimental Lakes Area in northwestern Ontario, Canada, was lowered experimentally by 2–3 m during each of three successive winters, and increased naturally but incompletely during the ensuing summers. Our objective was to compare the responses of the littoral and pelagic plant communities to this physical disturbance. Water-chemistry changes were muted, and neither nitrogen nor phosphorus concentration changed. Phytoplankton biomass, species assemblages, productivity, and nutrient status were largely unaffected except for small changes in species diversity and relative abundance of cyanobacteria and cryptophytes. Despite possible transient changes in functional and structural properties, the principal disruption for benthic algae was loss of colonizable surfaces. Floating-leaved and submersed macrophytes (hydrophytes) responded initially with large decreases in biomass and cover. The subsequent response of hydrophytes to drawdown varied: relative frequency of isoetids such as *Eriocaulon septangulare* decreased, while that of pondweeds such as *Potamogeton spirillus* increased. The trophic impacts of declining lake levels, whether due to hydroelectric reservoir manipulations or climate change, are likely to be much greater in the littoral zone than in the pelagic zone if major nutrients are unaltered.

Résumé : Le niveau de la surface de l'eau du lac 226 (L226) de la Région des lacs expérimentaux (nord-ouest de l'Ontario, Canada) a été abaissé expérimentalement de 2–3 m au cours de chacun de trois hivers successifs; il s'est rétabli naturellement, mais partiellement, pendant chacun des étés suivants. L'objectif était de comparer les réactions des communautés de plantes littorales et pélagiques à cette perturbation physique. La chimie de l'eau a peu changé et l'azote et le phosphore sont demeurés stables. La biomasse du phytoplancton, les associations d'espèces, la productivité et le statut trophique sont demeurés inchangés, à l'exceptions de petites modifications de la diversité spécifique et de l'abondance relative des cyanobactéries et des cryptophytes. Malgré certains changements transitoires de leurs propriétés fonctionnelles et structurales, la principale perturbation des algues benthiques a été la perte de surfaces à coloniser. Les macrophytes (hydrophytes) à feuilles flottantes et submergées ont affiché au départ une importante perte de biomasse et de couverture végétale. La réaction subséquente des hydrophytes à l'abaissement du niveau a varié : l'importance relative des plantes de type isoétide, telles qu'*Eriocaulon septangulare*, a diminué, alors que celles des potamots, tels que *Potamogeton spirillus*, a augmenté. L'impact trophique des réductions de niveau des lacs, qu'elles soient causées par les manipulations des réservoirs hydroélectriques ou par le changement climatique, risque d'être beaucoup plus important dans la zone littorale que dans la zone pélagique, lorsque les nutriments principaux restent inchangés.

[Traduit par la Rédaction]

Introduction

Fluctuations in water-surface elevation (or lake level) are one of the most important disturbances affecting aquatic ecosystems (Quennerstedt 1958; Paller 1997). Substantial changes in lake level can be due to natural causes such as drought, heavy precipitation, or even climate change (Greening and Gerritsen 1987; Wilcox and Meeker 1991). Water-level fluctuations can also be the deliberate result of hydroelectric power generation, efforts to enhance local fisheries and recreation, or attempts to control growths of nuisance aquatic macrophytes (Rorslett 1989; Paller 1997).

The influence of changes in lake level on phytoplankton and littoral benthic algae has received little attention. In an

Received 15 October 2004. Accepted 13 December 2004. Published on the NRC Research Press Web site at http://cjfas.nrc.ca on 18 May 2005.
J18361

M.A. Turner,[1] D.L. Findlay, L.L. Hendzel, W.A. Jansen, R.A. Bodaly, and S.E.M. Kasian. Experimental Lakes Area, Freshwater Institute, 501 University Crescent, Winnipeg, MB R3T 2N6, Canada.
D.B. Huebert. 35 Mansfield Crescent, Winnipeg, MB R2N 1R9, Canada.
L.M. Armstrong. Institute for Wetland and Waterfowl Research, Ducks Unlimited Canada, P.O. Box 1160, Stonewall, MB R0C 2Z0, Canada.

[1]Corresponding author (e-mail: turnermi@dfo-mpo.gc.ca).

 doi: 10.1139/F05-003 © 2005 NRC Canada

early review, Cooke (1980) suggested that an increase in algal blooms may be one of the most severe impacts of drawdown. Studies on the effects of lake-level fluctuations on benthic algae are also uncommon, though Ploskey (1986) implied that drawdown reduced periphyton biomass through desiccation.

In contrast, the effects of water-level fluctuations on aquatic macrophytes have received considerable attention (e.g., Quennerstedt 1958; Rorslett 1989; Paller 1997). Impacts on macrophytes have been highly variable, which is perhaps not surprising given the large variation in amount, timing, and duration of drawdown, as well as in lake-basin morphometry and nutrient status, and in the type of macrophyte community. There are, however, some features that are regularly reported. Quennerstedt (1958) postulated that as the amplitude of multiple drawdowns increased, the width of the littoral-zone vegetation would decrease. Drawdown usually leads to loss of macrophyte species richness, cover, and biomass (Tarver 1980; Rorslett and Johansen 1996). Such losses are often due to desiccation in summer and freezing and ice-scour in winter (Hellsten et al. 1996). However, the effect of a single drawdown can be reversed in one or two growing seasons by the rapid regrowth of macrophytes (Paller 1997). Another marked effect of drawdown is often a major change in species composition, which may occur after even a single drawdown (Rorslett 1989). The impacts of subsequent drawdowns are often less dramatic, owing to the replacement of drawdown-sensitive species with drawdown-resistant species (Rorslett 1989).

The purpose of our study was to compare the effect of experimental-lake-level drawdown on the benthic and planktonic plant communities of a small oligotrophic lake. We hypothesized that the drawdown and subsequent reflooding would cause resuspension of the previously inundated littoral sediments, releasing nutrients that would stimulate a phytoplankton bloom. We also expected that macrophytes and benthic algae would be impacted negatively both by the physical loss of habitat and by the shading expected to be caused by phytoplankton blooms and resuspension of native lake sediments. We used baseline data and concurrent data from nearby reference lakes for comparison. The principal importance of this study is its comparison of changes in the pelagic and littoral plant communities caused by drawdown that have not previously been well documented.

Methods

Study site

Lake 226 (L226) is a 16.1-ha double-basin lake (L226N and L226S) located on Precambrian granite in the Experimental Lakes Area (ELA) of northwestern Ontario (Beaty 1981). It is a soft-water, oligotrophic lake with a circumneutral pH (Fig. 1). The maximum depth of L226 in 1994 (pre-drawdown) was 14.7 m with a total lake volume of 9.6×10^5 m^3. The drainage-basin area is 97.2 ha with no permanent stream inflows (Beaty 1981). Although the lake had previously been subject to nutrient enrichment from 1973 to 1980, water chemistry and phytoplankton had returned to natural conditions before the onset of this experiment (1992–1994). For example, the epilimnetic chlorophyll *a* concentration averaged 14.1 μg·L^{-1} in L226N during the years of nutrient enrichment; in contrast, the mean open-water chlorophyll *a* concentration was 3.8 μg·L^{-1} during the pre-drawdown period (1992–1994) versus 5.2 μg·L^{-1} prior to nutrient enrichment (1971). Similarly, phytoplankton biomass averaged 4.6 mg·L^{-1} during nutrient enrichment and 0.8 mg·L^{-1} during the pre-drawdown period versus 0.5 mg·L^{-1} prior to enrichment.

Four ELA lakes (L224, L239, L240, and L373) were used as reference lakes, although different lakes and timelines were occasionally used as study components because of differences in availability of long-term biomonitoring data. All the lakes that were used, however, are located in the ELA and are subject to the same year-to-year changes in weather as the study lake.

To allow control of the lake level in a way that was typical of reservoirs supplying water for power production, a control structure was built at the outflow in the northeast corner of L226N (Fig. 1). This enabled the lake level to be drawn down during winter and allowed the lake to refill during spring and summer. During the winter of 1994–1995 the lake level was drawn down almost 2 m; during the winters of 1995–1996 and 1996–1997 the lake was drawn down approximately 3 m (Fig. 1). At drawdown levels of 1.7 and 3.1 m, the availability of hard surfaces (rock and some gravel or sand) in the littoral zone declined from 4.41 ha to 2.92 and 1.36 ha, respectively, i.e., to 66% and 31% of the pre-drawdown amount. In contrast, decreases in the profundal sediments were very small, with declines of only 2% and 3%, respectively (P. Cooley, North/South Consultants Inc., 83 Scurfield Boulevard, Winnipeg, MB R3Y 1G4). Although the lake was allowed to refill naturally each summer in 1995, 1996, or 1997, lake levels did not return to the initial lake level in any of these years (Fig. 1). This regime contrasted with the natural lake-level fluctuation of approximately 20 cm (K. Beaty, Freshwater Institute, 501 University Crescent, Winnipeg, MB R3T 2N6, personal communication).

Water chemistry

Epilimnetic water samples were taken at 0.5 m depth at stations overlying the deepest point in reference lakes 224, 239, and 373 and in each basin of L226. Samples were kept cool and stored in polyethylene bottles until water analyses were carried out within 24 h of collection according to Stainton et al. (1977). Total phosphorus (P) and nitrogen (N) were calculated as the sum of their total dissolved and particulate species. Monthly to weekly sampling during the ice-free season (May–October) yielded from 10 to 13 collections per year in each reference lake and from 12 to 26 collections in each of L226N and L226S (except for 1992, when only seven collections were made in each basin). Annual open-water means were derived from simple averages of these regular interval collections. A mean value for L226 was computed as the mean of the respective L226N and L226S means; this was also the practice for all other components of the study.

Phytoplankton

During each ice-free season from 1992 to 1997, phytoplankton was sampled at the deep stations in L226N and L226S (Fig. 1) and in reference lakes 224, 239, and 373

© 2005 NRC Canada

Fig. 1. Bathymetric map of experimental lake 226 (L226) illustrating the change in shoreline associated with a drawdown of 3.1 m below the historical reference lake level. The inset at the lower right shows changes in lake level from 1 January 1994 to 31 March 1998. Changes are shown relative to a long-term datum that was set equal to zero. The map also indicates approximate sampling locations for water chemistry, phytoplankton, and benthic algae and indicates the location of the outlet control structure. The location of the Experimental Lakes Area in Canada is shown on the map at the upper left.

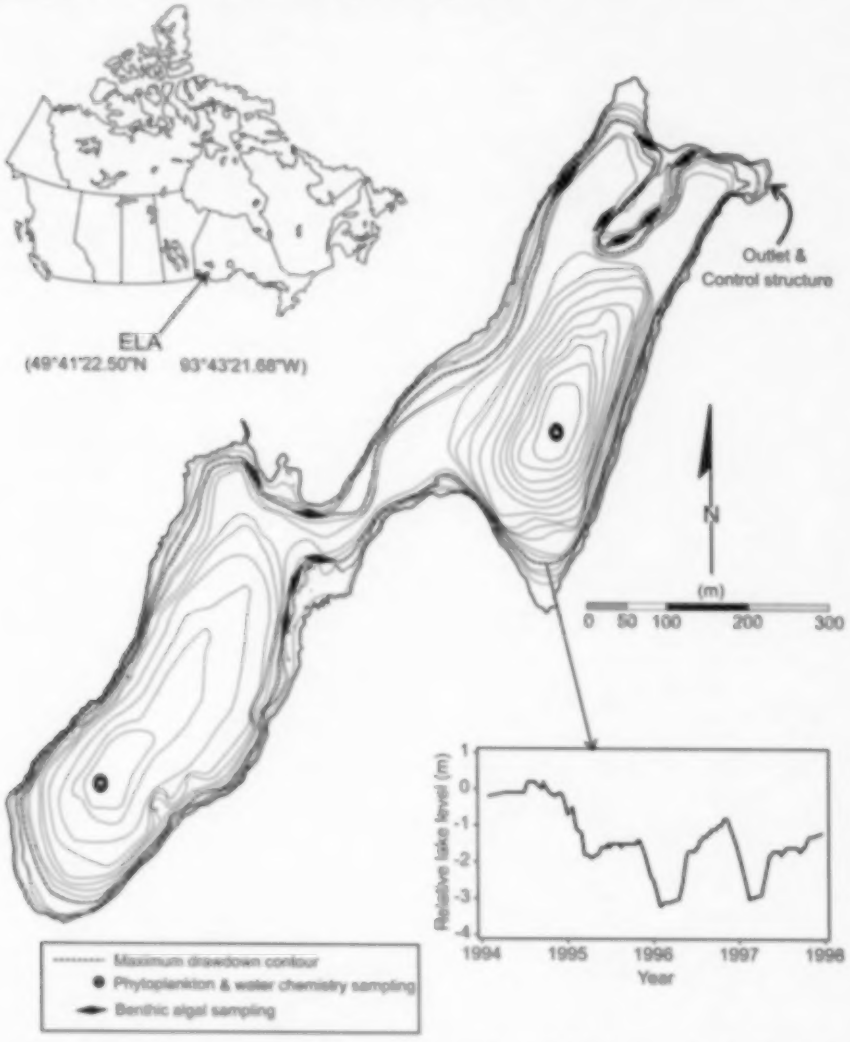

using a sampler that integrated the epilimnion (Shearer 1978). The number of monthly to weekly collections per year varied with the type of analysis: from 6 to 11 for algal composition, from 9 to 12 for productivity, and from 6 to 26 for nutrient-deficiency measures.

A 125-mL aliquot from each integrated sample was fixed in Lugol's solution for identification and enumeration of phytoplankton. One 10-mL subsample from each aliquot was allowed to settle for 24 h and counts were performed on an inverted microscope at magnifications of 125, 400, and 1200× with phase-contrast illumination (Utermohl technique, as modified by Nauwerck 1963). On occasion, net samples were taken with a 10 μm mesh net to aid species identification. Cell counts were converted to wet-weight biomass by approximating cell volume and assuming a specific gravity of 1. Estimates of cell volume for each species were obtained by routine measurements of up to 50 cells of an individual species and applying the geometric formula best fitted to the shape of the cell (Rott 1981). Simpson's index of diversity was calculated according to Washington (1984).

Epilimnetic phytoplankton nutrient status was measured on a subsample of each integrated sample. Seston composition ratios (carbon (C) : chlorophyll *a*, C:P, C:N, and N:P) were analysed as indicators of N and P deficiency (Hecky et al. 1993), limits having been derived experimentally (Healey and Hendzel 1980). Seston samples were analysed using the methods of Stainton et al. (1977). These physiological indicators of nutrient deficiency in the phytoplankton were so similar within each year that an annual ice-free season mean was calculated for each parameter.

© 2005 NRC Canada

Laboratory measurement of phytoplankton photosynthesis followed the procedure of Shearer et al. (1985) as modified by Fee et al. (1992). The integrated samples were inoculated with trace amounts of $NaH^{14}CO_3$ and dispensed into 60-mL glass-stoppered Pyrex® bottles. Samples were incubated in a water-filled rectangular incubator in a range of light levels (0 to ~980 $\mu E \cdot m^{-2} \cdot s^{-1}$) for 3 h at in-situ temperatures. Following incubation, an aliquot of each sample was removed, acidified to approximately pH 2.5, and bubbled with air for 20 min to remove all nonfixed $NaH^{14}CO_3$. Radioactivity was measured by liquid scintillation. Uptake of ^{14}C measured in dark bottles was subtracted from rates of uptake measured in the light. The maximum volumetric rate of photosynthesis (P_{opt}, mg $C \cdot m^{-3} \cdot h^{-1}$) divided by the concentration of chlorophyll *a* yielded P_{bm} (mg C·mg chlorophyll $a^{-1} \cdot h^{-1}$). Areal and volumetric phytoplankton photosynthesis was estimated using computer programs (Fee 1990) incorporating actual surface solar irradiance data and chlorophyll *a* concentrations. All rates were corrected for lake volumetric changes with depth.

Benthic algae

The bottom surface of the littoral zone in L226 and reference lakes 239 and 373 was largely rock, so scuba-based techniques (Turner et al. 1987) were used to measure the composition and metabolism of the natural biofilms on these rock surfaces (i.e., epilithon). Sampling was conducted monthly during July and August in each basin of L226 (1994–1997) and in reference lake 239 (1992–1997), and once per summer in reference lake 373 (1992–1997). On each occasion, epilithon was sampled on rock surfaces of low slope (<10%) at three unshaded locations (southern exposures) in the middle littoral zone of each lake or basin (Fig. 1). Because of the lake-level changes that occurred in L226N and L226S, actual sampling locations varied over the years. Similarly, although sampling locations were at 1–2 m water depth in all lakes, those in L226 were farther downslope during 1995–1997 relative to 1994. For all epilithic measures, data from replicate composite samples and (or) repeated sampling were averaged to report one midsummer mean for each lake or basin.

Epilithon for particulate-composition analyses was collected on each occasion by a diver using a quantitative scraping sampler (Turner et al. 1991). Three or 4 samples of epilithon (each 5 cm^2) were collected at each of the three sampling sites to yield a total of 9–12 samples. Replicate samples from each site were then combined to yield a location-specific sample that included 15 or 20 cm^2 of epilithon. Each of the three composites was adjusted to standard volume with lake water and then filtered through GF/C filters, dried overnight in the dark (C and N only), and frozen until analysis for particulate C, N, and P (Stainton et al. 1977).

To analyse the benthic algal taxonomy, aliquots of the three location-specific composite samples were combined to yield one sample per lake or basin on each sampling occasion. Samples were preserved by adding equal quantities of acid Lugol's solution and formaldehyde, acetic acid, and alcohol to achieve 4% final volume. To improve our effectiveness at detecting algae, prior to subsampling, these epilithic samples were sonicated at a frequency of 20 kHz for two 15-s intervals (Sonifier® cell disruptor with microtip, Model W140, Heat Systems – Ultrasonics Inc., Plainview, New York). Subsamples were analysed until 100 viable cells (chloroplast integrity was the criterion for viability) or 100 µm long filaments were enumerated. The methods used to identify algae and measure their abundance, algal biovolume, and Simpson's index of diversity were similar to those described earlier for phytoplankton. Additional details are presented in Turner et al. (1987, 1991). Only data for diatoms and cyanobacteria are presented because these regularly composed >90% of the algal biomass.

Rates of epilithic net photosynthesis were estimated in situ by sealing chambers to rock surfaces and measuring changes in dissolved inorganic carbon (DIC) in water overlying the isolated epilithon (Turner et al. 1987, 1991). DIC concentrations were determined using an infrared gas analyser. The rates measured thus reflected activities of the entire biofilm association rather than just the algal component. At each of the three different locations, samples were taken in four light conditions (including darkness) by using chambers that transmitted varying amounts of light, yielding a total of 12 samples per occasion. The maximum rate of net photosynthesis (P_{max}) was estimated as the mean areal rate of DIC uptake in the three samples receiving 100% of available light. Typically, epilithon in the middle littoral zone was light-saturated at in-situ irradiances >200 $\mu E \cdot m^{-2} \cdot s^{-1}$ (Turner et al. 1987), which was confirmed by examination of the intermediate-irradiance samples. Dark respiration (R_d) was measured as the mean areal rate of DIC release by epilithon in three samples incubated in the dark in parallel with net photosynthesis. The fraction of gross photosynthesis ($P_g = P_{max} + |R_d|$) consumed instantaneously by respiratory activities is given by the percentage ratio $R_d:P_g$, which varies from 0% to 100%.

Macrophytes

From 1994 through 1997, macrophyte cover was estimated once in each lake or basin between 26 July and 12 August in L226 and in reference lakes 239 and 240. Using a transect- and quadrat-sampling technique, 24 transects were spaced 100 m apart perpendicular to the shoreline of each lake. Cover was estimated for each transect at depths of 0.5, 1, 2, and 3 m using a combined cover value of all floating-leaved and submersed macrophytes (i.e., hydrophytes as in Hutchinson 1975) found within three replicate 0.25-m^2 quadrats. Percent cover was determined using a modified Braun–Blanquet scale (0 = 0%; 1 = 1%–5%; 2 = 6%–25%; 3 = 26%–50%; 4 = 51%–75%; 5 = 76%–99%; 6 = 100%; Barbour et al. 1987). Percent cover of emergent macrophytes (i.e., helophytes as in Hutchinson 1975) was estimated as the amount of space, viewed horizontally, occupied by helophytes along 10 m of shoreline, centred at each transect/shoreline intersection. One estimate of helophytes was made per transect.

Between 31 July and 17 August during 1994–1997, macrophyte biomass (in L226 only) was estimated by scuba divers using a transect- and quadrat-sampling technique. Transects were placed perpendicular to the shoreline using a stratified random design. Based on the initial estimate of macrophyte percent cover, each basin of L226 was divided into three zones (bays, north shore, and south shore). Six transects were then randomly placed among the three zones

© 2005 NRC Canada

in each basin, yielding a total of 12 transects. The number of transects within each zone was a reflection of the proportion of shoreline in that zone, so it was not necessary to "weight" any of the quadrat samples. Biomass was harvested within duplicate 0.25-m^2 quadrats at the shoreline and at 1, 2, 3, and 5 m. Harvested plant material was separated by species and by plant part, placed in paper bags, and dried at 85 ± 5 °C for 24 h. The aboveground material was then weighed to the nearest 1 mg to determine oven-dry weight. Voucher specimens were archived at the University of Manitoba (Winnipeg) herbarium.

Biomass estimates were calculated by multiplying the average biomass at a particular depth by the area of that depth interval and then summing the resultant values. For the whole-lake biomass estimates, it was assumed that plant biomass was uniform within a given depth interval. The deeper quadrat was used for each interval. Actual water depths, not 1994 depths, were used for all macrophyte data.

Statistical methods

Bootstrap-based randomization methods (Manly 1998) were used to compare the lakes prior to and during the drawdown period. Classical parametric tests were not used because it is difficult to test distributional assumptions when data sets are small. Randomization rather than non-parametric methods were chosen because actual values are considered in the calculation of p values, rather than simply their ordering.

For each characteristic, each year was treated as an observational unit and the difference between the data for the treatment lake and the average data for the reference lakes was constructed. These difference data were then used to calculate conventional two-sample t statistics for the changes accompanying drawdown. For each response, the true value of the t statistic was compared with the distribution of t statistics that was obtained by randomly (with replacement) resampling the raw data and assigning the observations to pre-drawdown versus during-drawdown data. Actual t statistics considered atypical of their randomization distributions (i.e., less than the 2.5th percentile or greater than the 97.5th percentile) were considered to be indicative of changes associated with drawdown. To avoid rejecting hypotheses that should be explored further during future studies, t statistics less than the 5th percentile or greater than the 95th percentile were considered to be "possibly indicative" of changes. Specifically, the bootstrap methods detailed in section 6.4 of Manly (1998) were used to conduct 1000 bootstrap simulations. The power of these analyses was lessened for the epilithic and macrophyte characteristics because there was only one year of pre-drawdown data for these parameters.

All analyses were conducted using SAS software (SAS Institute Inc. 1999). The tailored code developed to conduct the bootstrap sampling used PROC SURVEYSAMPLE.

Results

Water chemistry

Although some chemical parameters changed in response to winter drawdown, usually these changes were small relative to changes seen in the reference lakes (Table 1; Fig. 2). During 1995–1997, values of total P (Fig. 2*a*), N (Fig. 2*b*), particulate C (Fig. 2*c*), DIC (Fig. 2*d*), chlorophyll *a* (Fig. 2*f*), and pH (Fig. 2*j*) changed 10% or less relative to values during the pre-drawdown years of 1992–1994. Similarly, total suspended solids (unmeasured in the reference lakes) differed little, averaging 1.24 ± 0.07 $mg \cdot L^{-1}$ (mean ± standard deviation (SD), n = 3 years) during 1995–1997 versus 1.21 ± 0.06 $mg \cdot L^{-1}$ during the pre-drawdown years 1992–1994. Dissolved organic carbon decreased 24% during 1995–1997 versus 1992–1994 values, which was different from changes seen in the reference lakes (Fig. 2*e*; p = 0.041, Table 1). In contrast, conductivity increased (15%, Fig. 2*i*; p = 0.038, Table 1); the calcium concentration possibly increased (24%, Fig. 2*g*; p = 0.084, Table 1). There was a much larger increase (117%) in soluble reactive silica that was possibly significant (Fig. 2*h*; p = 0.061, Table 1), although the resulting concentration remained less than that in reference lake 239.

Phytoplankton

Phytoplankton composition in L226 prior to drawdown (1994) was generally similar to that observed in the three reference lakes (Fig. 3), though some algal groups were more abundant, reflecting L226's higher planktonic biomass (Fig. 3*a*) and productivity (Fig. 4*f*). From 1992 to 1994, L226 had an ice-free mean algal biomass of 0.8 $g \cdot m^{-3}$ compared with 0.4 $g \cdot m^{-3}$ for the three reference lakes (Fig. 3*a*). Chrysophytes were seasonally dominant (Fig. 3*g*), with smaller populations of cryptophytes (Fig. 3*h*), chlorophytes (Fig. 3*f*), diatoms (Fig. 3*e*), and dinoflagellates (Fig. 3*d*) present.

The effects of drawdown on the L226 phytoplankton were generally small. Changes in mean ice-free phytoplankton biomass following drawdown did not differ from those observed in the reference lakes (p = 0.13; Table 1). Chrysophytes were the predominant group both before and after drawdown (Fig. 3*g*); their relative biomass was little changed after drawdown and was similar to that in the reference lakes (Table 1). This was also the case for chrysophytes (Fig. 3*g*), dinoflagellates (Fig. 3*d*), diatoms (Fig. 3*e*), and chlorophytes (Fig. 3*f*). However, small differences were observed in the biomass of cyanobacteria (Fig. 3*c*; p = 0.029, Table 1) and possibly cryptophytes (Fig. 3*h*; p = 0.093, Table 1) following drawdown compared with the reference lakes. Species diversity (Fig. 3*b*), which had been similar in L226 and the reference lakes during two of the three open-water seasons prior to drawdown, declined following drawdown, which was significantly different from the reference lakes (p = 0.015, Table 1).

Particulate C : chlorophyll *a* ratios (Fig. 4*a*), a general indicator of nutrient status, indicated that the phytoplankton in L226 and the three reference lakes was severely nutrient-deficient, and this was unchanged following drawdown. Particulate C:P (Fig. 4*b*) and N:P ratios (Fig. 4*c*) indicated that the phytoplankton was severely P-deficient in L226 and in reference lakes 224, 239, and 373. After drawdown, there were no major changes in these indices in L226 in relation to the reference lakes (Table 1). Particulate C:N ratios (Fig. 4*d*) indicated that L226 phytoplankton exhibited moderate N deficiency during the study period. Although this deficiency did not change following drawdown, there was a significantly greater difference in C:N ratios between L226

© 2005 NRC Canada

Table 1. Results of bootstrap *t* tests comparing means for the treatment lake (L226) and reference lakes (L224, L239, L240, and L373) in the Experimental Lakes Area prior to treatment versus the period of drawdown.

	p	Nature of effect (if present, i.e., $p < 0.1$)[a]
Total phosphorus (P)	0.601	
Total nitrogen (N)	0.251	
Particulate carbon (C)	0.337	
Dissolved inorganic carbon[b]	0.395	
Dissolved organic carbon	0.041	<
Chlorophyll *a*	0.675	
Calcium	0.084	>
Soluble reactive silica	0.061	>
Conductivity	0.038	>
pH	0.046	>
C : chlorophyll *a*	0.697	
C:P	0.279	
N:P	0.158	
C:N	0.033	
Total algal planktonic biomass	0.131	
Planktonic algal diversity	0.015	<
Planktonic cyanobacteria	0.029	<
Planktonic dinoflagellates	0.888	
Planktonic diatoms	0.292	
Planktonic chlorophytes	0.709	
Planktonic chrysophytes	0.590	
Planktonic cryptophytes	0.093	>
P_{bm}	0.383	
P_{opt}	0.316	
Total epilithic biomass[c]	0.800	
Epilithic cyanobacteria[c]	0.224	
Epilithic diatoms[c]	0.450	
Epilithic diversity[c]	0.172	
Particulate C[c]	0.594	
R_d[c]	0.863	
P_{max}[c]	0.475	
R_d:P_g[c]	0.751	
Hydrophyte percent cover[d]	<0.05	<
Helophyte percent cover[e]	<0.01	<
Hydrophyte biomass[f]	0.07	<
Helophyte biomass[f]	0.09	<

Note: The following combinations of pretreatment years and reference lakes were generally used in the analyses: water chemistry: 1992–1994 and L224, L239, and L373; phytoplankton: 1992–1994 and L224, L239, and L373; benthic algae: 1994 and L239 and L373;[c] macrophytes: 1994 and L239 and L240.[d,e,f]

[a]The nature of the effect (if present) was either a greater or a lesser difference between the treatment lake and the reference lakes prior to drawdown (see the text for a more complete description of the effect).

[b]Pre-drawdown data for L373 were available and used in the analysis.

[c]Pre-drawdown data were available only for 1994, i.e., no treatment-lake data were collected in 1992 or 1993.

[d]Pre-drawdown data were available only for 1994 and data for the drawdown period were only available for 1995 and 1996; no reference-lake data were collected in 1992, 1993, or 1997.

[e]Pre-drawdown data were available only for 1994, i.e., no reference-lake data were collected in 1992 or 1993.

[f]There were no reference-lake data. The *t* test compares treatment-lake means before and during drawdown.

and the reference lakes ($p = 0.033$, Table 1), two of which briefly exhibited severe N deficiency.

Rates of phytoplankton photosynthesis were not noticeably affected by the drawdown (Figs. 4*e* and 4*f*; Table 1). This was true for both chlorophyll *a*-normalized (P_{bm}, Fig. 4*e*) and volumetric (P_{opt}, Fig. 4*f*) rates.

Benthic algae

During the midsummer prior to drawdown, total epilithic algal biomass in L226 averaged 0.64 mg·cm^{-2}, which was intermediate between that in reference lakes 239 and 373 (Fig. 5*a*). Although total epilithic biomass increased slightly following the drawdown of L226, the increase was not significant (Table 1). This was also true for particulate C (Fig. 5*e*; Table 1). For these and the other epilithic parameters, the power of the statistical analyses was curtailed by the availability of only one year of observations in L226 prior to drawdown.

The epilithon in L226 and the reference lakes was composed mainly of cyanobacteria (Fig. 5*b*) and diatoms (Fig. 5*c*). The relative biomass of cyanobacteria (predominantly *Lyngbya* spp.) was not detectably higher in L226 than in the reference lakes as a result of drawdown (Fig. 5*b*; Table 1). Similarly, the relative biomass of diatoms in L226 was usually lower than in the reference lakes during 1995–1997, although this was not an effect of drawdown (Fig. 5*c*; Table 1). Nor was there any detectable effect of drawdown on epilithic taxonomic diversity in L226 (Fig. 5*d*; Table 1).

In midsummer of 1994 prior to drawdown, P_{max} was 0.4 mmol C·m^{-2}·h^{-1} and remained largely unchanged following lake drawdown (Fig. 5*g*; Table 1). Although R_d more than doubled immediately following drawdown in L226, rates declined in 1996 and 1997 (Fig. 5*f*); as a result, there was no overall difference in the drawdown years compared with 1994 (Table 1). Similarly, despite a transient increase in the R_d:P_g ratio during 1995 (Fig. 5*h*), there was no difference between L226 and the reference lakes in the drawdown years (Table 1).

Macrophytes

Before drawdown, mean hydrophyte cover for the 0–3 m zone in L226 was estimated to be 14% in 1994 (Fig. 6*a*). Coverage decreased significantly in the drawdown years ($p < 0.05$, Table 1); coverage declined to 5% the summer following lake-level drawdown, and recovered somewhat in 1997. Helophyte coverage also declined ($p < 0.01$, Table 1) from an initial 14% to 3% in 1995, and remained low throughout the study (Fig. 6*b*). These patterns of change were in clear contrast to the two nearby reference lakes, where percent cover remained stable or increased during 1995–1996 (Figs. 6*a* and 6*b*). Unlike in the case of the epilithon, the magnitude of these impacts was sufficient to overcome the low power of the statistical analyses that was due to the availability of only one year of pre-drawdown data.

Prior to drawdown, L226 contained at least 20 species of aquatic macrophytes (Table 2). The dominant hydrophytes were the isoetids *Eriocaulon septangulare*, *Lobelia dortmanna*, and *Isoetes* spp. They contributed 43% of the total hydrophyte biomass (Fig. 6*d*) and occurred with a relative frequency of 39% (Table 3). Following drawdown, the relative frequency of barren substratum increased from 17%

© 2005 NRC Canada

Fig. 2. Selected water chemistry in the epilimnia of L226 (—) and three reference lakes 224 (◇ · · · · ◇), 239 (□ — — — □), and 373 (○– – – – ○) during the open-water periods of 1992–1997; because of the incomplete record prior to drawdown, data for L373 were not used in the statistical analyses. Annual open-water means are shown for each lake; values for each basin of L226 are connected by a vertical bar through the lake mean. A vertical line denotes the beginning of the experimental drawdown in L226.

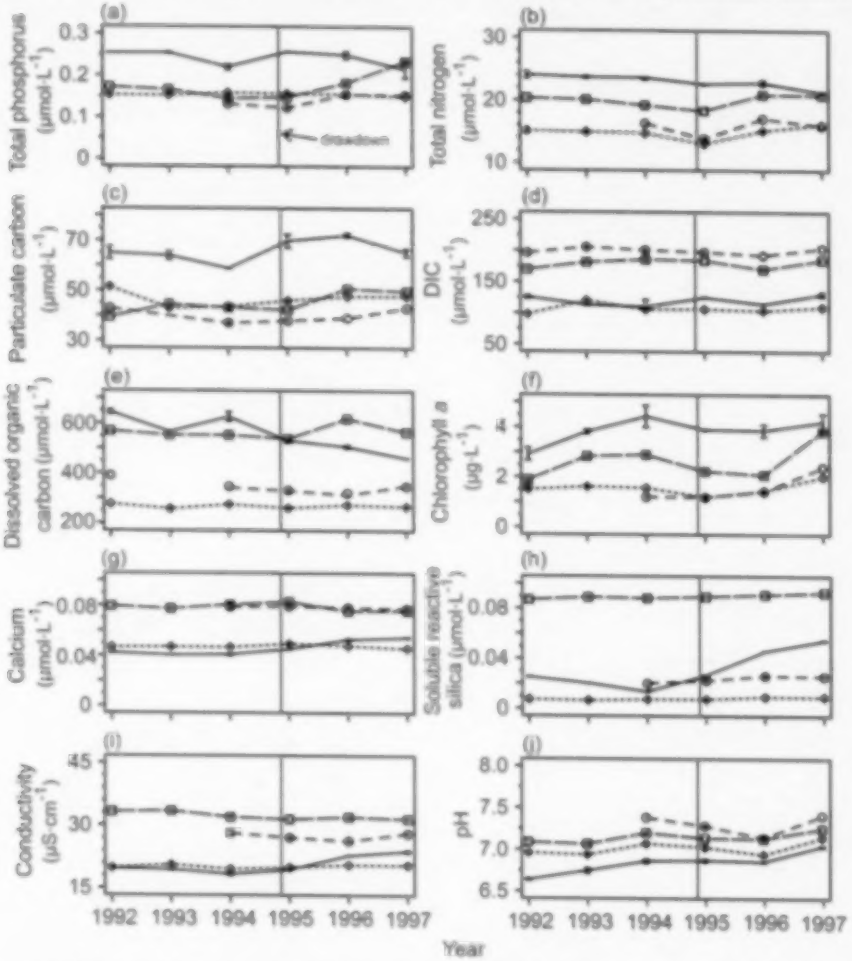

to 32%, and seven macrophyte species were no longer found in the lake (Table 2). Isoetids as a whole declined (Table 3), and by 1997 contributed only 11% to the estimated total hydrophyte biomass (Fig. 6*d*). In contrast to these declines in L226, the relative frequency of isoetids in nearby reference lakes was comparatively unchanged (Table 3). Equally dramatic was the almost complete loss of the helophyte community, most notably *Carex* spp., in terms of percent cover (Fig. 6*b*; $p < 0.01$, Table 1); the decline in areal biomass (Fig. 6c; $p = 0.09$, Table 1) was possibly significant. Species such as *Myriophyllum* spp., however, remained largely unaffected by drawdown (Table 2), and the pondweeds, particularly *Potamogeton spirillus*, actually increased in biomass and frequency. In 1994, pondweeds contributed 9% of macrophyte biomass, increasing to 75% in 1996 and 58% by 1997 (Fig. 6*d*); their relative frequency also increased substantially compared with that in the two reference lakes (Table 3).

In 1994, prior to drawdown, macrophyte areal biomass in L226 was estimated to be 4.6 g dry weight·m^{-2}, which is within the range of values reported for other oligotrophic lakes (Wile et al. 1985). Total aboveground biomass for the 0–5 m depth zone was estimated to be 73 kg dry weight for hydrophytes and 280 kg dry weight for helophytes. There was a possibly significant decrease in biomass of hydrophytes to 17% of this value in 1995 following initial lake-level drawdown (Fig. 6c; $p = 0.07$, Table 1); similarly the decline in helophyte biomass to 4% was possibly significant (Fig. 6c; $p = 0.09$, Table 1). There was little recovery in helophyte biomass, but by 1997, hydrophyte biomass had recovered to 49% of the pre-drawdown estimate (Fig. 6c).

Discussion

Water chemistry in L226 was typical of that in lakes within the ELA region (Beamish et al. 1976), with low levels of total P, total N, calcium, and conductivity. Although there were differences between pre- and post-drawdown water chemistry, these changes were generally small and did

© 2005 NRC Canada

Fig. 3. Total phytoplankton biomass (*a*), Simpson's index of diversity (*b*), and percent total biomass of cyanobacteria (*c*), dinoflagellates (*d*), diatoms (*e*), chlorophytes (*f*), chrysophytes (*g*), and cryptophytes (*h*) in L226 (—) and reference lakes 224 (◇ - - - - ◇), 239 (□ — — — □), and 373 (○– - - - ○). Annual open-water means are shown for each lake during 1992–1997; values for each basin of L226 are connected by a vertical bar through the lake mean. A vertical line denotes the beginning of the experimental drawdown in L226.

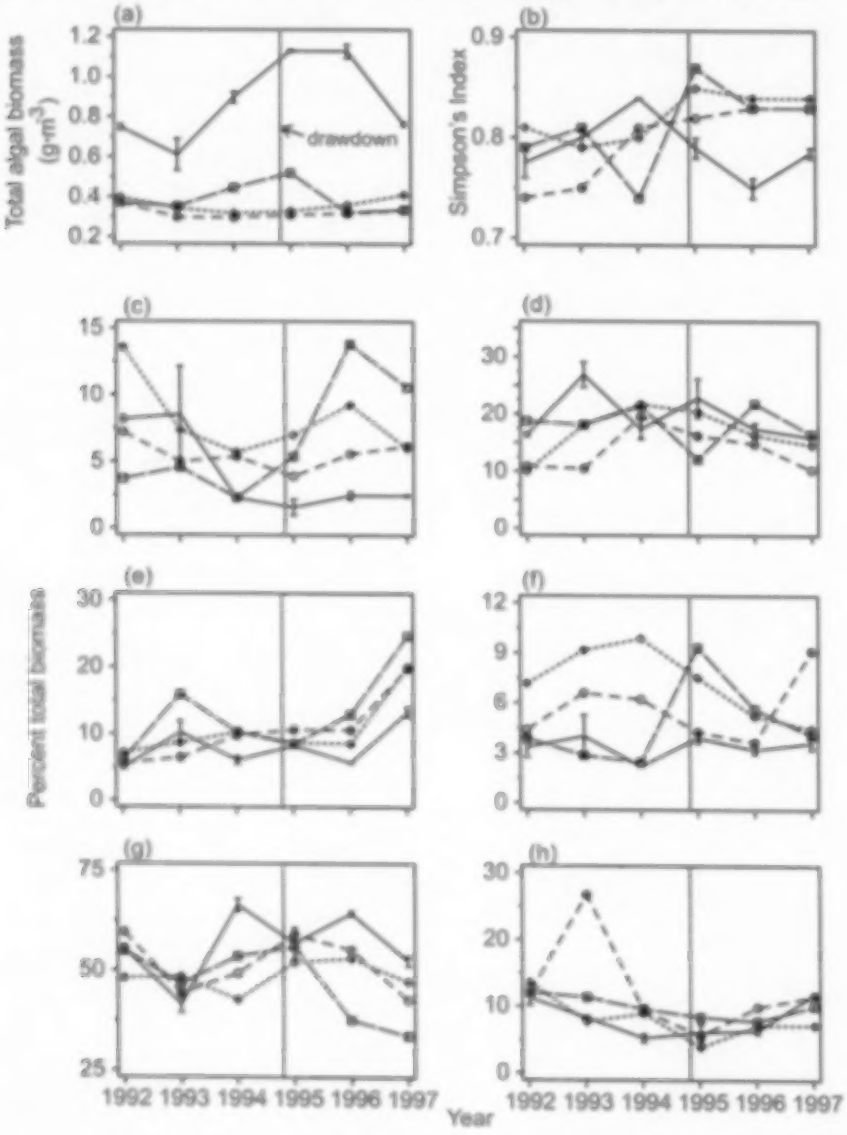

not alter the basic nutrient characterization of L226 as a soft-water, oligotrophic lake. After 3 years of drawdown, levels of conductivity, cations, and macronutrients such as N and P were still extremely low. Thus, our hypothesized resuspension of littoral sediments did not occur. Further evidence of this was that levels of total suspended solids remained unchanged after drawdown.

There are several plausible explanations for the small changes in water chemistry in L226. Perhaps the incomplete refilling of L226 dampened any nutrient release from the exposed lake sediments. We might also have observed lower levels of nutrient release compared with the inundation of soils in newly formed reservoirs because the reflooding of dried-out sediments with well-oxygenated water would likely not be as conducive to nutrient solubilization. Nutrient release may also have been prevented by the relatively small fetch of L226, which minimized wind action on the lake and prevented the expected resuspension of epilimnetic sediments. The substantial rockiness of the exposed lake bottom may have further diminished the potential for sediment resuspension. Observed increases in conductivity and calcium and silica concentrations (coupled with an increase in

© 2005 NRC Canada

Fig. 4. Metrics of phytoplankton nutrient status in L226 (—) and reference lakes 224 (◇ - - - - ◇), 239 (□ – – – □), and 373 (○– – – – – ○) during the open-water periods of 1992–1997; because of the incomplete record prior to drawdown, data for L373 were not used in the statistical analyses. Lines denote indices of nutrient deficiency rather than results of direct tests of nutrient deficiency. Chlorophyll *a*-normalized (Fig. 4*e*, P_{bm}) and volumetric (Fig. 4*f*, P_{opt}) rates of photosynthesis are also shown. Annual open-water means are shown for each lake; values for each basin of L226 are connected by a vertical bar through the lake mean. A vertical line denotes the beginning of the experimental drawdown in L226.

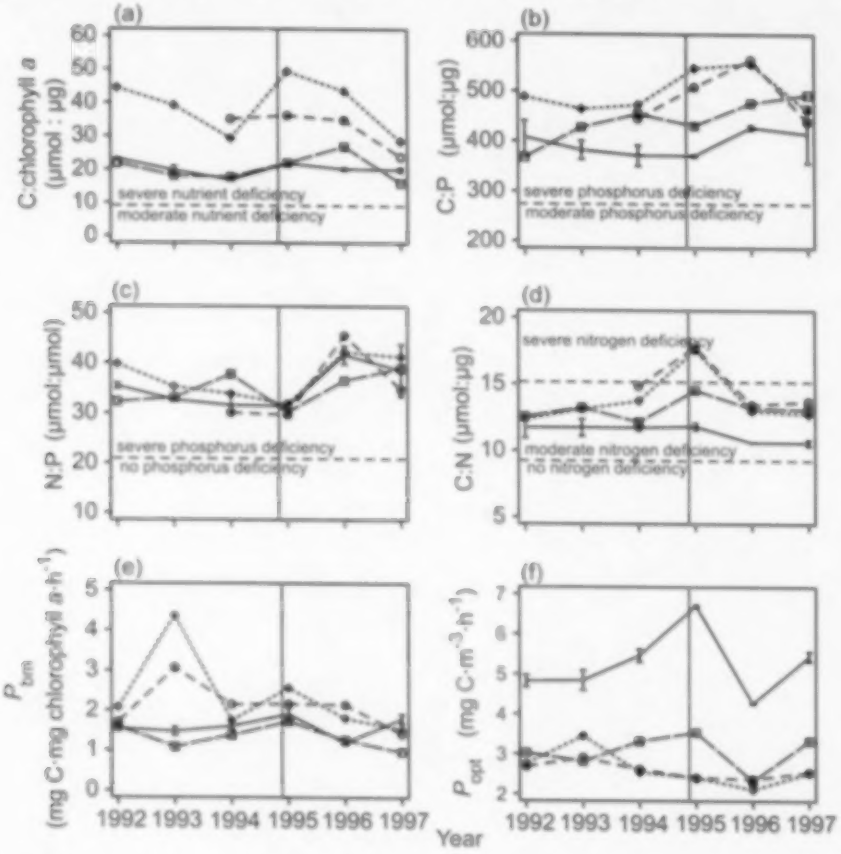

pH) may have been due to releases from the pore waters of drawdown areas. Decreases seen in dissolved organic carbon may have been due to the isolation and drying of a previously connected wetland as the lake level dropped. Whatever the reasons, the large increases in nutrient chemistry that we had anticipated did not occur.

The absence of large changes in levels of major nutrients meant that the phytoplankton bloom and subsequent cascade of effects that we had expected did not occur. There were no major effects of lake-level drawdown on phytoplankton-community composition at the group level except for small changes in the cyanobacteria and cryptophytes. Nor were any changes observed in phytoplankton photosynthesis or nutrient status. These results conflict with Cooke (1980), who suggested that an algal bloom would follow drawdown and reflooding, associated with considerable nutrient release upon reflooding, which did not occur. Although we did not observe a phytoplankton bloom, there was a small decrease in taxonomic diversity. One factor that could have contributed to this decrease is that a potentially large species bank for phytoplankton was reduced with the loss of about 70% of the previously inundated epilimnetic sediments at maximum drawdown.

There are two perspectives on the impact of lake-level drawdown on benthic algal associations in the littoral zone. The first is that responses (per unit area) were muted compared with the macrophyte changes. In contrast to the macrophytes, benthic algae have short turnover times and in some cases are more mobile. As a result, this community appeared to adapt more rapidly to drawdown per unit area of remaining colonizable surface without large long-term changes in biomass, species composition, or metabolism. The small increases in the sedimentary or epipelic character of the epilithon that were seen during the first year following drawdown (increases in respiration, abundance of blue-green algae, and particulate matter) may have been due to littoral-zone compression (i.e., the downward slumping of materials) or to the "deeper character" of the community studied. However, any changes seen in the L226 epilithon were temporary. The inference is that as long as hard littoral substrata

© 2005 NRC Canada

Fig. 5. Several compositional and metabolic measures of epilithon (biofilm on rock surfaces) in L226 (—) and reference lakes 239 (□ — — — □) and 373 (○- - - - ○) during July–August in 1992–1997; note that statistical analyses used only 1994 as a pre-drawdown year. Annual open-water mean rates of dark respiration (R_d) (*f*), maximum net photosynthesis (P_{max}) (*g*), and the balance between respiration and gross photosynthesis (R_d:P_g) (*h*) are shown for each lake. Values for each basin of L226 are connected by a vertical bar through the lake mean. A vertical line denotes the beginning of the experimental drawdown in L226.

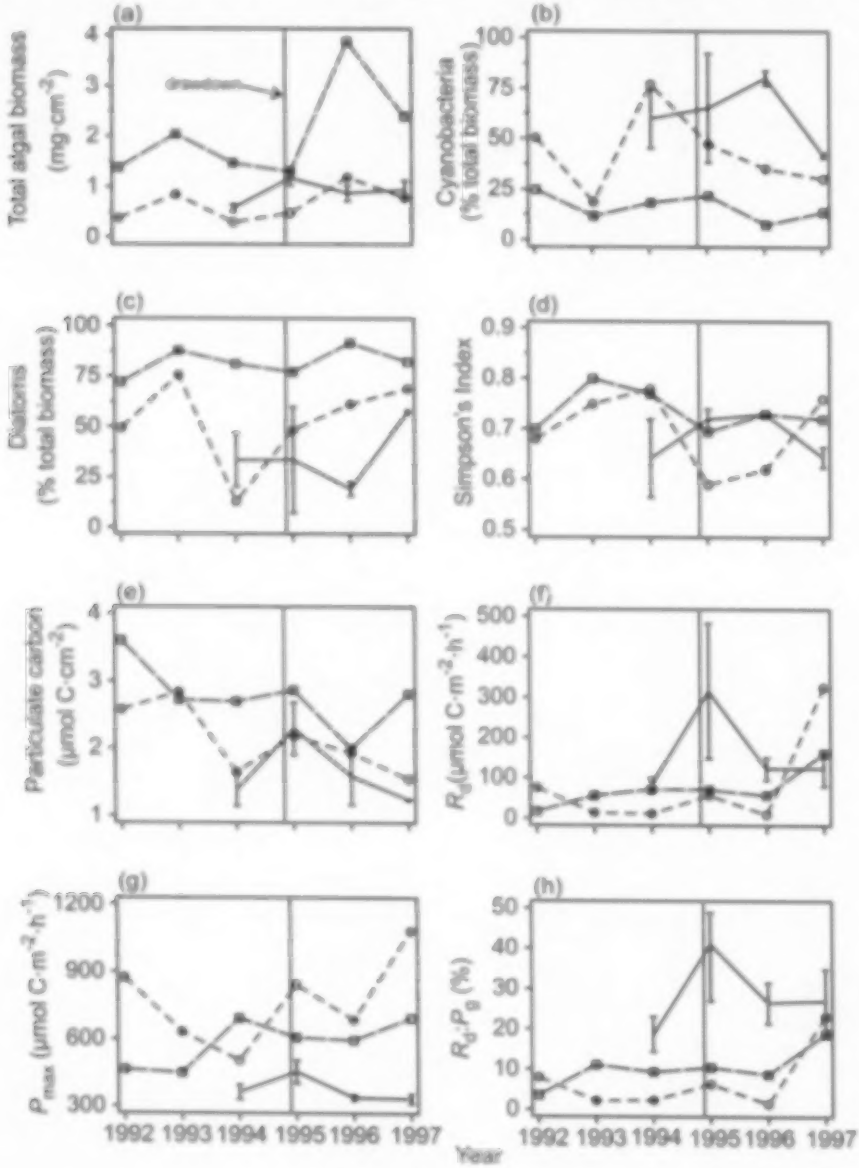

remained submerged and available for colonization, benthic algal composition and metabolism per unit area continued unchanged, at least partly because there were no large changes in waterborne availability of major nutrients. Had DIC increased in response to resuspension of littoral sediments coupled with a substantial increase in alkalinity, we might have expected benthic algal photosynthesis to increase. However, DIC remained constant and major changes did not occur, unlike other disturbances that have had major benthic algal impacts where DIC changed (Turner et al. 1991).

The second and more important concern for benthic algal communities following drawdown was the disruption of habitat and temporary loss of at least two-thirds of colonizable area. It is probable that as a result, the total benthic algal contribution to the lake's food web declined substantially (at least temporarily) following drawdown. Hard littoral surfaces contracted from 4.4 ha to as little as 1.4 ha (i.e., a de-

© 2005 NRC Canada

Fig. 6. Percent cover of hydrophytes (submersed and floating-leaved macrophytes) (*a*) and helophytes (emergent macrophytes) (*b*) in L226 (—) and reference lakes 239 (□ — — — □) and 240 (○- - - - ○) during 1994–1997. Average areal biomass of helophytes (—) and hydrophytes (- - - -) (*c*) and the percentages contributed by isoetids (—) and pondweeds (- - - -) (*d*) were also measured in L226. Initial lake-wide biomass was 280 ± 78 kg (mean ± SD) for helophytes and 73 ± 33 kg for hydrophytes. A vertical line denotes the beginning of the experimental drawdown in L226.

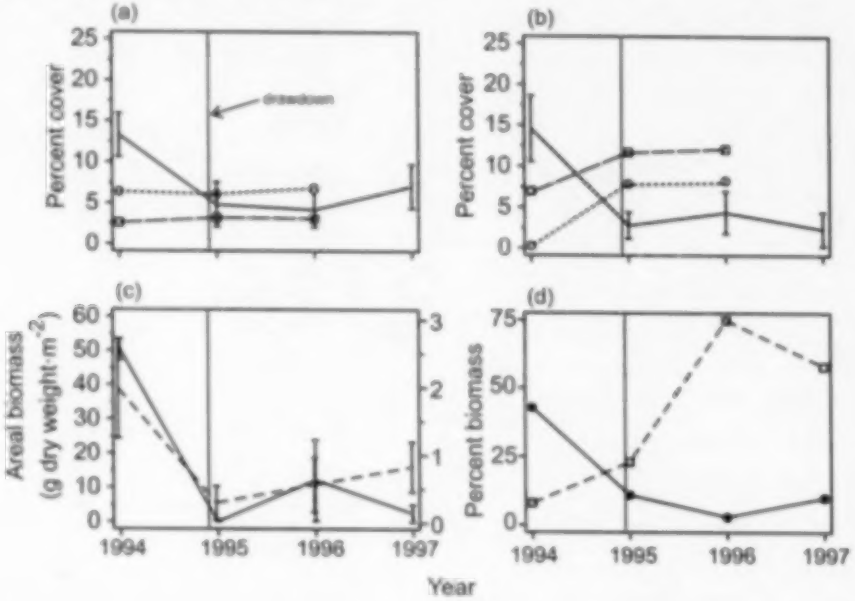

Table 2. Numbers of species and relative frequencies (%) of aquatic macrophytes in L226 from 1994 to 1997, separated on the basis of their response to drawdown.

	1994	1995	1996	1997
Number of species	20	17	15	13
Bare substratum[a]	16.7	27.1	31.0	32.2
Increase in frequency[b]	6.7	14.9	30.2	29.1
Little change in frequency[c]	31.6	40.8	29.1	32.8
Decrease in frequency[d]	18.6	8.4	2.4	5.9
Disappeared[e]	26.5	8.4	7.2	0

[a]Included all quadrats that contained no macrophytes.
[b]*Potamogeton spirillus*, *Sparganium fluctuans*, and *Najas flexilis*.
[c]*Eleocharis acicularis*, *Isoetes echinospora*, *Potamogeton amplifolius*, *Myriophyllum* spp., *Potamogeton epihydrus*, *Nitella* sp., *Dulichium arundinaceum*, and *Juncus pelocarpus*.
[d]*Eriocaulon septangulare* and *Nuphar variegatum*.
[e]*Lobelia dortmanna*, *Carex* spp., *Utricularia vulgaris*, *Iris versicolor*, *Equisetum fluviatile*, *Scirpus subterminalis*, *Potamogeton panormitanus*, *Utricularia cornuta*, and *Utricularia minor*.

Table 3. Relative frequencies[a] (%) of isoetids and pondweeds in L226 and reference lakes 239 and 240.

	1994		1995–1996/1997[b]	
Lake	Isoetids[c]	Pondweeds[d]	Isoetids	Pondweeds
239	53.7	5.4	49.4±1.8	4.1±0.4
240	71.6	1.4	61.9±0.4	2.2±1.5
226	38.5	26.4	18.5±8.2	46.4±11.3

[a]Do not include barren substratum.
[b]Parameters were only estimated in the reference lakes during 1994–1996. Values are given as the mean ± standard deviation.
[c]*Isoetes echinospora*, *Isoetes lacustris*, *Lobelia dortmanna*, and *Eriocaulon septangulare*.
[d]*Potamogeton epihydrus*, *P. spirillus*, *P. amplifolius*, and *P. panormitanus*.

cline in colonizable littoral surfaces to 31% of the pre-drawdown area). This contraction meant that any small increases in areal concentrations of epilithic algal biomass were insufficient to compensate for the substantial loss of colonizable surface. A further and potentially important loss of benthic algae that was unmeasured in our study could have occurred because of the loss of macrophytes as colonizable surfaces for epiphytic algae.

Macrophytes, especially the dominant isoetids found in L226 prior to drawdown, are relatively long-lived and slow to adapt to disturbance, and so were severely affected when drawdown occurred. There was a decrease in macrophyte species richness, cover, and biomass following the 2- to 3-m winter drawdowns in L226, while over the same time period, macrophyte cover was relatively consistent in the nearby reference lakes. The contrast between macrophyte cover in L226 and in the reference lakes corroborates the conclusion that drawdown caused the macrophyte decline. This result is consistent with the work of Paller (1997), who found that a 6-m drawdown resulted in the almost complete loss of aquatic macrophytes in Par Pond. Earlier studies with more or less severe drawdowns have yielded similar results (Rorslett 1989; Hellsten et al. 1996; Rorslett and Johansen 1996).

Declines in macrophyte biomass, cover, and species richness associated with winter drawdown are caused by the

© 2005 NRC Canada

desiccation of plant material and subsequent exposure to freezing temperature. In addition, compaction and erosion of the exposed littoral-zone sediment occurs during the following spring runoff, with a consequent loss in substratum fertility (Cooke 1980; Tarver 1980). For L226, these factors were compounded by the fact that the lake did not refill completely during the summer months, so there was also a physical loss of habitat. The 3-m drawdown, however, was insufficient to completely destroy the littoral macrophyte community. This is consistent with the work of Rorslett (1989), who found that fluctuations of 5–7 m were required to completely remove macrophytes from the littoral zone of oligotrophic lakes in Scotland and Norway.

The relative frequency and relative biomass of macrophytes in L226 were also altered in response to drawdown, consistent with the results found by others (Tarver 1980; Rorslett 1989). Rorslett (1989), in particular, classified macrophytes into drawdown-resistant or -sensitive species, based on plant strategy (as in Grime 1979). The suggestion that some species (e.g., isoetids) should be drawdown-sensitive, while others (e.g., ruderals or those growing in rubble) should be drawdown-resistant is consistent with our observations in L226. After drawdown there was a decline in isoetids, which are slow-growing perennial evergreens. In contrast, there was an increase in pondweeds, which are fast-growing ruderals with various strategies for vegetative reproduction. The pondweeds often overwinter as vegetative turions (winter buds) or as tubers buried in the sediment. Consequently, the relative frequency and biomass of pondweeds increased dramatically after drawdown. Interestingly, in 1997, after three winters of drawdown, there was a reversal of the decline of isoetids, which suggested that perhaps they were adapting to the drawdown regime and were beginning the return to a pre-drawdown community structure. Throughout the same time period, the relative frequency of isoetids and pondweeds in nearby reference lakes was remarkably consistent.

The considerable divergence between the littoral and pelagic plant communities in response to lake-level drawdown was also observed in the invertebrate communities of the experimental lake. Zoobenthos was impacted, while zooplankton was unaffected (M. Paterson, Freshwater Institute, 501 University Crescent, Winnipeg, MB R3T 2N6, personal communication). Clearly, efforts to understand the implications of fluctuations in lake level for small lakes should recognize that biota in the littoral zone are more likely to be impacted than pelagic communities. This divergence in plant responses follows, at least partly, from the lack of any substantial change in nutrient chemistry, in contrast to the substantial alteration and compression of littoral habitat that occurred.

In conclusion, water-fluctuation experiments are pertinent because of the increasing demand for hydroelectric power that has led to an increase in reservoir development. Such experiments may also provide a preview of the consequences of diminished precipitation caused by climate change. Such experiments are not so much about the loss of lake volume per se, but are more of an exploration of changes in the lake bottom, the colonization rate of aquatic plant communities onto new substrata, and the ability of these communities to withstand periods of desiccation and extreme weather.

Acknowledgements

Ken Beaty and Mark Lyng were instrumental in carrying out the hydrological requirements of this study. Eva Schindler provided the water-chemistry and phytoplankton-photosynthesis data. Staff of the ELA and the Freshwater Institute laboratories analysed the water-chemistry samples. Paul Cooley provided the base outline map in Fig. 1 showing the extent of maximum drawdown. The manuscript was markedly improved by the constructive comments of Helen Baulch and two anonymous reviewers. Financial support was provided by the Sustainable Fisheries Program of the Habitat Action Plan, and by Habitat Management of the Ontario Great Lakes Area, Department of Fisheries and Oceans.

References

Barbour, M.G., Burk, J.H., and Pitts, W.D. 1987. Terrestrial plant ecology. 2nd ed. Benjamin Cummings, New York.

Beamish, R.J., Blouw, L.M., and McFarlane, G.A. 1976. A fish and chemical study of 109 lakes in the Experimental Lakes Area (ELA), northwestern Ontario, with appended reports on lake whitefish ageing errors and the northwestern baitfish industry. Can. Fish. Mar. Serv. Tech. Rep. No. 607.

Beaty, K.G. 1981. Hydrometeorological data for the Experimental Lakes Area, northwestern Ontario, 1969 through 1978. Can. Data Rep. Fish. Aquat. Sci. No. 285.

Cooke, G.D. 1980. Lake level drawdown as a macrophyte control technique. Water Resour. Bull. **16**: 317–322.

Fee, E.J. 1990. Computer programs for calculating *in situ* phytoplankton photosynthesis. Can. Tech. Rep. Fish. Aquat. Sci. No. 1740.

Fee, E.J., Shearer J.A., Debruyn, E.R., and Schindler, E.U. 1992. The effect of lake size on phytoplankton photosynthesis. Can. J. Fish. Aquat. Sci. **49**: 2445–2459.

Greening, H.S., and Gerritsen, J. 1987. Changes in macrophyte community structure following drought in the Okefenokee Swamp. Aquat. Bot. **28**: 113–128.

Grime, J.P. 1979. Plant strategies and vegetation processes. John Wiley and Sons, New York.

Healey, F.P., and Hendzel, L.L. 1980. Physiological indicators of nutrient deficiency in lake phytoplankton. Can. J. Fish. Aquat. Sci. **37**: 442–453.

Hecky, R.E., Campbell, P., and Hendzel, L.L. 1993. The stoichiometry of carbon, nitrogen and phosphorus in particulate matter of lakes and oceans. Limnol. Oceanogr. **38**: 709–724.

Hellsten, S., Marttunen, M., Palomaki, R., Riihimaki, J., and Alasaarela, E. 1996. Towards an ecologically based regulation practice in Finnish hydroelectric lakes. Regul. Rivers Res. Manag. **12**: 535–545.

Hutchinson, G.E. 1975. A treatise on limnology. Vol. 3. John Wiley and Sons, Toronto.

Manly, B.F.J. 1998. Randomization, bootstrap and Monte Carlo methods in biology. Chapman & Hall, London.

Naumenck, A. 1963. Die Beziehungen zwischen Zooplankton und Phytoplankton in See Erken. Symb. Bot. Ups. **17**: 1–163.

Paller, M.H. 1997. Recovery of a reservoir fish community from drawdown related impacts. N. Am. J. Fish. Manag. **17**: 726–733.

Ploskey, G.R. 1986. Management of the physical and chemical environment: effects of water-level changes on reservoir ecosystems, with implications for fisheries management. *In* Reservoir fisheries management: strategies for the 80's. *Edited by* G.E.

© 2005 NRC Canada

Hall and M.J. Van Den Avyle. American Fisheries Society, Bethesda, Md. pp. 86–97.

Quennerstedt, N. 1958. Effects of water level fluctuation on lake vegetation. Verh. Int. Ver. Theor. Angew. Limnol. **13**: 901–906.

Rorslett, B. 1989. An integrated approach to hydropower impact assessment. Hydrobiologia, **175**: 65–82.

Rorslett, B., and Johansen, S.W. 1996. Remedial measures connected with aquatic macrophytes in Norwegian regulated rivers and reservoirs. Regul. Rivers Res. Manag. **12**: 509–522.

Rott, E. 1981. Some results from phytoplankton intercalibrations. Schweiz. Z. Hydrobiol. **43**: 43–62.

SAS Institute Inc. 1999. SAS OnlineDoc®. Version 8 [computer program]. SAS Institute Inc., Cary, N.C.

Shearer, J.A. 1978. Two devices for obtaining water samples integrated over depth. Can. Fish. Mar. Serv. Tech. Rep. No. 772.

Shearer J.A., Debruyn, E.R., Declercq, D.R., Schindler, D.W., and Fee, E.J. 1985. Manual of phytoplankton primary production methodology. Can. Tech. Rep. Fish. Aquat. Sci. No. 1341.

Stainton, M.P., Capel, M.J., and Armstrong, F.A.J. 1977. The chemical analysis of fresh water. 2nd ed. Can. Fish. Mar. Serv. Misc. Spec. Publ. No. 25.

Tarver, D.P. 1980. Water fluctuation and the aquatic flora of Lake Miccosukee. J. Aquat. Plant Manag. **18**: 19–23.

Turner, M.A., Jackson, M.B., Findlay, D.L., Graham, R.W., DeBruyn, E.R., and Vandermeer, E.M. 1987. Early responses of periphyton to experimental lake acidification. Can. J. Fish. Aquat. Sci. **44**(Suppl. 1): 135–149.

Turner, M.A., Howell, E.T., Summerby, M., and Hesslein, R.H. 1991. Changes in epilithon and epiphyton associated with experimental acidification of a lake to pH 5. Limnol. Oceanog. **36**: 1390–1405.

Washington, H.G. 1984. Review: diversity, biotic and similarity indices. A review with special relevance to aquatic ecosystems. Water Res. **186**: 652–694.

Wilcox, D.A., and Meeker, J.E. 1991. Disturbance effects on aquatic vegetation in regulated and unregulated lakes in northern Minnesota. Can. J. Bot. **69**: 1542–1551.

Wile, I., Miller, G.E., Hitchin, G.G., and Yan, N.D. 1985. Species composition and biomass of the macrophyte vegetation of one acidified and two acid-sensitive lakes in Ontario. Can. Field-Nat. **99**: 308–312.

© 2005 NRC Canada

The use of moored inverted echo sounders for monitoring meso-zooplankton and fish near the ocean surface

Mark V. Trevorrow

Abstract: This study evaluates the effectiveness of a 200-kHz inverted echo sounder for monitoring the abundance and behavior of near-surface zooplankton and fish. Data from both oceanic and littoral environments are examined: first from an 81-day deployment at Ocean Station Papa (OSP) in the northeast Pacific Ocean during the spring of 1996, and second from an 8-day deployment in the southern Strait of Georgia in September 1998. The analysis combines calibrated backscatter intensity, echo-amplitude statistics, and acoustic-scattering models to produce estimates of mean scatterer size and abundance. The identity of the various scatterer classes is deduced from local net trawls and reference to previous studies. At the OSP site the dominant scatterers were found to be euphausiids, pteropods, and myctophid fishes, with mean lengths of 15, 1.5, and 28 mm, respectively. At the Strait of Georgia site three fish size classes were identified: juvenile herring with mean length near 10 cm, juvenile salmon with mean length of 20 cm, and there was weak evidence for an adult salmon class. Overall, the acoustically derived abundance estimates were in reasonable agreement with the local net trawls and results from previous studies. The usefulness of sustained monitoring over diurnal and seasonal time scales is demonstrated with the OSP zooplankton data.

Résumé : Des données provenant de milieux littoraux et océaniques permettent d'évaluer une échosonde 200 kHz inversée pour l'observation en continu de l'abondance et du comportement du zooplancton et des poissons près de la surface. Les données océaniques proviennent d'un enregistrement de 81 jours à la station océanique Papa (OSP, dans le nord-est du Pacifique) au printemps 1996 et les données littorales d'un enregistrement de 8 jours dans le sud du détroit de Géorgie en septembre 1998. L'analyse combine l'intensité calibrée de la rétro-diffusion, les statistiques de l'amplitude de l'écho et des modèles de rétro-diffusion acoustique pour générer des estimations de la taille moyenne et de l'abondance des cibles de diffusion. L'identification des diverses classes de cibles se fait par déduction à partir de récoltes locales au chalut et d'études antérieures. Au site OSP, les cibles dominantes sont les euphausiidés, les ptéropodes et les poissons myctophidés, avec des longueurs respectives moyennes de 15, 1,5 et 28 mm. Au site du détroit de Géorgie, trois classes de poissons ont pu être identifiées, les jeunes harengs avec une longueur moyenne près de 10 cm, les jeunes saumons avec une longueur moyenne de 20 cm et de faibles indices d'une classe de saumons adultes. En général, les estimations d'abondance obtenues acoustiquement sont en assez bon accord avec les résultats de pêche locale au chalut et avec les études précédentes. Les données du zooplancton du site OSP font ressortir l'intérêt qu'il y a à faire des enregistrements en continu sur des échelles temporelles journalières et saisonnières.

[Traduit par la Rédaction]

Introduction

High-frequency (>20 kHz) acoustic backscatter systems are useful tools for monitoring near-surface biological and oceanographic processes. In particular, moored inverted echo sounders (IES) have the advantages of (*i*) continuous monitoring over extended periods of time, (*ii*) relatively high spatial and temporal resolution, and (*iii*) general immunity from avoidance problems encountered with nets and in-situ optical devices. The continuous monitoring capability is particularly useful in capturing daily cycles, seasonal trends, and isolated events, which are generally impractical or expensive to monitor from vessels. Of course, these advantages must be balanced against the inherent uncertainty common to all acoustic systems in the size and species composition of the scatterers, particularly for the simple, single-frequency system discussed here. However, when combined with occasional in-situ net samples and a background knowledge of the zooplankton and fish in a given environment, calibrated echo sounders can provide a quantitative spatial–temporal bridge between the net samples. Given the recently increasing interest in oceanic monitoring networks (e.g., Project Neptune in the northeast Pacific Ocean), it is timely to consider the capabilities and limitations of these single-point acoustic monitoring systems.

The use of moored or drifting IES systems for monitoring near-surface bubble and wave processes is well established (e.g., Thorpe 1986; Vagle and Farmer 1992; Trevorrow 2003). The same IES systems are also useful for profiling abundance and behavior of meso-zooplankton and small fish in

Received 15 April 2004. Accepted 21 October 2004. Published on the NRC Research Press Web site at http://cjfas.nrc.ca on 18 May 2005.
J18073

M.V. Trevorrow. Defence R&D Canada – Atlantic, P.O. Box 1012, Dartmouth, NS B2Y 3Z7, Canada (e-mail: Mark.Trevorrow@drdc-rddc.gc.ca).

 doi: 10.1139/F05-013 © 2005 NRC Canada

both oceanic and lake environments (e.g., Lord et al. 1976; Trevorrow and Tanaka 1997; Thomson and Allen 2000). In general, analysis of IES data on zooplankton and fish utilizes methods similar to those employed with vessel-mounted systems (summarized by Greene et al. 1989; MacLennan 1990; Foote 1991). There are two general regimes for acoustic scattering, with analytical approaches tailored to each. Meso-zooplankton often occurs at sufficiently high population densities to be considered quasi-continuous scattering layers rather than isolated targets. In this regime the volumetric backscatter strength is proportional to the zooplankter type and size and number of animals per unit volume (hereinafter called abundance to distinguish it from the animal mass density). Alternatively, for the case of larger, less abundant meso-zooplankton or fish, echoes will be more intermittent and strongly dependent on the scatterer's location relative to the IES beam. In either case, when evaluated only in terms of scattering strength, data from a single-beam echo sounder cannot be used to distinguish between different scatterer sizes (e.g., copepods versus euphausiids). For crustacean zooplankton a potential solution is to utilize multiple frequencies, as demonstrated, for example, by Holliday and Pieper (1980), Napp et al. (1993), and Wiebe et al. (1997). This does not work well for fish, however, because their scattering strength is largely frequency-independent. It turns out that examination of the echo-amplitude statistics, first proposed by Clay (1983) and Stanton (1985), provides additional information on the mean scatterer-target strength (TS). TS can be converted to scatterer size through appropriate acoustic scattering models. When combined with the volumetric scattering strength, mean abundances of the various scatterer classes can be extracted.

In this study the operational effectiveness of a single 200-kHz IES in two distinct oceanic environments is evaluated. The first example consists of data taken from a March-to-May 1996 deployment at Ocean Station Papa (OSP). OSP has been the site of ongoing oceanographic and zooplankton monitoring since the late 1950s (see Fulton 1983; Waddell and McKinnell 1995; Whitney and Freeland 1999), and specific oceanographic and zooplankton data were collected during the deployment and recovery cruises in March and May 1996. The second example consists of data from a littoral environment, collected during a shorter (8-day) deployment in September 1998 in the southern Strait of Georgia (SoG) near the mouth of the Fraser River (near Vancouver, British Columbia). This study will examine the combination of volume scattering strength and echo-amplitude statistics from these two sites, thereby showing that reasonable estimates of scatterer identity, size, and abundance can be extracted using a combination of acoustic and in-situ net data.

Instrumentation and analysis methods

Description of the instrument and basic data processing

The focus of this paper is data from a single self-contained 200-kHz IES. In the first example this IES was deployed in the spring of 1996 at OSP (50°N, 145°W), situated approximately 1400 km west of Vancouver Island in the northeast subarctic Pacific Ocean. The IES was deployed at the top of a subsurface mooring at a nominal depth of 42 m in a total water depth of approximately 4100 m. At OSP the instrument operated continuously from 0130 Universal Time (UT) 1 March until 1400 UT 20 May 1996. Oceanographic and zooplankton data were collected during the deployment and recovery cruises (February and May 1996) on board the *J.P. Tully*. Two years later the same IES was deployed in the southern SoG approximately 3.5 km north of the mouth of the Fraser River (49°08.33′N, 123°18.16′W). It was moored at 48 m depth in an overall water depth of 75 m and operated continuously from 1800 Pacific Daylight Time (PDT) on 8 September until 1430 on 16 September 1998. At the SoG site, reference conductivity–temperature–depth and fishery trawl data were collected by the vessels *Vector* and *W.E. Ricker*.

This 200-kHz IES was a prototype instrument developed at the Institute of Ocean Sciences, Sidney, British Columbia. It was designed to be a simple, low-power, self-contained system capable of deployments up to 1 year in length. The same instrument was used for studies of internal solitary waves near the Oregon coast and near-surface bubbles at OSP (see Trevorrow 1998, 2003). A very similar instrument was used by Thomson and Allen (2000) to image the nocturnal migration of zooplankton near Vancouver Island, and an updated version is described by Lemon et al. (2001). The electronics and batteries were contained in a 25 cm diameter by 80 cm long cylindrical pressure housing, supported either by streamlined syntactic foam flotation at OSP or by four 33 cm diameter plastic floats at the SoG site (Fig. 1). The 200-kHz transducer was mounted externally on the top, oriented vertically upward. The transducer beam width (total angle to –3 dB) was 4.6°. In both cases the IES operated continuously, transmitting a pulse of 0.5 ms duration at 1-s intervals. Echo amplitude was acquired with 8-bit resolution (48 dB dynamic range) in 200 cm × 21.5 cm depth bins, spanning a 10–53 m (OSP) or 15–58 m (SoG) upward range, in both cases including echoes from the sea surface. The raw IES data were stored internally on two standard PC harddrives with a total capacity of approximately 1 gigabytes. To reduce overall data-storage requirements in the longer OSP deployment, data from three successive pings were averaged. This prototype IES had no time-varying gain, which put some limits on detection of small zooplankton at greater range. In both deployments the receiver gain was configured as a compromise to resolve backscattering from both meso-zooplankton and near-surface bubble plumes, thus its dynamic range spanned volumetric backscatter levels between roughly –85 and –35 dB (re 1 m^{-1}) near the surface.

Quantitatively, the raw IES amplitude, A, can be converted to volumetric backscatter strength (S_v, dB re 1 m^{-1}) versus range (upward), r, using the standard sonar equation (e.g., Medwin and Clay 1998), i.e.,

$$S_v(r) = 20\log_{10}[A(r)] + K + 40\log_{10}(r) + 2\alpha_v r - 10\log_{10}[U(r)] \quad (1)$$

where K is the calibration coefficient, r is the range (= ½ct, where c is sound speed and t is time after transmission), α_v is acoustic absorption in seawater, and $U(r)$ is the insonified volume. Note that S_v is the deciBel equivalent of the volumetric backscatter cross section, s_v (m^{-1}), and any arithmetic operations (i.e., averaging) are performed on the cross-section data. The calibration coefficient, K, includes transmit power

© 2005 NRC Canada

Fig. 1. Photograph of the inverted echo sounder at the ocean surface during deployment at the Strait of Georgia site in September 1998. The 200-kHz transducer is the circular disk on the top, with the electronics and batteries contained within the 25 cm diameter by 80 cm long cylindrical pressure housing.

level, transducer sensitivity, preamplifier gains, and A/D conversion factors. Acoustic absorption in seawater is frequency- and environment-dependent, and for the typical water conditions at OSP has a value of 0.044 dB·m^{-1} (Francois and Garrison 1982), whereas under SoG conditions the absorption was 0.052 dB·m^{-1}. In terms of the equivalent solid angle of the transducer, ϕ (steradians), and the pulse duration, τ (= 500 μs), the insonified volume is given by

$$(2) \qquad V(r) = 1/3\,\phi[(r + 1/4\,c\tau)^3 - (r - 1/4\,c\tau)^3]$$

The equivalent solid angle of the transducer is related to the –3 dB total beam angle, θ_{3dB}, by the relation $\phi = 2\pi[1 - \cos(\frac{1}{2}\theta_{3dB})]$. For this IES the insonified volume increased from 0.2 m^3 at 10 m range to 3.5 m^3 at 45 m (the nominal ocean surface), and is thus small compared with the expected spatial scales of zooplankton and fish patchiness under study.

For the case of scattering from acoustically resolvable, isolated fish, it is customary to recast eq. 1 in terms of TS (dB re 1 m^2), i.e.,

$$(3) \qquad TS(r) = 20\log_{10}[A(r)] + K + 40\log_{10}[r] + 2\alpha_w r + BDL(\theta)$$

where BDL(θ) is the beam deviation loss, which for a circular piston transducer such as that used here is only a function of angle θ from the transducer axis. For this single-beam sonar it is impossible to determine θ for a particular target, thus the isolated-target analysis will use a pseudo-TS (pTS) quantity, defined by eq. 3 with BDL = 0. As discussed below, statistical methods can be used to compensate for the beam-pattern effect to produce averaged TS estimates.

The IES was calibrated using the backscatter target strength of tungsten-carbide spheres following methods outlined in Vagle et al. (1996). Given the calibrations and geometric variations in volume scattering strength, both the noise threshold and clipping levels were range-dependent. For this instrument the equivalent noise amplitude was found to be approximately 0.5 digital counts, corresponding to a S_v threshold increasing from –100 dB (re 1 m^{-1}) at 10 m range to –85 dB at 45 m range (near the ocean surface). Thus, weaker zooplankton scattering near the ocean surface will be lost in the noise. Similarly, the A/D clipping level of 255 counts corresponded to S_v from –43 dB at 10 m range to –28 dB at the ocean surface. This implies that features with higher volumetric cross section, such as dense fish schools or bubble plumes near the ocean surface, will be underestimated.

© 2005 NRC Canada

Echo-amplitude statistics

In addition to generating profiles of backscatter strength, supplemental information on the size and likely identity of the scatterers can be inferred from analysis of the echo-amplitude statistics. Specifically, this involves analyzing echo-amplitude probability density functions (PDFs), as described by Clay (1983), MacLennan (1990), and Wiebe et al. (1990). From observations of backscattering from a single fish or zooplankter, it has been found that echo amplitudes conform to Rician PDFs, specifically of the form

$$(4) \qquad w_R(e) = \frac{2e(1+\gamma)}{\sigma} \cdot \exp\left(-\frac{(1+\gamma)e^2 + \gamma\sigma}{\sigma}\right) \cdot I_0(q)$$

with $q = 2e \cdot \sigma^{-1/2} \cdot [\gamma(1+\gamma)]^{1/2}$, where e is the echo amplitude (the square root of either s_v or the cross-section equivalent of pTS), γ is the ratio of coherent to incoherent backscattered energy, σ is the mean backscatter cross section (units of m^2), and I_0 is the modified Bessel function. In this study all PDFs are normalized so that the integral over all echo amplitudes is 1. Note that $\gamma = 0$ corresponds to the well-known Rayleigh distribution. Clay and Heist (1984) and Wiebe et al. (1990) reported γ values for natural fish populations in the range 2–12, with larger and more active fish yielding smaller γ values. Dahl and Mathisen (1983) reported measurements for adult salmon conforming to Rayleigh distributions, i.e., with γ near 0.

There are two limiting cases for in-situ bioscattering with a single-beam IES: (1) single, well-resolved targets only occasionally found within the insonified volume (isolated scatterers), and (2) multiple scatterers with overlapping echoes within the insonified volume (overlapping-echo regime). These two limits exhibit dramatically different PDF shapes. For the case of the isolated scatterer, the echo-amplitude PDF has a maximum near zero and decreases rapidly with increasing echo amplitude. This is a result of the fact that with a single-beam sounder, a randomly distributed scatterer will give the majority of echoes away from the beam axis, and thus will have lower echo amplitude because of the BDL term in eq. 3. Mathematically, this isolated-scatterer PDF is the convolution of the Rician PDF for a single scatterer and the PDF due to beam-pattern effects, which takes the form

$$(5) \qquad w_E(e) = \int_0^1 \frac{w_T(\beta) \cdot w_R(e/\beta)}{\beta} \cdot d\beta$$

where $w_T(\beta)$ is the PDF for observing an amplitude β for scatterers randomly distributed in the transducer beam. Ehrenberg et al. (1984) determined an empirical relation for $w_T(\beta)$ for circular-piston transducers of radius r_t with the form

$$(6) \qquad w_T(\beta) = \frac{b_3}{(kr_t)^2(\beta + b_4)^{b_5}}$$

where $b_3 = 2.03$, $b_4 = 0.01$, and $b_5 = 0.83$ for $\beta > 0.005$. Thus, predicted PDFs can be generated through eqs. 4–6, given only two scatterer parameters, σ and γ. Observational PDFs are generated from pTS estimates using $e = e_{pTS} = 10^{pTS/20}$. Then a least-squares criterion is used to find best fit estimates for a particular data set. Using acoustic scattering models for various zooplankton and fishes, these best fit parameters (particularly σ) can be used to identify scatterer type and size. Note that it is entirely possible for the source PDF to be composed of more than one scatterer type, such that $w_R(e)$ in eq. 4 would be a normalized sum of multiple Rician replicas, i.e., with multiple σ, γ pairs. This adds to the complexity of the least-squares fitting process; however, in practice the PDF for a particular scatterer type will dominate over differing echo-amplitude ranges.

For the case of overlapping echoes, Stanton (1985) derived the PDF of the maximal echo amplitude, e_m, within a range bin using extremal statistics as

$$(7) \qquad p(e_m) = (\alpha e_m / E_{ms}) \cdot \exp(-e_m^2/2E_{ms}) \times [1 - \exp(-e_m^2/2E_{ms})]^{(\alpha-1)}$$

where E_{ms} is the mean-square echo amplitude and α is a shape parameter dependent on both the number of independent echo estimates within the range bin and the scatterer abundance relative to the insonified volume. In this case we will use $e_m = \max[s_v^{1/2}]$ within a given range bin (≈ a few metres in depth). For overlapping echoes, this PDF shape has a maximum at some finite (non-zero) echo amplitude. Non-overlapping echo regimes give a maximum PDF near zero, with $\alpha < 1$. Note that $\alpha = 1$ corresponds to a Rayleigh distribution, which is the expected distribution near the critical scatterer density. The transition between the two limits defines a critical abundance where there is (on average) one scatterer per insonified volume, i.e., at an abundance given by the inverse of the insonified volume, U, given in eq. 3 above. By searching for data PDFs at the transition between isolated- and overlapping-echo cases, the averaged scatterer TS can be extracted from the ratio of averaged s_v to the critical abundance at that point. The value of α from a least-squares fit of eq. 7 to the observed PDF turns out to be a useful quantifier of the relative criticality of the scatterers (Trevorrow and Tanaka 1997).

Zooplankton and fish scattering models

For zooplankton and fish, the link between acoustic backscatter and size–abundance distributions is provided by an acoustic-scattering model for a particular class of animals. A number of different models have been proposed in the literature (e.g., Johnson 1977, 1978; Holliday and Pieper 1980; Greene et al. 1989) that differ in applicability depending on acoustic frequency, species, size, and abundance. For this particular IES at OSP, the most relevant for crustacean meso-zooplankton is a size- and orientation-averaged model recommended by Stanton and Chu (2000), based on earlier models by Stanton et al. (1993). The motivation for using this model is that the acoustic backscatter for an individual zooplankter generally shows strong sensitivity to both size and orientation (i.e., swimming angle) relative to the beam, and generally a natural population exhibits distributions of both size and orientation. This model is appropriate where the combination of insonified volume and abundance creates echoes that have contributions from a large number of animals. For some larger zooplankters this is only marginally satisfied for this IES, as the insonified volumes and typical animal abundances are both of order 1. However, when dealing with ping-averaged quantities, as is necessary for the use of statistical analyses to extract averaged backscatter cross

© 2005 NRC Canada

Table 1. Summary of acoustically significant epipelagic and nocturnal migratory zooplankton species at Ocean Station Papa.

Class and species	Length (mm)	avTS at 200 kHz (dB re 1 m^2)	Typical abundance (m^{-3})		Expected S_v in May 1996 (dB re 1 m^{-1})
Euphausiids	15.0±3.0	–79.8	0.1–5.0		–90 to –73
Euphausia pacifica					
Thysanoessa longipes					
Thysanoessa spinifera					
Amphipods	6.0±2.0	–89.7	1.0–10		–90 to –80
Parathemisto pacifica					
Cyphocaris challengeri					
Pteropods	1.5±0.5	–76.0	0.5–2.0		–79 to –73
Limacina helicina					
Copepods			March 1996	May 1996	
Eucalanus bungii	5.5±1.0	–91.9	<1	1–5	–92 to –85
Neocalanus plumchrus	4.5±0.4	–95.6	<1	10–150	–85 to –74
Neocalanus flemingeri	4.2±0.3	–96.9	<1	5–30	–90 to –82
Metridia pacifica	2.2±0.2	–110.0	<1	1–50	–110 to –93
Oithona similis	1.0±0.2	–126.0	<50	100–1000	–106 to –96

Note: Lengths are given as the typical mean ± standard deviation of adult classes (includes C5 for copepods). Copepod abundance data are taken from Goldblatt et al. (1999), with other species' data compiled from Marlowe and Miller (1975), Mackas et al. (1993), and Waddell and McKinnell (1995). Average target strength (avTS) is calculated from a size- and orientation-averaged fluid-cylinder model assuming a horizontal aspect with 30° standard deviation. The pteropod TS is taken from Stanton et al. (1998). Modeled aspect ratios are taken as 15, 10, and 6 for euphausiids, amphipods, and copepods, respectively.

sections, it then becomes appropriate to use population-averaged models.

The specific model used here assumes that the larger crustacean zooplankton (amphipods and euphausiids) to be bent fluid cylinders with radius of curvature three times body length, a specific length to radius ratio that is dependent on species, a Gaussian length distribution (characterized by a mean and standard deviation), and a Gaussian orientation-angle distribution. Stanton et al. (1993) showed that this averaged model is insensitive to the amount of curvature, so only a nominal value is assumed. In the absence of any detailed in-situ information, a nominal orientation distribution is used for the euphausiids and amphipods, specifically using zero mean angle (horizontal) with a 30° standard deviation. For copepods a similar straight fluid-cylinder model with uniform angular distribution is assumed. For crustaceans the sound-speed and density contrasts in this fluid model are assumed to be 1.025 and 1.045. Given all these assumptions in combination with specific species-size data from net trawls, the averaged TS (avTS, units of dB re 1 m^2) per animal can be calculated using the model outlined in Stanton and Chu (2000).

A summary of the zooplankton species expected to be acoustically significant in the upper 30 m at OSP is provided (Table 1). Note that Goldblatt et al. (1999) present detailed copepod data from net samples taken at OSP on 1 March and 20 May 1996; however, they did not report abundance data on other species. The other major source is a database of net-sample results from the 1956–1980 weather-ship program reported by Waddell and McKinnell (1995). This table includes species that are normally resident in the epipelagic zone (*Oithona similis* and *Eucalanus bungii*) and those that exhibit diurnal vertical migration. It is appropriate to include *Neocalanus plumchrus* and *Neocalanus flemingeri* in this context, as they generally do not begin the deep seasonal migration (diapause) until late May, and generally exhibit only a minimal nocturnal migration (Mackas et al. 1993). The large copepods *Neocalanus cristatus* and *E. bungii* are generally confined to depths greater than 50 m at OSP (Mackas et al. 1993), although low abundances of *E. bungii* have been found in the upper 25 m (Marlowe and Miller 1975).

Also present and exhibiting nocturnal migration were two species of chaetognath (*Parasagitta elegans* and *Eukrohnia hamata*; see Goldblatt et al. 1999); however, these gelatinous-bodied animals have negligible acoustic TS. The avTS estimates are calculated using the above-described model, with the exception of the planktonic pteropod *Limacina helicina*. Stanton et al. (1998) showed that hard-shelled pteropods exhibit different scattering characteristics than the fluid-like crustaceans. In terms of avTS the pteropod has the highest value, followed closely by the euphausiids. The copepod avTS values are almost negligible by comparison, and because of the low abundance of adults in March 1996, their contribution to the observed S_v would have been negligible. Owing to their relatively high abundance in May 1996, only *N. plumchrus* and *N. flemingeri* approach the larger euphausiids and pteropods in their potential scattering contribution. The predicted S_v from the other copepod species would be roughly equal to or less than the instrumental noise level, making them largely undetectable with this IES.

With a single-frequency echo sounder it is impossible to separate these different species on the basis of volume scatter strength alone. One potential analytical approach would be to have detailed knowledge of the relative species composition, for example through colocated net trawls, and then to assume that the species composition remains fixed in time. The long IES time series could then be used to monitor changes in total abundance, related to total biomass under this assumption. However, it is unreasonable to expect that over a 90-day period covering the spring phytoplankton bloom, the species and size mixture would remain constant. Furthermore, from this particular deployment, detailed net-sample

© 2005 NRC Canada

data from the February and May 1996 cruises were only available for the copepods. An alternative approach would be to utilize scattering statistics, which can quantitatively separate different scattering classes. For example, since the euphausiids typically have near-critical abundances (one animal per insonified volume) for the IES beam, one would expect them to be separable from the supercritical copepod scattering when examined on an echo-amplitude statistical basis.

Similarly, estimating fish size and abundance from a single-beam echo sounder relies on the combination of volume scatter strength and echo-amplitude statistics. In this context robust and general fish scattering models are desired because the fish identity and size are only approximately known. For the generic fish observed with this IES, the simplest approach is to use a general, empirical formulation for fish TS as given by Love (1977),

$$(8) \qquad \mathrm{TS}(\mathrm{dB\ re\ 1\ m^2}) = 10\log_{10}[(4\pi)^{-1}\cdot\lambda^2\cdot b_1(L/\lambda)^{b_2}]$$

where λ is the acoustic wavelength (m), L is the overall fish length (m), and $b_1 = 0.048$ and $b_2 = 1.90$ (constants for ventral incidence). This expression is valid in the range $1 < L/\lambda < 100$, which sets the lower size limit for a 200-kHz sonar at 7.4 mm. Note that this relation is very nearly frequency-independent (i.e., exponent b_2 is near 2), so that extracting size information from multifrequency intensity would be essentially impossible. Similar empirical relations exist for other common fish species. For example, Foote (1987) presented an empirical relation for Atlantic herring (*Clupea harengus*) for 38-kHz dorsal-incidence echo sounders of the form

$$(9) \qquad \mathrm{TS}(\mathrm{dB}) = 20\log_{10}(L_{\mathrm{cm}}) - 71.9$$

where L_{cm} is the fish length in centimetres. We shall assume this relation to be applicable in ventral incidence at 200 kHz. A measure of the variability in TS among fish species can be seen from a comparison of these two relations: e.g., for a 20 cm long fish at 38 kHz, the eq. 8 estimate is –38.9 dB, while the eq. 9 estimate is –45.9 dB. This significant difference is likely due to the fact that herring have a smaller than average swim bladder. Both of these relations will be used to estimate lengths of myctophids, herring, and salmonids extracted from echo-amplitude PDF analysis both at OSP and in southern SoG.

Examples of echo-sounder results

Meso-zooplankton and myctophids at OSP

The basic IES data consist of a continuous time series of volume scatter strength versus range profiles looking upward toward the ocean surface. The first stage of analysis involved detecting the range to the ocean surface, which is then used as reference for further analysis. Zedel (1994) discusses techniques for detecting the ocean surface using echo sounders. At OSP the raw profiles were averaged into 3-s ensembles, smoothing out the effects of short waves but leaving relatively large excursions (up to ±2 m) in surface height due to ocean swell. By remapping the volume-scatter data to align with the detected surface, swell-wave displacements were removed. This allows ensemble averaging and display in depth versus time coordinates, as shown in Fig. 2, with an example from 6 March. This 16-h echogram is typical of the late-winter (March) nocturnal migration events recorded by this IES. The echogram shows a relatively low scattering level during daylight hours (i.e., before minute 120 (= 0400 UT = 1900 local) and after minute 840 (= 1600 UT = 0700 local)), with a dramatic increase in scattering strength in between. Within this nocturnal migratory scattering zone there appears to be a difference in texture between the near-surface (~8 m) and deeper layers, the scattering near 30 m depth being more *granular* and the near-surface scattering *smoother*. As will be shown below, this manifests itself as a distinct difference in echo-amplitude PDFs. Examining the upward and downward migration events in more detail (on a 3-s basis), a systematic vertical displacement of the upper boundary of the scattering layer was observed. Near sunset on 6 March there was an upward migration of 26 m over a 24-min period starting at 0414 UT, corresponding to an average speed of 1.8 cm·s^{-1}. At dawn (starting at 1518 UT) the averaged downward migration speed was 2.4 cm·s^{-1}. These migration speeds (near 2 cm·s^{-1}) were consistent over the entire 80-day data set. The strong near-surface scattering structures extending to a depth of 10 m in the latter half of Fig. 2 are plumes of small air bubbles injected by breaking surface waves.

The contrast between late-afternoon and nocturnal depth profiles is examined (Fig. 3). The daytime profile exhibits a low but measurable scattering strength, near –85 to –87 dB (re 1 m^{-1}), which approaches the noise threshold in the upper 5 m. In contrast, the nocturnal scattering profiles show a S_v that is approximately 10–12 dB higher, averaging approximately –77 dB from 5–30 m depth. The early-evening profile (0600 UT) shows a peak near 10 m depth; however, this peak appears to have migrated downward to near 25–30 m depth by 0800 UT. In both nocturnal profiles there is a definite avoidance of the upper 5 m. Note that at depths >15 m (denoted herein as the deeper layer) the nocturnal profiles show a *lumpy* character that is indicative of an isolated-scatterer regime, in contrast to the smoothness of the upper 15 m.

Examination of the echo-amplitude PDFs highlights differences in scattering character between the near-surface and deeper layers (Fig. 4). In both cases the probability densities span 2–3 orders of magnitude; however, the deeper layer shows a much wider spread of echo amplitudes. The near-surface PDF (Fig. 4*a*) seems to be well modeled by the strongly overlapping ($\alpha = 13.8$) extremal PDF. The excess scattering for $e_m \geq 3.6 \times 10^{-4}\cdot\mathrm{m}^{-1/2}$ comprises only 0.65% of the total. The fitted E_{ms} ($4.3 \times 10^{-9}\cdot\mathrm{m}^{-1}$) multiplied by the insonified volume at that range (2.5 m^3) gives an estimate of the average backscatter cross section of the target, specifically 1.06×10^{-8} m^2 or TS = –79.7 dB. This corresponds closely to the expected avTS of adult euphausiids (Table 1). The ping-averaged S_v in this depth bin (–77.5 dB re 1 m^{-1}) divided by this averaged euphausiid TS yields an average abundance of 1.7·m^{-3}, entirely consistent with our a priori expectations. As a check, the average number of scatterers per insonified volume (1.7·m^{-3} multiplied by 2.5 m^3) is 4.2, satisfying the assumption of overlapping scatterers.

In the deeper layer (Fig. 4*b*) the scattering statistics are more complicated, with a significantly higher echo-

© 2005 NRC Canada

Fig. 2. Volume scatter strength versus depth and time echogram at Ocean Station Papa (OSP) starting at 0200 UT on 6 March 1996. Depth profiles are referenced to the detected surface height within each ensemble (3 s) and then averaged over 40 successive ensembles (2 min).

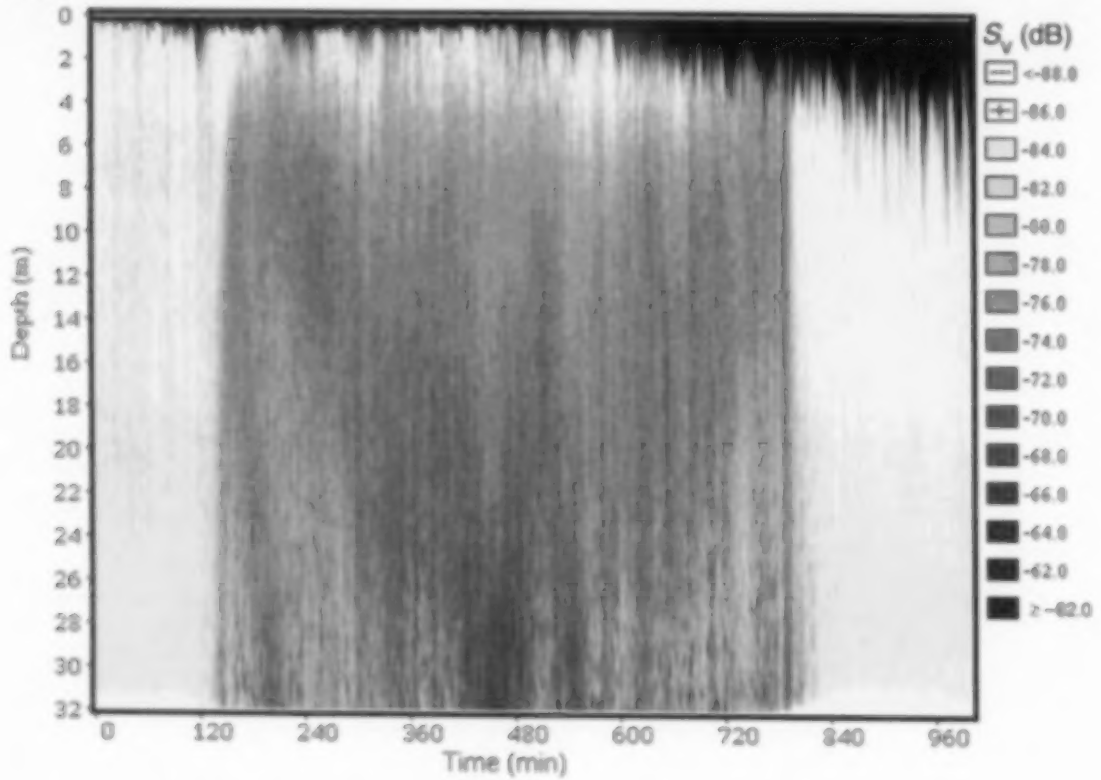

amplitude portion of the observed PDF unaccounted for by the single-scatterer model. In this case echo amplitudes $\geq 5 \times 10^{-4}$·m$^{-1/2}$ ($S_v \geq -66.0$ dB re 1 m^{-1}) comprised 9.8% of the total. This can be taken as a threshold dividing the two scatterer types, such that conditionally averaging over $S_v <$ −66.0 dB would exclude bias due to the secondary scatterer. Similar to the analysis of the near-surface layer, the best fit E_{ms} for the dominant scatterer corresponds to an average target cross section of 9.6×10^{-9} m^2 or TS = −80.2 dB, again suggesting that the scatterers are euphausiids, although they are possibly slightly smaller in mean size than those in the surface layer. Independently, the fitted α parameter from eq. 7 (= 1.12) shows near-critical density scattering, i.e., with an abundance equal to the reciprocal of the insonified volume at this range, or 3.6·m^{-3}. Dividing the conditionally averaged S_v in this depth interval (−74.8 dB re 1 m^{-1}) by this abundance yields an averaged TS of −80.4 dB, consistent with the previous estimates.

Looking more closely at this isolated-scatterer regime in the deeper layer, the echo-amplitude PDF based on pTS again shows a division into at least two distinct scatterer types (Fig. 5). In this analysis, echo amplitudes $<3.0 \times 10^{-4}$ m (pTS < −70.5 dB re 1 m^2) seem to be reasonably modeled by a combination of euphausiid and pteropod scattering. The pteropod contribution has been reduced to 50% of that of the euphausiids, putting their estimated abundance near 1.8·m^{-3}, consistent with the a priori expectation from Table 1. The larger, low-abundance scatterer has a fitted backscatter cross section of 5.0×10^{-7} m^2, or TS = −63.0 dB, much larger than expected from any known meso-zooplankton. The most likely source of this scattering is small myctophid fishes, of which the most abundant species known to inhabit the subarctic northeast Pacific Ocean is the northern lampfish, *Stenobrachius leucopsarus* (Pearcy and Laurs 1966; Norcross et al. 2003). These myctophids are commonly 20–60 mm in length depending on age, with yearling fish of 25 mm length the most abundant in late-winter trawls (Smoker and Pearcy 1970). Additionally, zooplankton trawls at OSP reported by Waddell and McKinnell (1995) showed occasional catches of larval fish (species not reported) of length 3–28 mm, with mean abundance near 0.09·m^{-3}. Using eq. 8 for fish of these sizes produces TS estimates in the range −58.5 to −49.5 dB, which are significantly larger than our present acoustic estimate. However, there is some evidence that myctophid swim bladders are reduced or atrophied (Butler and Pearcy 1972), and thus myctophids should have a reduced TS compared with other fish. If a TS versus length relation similar to eq. 9 for herring is used, the estimated TS for these myctophids would be in the range −65.9 to −56.3 dB, with the best fit TS corresponding to a 28 mm long fish. This is consistent with the present acoustic estimates.

The data and best fit Rician PDF in the myctophid scattering region appear to dominate above an echo-amplitude threshold of 3.5×10^{-4} m (TS = −69.1 dB; see Fig. 5), and

© 2005 NRC Canada

Fig. 3. Comparison of 30-min averaged volume scatter strength versus depth profiles before and during the zooplankton nocturnal migration at OSP on 6 March 1996 at 0200–0230 UT (●), 0600–0630 UT (□), and 0800–0830 UT (○) (minutes 0–30, 240–270, and 360–390 in Fig. 2); the broken line indicates instrumental noise level.

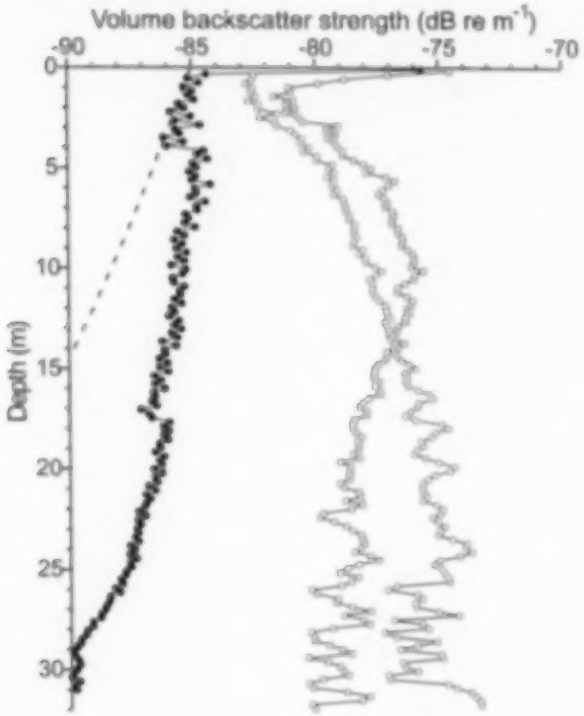

so echo integration above this threshold could be used to estimate myctophid abundance. However, this estimate would be biased, owing to the fact that the acoustically observable fraction ($e_{pTS} > 3.5 \times 10^{-4}$ m) represents only 22% of the total myctophid PDF. Alternatively, myctophid abundance can be estimated as a fraction of the total volume scattering using relative areas under the PDF curves. In this example the area under the observed PDF greater than this myctophid threshold is 9.2×10^{-3} (0.92%), with a similar area (0.88%) under the best fit Rician PDF. Thus, equating acoustic observation probability with actual abundance, the myctophid abundance can be taken as 0.9% of the euphausiid abundance (3.5·m^{-3} from above), or roughly 0.03·m^{-3}. As a consistency check, the sum of the volumetric scattering (i.e., the product of abundance and backscatter cross section) from the euphausiids and myctophids equals the simply averaged s_v in this depth region; specifically, 3.5·m^{-3} × 9.6×10^{-9}·m^2 + 0.03·m^{-3} × 5.0×10^{-7}·m^2 = 4.9×10^{-8}·m^{-1} (–73.1 dB), in agreement with the time- and range-averaged S_v, –72.7 dB.

A useful feature of a moored IES is its ability to monitor with high temporal resolution over extended periods of time. At OSP this capability can be used to monitor seasonal changes in the properties of the nocturnal migration (Fig. 6). This time series was computed by averaging s_v over a range of 10–20 m (nominally 22–32 m depth) and 10-min time intervals over the entire 80-day deployment. Range averaging

Fig. 4. Comparison of observed and model extremal probability density functions (PDFs) taken at 0600–1100 UT on 6 March 1996 at OSP from (*a*) the near-surface zone (6–8 m depth) and (*b*) the deeper zone (29–32 m depth). The solid line shows the best fit extremal PDF. In *a*, α = 13.8, $E_{rms} = 4.3 \times 10^{-9}$·m^{-1}, and in *b*, α = 1.12, $E_{rms} = 3.5 \times 10^{-6}$·m^{-1}. The echo-amplitude bin width is 5×10^{-5}·m$^{-1/2}$.

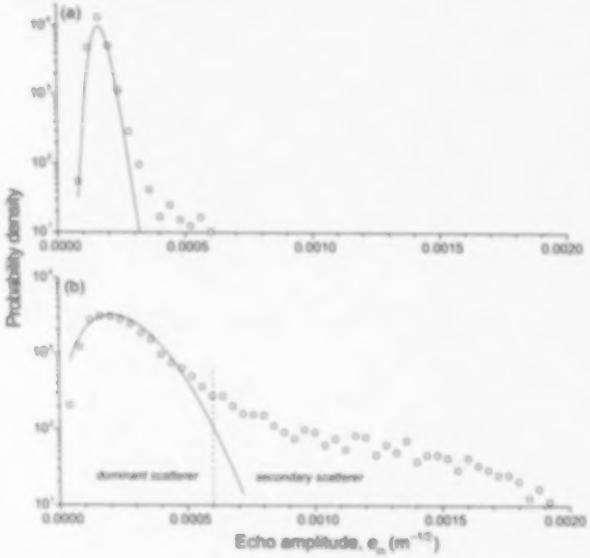

was performed only for the lower layer to avoid contamination from episodes of deep bubble injection. One immediately apparent change between March and May is a shortening of the nocturnal migration period due to the increasing duration of daylight. For example, on 1 March the nocturnal migration occurred between 0415 and 1540 UT, or over an interval of 11.4 h. By 16 May this nocturnal migration period was reduced to 0615–1315 UT, i.e., over an interval of 7.0 h. It appears that a S_v threshold of –85 dB (re 1 m^{-1}) would generally separate the diel- and nocturnal-migration periods, with occasional exceptions due to low migration abundances (e.g., year days 64 and 65). Another feature of the daily migrations is a scattering-strength peak coincident with the upward and downward migration events, presumably due to meso-zooplankton headed for the near-surface layer (<15 m depth) passing through the 22–32 m depth averaging zone. These peaks are more pronounced (S_v up to –71 dB) later in the year, suggesting that near-surface nocturnal scattering might be stronger later in the spring. Overall, there does not appear to be a clear seasonal trend in the mean nocturnal scattering strength, but rather a day-to-day fluctuation between roughly –84 and –76 dB. There appears to be a modest increase in daytime background scattering, from roughly –88 dB in March to near –85 dB in May.

It is useful to contrast the detailed scattering strength and statistics between the two ends of the OSP time series, with similarly analyzed results from 18 May (shown in Figs. 7, 8, and 9). The data from 18 May were selected because they are typical of the nocturnal migrations observed in May. Examination of the 30-min averaged profiles on 18 May

© 2005 NRC Canada

Fig. 5. Comparison of observed and Rician PDFs for scattering at 29–32 m depth at 0600–1100 UT on 6 March 1996 at OSP. Model Rician PDFs were calculated using eqs. 4–6 fitted to different regions of the observed PDF. The three model PDFs correspond to expectations for euphausiids (solid line, $\gamma = 0.0$, $\sigma = 1.2 \times 10^{-6}$ m^2, × 1), pteropods (broken line, $\gamma = 2.0$, $\sigma = 3.0 \times 10^{-8}$ m^2, × 0.5), and myctophids (~20 mm length, dotted line, $\gamma = 6.0$, $\sigma = 5.0 \times 10^{-7}$ m^2, × 0.04). The echo-amplitude bin width is 2×10^{-5} m.

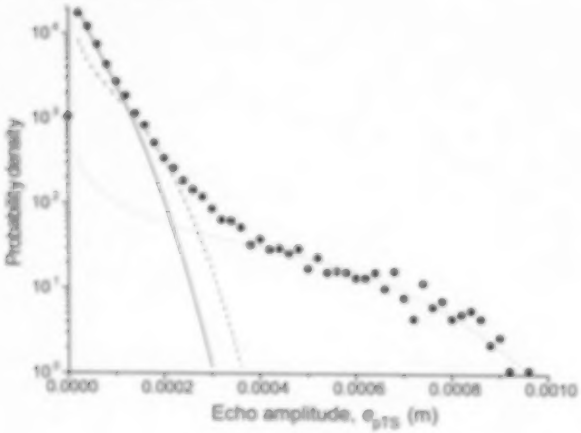

Fig. 6. Averaged volume scatter strength versus time for two 10-day periods: (*a*) late winter, 1–11 March, and (*b*) late spring, 6–16 May 1996. Volumetric backscatter cross-section data are averaged over 22–32 m depth and 10-min time intervals.

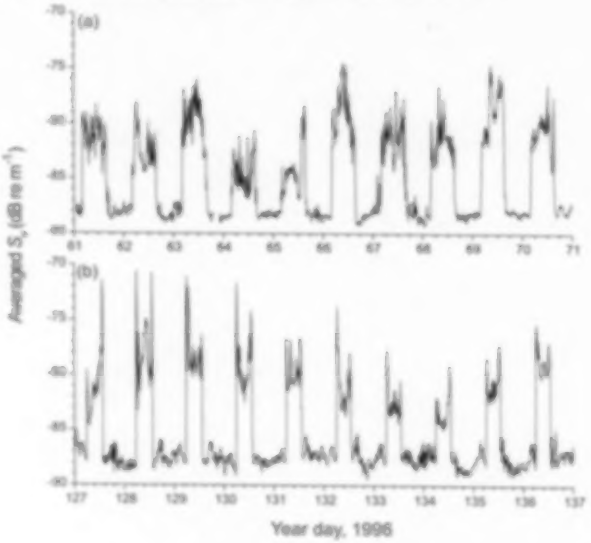

(Fig. 7) shows that there are two major differences from those in March. Firstly, the late-afternoon background scattering shows a stronger S_v (roughly 2–3 dB higher than that shown in Fig. 3), especially at depths >20 m. Secondly, scattering within the near-surface (3–10 m) layer is significantly stronger (approximately 3–5 dB higher) than that observed in the March profiles. In particular, in the 1130 UT profile (Fig. 7), note the strong scattering peak at 3–7 m depth. This near-surface peak ends at the bottom of the bubble-plume zone in the upper 2–3 m.

The echo-amplitude statistics for 18 May tell a similar story to those for 6 March. The maximal echo-amplitude PDF again shows a single-scatterer type in the near-surface layer (Fig. 8*a*), although slightly larger in mean-square scatterer amplitude with a lower degree of echo overlap ($\alpha = 4.0$ vs. 13.8 on 6 March). The E_{ms} of 1.2×10^{-8} m^{-1} corresponds to an averaged scatterer TS of –75.3 dB. With this mean TS, the averaged S_v of –73.0 dB at 5–8 m depth corresponds to an abundance of 2.1 m^{-3}. A partial explanation for this increase in TS is that the euphausiids and pteropods thought to make up this near-surface scattering layer have grown in size, or perhaps include fewer smaller or juvenile sizes. However, even a dramatic increase in mean euphausiid length from 15 to 20 mm, increasing avTS from –79.8 to –76.7 dB, cannot account entirely for this change. Another plausible explanation is an increase in the relative abundance of pteropods. In the lower layer the maximal echo-amplitude PDF (Fig. 8*b*) shows nearly complete dominance of isolated echo scattering ($\alpha = 0.38 < 1$), with no clear evidence for a smaller, dominant scatterer as seen in the 6 March data at this depth.

Looking at the echo-amplitude PDF based on pTS in this lower layer (Fig. 9) reveals a similar two-scatterer scenario. In this case echo amplitudes < 1.8×10^{-4} m (pTS < –74.9 dB re 1 m^2) are reasonably modeled by the smaller, dominant scatterer. In this analysis the dominant scatterer has a fitted backscatter cross section of 2.0×10^{-8} m^2, or TS = –77.0 dB, suggesting that the scatterers are probably a euphausiid–pteropod mixture similar to that in the upper layer. However, because the volumetric scattering now contains significant contributions from the larger, secondary scatterer, abundance estimates based on simply averaged s_v will be biased. This can be remedied by computing a conditionally averaged s_v. From previous extremal PDF analyses it was found that a S_v threshold of –66 dB (re 1 m^{-1}) separated the dominant- and secondary-scatterer contributions. At these depths (29–32 m) the conditionally averaged S_v was –77.7 dB. Using the dominant-scatterer TS estimated above, the estimated abundance of the euphausiid–pteropod mixture is thus 0.85 m^{-3}. This is much less than the critical-scatterer density at this range, in accordance with the implicit assumption of isolated scattering. The larger, secondary scatterer has a fitted backscatter cross section of 4.5×10^{-7} m^2, or TS = –63.5 dB, very similar to the 6 March result for myctophid fishes. However, the myctophids now contribute more strongly to the scattering. The total area under the data PDF for echo amplitudes $\geq 2.0 \times 10^{-4}$ m is 0.101, implying a 10% contribution to the total volumetric scattering, in contrast to the 0.9% contribution found at similar depths on 6 March. This implies that the estimated myctophid abundance is 0.09 m^{-3}, approximately three times higher than on 6 March. Again, a consistency check on the combined volumetric scattering from these two scatterer types yields an estimated S_v of –72.4 dB, very close to the simple range and time average in this zone.

Fish in the southern SoG

In contrast to the situation at OSP, very little evidence of zooplankton scattering was observed during the SoG deployment. It is probable that the mooring location was too close

© 2005 NRC Canada

Fig. 7. Comparison of 30-min averaged volume scatter strength versus depth profiles before and during the zooplankton nocturnal migration at OSP on 18 May 1996 at 0430–0500 UT (●), 0700–0730 UT (□), and 1130–1200 UT (○); the broken line indicates instrumental noise level. Up-migration on this day occurred near 0610 UT.

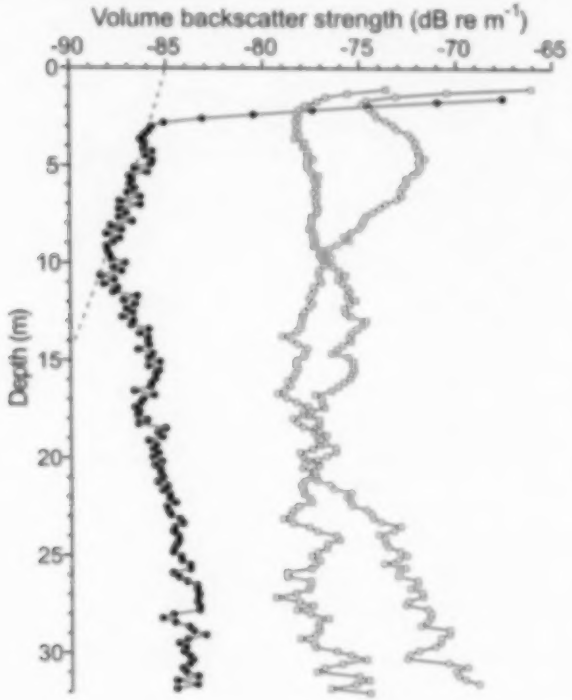

to shore (total water depth only 75 m) to sample the true pelagic zone, where a strong nocturnal migration of euphausiids was expected. Also, strong aggregations of the large copepod *N. plumchrus*, known to exist in great abundance on the margins of the Fraser River plume (Mackas and Loutit 1988), would not have been available in September as they would have already entered their deep seasonal migration (diapause). Instead, the IES captured many herring-schooling events during daylight hours, and large numbers of isolated echoes due to dispersed fish during the night. The daytime fish schools were observed at all depths, with the vertical dimension typically 5–10 m and duration in the beam 10–100 s. The typical volume scatter strength of these fish schools generally exceeded –30 dB (re 1 m^{-1}), close to and probably underestimated by the A/D clipping limit of the IES. Based on net trawls performed in this area (described below), these schools are presumed to be Pacific herring (*Clupea pallasii*). Schooling behavior is commonly observed in herring during daylight hours.

A typical example of fish aggregation and subsequent downward migration near dawn is shown in Fig. 10. The upward migration in the evening was not as clear. Near midnight, these fish typically began to congregate in loose shoals, generally located between the surface and 16 m depth. Figure 10 shows two such layers: one at 1–4 m depth in the first 30 min and the other at 8–16 m depth between minutes 15 and 45. Acoustically, these fish shoals have a distinctly different scattering texture from the zooplankton scattering seen at OSP, generally consisting of a series of isolated echoes with a duration of 1–2 s and a vertical extent of 2–3 range bins, equal to the pulse length. The equivalent S_v of these isolated fish echoes was in the range –70 to –56 dB (re

Fig. 8. Comparison of observed and model extremal PDFs taken at 0800–1200 UT on 18 May 1996 at OSP from (*a*) the near-surface zone (6–8 m depth) and (*b*) the deeper zone (20–32 m depth). The solid line shows the best fit extremal PDF. In *a*, α = 4.0, E_{ms} = 1.2 × 10^{-6}·m^{-1}, and in *b*, α = 0.38, E_{ms} = 5.0 × 10^{-7}·m^{-1} (solid line) and α = 2.0, E_{ms} = 4.0 × 10^{-9}·m^{-1} (broken line). The echo-amplitude bin width is 5 × 10^{-5}·m$^{-1/2}$.

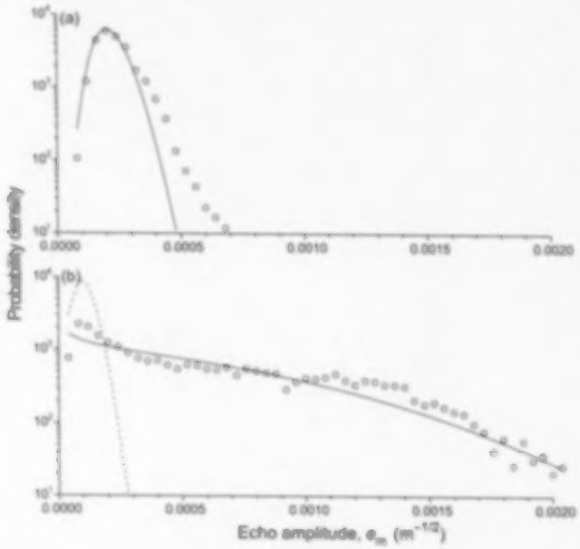

Fig. 9. Comparison of observed and Rician PDFs for scattering at 29–32 m depth at 0800–1200 UT on 18 May 1996 at OSP. Model Rician PDFs were calculated using eqs. 4–6 fitted to different regions of the observed PDF. The two model PDFs correspond to expectations for mixed euphausiids–pteropods (solid line, γ = 1.0, α = 2.0 × 10^{-8}·m^2, × 0.5) and myctophids (~20 mm length, broken line, γ = 4.0, α = 4.5 × 10^{-7}·m^2, × 0.25). The echo-amplitude bin width is 2 × 10^{-5} m.

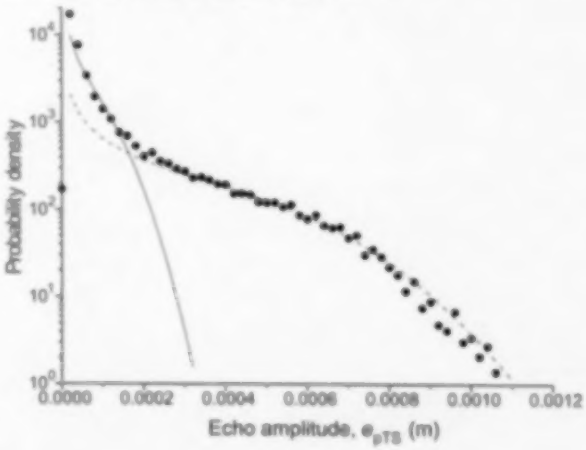

© 2005 NRC Canada

Fig. 10. Volume scatter strength versus depth and time echogram at the Strait of Georgia site starting at 0435 PDT on 12 September 1998. Depth profiles are referenced to the detected surface height. Volume scatter data are averaged over 15 pings (≈ 15 s).

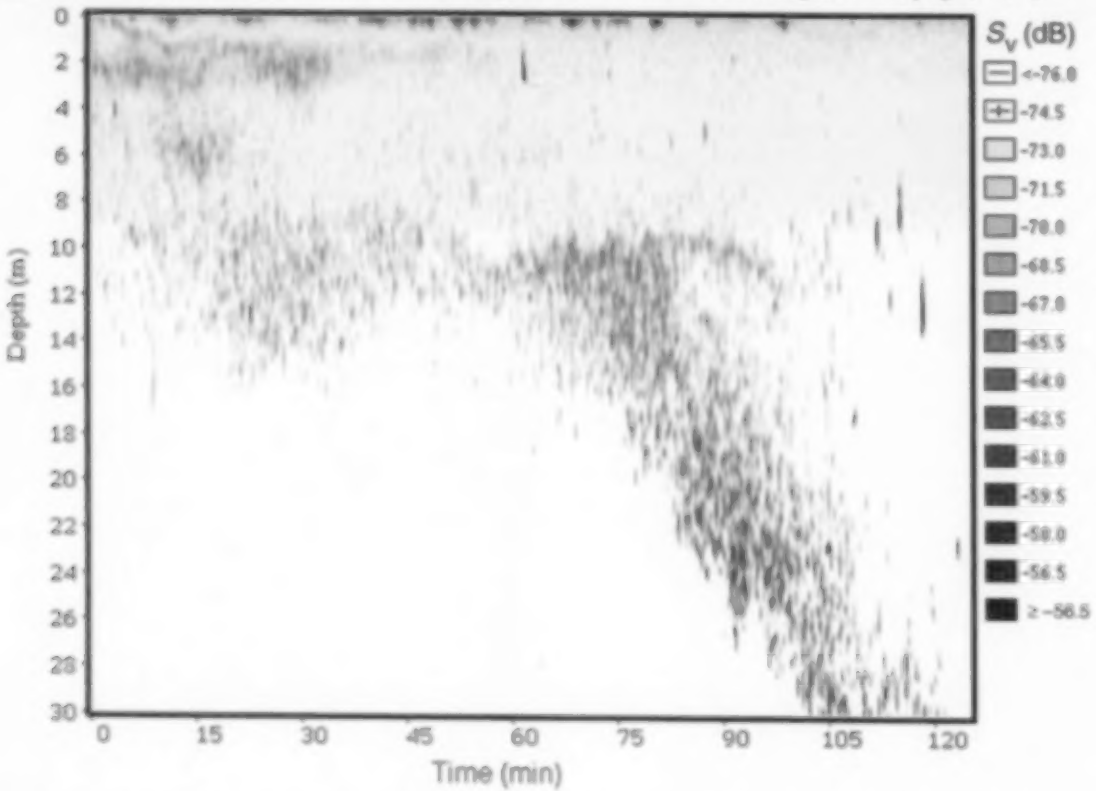

1 m^{-1}), clearly too large to be due to meso-zooplankton. The downward migration started at about 0535 (PDT), with an average speed of roughly 1 cm·s^{-1}. Several small fish balls, roughly 1–4 m high, can be seen as strong scatterers in the latter half of Fig. 10. Very few isolated fish echoes were observed during daylight hours.

On 16 September 1998 a series of net trawls was performed by the vessel *W.E. Ricker* in the southeastern SoG area, very near to the IES mooring (see Table 2). The focus of these trawls was to survey the abundance of migratory adult salmon, so only limited information was collected on other species. The trawls were conducted with a 12 m deep by 36 m wide rope trawl net, towed at a speed near 5 kn for approximately 30 min. Only a few adult salmon were caught during the six trawl sets, in spite of the large numbers (of the order of millions) of sockeye salmon (*Oncorhynchus nerka*) known to be moving into the Fraser River during this period. However, a significant number of herring were collected, particularly in trawl set 84, which likely captured a school. The majority of herring caught were young-of-the-year, with typical lengths from 8 to 12 cm. The trawls also captured a significant number of juvenile salmon (denoted as jacks in Table 2, a generic term covering all species), with lengths noted in the table. No zooplankton sampling was performed.

For these nocturnal fish echoes it is clearly appropriate to assume an isolated-echo regime and thus to analyze using pTS. A database of fish echoes was generated using a single-target selection criterion, i.e., searching from the surface to 30 m depth, targets echoes were selected with pTS > –60 dB (re 1 m^2), range dimension less than or equal to pulse length, and duration <4 s. Special care was taken to reject targets located within fish schools or near surface bubble plumes. Also, to better isolate individual herring from their schools, only data from nighttime periods (i.e., 2000–0600 PDT) were included in the statistical analyses. A total of 2293 fish echoes met this selection criterion over the 8 nights of monitoring. A comparison of the observed PDF with best fit Rician PDFs is shown for three generic fish classes, i.e., with lengths corresponding to juvenile herring, adult herring and (or) juvenile salmon, and adult salmon (Fig. 11). Similar to the zooplankton scattering at OSP, the observed probability densities span three orders of magnitude. General agreement between the observed and Rician PDFs is shown for the juvenile herring class for echo amplitudes up to 0.003 m (Fig. 11), corresponding to pTS up to –50 dB. The Rician PDF for this juvenile herring class produces an average backscatter cross section of 6.0×10^{-6}·m^2, or TS = –52.2 dB. Using eq. 9, this corresponds to a length of 10 cm, in reasonable agreement with the net samples. There is a clear change in scattering regime at echo amplitudes above 0.003 m (pTS = –50 dB), and this value could be used as a threshold to separate juvenile herring from other fish classes. Note that this juvenile herring class constitutes 80.7% of the total fish echoes.

Calculating abundances of these juvenile herring is problematic. It is conceivable that the same approach as for zoo-

© 2005 NRC Canada

Table 2. Trawl results from the vessel *W.E. Ricker* on 16 September 1998 in the southern Strait of Georgia.

Set	Start time	Start location	Distance and heading	Trawl depth	Adult salmon, with mean length	Other fish, with mean length
81	0658	49°01.05′N, 123°13.45′W	2.65 nm, 307°	Surface	1 sockeye, 58.4 cm; 1 chum, 81.5 cm; 1 chinook, 93.0 cm	52 herring; 9 jacks, 22 cm
82	0804	49°02.77′N, 123°16.68′W	1.99 nm, 315°	15 m	2 chum, 75.5 cm	287 herring; 13 jacks 22 cm
83	0928	49°07.52′N, 123°18.87′W	2.93 nm, 006°	Surface	None	3 jacks, 16 cm
84	1033	49°12.13′N, 123° 18.35′W	1.99 nm, 008°	30 m	1 chinook; 85.8 cm; 1 chum, 72.8 cm	5560 herring; 4 jacks, 22 cm
84	1211	49°17.66′N, 123°20.95′W	1.90 nm, 230°	60 m	None	199 herring; 5 jacks, 20 cm
86	1310	49°15.93′N, 123°25.40′W	2.58 nm, 230°	Surface	None	10 herring; 212 jacks, 19 cm

Note: Data courtesy of Dr. R. Sweeting of the Pacific Biological Station, Department of Fisheries and Oceans, Nanaimo, BC V9R 5K6.

plankton could be followed, i.e., calculating a conditionally averaged s_v, then dividing by the estimated mean fish cross section. However, during long periods of the nocturnal sampling there were no targets, so the average would be dominated by the instrumental noise level. An alternative approach is to calculate the total sampled volume, i.e., the volume of the conical IES beam from 30 m depth to the surface (158 m^3) multiplied by the total number of pings sampled (8 nights × 9 h at 1 ping·s^{-1}). This requires a correction for the potential overlap between the volume of water and (or) fish targets sampled by successive pings. Some hint of this can be extracted from the observation that the duration of fish echoes in the IES beam was up to three pings (3 s). Given the maximum beam diameter near the surface (3.6 m), samples will strictly be independent only for horizontal current or fish swimming speeds exceeding 1.2 m·s^{-1}. Of course, this requirement is less strict at greater depths and for fish swimming across the edges of the beam. Moreover, although it is too fast for juvenile herring swimming, currents in this region can easily reach this speed. Using this simple correction (dividing the number of pings by 3), the estimated nocturnal abundance of juvenile herring is (80.7% × 2293 fish) ÷ (86 400 pings × 158 m^3) = 1.3 × 10^{-4}·m^{-3}. However, since the net trawls were conducted during daylight hours, when the herring were largely found in schools, it would be inappropriate to compare abundances derived from total catch per unit trawl effort. It is conceivable that nocturnal trawls could be used to approximately calibrate the acoustically derived abundances, following methods proposed in Lord et al. (1976).

Above this juvenile herring threshold ($e_{pTS} > 0.003$) there is general agreement between the observed and Rician PDFs for the mixed adult herring – juvenile salmon class. The best fit Rician PDF for these intermediate-sized fish uses a backscatter cross section of 1.1 × 10^{-4}·m^2, or TS = –39.6 dB (re 1 m^2). Using eq. 9 for herring, this corresponds to a length of 41 cm, too large for adult herring, which are expected to be near 25 cm. However, using eq. 8 this TS corresponds to a fish length near 20 cm, in agreement with net-trawl results for juvenile salmon (jacks). The estimated abundance of jacks can be extracted from the observed PDF using the result that 18.4% of total targets have an echo amplitude corresponding to this intermediate size class, hence

Fig. 11. Comparison of observed and Rician PDFs for nocturnal (2000–0600 PDT) fish scattering at 2–30 m depth from 8 to 16 September 1998 at the Strait of Georgia site. Model Rician PDFs were calculated using eqs. 4–6 fitted to different regions of the observed PDF. The three model curves correspond to expectations for juvenile herring (solid line, $\gamma = 4.0$, $\sigma = 6.0 \times 10^{-6}$ m^2, × 1), adult herring and (or) juvenile salmon (broken line, $\gamma = 1.6$, $\sigma = 1.1 \times 10^{-4}$ m^2, × 0.45), and adult salmon (~50 cm length, dotted line, $\gamma = 1.0$, $\sigma = 2.0 \times 10^{-3}$ m^2, × 0.1). The echo-amplitude bin width is 5 × 10^{-4} m.

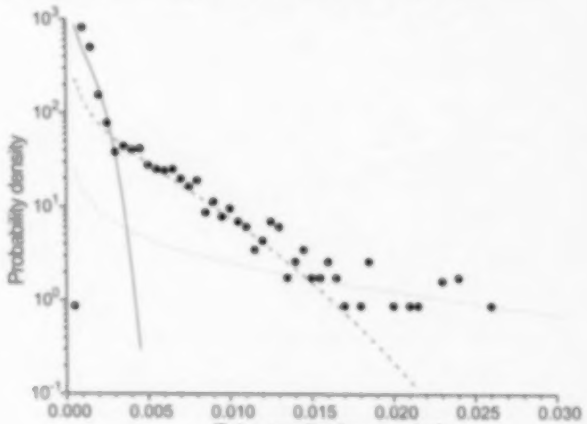

3.1 × 10^{-5}·m^{-3}. This is in reasonable agreement with the net trawls (Table 2), which recovered 246 jacks while sampling approximately 1.1 × 10^7 m^3 of water, yielding an estimated abundance of 2.2 × 10^{-5}·m^{-3}.

Additionally, at echo amplitudes above 0.016 m (pTS > –35.9 dB) there is some suggestion of a third, larger size class; however, only 0.9% of total fish echoes had amplitudes larger than this second threshold. The largest pTS observed was –31.7 dB. The best fit Rician PDF for this largest size class produced a cross section of 2.0 × 10^{-4} m^2, or TS = –27.0 dB, which is a reasonable value for an adult salmon of 60–80 cm length. However, the variance of the observed PDF at higher echo amplitudes and the corresponding mis-

© 2005 NRC Canada

match with the Rician PDF for the adult salmon class are much larger. This is presumably due to insufficient numbers of these larger targets being observed, and is a direct result of the small sampling volume of this narrow acoustic beam. At 0.9% of total targets, the estimated abundance is 1.4×10^{-6} m^{-3}. This is only about two times higher than the abundance found from the net trawls, which recovered a total of seven adult salmon, for an average abundance of 6.4×10^{-7} m^{-3}. Unfortunately, in spite of this apparent agreement in abundances, given the low percentage of total fish echoes and marginal confidence in the best fit PDF, the results for this adult salmon class should be considered suspect.

Discussion

Overall, this simple IES produced useful quantitative time series of meso-zooplankton and small fishes in both open oceanic and littoral environments. Through the combined use of echo intensity (i.e., volumetric backscatter cross section), echo-amplitude PDFs, and appropriate acoustic scattering models for the various scatterer types, reasonable estimates of mean TS and scatterer abundance were produced. A necessary foundation for this analysis was an acoustic calibration of the IES, including knowledge of the transducer beam pattern and limits imposed by electronic noise and A/D clipping. In the case of meso-zooplankton it was found to be useful to assume an overlapping-echo regime, deriving abundance from mean volumetric scattering strength. For fish with more isolated echoes, an echo-counting approach was found to be useful. Then, pulling together results from local zooplankton or fish trawls and relevant literature, it was possible to identify the likely species corresponding to the acoustically derived size classes. At the OSP site the dominant scatterers were found to be euphausiids, pteropods, and myctophid fish, with mean lengths of 15, 1.5, and 28 mm, respectively. At the SoG site, three fish size classes were identified: juvenile herring with mean length near 10 cm, juvenile salmon with mean length of 20 cm, and weak evidence for an adult salmon class with a probable size near 60 cm. Overall, the acoustically derived abundance estimates for both the crustacean zooplankton and myctophids at OSP and the juvenile fish at the SoG site were in reasonable agreement with the local net trawls and abundances from previous studies. This encourages general confidence in the acoustic scattering models that link animal type and size with acoustic parameters.

One particularly powerful aspect of moored-IES usage is the ability to monitor with high temporal and spatial resolution over extended periods of time. Even this simple instrument demonstrated a sampling resolution 20 cm in range by 1–3 s in time, with insonified volumes less than 3 m^3. At OSP this capability allowed examination of the nocturnal migration, and assessment of changes over an 80-day period from late winter through the spring bloom. A similar qualitative analysis of IES data by Thomson and Allen (2000) showed similar features of the nocturnal zooplankton and fish migration. Given identification of the species contributing to the volumetric scattering and some confidence in the acoustic scattering models, observations of diurnal and seasonal changes in volumetric scattering can be converted to useful biological information. At OSP no clear seasonal trend in mean nocturnal volume scatter strength was observed. However, some evidence was found for an increase in the mean size of the dominant scatterer (euphausiids) with a corresponding decrease in the mean abundance. An alternative explanation is a shift of the nocturnal scattering from euphausiid-dominated in March to pteropod-dominated in May. The abundance of myctophids apparently increased by a factor of 3 from March to May; however, the average acoustical size remained approximately constant. At the SoG site, the long sampling period was necessary to produce stable scattering statistics of low-abundance fish such as juvenile salmon, which had mean abundances $<10^{-4}$ m^{-3}. However, for very low abundance species, such as the adult salmon possibly seen in the SoG data, even the 8-night integration time was insufficient to produce reliable statistics. Furthermore, any changes in the abundance or spatial distribution of these fish over time scales of days to months will negate any gain from long integration periods. Thus, it must be concluded that a moored IES is not appropriate for monitoring low-abundance ($<10^{-5}$ m^{-3}) species such as adult salmon.

Clearly, these acoustic versus net-trawl comparisons could have been more closely coupled. For example, at OSP, trawls focused on the abundances and size distributions of the larger euphausiids, pteropods, and myctophids would have been useful. In the SoG case, both a length-frequency distribution for the herring and nighttime trawls to assess the dispersed herring abundance were required. In both cases the author had to rely on *trawls of opportunity* conducted by other researchers for other purposes. It is recommended that any future IES deployments be accompanied by specific net trawls focused on acoustically significant species.

One particular result that needs greater examination is the acoustic scattering from myctophid fishes. Some studies on their abundance and species distribution have been published (e.g., Pearcy and Laurs 1966; Norcross et al. 2003); however, the author was unable to find any detailed acoustic studies on these fishes. Of particular interest is that the swim bladders of older myctophids appear to be reduced or atrophied (Butler and Pearcy 1972), and thus myctophids should have a reduced TS compared with other fish. Myctophids appear to compensate for the lost buoyancy with a higher lipid content. Given the limited size-abundance data gleaned from the literature, it appears that a TS versus length relation for herring is a better match to the present data than the generic fish regressions from Love (1977). Note that Love's study included many freshwater fishes (cyprinids and salmonids), which generally have larger swim bladders than marine fish. Since herring have a slightly smaller swim bladder than most fish, this lends support for the explanation of a reduced swim bladder. Another discrepancy was that the acoustically estimated abundance of myctophids in this study was larger by a factor of about 3 than mean nocturnal abundances reported by both Pearcy and Laurs (1966) off the Oregon coast and Norcross et al. (2003) in the Alaskan gyre. A possible explanation for this difference is that the trawls sampled, and hence averaged, abundances over much larger volumes of water, generally covering the upper 50–100 m. If the myctophids were concentrated in denser layers (as observed from 15–30 m depth), then trawl estimates averaged over much greater depth intervals would be lower.

© 2005 NRC Canada

Net-trawl results from May 1996 suggested that adults of two copepod species (*N. plumchrus* and *N. flemingeri*) should have been observed acoustically, yet no clear evidence was found. This is due to several unfortunate features of their size and occurrence relative to the other scatterers. Firstly, their relatively high abundance (expected to be >20·m^{-3}) puts them well into the overlapping-echo regime. The analysis technique for overlapping echoes used an extremal echo-amplitude PDF that (as shown in cases like Fig. 8*b*) was thoroughly dominated by myctophid scattering. If adult copepod scattering were present, it would have been observed as a peak at low echo amplitudes (e.g., $\epsilon_m < 2 \times 10^{-4}$·m$^{-1/2}$). It can be speculated that in the absence of myctophids, a peak corresponding to large copepods might be resolved. There is a clear absence of any scatterer of that size shown here, in agreement with findings from Goldblatt et al. (1999) indicating daytime avoidance of the upper 15 m. Alternatively, if analyzed (inappropriately) as an isolated-echo PDF, then large copepods would show a Rician convolution PDF confined to $\epsilon_{pTS} < 4 \times 10^{-5}$ m (pTS < –88 dB), competing with the instrumental noise level. Some suggestion of a small-amplitude peak can be seen in Fig. 9 (essentially a single point at $\epsilon_{pTS} = 2 \times 10^{-5}$ m); however, this is not well separated from either the noise level or the euphausiid–pteropod PDF. The increase in the May versus March daytime backscatter level for depths >15 m suggests greater abundances of nonmigratory copepods. For example, assuming the daytime scattering to be due to *N. plumchrus*, the average S_v at 25–30 m depth in the 1130 UT profile in Fig. 7 (–83.6 dB re 1 m^{-1}) suggests an abundance of 16·m^{-3}, near the lower limit suggested by the net trawls. Clearly, because of the small size and relatively low abundance of the other smaller copepod species, their predicted S_v was less than or equal to the instrumental noise level, making them largely undetectable with this IES.

This particular IES had several shortcomings, which placed restrictions on data analysis. In the original instrument design, the requirements for low power consumption and large data-storage capability (by early-1990s standards) were the dominant factors, necessitating compromises in overall performance. The relatively low gain and limited dynamic range (48 dB) of the echo sounder resulted in poor signal to noise performance for sampling small zooplankton, particularly near the ocean surface, where systemic noise levels approached $S_v(z) < -85$ dB (re 1 m^{-1}). Additionally, this instrument did not have a time-varying gain to compensate for geometric spreading loss. These limitations essentially blinded the instrument to scattering from adult copepods, which were the most numerically abundant meso-zooplankton at OSP. Using modern electronics this could be improved through the use of 12- or 16-bit A/D converter electronics and more appropriate amplification. Furthermore, given the huge increases in modern digital data-storage capacity it should be possible to record 1 s ping (or faster) data within smaller depth bins (say 5–10 cm) over a greater maximum range (up to 100 m at 200 kHz should be achievable) over extended periods of time (i.e., months). This would allow tighter measurement of shorter surface waves and individual fish echoes. The increased data-storage capacity could also allow the addition of one or more different echo-sounder frequencies, such as a ~30-kHz channel that would be sensitive to fish but not to most crustacean zooplankton. Another specific limitation in both environments was the lack of measurements of near-surface currents, which prevented direct assessment of the water volume swept past the IES. This could be remedied in several ways, either with a current meter on a surface buoy, with a colocated acoustic Doppler current profiler, or (in well-understood littoral zones) with tidal-current models.

Acknowledgements

The instrument-development and experimental evaluations were supported by Fisheries and Oceans Canada through a number of programs during 1995–1999. The 1996 OSP mooring was supported in part by the Joint Global Ocean Flux Study (Canada). The author is grateful for the guidance and support of Dr. David Farmer, then at the Institute of Ocean Sciences (IOS). This work also benefited from many discussions with, and OSP zooplankton data provided by, Dr. David Mackas, also at IOS. Finally, the author acknowledges the early work of Paul Johnston (then at IOS) for electronics development and maintenance of the IES instrument.

References

Butler, J., and Pearcy, W. 1972. Swimbladder morphology and specific gravity of myctophids off Oregon. J. Fish. Res. Board Can. **29**(8): 1145–1150.

Clay, C. 1983. Deconvolution of the fish scattering PDF from the echo PDF for single transducer sonar. J. Acoust. Soc. Am. **73**: 1989–1994.

Clay, C., and Heist, B. 1984. Acoustic scattering by fish–acoustic models and a two parameter fit. J. Acoust. Soc. Am. **75**(4): 1077–1083.

Dahl, P., and Mathisen, O. 1983. Measurement of fish target strength and associated directivity at high frequency. J. Acoust. Soc. Am. **73**(4): 1205–1211.

Ehrenberg, J., Carlson, T., Traynor, J., and Williamson, N. 1984. Indirect measurement of the mean acoustic backscattering cross section of fish. J. Acoust. Soc. Am. **79**(4): 955–962.

Foote, K. 1987. Fish target strengths for use in echo integrator surveys. J. Acoust. Soc. Am. **82**(3): 981–987.

Foote, K. 1991. Summary of methods for determining fish target strength at ultrasonic frequencies. ICES J. Mar. Sci. **48**: 211–217.

Francois, R., and Garrison, G. 1982. Sound absorption based on ocean measurements. Part II: boric acid contribution and equation for total absorption. J. Acoust. Soc. Am. **72**: 1879–1890.

Fulton, J. 1983. Seasonal and annual variations of net zooplankton at Ocean Station P, 1956–1980. Can. Data Rep. Fish. Aquat. Sci. No. 374.

Goldblatt, R., Mackas, D., and Lewis, A. 1999. Mesozooplankton community characteristics in the NE subarctic Pacific. Deep-Sea Res. II, **46**: 2619–2644.

Greene, C., Wiebe, P., and Burczynski, J. 1989. Analyzing zooplankton size distributions using high-frequency sound. Limnol. Oceanogr. **34**(1): 129–139.

Holliday, D.V., and Pieper, R. 1980. Volume scattering strengths and zooplankton distributions at acoustic frequencies between 0.5 and 3 MHz. J. Acoust. Soc. Am. **67**(1): 135–146.

Johnson, R. 1977. Sound scattering from a fluid sphere revisited. J. Acoust. Soc. Am. **61**: 375–377

Johnson, R. 1978. Erratum: sound scattering from a fluid sphere revisited. J. Acoust. Soc. Am. **63**: 626.

© 2005 NRC Canada

Lemon, D.D., Gower, J.F.R., and Clarke, M.R. 2001. The acoustic water column profiler: a tool for long-term monitoring of zooplankton populations. *In* Proceedings of the MTS/IEEE International Conference Oceans 2001: An Ocean Odyssey, Honolulu, Hawai'i, 5–8 November 2001. Vol. 3. pp. 1904–1909.

Lord, G., Acker, W., Hartt, A., and Rothschild, B. 1976. An acoustic method for the high-seas assessment of migrating salmon. Fish. Bull. **74**(1): 104–111.

Love, R. 1977. Target strength of an individual fish at any aspect. J. Acoust. Soc. Am. **62**(6): 1397–1403.

Mackas, D., and Louttit, G. 1988. Aggregation of the copepod *Neocalanus plumchrus* at the margin of the Fraser River in the Strait of Georgia. Bull. Mar. Sci. **43**(3): 810–824.

Mackas, D., Sefton, H., Miller, C., and Raich, A. 1993. Vertical habitat partitioning by large calanoid copepods in the oceanic subarctic Pacific during spring. Prog. Oceanogr. **32**: 259–294.

MacLennan, D. 1990. Acoustical measurement of fish abundance. J. Acoust. Soc. Am. **87**: 1–15.

Marlowe, C., and Miller, C. 1975. Patterns of vertical distribution and migration of zooplankton at Ocean Station "P". Limnol. Oceanogr. **20**(5): 824–844.

Medwin, H., and Clay, C. 1998. Fundamentals of acoustical oceanography. Academic Press, San Diego.

Napp, J., Ortner, P., Pieper, R., and Holliday, D.V. 1993. Biovolume–size spectra of epipelagic zooplankton using a multi-frequency acoustic profiling system (MAPS). Deep-Sea Res. I, **40**(3): 445–459.

Norcross, B., McKinnell, S., Frandsen, M., Musgrave, D., and Sweet, S. 2003. Larval fishes in relation to water masses of the central north Pacific transitional areas, including the shelf break of west-central Alaska. J. Oceanogr. **59**: 445–460.

Pearcy, W., and Laurs, R. 1966. Vertical migration and distribution of mesopelagic fishes off Oregon. Deep-Sea Res. **13**: 153–165.

Smoker, W., and Pearcy, W. 1970. Growth and reproduction of the lanternfish *Stenobrachius leucopsarus*. J. Fish. Res. Board Can. **27**(7): 1265–1275.

Stanton, T. 1985. Density estimates of biological sound scatterers using sonar echo peak PDFs. J. Acoust. Soc. Am. **78**(5): 1868–1873.

Stanton, T., and Chu, D. 2000. Review and recommendations for the modeling of acoustic scattering by fluid-like elongated zooplankton: euphausiids and copepods. ICES J. Mar. Sci. **57**: 793–807.

Stanton, T., Chu, D., Wiebe, P., and Clay, C. 1993. Average echoes from randomly oriented random-length finite cylinders: zooplankton models. J. Acoust. Soc. Am. **94**(6): 3463–3472.

Stanton, T., Chu, D., Wiebe, P., Martin, L., and Eastwood, R. 1998. Sound scattering by several zooplankton groups. I. Experimental determination of dominant scattering mechanisms. J. Acoust. Soc. Am. **103**(1): 225–235.

Thomson, R., and Allen, S. 2000. Time series acoustic observations of macrozooplankton diel migration and associated pelagic fish abundance. Can. J. Fish. Aquat. Sci. **57**: 1919–1931.

Thorpe, S. 1986. Measurements with an automatically recording inverted echo-sounder, ARIES and the bubble clouds. J. Phys. Oceanogr. **16**: 1462–1478.

Trevorrow, M. 1998. Observations of internal solitary waves near the Oregon coast with an inverted echo-sounder. J. Geophys. Res. **103**(C4): 7671–7680.

Trevorrow, M. 2003. Measurements of near-surface bubble plumes in the open ocean with implications for high-frequency sonar performance. J. Acoust. Soc. Am. **114**(5): 2672–2684.

Trevorrow, M., and Tanaka, Y. 1997. Acoustic and in situ measurements of freshwater amphipods (*Jesogammarus annandalei*) in Lake Biwa, Japan. Limnol. Oceanogr. **42**(1): 121–132.

Vagle, S., and Farmer, D. 1992. The measurement of bubble size distributions by acoustical backscatter. J. Atmos. Oceanic Technol. **49**(9): 630–644.

Vagle, S., Foote, K., Trevorrow, M., and Farmer, D. 1996. Absolute calibrations of monostatic echosounder systems for bubble counting. IEEE J. Oceanic Eng. **21**(3): 298–305.

Waddell, B., and McKinnell, S. 1995. Ocean Station Papa detailed zooplankton data: 1956–1980. Can. Tech. Rep. Fish. Aquat. Sci. No. 2056.

Whitney, F., and Freeland, H. 1999. Variability in upper ocean water properties in the NE Pacific Ocean. Deep-Sea Res. II, **46**: 2351–2370.

Wiebe, P., Greene, C., Stanton, T., and Burczynski, J. 1990. Sound scattering by live zooplankton and micronekton: empirical studies with a dual beam acoustic system. J. Acoust. Soc. Am. **88**(5): 2346–2360.

Wiebe, P., Stanton, T., Benfield, M., Mountain, D., and Greene, C. 1997. High-frequency acoustic volume backscattering in the Georges Bank coastal region and its interpretation using scattering models. IEEE J. Oceanic Eng. **22**(3): 445–464.

Zedel, L. 1994. Deep ocean wave measurements using a vertically oriented sonar. J. Atmos. Oceanic Technol. **11**(1): 182–191.

© 2005 NRC Canada

Photodegradation-induced changes in dissolved organic matter in acidic waters

F.C. Wu, R.B. Mills, Y.R. Cai, R.D. Evans, and P.J. Dillon

Abstract: Photodegradation of dissolved organic matter (DOM) from stream waters was investigated using dissolved organic carbon (DOC) analysis, ultraviolet-visible absorbance, three-dimensional excitational emission matrix fluorescence, and high-performance size exclusion chromatography. The effects of altering pH and various iron concentrations on DOM characteristics during irradiation were examined. DOC concentration, absorbance, and fluorescence all decreased with increasing irradiation. These decreases were accompanied by a decrease in absorbance spectral slope and average molecular size and a blue-shift in fluorescence maximum; decreasing pH enhanced these changes. The photooxidation rate constants were wavelength dependent. For the ratio of the photooxidation rate constant at pH 4 to that at pH 8 under ultraviolet irradiation, there were two maxima at wavelengths of approximately 280 and 320 nm, respectively, indicating that aromatic fractions were most pH photosensitive. The isolated humic acid (HA) and fulvic acid (FA) fractions had different photodegradation characteristics in terms of the photooxidation rate constant and the effects of pH and iron. The results suggest that iron played a more significant role in the photodegradation of the HA fraction than that of the FA fraction and that the HA fraction was mainly responsible for the observed DOM photodegradation. The results indicate that DOM photodegradation in stream waters is strongly influenced by iron and acidity.

Résumé : Nous avons étudié la photodégradation de la matière organique dissoute (DOM) dans les eaux courantes par analyse du carbone organique dissous (DOC), l'absorbance à l'ultraviolet et au visible, la fluorescence avec matrice tridimensionnelle d'excitation/émission et la chromatographie d'exclusion de taille de haute performance. Nous avons examiné les effets du changement de pH et des diverses concentrations de fer durant l'irradiation sur les caractéristiques de la DOM. Les concentrations de DOC, l'absorbance et la fluorescence diminuent toutes avec l'accroissement de l'irradiation. Ces réductions s'accompagnent d'une diminution de la pente spectrale d'absorbance et de la taille moléculaire moyenne, ainsi que d'un glissement vers le bleu du maximum de fluorescence; la réduction du pH accentue ces changements. Les constantes du taux de photo-oxydation sont fonction de la longueur d'onde. Sous irradiation ultraviolette, il existe deux maximums du rapport de la constante du taux de photo-oxydation à pH 4 sur celle à pH 8, respectivement aux longueurs d'onde d'environ 280 nm et 320 nm, ce qui indique que les fractions aromatiques sont les plus photosensibles en fonction du pH. Les fractions isolées d'acide humique (HA) et d'acide fulvique (FA) possèdent des caractéristiques différentes de photodégradation, en ce qui a trait à la constante du taux de photo-oxydation et des effets du pH et du fer. Nos résultats indiquent que le fer joue un rôle plus significatif dans la dégradation des fractions HA que FA et que la fraction HA est en grande partie responsable de la photodégradation de la DOM observée; ils montrent que la photodégradation de la DOM en eau courante est fortement influencée par le fer et l'acidité.

[Traduit par la Rédaction]

Introduction

Recently, there have been several studies on factors that affect organic carbon fluxes in boreal ecosystems, aiding our knowledge of the role of boreal lakes and catchments in global carbon cycling and clarifying our understanding of dissolved organic matter (DOM) dynamics (Molot and Dillon 1996, 1997; Dillon and Molot 1997*a*). The DOM in boreal lakes is mainly derived from their catchments, and much of the organic matter is stored in sediments or lost to

Received 31 October 2003. Accepted 18 December 2004. Published on the NRC Research Press Web site at http://cjfas.nrc.ca on 18 May 2005.
J17817

F.C. Wu.[1] State Key Laboratory of Environmental Geochemistry, Institute of Geochemistry, Chinese Academy of Sciences, Guiyang/Guizhou 550002, China, and Environmental and Resource Studies Program, Trent University, Peterborough, ON K9J 7B8, Canada.
R.B. Mills and R.D. Evans. Environmental and Resource Studies Program, Trent University, Peterborough, ON K9J 7B8, Canada.
P.J. Dillon. Environmental and Resource Studies Program and Department of Chemistry, Trent University, Peterborough, ON K9J 7B8, Canada.
Y.R. Cai. Key Laboratory of Ore Deposit Geochemistry, Institute of Geochemistry, Chinese Academy of Sciences, Guiyang/Guizhou 550002, China.

[1]Corresponding author (e-mail: fcwu@mail.skleg.cn).

 doi: 10.1139/F05-009 © 2005 NRC Canada

the atmosphere following photodegradation (40%–70% of annual inputs) (Gennings et al. 2001). However, the mechanisms responsible for the transfer of organic matter from lake water to sediment and the atmosphere and changes in DOM properties that occur during these processes are poorly understood (Gennings et al. 2001).

A wealth of literature has established that both ultraviolet (UV) radiation and water acidity play an important role in the loss of dissolved organic carbon (DOC) and in changes in DOM properties in fresh and marine waters (Molot and Dillon 1997; Bertilsson and Tranvik 2000; Moran et al. 2000). Loss rates of DOC exposed to UV light in short-term incubations were similar to loss rates measured in long-term mass balance studies for seven lakes located in south-central Ontario, Canada (Molot and Dillon 1997). Gennings et al. (2001) subsequently found that experimental photooxidation rates were enhanced two- to three-fold in acidic waters when alkalinity was <0 μequiv.·L^{-1}. This is consistent with mass balance observations that atmospheric evasion is enhanced in acidic lakes.

The most likely mechanism for enhanced photodegradation of DOM in acidic waters is the photo-Fenton pathway (Zepp et al. 1992; Voelker et al. 1997). This pathway results in highly reactive hydroxyl radicals via two photochemically produced intermediates: ferrous iron and hydrogen peroxide. Reoxidation of ferrous iron by oxygen is inhibited at low pH, thus promoting the photo-Fenton reaction (Waite and Morel 1984). To further understand the mechanisms of DOM photodegradation in acidic waters, in this study, we examined changes in molecular and structural characteristics of DOM during photodegradation at various pHs using UV-visible (UV-Vis) absorbance, three-dimensional excitation emission matrix fluorescence spectroscopy (3DEEM), and high-performance size-exclusion chromatography (HPSEC). Experiments were carried out to determine whether there are characteristic differences in photodegradation between humic acid (HA) and fulvic acid (FA) fractions at various pHs. We also investigated whether iron plays a role in photodegradation by adding an agent (NaF) that forms a nonphotoreactive Fe(III) complex, which prevents or at least restricts iron from participating photochemically (Gao and Zepp 1998).

Materials and methods

Study site

The Dorset study area in south-central Ontario, Canada, is the site of long-term studies on the impacts of long-range atmospheric transport of acids and trace metals, climate change, and shoreline development on water quality of lakes and streams in forested catchments (Dillon et al. 1991; Dillon and Molot 1997*a*, 1997*b*). Study catchments are located in the District of Muskoka and Haliburton County on the southern edge of the Precambrian Shield and range in area from approximately 10 to 125 ha. The catchments are underlain by metamorphic silicate bedrock and are primarily forested with no upstream lakes. Soils in the catchments are brunisolic and podzolic. Descriptions of physiographic and regional meteorologic features are given in Dillon et al. (1991).

Methods

Water samples were collected from 11 headwater streams and four outflows of five lakes, i.e., Dickie (DE), Harp (HP), Plastic (PC), Blue Chalk (BC), and Red Chalk (RC), between March and April 2001. We chose to collect primarily headwater stream samples rather than lake water because the DOM in the study lakes has already received extensive UV radiation owing to their relatively long flushing times (1.6–5.7 years), resulting in the remaining DOM being relatively insensitive to irradiation (Molot and Dillon 1997). In contrast, DOM in streams has had little exposure to UV light and is much more "UV labile" (Molot and Dillon 1997).

The 15 stream samples were filtered through precombusted GF/F filters (Whatman, Maidstone, UK) before artificial UV irradiation experiments. A 20-L water sample was collected from each stream and filled into twelve 530 mL bags for irradiation experiments. After each day, one sample bag from irradiation and one bag from dark controls were taken for measurements of DOC concentration, UV-Vis absorbance, and 3DEEM fluorescence.

To examine the effect of pH on DOM photodegradation, we collected one water sample from HP 4 in June 2002 and we titrated its isolated HA and FA fractions to pH 4, 6, or 8 using reagent-grade H_2SO_4 or NaOH (Baker). The HA and FA fractions were isolated using XAD-8 resin (Thurman and Malcolm 1981) from a 20-L water sample. Based on DOC analysis, the isolated HA and FA fractions constituted 41% and 34%, respectively, of the total DOC in the original sample. NaF also was added to some of the samples to test whether or not iron levels were important in the photodegradation process. The samples at different pHs (pH = 4, 6, and 8) and fluoride treatment (0.01 mol·L^{-1}) were then subjected to UV radiation and dark control experiments similar to the whole stream water experiments described above. For each pH or fluoride treatment, there were six bags for photodegradation experiments and another six bags for dark controls. After each day, one bag from photodegradation experiments and one bag from dark controls were taken for DOC characterization analyses. Measurements were carried out twice, and the results were reported as the average of the two separate readings of the same bag.

The UV radiation chamber was assembled utilizing 40-W Q-Panel lights (Cleveland, Ohio); four UV-A 340 lamps emitting wavelengths of 315–400 nm and six UV-B 313 lamps emitting in the range of 280–315 nm were used. Lamps displayed emission maxima at 340 nm for UV-A and 300 nm for UV-B. A UV-A/UV-B light meter (model 3D V2.0, Solar Light Co., Philadelphia, Pennsylvania) was used to measure light intensity in the exposure chamber at the same height as the bag samples. Based on those measurements, the samples were irradiated with 20.0 ± 7.3 W UV-A·m^{-2} and 0.99 ± 0.26 W UV-B·m^{-2}. The irradiation used in this study was similar to that of Bertilsson and Tranvik (2000) who used radiation of 17.4 W UV-A·m^{-2} and 1.5 W UV-B·m^{-2}.

The chamber was enclosed within an environmental laboratory maintained at 10 °C to minimize secondary degradation or microbial production of organic matter. UV-transparent 530-mL sterile polyethylene Whirlpak bags (Nasco, Burlington, Ontario) were used for irradiation experiments; these bags were manually mixed and rotated twice a

© 2005 NRC Canada

day. The bags were completely transparent above 300 nm and had 90% transparency below 300 nm. They had been previously sterilized through an ethylene oxide process by the manufacturer and were cleaned with trace metal HNO_3 (Fisher Scientific Ltd., Nepean, Ontario) and Milli-Q water (Millipore Corp., Billerica, MA 01821) before the experiments. The exposed surface of a filled bag was 14 cm × 7.5 cm with a thickness of 0.8 cm. Bags were laid on their sides to maximize the exposure to UV radiation in the chamber. Incubation periods ranged from 4 to 6 days, and irradiation did not result in higher temperatures in the sample bags. Three bags containing Milli-Q water were exposed to similar experimental conditions as the samples in the same time frame to determine carbon leaching from the bags. The results indicated that DOC leaching from the bags was minimal after 6 days of irradiation (i.e., <0.2 mg·L^{-1}). Nonetheless, all data were corrected for leaching by subtracting the amount of carbon found in UV-exposed blanks on the same incubation day.

DOC concentrations were measured by high-temperature catalytic oxidation using potassium hydrogen phthalate as a standard (TOC 5000) (Shimadzu Co. Ltd., Kyoto, Japan). Total carbon and inorganic carbon standards with concentrations of 0, 5, 10, 25, and 50 mg·L^{-1} were used for calibration. System and Milli-Q water blanks were on average 0.025–0.050 and 0.072 mg C·L^{-1}, respectively. Total DOC was obtained by calculating the difference between total carbon and inorganic carbon.

UV-Vis absorbance spectra were obtained between 230 and 700 nm using a spectrophotometer (model CARY 400 Bio, Varian, Inc., Palo Alto, California) equipped with matching 2-cm quartz cells. Each sample was scanned three times and the resulting spectra were smoothed. The spectral slope was calculated from a linear least-squares regression of the plot of ln(absorbance) versus wavelength for the interval between 250 and 400 nm; all R^2 values were >0.90. The slope was then used to determine changes in the optical properties of DOM under irradiation. 3DEEM fluorescence was recorded using a spectrofluorometer (model SPEX, Jobin Yvon, Instruments S.A. Inc., Edison, New Jersey). Excitation wavelength (Ex) was set from 250 to 550 nm and emission wavelength (Em) from 250 to 700 nm applying a bandwidth of 2 nm for both. A 0.25-mm slit width was chosen for both Ex and Em. Matlab™ software was used to obtain the 3DEEM surface and contour plots in which Ex and Em wavelengths of the fluorescence maxima can be identified.

HPSEC was performed with a liquid chromatograph (Waters 600s, Waters Corporation, Milford, Massachusetts) with a photodiode array detector (Waters 996) connected to an autosampler (Waters 717$_{plus}$) (Wu et al. 2003). A Tsk-gel® column (7.8 mm × 30 cm and a particle size of 5 µm; model G2500PWXL, Tosohaas, Montgomeryville, Pennsylvania) was used for size exclusion. For each run, 30 µL of sample was injected onto the column with phosphate buffer (0.1 mol NaCl·L^{-1}, pH 6.8) as an eluent, and the flow rate was set at 0.5 mL·min^{-1}.

Total iron concentrations in the water samples and HA and FA isolates were analysed by high-resolution inductively coupled plasma mass spectrometry (model Element 2, Finnegan Mat Gmbh, Bremen, Germany). pH values were measured with a pH meter (model 825MP, Fisher Scientific Ltd.).

Statistical analyses

The slopes of the ln-linear regressions for DOC concentration, absorbance, and fluorescence intensity versus time were used to evaluate the DOM photodegradation rate constants (Gao and Zepp 1998; Reche et al. 1999; Gennings et al. 2001). Owing to the existence of time series autocorrelation, the reported correlation coefficient may be overstated.

To compare the difference between (*i*) irradiated and dark control stream samples, (*ii*) FA and HA fractions, (*iii*) various pH treatments, and (*iv*) fluoride treatments, we used analysis of variance (ANOVA) (Zar 1998). Owing to interaction between the samples, separate one-way ANOVA tests were used to discriminate between different levels of each treatment. Prior to the ANOVA, the assumptions of normality and homogeneity of variances were tested using the K–S test and Levene's test, respectively. Further testing using Pearson's correlation was performed to determine if there was a relationship between the concentration of iron, pH, and the rate of photodegradation in the 15 stream waters (Zar 1998).

Results and discussion

Photogradation of DOM: absorbance, fluorescence, DOC, and molecular size (MS)

Initial characterization of the stream waters is presented in Table 1. The streams represent a variety of chemical conditions with pH ranging from 4.5 to 7.2 and DOC from 2.7 to 10.8 mg·L^{-1}. RC 2 and DE 5 have the highest DOC concentrations and also tend to be more acidic with higher iron concentrations and fluorescence intensity. PC 0 has the highest pH with low DOC and iron concentration and low fluorescence intensity.

The data from the UV irradiation of HP 4 stream water manipulated to pH 4, 6, and 8 (Fig. 1) indicate that exposure to UV radiation generally resulted in decreased absorbance (Abs), fluorescence intensity, and DOC concentrations. This is consistent with other reports (Moran et al. 2000; Fukushima and Tatsumi 2001; Gennings et al. 2001) in which DOM was examined during photodegradation.

All first-order rate constants for irradiation were significantly different from those in the dark controls according to an ANOVA ($F_{[1,18]} = 6998.1$, $p = 0.00016$) with R^2 for ln(DOC), ln(Abs), and ln(Flu) versus time ranging from 0.85 to 0.98 (Fig. 1). This suggests that first-order kinetics is an appropriate approximation for DOM photodegradation in these short-term incubation experiments, an assumption also used by Molot and Dillon (1997) and Gennings et al. (2001). It is well known that pH affects DOM absorbance and fluorescence, but it seems that the photodegradation rate constants calculated may not be related to the original Abs and Flu data of the samples.

The rate constant for DOC loss (K_{DOC}) was 0.04·day^{-1} at pH 8, 0.07·day^{-1} at pH 6, and 0.12·day^{-1} at pH 4, the rate constant for fluorescence at Ex 350 nm and Em 450 nm (K_{Flu}) was 0.15·day^{-1} at pH 8, 0.30·day^{-1} at pH 6, and 0.43·day^{-1} at pH 4, and the rate constant for absorbance at 300 nm (K_{Abs}) was 0.26·day^{-1} at pH 8, 0.45·day^{-1} at pH 6, and 0.65·day^{-1} at pH 4. Thus, for the HP 4 sample, K_{DOC}, K_{Flu}, and K_{Abs} all increased as pH decreased from 8 to 6 to

© 2005 NRC Canada

Table 1. Water quality parameters of the stream water samples and their calculated photooxidation rate constants.

Sample*	Flu (QSU)	pH	DOC ($mg \cdot L^{-1}$)	Iron ($\mu g \cdot L^{-1}$)	K_{DOC} (day^{-1})
HP 3A	8.1	6.3	3.1	12.57	0.13
HP 4	11.8	6.3	5.6	84.84	0.45
HP 5	13.8	5.2	7.6	128.11	0.92
HP 0	9.8	5.7	5.2	32.07	0.24
DE 5	16.7	5.0	10.8	148.80	0.77
DE 8	15.9	5.2	9.1	123.82	0.42
DE 10	14.3	4.5	9.7	157.45	1.35
DE 0	13.3	5.3	8.1	69.93	0.57
PC 0	4.0	7.2	3.1	13.79	0.13
PC 1-03	17.8	6.8	9.2	128.04	0.51
BC 1	7.3	6.2	3.3	6.67	0.19
BC 0	2.7	6.2	2.7	2.43	0.46
RC 1	9.6	5.5	3.8	74.95	1.01
RC 2	18.0	4.5	10.7	112.73	0.51
RC 4	9.7	5.2	5.0	57.46	0.43
HA	14.1		6.4	399.50	
FA	11.5		18.4	244.90	

Note: Flu is the maximum fluorescence intensity and was standardized with quinine sulfate units (QSU); K_{DOC} is the photooxidation rate constant for DOC. Humic acid (HA) and fulvic acid (FA) were isolated from the HP 4 stream in June 2002 and were used for the pH and NaF manipulation experiment studies.

*HP, Harp Lake; DE, Dickie Lake; PC, Plastic Lake; BC, Blue Chalk Lake; RC, Red Chalk Lake.

4. This result supports previous findings that decreasing pH accelerates the photoreaction of DOM (Gao and Zepp 1998; Gennings et al. 2001; Anesio and Graneli 2003).

To test whether MS of DOM decreases as a result of photodegradation, we applied HPSEC. There was one major peak for the nonirradiated samples in the HPSEC chromatogram at pH 4, 6, and 8; with increasing irradiation, the peak was shifted to longer elution times (i.e., smaller MS) (Fig. 2). Generally, the retention time decreases with an increase in MS. Hence, the elution time in the HPSEC chromatogram demonstrates the relative order of MS. The area under the major peak rapidly decreased during the first day of irradiation. This suggests that the larger MS fractions were more UV photoreactive than the smaller MS fractions.

Wavelength and spectral dependence

Although DOM absorbance at all wavelengths decreased with increasing irradiation, the rate constants varied at different wavelengths (Fig. 3*a*). The highest K_{Abs} values occurred in the UV-B region (260–320 nm) and were shifted slightly to shorter wavelengths when pH changed from pH 8 to 6 to 4. This is similar to a recent study by Gao and Zepp (1998) who reported that DOM photodegradation within the Satilla River caused a decrease in UV and visible absorbance that occurred most rapidly in the UV-B region (280–320 nm). The ratio of K_{Abs} at pH 4 to that at pH 8 (Fig. 3*a*) shows that there were two major maxima at wavelengths of approximately 260–290 and 320–350 nm, respectively. These wavelengths indicate the occurrence of π–π^* electron transitions for aromatic compounds such as phenolic substances, aniline derivaties, benzoic acids, and polycyclic aromatic hydrocarbons in DOM (Traina et al. 1990). Therefore, the results indicate that while enhanced photodegradation occurred for all light-absorbing DOM fractions at low pHs, the aromatic fractions were the most pH sensitive. Similarly, Korshin et al. (1999) found two similar spectral maxima of humic substances in response to pH change using differential UV-Vis spectroscopy; those two maxima were also attributed to the characteristic response of many pure aromatic compounds.

The DOM absorbance spectral slope remained stable in the dark controls. However, it decreased slightly with increasing irradiation, and the decrease in spectral slope was significantly different among pH treatments during the 6-day incubation experiments (Fig. 3*b*) (for pH 4 and 8, $F_{[1,14]} = 21.2$, $p = 0.00055$; for pH 4 and 6, $F_{[1,14]} = 10809$, $p = 0.00018$). This is consistent with some previous reports (Morris and Hargreaves 1997; Gao and Zepp 1998) in which DOM samples from Pennsylvania and the coastal Satilla River irradiated by natural sunligh, were observed to have absorbance spectra that shifted, enhancing the ratios of UV-B to UV-A absorbance. Further decreasing pH enhanced this shift. On the other hand, an increase in spectral slope after irradiation also has been reported (e.g., Vodacek et al. 1997; Whitehead et al. 2000; Twardowski and Donaghay 2002). The reason for this discrepancy is not known. However, it may be related to the different origins of the DOM.

Similar to absorbance, the rate constants for fluorescence loss (K_{Flu}) varied at different excitation wavelengths, but they exhibited the highest sensitivity in the UV-A region (320–400 nm) (Fig. 4). This region is in the excitation wavelength range of the predominantly humic-like fluorescence peak of the DOM sample (Fig. 5), suggesting that humic-like fluorescence was preferentially photodegraded. The highest K_{Flu} values were shifted slightly towards shorter wavelengths with increasing acidity (Fig. 4), a change that is

© 2005 NRC Canada

Fig. 1. Natural logarithm of (*a*) absorbance at 350 nm (Abs), (*b*) fluorescence at excitation/emission 350/450 nm (Flu), and (*c*) dissolved organic carbon (DOC) as a fraction of the initial value versus UV exposure (days). The water sample was collected in June 2002 from the HP 4 (Harp Lake) stream. Both exposed and dark control data represent the average of two separate readings taken from the same bag. The trend lines are best-fit linear regression curves. ○, dark controls; ▲, pH 8; ●, pH 4; ■, pH 6.

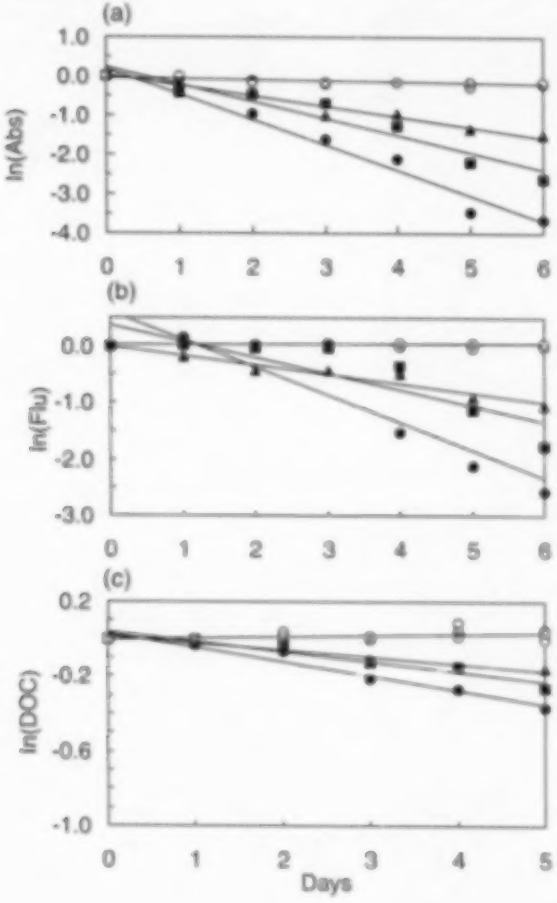

the predicted result of preferential photodegradation of the fluorophores with shorter wavelengths. The ratio of K_{Flu} at pH 4 to that at pH 8 shows that there was a broad peak at the excitation wavelength range from 280 to 400 nm, with two shoulders at approximately 280 and 320 nm (Fig. 4). This indicates that fluorophores excited at 280- to 400-nm wavelengths are more sensitive to enhanced photodegradation in acidic waters, with those excited at 280 and 320 nm being the most pH sensitive.

Del Castillo et al. (1999) found decreases in wavelengths for the emission maxima of humic fluorophores in the Orinoco River plume that they attributed to photodegradation. Moran et al. (2000) showed that Ex and Em maxima of humic substances decreased during long-term sunlight photodegradation. In this study, we observed similar

Fig. 2. High-performance size exclusion chromatograms of the photodegraded dissolved organic matter at pH 4. The water sample was collected in June 2002 from the HP 4 (Harp Lake) stream. The data represent the average of two separate readings from the same bag.

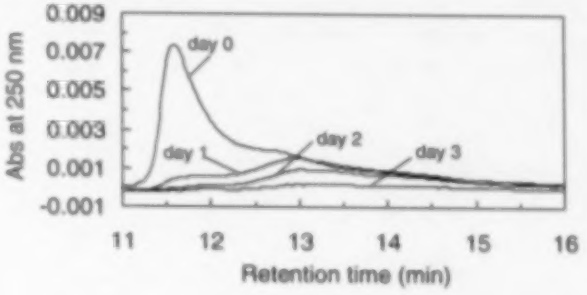

decreases in the maximum Ex and Em wavelengths during 6 days of irradiation (Fig. 5). The decrease was different between pH 4, 6, and 8 (for Ex wavelength: between pH 4 and 8, $F_{[1,14]} = 13.38$, $p < 0.0027$; between pH 4 and 6, $F_{[1,14]} = 1168$, $p < 0.00017$; for Em wavelength: between pH 4 and 6, $F_{[1,14]} = 5064$, $p < 0.0001$; between pH 4 and 8, $F_{[1,14]} = 10114$, $p < 0.0001$), being more pronounced in the more acidic waters. The maximum Ex/Em wavelengths decreased up to 21/18, 19/36, and 39/40 nm at pH 8, 6, and 4, respectively, after 6 days of irradiation. The Ex and Em wavelengths remained constant in dark controls. The decrease in Ex and Em wavelengths was consistent with the decrease in MS under UV irradiation, since larger MS DOM fractions are generally related to the longer maximum Ex and Em wavelengths, as reported in previous studies (Wu et al. 2002, 2003).

It appears that both K_{Abs} and K_{Flu} are wavelength dependent displaying local maxima in their spectra. This is consistent with the exposure of a complex mixture of DOM compounds of varying structures and characteristic fluorophores to a range of incident UV wavelengths. However, the enhanced photooxidation observed for fluorescence and absorbance is the same at low pH, a spectral shift being indicative of an increase in the ratio of UV-B to UV-A radiation. More significantly, the results suggest that the molecules absorbing and fluorescing at wavelengths of approximately 280 and 320 nm were most photosensitive to pH change, likely indicating that the aromatic fractions may play a significant role in the enhanced photodegradation of DOM in acidic waters.

Differences between HA and FA in photodegradation

To examine the possible differences between the HA and FA fractions and the role of photo-assisted Fenton reactions during their photodegradation at low pH, we conducted experiments at pH 4, 6, and 8 with the isolated HA and FA fractions. Fluoride solution was added to examine the effect of iron, as suggested by Gao and Zepp (1998).

The K_{Abs}, K_{Flu}, and K_{DOC} values for the isolated HA and FA fractions in dark controls were significantly smaller than those under UV irradiation (for the HA fraction: $F_{[1,18]} = 8.4$, $p = 0.0097$; for the FA fraction: $F_{[1,18]} = 1631.2$, $p = 0.00016$) (Fig. 6). However, the rate constants under UV ir-

© 2005 NRC Canada

Fig. 3. (*a*) Photodegradation rate constants for absorbance (K_{Abs}) versus wavelength at pH 4, 6, and 8. ▲, pH 8; ●, pH 4; ■, pH 6; ○, pH 4/pH 8. (*b*) Changes in absorbance spectral slope (S) with increasing UV irradiation time (days). Solid bars, pH 4; stippled bars, pH 6; open bars, pH 8. The error bars represent the standard errors of two independent observations. The water sample was collected in June 2002 from the HP 4 (Harp Lake) stream.

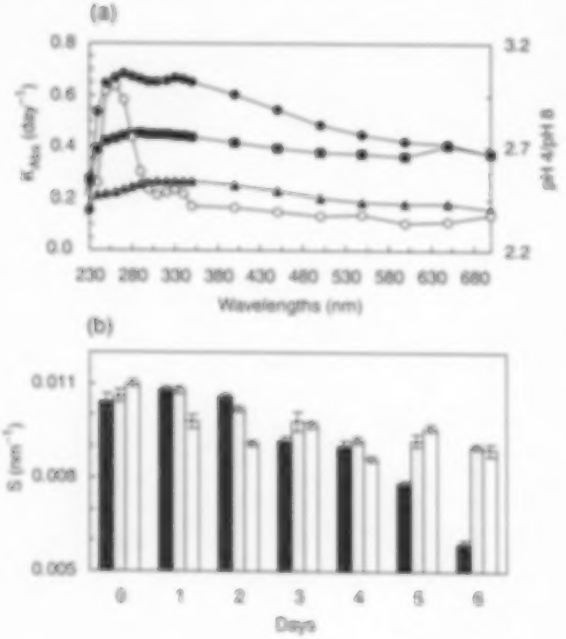

Fig. 4. Photodegradation rate constants for fluorescence (K_{Flu}) versus excitation wavelength at pH = 4, 6, and 8. ▲, pH 8; ●, pH 4; ■, pH 6; ○, pH 4/pH 8. The water sample was collected in June 2002 from the HP 4 (Harp Lake) stream.

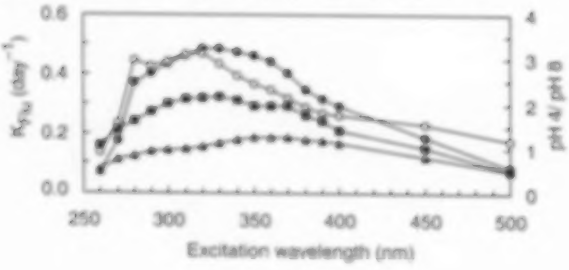

radiation were significantly different between pH 4, 6, and 8 for the HA fraction (for pH 4 and 8: $F_{[1,6]} = 163.5$, $p < 0.00023$; for pH 4 and 6: $F_{[1,6]} = 118.5$, $p < 0.00026$), being considerably larger at pH 4 than those at pH 6 and 8. On the contrary, rates were similar at pH 4, 6, and 8 for the FA fraction (for pH 4 and 6: $F_{[1,6]} = 0.82$, $p = 0.39$; for pH 4 and 8: $F_{[1,6]} = 0.29$, $p = 1.33$). These results indicate that photooxidation of the HA fraction was more sensitive to pH changes than that of the FA fraction. HA is typically more

Fig. 5. Excitation and emission (Ex and Em) wavelengths of fluorescence maxima with increasing UV irradiation time (days). Solid bars, pH 4; stippled bars, pH 6; open bars, pH 8. The error bars represent the standard errors of two independent observations. The water sample was collected in June 2002 from the HP 4 (Harp Lake) stream.

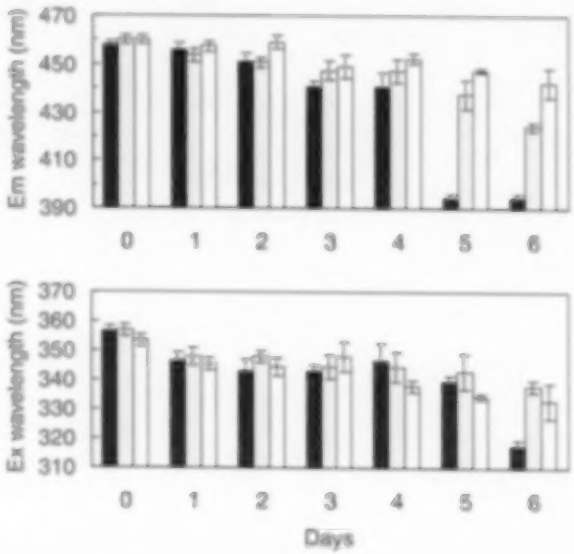

aromatic than FA (Gron et al. 1996), and so the results are consistent with those seen in the HP 4 stream.

The addition of fluoride to the HA and FA fractions had a different effect for each acid. For the HA fraction, the addition of 10 mmol NaF·L^{-1} significantly decreased the degradation rate constants at all pH treatments ($F_{[1,18]} = 1424$, $p < 0.0001$) (Fig. 6); however, for the FA fraction, the addition of NaF did not decrease the rate constants ($F_{[1,18]} = 0.006$, $p = 0.98$). It has been reported that the addition of fluoride decreases the rate of DOM photodegradation and eliminates the pH effect as fluoride binds the active iron, which otherwise participates in the photo-Fenton process (Gao and Zepp 1998; Gennings et al. 2001). However, the results presented here suggest that this is only true for the HA fraction and not for the FA fraction. It appears that iron may not play an important role in FA photodegradation.

In the photo-Fenton reaction, the hydroxyl radical reacts with aromatic hydrocarbons by adding to the aromatic ring, resulting in a substituted hydrocyclohexadienyl radical, and thus favours reaction with aromatic moieties. The reaction of this carbon radical depends on environmental conditions such as pH, aromaticity, and redox potential (Chen and Pignatello 1997). Gron et al. (1996), using ^{13}C NMR analysis, found that on average, HA consists of 51% aromatic carbon, while FA consists of 14%–20% aromatic carbon. Fukushima and Tatsumi (2001) found that the majority of Fe(III)–DOM complexes, and therefore reaction sites for photooxidation, were in the largest MS fractions. This agrees with our HPSEC results presented earlier in which larger MS fractions were photodegraded more rapidly than lower MS fractions (Fig. 2) and that the rate constants for the HA fraction were considerably larger than those for the FA frac-

© 2005 NRC Canada

Fig. 6. Photodegradation rate constants (K) of the isolated (a) humic acid and (b) fulvic acid at pH 4, 6, and 8 and the effect of the addition of fluoride. The K_{Abs}, K_{Flu}, and K_{DOC} are the photooxidation rate constants for absorbance at 350 nm, fluorescence at excitation/emission 350/450 nm, and dissolved organic carbon (DOC) decay, respectively. The error bars represent the standard errors of two independent observations. Solid bars, pH 4; stippled bars, pH 6; open bars, pH 8.

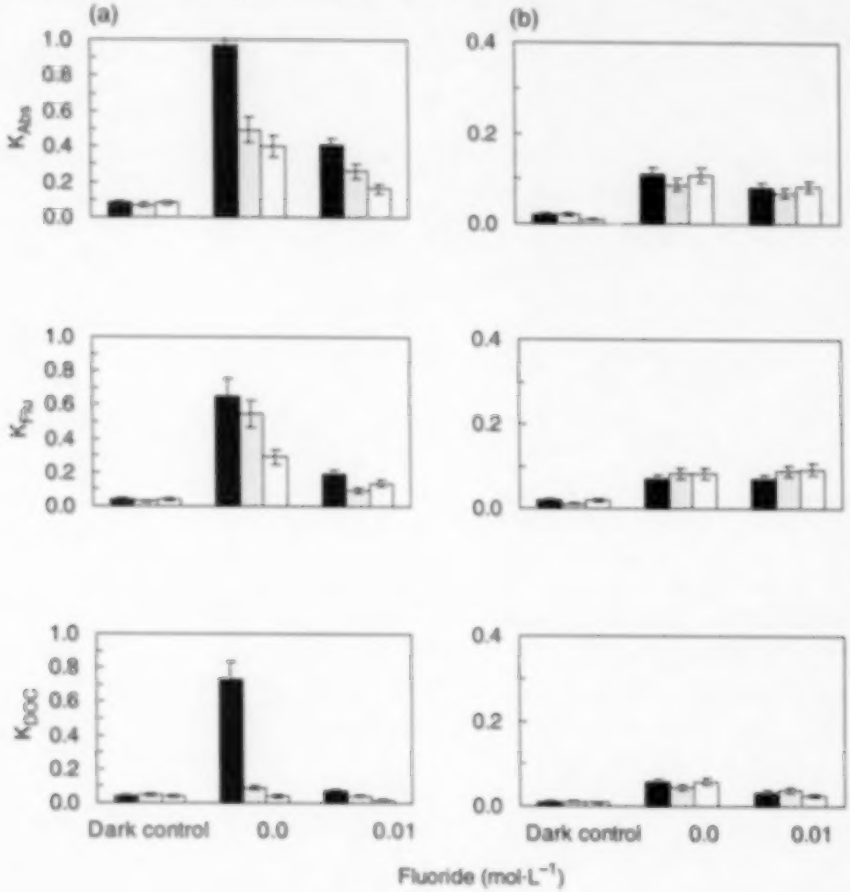

tion at all pHs (Fig. 6). In our study streams, the iron to DOC concentration ratio in the HA fraction was much higher than in the FA fraction (Table 1). Hence, the higher aromatic content and relative higher iron concentration in the HA fraction may contribute to its greater pH photosensitivity. Thus, the results presented here indicate that HA may be the primary target for DOM photodegradation in acidic waters.

Relationships between photooxidation rate constants, pH, and iron concentrations

For the 15 stream samples in the Dorset area, there was a significant negative correlation between pH and K_{DOC} (R = 0.39, $p < 0.01$). In a similar study of 24 North American lakes (Reche et al. 1999), there was a slightly negative correlation between loss of absorbance at 440 nm and pH (R = –0.38, p = 0.06) for lakes where pH ranged between 4 and 7. Furthermore, the correlation between K_{DOC} and iron concentrations for these samples was also strong (R = 0.52, $p <$ 0.01). Since the primary photoproduct of DOM degradation is CO_2, the results found by Bertilsson and Tranvik (2000) that dissolved inorganic carbon production is negatively related to pH and positively related to iron concentration are no surprise. These results provide supportive evidence to the current findings that pH and iron are two factors influencing photodegradation of DOM.

Since the GF/F filtration used in this study did not remove all microbes from the water and experiments were not performed under sterile conditions, some of the DOM may have been microbially consumed and respired. It has been reported that bacteria consume humic components at a relatively low rate (Moran and Hodson 1990) and microbes consume primarily low-MS photoproducts (Miller et al. 1997; Moran and Zepp 1997; Bertilsson and Tranvik 1998). However, the contribution of microbial consumption in situ relative to DOM photodegradation is largely unknown. Previous studies have shown that bacterial consumption rates of several low molecular weight photoproducts were much lower than low molecular weight product rates (Bertilsson and Tranvik 1998) and thus photoproducts accumulated in

© 2005 NRC Canada

short-term incubations using artificial UV lamps. In mass balance studies, Dillon and Molot (1997*a*) and Gennings et al. (2001) suggested that a main portion of the autochthonous and allochthonous DOM degraded was a result of photooxidation rather than consumption by the pelagic microbial community.

Molot and Dillon (1997) found that DOC photooxidation rates in incubations for up to 11 days were similar to loss rates measured in 12-year mass balance studies. They suggested that photooxidation has the potential to remove most of the allochthonous DOC lost in surface water. Beyond the impact that increased UV has on the quantity of DOM, irradiation also alters the quality of DOM found in surface waters. This study has shown that such processes are largely dependent on environmental conditions. In particular, acidity and iron concentration are key factors in the aging and transformation of DOM in lakes and streams.

Acknowledgements

The authors thank the Natural Sciences and Engineering Research Council of Canada, Inco Ltd., and 973 Project (2002CB412300) for financial support of this research.

References

Anesio, A.M., and Graneli, W. 2003. Increased photoreactivity of DOC by acidification: implications for the carbon cycle in humic lakes. Limnol. Oceanogr. **48**: 735–744.

Bertilsson, S., and Tranvik, L.J. 1998. Photochemically produced carboxylic acids as substrates for freshwater bacterioplankton. Limnol. Oceanogr. **43**: 885–895.

Bertilsson, S., and Tranvik, L.J. 2000. Photochemical transformation of dissolved organic matter in lakes. Limnol. Oceanogr. **45**: 753–762.

Chen, R., and Pignatello, J. 1997. Role of quinone intermediates as electron shuttles in Fenton and photo-assisted Fenton oxidations of aromatic compounds. Environ. Sci. Technol. **31**: 2399–2406.

Del Castillo, C.E., Coble, P.G., Morel, J.M., Lopez, J.M., and Corredor, J.E. 1999. Analysis of the optical properties of the Orinoco River plume by absorption and fluorescence spectroscopy. Mar. Chem. **66**: 35–51.

Dillon, P.J., and Molot, L.A. 1997*a*. Dissolved organic and inorganic carbon mass balances in central Ontario lakes. Biogeochemistry, **36**: 29–42.

Dillon, P.J., and Molot, L.A. 1997*b*. Effect of landscape form on export of dissolved organic carbon, iron, and phosphorus from forested stream catchments. Water Resour. Res. **33**: 2591–2600.

Dillon, P.J., Molot, L.A., and Scheider, W.A. 1991. Phosphorus and nitrogen export from forested catchments in central Ontario. J. Environ. Qual. **20**: 857–864.

Fukushima, M., and Tatsumi, K. 2001. Degradation characteristics of humic acid during photo-Fenton process. Environ. Sci. Technol. **35**: 3683–3690.

Gao, H., and Zepp, R.G. 1998. Factors influencing photoreactions of dissolved organic matter in a coastal river of the southeastern United States. Environ. Sci. Technol. **32**: 2940–2946.

Gennings, C., Molot, L.A., and Dillon, P. 2001. Enhanced photochemical loss of organic carbon in acidic waters. Biogeochemistry, **52**: 339–354.

Gron, C., Wassenaar, L., and Krog, M. 1996. Origin and structures of groundwater humic substances from three Danish aquifers. Environ. Int. **22**: 519–534.

Korshin, G.V., Benjamin, M.M., and Li, C.W. 1999. Use of differential spectroscopy to evaluate the structure and reactivity of humics. Water Sci. Technol. **40**: 9–16.

Miller, W.L., Moran, M.A., and Zepp, R.G. 1997. Interaction of photochemical and microbial processes in the degradation of refractory dissolved organic matter from a coastal marine environment. Limnol. Oceanogr. **42**: 1317–1324.

Molot, L.A., and Dillon, P.J. 1996. Storage of terrestrial carbon in boreal lake sediments and evasion to the atmosphere. Global Biogeochem. Cycles, **10**: 483–492.

Molot, L.A., and Dillon, P.J. 1997. Photolytic regulation of dissolved organic carbon in northern lakes. Global Biogeochem. Cycles, **11**: 357–365.

Moran, M.A., and Hodson, R.E. 1990. Bacterial production on humic nonhumic components of dissolved organic carbon. Limnol. Oceanogr. **35**: 1844–1756.

Moran, M.A., and Zepp, R.G. 1997. Role of photoreactions in the formation of biologically labile compounds from dissolved organic matter. Limnol. Oceanogr. **42**: 1307–1316.

Moran, M.A., Sheldon, W.M., and Zepp, R.G. 2000. Carbon loss and optical property changes during long-term photochemical and biological degradation of estuarine dissolved organic matter. Limnol. Oceanogr. **45**: 1254–1264.

Morris, D.P., and Hargreaves, B.R. 1997. The role of photochemical degradation of dissolved organic carbon in regulating the UV transparency of three lakes on the Pocono Plateau. Limnol. Oceanogr. **42**: 239–249.

Reche, I., Pace, M.L., and Cole, J.J. 1999. Relationship of trophic and chemical conditions to photobleaching of dissolved organic matter in lake ecosystems. Biogeochemistry, **44**: 259–280.

Thurman, E.N., and Malcolm, R.L. 1981. Preparative isolation of aquatic humic substances. Environ. Sci. Technol. **15**: 463–466.

Traina, S.J., Novak, J., and Smeck, N.E. 1990. An ultraviolet absorbance method of estimating the percent aromatic carbon content of humic acid. J. Environ. Qual. **19**: 151–153.

Twardowski, M.S., and Donaghay, P.L. 2002. Photobleaching of aquatic dissolved materials: absorption removal, spectral alteration, and their interrelationship. J. Geophys. Res. **107**(C8): 6.1–1.12.

Vodacek, A., Blough, N.V., DeGrandpre, M.D., Peltzer, E.T., and Nelson, R.K. 1997. Seasonal variation of CDOM and DOC in the Middle Atlantic Bright: terrestrial inputs and photooxidation. Limnol. Oceanogr. **42**: 674–686.

Voelker, B.M., Morel, F.M.M., and Sulzberger, B. 1997. Iron redox cycling in surface waters; effects of humic substances and light. Environ. Sci. Technol. **31**: 1004–1011.

Waite, T.D., and Morel, F.M.M. 1984. Photoreactive dissolution of colloidal iron oxides in natural waters. Environ. Sci. Technol. **18**: 860–868.

Whitehead, R.F., de Mora, S., Demers, S., Gosselin, M., Montfort, P., and Mostajir, B. 2000. Interactions of ultraviolet-B radiation, mixing, and biological activity on photobleaching of natural chromophoric dissolved organic matter: a mesocosm study. Limnol. Oceanogr. **45**: 278–291.

Wu, F.C., Evans, R.D., and Dillon, P.J. 2002. High-performance liquid chromatographic fractionation and characterization of fulvic acid. Anal. Chim. Acta, **464**: 47–55.

Wu, F.C., Evans, R.D., and Dillon, P.J. 2003. Separation and characterization of NOM by high-performance liquid chromatogra-

© 2005 NRC Canada

phy and on-line three dimensional excitation emission matrix fluorescence detection. Environ. Sci. Technol. **37**: 3687–3693.

Zar, J.H. 1998. Biostatistical analysis. 4th ed. Prentice Hall, Englewood Cliffs, N.J.

Zepp, R.G., Faust, B.C., and Hoigne, J. 1992. Hydroxyl radical formation in aqueous reaction (pH = 3–8) of iron(II) with hydrogen peroxide: the photo-Fenton. Environ. Sci. Technol. **26**: 313–319.

© 2005 NRC Canada

Automatic calculation of the sensitivity of Bayesian fisheries models to informative priors

Russell B. Millar and Wayne S. Stewart

Abstract: The derivatives of Bayes estimators, with respect to changes in hyper-parameters of the prior density, are posterior covariances. Hence, these derivatives can be readily estimated from a posterior sample and the calculation is shown to be especially straightforward for parameters having a marginal prior that is of exponential family form. Three examples are given. The first fits a Ricker curve to stock–recruit data and, for several important management parameters, examines the sensitivity of the Bayes estimates to the informative log-normal priors placed on the maximum annual reproductive rate and density-dependent compensation parameters. Using the WinBUGS software, it is demonstrated that these derivatives can easily be estimated by a minor addition to the program code. The utility of the estimated sensitivities is examined by refitting the Ricker model using a range of different priors. The second example revisits a hierarchical model that was used to perform a meta-stock assessment on several US West Coast rockfish (*Sebastes* spp.) stocks, and examines the sensitivity of the Bayes estimate of bulk catchability to the hyper-prior. The final example looks at an example from the literature and uses summary statistics provided therein to determine the sensitivity of model parameters to their prior means.

Résumé : Les valeurs dérivées des estimateurs bayésiens, en ce qui a trait aux changements dans les hyper-paramètres de la densité a priori, sont des covariances a posteriori. Ces valeurs dérivées peuvent donc être facilement calculées à partir d'un échantillon a posteriori et le calcul est particulièrement direct pour les paramètres qui ont une densité marginale a priori qui est de forme de la famille exponentielle. Nous présentons trois exemples. Le premier ajuste une courbe de Ricker à des données de stock–recrues et examine, pour plusieurs paramètres d'intérêt pour la gestion, la sensibilité des estimés bayésiens aux densités informatives à priori log-normales attribuées au taux reproductif annuel maximal et aux paramètres de compensation reliés à la densité. Nous démontrons à l'aide du logiciel WinBUGS que ces valeurs dérivées peuvent s'estimer facilement en faisant une addition mineure au code du programme. Nous examinons l'utilité des sensibilités estimées en ajustant de nouveau le modèle de Ricker et en utilisant une gamme de différentes distributions a priori. Le second exemple réexamine un modèle hiérarchique utilisé pour faire une étude de méta-stock de plusieurs stocks de sébastes (*Sebastes* spp.) de la côte occidentale des É.-U. et évalue la sensibilité de l'estimé bayésien de la capturabilité globale à la distribution hyper a priori. Le dernier exemple examine une étude tirée de la littérature et utilise les statistiques générales qu'on y trouve pour déterminer la sensibilité des paramètres du modèle à leurs moyennes a priori.

[Traduit par la Rédaction]

Introduction

The Bayesian approach has found favor in fisheries science for two primary reasons, the relative ease with which complex models can be fitted and its ability to incorporate prior knowledge (and hence prior uncertainty) about all unknown parameters. This is particularly relevant to fisheries science, where data are often information-poor but prior knowledge, in some form or other, is abundant.

Prior knowledge is incorporated in a logically rigorous manner via application of Bayes' rule:

$$\pi(\boldsymbol{\theta}|\,y) = \frac{\pi(\boldsymbol{\theta})f(y|\boldsymbol{\theta})}{f(y)}$$

where $\pi(\boldsymbol{\theta}|\,y)$ is the posterior density of the parameters given the data y, $\pi(\boldsymbol{\theta})$ the prior density, $f(y|\boldsymbol{\theta})$ the likelihood, and $f(y)$ the (marginal) density of the data. The Bayesian paradigm therefore takes information from two sources, the data via the likelihood, $f(y|\boldsymbol{\theta})$, and the prior, $\pi(\boldsymbol{\theta})$. Bayes' rule is attributed to the Presbyterian minister Thomas Bayes and his work "Essay Towards Solving a Problem in the Doctrine of Chances" published posthumously by his friend Richard Price in 1763 (Dale 1999).

Dependence on the prior often draws strong criticism from those who follow the frequentist paradigm because they regard the justification of any a priori distribution, informative or "non-informative" (Kass and Wasserman 1996; Millar 2002), as an overwhelming difficulty. However, it can also be argued that the frequentist paradigm is not as objective as it may appear. Classical fisheries models often assign fixed values to certain unknown parameters when there is, in fact, some uncertainty about their true value. For example,

Received 26 April 2004. Accepted 13 December 2004. Published on the NRC Research Press Web site at http://cjfas.nrc.ca on 20 May 2005.
J18088

R.B. Millar[1] and W.S. Stewart. Department of Statistics, Private Bag 92019, University of Auckland, Auckland, New Zealand.

[1]Corresponding author (e-mail: millar@stat.auckland.ac.nz).

 doi: 10.1139/F04-240 © 2005 NRC Canada

Fleischman and Burwen (2003) implemented a (frequentist) maximum-likelihood model of a mixed fishery in which they made the standard assumption that baseline information about the component species was known exactly. They then followed this with a Bayesian version of their model in which uncertainty about the baseline information was explicitly modeled. Further examples of the frequentist inclination to fix the value of unknown quantities are given by McAllister and Ianelli (1997), including models used to advise managers about total allowable catches where the use of fixed values of natural mortality rate, recruitment, and selectivity gives a false impression of uncertainty in the resulting inference.

Prior knowledge may come from a variety of sources, including related analyses on the same fishery, expert opinion, and formal meta-analyses (Gelman et al. 1995) over similar fisheries (e.g., Harley and Myers 2001). However, regardless of the origins of the prior knowledge, it will be contentious. Moreover, in the case of a frequentist meta-analysis (e.g., Myers et al. 1999) the parameters of the prior distribution that is induced from the analysis will have associated standard errors. If this induced prior is used in a subsequent Bayesian model then it is necessary to ask how sensitive the conclusions would be to a 1 or 2 standard deviation change, say, to the parameters of that prior.

Assessing the sensitivity of posterior inference to informative priors is a vital part of the analysis. We show here that this task can be easily automated in many cases. In the next section we discuss the three main approaches to sensitivity analysis and then focus on one of them, parametric local sensitivity analysis. This approach quantifies sensitivity as the derivative, with respect to hyper-parameters of the prior, of the Bayes estimate of the parameter(s) of interest. These derivatives have been formulated by Geweke (1999) and independently by Millar (2004), who corrects Geweke's second derivative formula.

The methodology herein is first applied to the Bayesian modeling of spawner and recruitment data. Log-normal marginal priors are used on two of the model parameters, and sensitivities of the Bayes estimates of management parameter to the prior means are estimated. One of the log-normal priors is the frequentist-derived prior for maximum reproductive rate of pink salmon (*Oncorhynchus gorbuscha*) given by Myers et al. (1999), and sensitivity with respect to uncertainty in estimation of this prior is assessed. The second example looks at sensitivity to hyper-priors in the meta-stock assessment model of Millar and Methot (2002). The third example looks at the mixture model of Fleischman and Burwen (2003) and demonstrates that, especially when normal priors are used, it is possible to deduce the sensitivity to prior specification using simple posterior summary statistics. Consequently, sensitivity can easily be evaluated for previously published Bayesian analyses that have provided the values of the required summary statistics.

Methods

Bayesian sensitivity analysis

There are essentially three approaches to quantifying sensitivity (Ríos Insua and Ruggeri 2000) of the posterior distribution to the prior: (*i*) ad-hoc (informal) methods, (*ii*) global sensitivity analysis, and (*iii*) local sensitivity analysis.

The modeler, when applying the informal approach, simply uses a selection of alternative priors and observes a range of posterior distributions (Berger 2000). Global sensitivity analysis typically uses an infinitely large class of alternative priors in determining the range in posterior output and consequently is implemented via complex mathematical calculations. Typically, a baseline prior is elicited (Berger 2000) and various classes of alternatives are defined as perturbations from the baseline. For example, in the ϵ-contamination class, ϵ determines the degree of contamination (i.e., mixing) of the baseline prior by an extreme alternative prior. The class is obtained by allowing ϵ to vary from zero to unity.

Local sensitivity analysis (Gustafson 2000) uses differential calculus or functional analysis to determine sensitivity. The essence of the methodology is to use functional differentiation to "differentiate" a posterior with respect to infinitesimal perturbations in the baseline prior. In general, the use of functional differentiation allows local sensitivity to consider arbitrary forms of perturbation in the baseline prior.

The general forms of global and local sensitivity require complicated mathematical concepts and are little used in practice. This paper will focus on parametric local sensitivity, where derivatives are used to find the rate at which the Bayes estimator of some parameter of interest changes with respect to hyper-parameters of the joint prior density. In particular, the derivative is straightforward to evaluate when the hyper-parameters are the natural parameters of an exponential family marginal prior.

Local sensitivity of Bayes estimators

The method is easily motivated and demonstrated by considering the simple case of independent and identically distributed (iid) normal data and a conjugate normal prior. That is, $\theta \sim N(\mu_0, \sigma_0^2)$, $y_i|\theta \sim N(\theta, \sigma^2)$, $i = 1 \ldots n$, and σ is assumed to be known. The posterior is (Lee 1997)

$$\theta|\mathbf{y} \sim N(\mu_1, \sigma_1^2)$$

where

$$\sigma_1^2 = \left\{ \frac{1}{\sigma_0^2} + \frac{n}{\sigma^2} \right\}^{-1}$$

$$\mu_1 = \sigma_1^2 \left\{ \frac{\mu_0}{\sigma_0^2} + \frac{n\bar{y}}{\sigma^2} \right\}$$

The rate at which the mean of the posterior changes with respect to the mean of the prior is therefore

$$\frac{\partial \mu_1}{\partial \mu_0} = \frac{\sigma_1^2}{\sigma_0^2}$$

which is simply the ratio of the posterior variance to the prior variance.

More generally, for an arbitrary prior and likelihood, letting $\boldsymbol{\theta} = (\theta_1, \ldots, \theta_i, \ldots, \theta_p)$ be the vector of unknown model parameters with prior $\pi(\boldsymbol{\theta})$, and $g(\boldsymbol{\theta})$ the parameter of interest, Geweke (1999) and Millar (2004) have shown that

© 2005 NRC Canada

$$(1)\qquad \frac{\partial E(g(\boldsymbol{\theta})|\mathbf{y})}{\partial \gamma} = \mathrm{cov}\left(g(\boldsymbol{\theta}), \frac{\partial \log(\pi(\boldsymbol{\theta}))}{\partial \gamma}\middle| \mathbf{y}\right)$$

where γ is a hyper-parameter of $\pi(\boldsymbol{\theta})$. Moreover, Millar (2004) has shown that eq. 1 simplifies when γ is the canonical parameter of an exponential family marginal prior density (Appendix A) that is a priori independent of any other model parameters. The exponential family includes normal, exponential, gamma, Poisson, and binomial densities.

If parameter θ_i has a prior $N(\mu_0, \sigma_0^2)$ distribution then μ_0 is the canonical parameter and, assuming that θ_i is a priori independent of any other model parameters, eq. 1 simplifies to

$$(2)\qquad \frac{\partial E(g(\boldsymbol{\theta})|\mathbf{y})}{\partial \mu_0} = \frac{\mathrm{cov}(g(\boldsymbol{\theta}), \theta_i|\mathbf{y})}{\sigma_0^2}$$

If the parameter of interest is θ_i (i.e., $g(\boldsymbol{\theta}) = \theta_i$) then the right-hand side of eq. 2 is, once again, the ratio of posterior variance to prior variance. That is, the sensitivity result obtained in the conjugate iid normal example holds more generally, regardless of the form of the likelihood, $f(\mathbf{y}|\boldsymbol{\theta})$, and the number of other parameters.

Sensitivity results can also be easily obtained for priors that are transformations of exponential family densities, such as a log-normal or inverse-gamma density. For example, if θ_i has a log-normal prior distribution then $\log(\theta_i)$ has a $N(\mu_0, \sigma_0^2)$ prior and, hence, from eq. 2

$$(3)\qquad \frac{\partial E(g(\boldsymbol{\theta})|\mathbf{y})}{\partial \mu_0} = \frac{\mathrm{cov}(g(\boldsymbol{\theta}), \log(\theta_i)|\mathbf{y})}{\sigma_0^2}$$

Moreover, if we are interested in the sensitivity of $E(g(\boldsymbol{\theta})|\mathbf{y})$ with respect to $E(\theta_i)$ then we can calculate it through the chain rule. For a log-normal prior this gives

$$(4)\qquad \frac{\partial E(g(\boldsymbol{\theta})|\mathbf{y})}{\partial E(\theta_i)} = \frac{\partial E(g(\boldsymbol{\theta})|\mathbf{y})}{\partial \mu_0}\left(\frac{\partial E(\theta_i)}{\partial \mu_0}\right)^{-1} = \frac{\mathrm{cov}(g(\boldsymbol{\theta}), \log(\theta_i)|\mathbf{y})}{\sigma_0^2 E(\theta_i)}$$

because $E(\theta_i) = \exp(\mu_0 + 0.5\sigma_0^2)$ and so $\partial E(\theta_i)/\partial \mu_0 = E(\theta_i)$. Here the sensitivity is with respect to change in the prior mean of θ_i arising from a change to hyper-parameter μ_0.

Millar (2004) shows that the second-order derivatives of $E(g(\boldsymbol{\theta}))$ are given as third-order posterior moments. These will not be considered here.

Examples

Example 1: Ricker stock–recruit model

The sensitivity of a Ricker stock and recruitment model was investigated using the pink salmon data found in Quinn and Deriso (1999, p. 105). These data span the years 1960–1989 (Fig. 1).

The Ricker stock–recruit model can be written as

$$(5)\qquad R_t = \alpha S_t e^{-\beta S_t} e^{\varepsilon_t}$$

where R_t is the observed number of recruits resulting from S_t spawners, α is the slope at the origin (maximum annual reproductive rate), β quantifies the density-dependent compensation in recruitment, and ε_t are iid normally distributed errors with mean zero. Rearranging and taking logarithms gives the linear equation

$$(6)\qquad y_t = \log\left(\frac{R_t}{S_t}\right) = a - \beta S_t + \varepsilon_t$$

where $a = \log(\alpha)$.

The stock–recruit meta-analysis of Myers et al. (1999) provides an informative log-normal prior for α, $\alpha \sim LN(\mu_a, \sigma_a^2)$, where $\mu_a = 1.22$ and $\sigma_a^2 = 0.12$ are the mean and variance of a, respectively. The meta-analysis was implemented under the frequentist paradigm by fitting a variance components model using maximum likelihood. The standard error of μ_a was 0.07 (Myers et al. 1999; Table 1).

For this stock–recruit model, the parameters of interest are α and the derived management parameters

$$(7)\qquad R_{\max} = \frac{\alpha}{\beta e}$$

$$(8)\qquad S_{\max} = \frac{1}{\beta}$$

where $R_{\max}$, the maximal value of recruitment (from eq. 5), is obtained when the number of spawners equals $S_{\max}$. Parameter β was originally given a non-informative (i.e., very low precision) normal prior; however, even when the informative prior was employed on a, its posterior sample in-

Fig. 1. (*a*) Spawner, S, and recruitment, R, data for the pink salmon (*Oncorhynchus gorbuscha*) stock from Quinn and Deriso (1999, p. 105). (*b*) Spawners plotted against $\log(R/S)$, showing the lack of information in these data in the absence of prior knowledge about the intercept or slope parameters of eq. 5.

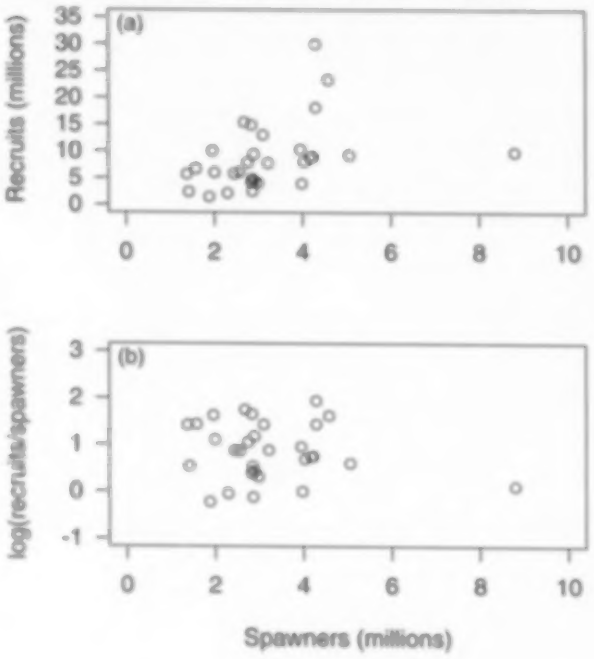

© 2005 NRC Canada

Table 1. Summary posterior statistics for the parameters of interest in example 1, from a posterior sample of size 100 000: α (maximum annual reproductive rate), R_{max} (maximal recruitment), and S_{max} (optimal number of spawners).

	Mean	Standard deviation	MCMC[a] error of the mean	2.5% quantile	Median	97.5% quantile
S_{max}	11.39	6.85	0.036	4.72	9.56	29.34
R_{max}	13.54	6.28	0.030	7.41	11.85	29.81
α	3.45	0.62	0.004	2.48	3.36	4.88

[a]Markov chain Monte Carlo code.

cluded near-zero values, which gave large values of S_{max} and R_{max}, well in excess of all of the stock and recruitment values in the data (Fig. 1). Such values were considered implausible and this initiated a reevaluation of the prior on β. In the above model, spawning-stock size is an explanatory variable and as such can legitimately be used to provide prior information about S_{max}. On the basis of the range of observed spawner abundances, 10% and 90% percentiles for the prior distribution of S_{max} were chosen to be 1 and 10 m, respectively. Assuming a log-normal distribution, and denoting $s = \log(S_{max})$, these percentiles give $s \sim N(\mu_s = 1.1513, \sigma_s^2 = 0.8070)$. Equivalently, $\log(\beta) \sim N(-1.1513, 0.8070)$ from eq. 8.

Here the informative log-normal prior on α was taken from the literature, and a vaguely informative log-normal prior was placed on S_{max}. Sensitivity will be examined with respect to these two priors. The sensitivities of the Bayes estimates to change in $E(\alpha)$ or $E(S_{max})$ can be calculated using eq. 4. For example, putting $g(\boldsymbol{\theta}) = R_{max}$ and $\theta_i = S_{max}$ gives

$$\frac{\partial E(R_{max}|\,\boldsymbol{y})}{\partial E(S_{max})} = \frac{\mathrm{cov}(R_{max}, s|\,\boldsymbol{y})}{\sigma_s^2 E(S_{max})} \quad (9)$$

Evaluation of the desired derivatives is easily facilitated by a minor addition to the Markov chain Monte Carlo (MCMC) code used to sample from the posterior. Here it was desired to model the sensitivity of Bayes estimates of S_{max}, R_{max}, and α with respect to the priors on α and S_{max}. Hence, a vector $\boldsymbol{D}$ was defined having first three elements equal to the three parameters of interest: $\boldsymbol{D}[1] = S_{max}$; $\boldsymbol{D}[2] = R_{max}$; $\boldsymbol{D}[3] = \alpha$. The remaining elements of $\boldsymbol{D}$ were defined to be

$$\boldsymbol{D}[4] = \frac{a}{\sigma_a^2 E(\alpha)}$$

$$\boldsymbol{D}[5] = \frac{s}{\sigma_s^2 E(S_{max})}$$

$$\boldsymbol{D}[6] = \frac{a}{\sigma_a^2}$$

$$\boldsymbol{D}[6] = \frac{s}{\sigma_s^2}$$

With the above vector defined, quantities such as eq. 9 can be evaluated as posterior covariances. For example,

$$\frac{\partial E(S_{max}|\,\boldsymbol{y})}{\partial E(\alpha)} = \mathrm{cov}(\boldsymbol{D}[1], \boldsymbol{D}[4])$$

$$\frac{\partial E(R_{max}|\,\boldsymbol{y})}{\partial E(S_{max})} = \mathrm{cov}(\boldsymbol{D}[2], \boldsymbol{D}[5])$$

Moreover, the derivative with respect to change in $E[a]$ and $E[s]$ can also be evaluated. For example, the derivative of the Bayes estimate of S_{max} with respect to $E[a]$ is just $\mathrm{cov}(\boldsymbol{D}[1], \boldsymbol{D}[6])$.

The model was implemented in WinBUGS (Spiegelhalter et al. 1999). To aid "burn in", 5000 iterations were discarded before vector $\boldsymbol{D}$ was monitored for 100 000 iterations. The convergence diagnosis and output analysis (CODA; Plummer et al. 2004) library was loaded into R software (R Development Core Team 2004) and the MCMC output from WinBUGS was analyzed for convergence. Various convergence diagnostics (Geweke 1992; Gelman and Rubin 1992; Raftery and Lewis 1992; Heidelberger and Welch 1983) were employed and they showed no statistically significant evidence against convergence of the posterior sample.

In addition to specification of vector $\boldsymbol{D}$, the WinBUGS code was extended to implement the model for a sequence of differing prior means on a (Appendix B). The sequence was equal-spaced and of length 21, with the lower and upper bounds of the sequence corresponding to a halving and a doubling of the scale of the log-normal prior on α, respectively. That is, the lower-bound prior used $\mu_a = 1.22 + \log(2) = 0.53$ and the upper-bound prior used $\mu_a = 1.22 + \log(2) = 1.91$. Running the code provides 21 simultaneous different Bayes estimators of each of the parameters of interest, corresponding to the 21 different priors (Fig. 2). This procedure was repeated for an equal-spaced sequence of prior means on s.

The observed Bayes estimates of S_{max}, R_{max}, and α were 11.39 m, 13.54 m, and 3.45, respectively (Table 1). The posterior covariances were calculated by monitoring the $\boldsymbol{D}$ vector and loading it into the R software. From these, the derivatives of the Bayes estimates of S_{max}, R_{max}, and α, with respect to the prior mean of a, were calculated to be –5.94 m, –3.83 m, and 0.87, respectively (Table 2). The derivatives give an accurate linear approximation to the actual change in the Bayes estimates over the range of priors constructed above (Fig. 2).

Recall that the prior mean of a for the baseline prior, 1.22, was determined from a variance-components model and was estimated to have standard error of 0.07 (Myers et al. 1999). Multiplying the above derivatives by 0.07 gives a linear approximation to the change in the three Bayes estimators caused by a 1 standard error change in the prior mean of a. These values are approximately, 0.4 m, 0.3 m, and 0.06, respectively. The changes are an order of magnitude smaller than the posterior standard deviations (Table 1) of S_{max},

© 2005 NRC Canada

Fig. 2. Observed Bayes estimates of the parameters of interest over a range of prior means for $a = \log(\alpha)$ (logarithm of the maximum annual reproduction rate) and S_{max} (optional number of spawners), and the first-order approximation (solid line) obtained using derivatives from Table 2. R_{max} denotes maximal recruitment.

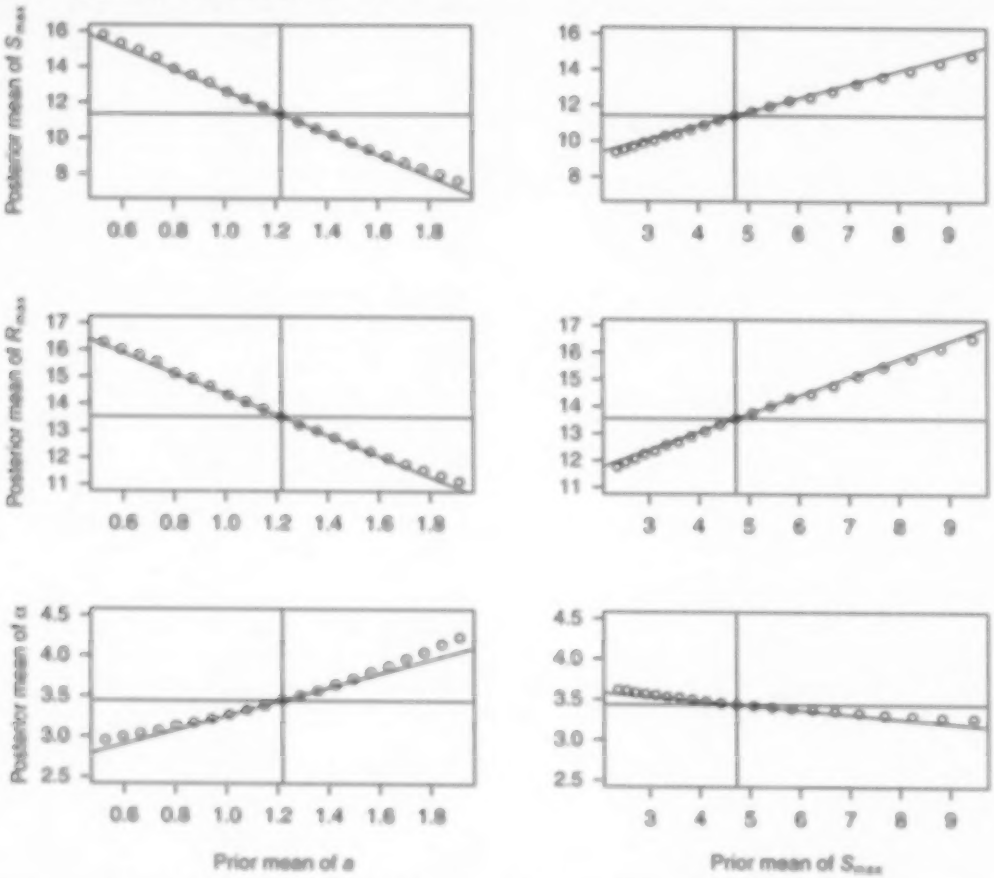

Table 2. Posterior covariances between ($D[1]$, $D[2]$, $D[3]$) and ($D[4]$, $D[5]$, $D[6]$, $D[7]$), which give the derivative of the Bayes estimates of S_{max} (optimal number of spawners), R_{max} (maximal recruitment), and α (maximum annual reproductive rate) with respect to the prior means of α, S_{max}, a ($= \log(\alpha)$), and s ($= \log(S_{max})$), respectively.

Parameter of interest		Derivative with respect to: $E[\alpha]$	$E[S_{max}]$	$E[a]$	$E[s]$
		$D[4]$	$D[5]$	$D[6]$	$D[7]$
S_{max}	$D[1]$	−1.65	0.77	−5.94	3.65
R_{max}	$D[2]$	−1.07	0.68	−3.83	3.21
α	$D[3]$	0.24	−0.054	0.87	−0.26

R_{max}, and α, respectively, and hence it would be reasonable to say that posterior inference is not sensitive to uncertainty in the estimation of the prior mean of a.

The Bayes estimates were sensitive to the prior imposed on S_{max}. In particular, the Bayes estimate of S_{max} is 77% sensitive to its prior mean (Table 2; Fig. 2). The prior on S_{max} was employed to restrict implausibly large posterior values of S_{max} and was intended to be vaguely informative. The actual prior used was specified without expert opinion and hence could be considered rather arbitrary. These sensitivity results show that this somewhat arbitrary prior was having a large influence on the Bayes estimates, and hence it would have to be concluded that posterior inference using this model cannot be justified.

Example 2: hierarchical meta-assessment model

Millar and Methot (2002) implemented a hierarchical model for the bulk catchability, Q, of US West Coast rockfish (*Sebastes* spp.). Bulk catchability was defined as the ratio between swept-area biomass (of the survey trawl) and actual biomass, and was widely believed to be substantially different from unity because of gear avoidance and the inability of the survey trawl to sample all of the suitable rockfish habitat. Specifically, with $q = \log(Q)$ denoting log-catchability, it was assumed that the q value of a randomly chosen rockfish species was normally distributed with mean μ_q and variance σ_q^2. The informative hierarchical prior used by Millar and Methot (2002) was given by

$$\mu_q \sim N(\gamma, 1)$$

$$\sigma_q^2 \sim \Gamma^{-1}(1, 1)$$

© 2005 NRC Canada

Table 3. Prior and posterior summary statistics for the regression parameters used in the mixture-model analyses of hydroacoustic data on 3 separate weeks (from Table 1 of Fleischman and Burwen 2003).

	β_0		β_1		δ	
	Mean	SD	Mean	SD	Mean	SD
Prior	2.88	0.18	0.0319	0.0029	–0.33	0.11
Posteriors						
Week 1	2.84	0.10	0.0338	0.0027	–0.36	0.09
Sensitivity	0.3		0.9		0.7	
Week 2	2.81	0.10	0.0330	0.0027	–0.38	0.09
Sensitivity	0.3		0.9		0.7	
Week 3	2.81	0.09	0.0356	0.0026	–0.30	0.09
Sensitivity	0.3		0.8		0.7	

Note: Sensitivity is the derivative of the posterior mean to the prior mean and is calculated as the ratio of posterior variance to prior variance (it is given to 1 decimal place, owing to round-off in the tabulated values).

with $\gamma = -1$. With this prior, Millar and Methot (2002) fitted the model using the Metropolis–Hastings algorithm, and the Bayes estimate of Q was calculated to be 0.34.

We obtained the computer program used by Millar and Methot (2002) and refitted the above model. The prior variance of μ_q is unity, and hence the derivative of the Bayes estimator of Q with respect to γ is simply given by $\text{cov}(Q, \mu_q|y)$, which was computed to be 0.07.

To demonstrate the applicability of the derivative, consider an alternative prior that doubles the scale of the prior on Q. This corresponds to increasing γ by $\log(2) = 0.693$, that is,

$$\mu_q \sim N(-0.307, 1)$$

Using the calculated derivative of 0.07, linear approximation gives a Bayes estimate for Q of 0.39 ($= 0.34 + 0.693 \times 0.07$) under this alternative prior. Refitting under this alternative prior, the Bayes estimator of Q was computed to be 0.38.

Example 3: mixed-species model for hydroacoustic data

Fleischman and Burwen (2003) applied mixed-fishery models to measurements of hydroacoustic scatter to estimate the relative composition of chinook salmon (*Oncorhynchus tshawytscha*) and sockeye salmon (*Oncorhynchus nerka*) at a site in the Kenai River, Alaska. Their first analysis used the maximum-likelihood approach to mixed-fishery analysis (Millar 1987). The mixture approach gives (asymptotically) unbiased estimates of composition and is preferable to the use of uncorrected classification proportions (Millar 1990). The analysis made the standard assumption that the baseline information about each species was known without error; that is, that the statistical distribution of hydroacoustic scatter from each of the two species was known exactly. However, their second analysis was a Bayesian implementation of the mixture model and was used to investigate the sensitivity to the above assumption about known baseline information.

The mixture models used echo-length standard deviation y as the response variable and it was modeled as a two-component mixture (one component from each of the two species of salmon), with mixing weights equal to the proportions of each salmon species. Within each species, the response variable was modeled as a linear function of fish length. In this regression, a common slope parameter, β_1, was used for both species, but different intercepts were assumed. The intercept parameter for chinook salmon was denoted β_0, and that for sockeye salmon was denoted $\beta_0 + \delta$. The length distribution of each species was assumed to be a mixture of the length distributions of three different age classes.

The Bayesian model of Fleischman and Burwen (2003) placed independent and highly informative normal priors on parameters β_0, β_1, and δ to represent the baseline information derived from previous experiments that measured the hydroacoustic signal from tethered fish. The proportion of chinook salmon, π_C, was given a flat prior on [0,1], as were the proportions of each age class within each species. Auxiliary data were used to provide informative priors on the length distributions at age for each species. Three sets of mixture data were analyzed for 3 separate weeks and posteriors were generated for each of these.

Table 1 of Fleischman and Burwen (2003) gives the prior and posterior standard deviations of β_0, β_1, and δ. Hence, because these parameters were given normal priors, the derivative of their posterior mean (i.e., Bayes estimate) with respect to their prior mean is, from eq. 2, just the ratio of posterior variance to prior variance (Table 3). It is seen that in all 3 weeks, the Bayes estimate of β_1 is highly sensitive to its prior mean, with a derivative always at least 0.8. Parameter δ is also sensitive to its prior mean, with a derivative of about 0.7.

In this example, the parameter of primary interest is the proportion of chinook salmon, π_C, and therefore it would be of more interest to evaluate the sensitivity of π_C to the informative priors used on β_0, β_1, and δ. This is not possible using the summary information provided in Fleischman and Burwen (2003). Nonetheless, it would be trivial to calculate from the posterior sample. For example, the derivative of the Bayes estimate of π_C with respect to the prior mean β_0 is, from eq. 2, simply the posterior covariance between π_C and β_0 divided by the prior variance of β_0.

Discussion

The formal use of prior information by Bayesian models has been promoted as an advantageous feature of the Bayesian paradigm compared with the traditional frequentist

© 2005 NRC Canada

approach (Hilborn and Liermann 1998). However, informative priors can be highly contentious and it is important to determine if posterior inference is sensitive to the range of defensible informative priors that could used. An informal sensitivity analysis that refits the model for several different priors can easily be performed, notwithstanding the additional computational cost. However, we have shown here that a parametric form of local sensitivity can be implemented, at no additional computational expense. It calculates derivatives of Bayes estimates with respect to parametric change in the prior and provides readily interpretable quantitative summaries of sensitivity to prior specification.

The formula for local sensitivity is particularly convenient when sensitivity is with respect to parameters that have an exponential family prior, a priori independent of other model parameters. In the simplest case, if a parameter has a normal prior then the sensitivity of its Bayes estimate to its prior mean is simply the ratio of posterior variance to prior variance. This simple result enables sensitivity to prior specification to be deduced for some previously published Bayesian analyses, including the analysis of Fleischman and Burwen (2003), which was covered in example 3 herein, and the Bayesian surplus production analysis of Hoenig et al. (1994).

In the stock–recruit example, an estimate of uncertainty in the prior mean of parameter a (logarithm of maximum annual reproductive rate) was known, and posterior inference was seen to be relatively insensitive to this uncertainty. Similarly, in the mixture model example (Fleischman and Burwen 2003), the high sensitivity to the prior means of the baseline information will not be of concern if this baseline information is well estimated from the experiments with tethered fish.

In addition to the prior on a, the stock–recruit example also deployed a rather arbitrary prior on parameter S_{max} (optimal number of spawners) that was intended to be vaguely informative. This prior would be difficult to defend and a wide range of alternative priors could be postulated. For example, some readers might prefer a prior that halves or doubles the scale of the one used. It was seen that the derivative of the Bayes estimate of S_{max} with respect to its prior mean was 0.77. Given the wide range of plausible alternative priors it must be concluded that posterior inference from this model is sensitive to prior specification. This inference should not be used until prior knowledge about S_{max} is better determined.

Within the WinBUGS software, estimation of local sensitivity can be facilitated by defining an appropriate $\boldsymbol{D}$ vector. The derivatives of Bayes estimates are then obtained as posterior covariances of elements of $\boldsymbol{D}$. At present, WinBUGS 1.4 does calculate correlations during MCMC sampling, but unfortunately does not make the values of these correlations, or the associated covariances, available to the user. Thus, the covariances were calculated external to WinBUGS. We are currently exploring implementation options for fully automating, without the requirement of explicitly specifying $\boldsymbol{D}$, calculation of the sensitivities in real time within MCMC software.

The derivatives of the Bayes estimates are calculated using observed posterior covariances calculated from a posterior sample, and hence are estimates of the true posterior covariance. We calculated the MCMC sampling error of the observed posterior covariances by modeling the cross-terms (in the equation for sample covariance) using an autoregressive function within the R package. For all of the posterior covariances calculated herein, the coefficient of variation due to MCMC sampling was no more than 1%.

We close by remarking that specification of so-called noninformative priors is also contentious in all but the simplest of models. However, in this context, one is not concerned with sensitivity with respect to hyper-parameters, but rather with respect to the functional form of the prior (Kass and Wasserman 1996; Millar 2002).

References

Berger, J.O. 2000. Bayesian robustness. *In* Robust Bayesian analysis. *Edited by* D. Ríos Insua and F. Ruggeri. Springer-Verlag, New York. pp. 1–32.

Dale, A.I. 1999. A history of inverse probability from Thomas Bayes to Karl Pearson. Springer-Verlag, New York.

Fleischman, S.J., and Burwen, D.L. 2003. Mixture models for the species apportionment of hydroacoustic data, with echo-envelope length as the discriminatory variable. ICES J. Mar. Sci. **60**: 592–598.

Gelman, A., and Rubin, D.B. 1992. Inference from iterative simulation using multiple sequences. Stat. Sci. **7**: 457–472.

Gelman, A., Carlin, J.B., Stern, H.S., and Rubin, D.B. 1995. Bayesian data analysis. Chapman & Hall/CRC, New York.

Geweke, J. 1992. Evaluating the accuracy of sampling-based approaches to calculating posterior moments. *In* Bayesian statistics 4. *Edited by* J.M. Bernardo, J.O. Berger, A.P. Dawid, and A.F.M. Smith. Clarendon Press, Oxford, UK. pp. 169–193.

Geweke, J. 1999. Simulation methods for model criticism and robustness analysis. *In* Bayesian statistics 6. *Edited by* J.M. Bernardo, J.O. Berger, A.P. Dawid, and A.F.M. Smith. Clarendon Press, Oxford. pp. 275–299.

Gustafson, P. 2000. Local robustness in Bayesian analysis. *In* Robust Bayesian analysis. *Edited by* D. Ríos Insua and F. Ruggeri. Springer-Verlag, New York. pp. 71–88.

Harley, S.J., and Myers, R.A. 2001. Hierarchical Bayesian models of length-specific catchability of research trawl surveys. Can. J. Fish. Aquat. Sci. **58**: 1569–1584.

Heidelberger, P., and Welch, P.D. 1983. Simulation run length control in the presence of an initial transient. Operations Res. **31**: 1109–1144.

Hilborn, R., and Liermann, M. 1998. Standing on the shoulders of giants: learning from experience in fisheries. Rev. Fish Biol. Fish. **8**: 273–283.

Hoenig, J.M., Warren, W.G., and Stocker, M. 1994. Bayesian and related approaches to fitting surplus production models. Can. J. Fish. Aquat. Sci. **51**: 1823–1831.

Kass, R.E., and Wasserman, L. 1996. The selection of prior distributions by formal rules. J. Am. Stat. Assoc. **91**: 1343–1370.

Lee, P.M. 1997. Bayesian statistics: an introduction. Redwood Books, Trowbridge, Wiltshire, UK.

McAllister, M.K., and Ianelli, J.N. 1997. Bayesian stock assessment using catch-age data and the sampling–importance resampling algorithm. Can. J. Fish. Aquat. Sci. **54**: 284–300.

Millar, R.B. 1987. Maximum likelihood estimation of mixed stock fishery composition. Can. J. Fish. Aquat. Sci. **44**: 583–590.

Millar, R.B. 1990. Comparison of methods for estimating mixed stock fishery composition. Can. J. Fish. Aquat. Sci. **47**: 2235–2241.

Millar, R.B. 2002. Reference priors for Bayesian fisheries models. Can. J. Fish. Aquat. Sci. **59**: 1492–1502.

© 2005 NRC Canada

Millar, R.B. 2004. Sensitivity of Bayes estimators to hyper-parameters, with an application to maximum yield from fisheries. Biometrics, **60**: 536–542.

Millar, R.B., and Methot, R.D. 2002. Age-structured meta-analysis of U.S. West Coast rockfish (Scorpaenidae) populations and hierarchical modeling of trawl survey catchabilities. Can. J. Fish. Aquat. Sci. **59**: 383–392.

Myers, R.A., Bowen, K.G., and Barrowman, N. 1999. Maximum reproductive rate of fish at low population sizes. Can. J. Fish. Aquat. Sci. **56**: 2404–2419.

Plummer, M., Best, N.G., Cowles, M.K., and Vines, S.K. 2004. CODA: output analysis and diagnostics for MCMC (http://www.fis.iarc.fr/coda/).

Quinn, T.J., and Deriso, R.B. 1999. Quantitative fish dynamics. Oxford University Press, New York.

R Development Core Team. 2004. R: a language and environment for statistical computing. R Foundation for Statistical Computing (http://www.R-project.org).

Raftery, A.E., and Lewis, S.M. 1992. One long run with diagnostics: implementation strategies for Markov chain Monte Carlo. Stat. Sci. **7**: 493–497.

Ríos Insua, D., and Ruggeri, F. 2000. Robust bayesian analysis. Vol. 152. Springer-Verlag, New York.

Spiegelhalter, D.J., Thomas, A., and Best, N.G. 1999. WinBUGS. Version 1.2. User manual. MRC Biostatistics Unit, Cambridge, UK.

Appendix A

The examples herein all demonstrated sensitivity with respect to normal or log-normal priors. More generally, Millar (2004) showed that if θ_i comes from an exponential family of the form

$$\pi(\theta_i;\gamma,\phi) = \exp\left\{\frac{\gamma\theta_i - b(\gamma)}{a(\phi)} + c(\theta_i,\phi)\right\}$$

then

$$\frac{\partial E(g(\boldsymbol{\theta})|\boldsymbol{y})}{\partial\gamma} = \frac{\mathrm{cov}(g(\boldsymbol{\theta}),(\theta_i)|\boldsymbol{y})}{a(\phi)}$$

Here, γ is the canonical parameter and $a(\phi)$ is typically a nuisance parameter.

Appendix B. WinBUGS code for example 1

The code uses a loop to simultaneously fit the model with multiple priors. Vector ***D*** is used to facilitate easy computation of the sensitivities.

```
model{
#10% and 90% bounds for ad hoc prior on Smax (millions)
Bound10<-1; Bound90<-10
pri.mean.log.Smax<-(log(Bound10)+log(Bound90))/2
pri.mean.log.beta<-pri.mean.log.Smax
#Note: The 90% percentile of a std normal is 1.281552
pri.var.log.beta<-pow((log(Bound90)-log(Bound10))/(2* 1.281552),2)
pri.prec.log.beta<-1/pri.var.log.beta
#Informative prior on a = log(alpha), from Myers et al. (1999)
pri.mean.log.alpha<-1.22
pri.var.log.alpha<-0.12
pri.prec.log.alpha<-1/pri.var.log.alpha
# j indexes the priors, P = Number of priors
inc <-log(2)*2/(P-1)
for(j in 1:P){
 tau[j] ~ dgamma(1.0E-3, 1.0E-3)
 #sequence of P prior means for log(alpha), with increment inc
 mus[j]<-pri.mean.log.alpha+(j-1-(P-1)/2)*inc
 alphas[j] ~ dlnorm(mus[j],pri.prec.log.alpha)
 log.alphas[j]<-log(alphas[j])
 betas[j] ~ dlnorm(pri.mean.log.beta, pri.prec.log.beta)
 Rmaxs[j]<-alphas[j]/(exp(1)*betas[j])
 Smaxs[j]<-1/betas[j]
 for(k in 1:N){
  Y[j,k]<- log(R[k]/S[k])
  expected[j,k] <- log.alphas[j] - betas[j]*S[k]/1000 #Spawners in millions
  Y[j,k]~dnorm(expected[j,k],tau[j])
  }
}
D[1]<-Smax
D[2]<-Rmax
D[3]<-alpha
```

© 2005 NRC Canada

```
D[4]<-a/(pri.var.log.alpha*exp(pri.mean.log.alpha+0.5*pri.var.log.alpha))
D[5]<-s/(pri.var.log.beta*exp(-pri.mean.log.beta+0.5*pri.var.log.beta))
D[6]<-a/pri.var.log.alpha
D[7]<-s/pri.var.log.beta
#Parameters of interest
alpha<-alphas[(P+1)/2]
a<-log(alpha)
beta<-betas[(P+1)/2]
Smax<-1/beta
s<-log(Smax)
Rmax<-alpha/(exp(1)*beta)
}
############ DATA ###################
list(N = 30,P = 21,
R = c(2446,14934,10031,8050,7884,4430,13086,6051,7801,5846,6101,4175,2541,2194,1512,
6704,5742,8809,4062,9277,15452,10343,8950,30011,3999,9917,4906,18215,9461,23359), S =
c(1418,2835,1957,4033,2750,2891,3098,2001,3215,2443,2561,2834,2859,2295,1880,
1579,1373,4183,2984,5059,2669,3949,4219,4290,3976,8799,2856,4289,2892,4577))
############INITS#######################
list(tau = c(1,1,1,1,1,1,1,1,1,1,1,1,1,1,1,1,1,1,1,1,1),
  alphas = c(4,4,4,4,4,4,4,4,4,4,4,4,4,4,4,4,4,4,4,4,4))
```

© 2005 NRC Canada

Comparison of size-at-age of larval Atlantic cod (*Gadus morhua*) from different populations based on size- and temperature-dependent growth models

A. Folkvord

Abstract: This study presents the first intraspecific evaluation of larval growth performance across several different experimental scales, environments, and regions of a marine fish species. Size- and temperature-dependent growth models for larval and early juvenile Atlantic cod (*Gadus morhua*) are developed based on selected laboratory experiments with cod fed in excess. Observed sizes-at-age of cod from several experiments and stocks are compared with predictions from the models using initial size and ambient temperature history as inputs. Comparisons with results from other laboratory experiments reveal that the model predictions represent relatively high growth rates. Results from enclosure experiments under controlled seminatural conditions generally provide growth rates similar to those predicted from the models. The models therefore produce suitable reference growth predictions against which field-based growth estimates can be compared. These comparisons suggest that surviving cod larvae in the sea typically grow at rates close to their size- and temperature-dependent capacity. This suggests that climatic influences will strongly affect the year-to-year variations in growth of cod during their early life history owing to their markedly temperature-dependent growth potential.

Résumé : Cette étude présente la première évaluation intraspécifique de la performance de la croissance larvaire d'une espèce de poisson marin sur plusieurs échelles expérimentales différentes et dans divers environnements et régions. L'élaboration de modèles de croissance de larves et de très jeunes morues franches (*Gadus morhua*) en fonction de la taille et de la température se base sur des expériences en laboratoire choisies dans lesquelles les morues sont nourries en excès. Les tailles de la morue observées en fonction de l'âge dans plusieurs expériences et stocks sont alors comparées aux prédictions des modèles qui utilisent la taille initiale et la température ambiante expérimentée comme variables d'entrée. Des comparaisons avec les résultats d'autres expériences de laboratoire indiquent que les prédictions des modèles représentent des taux de croissance relativement élevés. Les résultats d'expériences en enclos dans des conditions contrôlées semi-naturelles fournissent généralement des taux de croissance semblables à ceux que prédisent les modèles. Les modèles fournissent donc des prédictions de référence adéquates de la croissance aux fins de comparaison avec les estimations de croissance déterminées en nature. Ces comparaisons indiquent que les larves de morue qui survivent dans la mer croissent généralement à des taux qui s'approchent de leur potentiel, compte tenu de leur taille et de la température. On peut donc croire que les influences climatiques affecteront fortement la variation d'une année à l'autre de la croissance des morues au début de leur cycle biologique à cause de leur potentiel de croissance fortement dépendant de la température.

[Traduit par la Rédaction]

Introduction

Fish larvae exhibit highly variable growth rates when raised at different temperatures and food levels (Houde 1989; Letcher and Bengtson 1993; Otterlei et al. 1999). Larval survival has also been shown to depend on food availability, where slow-growing and poorly conditioned larvae either directly or indirectly suffer elevated starvation-related mortality (Ellertsen et al. 1981; Werner and Blaxter 1981; Jonas and Wahl 1998). Growth and condition are closely linked in fish larvae and high priority is given to the allocation of energy to growth (Pedersen 1997; Finn et al. 2002). This may be a reflection of the high mortality associated with smaller sizes in the larval stage (McGurk 1986; Miller et al. 1988), where the advantage of growing faster (and bigger) outweighs the benefits of depositing energy storage for subsequent periods of food shortage. One of the consequences is that the time period from onset of food deprivation to starvation mortality does not increase noticeably with size in the larval stage (Miller et al. 1988; Jordaan and Brown 2003).

Size-at-age provides an integrated measure of the past feeding history and growth of surviving larvae. Specifically, smaller sizes-at-age than possible given the predicted capacity for growth at the prevailing environmental conditions indicate previous periods of food limitation that may have been associated with elevated mortality. A similar approach

Received 23 April 2004. Accepted 17 December 2004. Published on the NRC Research Press Web site at http://cjfas.nrc.ca on 20 May 2005.
J18084

A. Folkvord. Department of Biology, University of Bergen, 5020 Bergen, Norway (e-mail: arild.folkvord@bio.uib.no).

 doi: 10.1139/F05-008 © 2005 NRC Canada

has been applied in clinical medicine, where reference growth curves, indicating expected growth performances, are in common use to assess growth and development of infants (Onis et al. 1997; Victora et al. 2000). The problem of using size-at-age as a comparative measure in larval fish is that growth is strongly influenced by temperature conditions, making simple comparisons difficult (Øiestad 1984). Rather than a growth relationship in which size depends only on age as in homeotherms such as humans (Victora et al. 2000), ambient temperature must also be included in reference growth curves for fish. Temperature-corrected growth models for juvenile and adult fish have been used to compare growth rates of fish from different stocks (Brander 1995), but to date, no comprehensive comparisons of growth performance have been undertaken for the early life stages of a marine fish species. Here, I present a new approach to evaluate growth performance in young fish using Atlantic cod (*Gadus morhua*) as a model species.

Previously developed age-based growth models for cod larvae that are appropriate for constant temperature conditions (e.g., Campana and Hurley 1989; Otterlei et al. 1999) lack the flexibility needed when comparing offspring from variable temperature conditions. Therefore, the purpose of this study is firstly to provide general size-based models for growth in larval cod that incorporate temperature and initial size as input variables so that comparisons can be made across different experimental scales, environments, and regions. The models will then be compared with other laboratory studies to confirm that the model predictions are based on data from the highest laboratory growth rates available. Thereafter, the model will be validated against observation from enclosure studies under seminatural conditions that are characterized by high survival and growth rates (Øiestad 1984). Finally, the model outputs will be compared against growth estimates from the field obtained through otolith microstructure analysis. The growth performance of the larvae from the different environments is evaluated using a common metric, and the robustness of the model outputs is also investigated through evaluation of initial assumptions and temperature relationships. To my knowledge, this is the first attempt to evaluate the growth performance of surviving fish larvae from several field locations and environments relative to their size- and temperature-dependent growth potential. Based on the importance of size-dependent mortality in marine fish larvae (e.g., Miller et al. 1988; Bailey and Houde 1989; Houde 1997), it is hypothesized that surviving cod larvae at sea are generally characterized by relatively high growth rates.

Materials and methods

Model development

Size- and temperature-dependent growth (STDG) models are reparameterized from previously published Gompertz-type age- and temperature-dependent growth (ATDG) models (Otterlei et al. 1999). The models are based on data from extensive laboratory experiments with northeast Arctic (NA) cod and Norwegian coastal (NC) cod conducted over two seasons. The cod larvae were fed natural plankton in excess at constant temperatures in the range 4–14 °C under a daily and seasonally fluctuating light cycle. Larvae were sampled weekly over a 2-month period each year and measured for length and weight (range approximately 0.02–200 mg dry weight (DW) and 3.5–45 mm live standard length (SL)). The lower temperature groups did not cover the same size range, and the model is therefore not adequately documented outside the size range of 0.03–50 mg DW for the entire temperature range. The original ATDG models indicated an asymmetric dome-shaped relationship between age and growth rate at the given temperatures, and the models explained more than 95% of the variability in size-at-age (see Otterlei et al. (1999) for further details). In this study, third-degree polynomial models are thus selected as the basis for the STDG models to accommodate for this initial increase and subsequent relatively slower decline in growth rate with increasing fish size. The daily specific growth rate (SGR) (percent per day) is given as

$$(1) \qquad \mathrm{SGR} = c_0 + c_1 \ln\mathrm{DW} + c_2(\ln\mathrm{DW})^2 + c_3(\ln\mathrm{DW})^3$$

with $c_i = a_i + b_i\mathrm{Temp}$, where Temp is the average daily temperature (°C) and ln DW is the natural log of the estimated stock-specific larval dry weight (mg) on a given day. A quadratic temperature term is not used, since a previous study has shown that the temperature effect on growth was approximately linear in the temperature range of the original data (Otterlei et al. 1999).

The parameters of the models are estimated by stepwise nonlinear procedures (StatSoft Inc. 1995) using the daily temperature-specific growth rates and dry weights from the ATDG models as inputs (Otterlei et al. 1999). Nonsignificant terms of eq. 1 were excluded in the final models. In this paper, specific growth rate is defined as

$$(2) \qquad \mathrm{SGR} = 100 \cdot (e^{g} - 1)$$

where g is the instantaneous growth coefficient either obtained by derivation of the Gompertz size-at-age function (Otterlei et al. 1999) or defined as

$$(3) \qquad g = (\ln\mathrm{DW}_2 - \ln\mathrm{DW}_1)/(t_2 - t_1)$$

where DW_i is the dry weight at time t_i. Separate models are fitted to the data for NA cod and NC cod, and only significant parameters are included in the final models.

Data selection

The following criteria were applied when selecting data sets to be included in the comparative analysis: (*i*) the larval groups were not fed restricted diets and the fish exhibited significant positive growth (only data from highest food levels were used from laboratory and enclosure studies), (*ii*) the data were available from personal sources and (or) published in peer-reviewed journals, (*iii*) the durations of the experiments were beyond 3 weeks and beyond period of initial starvation mortality, (*iv*) initial and (or) final sizes were available, including information on shrinkage correction, (*v*) at least two measurements of size-at-age (or an alternative model output) from the same population were available (single cross-sectional data were used on two occasions for field studies), (*vi*) data where both the larval sizes and temperatures were outside the main range of the model domain at any given time were not included (cases where either the temperature exceeded the 4–14 °C range or the larval size exceeded the 0.03–50 mg DW range are mentioned explic-

© 2005 NRC Canada

itly), (*vii*) temperature data were presented in the paper or could be approximated from other sources (e.g., internet, see below), and (*viii*) the larval groups had only been feeding on live plankton. These criteria were chosen to select good-quality data from well-growing known-aged laboratory and enclosure groups as well as aged groups from the field. It was not the intention of this study to present a complete review of all published experimental growth results of larval cod; rather, the intention was to select those studies that a priori could be expected to contain growth rates that best described the growth potential. Two model predictions are also included using the original data underlying the ATDG and STDG models, the 6 and 10 °C NC cod data, which represent the series with the poorest and best fit to the original ATDG models, respectively (Otterlei et al. 1999). In total, 40 data series from 25 studies are included in this study (Table 1).

Data analysis

The models were initialized with the average initial sizes-at-age as inputs. In cases where several replicate units were used in the experiment, the average of the replicates was used. Since the STDG models like the ATDG models produce monotonically increasing sizes, the initial growth rates were taken to represent the embryonic growth (Otterlei et al. 1999). To correct for variable amounts of yolk included in the published initial dry weights, I used the following approximation to relate early embryonic weight to total larval weight (including yolk) based on data from cod larvae kept at 7 °C (Solberg and Tilseth 1987):

$$\text{EDW} = \text{TDW}(0.7 + 0.05\text{DPH}) \quad (4)$$

where EDW is embryo dry weight, TDW is total dry weight including yolk, and DPH is days posthatching. For larvae older than 6 days, the EDW is set equal to the total dry weight (termed DW hereafter). If daily temperature estimates were not available, linear interpolations between days were used to obtain the data for the models. If depth-stratified temperature data were available, the distribution of larvae in the water column determined whether the mean water temperature of the water column or the temperatures at specific depths (maximum temperatures) were used. The models were run with temperatures ranging from 2 to 16 °C, slightly outside the range of 4–14 °C from which the model was developed (Table 1). The model was also run for sizes exceeding the 50 mg DW as long as the temperature at this point was between 8 and 14 °C (see above). When the average initial weights are unknown, i.e., for field data, an initial DW of 45 µg was used (corresponding to 4.4 mm live SL). No correction for shrinkage was used when the same fixation had been used throughout a study. The model predictions were calculated throughout the period of investigation on a daily basis with the daily temperature history and estimated size each day as inputs. All of the laboratory and mesocosm studies are based on known-age material, while the field material has been aged by use of otolith microstructure analysis (Campana 1992). Average estimated ages of larvae from the different data series are used to estimate mean hatch dates and corresponding temperature histories.

No size-dependent mortality corrections were applied to any of the data sets. Typically, the apparent growth rates of a cohort are overestimates of individual growth rates when smaller individuals in a cohort of larvae have relatively higher mortality (Folkvord 1997). In papers where lengths were reported as the size measure instead of DW, I used the following length to weight relationships when no other relationship was presented in the paper:

$$\ln\text{DW} = -9.38 + 4.55 \ln\text{SL} - 0.2046(\log\text{SL})^2 \quad (5)$$

$$\ln\text{SL} = 2.296 + 0.277 \ln\text{DW} - 0.005128(\log\text{DW})^2 \quad (6)$$

where SL is live standard length (mm) and DW is dry weight (mg) from frozen specimens (data from Folkvord et al. 1999; $n = 509$, $r^2 = 0.995$, SE of the estimate = 0.130 and 0.035, respectively). Total length was estimated from SL with the relationship

$$\text{TL} = -0.20 + 1.082\text{SL} \quad (7)$$

where TL is live total length (mm) (R.N. Finn, Department of Biology, University of Bergen, N-5020 Bergen, Norway, unpublished data).

Separate STDG models are used for offspring of NA cod and NC cod. For the other laboratory studies with offspring from other populations, I compare their growth rates against the NC cod model outputs, since this is the model that predicts the highest growth rates. The sizes-at-age are estimated for the duration of the experiments or to a maximum of 90 DPH. The model outputs are compared directly with the observed size-at-age for the included studies. In addition, I calculate the growth performance in the different studies relative to model predictions as

$$\text{Growth ratio} = \frac{\text{average observed SGR}}{\text{average modeled SGR}} \quad (8)$$

where common initial weights and respective final weights are used. The growth ratio thus represents the average proportional daily growth rate of the observed versus modeled growth rates. The same growth performance measure was used when comparing the effects of changing the initial size or the subsequent temperature history. In this case, the modified growth rate was divided by the original growth rate.

To evaluate the effect of initial size on the size predictions of the field data, three initial sizes (30, 45, and 67.5 µg) were used in a 70-day, 6 °C simulation. These weights were termed lower, middle, and upper initial size estimates, and the relative initial size ratio was 1.5 between middle and lower and upper and middle. In addition, I ran a test of the temperature sensitivity by adding 1 °C to or subtracting 1 °C from the estimated temperature for Georges Bank from Campana and Hurley (1989) throughout the 90-day period. In both cases, the effect of the parameter change was estimated by relative difference in final weights and the change in growth ratio.

Results

STDG models

For both the NC and NA data series, a five-parameter STDG model explained nearly all of the variability of the estimated growth rates of the ATDG models (Otterlei et al. 1999) (stepwise nonlinear estimation, $r^2 > 0.997$, $n = 434$ and 451 for NC cod and NA cod, respectively). The models predict a maximum growth rate prior to initiation of metamorphosis (at around 0.7 mg DW and 9 mm SL) and a linear

© 2005 NRC Canada

Table 1. Sources of growth- and size-at-age data of larval and juvenile cod (*Gadus morhua*) used in the study.

Reference	Study code	Area or place of study	Temperature (°C)	Initial DW used (µg)	Duration (days)	Fixation and measures	Comments (temperature data from paper unless specified otherwise)
Laboratory studies							
Laurence 1978	L1	Rhode Island, USA	4, 7, 10	36–43 on day 0	35–49	Not specified	First pioneering laboratory growth study on larval cod
Laurence et al. 1981	L2	Rhode Island, USA	7	44 on day 0	42	Fixed in formalin	Low survival in highest prey density group (sampled to extinction)
Buckley et al. 1993	L3	Rhode Island, USA	7[a]	35 on day 0	42	Fresh for SL, frozen for DW	31%–44% survival in high prey density group
Otterlei et al. 1999	L4	Bergen, Norway	6, 10 (4, 8, 12, 14 not shown here)	30 on day 0	56	Fresh for SL, frozen for DW	5%–45% survival, basis for growth models, otoliths removed before DW measurements, only NC cod data shown here
Folkvord et al. 1999	L5	Bergen, Norway	8	38 on day 0	56	Fresh for SL, frozen for DW	47%–65% survival of NA cod, six replicates, used SL–DW relationship from this study
Baskerville-Bridges and Kling 2000	L6	Maine, USA	10–11, experiment I	30 on day 0	44	Fresh for SL, frozen for DW	Fed rotifers and *Artemia* (from day 22 or 16), 29%–36% survival (experiments I and II in paper)
			7–8, experiment II		36		
Puvanendran and Brown 2002	L7	Newfoundland, Canada	8	48 on day 0	42	Fresh for SL and DW	High light intensity and 24:0 light cycle gave best growth, 30%–40% survival
Mesocosm studies							
Ellertsen et al. 1981	E1	Fladevigen, Norway	4.5–9.9	50 on day 11	52	4% buffered formaldehyde	First group 1976, first mesocosm study of NC larval cod growth in a century, 10% survival
Pedersen et al. 1989	E2	Tromsø, Norway	2.0–11.5 (max. temperature)	34 on day 4	50	4% buffered formaldehyde	Low initial temperatures in 1987, 7% survival, several releases[b]
Olsen et al. 1991	E3	Tromsø, Norway	6.1–14.7 (mean temperature)	75 on day 11	70	4% buffered formaldehyde	Rapid growth in 1989, larval DW estimated from SL[b]
Blom et al. 1991	E4	Øygarden, Norway	3.7–11.9 (mean temperature)	61 on day 6	80	4% buffered formaldehyde	1988 NC cod data, last samples taken with dip net, 23% survival to metamorphosis
Blom et al. 1994	E5	Øygarden, Norway	5.8–9.8	32 on day 2	45	4% buffered formaldehyde	Average of two strains of NC cod in 1991, 23% survival[c]
Folkvord et al. 1994	E6	Austevoll, Norway	6.8–11.2 (max. temperature)	33 and 34 on day 4 and day 5	40, 29	4% buffered formaldehyde	1985 cohorts 1 and 2 with NC cod, 40% and 15% survival
van der Meeren et al. 1994	E7	Austevoll, Norway	4.4–12.2, 7.4–12.3	44 and 42, 42 and 40 on day 2	48, 36	Fresh for WW and DW	1993 data (experiments I and II) on NC and NA cod, 28%–83% survival

© 2005 NRC Canada

Table 1 (*concluded*).

Reference	Study code	Area or place of study	Temperature (°C)	Initial DW used (μg)	Duration (days)	Fixation and measures	Comments (temperature data from paper unless specified otherwise)
Field studies							
Bolz and Lough 1988	F1	Georges Bank, Northwest Atlantic	4.6–10.2	45 on day 0	90	Corrected for shrinkage	Temperature data from Campana and Hurley (1989), sampling with 61-cm Bongo net and 1- to 10-m MOCNESS and an otter trawl for larger cod
Campana and Hurley 1989	F2	Browns and Georges banks, Northwest Atlantic	5.3–8.4, 5.1–9.9	45 on day 0	120 (90 used)	Not corrected for shrinkage	First age- and temperatue-dependent growth model for field larvae, 3 mm TL at day 0, sampling with 61-cm Bongo net
Meekan and Fortier 1996	F3	Scotian Shelf, Northwest Atlantic	7.6–2.3, 8.0–3.1	45 on day 0	80	Fresh for SL	Temperature data from Department of Fisheries and Oceans, S1 and S2 cohorts, sampling with 2-m^2 trawls
Suthers and Sundby 1996	F4	Browns Bank and northern Norway, Northeast Atlantic	2.5–6.0, 5.9–8.7	45 on day 0	90, 80	Not corrected for shrinkage	Data from both sides of the Atlantic, temperature data for Browns Bank from Department of Fisheries and Oceans and for Northeast Atlantic from Sundby (2000), sampling with 5- and 10-m^2 midwater trawls, respectively
Begg and Marteinsdottir 2000	F5	Northwest Iceland, North Atlantic	7.5–10.6, 3.0–8.2	45 on day 0	93, 84	Modeled fresh TL	Data from 1988, northern and southern area, used 57.5 and 45 mm as reported final TL; sampling with a 324-m^2 pelagic trawl
Anderson and Dalley 2000	F6	Grand Banks, Northwest Atlantic	3.7–7.8, 5.5–8.8	45 on day 0	65, 68	Fresh for TL	Data from cold year (1997) and warm year (1996), authors used 3.5 mm TL on day 0, sampling with 61-cm Bongo net and 73-m^2 IYGPT trawl

Note: L, E, and F denote laboratory, enclosure, and field studies, respectively. NA, northeast Arctic cod; NC, Norwegian coastal cod. Initial weights have been corrected for presence of yolk. SL, standard length; DW, dry weight; WW, wet weight; TL, total length.

[a]L. Buckley, University of Rhode Island/National Oceanic and Atmospheric Administration (URI/NOAA) Cooperative Marine Education and Research Program, Graduate School of Oceanography, Narragansett, RI 02882, USA.

[b]T. Pedersen, Norwegian College of Fisheries Science, University of Tromsø, 9001 Tromsø, Norway.

[c]G. Blom, Department of Biology, University of Bergen, N-5020 Bergen, Norway.

© 2005 NRC Canada

Fig. 1. Plots of size- and temperature-dependent growth models for (*a*) Norwegian coastal (NC) Atlantic cod (*Gadus morhua*) and (*b*) northeast Arctic (NA) cod. Equation for each relationship: NC cod, specific growth rate (SGR) = 1.20 + 1.80·temperature – 0.078·temperature·ln DW – 0.0946·temperature·(ln DW)^2 + 0.0105·temperature·(ln DW)^3; NA cod, SGR = 1.08 + 1.79·temperature – 0.074·temperature·ln DW – 0.0965·temperature·(ln DW)^2 + 0.0112·temperature·(ln DW)^3. DW, dry weight.

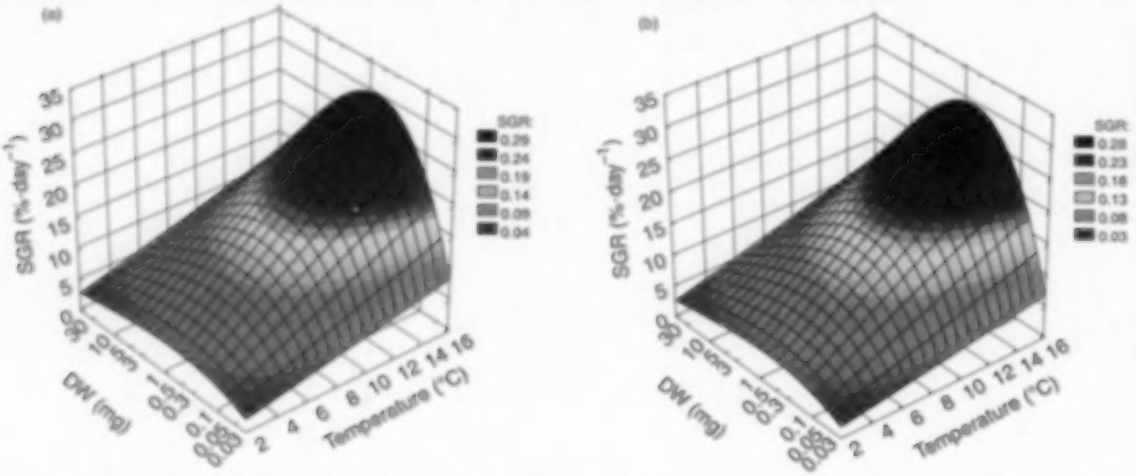

increase in growth rate with temperature at any given size within the model domain (Fig. 1). At the upper size range, minimum predicted growth rates were found at 450 and 600 mg DW (55–59 mm SL) for the NA cod and NC cod, respectively. Beyond these sizes, the predicted growth rates slowly started to increase again. This is unrealistic, and the models should therefore not under any circumstance be used beyond the size of minimum growth rate. At 0 °C, the models predict size-independent growth rates slightly above 1%·day^{-1}, but further experimentation is needed at low temperatures to verify if this is realistic. At the high end of the temperature spectrum, the growth will eventually cease when temperature approaches lethality for cod (approximately 16 °C for newly hatched larvae (Iversen and Danielssen 1984) and above 20 °C for early juveniles (Otterlei 2000)), while the STDG models will still predict linearly increasing growth rates with increasing temperature. The models should thus be used with caution at temperatures below 4 °C and above 14 °C for which data were available to parameterize the STDG models, although maximum growth of early cod juveniles has been observed at 16–18 °C (Otterlei 2000). The estimated daily NC cod growth rates were typically between 0.2% and 0.5% higher than the NA cod growth estimates within the data range used. Overall, the STDG models were considered to be suitable alternative parameterizations of the original ATDG models, since they were easier to implement in situations with changing temperature. In the ADTG models, a new age-at-size has to be calculated every time the temperature changes to reflect the age that the larvae should have as if it had been growing at the same temperature throughout. Otherwise, the larvae will have the "wrong" size according to the current age and temperature to be used in the ATDG model. The STDG models are used in the remainder of this study.

Comparative analyses of laboratory studies

The STDG models often predicted larger sizes than the observed sizes-at-age in the laboratory studies. This was especially true for the oldest study included in the analysis (Laurence 1978) (Fig. 2*a*). In this study, the final size-at-age predicted by the STDG model was up to 10 times higher than the observed size-at-age. Subsequent experiments in the same laboratory showed a much closer correspondence between predicted and observed size-at-age (Laurence et al. 1981; Buckley et al. 1993) (Fig. 2*b*). Strong correlations were also found between the model and the original data underlying the model for NC cod at 10 °C (best series fit), while the model initially underestimated the growth somewhat for NC cod at 6 °C, the poorest fit of the original data series (Otterlei et al. 1999) (Fig. 2*c*). Subsequent studies from the same laboratory (Folkvord et al. 1999) (Fig. 2*d*) and other laboratories (Baskerville-Bridges and Kling 2000; Puvanendran and Brown 2002) (Figs. 2*e* and 2*f*), on the other hand, indicate that the model predictions are representing relatively high larval cod growth rates. In the first experiment by Baskerville-Bridges and Kling (2000), a reduction in observed growth relative to the model in the latter half of the experiment coincides with the transition in feeding from rotifers to *Artemia*.

Validation of growth potential in enclosure studies

Observed growth rates from the enclosure studies were in general in agreement with the high predicted growth rates from the STDG models (Fig. 3). The first mesocosm study carried out in Flødevigen, Norway, in the mid-1970s was no exception (Ellertsen et al. 1981), although relatively higher growth rates were obtained in the same mesocosm in a later study (Clemmesen et al. 2003) (Figs. 3*a* and 3*b*). Subsequent experiments in larger enclosures (macrocosms) confirmed the good agreement between the NC cod STDG model and observed growth patterns (Blom et al. 1991, 1994; Folkvord et al. 1994) (Figs. 3*c* and 3*d*). In the study by Folkvord et al. (1994), the highest growth rates were observed and predicted for the second cohort released 10 days after the first cohort at somewhat elevated ambient temperatures due to the spring season temperature increase. Up to 10-fold differences in

© 2005 NRC Canada

Fig. 2. Observed (points) and predicted (lines) sizes-at-age (dph, days posthatch) from different laboratory studies. Within each panel, the dotted line and triangles represent the higher average temperature series, the solid line and squares the midtemperature series, and the dashed line and circles the lower average temperature series. Data from (*a*) L1, (*b*) L2 (solid line) and L3 (dashed line), (*c*) L4 (10 °C (dotted line) and 6 °C (dashed line)), (*d*) L5, (*e*) L6 (experiment I (dotted line) and experiment II (solid line)), and (*f*) L7.

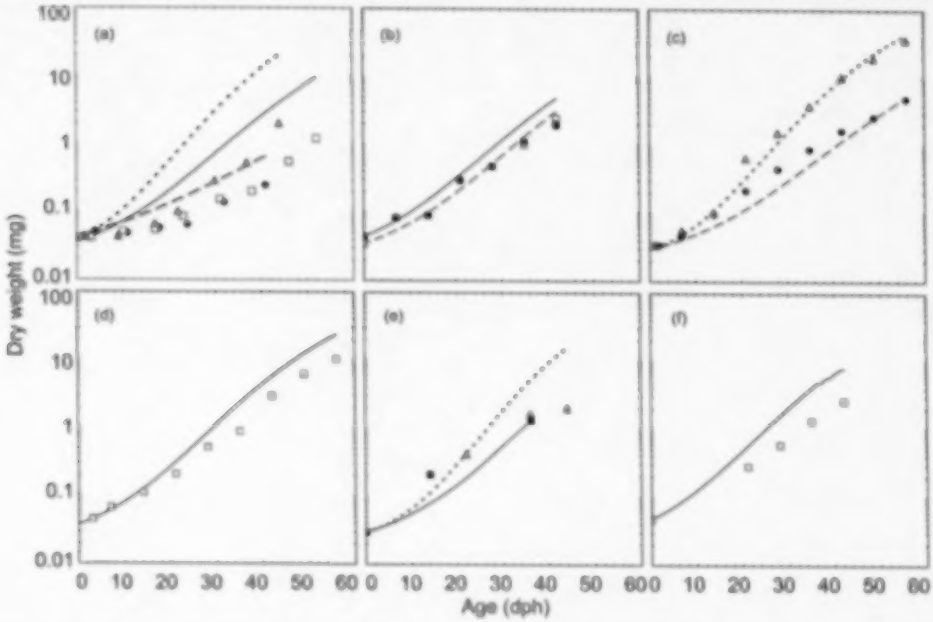

size-at-age were observed between years in one of the mesocosms in northern Norway (Pedersen et al. 1989; Olsen et al. 1991), but according to the STDG model, this was mainly attributable to the differences in ambient temperature between years (Fig. 3*b*). Experiments in bag enclosures generally yielded very similar model predictions compared with observed final sizes (Suthers et al. 1999; van der Meeren and Jørstad 2001; van der Meeren and Moksness 2003) (Figs. 3*f*–3*h*), although the observed growth in the study by Finn et al. (2002) was somewhat slower initially than predicted. On the other hand, higher than expected growth rates were observed for NC cod in the study by van der Meeren et al. (1994), where offspring were over twice as heavy as predicted at the end of the experiment in both series studied (Fig. 3*e*). The same was the case for offspring of NA cod simultaneously reared in the same enclosures (data not shown). Overall results from the enclosure studies generally confirmed an acceptable accuracy of the size-at-age predictions of the STDG models, indicating that they provided useful representations of the growth potential in larval cod.

Growth performance of cod larvae at sea

The STDG model predicted a somewhat slower initial growth than reported by Bolz and Lough (1988) in their study of fish from the Georges Bank (Fig. 4*a*). Observed and predicted size-at-age converged as the fish became larger, however. In contrast, the predictions from the Campana and Hurley (1989) model, using the same temperature field, were relatively similar initially when taking into account that they had not corrected the larval lengths for shrinkage and that the model was initialized with a TL at hatching of 3 mm (Fig. 4*a*). However, for older cod larvae, an increasing discrepancy is noted between the predictions from the Campana and Hurley (1989) model and the STDG and Bolz and Lough (1988) model predictions (Fig. 4*a*). This is largely due to a low predicted growth from the Campana and Hurley (1989) model in older larvae at relatively higher temperatures in the latter part of the study (Figs. 4*a* and 4*b*). The Campana and Hurley (1989) model has a temperature optimum at 5.9 °C, and at 4 °C, the growth pattern of the Campana and Hurley (1989) model is initially similar to that predicted from the STDG model (Fig. 4*b*). However, at a constant temperature of 9 °C, the models produce clearly divergent results (Fig. 4*b*).

Meekan and Fortier (1996) presented data from late autumn – early winter spawning cod, which, in contrast with the other cod in this review, experienced a significant temperature decrease during their early life history. There were no temperature series presented in the paper, but using the data from a hydrographical station in the area (data source: Department of Fisheries and Oceans Canada, average of 20 and 30 m at subarea 11, Emerald Bank; http://www.mar.dfo-mpo.gc.ca/science/ocean/tsdata.html), the two surviving cohorts show a size-at-age close to the predicted sizes (Fig. 4*c*). The cohort with the largest size-at-age (1992–1993) came from the warmest of the two years in the study, which was about 1 °C warmer during the first 2 months of the larval period (Meekan and Fortier 1996).

Growth data from both the eastern and western Atlantic were presented by Suthers and Sundby (1996). Although the day length differences experienced off the Canadian and Norwegian coasts may favor growth of cod from the latter region, the ambient temperature differences in the two regions seem to be the main factor explaining the observed differences in growth (Fig. 4*d*). In both cases, the

© 2005 NRC Canada

Fig. 3. Observed (points) and predicted (lines) sizes-at-age (dph, days posthatch) from different enclosure studies. Within each panel, the dotted line and triangles represent the higher average temperature series, the solid line and squares the midtemperature series, and the dashed line and circles the lower average temperature series. Thicker lines of same type in the same panel indicate size- and temperature-dependent growth predictions versus model predictions from the source paper (regular thickness) and solid symbols represent heavier initial weights. Data from (*a*) E1, (*b*) E2 (dashed line) and E3 (dotted line), (*c*) E4 (dashed lines) and E5 (solid line), (*d*) E6 (cohort 1 (solid line) and cohort 2 (dotted line)), (*e*) E7 (experiment I (solid line) and experiment II (dotted line)) (only Norwegian coastal (NC) Atlantic cod (*Gadus morhua*) data shown), (*f*) E8 (NC cod (dotted line) and northeast Arctic (NA) cod (thick dotted line)), (*g*) E9 (NC cod (dotted line) and NA cod (thick dotted line)), (*h*) E10 (dotted line) and E12 (solid line), and (*i*) E11 (mesocosm 1 (solid line) and mesocosm 2 (dotted line)).

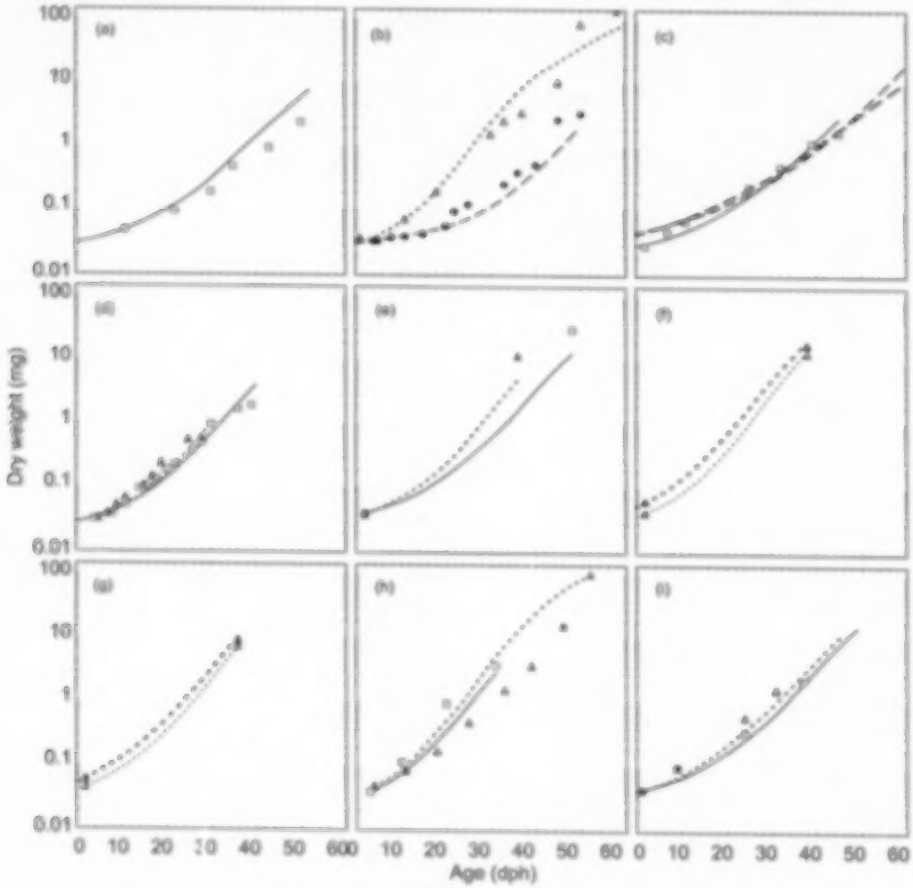

observed sizes-at-age were higher than predicted based on the STDG models (Fig. 4*d*). The same was also the case for the selected data from Begg and Marteinsdottir (2000) off the coast of Iceland. A good agreement was evident using the data from the southern (and warmer) part of the coast, while the cod from the northern (and colder) regions had apparently been growing much better than expected (Fig. 4*e*). This discrepancy was also present using the data from a cold year (1997) and a warm year (1996) off Newfoundland (Anderson and Dalley 2000). Again, a relatively good agreement was seen between observed and predicted size in the warm year, while the fish from the cold year seemed to have been growing much better than expected (Fig. 4*f*).

Comparison of growth performance of cod from different spatial scales

When comparing the growth performance in the various studies conducted at different scales, it is clear that the STDG models are based on some of the best-performing laboratory groups in the literature (Fig. 5*a*). The data of the larval groups from Laurence (1978), which have been used in several modeling studies, appear as the poor-performing outliers in this case, obtaining less than 70% of the average daily growth rate of the better performing groups. The best growth performance was found in the recent paper by Baskerville-Bridges and Kling (2000) (experiment II), which had marginally better average growth rate than expected (growth ratio of 1.01). Higher growth ratios are seen in the enclosure data series, which generally confirm the high growth rates experienced in these systems (Fig. 5*b*). In addition, the survival rates from some of these enclosure studies are among the highest reported for cod larvae in the literature (Table 1). Summarizing the results from the field investigations, it becomes clear that the surviving larvae in general

© 2005 NRC Canada

Fig. 4. Observed (points) and predicted (lines) sizes-at-age (dph, days posthatch) from different field studies. Within each panel, the dotted line represents the higher average temperature series, the solid line the midtemperature series, and the dashed line and circles the lower average temperature series. Thicker lines of same type in the same panel indicate size- and temperature-dependent growth model predictions versus model predictions from the source paper (regular thickness). Data from (*a*) F1 (solid line) and F2 (dashed line), (*b*) F2 (9 °C (dotted line), 6 °C (solid line), and 4 °C (dashed line)), (*c*) F3 (warmer 1992–1993 season (solid circles) and colder 1991–1992 season (open circles)), (*d*) F4 (Norwegian coast (solid line) and Canadian coast (dashed line)), (*e*) F5 (southern Iceland (solid line) and northern Iceland (dashed line)), and (*f*) F6 (warmer 1996 season (solid line) and colder 1997 season (dashed line)). SL, standard length.

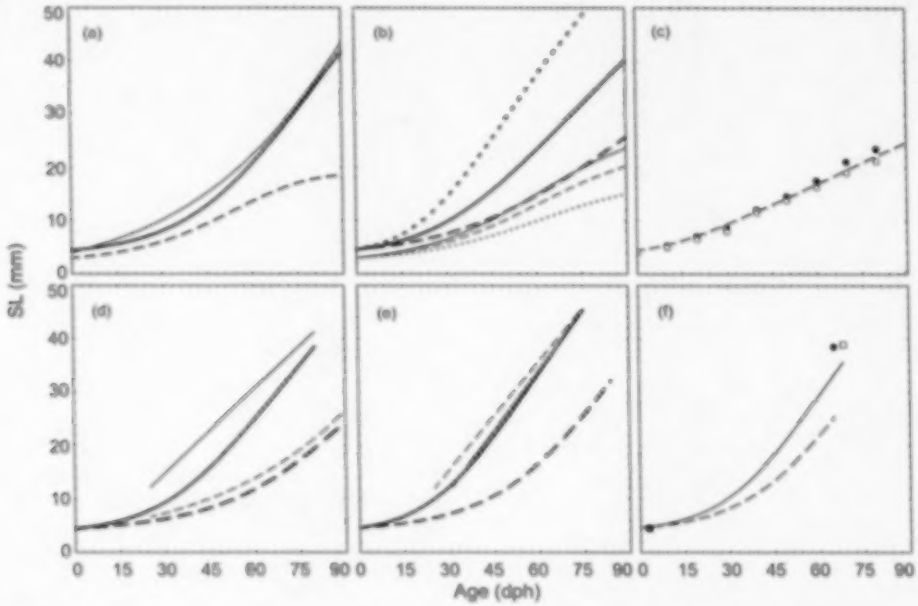

have been growing at rates close to their estimated potential (Fig. 5c). The only exception seems to be the output from the Campana and Hurley (1989) model, which clearly predicts a lower average growth than reported from the original data (Bolz and Lough 1988). The two instances of very high growth rates in the field are both based on data from cod stocks in cold-water environments (see below).

Effects of changes in initial size and temperature on subsequent growth

In the field studies, the initial sizes of the fish were generally unknown. The start weight was therefore set to 45 µg, which is somewhat above average for the laboratory and enclosure studies (Table 1). A preliminary sensitivity analysis was undertaken to evaluate the effects of changing the initial weights. Permitting 50% initial weight differences (45 versus 30 µg, middle versus lower, and 67.5 versus 45 µg, upper versus middle) generated weight differences of 100%–150% after 30–40 days. The difference in sizes increased initially due to the increasing growth rate with size for smaller larvae and then declined after the size of maximum growth had been attained (Fig. 6). In the example with cod growing at 6 °C, the size differences were reduced back close to the original size difference within a 70-day period (largest group being 50%–80% heavier). The corresponding growth ratios were 1.00 (upper/middle) and 1.05 (middle/lower) when using the respective initial weights and 1.06 and 1.12 when a using a common (and incorrect) initial weight. Thus, a 50% error in the initial weight estimate would only generate a growth ratio difference of about 0.06 when calculated over a 70-day period. Running the same simulation at higher temperatures tended to increase the initial size difference at a younger age but diminished the subsequent differences between the groups more rapidly as well.

The effects of under- or overestimating the temperature history were simulated by altering the temperature for Georges Bank by 1 °C up or down. A 1 °C elevation throughout the study period increased the final weight by 50%, while a 1 °C reduction throughout the growth period led to a 40% reduction in final weight compared with the original predictions. The corresponding growth ratios changed from 1.02 to 0.97 and 1.10, respectively, approximately the same effect on the growth ratio as reported for the change in initial size.

Discussion

STDG model justification

This study presents the first intraspecific evaluation of larval growth performance of a marine fish species across different experimental scales, environments, and regions. The development of STDG models based on larvae fed in excess has allowed the comparison of growth performances of larval groups from widely different systems and environments. Although temperature-dependent growth models for cod larvae have been presented earlier (e.g., Campana and Hurley 1989; Otterlei et al. 1999), they have been parameterized as age-based models and (or) have been based on data where feeding conditions have been confounded with temperature.

© 2005 NRC Canada

Fig. 5. Growth ratios from (*a*) laboratory, (*b*) enclosure, and (*c*) field studies (defined as the ratio of average observed daily growth rate versus average daily predicted growth rate). Numbers in the bars refer to the respective studies, with the lowest positioned number in a given bar referring to the study with the lowest value in that bar. The vertical line at 1.0 refers to the ratio where the observed average growth rate equals the predicted average growth rate.

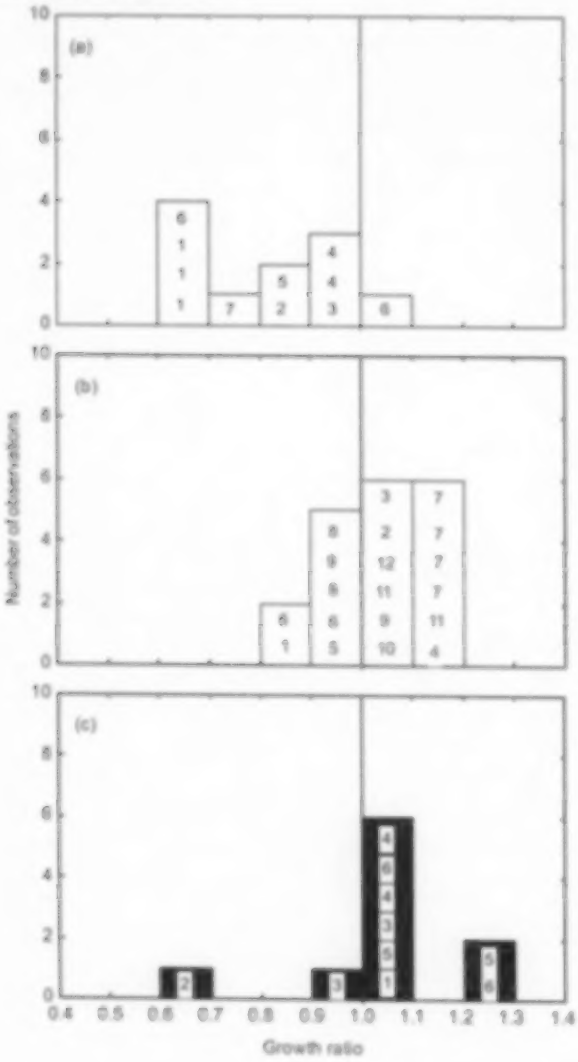

Fig. 6. Progression of size (solid lines) and growth ratios (dotted lines) (ratio of average observed value versus average predicted value) based on an above-average (upper; thick lines) initial weight (67.5 μg) or a below-average (lower; thin lines) initial weight (30 μg) relative to a mean initial weight (middle) of 45 μg. Simulations are run at 6 °C constant temperature. dph, days posthatch.

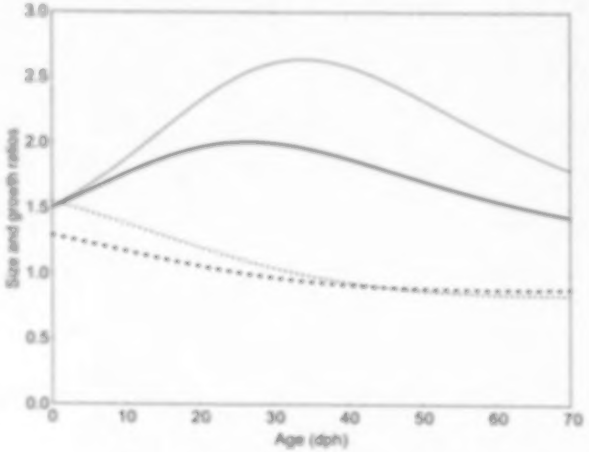

Age-based models impose certain critical assumptions when the larvae have been growing at changing temperatures, since the age-at-size will need to be adjusted as the fish move from one temperature field to another. For example, a larva that has been growing at 8 °C will in the ATDG model need to be reassigned a younger age (at a given size) when it moves into warmer waters (or an older age if moves into colder waters) to obtain the correct size-at-age according to the ATDG model. The impact of changes in age-at-size within the original model specifications is unclear. Furthermore, models based on field-sampled material where temperature and potentially confounding factors such as food level and larval size effects are not separated (Campana and Hurley 1989) are not well suited as reference growth curves either. One of the advantages of comparing the observed size-at-age with the temperature-dependent growth potential from STDG models is that the residuals can possibly serve as indirect measures of feeding conditions during the larval period.

Comparisons with several laboratory studies confirm that the underlying data for the models represent some of the most rapid laboratory growth rates for cod available after 25 years of cod larval culture. As such, the models should have utility for predicting the temperature- and size-dependent growth potential of cod larvae. The comparison of observed versus predicted growth in enclosure studies also supports the applicability of the STDG models. Enclosure systems typically have been characterized by high growth and survival rates in the absence of predators when food levels have been in excess of 10 prey·L^{-1} (Øiestad 1984, 1990). The close correspondence between enclosure observations and predictions further suggests that the STDG outputs are realistic estimates of larval growth potential in cod.

Growth performance of field-caught larvae

Consistent with expectations, the surviving cod larvae from the field seem to have been growing at rates close to their estimated capacity. This is the case for populations from both sides of the Atlantic and from several years of study (e.g., Suthers and Sundby 1993; Meekan and Fortier 1996). Incorporation of temperature in the growth models seems to explain to a large extent the difference in size-at-age reported by Suthers and Sundby (1996). Temperature-mediated differences in growth were also indicated between years (Meekan and Fortier 1996). In their study, the higher growth rate found for the 1992–1993 cohort also initially ex-

© 2005 NRC Canada

perienced higher temperatures than the 1991–1992 cohort. The finding that a stronger selection for survival took place in the warmer year is still worth noting, since the fish will be more susceptible to starvation-related mortality during food shortage at high-temperature conditions compared with at low-temperature conditions (McGurk 1984). The selective mortality took place after day 40 from hatching at a larval size greater than 10 mm (Meekan and Fortier 1996), however, and at this size, predation mortality may be more important than starvation as a mortality agent. Since no data on selective mortality were available from other field studies, it is not possible at this stage to conclude whether the high growth of the survivors is due to generally high growth rates or if this is the result of a very strong selection for larger size-at-age.

Internal and external influences on larval growth

Several studies have previously shown larval mortality to decrease with larval size (Bailey and Houde 1989; Houde 1997), and mortality rates in fish larvae have been suggested to be especially high considering their size (McGurk 1986). The finding that surviving cod larvae seem to be growing at rates close to their maximum capacity may reflect the importance of growing fast during the larval stage. This may not always be the case with smaller larvae, however. Buckley et al. (2004) sampled larvae smaller than 10 mm on the Georges Bank and concluded, using RNA/DNA ratios as indirect measures of recent growth, that larvae found at temperatures around 8 °C were growing slower than those at 7 °C. The question still remains if these larvae at higher temperatures suffered subsequent higher mortalities and failed to contribute to recruitment. Since fish larvae typically do not deposit significant amounts of energy storage in livers and muscle as do older fish, the resilience of larvae to starvation mortality does not improve much during the larval stage (Hunter and Coyne 1982; Jordaan and Brown 2003). Thus, a food shortage, especially at relatively high temperatures, can rapidly result in increased mortality. This does not have to imply direct starvation mortality, since elevated temperatures may increase the consumption of co-occurring predators as well.

The population genetic effects on the temperature relationship are still largely unresolved. Relatively small differences were observed between NA cod and NC cod, and contrary to the predictions from the countergradient hypothesis (Conover and Schultz 1997), offspring from the northern stock grew slower than the southern (NC cod) offspring (Otterlei et al. 1999). The difference in growth between offspring from the two stocks was comparable with the growth difference caused by a 0.5 °C difference in rearing temperature. The diversity of the genetic material underlying these studies is small, however, and broader parental coverage is needed before this matter can be properly resolved. As pointed out by Suthers and Sundby (1996), environmental factors other than temperature may also influence the growth of cod populations. Cod stocks from the eastern and western side of the Atlantic experience up to 48% difference in day length, and this may also explain part of the differences in observed growth rates. Although prolonged day lengths have been shown to generate increased growth rates of larval cod in the laboratory (Puvanendran and Brown 2002), these effects are generally of a smaller magnitude than those generated by differences in ambient temperature. A growth ratio of 1.15 was obtained for larval groups reared at 24:0 versus 16:8 day length (Puvanendran and Brown 2002), while the estimated growth ratio was 1.40 between cod from the eastern and western Atlantic temperature environments, which had a 3–3.5 °C temperature difference in addition to the same day length difference of approximately 50% (Suthers and Sundby 1996). The apparent applicability of the NC cod STDG model across regions and populations therefore suggests ambient temperature to be a major contributor to differences in growth rates between populations. Further investigations into differences in population-specific growth responses are strongly encouraged, however, since such differences have been documented in other species (Conover and Schultz 1997).

Fig. 7. Growth ratios at different temperatures from short-term experiments by Steinarsson and Björnsson (1999). Different symbols refer to larval groups with different initial weights: 0.046 mg (●), 0.107 mg (□), 0.140 mg (○), and 0.095 mg (▲).

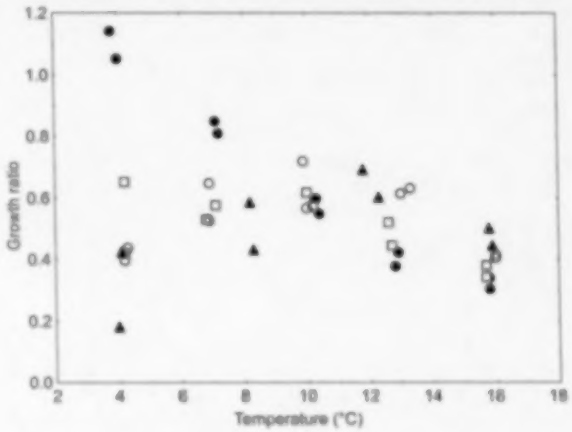

Model evaluation and comparison

None of the originally selected cod growth papers enabled a comprehensive comparison of model performance across the entire reported temperature range. In a series of short-term experiments, however, Steinarsson and Björnsson (1999) reared young cod larvae at temperatures ranging from 3.8 to 16.0 °C. Although these experiments did not meet the selection criteria for individual growth studies used here (owing to short duration), the data from Steinarsson and Björnsson (1999) enabled a comparison with the STDG model across the entire temperature range. Comparing growth performances from their experiments with predicted growth performances from the STDG model reveals a wider range in performances at 4 °C and a relatively lower growth performance at 16 °C (Fig. 7). Overall, the growth rates in these experiments were substantially lower than predicted by the model, with growth ratios averaging about 0.6. This is most likely not due to the origin of larvae (from Icelandic populations), since larvae sampled from Icelandic waters were growing as fast as the model predictions (Begg and Marteinsdottir 2000). Two of the data series had the highest growth ratios at around 10 °C, while the two others had the highest growth ratios at 4 and 12 °C, respectively. The highest mortality

© 2005 NRC Canada

rates were also observed at 16 °C (Steinarsson and Björnsson 1999), suggesting that for young cod larvae, temperatures above 14 °C are suboptimal for growth and survival. Temperatures above 12 °C have previously been shown to be detrimental to developing cod embryos, while the tolerance to higher temperatures increases after hatching (Iversen and Danielssen 1984). At temperatures below 14 °C, the average growth ratios predicted from the STDG model were relatively constant and averaged 0.54–0.62 throughout the 4–14 °C temperature range (data grouped in 4, 7, 10, and 13 °C temperature groups; Kruskal–Wallis test, $p > 0.8$, Kruskal–Wallis test, $p < 0.05$ when including the 16 °C group). Although noticeable variability in growth ratios was observed between groups in these short-term experiments, the overall similar growth ratio in the temperature range 4–14 °C suggests that the temperature effect of the STDG models was appropriately parameterized.

The predictions from the Campana and Hurley (1989) model stand out as the case where cod larvae at sea are growing relatively slowly compared with their growth potential. This study was the first of its kind, linking the ambient temperature history of field-caught larvae with an age-based model. There are some potential methodological problems with the data material underlying the construction of this model. Samples were taken with 0.61-m Bongo nets, a gear not suitable for quantitative sampling of cod larvae larger than 10–12 mm (Campana and Hurley 1989; Suthers and Frank 1989). Larger larvae are underrepresented in the samples, and it is thus not surprising that growth rate apparently declines rapidly with age. To what extent this avoidance effect is confounded by temperature is unclear, but since the larger individuals will be very important in determining the apparent growth rate at older ages, further investigations into this matter are strongly recommended. The initial larval size used by Campana and Hurley (1989) is 3 mm TL, which was significantly smaller than sizes reported by Bolz and Lough (1988) for cod larvae in the same area. Although Campana and Hurley (1989) considered the Bolz and Lough (1988) correction of 30% shrinkage to be excessive, comparisons with length measurements of live cod larvae in the laboratory that typically are between 4 and 5 mm TL at hatch (e.g., Folkvord et al. 1999; Puvanendran and Brown 1999), seem to support the correction used by Bolz and Lough (1988). The implication of the Campana and Hurley (1989) model is that cod larvae are increasingly food limited with increasing temperature. This still may be a valid point (Buckley et al. 2004), but to what extent these larvae survive to older stages still remains an open question. The fact that the Campana and Hurley (1989) model does not permit cod to grow beyond 18 mm at 9 °C indicates limitations of the model. This is not an unrealistic ambient temperature for cod to experience during their early juvenile stage in the Georges Bank area. On the other hand, the STDG model supports the growth pattern presented in Bolz and Lough (1988) during the first 90 days after hatching, suggesting that the predictions based on the Campana and Hurley (1989) model underestimate growth, especially during the latter part of the study period.

The apparent high growth rate of field-caught cod at low temperatures also needs some clarification. Since the estimated ages used in these studies are based on otolith microstructure analysis, there is a possibility of age underestimation due to slow otolith growth (Otterlei et al. 2002). Studies of the otolith growth of the larvae used to parameterize the STDG and ATDG models have shown that the daily incremental growth at temperatures below 6 °C is very narrow and well below the practical resolution limit of light microscopy analysis (Otterlei et al. 2002). At 4 °C, the average daily radial otolith growth during the first 3 weeks was less than 0.4 µm. The groups from the colder regions and years in the papers by Begg and Marteinsdottir (2000) and Anderson and Dalley (2000) both originated in temperatures around or below this level. A significant underestimation of age is thus possible, where apparent growth will incorrectly be confounded by initial ambient temperature. In the case of the study of Begg and Marteinsdottir (2000), a positive growth effect of the northern stocks may partly be due to longer periods of daylight for feeding (Suthers and Sundby 1996). The possibility that population-specific growth performances exist cannot be ruled out either (see above), but the laboratory experiments with offspring from the same stocks (Laurence 1978; Steinarsson and Björnsson 1999; Puvanendran and Brown 2002) do not provide evidence of offspring from these stocks responding differently to temperature or performing better than predicted by the STDG model.

Although the STDG model in general predicted the growth pattern with good accuracy, there are a few data series that warrant further comments. The observed size-at-age in Finn et al. (2002) was lower than expected initially and vice versa at the end. For the latter, it should be noted that the data at this point are outside the main model domain. As such, the growth capacity of larger individuals may well be higher than predicted by the model. An indication of this being the case is also present in a data set with even higher rearing temperatures (1992 data from van der Meeren et al. (1994), which were outside the size and temperature range of model). Shifts in temperature for maximum growth have also been shown in cod and other species (Hallaråker et al. 1995; Otterlei 2000), and the early juvenile cod may thus have a higher growth potential than predicted by the model at temperatures above 10 °C. However, a similar pattern as observed in Finn et al. (2002) may also to some extent be created by sampling effects. Selective sampling of smaller individuals is a common problem in cylindrical bag enclosures owing to the lack of suitable sampling gear, and in many cases, the final sizes at termination of the experiment are the only unbiased estimates of size-at-age (T. van der Meeren, Institute of Marine Research, Austevoll, 5392 Storebø, Norway, personal communication). In a recent paper by van der Meeren and Moksness (2003), larger than expected larvae were found initially in similar-type enclosures. Consequently, this discrepancy does not seem to be related to rearing in bag enclosures as such. In addition, group-specific growth responses may very well vary from the average deterministic predictions from the STDG model. Periods of relatively low growth may be compensated for by extraordinary high growth rates, as have been documented for adult cod (Pedersen and Jobling 1989). At the same time, fast growth events caused by development or improvements in food availability may continue for several subsequent days, resulting in a noticeable growth burst (Juanes and Conover

© 2005 NRC Canada

1994). These effects are expected to be more pronounced at smaller time scales, however, and integration of growth over longer time periods is expected to more accurately reflect the overall true growth performance.

A special consideration is given to the initial sizes of larvae used in the field studies, since these are usually unknown. In this paper, an initial weight of 45 μg was used (yolk excluded), and this represents a relatively heavy embryo at hatching. Using a lower initial weight in field examples would increase the estimates of cod larvae growth in the field. With respect to the main conclusions of this paper, this strengthens the claim that the surviving larvae are indeed growing very well. When plotting the effects of a 50% increase of initial weight, we can see that the relative size difference increases initially. This is due to the increasing growth rate with size up to the size at maximum growth rate (about 0.7 mg DW for both NA and NC cod). As the larvae pass the size of maximum growth capacity, the relatively smaller larvae tend to catch up somewhat as the growth of the larger larvae slows down. A size-specific growth rate pattern like this would also generate an increase in the coefficient of variation with size in a cohort of larvae followed by a decrease in the coefficient of variation for the same reasons (Huston and DeAngelis 1987). Thus, one should be careful about inferring selective mortality based only on patterns in mean–variance relationships (Miller 1997). It can be noted that the size ratio will converge as the age of comparison increases, however, and by day 60, the relative size difference between the mean initial weight and a lower initial weight is back to what it was at the outset. The differences in growth rates have also stabilized, and the growth ratio calculations are therefore quite robust against variations in initial size.

An indication of the robustness of the STDG models to predictions at the outer range of the model domain can be found by comparing them with other model predictions. Björnsson and Steinarsson (2002) presented a model for juvenile and adult Icelandic cod based on experiments where the fish had been fed in excess. Their model was applicable for juveniles with a wet weight of 1–2 g up to adult cod weighing several kilograms. The STDG models and the Björnsson and Steinarsson (2002) model yielded comparable growth estimates at a fish size of 450–600 mg DW, which were the sizes of minimal growth predicted by the STDG models (Fig. 8). The differences in estimated daily specific growth rates were less than 0.4% for the NA cod model and less than 1% for the NC model at temperatures of 4–16 °C. This may facilitate the generation of growth trajectories from hatching to spawning by using the STDG models until 450–600 mg DW and the Björnsson and Steinarsson (2002) model thereafter.

Fig. 8. Comparison of temperature-specific growth predictions for northeast Arctic Atlantic cod (*Gadus morhua*) of 450 mg using the size- and temperature-dependent growth model (●) and the model presented by Björnsson and Steinarsson (2000) (□). SGR, specific growth rate.

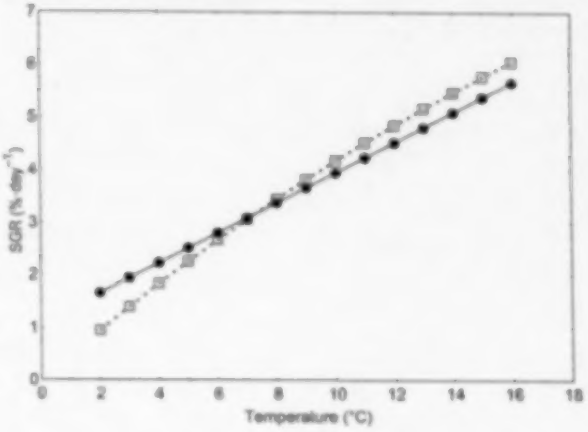

Final remarks

This study has shown that ambient temperature is an important factor in determining the size-at-age of larval cod in natural cod stocks. Previous studies have shown that juvenile cod size at the 0-group stage are strongly correlated with regional temperature indices (Ottersen and Loeng 2000). I suggest that these correlations may be determined during the larval stage owing to the marked temperature-dependent growth at this stage. The growth response to temperature in fishes is most pronounced at early stages (Post and Lee 1996), and thus, changes in ambient temperature during these stages may generate large growth differences that carry on into later stages. Temperature versus recruitment correlations have been found to vary with region in cod, where positive correlations are found in northern, colder waters, while the correlation tends to be negative at the southern borders of the cod distributional area (Planque and Frédou 1999). A lower recruitment of cod in the North Sea is seen in relatively warm years (Beaugrand et al. 2003), and the plankton concentration is shown to be inversely related to ambient temperature. It is suggested that this will reduce larval and early juvenile survival owing to increasing metabolic costs at times when plankton energy is in short supply. Whether this reduced survival is accompanied by a reduced growth of the survivors (recruits) remains to be documented. On the other hand, the NA cod stock will typically benefit from higher temperatures caused by increased advection of relatively warm Atlantic water with abundant suitable plankton (Sundby 2000). Significant growth responses to climatic changes thus seem likely as surviving cod respond to improved feeding conditions and elevated temperature conditions.

In summary, the development of the STDG models enabled a broad comparison of growth performance of the youngest stages of cod. The results so far indicate that the surviving larvae have been growing at rates close to their maximum temperature- and size-dependent capacity, but several questions still remain. How common is a temperature-dependent mortality risk due to increased energetic demands in cod larvae? To what extent are there population differences in responses to temperature? What are the consequences of climate changes on growth and recruitment variability in this species? For all of these questions and many more, the documentation of the growth potential and to what extent this is achieved under the prevailing conditions should enable us to provide more qualified answers as well as new challenging questions.

© 2005 NRC Canada

Acknowledgements

I am indebted to Dr. Erling Otterlei and Gunnar Nyhammer, who took on the effort of extensive cod rearings in the laboratory. Prof. Gudrun Marteinsdottir and Dr. Geir Blom, Dr. Larry Buckley, Dr. Nigel Finn, Dr. Torstein Pedersen, Dr. V. Puvanendran, Dr. Iain Suthers, and Dr. Terje van der Meeren are thanked for providing additional information from their publications and Prof. Ken Frank for providing references to Canadian hydrography data. This study was supported by Norwegian Research Council grants 108920/120 and 130192/140 and a study leave grant from the University of Bergen to the Chesapeake Biological Laboratory, University of Maryland. The paper benefited from discussions with members of the ICES WG in recruitment processes and by constructive comments by Prof. Ed Houde, Dr. Tom Miller, and Clelia Booman.

References

Anderson, J.T., and Dalley, E.L. 2000. Interannual differences in hatching times and growth rates of pelagic juvenile cod in Newfoundland waters. Fish. Res. **46**: 227–238.

Bailey, K.M., and Houde, E.D. 1989. Predation on eggs and larvae of marine fishes and the recruitment problem. Adv. Mar. Biol. **25**: 1–83.

Baskerville-Bridges, B., and Kling, L.J. 2000. Larval culture of Atlantic cod (*Gadus morhua*) at high stocking densities. Aquaculture, **181**: 61–69.

Beaugrand, G., Brander, K.M., Lindley, J.A., Souissi, S., and Reid, P.C. 2003. Plankton effect on cod recruitment in the North Sea. Nature (Lond.), **426**: 661–664.

Begg, G.A., and Marteinsdottir, G. 2000. Spawning origins of pelagic juvenile cod *Gadus morhua* inferred from spatially explicit age distributions: potential influences on year-class strength and recruitment. Mar. Ecol. Prog. Ser. **202**: 193–217.

Björnsson, B., and Steinarsson, A. 2002. The food-unlimited growth rate of Atlantic cod (*Gadus morhua*). Can. J. Fish. Aquat. Sci. **59**: 494–502.

Blom, G., Otterå, H., Svåsand, T., Kristiansen, T.S., and Serigstad, B. 1991. The relationship between feeding condition and production of cod fry (*Gadus morhua* L.) in a semi-enclosed marine ecosystem in western Norway, illustrated by use of a consumption model. ICES Mar. Sci. Symp. **192**: 176–189.

Blom, G., Svåsand, T., Jørstad, K.E., Otterå, H., Paulsen, O.I., and Holm, J.C. 1994. Comparative survival and growth of two strains of Atlantic cod (*Gadus morhua*) through the early life stages in a marine pond. Can. J. Fish. Aquat. Sci. **51**: 1012–1023.

Bolz, G.R., and Lough, R.G. 1988. Growth through the first six months of Atlantic cod, *Gadus morhua*, and haddock, *Melanogrammus aeglefinus*, based on daily otolith increments. Fish. Bull. U.S. **86**: 223–235.

Brander, K. 1995. The effect of temperature on growth of Atlantic cod (*Gadus morhua* L.). ICES J. Mar. Sci. **52**: 1–10.

Buckley, L.J., Smigielski, A.S., Halavik, T.A., Burns, B.R., and Laurence, G.A. 1993. Growth and survival of the larvae of three temperate marine fish species at discrete prey densities. II. Cod (*Gadus morhua*), winter flounder (*Pseudopleuronectes americanus*), and silver hake (*Merluccius bilinearis*). *In* Physiological and biochemical aspects of fish development. *Edited by* B.T. Walther and H.J. Fyhn. University of Bergen, Bergen, Norway. pp. 183–195.

Buckley, L.J., Caldarone, E.M., and Lough, G. 2004. Optimum temperature and food-limited growth on larval Atlantic cod (*Gadus morhua*) and haddock (*Melanogrammus aeglefinus*) on Georges Bank. Fish. Oceanogr. **13**: 134–140.

Campana, S.E. 1992. Measurement and interpretation of the microstructure of fish otoliths. *In* Otolith microstructure examination and analysis. *Edited by* D.K. Stevenson and S.E. Campana. Can. Spec. Publ. Fish. Aquat. Sci. No. 117. pp. 59–71.

Campana, S.E., and Hurley, P.C.F. 1989. An age- and temperature-mediated growth model for cod (*Gadus morhua*) and haddock (*Melanogrammus aeglefinus*) larvae in the Gulf of Maine. Can. J. Fish. Aquat. Sci. **46**: 603–613.

Clemmesen, C., Bühler, V., Carvalho, G., Case, R., Evans, G., Hauser, L., Hutchinson, W.F., Kjesbu, O.S., Mempel, H., Moksness, E., Otterå, H., Paulsen, H., Thorsen, A., and Svåsand, T. 2003. Variability in condition and growth of Atlantic cod larvae and juveniles reared in mesocosms: environmental and maternal effects. J. Fish Biol. **62**: 706–723.

Conover, D.O., and Schultz, E.T. 1997. Natural selection and the evolution of growth rate in the early life history: what are the trade offs? *In* Early life history and recruitment in fish populations. *Edited by* R.C. Chambers and E.A. Trippel. Chapman and Hall Ltd., London, UK. pp. 305–332.

Ellertsen, B., Moksness, E., Solemdal, P., Tilseth, S., Westgård, T., and Øiestad, V. 1981. Growth and survival of cod larvae in an enclosure. Experiments and a mathematical model. Rapp. P.-v. Réun. Cons. Int. Explor. Mer, **178**: 45–57.

Finn, R.N., Rønnestad, I., van der Meeren, T., and Fyhn, H.J. 2002. Fuel and metabolic scaling during the early life stages of Atlantic cod *Gadus morhua*. Mar. Ecol. Prog. Ser. **243**: 217–234.

Folkvord, A. 1997. Ontogeny of cannibalism in larval and juvenile fish with special emphasis on Atlantic cod, *Gadus morhua* L. *In* Early life history and recruitment in fish populations. *Edited by* R.C. Chambers and E.A. Trippel. Chapman and Hall Ltd., London, UK. pp. 335–366.

Folkvord, A., Øiestad, V., and Kvenseth, P.G. 1994. Growth patterns of three cohorts of Atlantic cod larvae (*Gadus morhua* L.) studied in a macrocosm. ICES J. Mar. Sci. **51**: 325–336.

Folkvord, A., Otterlei, E., and Svardal, A. 1999. Alkylerte fenolers hormonelle virkning på torsk — generasjonseffekter. Vekst, overlevelse og kjønnsdifferensiering. Institutt for Fiskeri- og Marinbiologi (IFM) Rapp. **15**: 1–11.

Hallaråker, H., Folkvord, A., and Stefansson, S.O. 1995. Growth of juvenile halibut (*Hippoglossus hippoglossus* L.) related to temperature, day length and feeding regime. Neth. J. Sea Res. **34**: 139–147.

Houde, E.D. 1989. Comparative growth, mortality, and energetics of marine fish larvae: temperature and latitudinal effects. Fish. Bull. U.S. **87**: 471–495.

Houde, E.D. 1997. Patterns and trends in larval-stage growth and mortality of teleost fish. J. Fish Biol. **51**: 52–83.

Hunter, J.R., and Coyne, K.M. 1982. The onset of schooling in northern anchovy larvae, *Engraulis mordax*. Calif. Coop. Oceanic Fish. Invest. Rep. No. 23. pp. 246–251.

Huston, M.A., and DeAngelis, D.L. 1987. Size bimodality in monospecific populations: a critical review of potential mechanisms. Am. Nat. **129**: 678–707.

Iversen, S.A., and Danielssen, D.S. 1984. Development and mortality of cod (*Gadus morhua* L.) eggs and larvae in different temperatures. Flødevigen Rapp. **1**: 49–65.

Jonas, J.L., and Wahl, D.H. 1998. Relative importance of direct and indirect effects of starvation for young walleyes. Trans. Am. Fish. Soc. **127**: 192–205.

© 2005 NRC Canada

Jordaan, A., and Brown, J.A. 2003. The risk of running on empty: the influence of age on starvation and gut fullness in larval Atlantic cod (*Gadus morhua*). Can. J. Fish. Aquat. Sci. **60**: 1289–1298.

Juanes, F., and Conover, D.O. 1994. Rapid growth, high feeding rates, and early piscivory in young of the year bluefish (*Pomatomus saltatrix*). Can. J. Fish. Aquat. Sci. **51**: 1752–1761.

Laurence, G.C. 1978. Comparative growth, respiration and delayed feeding abilities of larval cod (*Gadus morhua*) and haddock (*Melanogrammus aeglefinus*) as influenced by temperature during laboratory studies. Mar. Biol. **50**: 1–7.

Laurence, G.C., Smigielski, A.S., Halavik, T.A., and Burns, B.R. 1981. Implications of direct competition between larval cod (*Gadus morhua*) and haddock (*Melanogrammus aeglefinus*) in laboratory growth and survival studies at different food densities. Rapp. P.-V. Reun. Cons. Int. Explor. Mer, **178**: 304–311.

Letcher, B.H., and Bengtson, D.A. 1993. Effects of food density on growth and on patterns of prey depletion by larval silverside fish, *Menidia beryllina* (Cope) — a laboratory investigation with image analysis. J. Exp. Mar. Biol. Ecol. **167**: 197–213.

McGurk, M.D. 1984. Effects of delayed feeding and temperature on the age of irreversible starvation and on the rates of growth and mortality of Pacific herring larvae. Mar. Biol. **84**: 13–26.

McGurk, M.D. 1986. Natural mortality of marine pelagic fish eggs and larvae: role of spatial patchiness. Mar. Ecol. Prog. Ser. **34**: 227–242.

Meekan, M.G., and Fortier, L. 1996. Selection for fast growth during the larval life of Atlantic cod *Gadus morhua* on the Scotian Shelf. Mar. Ecol. Prog. Ser. **137**: 25–37.

Miller, T.J. 1997. The use of field studies to investigate selective processes in fish early life history. *In* Early life history and recruitment in fish populations. *Edited by* R.C. Chambers and E.A. Trippel. Chapman and Hall Ltd., London, UK. pp. 197–223.

Miller, T.J., Crowder, L.B., Rice, J.A., and Marschall, E.A. 1988. Larval size and recruitment mechanisms in fishes: toward a conceptual framework. Can. J. Fish. Aquat. Sci. **45**: 1657–1670.

Øiestad, V. 1984. Criteria for condition evolved from enclosure experiments with cod larva populations. Fiødevigen Rapp. **1**: 213–229.

Øiestad, V. 1990. Specific application of meso- and macrocosms for solving problems in fisheries research. *In* Enclosed experimental ecosystems: a review and recommendations. *Edited by* C. Lalli. Springer-Verlag, Berlin. pp. 136–154.

Olsen, R.E., Henderson, R.J., and Pedersen, T. 1991. The influence of dietary lipid classes on the fatty acid composition of small cod *Gadus morhua* L. juveniles reared in an enclosure in northern Norway. J. Exp. Mar. Biol. Ecol. **148**: 59–76.

Onis, M.de, Garza, C., and Habicht, J.-P. 1997. Time for a new growth reference. Pediatrics, **100**: 1–2.

Otterlei, E. 2000. Temperature- and size-dependent growth of larval and early juvenile cod (*Gadus morhua* L.). Dr. scient. thesis, University of Bergen, Norway.

Otterlei, E., Nyhammer, G., Folkvord, A., and Stefansson, S.O. 1999. Temperature- and size-dependent growth of larval and juvenile cod (*Gadus morhua*): a comparative study between Norwegian coastal cod and northeast Arctic cod. Can. J. Fish. Aquat. Sci. **56**: 2099–2111.

Otterlei, E., Folkvord, A., and Nyhammer, G. 2002. Temperature dependent otolith growth of larval and early juvenile cod (*Gadus morhua*). ICES J. Mar. Sci. **59**: 851–860.

Ottersen, G., and Loeng, H. 2000. Covariability in early growth and year-class strength of Barents Sea cod, haddock, and herring: the environmental link. ICES J. Mar. Sci. **57**: 339–348.

Pedersen, B.H. 1997. The cost of growth in young fish larvae, a review of new hypotheses. Aquaculture, **155**: 259–269.

Pedersen, T., and Jobling, M. 1989. Growth rates of large, sexually mature cod, *Gadus morhua*, in relation to condition and temperature during an annual cycle. Aquaculture, **81**: 161–168.

Pedersen, T., Eliassen, J.E., Eilertsen, H.C., Tande, K.S., and Olsen, R.E. 1989. Feeding, growth, lipid composition, and survival of larval cod (*Gadus morhua* L.) in relation to environmental conditions in an enclosure at 70° in northern Norway. Rapp. P.-V. Reun. Cons. Int. Explor. Mer, **191**: 409–420.

Planque, B., and Frédou, T. 1999. Temperature and the recruitment of Atlantic cod (*Gadus morhua*). Can. J. Fish. Aquat. Sci. **56**: 2069–2077.

Post, J.R., and Lee, J.A. 1996. Metabolic ontogeny of teleost fishes. Can. J. Fish. Aquat. Sci. **53**: 910–923.

Puvanendran, V. and Brown, J.A. 1999. Foraging, growth and survival of Atlantic cod larvae in different prey concentrations. Aquaculture, **175**: 77–92.

Puvanendran, V., and Brown, J.A. 2002. Foraging, growth and survival of Atlantic cod larvae reared in different light intensities and photoperiods. Aquaculture, **214**: 131–151.

Solberg, T., and Tilseth, S. 1987. Variations in growth pattern among yolk-sac larvae of cod (*Gadus morhua* L.) due to differences in rearing temperature and light regime. Sarsia, **72**: 347–349.

StatSoft Inc. 1995. Statistica for Windows (computer program manual). StatSoft Inc., Tulsa, Okla.

Steinarsson, A., and Björnsson, B. 1999. The effects of temperature and size on growth and mortality of cod larvae. J. Fish Biol. **55**: 100–109.

Sundby, S. 2000. Recruitment of Atlantic cod stocks in relation to temperature and advection of copepod populations. Sarsia, **85**: 277–298.

Suthers, I.M., and Frank, K.T. 1989. Inter-annual distributions of larval and pelagic juvenile cod (*Gadus morhua*) in southwestern Nova Scotia determined with two different gear types. Can. J. Fish. Aquat. Sci. **46**: 591–602.

Suthers, I.M., and Sundby, S. 1993. Dispersal and growth of pelagic juvenile Arcto-Norwegian cod (*Gadus morhua*), inferred from otolith microstructure and water temperature. ICES J. Mar. Sci. **50**: 261–270.

Suthers, I.M., and Sundby, S. 1996. Role of the midnight sun: comparative growth of pelagic juvenile cod (*Gadus morhua*) from the Arcto-Norwegian and a Nova Scotian stock. ICES J. Mar. Sci. **53**: 827–836.

Suthers, I.M., van der Meeren, T., and Jørstad, K.E. 1999. Growth histories derived from otolith microstructure of three Norwegian cod stocks co-reared in mesocosms: effect of initial size and prey size changes. ICES J. Mar. Sci. **56**: 658–672.

van der Meeren, T., and Jørstad, K.E. 2001. Growth and survival of Arcto-Norwegian and Norwegian coastal cod larvae (*Gadus morhua* L.) reared together in mesocosms under different light regimes. Aquacult. Res. **32**: 549–563.

van der Meeren, T., and Moksness, E. 2003. Growth and mortality patterns evaluated from otolith microstructure in Atlantic cod *Gadus morhua* larvae reared on different feeding regimes in mesocosms. Mar. Ecol. Prog. Ser. **264**: 95–107.

van der Meeren, T., Jørstad, K.E., Solemdal, P., and Kjesbu, O.S. 1994. Growth and survival of cod larvae (*Gadus morhua* L.): comparative enclosure studies of Northeast Arctic cod and coastal cod from western Norway. ICES Mar. Sci. Symp. **198**: 633–645.

Victora, C.G., Onis, M. de, Garza, C., Cole, T., Frongillo, E.A., Cameron, N., Shekar, M., Yip, R., Bhatnagar, S., Burger, H., Delgado, H.L., Dada, O.A., Gross, B., Hofvander, Y., Lavin,

© 2005 NRC Canada

P.A., and Tang, G.H. 2000. Growth patterns of breastfed infants in seven countries. Acta Paediatr. **89**: 215–222.

Werner, R.G., and Blaxter, J.H.S. 1981. The effect of prey density on mortality, growth and food consumption in larval herring (*Clupea harengus* L.). Rapp. P.-V. Reun. Cons. Int. Explor. Mer, **178**: 405–408.

© 2005 NRC Canada

Risk analysis for species introductions: forecasting population growth of Eurasian ruffe (*Gymnocephalus cernuus*)

John M. Drake

Abstract: The North American distribution of the Eurasian ruffe (*Gymnocephalus cernuus*), an ecologically important and costly invasive fish, is presently limited to the Laurentian Great Lakes. Risk analyses for accidental introductions of ruffe to inland lakes should focus on the chance of establishment for small introductions such as those that would result from transporting ruffe as bait. Here I use Akaike's Information Criterion to select a population growth model for ruffe based on observed population dynamics during the invasion of Loch Lomond, Scotland. This population is regulated by a high carrying capacity and Allee effects were undetected. Parameter estimates obtained from this population forecast that the chance of establishment for possible introductions of ruffe to inland lakes in North America is high. A model for ruffe winter survival suggests that survivorship between introductions and spawning may be an important determinant of establishment success, but that the chance of establishment is high for introductions of only a few individuals. To prevent invasions of ruffe in inland waters, release of ruffe, whether intentional or accidental, should not be tolerated.

Résumé : La répartition nord-américaine du poisson eurasiatique, la grémille (*Gymnocephalus cernuus*), une espèce d'importance écologique et un envahisseur coûteux, se limite actuellement aux Grands Lacs laurentiens. Les analyses de risque d'introductions accidentelles dans les lacs de l'intérieur du continent devraient se concentrer sur la probabilité d'établissement de petites introductions, comme, par exemple, celles qui résulteraient du transport de grémilles pour servir d'appât. Le critère d'information d'Akaike permet de choisir un modèle de croissance pour la grémille d'après la dynamique de la population observée lors de l'invasion du Loch Lomond, Écosse. La population est contrôlée par un stock limite élevé et aucun effet Allee n'a été détecté. L'utilisation des estimations de paramètres obtenues dans cette étude pour prédire la probabilité d'un établissement lors d'introductions possibles de grémilles dans les lacs continentaux d'Amérique du Nord indique que la probabilité d'établissement est forte. Un modèle de la survie de la grémille à l'hiver indique que la survie entre l'introduction et la fraie peut être un important facteur déterminant du succès de l'établissement; cependant, la probabilité d'un établissement est forte même lors de l'introduction d'un petit nombre d'individus. Afin de prévenir l'invasion des eaux continentales par la grémille, on ne peut tolérer ni la libération volontaire, ni la libération accidentelle de grémilles.

[Traduit par la Rédaction]

Introduction

Biological invasions of non-indigenous freshwater fishes, invertebrates, and plants have had considerable effects on the composition of North American freshwater ecosystems (Lodge 2001; Rahel 2002), are an important driver of declines in biodiversity (Sala et al. 2000), and impose considerable economic costs, for control and due to lost productivity (Leung et al. 2002). Risk-analysis methodology for intentional and unintentional introductions of non-indigenous species is therefore an important research frontier in applied ecology (National Research Council 2002).

The Eurasian ruffe (*Gymnocephalus cernuus*) was unintentionally introduced into the Great Lakes around 1986 (Pratt et al. 1992), probably in discharged ballast water, and has subsequently spread to other regions of the Great Lakes, including populations on the south and north shores of Lake Superior and at Thunder Bay River on Lake Huron (United States Geological Survey non-indigenous aquatic species database (available at http://nas.er.usgs.gov)). The ruffe is a demersal freshwater and brackish-water species that has been invasive in other parts of the world, including the United Kingdom and Eastern Europe (Froese and Pauly 2003). The distribution of ruffe in North America is presently limited to the Great Lakes, probably because vectors of dispersal to inland waters are primarily anthropogenic and because considerable effort has been invested in management of the ruffe since its discovery in North America. Eco-

Received 30 April 2004. Accepted 10 January 2005. Published on the NRC Research Press Web site at http://cjfas.nrc.ca on 20 May 2005.
J18098

J.M. Drake.[1] Department of Biological Sciences, University of Notre Dame, Notre Dame, IN 46556, USA.

[1]Present address: National Center for Ecological Analysis and Synthesis, Suite 300, 735 State Street, Santa Barbara, CA 93101, USA (e-mail: drake@nceas.ucsb.edu).

 doi: 10.1139/F05-014 © 2005 NRC Canada

logical impacts of ruffe include predation on eggs of other fish species (Selgeby 1998) and competition with native fishes (Savino and Kolar 1996; Fullerton et al. 2000); ruffe could also impose high economic costs if its effect on the yellow perch (*Perca flavescens*) fishery is as severe as predicted (Leigh 1998). For these reasons, the prevention of future ruffe invasions in uninfested inland ecosystems is a current management objective. To accomplish this goal, prospective risk analyses for ruffe invasions should focus on the chance and rate of establishment of ruffe in inland lakes under different management scenarios.

As a preliminary assessment of the risk of establishment for small, unintentional introductions of ruffe, I conducted a demographic analysis based on the establishment and expansion of ruffe in Loch Lomond, Scotland (56°05′00″N, 004°36′00″W). Previous authors have suggested that stochastic population-growth models could be used to quantify establishment risk for intentional and unintentional introductions of non-indigenous species (Wilson 2000; National Research Council 2002), and similar techniques are already commonplace for assessing risk of extinction (Beissinger and McCullough 2002; Morris and Doak 2002). Although the ruffe population in the Great Lakes is likely beyond eradication, and possibly beyond control, invasion of other ecosystems, including many inland lakes, might still be avoided. In this paper I use a stochastic model of population growth to determine the chance of establishment for introductions of ruffe in such ecosystems as a function of the initial number of individuals introduced. I find no evidence for Allee effects and negligible effects of environmental variability, which suggests that ruffe are unlikely to exhibit long time lags between introduction and population growth. Survival between introduction and post-introduction spawning is therefore likely a crucial transition in ruffe invasions. To examine this transition, I develop a simple model for winter survival and find that establishment probability remains high for introductions of more than a few individuals. This finding is relatively insensitive to estimation error in adult mortality rate and sex ratio of the donor population.

Methods

Adams and Maitland (1998) reported a time series for ruffe caught on screens at the Ross Priory Pumping Station on the south shore of Loch Lomond between 1982 and 1996. Although these data do not accurately reflect the relative abundances of different species in Loch Lomond because of different species-specific catch rates, they do accurately represent fluctuations within a species over time (Adams and Maitland 1998). These data (Fig. 1) exemplify the rapid population growth that is a common characteristic of the first phase of an invasion (Shigesada and Kawasaki 1997), but also vary considerably from year to year throughout the time series. This variability is important for two reasons. First, it obscures the predominant drivers of population growth, for instance whether or not the population is influenced by density-dependent factors. Second, it renders plausible the possibility that though the population might initially increase in abundance, it could eventually fail as a result of boom-and-bust cycles and (or) because the population fails to endure environmental fluctuations. Below, I consider the evidence from the observed dynamics of the Loch Lomond population for each of these hypotheses and quantify the chance of establishment for possible future introductions of ruffe in inland waters.

Fig. 1. Population dynamics of invasive Eurasian ruffe (*Gymnocephalus cernuus*) in Loch Lomond, Scotland. Data are from Adams and Maitland (1998).

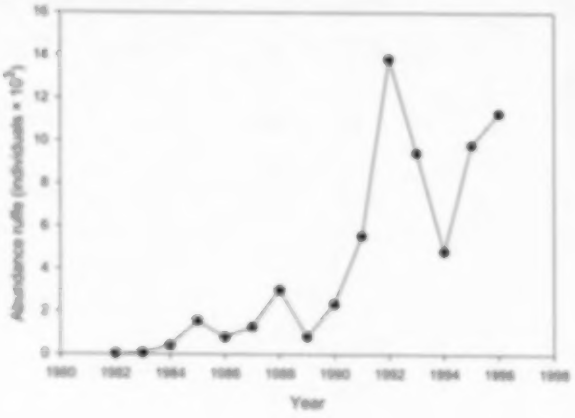

Random fluctuations in population-growth rate are usually represented as the combination of two interacting stochastic processes. Demographic stochasticity refers to the effect of variation in individual fitness on population dynamics and results from growth of a population of discrete individuals (Engen et al. 1998; Lande et al. 2003). In contrast, environmental stochasticity refers to random fluctuations in population vital rates over time (Engen et al. 1998; Lande et al. 2003). Below, I assume that effects of demographic stochasticity and random variation in sex ratio on long-term population dynamics (i.e., persistence) are negligible. For most fish species, including the ruffe, this assumption is justified because high individual fertilities overwhelm the effects of individual variation in fertility. Measured fecundities of ruffe range from tens to hundreds of thousands of eggs per individual, depending on size (Kolomin 1977; Ogle 1998). The estimated average annual fecundity of ruffe in North America (~45 000) is consistent with this range (Selgeby and Ogle 1992). Similarly, highly predictable, long life-spans (7–11 years; Kolomin 1977) result in relatively low variation in survival rates of mature individuals. For this reason, larval survival rate is a much more important determinant of long-term population growth in species such as the ruffe. At this developmental stage, however, there are sufficient individuals (even if only one female has spawned) that individual variation in survival is overwhelmed by fluctuations in average survival from year to year, i.e., demographic stochasticity is overwhelmed by environmental variation. This phenomenon is well known in fisheries research and is captured in the concept of year-class strength. Thus, the first model developed below focuses on environmental stochasticity, but shows that these fluctuations are unlikely to have an important effect on establishment probability; a second model is developed to study effects of individual variation and sex ratio on winter survival.

© 2005 NRC Canada

Model for long-term persistence

Population dynamics of seasonally reproducing species in a fluctuating environment can be represented by the stochastic difference equation

$$N_{t+1} = f(N_t) + \varepsilon \quad (1)$$

where N_t is the population size at time t, ε is a random perturbation due to environmental variability, and $f(N_t)$ is a continuously differentiable, possibly density-dependent model for the mean change in population size. An approximation to eq. 1 is the diffusion process characterized by an infinitesimal mean, μ, and variance, σ^2 (Dennis et al. 1991). This modeling framework commonly serves as a basis for inference and for forecasting extinction dynamics, on the assumption that the growth of small populations will be nearly exponential. After testing for Allee effects, it is assumed that this approximation holds for invading populations of ruffe.

Following the convention of log-transforming models and data so that exponential growth is more simply represented as a linear autoregressive process and residuals exhibit constant variance (Lande and Orzack 1988; Dennis et al. 1991; Morris and Doak 2002), a model was selected by fitting the observed data to the following common population-dynamical models: constant population growth rate (exponential population growth), Ricker model, theta-logistic model, and an Allee effect model (Table 1). Assuming that environmental variation in the transformed time series is distributed normally, maximum-likelihood estimates of parameter values are obtained by fitting least squares (Morris and Doak 2002). Parameter estimation was conducted with PROC NLIN in SAS version 8.2 (SAS Institute Inc. 1999). Model selection was determined by the smallest Akaike's Information Criterion (AIC) adjusted for small data sets (AIC_c; Burnham and Anderson 2002). AIC selects the model that minimizes the expected Kullback–Leibler distance between a complete representation of the data-generating process and its approximate representation by a parameterized model (Burnham and Anderson 2002). This can be conceptualized as a formalized procedure for selecting the most likely model (in terms of posterior likelihood) with a penalty to correct for bias caused by model complexity. Using this procedure, I determined that the Ricker model provided the best fit to the observed data.

For forecasting population establishment, I used a density-independent model of population growth in a variable environment (Dennis et al. 1991). This model assumes that Allee effects, carrying capacity, random fluctuations in sex ratio, and demographic stochasticity are negligible (see Møller and Legendre 2001; Dennis 2002; Engen et al. 2003). Data were not available to estimate fluctuations in sex ratio or demographic stochasticity, so these phenomena were studied in an exploratory way using a second model. The following observations justify the decision to use a density-independent model for long-term forecasts.

First, the success or failure of the introduced population depends primarily on population growth during the years immediately following introduction, i.e., during the exponential-growth phase of the approach to carrying capacity. If recruitment during such years is poor as a consequence of environmental fluctuations, then the invasion may

Table 1. Models used to forecast the chance of establishment for introductions of Eurasian ruffe (*Gymnocephalus cernuus*) to inland lakes in North America. AIC = Akaike's Information Criterion.

	Parameter			Model fit			
Model	r	κ	θ	SSE[a]	df[b]	AIC_c	Reference
Exponential: $\ln(N_{t+1}/N_t) = r$	0.4642			11.2733	14	41.79	Dennis et al. 1991
Ricker[c]: $\ln(N_{t+1}/N_t) = r(1 - N_t/\kappa)$	0.8817	8104.5		8.3834	14	40.95	Morris and Doak 2002
Theta-logistic: $\ln(N_{t+1}/N_t) = r[1 - (N_t/\kappa)^\theta]$	2.9687	6189.1	0.1337	6.8673	14	42.20	Morris and Doak 2002
Allee effect: $\ln(N_{t+1}/N_t) = \ln(N_t) + r - \kappa N_t$	0.8817	1.09×10^{-4}	1.09×10^{-4}	8.3834	14	45.00	Morris and Doak 2002

[a]Sum of squared errors.
[b]Uncorrected total degrees of freedom.
[c]Best fit overall.

© 2005 NRC Canada

fail. Linearizing the Ricker model around $N_0 = 0$ yields $\ln(N_{t+1}/N_t) = r$, indicating that exponential growth is a good approximation to the Ricker model during this phase of invasion. Second, population estimates for ruffe in Loch Lomond are relative (depending on the sampling rate) and are not absolute measures of abundance. Since the sampling rate is unknown, one cannot determine the true carrying capacity of Loch Lomond. Furthermore, the carrying capacity of the Great Lakes (or even of just Lake Superior) is likewise unknown. However, it certainly is very large, and standard results (e.g., Tier and Hanson 1981) indicate that it will therefore have a negligible effect on the chance of extinction within ecological time scales. Even for introductions to smaller inland lakes, carrying capacity is unlikely to affect the chance of establishment, as ruffe populations likely can attain high densities without adverse affects on individuals.

The population growth rate, r, was obtained from the best fit (Ricker) model (Table 1). Observe that the Ricker model can be rescaled by defining $N_t^* = N_t/\kappa$, resulting in the two-parameter model $\ln(N_{t+1}^*/N_t^*) = r(1 - N^*)$, leaving the value of r unchanged. The mean of the diffusion process is approximately this value less the variance divided by 2 (Dennis et al. 1991). The variance was estimated by mean squared error of the best fit model (Morris and Doak 2002). Uncertainty in parameter estimates was propagated throughout these estimates using estimators derived by Dennis et al. (1991).

Finally, I considered two additional models. First, I supposed that population dynamics might exhibit density-dependent time lags, which can be modeled as autoregressive processes (Turchin 2003). Time lags are important because, when coupled with demographic stochasticity and environmental variability, they can result in non-negligible probabilities of extinction even at population sizes near carrying capacity (Belovsky et al. 1999). Additionally, density-dependent time lags are the most likely mechanism for the boom-and-bust cycles commonly observed in biological invasions. I used the partial rate correlation function (PRCF) as a probe for density-dependent time lags in population growth and sequential-blocks cross-validation (validation block size of one data point) as described by Turchin (2003) for selection of autoregressive models.

Second, Adams and Maitland (1998) suggest that the Loch Lomond population grew exponentially (constant growth rate) during the period 1982–1992 and stabilized thereafter. Although I found more support for the Ricker (density-dependent) model than for the exponential-growth model, it does not follow that this is the best two-parameter model for density dependence. Alternatively, the growth of ruffe populations is perhaps better characterized by a "ceiling" model in which the population grows exponentially until it reaches a ceiling, at which time it abruptly ceases to increase (Foley 1994). The Ricker model considered above might fit such a model quite poorly. Therefore, to test for this possibility I compared the observed log-transformed interannual population-growth rates given by $X_t = \ln(N_t/N_{t-1})$, where N_t is the population size at time t, before and after 1993, with a two-tailed t test for populations with unequal variances.

Model for winter survival

The model considered above reflects the effect of fluctuating environments on long-term persistence of an introduced population, conditional on persistence to spawning in the first year following introduction. Importantly, because the number of initially introduced individuals is small, demographic stochasticity and random fluctuations in sex ratio could have a profound effect on persistence at this phase of establishment. Some insight into this process can be obtained by considering an introduction of individuals that is a random sample of a donor population, after the spring spawning and before winter mortality occurs. Ignoring the possibilities of a late-season spawn (Fedorova and Vetkasov 1974; Kolomin 1977) and hermaphroditism (Butskaya 1976), the probability of successful spawning is determined by the chance that at least one male and one female survive through the winter. Representing winter mortality by δ with a subscript to indicate sex, the chance that at least one female survives is $(1 - \delta_F^F)$ and the chance that at least one male survives is $(1 - \delta_M^M)$, where F is the number of females and M is the number of males. Here we assume that adult mortality is not age-dependent, though extending this model to include age structure would be straightforward. For F females and M males, the joint probability of at least one male and one female surviving is

$$(2) \qquad (P_{\text{mate}}|M, F) = (1 - \delta_F^F)(1 - \delta_M^F)$$

The total chance of mating, conditional on N and assuming no Allee effects, is given by

$$(3) \qquad (P_{\text{mate}}|N) = (P_{\text{mate}}|M, F)(P_{M,F}|N)$$

If the N introduced individuals are drawn from a population with sex ratio of ϕ males per female, the probability of M males and F females is given by the binomial distribution with parameter $p = (1 + \phi)^{-1}$. Since $M = N - F$, the total chance of mating, given an introduction of N individuals of unknown sex is

$$(4) \qquad (P_{\text{mate}}|N) = \sum_{F=1}^{N} (1 - \delta_F^F)(1 - \delta_M^{N-F}) \binom{N}{F} p^F (1 - p)^{N-F}$$

Holding all other parameters constant, this formula takes its maximum value at $p = 0.5$, i.e., where the sex ratio is equal to 1.

Results

Model selection

Goodness-of-fit statistics (AIC_c) for the log-transformed linear, Ricker, theta-logistic, and Allee effect models are given in Table 1. The Ricker model provided the best fit to these data (Table 1). Model selection was based on the lowest AIC_c value. The difference between the estimated AIC_c value for the Ricker model and the next best model (exponential population growth) was 0.837, indicating that support for the Ricker model against the exponential-growth model was only about 2.3 to 1. The PRCF showed a significant negative spike (PRCF $\leq 2/\sqrt{t}$, where t is the number of data points; Turchin 2003) at a time lag of 1 year, indicating dependence only on the population size in the previous year.

© 2005 NRC Canada

Fig. 2. Estimated chance of establishment for small introductions of ruffe determined from stochastic population-growth models (solid line) with 95% confidence intervals (broken lines).

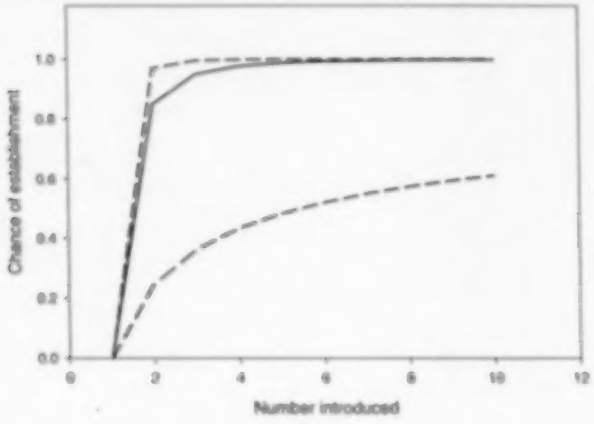

Sequential-block cross-validation showed that higher order (lagged) models were not warranted by these data. Additionally, there was insufficient evidence for the ceiling model ($P = 0.131$), though it is interesting that the average X value from 1993 to 1996 was not significantly different from zero ($P = 0.879$), which is consistent with the carrying capacity implicit in the Ricker model having been reached. The lack of first-order autocorrelation among the residuals ($P = 0.989$) confirms that observations were independent, thus satisfying the assumptions of the model (Dennis et al. 1991).

Forecasting long-term persistence

The maximum-likelihood estimate of the population-growth parameter, r, in the Ricker model is 0.8817 (95% confidence interval 0.2207, 1.5426). Maximum and minimum observed values for X_t were 2.156 and −1.284, respectively. The maximum-likelihood estimate for environmental variation, σ_e, is 0.599. The chance of establishment, π_{est}, defined as the complement of the chance of extinction, is given by the equation (Dennis et al. 1991)

$$\pi_{est} = \begin{cases} 0 & \mu \le 0 \\ 1 - \exp[-2\mu \ln(N_0)/\sigma^2] & \mu > 0 \end{cases} \quad (5)$$

where $\mu = r - \sigma^2/2$ and N_0 is the initial number of females introduced (assuming an adequate number of males is introduced for fertilization to occur). This result is presented with approximate 95% confidence intervals reflecting uncertainty in the parameter estimates (Fig. 2; Dennis et al. 1991).

Winter survival

To understand the effects of changes in mortality and sex ratio on the chance of persistence to first spawning, I evaluated eq. 4 for different values of the parameters δ and p. The effect of increasing mortality while holding sex ratio constant is to diminish the chance of persistence for an introduction of a given size, consistent with intuition (Fig. 3*a*). However, even for very high levels of winter mortality, the chance that one male and one female survive is unacceptably high even for very small introductions (e.g., 30% chance of

Fig. 3. Estimated chance of winter survival and reproduction for small introductions of ruffe. Results are relatively insensitive to (*a*) adult mortality and (*b*) sex ratio. Estimates in *a* were obtained by evaluating eq. 4 at different values of $\delta_M = \delta_F = \delta$, holding sex ratio constant ($\phi = 1$). Estimates in *b* were obtained by evaluating eq. 4 at different values of p, holding adult mortality constant ($\delta = 0.2$).

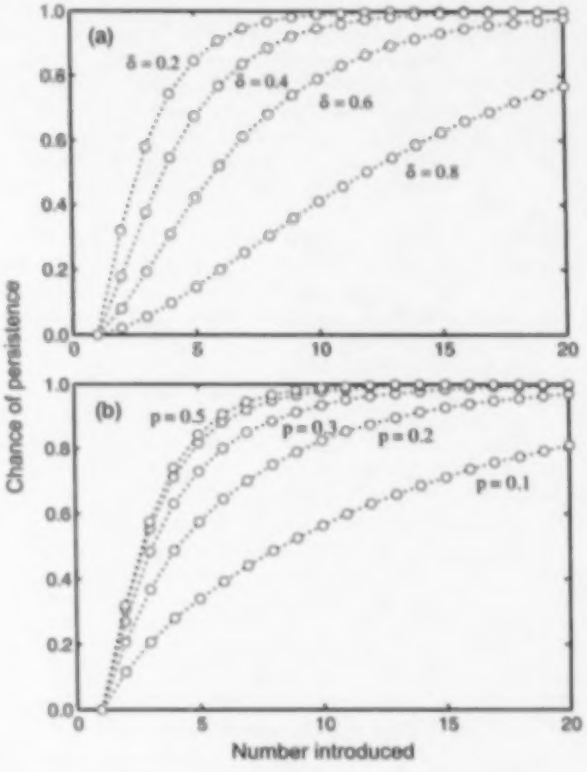

persistence for an introduction of eight individuals). A skewed sex ratio in the donor population had a less pronounced effect on the chance of persistence than did winter mortality (Fig. 3*b*). The uppermost line (Fig. 3*b*) represents introduction from a population with a sex ratio of $\phi = 1$, showing that the chance of mating is highest when males and females are in equal proportions. However, to vastly change this result, highly skewed sex ratios are required, as represented by the bottom two lines, which correspond to $\phi = 4$ and $\phi = 9$, respectively. Since the processes underlying Figs. 2 and 3 are independent, these probabilities can be multiplied to obtain a joint probability of persistence. Clearly, the phase represented by Fig. 3 (winter mortality and biased sex ratio in the donor population) will overwhelm the joint probability for most introduced populations.

Discussion

The results of this study support the tentative conclusion of Adams and Maitland (1998) that the ruffe population in Loch Lomond is density regulated and moreover that is has approximately stabilized. However, according to model forecasts, lakes with even small introductions are at considerable

© 2005 NRC Canada

risk for invasion. The estimated chance of long-term persistence for an introduction of just two females prior to spawning (assuming that a male is also introduced, to ensure reproduction) is 0.85. If introduction occurs after spawning so that winter survival is the crucial factor determining establishment success, the chance of persistence is diminished but still unacceptably high for introductions of even modest size (e.g., 30% chance of establishment for $N_0 = 8$). While zero tolerance to introductions of non-indigenous species is probably not generally feasible, if invasions of ruffe are to be prevented, introductions of any size should not be tolerated. If during model fit it had been assumed that the Loch Lomond population was not regulated (i.e., if an exponential model had been assumed), the chance of establishment would have been estimated as even higher and would have been overestimated.

As with all modeling exercises, the results obtained here depend on assumptions that are approximations of the real data-generating process. I suggest that taken together the two models studied here provide a reasonably robust framework for understanding the effect of size of the introduced population on the chance of establishment for ruffe. In particular, even under a management policy with high tolerance for invasions (the opposite of a risk-averse or precautionary policy) the most severe models estimate that the chance of establishment is unacceptably high for even very small introductions. Including additional biological details is unlikely to affect this outcome for the following reasons.

Factors not considered by the model for long-term persistence are Allee effects (which were tested for but not detected and for which the power to detect is probably low), demographic stochasticity, and fluctuations in sex ratio. I have argued that for species like ruffe and other fishes with per-capita annual fecundities in the tens of thousands, environmental stochasticity in larval survival will overwhelm demographic stochasticity and fluctuations in sex ratio (cf. Engen et al. 2003). This life history contrasts with the life histories of other groups, particularly birds, for which much of the recent theory about demographic stochasticity and fluctuating sex ratio was developed (Sæther et al. 1998; Engen et al. 2003), and is consistent with the idea that fluctuating environments will affect species differently depending on life history. Detection, estimation, and analysis of Allee effects present a much more challenging problem. In Lake Superior, aggregation during spawning probably removes any effect of mate limitation. It remains to be determined if ruffe are regulated by Allee effects from other sources. The failure to detect Allee effects in this analysis is consistent with a Bayesian meta-analysis, which yielded little evidence for depensation in four other taxonomic groups of fish (salmonids, gadiforms, clupeiforms, and pleuronectiforms; Liermann and Hilborn 1997), suggesting that Allee effects may be rare in fish species generally. How often and under what conditions Allee effects occur in fish are important topics for future research.

In contrast to the model for long-term persistence, the model for winter survival explicitly considers effects of demographic stochasticity (individual heterogeneity in winter survival) and sex ratio, but does not consider environmental variability. Here, the major limitations are ignorance of the correct model structure and uncertainty in parameter estimates. For these reasons this model should be viewed as a thought experiment rather than as a representation of this particular system. Interpreted this way, this model shows that either a severely biased sex ratio in the donor population or extremely high winter mortality is required for demographic stochasticity and fluctuations in sex ratio to greatly influence the chance of establishment. Despite limitations, these models support relatively strong inferences from the perspective of potential policy. Considered together, they suggest that even under extreme conditions, the chance of establishment is around 10% for an introduction of just four individuals.

Additionally, these results rely on the premise that data from ruffe populations in Loch Lomond and within the species' native range are representative of demography in North America. Unfortunately, long-term data from other invaded ecosystems are not available to compare ruffe demography in different regions and to assess heterogeneity among lakes. In the absence of better data, it is not unreasonable to consider Loch Lomond a surrogate for North American lakes. Loch Lomond is monomictic and has average depth of 37 m. Minimum and maximum temperatures from biweekly sampling over 5 years (1996–2001) are 5.5 ± 1.2 and 16.5 ± 0.75 °C (mean ± standard deviation (SD)), respectively; Adams and Maitland 2001). While minor differences among lakes are inevitable even within a region, these characteristics are broadly consistent with the features of many North American lakes and differences are unlikely to greatly affect population dynamics.

Future analyses of invasion risk should focus on characterizing uncertainty in forecasts, estimates of which should accompany recommendations for management. More importantly, an outstanding problem in invasion biology is why so many introduced populations fail to establish, especially when many exhibit high population-growth rates (Williamson 1996). Clearly the phenomena modeled here (small population sizes and environmental variation) are not sufficient to explain the low rates of establishment commonly observed. It follows, therefore, that without further understanding of the biological mechanisms that limit population establishment, model projections cannot be expected to provide reliable estimates of invasion risk. In this respect the estimates obtained here should be interpreted as an upper bound on invasion risk for ruffe. Until lower bounds are determined, these are also our best estimates.

Acknowledgements

I thank K.L.S. Drury, D.M. Lodge, and two anonymous reviewers for comments on an earlier version of the manuscript. This work was funded by grants from the US Environmental Protection Agency's Science to Achieve Results program (USEPA STAR) (to David Lodge), a USEPA STAR Graduate Research Fellowship (to John Drake), and a University of Notre Dame Schmitt Research Fellowship (to John Drake).

References

Adams, C.E., and Maitland, P.S. 1998. The ruffe population of Loch Lomond, Scotland: its introduction, population expansion, and interaction with native species. J. Gt. Lakes Res. **24**: 249–262.

© 2005 NRC Canada

Adams, C.E., and Maitland, P.S. 2001. Invasion and establishment of freshwater fish populations in Scotland — the experience of the past and lessons for the future. Glasg. Nat. **23**: 35–43.

Beissinger, S.R., and McCullough, D.R. (*Editors*). 2002. Population viability analysis. University of Chicago Press, Chicago, Ill.

Belovsky, G.E., Mellison, C., Larson, C., and Van Zandt, P.A. 1999. Experimental studies of extinction dynamics. Science (Wash., D.C.), **286**: 1175–1177.

Burnham, K.P., and Anderson, D.R. 2002. Model selection and multimodel inference: a practical information–theoretic approach. 2nd ed. Springer-Verlag, New York.

Butskaya, N.A. 1976. On the large-scale intersexuality of the ruffe *Acerina cernua* of the eastern part of the Gulf of Finland. J. Ichthyol. (Engl. Transl. Vopr. Ikhtiol.), **16**: 737–745

Dennis, B. 2002. Allee effects in stochastic populations. Oikos, **96**: 389–401.

Dennis, B., Munholland, P.L., and Scott, J.M. 1991. Estimation of growth and extinction parameters for endangered species. Ecol. Monogr. **61**: 115–143.

Engen, S., Bakke, Ø., and Islam, A. 1998. Demographic and environmental stochasticity — concepts and definitions. Biometrics, **54**: 39–45.

Engen, S., Lande, R., and Sæther, B.-E. 2003. Demographic stochasticity and Allee effects in populations with two sexes. Ecology, **84**: 2378–2386.

Fedorova, G.V., and Vetkasov, S.A. 1974. Biological characteristics and abundance of Lake Ilmen ruffe. J. Ichthyol. (Engl. Transl. Vopr. Ikhtiol.), **13**: 943–946.

Foley, P. 1994. Predicting extinction times from environmental stochasticity and carrying capacity. Conserv. Biol. **8**: 124–137.

Froese, R., and Pauly, D. (*Editors*). 2003. FishBase [online]. World Wide Web electronic publication. Available from http://www.fishbase.org [version 26 October 2003].

Fullerton, A.H., Lamberti, G.A., Lodge, D.M., and Goetz, F.W. 2000. Potential for resource competition between Eurasian ruffe and yellow perch: growth and RNA responses in laboratory experiments. Trans. Am. Fish. Soc. **129**: 1331–1339.

Kolomin, Y.M. 1977. The Nadym River ruffe, *Acerina cernua*. J. Ichthyol. (Engl. Transl. Vopr. Ikhtiol.), **17**: 345–349.

Lande, R., and Orzack, S.H. 1988. Extinction dynamics of age-structured populations in a fluctuating environment. Proc. Natl. Acad. Sci. U.S.A. **85**: 7418–7421.

Lande, R., Engen, S., and Sæther, B.-E. 2003. Stochastic population dynamics in ecology and conservation. Oxford University Press, Oxford.

Leigh, P. 1998. Benefits and costs of the ruffe control program for the Great Lakes fishery. J. Gt. Lakes Res. **24**: 351–360.

Leung, B., Lodge, D.M., Finnoff, D., Shogren, J.F., Lewis, M., and Lamberti, G. 2002. An ounce of prevention or a pound of cure: bioeconomic risk analysis of invasive species. Proc. R. Soc. Lond. B Biol. Sci. **269**: 2407–2413.

Liermann, M., and Hilborn, R. 1997. Depensation in fish stocks: a hierarchic Bayesian meta-analysis. Can. J. Fish. Aquat. Sci. **54**: 1976–1984.

Lodge, D.M. 2001. Lakes. *In* Global biodiversity in a changing environment: scenarios for the 21st century. *Edited by* F.S. Chapin III, O. Sala, and E. Huber-Sanwald. Springer-Verlag, New York, pp. 277–313.

Morris, W.F., and Doak, D.F. 2002. Quantitative conservation biology: theory and practice of population viability analysis. Sinauer Associates, Sunderland, Mass.

Møller, A.P., and Legendre, S. 2001. Allee effect, sexual selection and demographic stochasticity. Oikos, **92**: 27–34.

National Research Council. 2002. Predicting invasions of nonindigenous plants and plant pests. National Academy Press, Washington, D.C.

Ogle, D.H. 1998. A synopsis of the biology and life history of ruffe. J. Gt. Lakes Res. **24**: 170–185.

Pratt, D.M., Blust, W.H., and Selgeby, J.H. 1992. Ruffe, *Gymnocephalus cernuus*: newly introduced in North America. Can. J. Fish. Aquat. Sci. **49**: 1616–1618.

Rahel, F.J. 2002. Homogenization of freshwater faunas. Annu. Rev. Ecol. Syst. **33**: 291–315.

Sæther, B.-E., Engen, S., Islam, An., McCleery, R., and Perrins, C. 1998. Environmental stochasticity and extinction risk in a population of small song bid, the great tit. Am. Nat. **151**: 441–450.

Sala, O.E., Chapin, F.S., III, Armesto, J.J., Berlow, R., Bloomfield, J., Dirzo, R., et al. 2000. Global biodiversity scenarios for the year 2100. Science (Wash., D.C.), **287**: 1770–1774.

SAS Institute Inc. 1999. SAS®. Version 8.2 [computer program]. SAS Institute Inc., Cary, N.C.

Savino, J.F., and Kolar, C.S. 1996. Competition between nonindigenous ruffe and native yellow perch in laboratory studies. Trans. Am. Fish. Soc. **125**: 562–571.

Selgeby, J. 1998. Predation by ruffe (*Gymnocephalus cernuus*) on fish eggs in Lake Superior. J. Gt. Lakes Res. **24**: 304–308.

Selgeby, J.H., and Ogle, D.H. 1992. Trophic relations of ruffe and the status of ongoing research in the St. Louis River Estuary, Lake Superior, 1991. Lake Superior Committee, Great Lakes Fishery Commission, Ann Arbor, Mich.

Shigesada, N., and Kawasaki, K. 1997. Biological invasions: theory and practice. Oxford University Press, Oxford.

Tier, C., and Hanson, F.B. 1981. Persistence of density dependent stochastic populations. Math. Biosci. **53**: 89–117.

Turchin, P. 2003. Complex population dynamics: a theoretical/empirical synthesis. Princeton University Press, Princeton, N.J.

Williamson, M. 1996. Biological invasions. Chapman & Hall, London.

Wilson, E.O. 2000. On the future of conservation biology. Conserv. Biol. **14**: 1–3.

© 2005 NRC Canada

Age validation of canary rockfish (*Sebastes pinniger*) from off the Oregon coast (USA) using the bomb radiocarbon method

Kevin R. Piner, Owen S. Hamel, Jennifer L. Menkel, John R. Wallace, and Charles E. Hutchinson

Abstract: The alternating translucent and opaque banding pattern in canary rockfish (*Sebastes pinniger*) otoliths, aged using a break-and-burn methodology, are annual markings. To validate age assignment, we compared measured radiocarbon levels in canary rockfish otolith cores with a reference chronology developed from known age Pacific halibut (*Hippoglossus stenolepis*). An average 2- to 3-year phase shift was detected between the canary rockfish and a Pacific halibut reference chronology that was likely the result of differences in the regional oceanography or underageing bias. The assumption of ageing bias consistency was tested with two sampling designs. The first design controled for age-related ageing error, and the second design related birth year to estimated age. No change in the magnitude of ageing bias as a function of age was detected.

Résumé : Le patron de bandes alternées translucides et opaques dans les otolithes du sébaste canari (*Sebastes pinniger*), analysé par la méthode de cassure et de brûlage, représente des marques annuelles. Afin de valider la détermination de l'âge, nous avons utilisé des mesures de concentrations de radiocarbone dans des carottes des otolithes de sébastes canaris que nous avons comparées à une chronologie de référence élaborée chez des flétans du Pacifique (*Hippoglossus stenolepis*) d'âge connu. Il existe un décalage moyen de 2–3 ans entre les résultats obtenus chez le sébaste et la chronologie de référence du flétan, qui s'explique soit par des différences océanographiques régionales, soit par une erreur de sous-estimation de l'âge. La possibilité d'une erreur systématique dans la détermination de l'âge a été vérifiée à l'aide de deux plans d'échantillonnage. Le premier plan tient compte des erreurs de détermination associées à l'âge et le second plan met en relation l'année de la naissance et l'âge estimé. Nous n'avons pas détecté de changement dans l'importance de l'erreur de détermination de l'âge en fonction de l'âge.

[Traduit par la Rédaction]

Introduction

Canary rockfish (*Sebastes pinniger*) are found on the continental shelf off the west coast of the United States, Canada, and Alaska. They are a long-lived species, reported to live in excess of 50 years (Crone et al. 1999). Larvae are initially pelagic until settling into nearshore rocky habitat during the summer of their first year of life (Boehlert 1980; Crone et al. 1999). The species appears to undergo an ontogenetic migration to deeper waters with increasing age (Love et al. 2002), and the majority of the population is found at depths shallower than 250 m (Boehlert 1980; Crone et al. 1999).

The canary rockfish population was estimated to be below 10% of the unexploited stock size in 2002 (Methot and Piner 2002). The stock is currently managed under a rebuilding plan that allows for catches in the near future to be only a small fraction of the historical catch to achieve stock rebuilding. Canary rockfish were once a targeted fishery, but because of the low stock size they are currently taken as nontargeted catch. The low population size of canary rockfish constrains the harvest of other species because of the multispecies nature of the fisheries in this region. Rebuilding from the current population level to a target of 40% of unexploited stock size is estimated to take several decades. Age

Received 16 January 2004. Accepted 29 September 2004. Published on the NRC Research Press Web site at http://cjfas.nrc.ca on 26 May 2005.
J17923

K.R. Piner,[1] **O.S. Hamel,**[2] **and J.R. Wallace.** National Marine Fisheries Service, Northwest Fisheries Science Center, 2725 Montlake Boulevard East, Seattle, WA 98112, USA.
J.L. Menkel. Pacific States Marine Fisheries Commission, Northwest Fisheries Science Center, 2032 South East OSU Drive, Newport, OR 97365, USA.
C.E. Hutchinson. National Marine Fisheries Service, Alaska Fisheries Science Center, P.O. Box 15700 Seattle, WA 98115-0070, USA.

[1]Present address: National Marine Fisheries Service, Southwest Fisheries Science Center, 8604 La Jolla Shores Drive, La Jolla, CA 92037, USA.
[2]Corresponding author (e-mail: owen.hamel@noaa.gov).

 doi: 10.1139/F05-082 © 2005 NRC Canada

composition and longevity information have helped shape the view of current stock status of canary rockfish and its future prospects for recovery, but the accuracy of the ages is unknown. Bomb radiocarbon (^{14}C) validation of the ageing method for this long-lived species is likely the best available method to test this assumption.

Bomb radiocarbon validation (Kalish 1993, 1995) refers to the use of the nearly synchronous increase in the ^{14}C levels in marine calcareous structures formed during the 1950s–1970s as a dated marker. This rapid increase in surface oceanic and atmospheric ^{14}C levels was due to atmospheric testing of nuclear weapons (Nydal 1993). This phenomenon offers fishery biologists a means to assess the accuracy of age estimates for fish born during this period to within ±1–3 years (Campana 2001). The birth years 1955–1975 are of most interest, as they encompass the period of rapid rise to the peak in radiocarbon levels. The validation method typically relies on determining ^{14}C levels in otolith material from the first year of life and developing a time series of increasing ^{14}C levels with known or estimated birth years. Age assignments can be judged on their accuracy (validation) by comparing core ^{14}C time series to a reference time series of known ^{14}C levels (Kalish et al. 2001) during the same period. The drawbacks of this method include high costs and difficulties in locating fish born during the desired period. The advantages include validation of the ageing method across several age classes. For many long-lived species, this can be across 30–40 years. This method assumes that the rate of increase, and especially the timing of the initial increase in the ^{14}C of the validation chronology, is the same as the reference chronology used for comparison. The method also assumes that the magnitude of any ageing bias is consistent across all ages used in the study (Campana and Jones 1998).

The objective of this work was to use ^{14}C levels measured in canary rockfish otolith cores from fish collected during the 1990s to validate the ageing method currently used to produce age composition data for canary rockfish stock assessments. To validate the age assignment, we compared the canary rockfish ^{14}C chronology with a chronology developed from known age individuals of Pacific halibut (*Hippoglossus stenolepis*) (Piner and Wischniowski 2004). Using a simple sampling design, we also evaluated the assumption that the magnitude of ageing error is independent of age.

Methods

Sample collection

Biologists from the Oregon Department of Fish and Wildlife have routinely collected both sagittal otoliths from fish taken by trawlers operating in the eastern Pacific at approximately 45°N. One otolith was initially used to determine the age through annuli counts, while the second otolith was archived. The annuli in this study were the translucent winter growth bands. All ages were estimated using a break-and-burn method, in which the otolith was broken in half through the focus and then charred with an alcohol flame. The charring enhances the contrast between the opaque and translucent regions in the otolith.

Each otolith was aged at least one additional time by an independent reader. The first age (Tables 1 and 2) was the production age and has been used in all canary rockfish stock assessments (Crone et al. 1999; Methot and Piner 2002). Because of the importance of the age information to the stock assessments, we used the first age as the basis for the analysis to determine ageing accuracy. The second age was produced at a later date by a second reader working in the same laboratory as the first reader. A third age was produced at a later date by a third reader working in an independent laboratory. The first age used the freshest burn, while subsequent readings were potentially more difficult because charring from the burn may have faded with time.

Sample preparation

Otolith cores were removed to obtain material deposited prior to the first annulus, which encompassed the first year's growth. Each otolith core was removed following procedures similar to those of Campana and Jones (1998). The core size corresponding to the first year of growth was measured in young canary rockfish using imaging software and used to estimate the diameter of the first year of otolith growth in adult fish. The otolith section that approximated the core measurements was removed using a slow-speed isomet saw. A Dremel™ (Mount Prospect, Illinois) variable-speed drill and a variable-speed lapping wheel with 320 grit sanding paper were used to remove any additional material beyond the first annulus. Both the sanding paper and Dremel tips were changed for each otolith to prevent cross-contamination. An iterative process of otolith material removal followed by visual inspection under × 30 to × 60 magnification was used to produce the final core. Final otolith cores were subsequently cleaned in an ultrasonic bath, dried, weighed, and packaged in glass vials before being sent to the Woods Hole Accelerator Mass Spectroscopy laboratory (Gagnon et al. 2000) for assay. Each core was assayed for both $\delta^{14}C$ and $\delta^{13}C$. The $\delta^{13}C$ values were used to correct for isotopic fractionization, and the subsequent values of ^{14}C were then reported as $\Delta^{14}C$, which was defined as the adjusted per mil deviation (‰) from the radiocarbon activity of 19th-century wood (Stuiver and Polach 1977).

Assumption of ageing bias consistency

To test the assumption that the magnitude of ageing bias did not change as a function of age, we selected otoliths from 28 canary rockfish using two sampling designs. The first design group consisted of 19 otoliths selected from a sample frame of canary rockfish collected during 1993 whose estimated birth years were from 1949 to 1974 (Table 1). In this design, the youngest fish were the most recent cohorts, and the ages from annuli counts and the estimated birth years were linearly related. The second design group consisted of nine fish from a sampling frame of canary rockfish collected during the 1990s, with ages based on an annuli count of approximately 30 years. The estimated birth dates in this design component fell between 1957 and 1970 (Table 2). Because samples in the second design were selected from the same age group, this design controlled for ageing error changing as a function of age. The birth years in the second design did not need to extend back before the period

© 2005 NRC Canada

Table 1. The temporal, biological, and chemical information used in the validation of canary rockfish (*Sebastes pinniger*) ages from fish that were collected in the same year and over a range of ages and used in the test of ageing error consistency.

Sample No.	Collection year	Birth year	Total length (cm)	Sex	Core weight (mg)	First age	Second age	Third age	$\delta^{13}C$ (‰)	$\Delta^{14}C \pm$ error (‰)
1	1993	1949	54	M	14.8	44	44	45	–2.47	–109.3±4.5
2	1993	1951	53	M	12.2	42	41	na	–3.00	–97.8±3.4
3	1993	1954	53	M	9.7	39	44	na	–2.85	–104.8±6.2
4	1993	1956	52	M	21.5	37	38	37	–2.35	–100.4±2.9
5	1993	1958	51	M	14.1	35	37	na	–2.55	–103.0±4.2
6	1993	1959	51	M	11.0	34	34	35	–1.67	–98.0±3.6
7	1993	1959	51	M	25.3	34	33	na	–3.02	–81.3±3.0
8	1993	1961	51	M	15.5	32	31	na	–2.72	–76.2±4.8
9	1993	1962	50	M	18.2	31	31	31	–2.38	–41.9±3.8
10	1993	1962	52	M	21.6	31	32	na	–2.50	–75.1.0±3.8
11	1993	1963	52	M	15.5	30	31	32	–2.42	–92.6±3.4
12	1993	1964	54	M	17.1	29	30	28	–1.80	–88.0±2.9
13	1993	1965	59	F	16.1	28	29	na	–2.85	–93.0±3.7
14	1993	1966	54	M	15.1	27	27	31	–2.00	–73.9±3.1
15	1993	1967	55	F	17.8	26	26	26	–2.12	–7.4±5.5
16	1993	1968	52	M	18.7	25	25	26	–2.90	10.1±3.2
17	1993	1970	51	M	11.7	23	23	24	–2.59	0.8±3.4
18	1993	1972	55	M	18.9	21	23	na	–2.47	19.8±3.3
19	1993	1974	50	M	11.9	19	19	23	–2.83	18.9±4.1

Note: $\delta^{13}C$ ($^{13}C/^{12}C$) was used to correct for isotopic fractionation to produce $\Delta^{14}C$, which is the per mil deviation from the radiocarbon concentration of 19th-century wood. na, data is not available.

Table 2. The temporal, biological, and chemical information used in the validation of canary rockfish (*Sebastes pinniger*) ages from fish that were collected from a range of years and of a similar age and used in the test of parallelism of the uptake rates.

Sample No.	Collection year	Birth year	Total length (cm)	Sex	Core weight (mg)	First age	Second age	$\delta^{13}C$ (‰)	$\Delta^{14}C \pm$ error (‰)
20	1990	1957	54	M	21.6	33	35	–2.17	–104.9±3.7
21	1990	1960	59	F	14.2	30	30	–2.7	–79.9±3.1
22	1992	1962	59	F	19.2	30	31	–2.90	–89.2±3.1
23	1993	1962	54	F	15.0	31	30	–2.56	–36.8±4.0
24	1994	1963	53	M	11.8	31	31	–2.99	–106.2±3.0
25	1994	1965	52	M	12.5	29	30	–2.85	–82.7±3.8
26	1997	1967	53	M	12.2	30	30	–2.79	8.3±4.1
27	1998	1969	50	M	11.8	29	29	–2.69	–28.3±3.5
28	1999	1970	54	M	10.2	29	32	–3.28	30.0±3.5

Note: $\delta^{13}C$ ($^{13}C/^{12}C$) was used to correct for isotopic fractionation to produce $\Delta^{14}C$, which is the per mil deviation from the radiocarbon concentration of 19th-century wood.

of initial increase, because $\Delta^{14}C$ is largely uninformative with respect to age in the prebomb period. If ageing error changed as a function of age, then a comparison of the two sampling design chronologies should show a phase shift that increased or decreased with age.

Validation of ageing method

To validate the age assignments, we compared the $\Delta^{14}C$ chronology derived from canary rockfish with a reference curve of $\Delta^{14}C$ developed from Pacific halibut (Piner and Wischniowski 2004) that were collected in the northeast Pacific (52°N–60°N). To facilitate the comparison of chronologies, we estimated predicted levels of $\Delta^{14}C$ for both data sets using logistic curves estimated in AD Model Builder (Otter Research Ltd., Sidney, British Columbia) by minimizing the weighted sum of the variance in each direction. This method required the ratio of the variances to be fixed. The logistic was parameterized as the following equation, setting the lower asymptote (y_{min}) to be the lowest value observed in that data set:

$$\hat{y} = y_{min} + \frac{k}{1 + \exp[b(a - x)]}$$

where $y = \Delta^{14}C$, x = birth year, and the parameters k (absolute range of increase), a (temporal midpoint of increase), and b (shape parameter) were estimated.

For the canary data, we assumed errors in both of the coordinates that represented both process and measurement error in $\Delta^{14}C$ and measurement error in the birth year estimates. We assumed that the errors were normally distributed. The ratio of the variances was estimated by comparing the variance around the upper asymptote for the halibut data (to estimate variability in $\Delta^{14}C$), including all data for esti-

© 2005 NRC Canada

Fig. 1. The $\Delta^{14}C$ chronologies derived from otoliths taken from canary rockfish, *Sebastes pinniger* (●), and from Pacific halibut, *Hippoglossus stenolepis* (○) (Piner and Wischniowski 2004). Lines represent a logistic fit to each series. Birth years were determined from otolith annuli counts. Errors bars representing radiocarbon measurement error have been removed from samples prior to 1965 to improve the legibility of the figure.

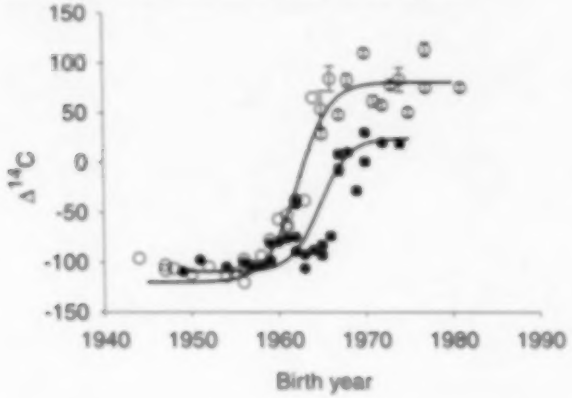

mated birth years of 1968 and above (variance = 417.8), with the average coefficient of variation (CV) from an independent double-read analysis of canary rockfish (0.103, n = 74) (Crone et al. 1999), multiplied by the average estimated age of 31, and then squared (to estimate variability in the estimate of birth year, variance = 10.1). For the Pacific halibut data, for which the birth years are known (Piner and Wischniowski 2004), we assumed error only in $\Delta^{14}C$. A synchronous increase in $\Delta^{14}C$ values was interpreted as evidence that the ages used to develop the time series were accurate. The phase shift between the years of initial rise in the two curves was estimated as the difference between the timing at 20% increase in each curve.

Results

General

Fish were between 19 and 44 years of age and ranged from 50 to 59 cm total length (Tables 1 and 2). The average core weight of all otoliths was 15.6 mg (standard deviation, SD = 4.0). The second age reading (Tables 1 and 2) produced significantly older ages (average difference = 0.6 years) than the first reading (p = 0.02, n = 28, paired t test). The third age reading also produced significantly older ages (average difference = 1.2 years) than the first reading (p = 0.03, n = 11, paired t test).

While the first data points that are obviously above the prebomb levels occurred at the same time for both Pacific halibut and canary rockfish (Fig. 1), a second group of canary rockfish observations between estimated birth years 1962 and 1965 contained $\Delta^{14}C$ levels consistent with prebomb levels and were quite different from the halibut chronology. Otolith cores formed prior to 1959 based on otolith age contained very low levels of $\Delta^{14}C$ (minimum = –109.3‰ in 1949), similar to halibut. Otolith cores from canary rockfish with estimated birth years from 1959 to 1969 showed increased radiocarbon values, with a possible local maximum at –36.8‰ in 1962. The peak $\Delta^{14}C$ values occurred in 1969 at 30.0‰. The maximum values of $\Delta^{14}C$ in the otolith cores were substantially less than those reported for Pacific halibut.

Fig. 2. The $\Delta^{14}C$ chronologies from canary rockfish, *Sebastes pinniger*, otoliths used to validate the assumption that the magnitude of the ageing bias did not change as a function of age. The test included two sample designs: samples of approximately the same age (○) and samples that linearly related birth year to age (●). All ages were determined from otolith annuli counts.

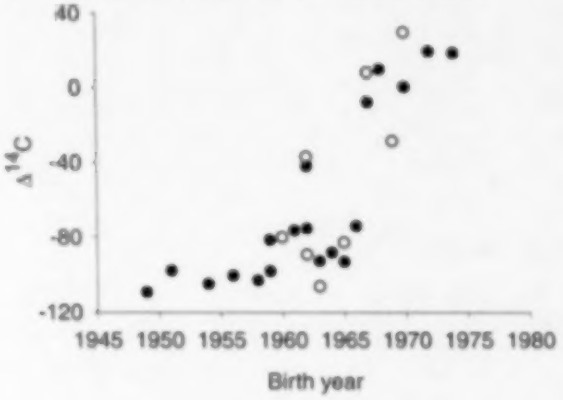

Assumption of ageing bias consistency

We could not document that the magnitude of the potential ageing bias changed as a function of age. Despite the highly variable data, the patterns of change in $\Delta^{14}C$ values from otolith cores taken from both sampling designs were nearly identical (Fig. 2). Because we could not document evidence of an ageing bias changing as a function of age, the two data sets were combined and subsequently compared with the halibut data.

Validation of ageing methods

There was considerable variability around the functional form that described the change in $\Delta^{14}C$ with estimated birth year. The variance in $\Delta^{14}C$ used to estimate the logistic was assumed to be 10 times the variance in birth year based on the estimates of variance in each described above (ratio = 41.2) and after inflating the variance in the birth year estimate to account for between-otolith variance, which was not captured by the double-read analysis. The shape of the fitted canary rockfish $\Delta^{14}C$ logistic curve (b = 0.61) was similar to that of the halibut reference curve (b = 0.55) (Fig. 1). The difference in the average timing of the first increase, represented by the timing of 20% of the total increase of the logistic a' was 2.8 years between the canary rockfish curve (a' = 1962.6) and the Pacific halibut curve (a' = 1959.8). This was nearly identical to the difference (2.5 years) between the midpoints of the canary curve (a = 1964.8) and halibut curve (a = 1962.3). A 2.8-year phase shift represents <10% of the median age of the fish used in this study. The other estimated logistic parameters were k = 200.6 and k = 133.2 for halibut and canary rockfish, respectively. The estimated parameters and differences were insensitive to the assumption of the ratio between the variance in $\Delta^{14}C$ and the variance in estimated birth year. Using a variance ratio of either 40 or 100 instead of 10 resulted in very similar curves,

© 2005 NRC Canada

with identical 2.8-year phase shifts at the point of 20‰ increase.

The strength of upwelling at 45°N (Smith et al. 2001), as measured by the amount of offshore Ekman transport in the surface layer (http://www.pfeg.noaa.gov), appeared to have little correlation with the residual pattern about the logistic fit to the canary rockfish data (Fig. 3). The residuals were an estimate of the direction and magnitude of the deviation of the observed $\Delta^{14}C$ value from that predicted by the logistic curve. Anomalously low $\Delta^{14}C$ levels, as measured by large negative residuals in the fit of the canary logistic curve, show no strong relationship to either the strength of upwelling in the year of otolith formation or to upwelling in the prior year.

Discussion

This work supports the conclusion that the alternating translucent and opaque banding pattern within the canary rockfish otolith represents annual markings. It seems doubtful that the annuli from the break-and-burn method used to age canary rockfish are anything but annual marks, as the reconstructed time series of ^{14}C values from the canary rockfish otolith cores approximates that of the halibut reference curve with an average 2- to 3-year delay. The delay can be explained by measurement error due to ageing inaccuracy, process error resulting from a reference chronology that does not match the expectations for oceanic conditions on the Oregon continental shelf, or a combination of both sources. The first observed increase in ^{14}C occurs at the same estimated birth year for canary rockfish as for Pacific halibut, but after 1962 the ^{14}C levels in the canary rockfish chronology declined to near prebomb levels. This indicates either that there may be a mix of correctly aged and underaged canary rockfish (with no overageing) or that oceanographic conditions experienced by canary rockfish and Pacific halibut were substantially different after 1962.

The canary rockfish samples were collected off the Oregon coast (USA), while the reference chronology was derived from samples taken in the Gulf of Alaska and along the west coast of British Columbia, Canada (Piner and Wischniowski 2004). The Oregon shelf is characterized by complex and temporally variable oceanographic processes. Wind stress and freshwater runoff, primarily Columbia River outflow, are important to the circulation patterns that can vary weekly, seasonally, and interannually (Smith et al. 2001). Interannual variations are influenced by the El Niño Southern Oscillation (ENSO) phenomenon. ENSO events can introduce anomalous water masses onto the continental shelf off Oregon (Huyer and Smith 1985), although not all ENSO events are strong enough to be felt that far north (Enfield and Allen 1980; Mysak 1986). Seasonal, oceanographic processes include downwelling (Austin and Barth 2002) and upwelling (Huyer 1977, 1983) that are also affected by ENSO events. Upwelling is typically sporadic, occurring during any season where winds are predominantly from the north. Upwelling off the Oregon coast can result in the movement of 8 °C waters from below the pycnocline onto the shelf (Mooers et al. 1976; Huyer 1977). Waters upwelled from below these density fronts may contain carbon of an earlier origin, resulting in anomalously low ^{14}C levels of $\Delta^{14}C$ and potentially a delay in the timing of increase. The complicated oceanographic processes occurring along the Oregon coast are different from those occurring off the coasts of Alaska and British Columbia. The effects of these oceanographic differences on the shape of the radiocarbon chronologies are not clear.

Fig. 3. The residuals (observed – predicted) from the fit of the logistic to the canary rockfish, *Sebastes pinniger*, $\Delta^{14}C$ chronology plotted against (*a*) the yearly mean upwelling index from the year of otolith material formation and (*b*) the yearly mean upwelling index from the prior year. The upwelling index is the average of the monthly measures of the surface Ekman transport, with the units of $m^3 \cdot s^{-1} \cdot 100\ m^{-1}$ of coastline. The upwelling data is available through the Pacific Fisheries Environmental Laboratory (http://www.pfeg.noaa.gov).

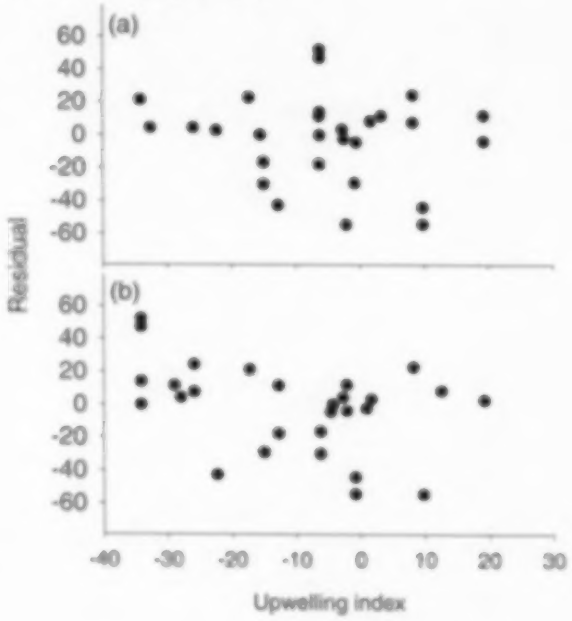

The low prebomb levels of ^{14}C measured in canary rockfish otoliths suggest that upwelling of depleted ^{14}C waters onto the continental shelf is an important oceanographic process along the Oregon coast. Nearly identical levels of prebomb ^{14}C were also measured in Pacific halibut (Piner and Wischniowski 2004) and yelloweye rockfish, *Sebastes ruberrimus*, (Kerr et al. 2004) derived from the continental shelf off Canada and Alaska, suggesting that those areas may have been similarly affected by seasonal upwelling. Similar effects on the ^{14}C chronologies due to upwelling have been reported for corals in both the Atlantic and Pacific oceans (Toggweiler et al. 1991; Druffel 1996). Although the year-to-year variability in the distribution of isopycnals along the Oregon coast is less than the seasonal variability (Huyer 1977), the period 1960–1964 was characterized by below average upwelling at 42°N–45°N (Smith et al. 2001). Conversely, the estimated birth years corresponding to 1962–1964 contain some of the most anomalously low ^{14}C levels that were measured in canary rockfish, which suggests that variability in upwelling alone cannot explain these

© 2005 NRC Canada

anomalies. The low postbomb maximum levels of ^{14}C in canary rockfish indicate that canary larvae and juveniles are not in contact with water masses with significant atmospheric influence, such as from direct freshwater input (Campana and Jones 1998), or that the series did not capture the peak radiocarbon level.

Ageing error could have produced the measured delay in timing of ^{14}C increase. Previous ageing precision work (Crone et al. 1999) concluded that age reproducibility is low, ranging from 25% agreement for ages 6–13 to 16% for ages >25. The relatively low between-readers agreement, even on the youngest ages, precludes treating any single data point as known without error. The average CV calculated over all double and triple reads for the otoliths used in this study was 3.0%. Repeated age readings on the otoliths reported in this study produced ages older than the first age. If the second or third ages had been used, the apparent bias in ageing would be lessened, but not eliminated. This supports the assertion that measurement error in the form of an underageing bias is a likely factor contributing to the delay in the canary rockfish chronology relative to the Pacific halibut. Without a chronology of dissolved inorganic carbon (Kalish et al. 2001) from the areas inhabited by canary rockfish juveniles, however, the processes of upwelling or underageing are confounded and cannot be separated in this study.

This study used a simple sampling design to evaluate the assumption that the magnitude of the ageing bias did not change as a function of age. Although not carried out in this study, the sampling design that controlled for ageing error could be used to statistically test for equality of the rate of change measured in canary rockfish and a reference chronology by eliminating the confounding problem of ageing error changing as a function of age. The assumption of equality in the timing of increase between reference and test species is supported by the similarity between the ^{14}C functional forms from other published studies, including species from the Atlantic (Campana 1997; Kalish et al. 2001), Gulf of Mexico (Baker and Wilson 2001), and the northeast Pacific (Piner and Wischniowski 2004).

We could not document a violation of the assumption that the processed cores were not contaminated by more recently formed otolith material. The effects of large errors in the processing of otolith cores from cohorts close to the period of the initial rise would have resulted in the inclusion of otolith material from more recent years with presumably higher values of ^{14}C. Such errors would result in greater than expected measured $\Delta^{14}C$ levels; however, the largest deviations from the expected were in the opposite direction. Small errors in processing would result in only small increases in ^{14}C levels observed, and any minor error would have little effect on the conclusions of this study.

This work provides the first time series of ^{14}C levels measured in a fish species on the continental shelf off Oregon, USA. Although uncertainty exists in the measured ^{14}C levels as well as the year of material formation, this work provides an important history of oceanographic conditions, making these results of a broader interest than simply to fisheries science. The ageing work underlying the ^{14}C chronology is the product of the standard ageing effort that is done to support stock assessments. Although the hypothesis of underageing and oceanographic influences cannot be separated in this study, stock assessments using underaged samples can increase the likelihood of overfishing (Lai and Gunderson 1987). The current canary rockfish assessment combines ages >25 into a single group (Methot and Piner 2002), so the effect of underageing of the old fish used in this study may not be critical to the assessment results. However, if underageing occurs in the youngest ages, it could potentially alter the estimation of important biological process, such as growth and recruitment. To improve the subsequent stock assessments, we should direct future validation efforts at younger age classes.

Acknowledgements

We are grateful to our colleagues at the Northwest Fisheries Science Center, Alaska Fisheries Science Center, and the Cooperative Ageing Project for their cooperation and helpful suggestions. Christian Reiss was invaluable in providing oceanographic expertise. We are also indebted to several anonymous reviewers for helpful critiques of this work. The National Science Foundation partially supported this work through the Cooperative Agreement OCE-9807266 grant.

References

Austin, J.A., and Barth, J.A. 2002. Drifter behavior on the Oregon–Washington shelf during downwelling favorable winds. J. Phys. Ocean. **32**: 3132–3144.

Baker, S.M., and Wilson, C.A. 2001. Use of bomb radiocarbon to validate otolith section ages of red snapper *Lutjanus campechanus* from the northern Gulf of Mexico. Limnol. Oceanogr. **46**(7): 1819–1824.

Boehlert, G.W. 1980. Size composition, age composition, and growth of canary rockfish, *Sebastes pinniger*, and splitnose rockfish, *S. diploa*, from the 1977 rockfish survey. Mar. Fish. Rev. **42**(3–4): 57–63.

Campana, S.E. 1997. Use of radiocarbon from nuclear fallout as a dated marker in the otoliths of haddock, *Melanogrammus aeglefinus*. Mar. Ecol. Prog. Ser. **150**: 49–56.

Campana, S.E. 2001. Accuracy, precision and quality control in age determination, including a review of the use and abuse of age validation methods. J. Fish Biol. **59**:197–242.

Campana, S.E., and Jones, C.M. 1998. Radiocarbon from nuclear testing applied to age validation of black drum, *Pogonias cromis*. Fish. Bull. **96**: 185–192.

Crone, P.R., Piner, K.R., Methot, R.D., Conser, R.J., and Builder, T.L. 1999. Status of the canary rockfish resource off Oregon and Washington in 1999. *In* Appendix to the status of the Pacific coast groundfish fishery through 1999 and recommended acceptable biological catches for 2000. Pacific Fishery Management Council, Portland, Ore.

Druffel, E.R.M. 1996. Post-bomb radiocarbon records of surface corals from the tropical Atlantic ocean. Radiocarbon, **38**(3): 563–572.

Enfield, D.B., and Allen, J.S. 1980. On the structure and dynamics of monthly mean sea level anomalies along the Pacific Coast of North and South America. J. Phys. Ocean. **10**: 557–578.

Gagnon, A.R., McNichol, A.P., Donoghue, J.C., Stuart, D.R., and von Reden, K. 2000. The NOSAMS sample preparation laboratory in the next millennium: progress after the WOCE program. Nucl. Instrum. Methods Phys. Res. B, **172**: 409–415.

© 2005 NRC Canada

Huyer, A. 1977. Seasonal variation in temperature, salinity, and density over the continental shelf off Oregon. Limnol. Oceanogr. **22**(3): 442–453.

Huyer, A. 1983. Coastal upwelling in the California current system. Prog. Oceanogr. **12**: 259–284.

Huyer, A., and Smith, R.L. 1985. The signature of El Nino off Oregon, 1982–1983. J. Geophys. Res. **90**: 7133–7142.

Kalish, J.M. 1993. Pre- and post-bomb radiocarbon in fish otoliths. Earth Planet. Sci. Lett. **114**: 549–545.

Kalish, J.M. 1995. Application of the bomb radiocarbon chronometer to the validation of redfish *Centroberyx affinis* age. Can. J. Fish. Aquat. Sci. **52**: 1399–1405.

Kalish, J.M., Nydal, R., Nedreaas, K.H., Burr, G.S., and Eine, G.L. 2001. A time history of pre- and post-bomb radiocarbon in the Barents sea derived from Arcto-Norwegian cod otoliths. Radiocarbon, **43**: 843–855.

Kerr, L.A., Andrews, A.H., Frantz, B.R., Coale, K.H., Brown, T.A., and Cailliet, G.M. 2004. Radiocarbon in otoliths of yelloweye rockfish (*Sebastes ruberrimus*): a reference time series for the coastal waters of southeast Alaska. Can. J.Fish. Aquat. Sci. **61**: 443–451.

Lai, H.L., and Gunderson, D.R. 1987. Effects of ageing errors on estimates of mortality and yield per recruit for walleye pollock (*Theragra chalcogramma*). Fish. Res. **5**: 287–302.

Love, M.S., Yoklavich, M., and Thorsteinson, L. 2002. The rockfishes of the Northeast Pacific. University of California Press, Los Angeles, Calif.

Methot, R., and Piner, K. 2002. Stock assessment of canary rockfish off California, Oregon and Washington in 2001. *In* Status of the Pacific Coast groundfish fishery through 2002; stock assessment and fishery evaluation. Vol. I. Pacific Fishery Management Council, Portland, Ore.

Mooers, C.N.K, Collins, C.A., and Smith, R.L. 1976. The dynamic structure of the frontal zone in the coastal upwelling region off Oregon. J. Phys. Ocean. **6**(1): 3–21.

Mysak, L.A. 1986. El Nino, interannual variability and fisheries in the northeast Pacific Ocean. Can. J. Fish. Aquat. Sci. **43**: 464–497.

Nydal, R. 1993. Application of bomb ^{14}C as a tracer in the global carbon cycle. Trends Geophys. Res. **2**: 355–364.

Piner, K.P., and Wischniowski, S.G. 2004. Pacific halibut (*Hippoglossus stenolepis*) chronology of bomb radiocarbon in otoliths from 1944–1981 and a validation of ageing methods. J. Fish Biol. **64**: 1060–1071.

Smith, R.L., Huyer, A., and Fleischbein, J. 2001. The coastal ocean off Oregon from 1961 to 2000: Is there evidence of climate change or only of Los Niños? Progr. Oceanogr. **49**: 63–93.

Stuiver, M., and Polach, H.A. 1977. Discussion: Reporting of 14C data. Radiocarbon, **19**: 355–363.

Toggweiler, J.R., Dixon, K., and Broecker, W.S. 1991. The Peru upwelling and the ventilation of the south Pacific thermocline. J. Geophys. Res. **96**(C11): 20467–20497.

© 2005 NRC Canada

Inferring sedimentary chlorophyll concentrations with reflectance spectroscopy: a novel approach to reconstructing historical changes in the trophic status of mountain lakes

Biplob Das, Rolf D. Vinebrooke, Arturo Sanchez-Azofeifa, Benoit Rivard, and Alexander P. Wolfe

Abstract: Reflectance spectroscopy has made it possible to rapidly and nondestructively assess the chlorophyll content of plants and natural waters. However, to date this approach has not been applied to chlorophyll and chlorophyll derivatives preserved in lake sediments. Here, we explore the relationships between visible-near-infrared spectral properties of lake sediments and measured pigment concentrations for lakes that have been exposed recently to anthropogenic nitrogen deposition. Down-core decreases in pigment concentrations and changes in reflectance properties effectively chronicle increases in whole-lake primary production since 1950. Specifically, reflectance spectra of sediments from four alpine lakes in Rocky Mountain National Park (Colorado Front Range, USA) preserve salient troughs near 675 nm that covary in magnitude with concentrations of chlorophyll *a* and associated pheopigments. The area of the trough in reflectance between 600 and 760 nm best explains the sum of total chlorophyll *a* and its derivatives ($r^2 = 0.82$, $n = 23$, $P < 0.01$). This result suggests that chlorophyll *a* preserved in lake sediments can be remotely sensed using a simple index derived from reflectance spectroscopy, thus providing a new paleolimnological strategy for rapid exploratory assessments of changing lake trophic status.

Résumé : La spectroscopie de réflectance permet de déterminer rapidement et sans destruction le contenu en chlorophylle des plantes et des eaux naturelles. Cette méthodologie n'a cependant pas été utilisée jusqu'à maintenant pour mesurer la chlorophylle et ses dérivés conservés dans les sédiments lacustres. Nous examinons ici les relations entre les propriétés spectrales dans le visible et l'infrarouge adjacent des sédiments lacustres, d'une part, et les concentrations de pigments mesurés, d'autre part, dans des lacs qui ont été exposés récemment à la déposition d'azote d'origine anthropique. La réduction des concentrations de pigments vers le bas des carottes de sédiments et les changements des propriétés de réflectance représentent concrètement l'augmentation de la production primaire à l'échelle du lac entier depuis 1950. De manière plus spécifique, les spectres de réflectance des sédiments de quatre lacs alpins du Parc national des Montagnes Rocheuses (versant oriental du Colorado, Colorado Front Range, É.-U.) conservent des creux évidents près de 675 nm, dont l'importance est en covariance avec les concentrations de chlorophylle *a* et des phéopigments associés. La surface du creux dans la réflectance entre 600 nm et 760 nm explique le mieux la somme de la chlorophylle *a* totale et de ses dérivés ($r^2 = 0{,}82$, $n = 23$, $P < 0{,}01$). Ce résultat indique que la chlorophylle *a* conservée dans les sédiments lacustres peut être mesurée à distance à l'aide d'un indice simple provenant de la spectroscopie de réflectance, fournissant ainsi une nouvelle stratégie de paléolimnologie pour évaluer rapidement, et de façon exploratoire, le statut trophique changeant d'un lac.

[Traduit par la Rédaction]

Introduction

Among the most important applications of paleolimnology is the reconstruction of historical changes in lake trophic status, including those pertaining to cultural eutrophication (Hall and Smol 1999). To this end, robust methodologies have been developed using diatoms (Reavie et al. 1995; Bennion et al. 1996), sediment geochemistry (Engstrom et al. 1985; Schelske et al. 1986), and combined multiproxy approaches (Fritz et al. 1993; Anderson and Rippey 1994). Sedimentary pigments (chlorophylls, carotenoids, and their derivatives) are of considerable utility in this objective, in

Received 6 February 2004. Accepted 31 December 2004. Published on the NRC Research Press Web site at http://cjfas.nrc.ca on 25 May 2005.
J17956

B. Das, A. Sanchez-Azofeifa, B. Rivard, and A.P. Wolfe.[1,2] Department of Earth and Atmospheric Sciences, University of Alberta, Edmonton, AB T6G 2E3, Canada.
R.D. Vinebrooke. Freshwater Biodiversity Laboratory, Department of Biological Sciences, University of Alberta, Edmonton, AB T6G 2E3, Canada.

[1]Corresponding author (e-mail: alexw@unis.no).
[2]Present address: The University Centre in Svalbard, P.O. Box 156, N-9171 Longyearbyen, Norway.

 doi: 10.1139/F05-016 © 2005 NRC Canada

Fig. 1. Location maps of the investigated sites in the Colorado Rocky Mountains (USA), showing (*a*) Pristine Lake, Mount Zirkel Wilderness Area, in relation to Rocky Mountain National Park, and (*b*) the four study lakes located in Rocky Mountain National Park.

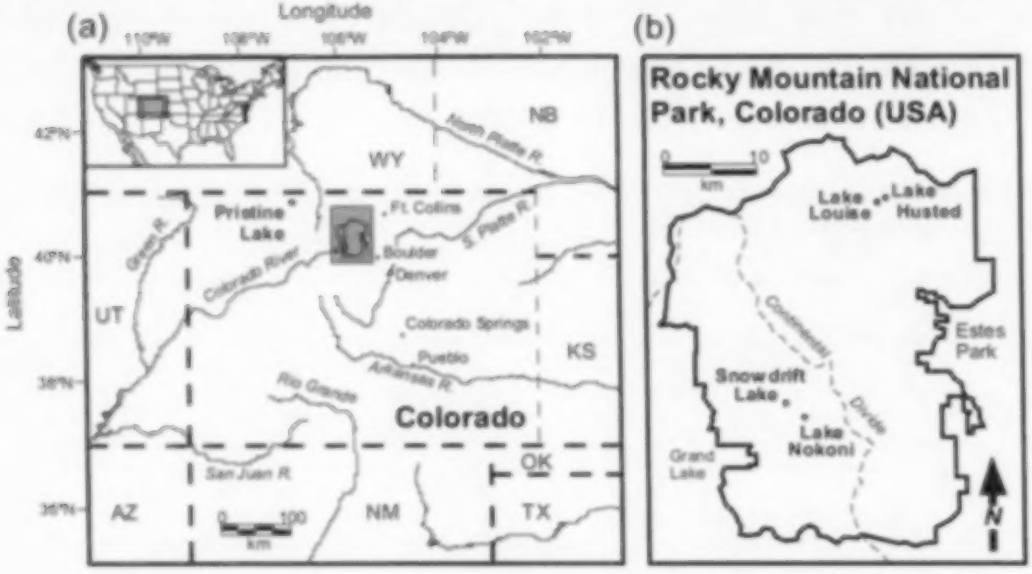

part because they enable the quantification of past production by algal groups that do not produce morphological fossils (Millie et al. 1993; Leavitt and Hodgson 2001). However, the analysis of sedimentary pigments is expensive and labor intensive, which ultimately limits the attainable spatial and temporal resolution of analyses. Because lake primary production is also linked to climate (Schindler et al. 1990; Hobbie et al. 1999; Flanagan et al. 2003), the development of techniques that facilitate the rapid assessment of lake trophic changes from the sediment record is increasingly of broad relevance.

Reflectance spectroscopy is a powerful tool for lake sediment analysis, in part because it is rapid, reagent-free, and nondestructive (Korsman et al. 1999, 2001). To date, applications include calibration of visible-near-infrared (VNIR; 400–2500 nm) spectra to air temperatures for paleoclimate reconstruction (Rosén et al. 2000) and use of the near-infrared band (NIR; 780–2500 nm) to infer organic and inorganic sediment constituents (Nilsson et al. 1996; Malley et al. 1999). In paleoceanography, green reflectance (550 nm) has been used as a quantitative measure of sediment color (Peterson et al. 2000). However, these studies have not explored explicitly the relationships between localized spectral features and sediment geochemical composition. On the other hand, the spectral properties of chlorophylls in natural waters have been examined more closely (Gitelson 1992; Rundquist et al. 1996; Schalles et al. 1998). These studies reveal consistent absorption by algal chlorophylls in the red bandwidth of the electromagnetic spectrum (600–700 nm), which broadly parallels the spectral behavior of chlorophylls in higher plants (Gitelson and Merzlyak 1997; Richardson et al. 2002) and bryophytes (Lovelock and Robinson 2002). Similarly, red absorption is fundamental in remote sensing of phytoplankton (Richardson 1996) and macroalgae (Guillaumont et al. 1997) in marine environments.

The present study builds on these observations by assessing a new application of VNIR reflectance spectroscopy: the prediction and reconstruction of sedimentary chlorophyll concentrations in lake sediments. Specifically, we explore the use of simple reflectance indices to infer concentrations of sedimentary chlorophyll *a* and its derivatives for a set of mountain lakes, exploiting a priori knowledge of the absorption spectra of these pigments (Gitelson 1992; Rundquist et al. 1996; Schalles et al. 1998).

Materials and methods

Study sites and sediment cores

The primary materials used in this study are sediments from four lakes situated in Rocky Mountain National Park (RMNP), Colorado Front Range, USA (Fig. 1). Sediments from a fifth site, in the Mount Zirkel Wilderness Area approximately 80 km to the northwest, are used to validate observations from the other four lakes. The study sites are typical midcontinental alpine lakes characterized by clear (Z_{Secchi} > 5 m), chemically dilute (conductivities <10 $\mu S \cdot cm^{-1}$), and slightly acidic (pH 6.2–6.5) waters. The lakes have short ice-free seasons (July–October). All five catchments occupy high elevation cirques (3200–3400 m above sea level) of last glacial (Pinedale) age and are situated at or slightly above the alpine tree line. The dominant catchment substrates are bedrock (Precambrian granites, gneisses, and quartz monzonites) and talus derived from these lithologies. Although the lakes are oligotrophic (total phosphorus, TP < 0.01 $mg \cdot L^{-1}$), inorganic nitrogen concentrations (NO_3^- + NH_4^+) are well above natural background levels (Table 1).

Short (22–40 cm total length), undisturbed sediment cores were obtained from the deepest midpoint of each lake basin using a modified Kajak–Brinkhurst apparatus (Glew 1989) and extruded in consecutive 0.5- or 1.0-cm increments once

© 2005 NRC Canada

Table 1. Site characteristics and water chemistry of the studied lakes.

Lake name	Latitude (°N)	Longitude (°W)	Elevation (m a.s.l.)	Area (ha)	Depth (Z_{max}; m)	$[NO_3^-]$ ($mg \cdot L^{-1}$)	$[NH_4^+]$ ($mg \cdot L^{-1}$)	[TP] ($mg \cdot L^{-1}$)
Rocky Mountain National Park								
Louise	40°30′28″	105°37′13″	3360	2.7	8	1.026	0.031	0.009
Husted	40°30′56″	105°36′50″	3350	4.0	11	0.267	0.033	0.005
Snowdrift	40°20′30″	105°44′11″	3390	3.2	14	0.107	0.015	0.004
Nokoni	40°15′15″	105°43′50″	3290	7.6	38	0.078	0.023	0.003
Mount Zirkel Wilderness Area								
Pristine	40°41′27″	107°40′53″	3370	2.4	9	0.658	0.019	0.011

Note: TP, total phosphorus; m a.s.l., metres above sea level.

Fig. 2. Comparison of reflectance spectra (%*R* from 400 to 700 nm) between (*a*) chlorophyll *a* dilutions of lake water with living *Chlorella* spp. cells (Schalles et al. 1998) (numbers are chlorophyll *a* concentrations ($\mu g \cdot L^{-1}$)) and (*b*) the upper lake sediment samples from the present study. The region of chlorophyll absorption is clearly identifiable in both examples. In (*c*), representative spectra (%*R* from 450 to 900 nm) are illustrated for the most recent (1.75 cm, ~1990) and oldest (10.0 cm; pre-industrial) sediments from Lake Louise. The first derivative of these spectra is shown in (*d*). The key wavelengths used in defining spectral indices for chlorophyll prediction are indicated in panel (*c*).

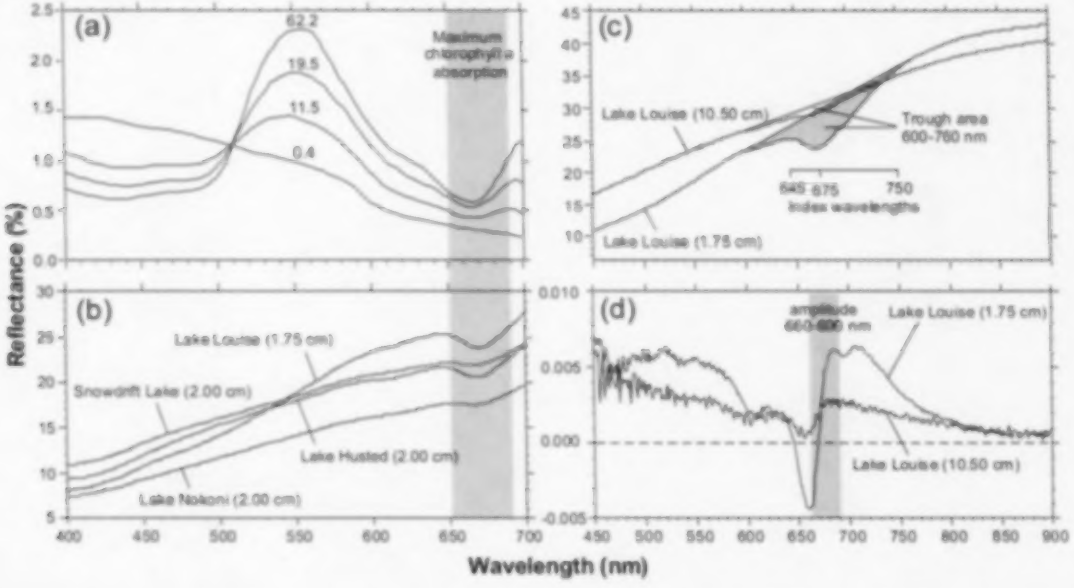

returned to shore (Glew 1988). Spectral and pigment analyses were conducted on 23 core depths from the RMNP lakes (Lake Louise: eight samples; lakes Husted, Snowdrift, and Nokoni: five samples each). VNIR reflectance spectra were obtained from an additional 17 depths in the Pristine Lake core. These samples include both pre- and post-1950 sediments from each lake. Each core has been dated using excess ^{210}Pb activities determined by α spectroscopy, to which the constant rate of supply model has been applied (Wolfe et al. 2003). Because our objective is to focus on stable inventories of sedimentary algal pigments, samples from the uppermost 1.5 cm of the cores were not analyzed. This represents the zone of most intense sediment redox cycling and hence of maximum potential chemical instability among pigments (Leavitt and Hodgson 2001).

The recent paleolimnology of this region has been examined in considerable detail (Baron et al. 2000; Wolfe et al. 2001, 2002), revealing a suite of recent ecological and biogeochemical changes that reflect initial ecosystem responses towards enhanced anthropogenic deposition of fixed nitrogen from industrial, agricultural, and automotive sources. These stratigraphic shifts, which include increased representations of mesotrophic diatom taxa (e.g., *Asterionella formosa*), declining sediment C:N and $\delta^{15}N$ values, and greater autochthonous organic matter production, have accelerated markedly since approximately 1950 AD.

Sediment spectral reflectance

For the analysis of sediment spectral reflectance, small (0.2–1.0 g dry mass), freeze-dried samples were first ground (agate mortar and pestle) then sieved (<125 μm). Samples were stored in the dark at 4 °C following collection. Reflectance spectra were measured with a FieldSpec Pro® spectroradiometer (Analytical Spectral Devices Inc., Boul-

© 2005 NRC Canada

Fig. 3. Visible-near-infrared (VNIR) reflectance spectra (450–900 nm) of sediments from four lakes in Rocky Mountain National Park: (*a*) Lake Louise, (*b*) Lake Husted, (*c*) Snowdrift Lake, and (*d*) Nokoni Lake, subdivided as pre- and post-dating ~1950 AD, as determined by sediment ^{210}Pb activities and constant rate of supply depth–age models (Wolfe et al. 2003). Dashed vertical lines indicate 675 nm.

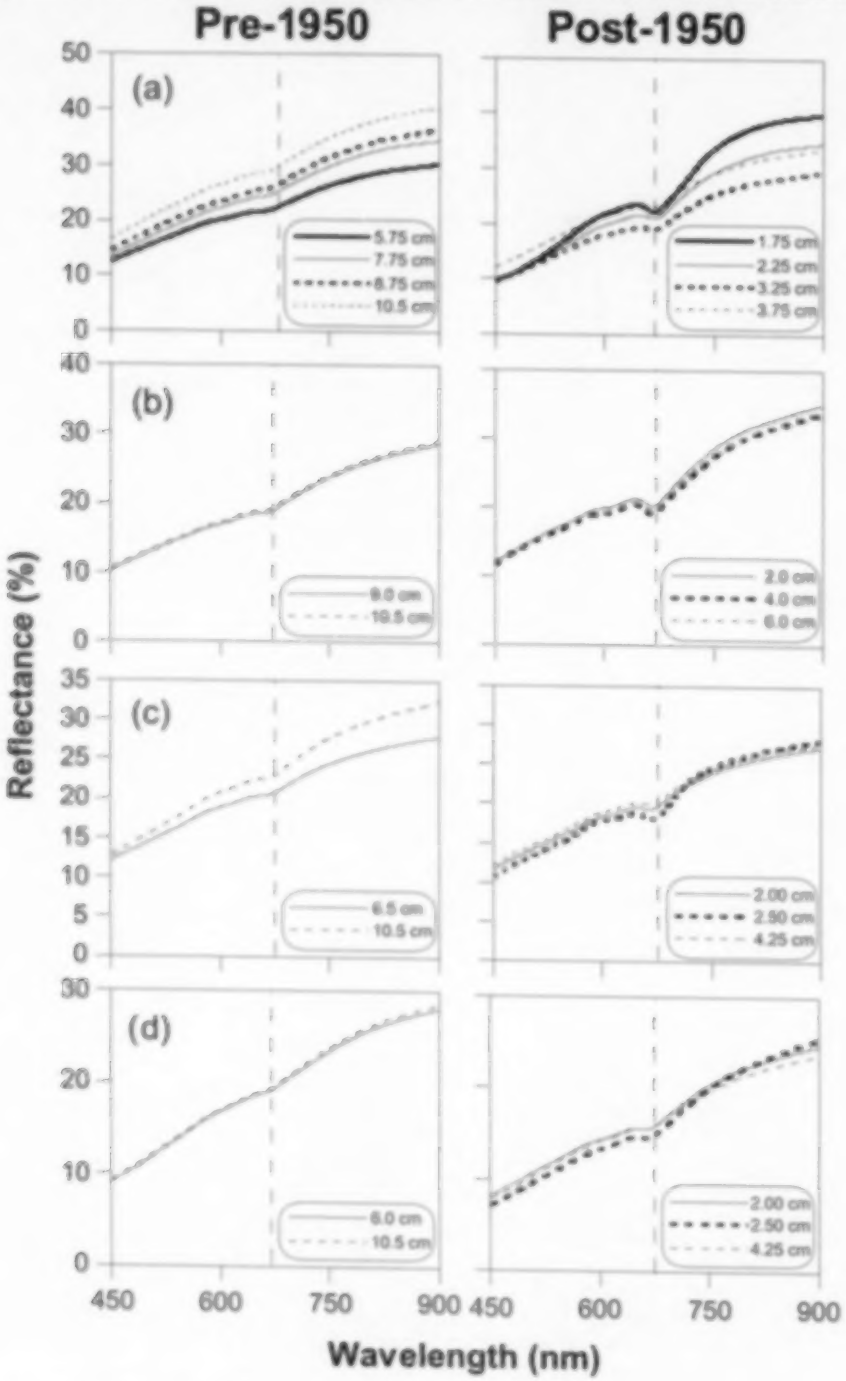

der, Colorado, USA) over the 350- to 2500-nm range. The VNIR portion of the spectrum (350–1050 nm) was quantified using a 512-channel silicon photodiode array overlain with an order separation filter. Each channel, an individual detector itself, is geometrically positioned to receive light within a narrow (approximately 1.4 nm) bandwidth. Light

© 2005 NRC Canada

Fig. 4. Stratigraphies of organic content, selected pigment concentrations, and related parameters from four lakes in Rocky Mountain National Park: (*a*) Lake Louise, (*b*) Lake Husted, (*c*) Snowdrift Lake, and (*d*) Nokoni Lake. At right is the area of the reflectance trough between 600 and 760 nm, the most robust predictive index of sediment chlorophyll concentrations. OM, organic matter.

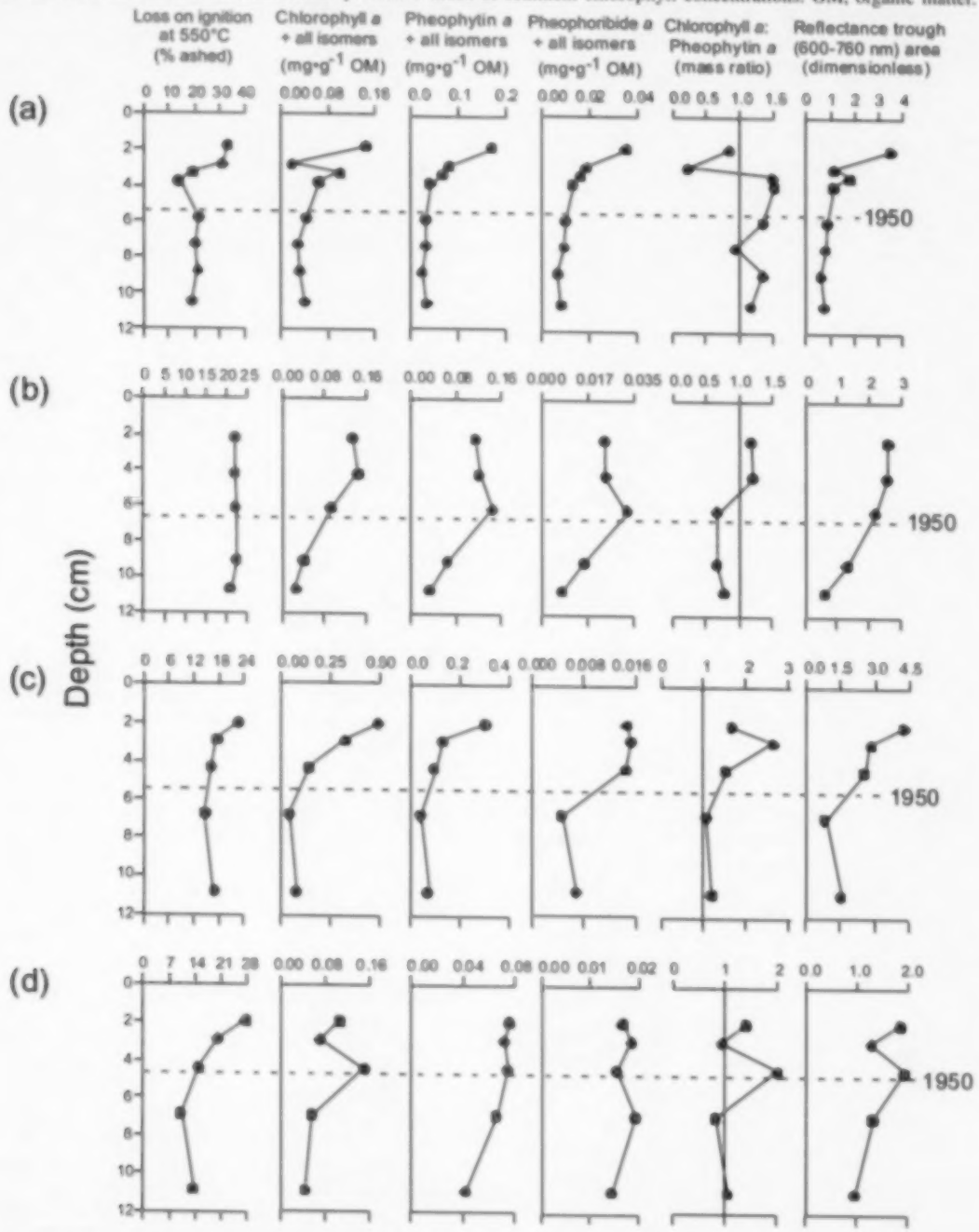

was brought to the instrument using a Lowel Pro® (Brooklyn, New York, USA) lamp with an effective view of approximately 45°. Working distance to the sample surface was ~16.5 cm. Light energy was collected through bundled optical fibers with a conical view of ~15°. Reflectance was standardized to a white reference panel (spectralon) between each measurement. Percent reflectance (R) was computed as $(R_{sample}/R_{reference}) \times 100$ for the spectral region of greatest interest, 450–900 nm.

Pigment analysis

Sedimentary pigment concentrations were quantified us-

© 2005 NRC Canada

Table 2. Correlation coefficients for linear regressions between various spectral indices and sediment pigment concentrations.

Spectral index	Fraction of sedimentary pigments		
	Chlorophyll *a* + isomers	Pheophorbide *a* + pheophytin *a*	Chlorophyll *a* + derivatives
Reflectance trough area 600–760 nm	0.84**	0.94**	0.92**
Amplitude of reflectance 675–750 nm	0.74*	0.88**	0.83**
Amplitude of first derivative 660–690 nm	0.66*	0.86**	0.82**
Ratio of reflectance 645/675 nm	0.63*	0.67*	0.68*
Ratio of reflectance 675/750 nm	–0.57*	–0.71*	–0.68*
First derivative value at 675 nm	–0.39	–0.58	–0.56
Amplitude of reflectance 645–675 nm	0.27	0.44	0.38

Note: *, $P < 0.05$; **, $P < 0.01$.

ing reverse-phase high-performance liquid chromatography (HPLC; Vinebrooke et al. 2002). Pigments were extracted by soaking freeze-dried sediments in acetone, methanol, and deionized water (80:15:5 by volume) for 24 h in darkness at 10 °C. Extracts were then filtered (0.2-μm pore nylon), dried under N_2, and stored in the dark at –20 °C until analysis. Dry extracts were reconstituted with an injection solution (70% acetone – 25% ion-pairing reagent – 5% methanol) containing Sudan II (3.2 mg·L^{-1}) as the internal reference. The ion-pairing reagent consisted of 0.75 g tetrabutyl ammonium acetate and 8.00 g ammonium acetate in 100 mL deionized water. Pigments were separated on an HP 1100 HPLC (Hewlett-Packard Ltd., Mississauga, Ontario, Canada) equipped with a Rainin 200 C18 column (10-cm length, 5-μm particle size). Pigments were detected with an in-line diode array detector (435-nm detection wavelength) and a fluorescence detector (435-nm excitation wavelength, 667-nm detection wavelength). Analytical separation included isocratic delivery (1.0 mL·min^{-1}) of mobile phase A (10% ion-pairing reagent in methanol) for 1.5 min, a linear succession to 100% solution B (27% acetone in methanol) for 7 min, and isocratic retention for 12.5 min. The column was re-equilibrated between samples by continuous isocratic delivery for 3 min, a linear return to 100% solution A over 3 min, and a final isocratic delivery for 4 min. Pigment concentrations were quantified using equations derived from dilution series of authentic standards from the US Environmental Protection Agency (National Exposure Research Laboratory, Cincinnati, Ohio) or commercially available standards (Sigma Chemical Co., St. Louis, Missouri, USA). All pigment concentrations are expressed as their mass per gram organic matter (mg·g^{-1} OM), which was determined by mass loss on ignition at 550 °C for 2 hours (Heiri et al. 2001). Normalization of pigment concentrations to organic content eliminates any potential biasing from dilution by inorganic sediment constituents (Leavitt 1993; Vinebrooke et al. 2002).

Spectral indices and regression

From the sediment reflectance spectra obtained for the 23 samples that were also analyzed for pigments, seven indices were calculated to summarize the large volume of spectral information. The selection of wavelengths used in defining the following indices is based on comparative observations of the general patterns of R observed in both time frames (e.g., Fig. 2). The first two indices are the amplitudes (maximum–minimum) of R shifts between 645 and 675 nm and between 675 and 750 nm. The third and fourth indices are ratios of reflectance between the same wavelengths: R_{645}/R_{675} and R_{675}/R_{750}. The fifth and sixth indices are based on the first derivative of R (R'): both the value of R' at 675 nm and amplitude of R' between 660 and 690 nm were calculated. The final index is the dimensionless area between a straight line joining R values at 600 and 760 nm and the underlying curve; this trough in R is recognized in all spectra.

Univariate linear regression analyses were performed using each of the spectral indices as an explanatory variable of the following representative fractions of HPLC-derived pigment concentrations: chlorophyll *a* + all chlorophyll *a* isomers (i.e., primary chlorophyll *a*), pheophytin *a* + pheophorbide *a* (pheopigments from chlorophyll *a* degradation), and the sum of these two fractions (primary and degraded chlorophyll *a*). All regressions were performed with SPSS v. 10.0 (Norusis 2000). The distributional properties of the data could not be evaluated owing to the lack of replication of the independent variable. However, log-transformation of the data prior to regression analysis generated regression or correlation coefficients that were highly similar to those presented here using the raw data. Therefore, we were confident in the robustness of our statistical analyses regarding the assumptions of normality and homogeneity of variance.

Results and discussion

Spectral characteristics of RMNP lake sediments

The most prominent feature of VNIR reflectance spectra obtained from RMNP lake sediments is a trough centered on 675 nm that is attributed to the presence of chlorophylls. This trough is seen in both natural waters inoculated with *Chlorella* spp. (Schalles et al. 1998) and RMNP lake sediments (Figs. 2*a*, 2*b*). We confirmed that the reflectance trough in the lake sediments was solely attributable to chlorophyll by organic extraction of the pigment and its derivatives (Vinebrooke et al. 2002) and subsequent VNIR analysis of the dried sediment residue, which no longer retained a reflectance trough at 675 nm. Therefore, differences between the spectral signatures of chlorophyll-amended water (Fig. 2*a*) and lake sediments (Fig. 2*b*) arise from the markedly different reflectance properties of the media (aqueous versus par-

© 2005 NRC Canada

Fig. 5. Regressions (n = 23) between the three most highly predictive spectral indices and representative categories of sedimentary pigments: (a–c) reflectance trough area (600–760 nm); (d–f) amplitude of raw reflectance (R) (675–750 nm); and (g–i) amplitude of the first derivative of reflectance (660–690 nm). OM, organic matter.

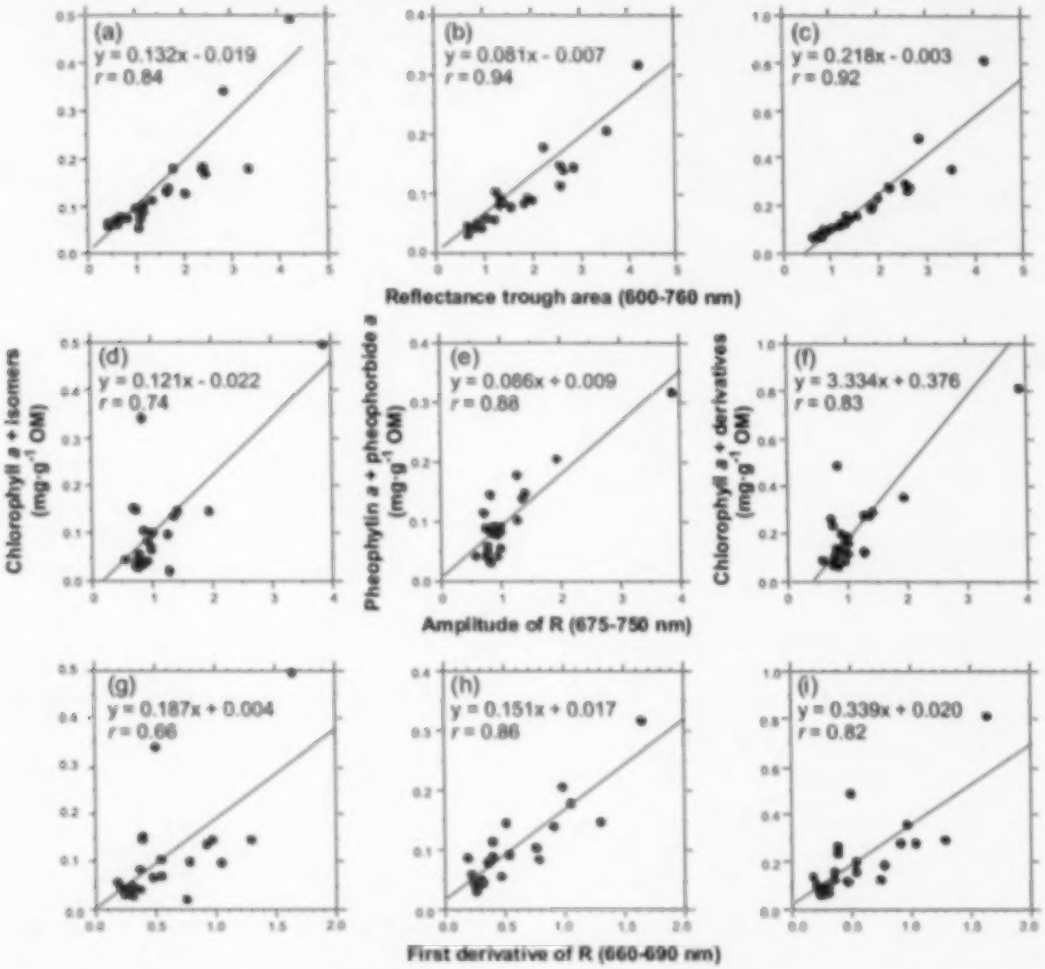

ticulate) in which chlorophyll is diluted rather than the spectral behavior of chlorophyll itself. Further differences between algal and sedimentary spectral reflectance signatures occur around 550 nm (Figs. 2*a*, 2*b*) and are likely attributable to accessory nonchlorophyll pigments contained in the algal cells. HPLC analyses revealed relatively low carotenoid concentrations in RMNP lake sediments, suggesting partial degradation of these compounds. Furthermore, the development of this trough does not appear related in any way to background values of R, which progressively increase between 450 and 900 nm. Between-lake differences in the values of R (Fig. 2*b*) likely reflect subtle variations in the reflective properties of sediment mineral components.

Comparison of recent and old sediments from Lake Louise (Figs. 2*c*, 2*d*) and the other lakes (Fig. 3) showed that chemical changes associated with algal death, sedimentation, and decomposition did not induce substantial shifts in the wavelength of minimum red reflectance. Indeed, pre- and post-1950 sediments from the four mountain lakes exhibited reflectance spectra that are very similar, except for the 675-nm trough, which is more pronounced following 1950 (Fig. 3). Although the preservation of chlorophyll reflectance features in sediment has been recognized for some time (Schalles et al. 2000), these have not previously been calibrated to quantitative sedimentary pigment concentrations.

Fossil pigment stratigraphy

The organic content of sediments from the four RMNP lakes varies between 10% and 35%, and, with the exception of Lake Husted, increases towards the mud–water interface. Chlorophyll *a* and associated pheopigments are consistently preserved in all samples analyzed. For this reason, and given that our primary interest lies in whole-lake algal production, only chlorophyll *a* and its degradation products are considered further. With few exceptions, the stratigraphic trend in concentrations of these pigments is an increase towards the surface of each of the analyzed cores (Fig. 4). Concentrations of total sediment chlorophyll *a* and derivatives range

© 2005 NRC Canada

Fig. 6. (*a*) Comparison of measured (by high-performance liquid chromatography (HPLC)) and predicted total concentrations of chlorophyll *a* + derivatives obtained using the regression of Fig. 5*a* and (*b*) plot of corresponding residuals. OM, organic matter.

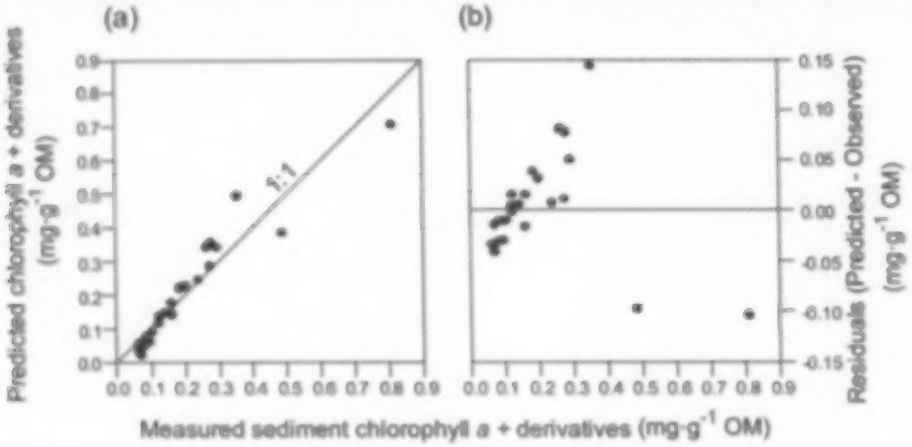
(a)
(b)
Predicted chlorophyll a + derivatives (mg·g-1 OM)
1:1
Residuals (Predicted - Observed) (mg·g-1 OM)
Measured sediment chlorophyll a + derivatives (mg·g-1 OM)

from < 0.1 mg·g^{-1} OM in pre-1950 sediments to a maximum of 0.9 mg·g^{-1} OM at the surface in Snowdrift Lake. These values are typical for oligotrophic lake sediments, as is the relatively large degree of between-lake variability in sediment pigment concentrations (Vinebrooke et al. 2002). Clearly, neither the production nor the preservation of algal pigments is uniform across the sediment surface, and this mandates a critical assessment of the possibility that consistent between-lake stratigraphic trends (Fig. 4) are merely preservational artifacts.

An appropriate approach to assessing diagenesis is by comparing chlorophyll *a* concentrations to those of its principal degradation product, pheophytin *a* (Vinebrooke et al. 2002). Our data do not reveal high pheophytin *a* concentrations in samples of low chlorophyll *a* concentration, the expected pattern if diagenetic processes were modulating the down-core distribution of pigments. Indeed, the chlorophyll *a*/pheophytin *a* ratio does not show any consistent stratigraphic trends among the four lakes (Fig. 4). Pheophorbide *a* concentrations, which have widely been interpreted as proxies for algal grazing by invertebrates (e.g., Leavitt et al. 1994), are several fold lower than those of pheophytin *a* in RMNP lake sediments. However, both pheopigments have very similar down-core stratigraphies (Fig. 4). This does not support the regulation of pheophorbide *a* as a unique by-product of grazed algal standing crop, even more so since the four lakes have markedly different fish stocking histories (Wolfe et al. 2003), which constitutes the dominant regulator of invertebrate herbivory. The production of pheophorbide *a* in the absence of grazing has been recognized in marine ecosystems (Head et al. 1994) and can therefore be suspected for lakes. Thus, the stratigraphic profiles of both pheopigments can be simply attributed to greater sources of reactive chlorophyll *a* in the most recently deposited sediments, in turn due to increased algal standing crop. Although pigment degradation is clearly occurring in the sediments of the RMNP lakes (incompleteness of carotenoid record, abundance of pheopigments), this does not appear to obscure the primary environmental signal suggested by the pigment stratigraphy: progressive increases in algal production and sedimentation over recent decades.

Regression between spectral indices and sedimentary pigments

For the 23-sample population, seven reflectance indices were regressed against three categories of sedimentary pigments: chlorophyll *a* and its isomers; pheopigments from chlorophyll *a* degradation (pheophytin *a* + pheophorbide *a*); and the sum of the first two classes (hereafter chlorophyll *a* + derivatives). Of the indices, only two failed to produce significant correlations (the first derivative value at 675 nm and the amplitude of reflectance change between 645 and 675 nm). All other spectral indices were significantly ($P < 0.05$) correlated to all three categories of sedimentary pigment concentrations expressed per unit organic matter (Table 2). These correlations do not differ appreciably when sedimentary pigment concentrations are expressed per unit dry mass of sediment. The three most highly correlated indices are as follows: reflectance trough area between 600 and 760 nm, the amplitude of R between 675 and 750 nm, and the amplitude of R' between 660 and 690 nm. The regressions obtained from these three indices and the three pigment categories are illustrated in Fig. 5.

Interestingly, spectral indices are more closely correlated to the sum of pheopigments than to their precursor, chlorophyll *a*. However, the correlation coefficients are similar for both pigment classes (Table 2), suggesting that both chlorophyll and its degradation products have similar reflectance properties. This implies that diagenesis of sediment organic matter is unlikely to significantly alter the portions of reflectance spectra that relate most strongly to algal production (i.e., 600–760 nm).

Development of predictive models

The strength of the above relationships allows the development of simple inference models based on the three most statistically robust spectral predictors of sedimentary pigments. These models are directed towards the reconstruction

© 2005 NRC Canada

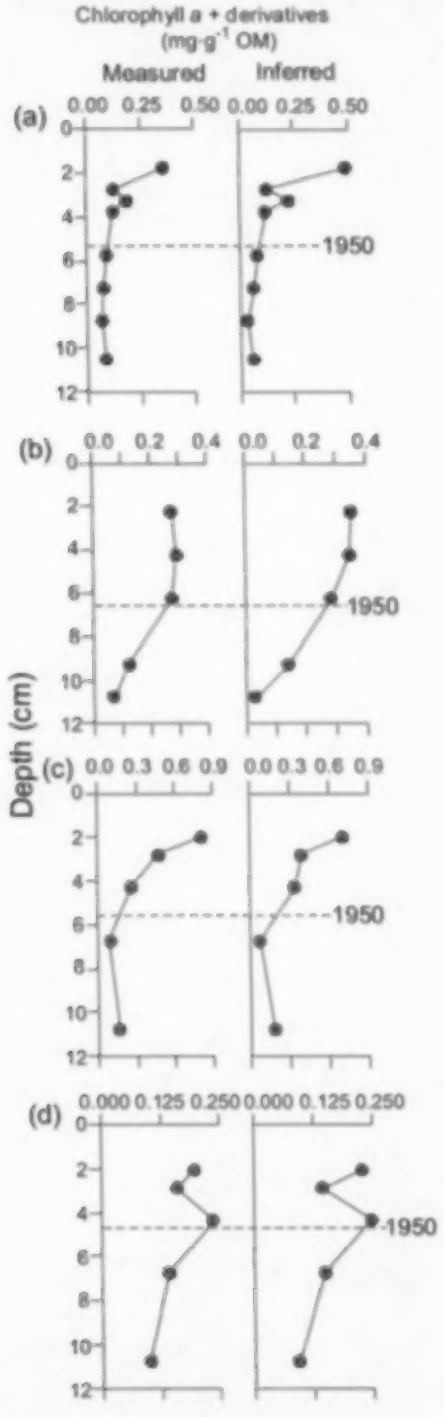

Fig. 7. Down-core comparisons of measured and inferred sediment concentrations of total chlorophyll *a* + derivatives from (*a*) Lake Louise, (*b*) Lake Husted, (*c*) Snowdrift Lake, and (*d*) Nokoni Lake. Inferred values are based on the reflectance trough area index (600–760 nm). OM, organic matter.

of the most inclusive pigment category, chlorophyll *a* + derivatives, which is believed to best reflect total algal abundance and hence be of greatest potential utility for reconstructing lake trophic evolution. Linear regressions developed between spectral indices and pigment categories were applied to the 23 reflectance spectra and measured versus inferred values of chlorophyll *a* + derivatives were graphed (Fig. 6). The total integrated area of the reflectance trough from 600 to 760 nm was the best predictor of all three classes of sedimentary chlorophyll concentrations considered (Table 2). This index was particularly successful in producing a cluster of points closely surrounding the 1:1 line at concentrations <0.3 mg·g^{-1} OM and a reduced scatter and trend in corresponding residuals (Fig. 6). Although more work is clearly needed for sediments with higher chlorophyll *a* concentrations, our analyses show that simple spectral indices are potentially sensitive to changes of sediment chlorophyll *a* + derivatives in the order of ±0.15 mg·g^{-1} OM.

Another way of depicting this data is to plot stratigraphically both measured and inferred values alongside each other (Fig. 7). This enables the largest mismatches to be readily identified, for example the model's overestimation at the top of the Lake Louise core and underestimations in the two most recent samples from Snowdrift Lake. However, with the exception of these points, the reflectance trough index faithfully reproduces measured sediment pigment concentrations with remarkable degrees of accuracy and precision. This implies that overall trends in sedimentary chlorophyll concentrations may be reconstructed in the absence of HPLC measurements. However, the inferred values shown here (Fig. 7) do not constitute reconstructions in the strict sense, because they represent the same samples used in the inference model's development (Fig. 6). To avoid this element of circularity, we now apply the model to a fifth lake outside the calibration set and for which there exist several independent lines of evidence for increased production.

Application to lake trophic reconstruction

Pristine Lake receives significant amounts of nitrogen deposition originating from coal-fired power plants in the lower Yampa River valley, notably at Hayden and Craig (Turk and Campbell 1987). These emissions are transported to the Mount Zirkel Wilderness Area by prevailing westerly winds. Inorganic N deposition rates in the region thus exceed 4 kg N·ha^{-1}·year^{-1} (Williams and Tonnessen 2000). This is directly comparable with RMNP lakes east of the Continental Divide, which are affected by N emissions from the Front Range urban corridor (Baron et al. 2000).

Sediments from Pristine Lake record a large increase in total diatom concentrations since 1950, associated with increased abundances of the mesotrophic planktonic taxa *Asterionella formosa* and *Fragilaria tenera* (*Synedra* sensu lato) (Fig. 8*a*). Sedimentary chlorophyll *a* + derivatives were inferred by NIRS for 17 intervals in the Pristine Lake core using the model derived from reflectance trough area (600–760 nm). This reconstruction yields estimates ranging from < 0.05 mg·g^{-1} OM before 1950 to values up to 0.4 mg·g^{-1} OM in the last decade (Fig. 8*b*). Reflectance-inferred increases in chlorophyll concentrations were correlated significantly with other proxies of lake enrichment, including relative frequencies of *Asterionella formosa* (r = 0.75, P <

© 2005 NRC Canada

Fig. 8. (*a*) Conventional paleolimnological proxies and corresponding ^{210}Pb ages for Pristine Lake in the Mount Zirkel Wilderness Area and (*b*) reconstructed total sediment chlorophyll *a* + derivatives inferred from the reflectance trough area index. Protocols for diatom analysis, organic carbon, and dating are described elsewhere (Wolfe et al. 2003). OM, organic matter.

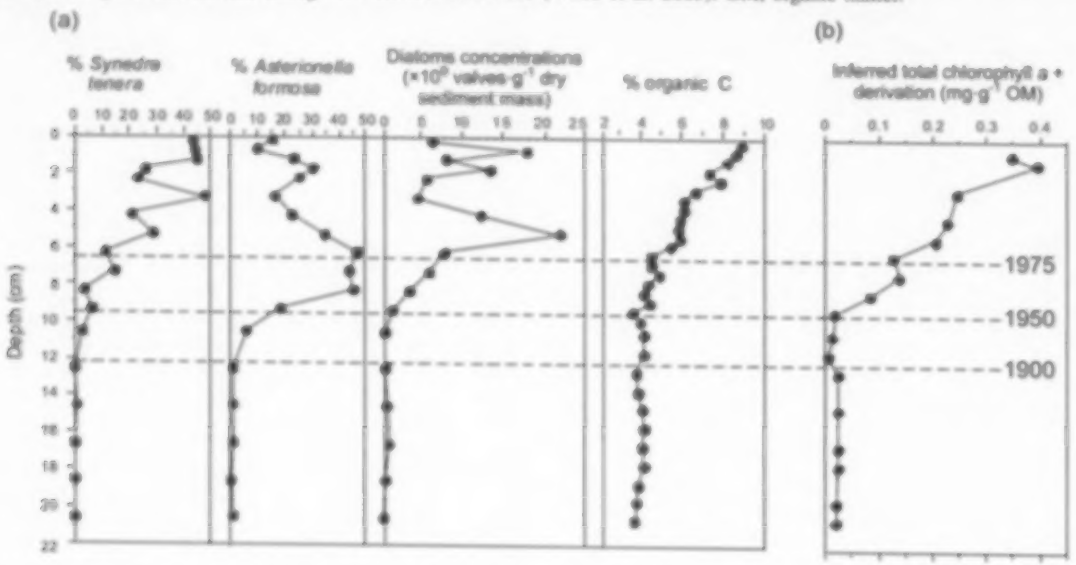

0.01) and *Fragilaria tenera* ($r = 0.82$, $P < 0.01$), as well as organic carbon content ($r = 0.88$, $P < 0.01$). These changes (Fig. 8*a*) are directly comparable to those documented from five RMNP lakes, including those considered previously here (Wolfe et al. 2003). Moreover, the inferred sedimentary chlorophyll stratigraphy matches the chronology of regional energy development and population growth exceptionally well.

It is interesting to note that the parallel behavior of diatom and inferred sedimentary chlorophyll concentrations observed before 1975 appears to collapse in subsequent decades. This may suggest the progressive replacement of diatoms by nonsiliceous algal groups as resource ratios continue to shift. Irrespective of these finer points of interpretation, which remain to be confirmed, the data unequivocally support the contention that VNIR spectral data may produce realistic reconstructions of trends in sedimentary chlorophyll concentration, which is a more integrative measure of whole-lake production relative to proxies such as diatom concentrations (Vinebrooke et al. 2002). In the case of Pristine Lake, the remotely sensed data corroborate diatom-based inferences of recent nutrient enrichment, together providing a powerful case that this lake has markedly deviated from its natural, pre-industrial, trophic state.

In summary, the results of this investigation confirm that reflectance spectroscopy is a powerful tool in paleolimnology (Korsman et al. 2001). Specific regions of sediment reflectance, notably in the red portion of the spectrum, demonstrably relate to sedimentary concentrations of chlorophyll *a* and its degradation products. Simple models can be developed to infer sediment photosynthate concentrations and thereafter be applied to the reconstruction of changing lake trophic regimes. This method does not supplant wet chemical methods, which remain necessary for the quantification of trace pigments such as carotenoids. Rather, VNIR methods enable rapid and nondestructive, semiquantitative assessments of bulk sediment chlorophyll concentrations. For many paleolimnological applications, including studies of eutrophication (Hall and Smol 1999) and animal-derived nutrient fluxes (Finney et al. 2000), this information may nonetheless be critical.

Measured pigment concentrations associated with total primary production (i.e., chlorophyll *a* and its derivatives) have increased over recent decades in all four investigated RMNP lakes, in agreement with additional proxies such as diatoms, nitrogen stable isotopes, and organic matter provenance (Wolfe et al. 2002, 2003). The results from Pristine Lake in the Mount Zirkel Wilderness Area confirm that recent nutrient enrichment is widespread in the Colorado Rocky Mountains. Similar observations have now also been documented from the Beartooth–Absaroka Wilderness of Montana and Wyoming (Saros et al. 2003), as well as from Sequoia and Yosemite National Parks in the Sierra Nevada (Sickman et al. 2003). All of these regions are congressionally designated Class I wildernesses under the Clean Air Act, which in principle specifically mandates protection from human-induced ecological changes. Nonetheless, recent observations collectively constitute a mounting body of evidence indicating that midcontinental alpine lakes are changing directionally in response to increased nutrients transported atmospherically from a variety of anthropogenic sources.

Acknowledgements

This research was supported by the Natural Sciences and Engineering Research Council of Canada (Discovery Grants to APW, RDV, and BR). The staff of Rocky Mountain National Park and the US National Park Service (Department of the Interior) are thanked for facilitating the collection of

© 2005 NRC Canada

sediment cores from study lakes. Sheri Lee-Foley assisted with reflectance spectroscopy, which was conducted in the Earth Observation Systems Laboratory (EOSL) at the University of Alberta. We further thank Sybille Wunsam for counting diatoms from Pristine Lake, as well as Jack Cornett and Janice Lardner for generating ^{210}Pb chronologies.

References

Anderson, N.J., and Rippey, B. 1994. Monitoring lake recovery from point-source eutrophication: the use of diatom-inferred total epilimnetic phosphorus and sediment chemistry. Freshw. Biol. **32**: 625–639.

Baron, J.S., Rueth, H.M., Wolfe, A.P., Nydick, K., Allstott, E.J., Minear, J.T., and Moraska, B. 2000. Ecosystem responses to nitrogen deposition in the Colorado Front Range. Ecosystems, **3**: 352–368.

Bennion, H., Juggins, S., and Anderson, N.J. 1996. Predicting epilimnetic phosphorous concentrations using an improved diatom-based transfer function and its application to lake management. Environ. Sci. Technol. **30**: 2004–2007.

Engstrom, D.R., Swain, E.B., and Kingston, J.C. 1985. A palaeolimnological record of human disturbance from Harvey's Lake, Vermont: geochemistry, pigments and diatoms. Freshw. Biol. **15**: 261–288.

Finney B.P., Gregory-Eaves, I., Sweetman, J., Douglas, M.S.V., and Smol, J.P. 2000. Impacts of climatic change and fishing on Pacific salmon abundances over the past 300 years. Science (Washington, D.C.), **290**: 795–799.

Flanagan, K.M., McCauley, E., Wrona, F., and Prowse, T. 2003. Climate change: the potential for latitudinal effects on algal biomass in aquatic ecosystems. Can. J. Fish. Aquat. Sci. **60**: 635–639.

Fritz, S.C., Kingston, J.C., and Engstrom, D.R. 1993. Quantitative trophic reconstructions from sedimentary diatom records: a cautionary tale. Freshw. Biol. **30**: 1–23.

Gitelson, A.A. 1992. The peak near 700 nm on radiance spectra of algae and water: relationships of its magnitude and position with chlorophyll concentration. Int. J. Remote Sens. **13**: 3367–3373.

Gitelson, A.A., and Merzlyak, M.N. 1997. Remote estimation of chlorophyll content in higher plant leaves. Int. J. Remote Sens. **18**: 2691–2697.

Glew, J.R. 1988. A portable extruding device for close interval sectioning of unconsolidated core samples. J. Paleolimnol. **1**: 235–239.

Glew, J.R. 1989. A new trigger mechanism for sediment samplers. J. Paleolimnol. **2**: 241–243.

Guillaumont, B., Bajjouk, T., and Talec, P. 1997. Seaweed and remote sensing: a critical review of stressors and data processing. *In* Progress in phycological research 12. *Edited by* F.E. Round and D.J Chapman. Biopress, Bristol, UK. pp. 213–282.

Hall, R.I., and Smol, J.P. 1999. Diatoms as indicators of lake eutrophication. *In* The diatoms: applications for the earth and environmental sciences. *Edited by* E.F. Stoermer and J.P. Smol. Cambridge University Press, Cambridge, UK. pp. 128–168.

Head, E.J., Hargrave, B.T., and Rao, D.V.S. 1994. Accumulation of a pheophorbide *a*-like pigment in sediment traps during late stages of a spring bloom: a product of dying algae? Limnol. Oceanogr. **39**: 176–181.

Heiri, O, Lotter, A.F., and Lamcke, G. 2001. Loss on ignition as a method for estimating organic and carbonate content in sediments: reproducibility and comparability of results. J. Paleolimnol. **25**: 101–110.

Hobbie, J.E., Peterson, B.J., Bettez, N., Deegan, L., O'Brien, W.J., Kling, G.W., Kipphut, G.W., Bowden, W.B., and Hershey, A.E.1999. Impact of global change on the biogeochemistry and ecology of an Arctic freshwater system. Polar. Res. **18**: 207–214.

Korsman, T., Nilsson, M.B., Landgren, K., and Renberg, I. 1999. Spatial variability in surface sediment composition characterized by near-infrared (NIR) reflectance spectroscopy. J. Paleolimnol. **21**: 61–71.

Korsman, T., Renberg, I., Dåbakk, E., and Nilsson, M.B.2001. Near-infrared spectroscopy (NIRS) in paleolimnology. *In* Tracking environmental changes using lake sediments. Vol. 2. *Edited by* W.M. Last and J.P. Smol. Kluwer, Dordrecht, the Netherlands. pp. 299–317.

Leavitt, P.R. 1993. A review of factors that regulate carotenoid and chlorophyll deposition and fossil pigment abundance. J. Paleolimnol. **9**: 109–127.

Leavitt, P.R., and Hodgson, D.A. 2001. Sedimentary pigments. *In* Tracking environmental changes using lake sediments. Vol. 3. *Edited by* J.P. Smol, H.J.B. Birks, and W.M. Last. Kluwer, Dordrecht, the Netherlands. pp. 295–325.

Leavitt, P.R., Sanford, P.R., Carpenter, S.R., and Kitchell, J.F. 1994. An annual fossil record of production, planktivory and piscivory during whole-lake experiments. J. Paleolimnol. **11**: 133–149.

Lovelock, C.E., and Robinson, S.A. 2002. Surface reflectance properties of Antarctic moss and their relationship to plant species, pigment composition and photosynthtic function. Plant Cell Environ. **25**: 1239–1250.

Malley, D.F., Rönicke, H., Findlay, D.L., and Zippel, B. 1999. Feasibility of using near-infrared reflectance spectroscopy for the analysis of C, N, P, and diatoms in lake sediments. J. Paleolimnol. **21**: 195–306.

Millie, D.F., Paerl, H.W., and Hurley, J.P. 1993. Microalgal pigment assessments using high-performance liquid chromatography: a synopsis of organismal and ecological applications. Can. J. Fish Aquat. Sci. **50**: 1513–1527.

Nilsson M.B., Dåbakk, E., Korsman, T., and Renberg, I. 1996. Quantifying relationships between near-infraed reflectance spectra of lake sediments and water chemistry. Environ. Sci. Technol. **30**: 2586–2590.

Norusis, M.J. 2000. SPSS 10.0 guide to data analysis.Prentice-Hall, Inc., Upper Saddle River, N.J., USA.

Peterson, L.C., Haug, G., Hughen, K.A., and Röhl,U. 2000. Rapid changes in the hydrologic cycle of the tropical Atlantic during the last glacial. Science (Washington, D.C.), **290**: 1947–1951.

Reavie, E.D., Hall, R.I., and Smol,J.P. 1995. An expanded weighted-averaging model for inferring past total phophorus concentrations from diatom assemblages in eutrophic British Columbia lakes. J. Paleolimnol. **14**: 49–67.

Richardson, A.D., Duigan, S.P., and Berlyn, G.P. 2002. An evaluation of noninvasive methods to estimate foliar chlorophyll content. New Phytol. **153**: 185–194.

Richardson, L.L. 1996. Remote sensing of algal bloom dynamics. Bioscience, **46**: 492–501.

Rosén, P., Dåbakk, E., Renberg, I., Nilsson, M., and Hall, R.I. 2000. Near-infrared spectrometry (NIRS): a new tool for inferring past climate change from lake sediments. Holocene, **10**: 161–166.

Rundquist, D.C., Han, L., Schalles, J.F., and Peake,J.F. 1996. Remote measurement of algal chlorophyll in surface waters: the case for the first derivative of reflectance near 690 nm. Photogramm. Eng. Remote Sens. **62**: 195–200.

Saros, J.E., Interlandi, S.J., Wolfe, A.P., and Engstrom, D.R. 2003. Recent changes in the diatom community structure of lakes in

© 2005 NRC Canada

the Beartooth Mountain Range, USA. Arct. Antarct. Alp. Res. **35**: 18–23.

Schalles, J.F., Gitelson, A.A., Yacobi, Y.Z., and Kroenke, A.E. 1998. Estimation of chlorophyll *a* from time series measurements of high spectral resolution reflectance in an eutrophic lake. J. Phycol. **34**: 383–390.

Schalles, J.F., Rundquist, D.C., and Schiebe, F.R. 2000. The influence of suspended clays on phytoplankton reflectance signatures and the remote estimation of chlorophyll. Verh. Int. Ver. Theor. Angew. Limnol. **27**: 1–7.

Schelske, C.L., Stoermer, E.F., Fahnenstiel, G.L., and Haibach, G.L. 1986. Phosphorus enrichment, silica utilization, and biogeochemical silica depletion in the Great lakes. Can. J. Fish. Aquat. Sci. **43**: 407–415.

Schindler, D.W., Beaty, K.G., Fee, E.J., Cruikshank, D.R., DeBruyn, E.D., Findlay, D.L., Lindsay, G.A., Shearer, J.A., Stainton, M.P., and Turner, M.A. 1990. Effects of climatic warming on lakes of the central boreal forest. Science (Washington, D.C.), **250**: 967–970.

Sickman, J.O., Melack,J.M., and Clow, D.W. 2003. Evidence for nutrient enrichment of high-elevation lakes in the Sierra Nevada, California. Limnol. Oceanogr. **48**: 1885–1892.

Turk, J.T., and Campbell, D.H. 1987. Estimates of acidification of lakes in the Mt. Zirkel Wilderness Area, Colorado. Wat. Resour. Res. **23**: 1757–1751.

Vinebrooke, R.D., Dixit, S.S., Graham, M.D., Gunn, J.M., Chen, Y.W., and Belzile, N. 2002. Whole-lake algal responses to a century of acidic deposition on the Canadian Shield. Can. J. Fish. Aquat. Sci. **59**: 483–493.

Williams, M.W., and Tonnessen, K.A. 2000. Critical loads for inorganic nitrogen deposition in the Colorado Front Range, USA. Ecol. Appl. **10**: 1648–1665.

Wolfe, A.P., Baron, J.S., and Cornett, R.J. 2001. Anthropogenic nitrogen deposition induces rapid ecological changes in alpine lakes of the Colorado Front Range (USA). J. Paleolimnol. **25**: 1–7.

Wolfe, A.P., Kaushal, S.K., Fulton, J.R., and McKnight, D.M. 2002. Spectrofluorescence of lake sediment fulvic acids and historical changes of lacustrine organic matter provenance in response to atmospheric nutrient enrichment. Environ. Sci. Technol. **36**: 3217–3223.

Wolfe, A.P., Van Gorp, A.C., and Baron, J.S. 2003. Recent ecological and biogeochemical changes in alpine lakes of Rocky Mountain National Park (Colorado, USA): a response to anthropogenic nitrogen deposition. Geobiology, **1**: 153–168.

© 2005 NRC Canada

A model of total swimming costs in turbulent flow for juvenile Atlantic salmon (*Salmo salar*)[1]

Eva C. Enders, Daniel Boisclair, and André G. Roy

Abstract: Juvenile Atlantic salmon (*Salmo salar*) live in rivers characterized by highly turbulent flows. In these environments, flow turbulence is associated with a wide range of instantaneous flow velocities, which may affect the energetic costs of habitat utilization of juvenile Atlantic salmon. The purpose of our work was to develop a swimming costs model for juvenile Atlantic salmon that especially accounts for the effects of velocity fluctuations in turbulent environments. We estimated the total swimming costs of fish in a respirometer in which we produced five turbulent flow conditions, each characterized by a mean and a standard deviation of flow. Respirometry experiments were conducted at water temperatures of 10, 15, and 20 °C with fish ranging in size between 4.3 and 17.6 g at three mean flow velocities (18, 23, and 40 cm·s^{-1}) and three standard deviations of flow velocity (5, 8, and 10 cm·s^{-1}). Our results confirmed that total swimming costs increased with an increase of water temperature, body mass, mean flow velocity, and standard deviation of flow velocity (R^2 = 0.93). Water temperature, body mass, mean flow velocity, and standard deviation of flow velocity contributed respectively 2%, 31%, 46%, and 14% to the explained variation in total swimming costs.

Résumé : Les juvéniles du saumon atlantique (*Salmo salar*) vivent dans les rivières caractérisées par des écoulements fortement turbulents. Dans ces environnements, la turbulence de l'écoulement est associée à un vaste étendu des vitesses instantanées, ces dernières pourraient affecter les coûts énergétiques des juvéniles du saumon atlantique lors de l'utilisation de l'habitat. Le but de notre travail était de développer un modèle de coût de nage des juvéniles du saumon atlantique qui tient spécialement compte des effets des fluctuations de vitesse dans un environnement turbulent. Nous avons estimé les coûts totaux de nage de poisson dans un respiromètre dans lequel nous avons produit cinq conditions turbulentes, chacune caractérisée par une moyenne et un écart-type distincts de la vitesse de l'écoulement. Les expériences respirométriques ont été réalisées à 10, 15 et 20 °C en utilisant des poissons d'une taille variant de 4,3 à 17,6 g, à trois vitesses moyennes (18, 23 et 40 cm·s^{-1}) et à trois écart-types de vitesse (5, 8 et 10 cm·s^{-1}). Nos résultats confirment que les coûts totaux de nage augmentent avec une augmentation de la température de l'eau, de la masse corporelle, de la vitesse moyenne et de l'écart-type de vitesse (R^2 = 0,93). La température de l'eau, la masse corporelle, la vitesse moyenne et l'écart-type de vitesse contribuent respectivement pour 2, 31, 46 et 14 % de la variation expliquée dans les coûts totaux de nage.

Introduction

Bioenergetics models may be applied to assess fish habitat quality and spatial distribution (Fausch 1984; Nislow et al. 2000). In a habitat with favorable growth conditions, fish obtain a positive balance between the energetic gains through food consumption, the energetic costs for metabolism, and the losses from excretion and egestion (Fausch 1984; Hill and Grossman 1993). Increased growth may lead to fitness advantages with respect to foraging abilities and competitive capacities (Hill and Grossman 1993; Cutts et al. 1998), overwinter survival (Cunjak and Therrien 1998; Morgan et al. 2000), and age of first reproduction (Hutchings and Jones 1998; Morgan et al. 2002). However, the precision of the predictions of bioenergetics models depends on the reliability of the submodels used to estimate the different components of fish energy budget (Hansen et al. 1993; Ney 1993). Activity metabolism may represent up to 40% of the energy budget (Brett and Groves 1979; Boisclair and Leggett 1989). Consequently, the precise quantification of the activity me-

Received 5 April 2004. Accepted 17 December 2004. Published on the NRC Research Press Web site at http://cjfas.nrc.ca on 26 May 2005.
J18061

E.C. Enders[2,3] **and D. Boisclair.** Département de sciences biologiques, Université de Montréal, C.P. 6128, Succursale Centre-ville, Montréal, QC H3C 3J7, Canada.
A.G. Roy. Département de géographie, Université de Montréal, C.P. 6128, Succursale Centre-ville, Montréal, QC H3C 3J7, Canada.

[1]Contribution to the program of CIRSA (Centre Interuniversitaire de Recherche sur le Saumon Atlantique).
[2]Corresponding author (e-mail: enderse@dfo-mpo.gc.ca).
[3]Present address: Fisheries and Oceans Canada, Ecological Sciences Section, 80 East White Hills Road, P.O. Box 5667, St. John's, NL A1C 5X1, Canada.

 doi: 10.1139/F05-007 © 2005 NRC Canada

tabolism is of great interest to obtain appropriate predictions from bioenergetics models (Boisclair and Leggett 1989; Hansen et al. 1993; Ney 1993).

Estimation of the activity metabolism requires the description of the movements performed by the fish in their natural environment (i.e., number, duration, and speed of movements) and the quantification of the energetic costs of performing these movements. Generally, the energy expenditures associated with the movements of stream-dwelling fish are estimated by models derived from respirometry experiments with fish swimming at a steady speed in a flume designed to minimize flow heterogeneity (Brett 1964; Beamish 1978). However, in their natural environment, stream-dwelling fish are often confronted with a highly turbulent flow that may affect their activity metabolism. For instance, Pavlov et al. (2000) have shown that the sustained swimming speed and the critical swimming speed of gudgeon (*Gobio gobio*) and roach (*Rutilus rutilus*) decrease with an increase of turbulence intensity (standard deviation/mean flow velocity). This suggests that the activity metabolism increases with an increase of turbulent intensity (Pavlov et al. 2000). In contrast, Liao et al. (2003) demonstrated that adult rainbow trout (*Oncorhynchus mykiss*) swimming behind an obstacle producing a regular vortex shedding use the energy of these vortices to maintain their position in turbulent flows while reducing their muscle activity. This indicates that activity metabolism of fish using vortices that occur in turbulent flows may be lower than in the absence of such vortices. However, in natural gravel-bed rivers, vortex shedding may be more dynamic and more variable in location, occurrence, and intensity than under a controlled laboratory situation. Therefore, it may be more difficult for stream-dwelling fish to benefit from vortices in natural flow environments. Furthermore, in natural gravel-bed rivers, we also observe large-scale flow structures that extend over the entire water column. They may be seen as a temporal succession of quasi-periodic pulses of high- and low-speed fluid lasting several seconds (Roy and Buffin-Bélanger 2001; Roy et al. 2004). The high-speed pulses are generally directed towards the river bed whereas the low-speed pulses develop towards the water surface. Measurements of these turbulent flow structures suggest that the flow velocity can change three- to eightfold relative to the mean flow velocity within 1–5 s (Roy et al. 1999). These large-scale flow structures vary in length between three and five times the water depth (Roy et al. 2004). Fish are confronted by these flow fluctuations, and in a preliminary study, we showed that the cost of swimming in such a temporally fluctuating flow may be two to four times the values predicted by steady-swimming models (Enders et al. 2003). However, the energetic cost of swimming under turbulent flow conditions was estimated using only a single water temperature and fish body mass. In the present study, we conducted experiments under a wider range of water temperature, body mass, mean flow velocity, and turbulent conditions.

The objectives of this study were to (*i*) evaluate the effect of fish body mass, water temperature, mean flow velocity, and descriptors of flow turbulence on the energetic cost of swimming in fish, (*ii*) develop swimming costs models for fish swimming under turbulent flow conditions, (*iii*) assess the relative power of different descriptors of flow turbulence in predicting total swimming costs, and (*iv*) compare the prediction of turbulent swimming models with existing forced-swimming models over a range of abiotic conditions.

Material and methods

We attained our objectives by performing a total of 104 respirometry experiments during which we subjected individual fish ranging from 4.3 to 17.6 g wet mass to turbulent flow conditions. Respirometry experiments were conducted at 10, 15, and 20 °C. We estimated total swimming costs under four turbulent flow conditions defined by the combination of two means (18 and 23 cm·s^{-1}) and two standard deviations (5 and 8 cm·s^{-1}) of flow velocity. Eight respirometry experiments, each involving a fish of a different mass, were performed for each combination of water temperature and flow condition (further referred to as suite of experiments). In addition to these 12 suites of experiments (3 water temperatures × 4 flow conditions), we conducted another suite of eight experiments at 15 °C and under a turbulent flow condition characterized by a mean flow velocity of 40 cm·s^{-1} and a standard deviation of flow velocity of 10 cm·s^{-1}.

Fish

We evaluated the energetic cost of swimming in a turbulent flow using juvenile Atlantic salmon (*Salmo salar*; ages 1+ and 2+). The body mass (wet) of the juvenile Atlantic salmon (JAS) ranged from 4.3 to 17.6 g. JAS are particularly suitable for this study because their natural habitat comprises riffle sections in gravel-bed rivers that are characterized by a highly turbulent flow. JAS are drift feeders and undertake feeding motions from the riverbed towards the water surface to capture drifting invertebrates (Kalleberg 1958). During these motions, JAS experience rapid changes in flow velocities and structure.

JAS were provided by the Pisciculture de Tadoussac (operated by the Société de la Faune et des Parcs du Québec, Canada). These fish are the offspring from the crossing of wild genitors originating from the Sainte-Marguerite River (Saguenay Region, Quebec, Canada). The juveniles were transferred to the Université de Montréal where they were kept in 500-L Living Stream aquaria (LSW 700) (Frigid Units Inc., Toledo, Ohio). Fish were adapted for a period of 1 month at the targeted water temperatures (10, 15, and 20 °C ± 0.5 °C) before starting a suite of experiments. Fish were fed daily with commercial food pellets (Corey Feed Mills Ltd., Fredericton, New Brunswick).

Respirometry

The details of the experimental design and procedure that we employed are fully described in Enders et al. (2003). They are only summarized here. The respirometer consisted of a Plexiglas© box that could be hermetically sealed. The respirometer contained two pumps (further referred to as pumps 1 and 2) and a bottle-shaped swimming chamber. The narrow neck of the swimming chamber was connected to pump 1 (Jacobs Canada Inc., Mississauga, Ontario) that generated the turbulent flow in the swimming chamber. Pump 2 (Powerhead, Montréal, Quebec) transferred water from the respirometer to an oxygen meter (Intap, model 565) (Mettler

© 2005 NRC Canada

Table 1. Mean flow velocity, standard deviation of the flow velocity, and minimum and maximum values measured for the streamwise (u), vertical (v), and lateral (w) velocity components at five different flow conditions, turbulence intensity (TI; standard deviation (u_{SD})/mean velocity ($\bar{u}$)), and turbulent kinetic energy (TKE).

Velocity vector	Low velocity, low turbulence	Low velocity, medium turbulence	Medium velocity, low turbulence	Medium velocity, medium turbulence	High velocity, high turbulence
$\bar{u}$ (cm·s^{-1})	18.1	18.3	23.1	23.1	40.7
u_{SD} (cm·s^{-1})	5.1	8.2	5.1	8.0	10.3
u_{min} (cm·s^{-1})	3.6	0.5	5.0	0.7	2.5
u_{max} (cm·s^{-1})	34.6	39.7	35.2	43.7	76.6
$\bar{v}$ (cm·s^{-1})	0.1	0.0	0.0	0.0	–2.1
v_{SD} (cm·s^{-1})	4.9	7.0	5.0	7.4	14.8
v_{min} (cm·s^{-1})	–21.9	–24.8	–22.9	–29.9	–74.7
v_{max} (cm·s^{-1})	21.9	23.7	21.5	29.8	51.0
$\bar{w}$ (cm·s^{-1})	0.2	0.1	0.0	0.3	3.1
w_{SD} (cm·s^{-1})	5.5	7.6	5.5	7.5	12.4
w_{min} (cm·s^{-1})	–21.9	–26.0	–27.4	–28.2	–49.4
w_{max} (cm·s^{-1})	23.3	26.6	26.5	30.7	56.0
TI*	0.27	0.44	0.22	0.34	0.25
TKE (g·cm^{-1}·s^{-2})	66.8	139.4	68.8	143.6	416.2

*Unitless.

Toledo, Mississauga, Ontario). The energetic cost of swimming against a turbulent flow was quantified by measuring the oxygen depletion over time with the oxygen meter (±0.01 mg O_2·L^{-1}).

Turbulent flow

The turbulent flow within the swimming chamber was created by modulating the electric current that powered pump 1. The flow in the swimming chamber was quantified using an acoustic Doppler velocimeter (ADV) (Sontek, San Diego, California). The turbulent flow was measured in the absence of the fish to avoid interference caused by its body and movements. The ADV allowed us to record the three orthogonal velocity components of the flow (streamwise (u), vertical (v), and lateral (w)). The instantaneous velocities of the three orthogonal velocity components were measured at a frequency of 25 Hz. The ADV also permitted us to define the settings of the components of the electric current that could create five different flow conditions (Table 1). The flow conditions are characterized by a selected combination of three mean streamwise flow velocities ($\bar{u}$; low flow velocity = 18 cm·s^{-1}, medium flow velocity = 23 cm·s^{-1}, and high flow velocity = 40 cm·s^{-1}) and three standard deviations of the streamwise flow velocity (u_{SD}; low turbulence = 5 cm·s^{-1}, medium turbulence = 8 cm·s^{-1}, and high turbulence = 10 cm·s^{-1}). The settings for the five turbulent flow conditions were selected because they are within the range of mean flow velocities (5–40 cm·s^{-1}) (DeGraaf and Bain 1986; Guay et al. 2000) and of standard deviations of flow velocity (4–14 cm·s^{-1}) observed at the focal point used by JAS under natural conditions (Enders et al. 2005).

Velocity time series were recorded for 5 min at the beginning and end of each suite of respirometry experiments. This strategy was adopted to verify the stability and repeatability of the flow created by our apparatus for given settings of the components of the electric current that powered pump 1. The stability of the five experimental flow conditions was tested using Student's t test. Such t tests were performed to compare the mean streamwise flow velocities recorded before and after a suite of experimental observations. The repeatability of the specific turbulent flow condition produced at different water temperatures was tested using a one-way analysis of variance (ANOVA) comparing the mean streamwise flow velocities. During this analysis, the velocity time series obtained before and after a suite of experimental observations were used as replicates. The stability and repeatability of the standard deviations of the streamwise flow velocities were tested using the Levene's test of the homogeneity of variance using the same procedure.

We obtained the means and standard deviations for the velocity components (u, v, w) for each flow condition. From the means and standard deviations for u, we calculate the turbulence intensity (TI; standard deviation (u_{SD})/mean velocity ($\bar{u}$)). We also used the three velocity components provided by the ADV to calculate the turbulent kinetic energy (TKE) (grams per centimetre per second squared):

$$(1) \qquad \text{TKE} = 1/n \sum_{i=1}^{n} 0.5\rho(u_i'^2 + v_i'^2 + w_i'^2)$$

where n is the number of instantaneous velocity fluctuations (7500 measurements per velocity time series), ρ (grams per cubic centimetre; depending on water temperature used in our experiments) is the water density, and u_i', v_i', and w_i' (centimetres per second) represent the instantaneous velocity fluctuation of the three velocity components.

The five different flow conditions created by our apparatus during the experiments corresponded to the targeted means (18, 23, and 40 cm·s^{-1}) and standard deviations (5, 8, and 10 cm·s^{-1}) of flow velocity. Mean flow velocities were always within 1.8%, 0.4%, and 1.7% of the targeted values for the low, medium, and high flow velocities, respectively (Table 1). The standard deviation of the streamwise flow velocity was 5.1, 8.1, and 10.3 cm·s^{-1} for the low, medium, and

© 2005 NRC Canada

high turbulence condition, respectively, and did not vary by more than 4.3% among experiments. Mean vertical and lateral flow velocities were close to 0 $cm \cdot s^{-1}$ (–2.1 to 3.1 $cm \cdot s^{-1}$). The corresponding standard deviation of the vertical and lateral flow velocity ranged from 4.9 to 14.8 $cm \cdot s^{-1}$. TI of the five different flow conditions varied between 0.22 (medium flow velocity and low turbulence) and 0.44 (low flow velocity and medium turbulence). TKE ranged from 66.8 $g \cdot cm^{-1} \cdot s^{-2}$ (low flow velocity and low turbulence) to 416.2 $g \cdot cm^{-1} \cdot s^{-2}$ (high flow velocity and high turbulence) (Table 1).

For any given flow condition, $\bar{u}$ and u_{SD} did not vary significantly among the recordings performed before and after a suite of experimental observations (stability test for $\bar{u}$: $0.42 < p < 0.98$, variation = 0.0%–0.3%; stability test for u_{SD}: $0.12 < p < 0.94$, variation = 0.2%–2.1%). Similarly, the characteristics of specific flow conditions produced at different water temperatures did not vary significantly among experiments (stability test for $\bar{u}$: $0.39 < p < 0.99$, variation = 0.1%–0.9%; stability test for u_{SD}: $0.17 < p < 0.69$, variation = 0.1%–2.3%). These results suggest that the flows created by our apparatus were stable and repeatable.

Total swimming costs

A single fish was selected at random from our stock of experimental fish, kept separately, and not fed for 2 days before the experiment to avoid increased metabolic rates due to digestion (Brett and Groves 1979). The fish was introduced into the swimming chamber 24 h before the beginning of the experiment to allow it to adapt to the experimental conditions. The initial oxygen concentration was measured at the beginning of the experiment and subsequently at every 30 min until the end of an experiment. We monitored fish behavior during each experiment using a web cam (Sony Electronics Inc., Oradell, New Jersey) to ensure that fish were continuously swimming. An experiment ended after 6 h for the low and medium flow velocity experiments and after 3 h for the high flow velocity experiments. No observation was made below 7.6 mg $O_2 \cdot L^{-1}$ to minimize the influence of low oxygen concentration on the fish behavior (Beamish 1978). At the end of an experiment, the fish was removed from the respirometer, anaesthetized (clove oil, 0.6 $mg \cdot L^{-1}$), weighed (grams wet), and measured (total body length, centimetres). The biological oxygen demand (BOD) was determined within 3 h of an experiment using the same procedure but without fish. We estimated the total oxygen consumption rate (sum of standard metabolic rate plus net swimming costs) of fish ($\dot{V}O_2$) (milligrams of oxygen per hour) as

$$(2) \qquad \dot{V}O_2 = \Delta O_2 / \Delta t V_w - \mathrm{BOD}$$

where ΔO_2 is the difference in oxygen concentration between two consecutive oxygen concentration measurements (milligrams of oxygen per litre), Δt is the time interval of 0.5 h between two consecutive oxygen concentration measurements, V_w (litres) is the volume of water in the respirometer excluding the solid volume of pumps, swimming chamber, and fish, and BOD is the biological oxygen demand by microorganisms in the water (milligrams of oxygen per hour). The BOD was always below the detection limit of the oxygen sensor. As we measured oxygen concentration within the swimming chamber at 30-min intervals over 3 or 6 h, we obtained 6 or 12 $\dot{V}O_2$ values per experiment, respectively. We then calculated the mean (further referred to as total swimming costs C_R (milligrams of oxygen per hour)) of the 12 or 6 $\dot{V}O_2$ values obtained for each experiment.

Prior to statistical analyses, the obtained total swimming costs and body mass values were log transformed and the residuals were tested for normality using graphical probability plots. Homogeneity of variance was tested using Levene's test. Statistical analyses of total swimming cost data were performed on two groupings of our experiments. The first grouping (further referred to as G1) comprised 96 experiments (8 fish masses × 3 water temperatures × 4 flow conditions). G1 allowed us to test the variability of total swimming costs with water temperature, mean flow velocity (18 and 23 $cm \cdot s^{-1}$), and standard deviation of flow velocity (5 and 8 $cm \cdot s^{-1}$) using a three-way ANOVA. During this analysis, fish body mass was used as a covariate. The second grouping (further referred to as G2) consisted of 40 experiments performed at 15 °C using eight fish masses and five flow conditions (mean flow of 18 and 23 $cm \cdot s^{-1}$ and standard deviation of 5 and 8 $cm \cdot s^{-1}$ together with mean flow of 40 $cm \cdot s^{-1}$ and standard deviation of 10 $cm \cdot s^{-1}$). G2 was used to test the significance of the effect of mean flow and standard deviation of flow on total swimming costs over a wider range of flow turbulence than with G1 but at a single water temperature. This analysis was performed with a two-way ANOVA using fish mass as a covariate.

The relationship between total swimming costs and body mass, water temperature (only for G1), and flow characteristics was assessed using multiple regression analyses. Three different types of models were explored. These models were defined by the variable(s) used to represent flow. Following this procedure, flow characteristics were alternately represented by (*i*) the mean and the standard deviation of flow velocity, (*ii*) the turbulence intensity, and (*iii*) the turbulent kinetic energy.

Results

Total swimming costs

The oxygen depletion in the respirometer was linear over time during all experiments ($0.89 < r^2 < 1.0$, $p < 0.001$). Consequently, no relationship between oxygen consumption rates C_R and time since the beginning of an experiment was observed ($0.01 < r^2 < 0.13$, $0.24 < p < 1.0$) (Fig. 1). Within-experiment variation in C_R ranged from 3.8% to 11.6%. The total swimming costs varied 9.3-fold among our experiments (1.6–14.9 mg $O_2 \cdot h^{-1}$) (Table 2). Data comprised in our first grouping of experiments (G1) indicated that total swimming costs increased twofold as fish mass increased from 5 to 15 g. As expected, total swimming costs increased with water temperature (Fig. 2). For instance, depending on the flow conditions, the total swimming costs of a 10-g fish increased by 10.5%–16.9% as water temperature increased from 10 to 20 °C. Total swimming costs also tended to increase with mean flow velocity and with the standard deviation of flow velocity (Fig. 3). Hence, the total swimming costs of a 10-g fish increased, on average, by 61.4% as mean flow velocity

© 2005 NRC Canada

Fig. 1. Oxygen consumption rates during the experimental period of four juvenile Atlantic salmon (*Salmo salar*): a 5.3-g fish at 10 °C, $\bar{u}$ = 18 cm·s^{-1}, and u_{SD} = 5 cm·s^{-1} (solid circles); a 9.6-g fish at 15 °C, $\bar{u}$ = 23 cm·s^{-1}, and u_{SD} = 5 cm·s^{-1} (open circles); a 15.0-g fish at 20 °C, $\bar{u}$ = 23 cm·s^{-1}, u_{SD} = 8 cm·s^{-1} (solid triangles); and a 11.6-g fish at 15 °C, $\bar{u}$ = 40 cm·s^{-1}, and u_{SD} = 10 cm·s^{-1} (open triangles). Regression lines of the linear relationship between time and oxygen consumption rates are presented.

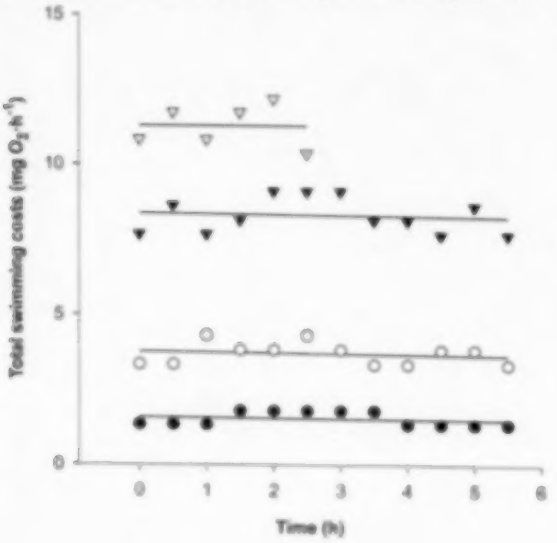

increased from 18 to 23 cm·s^{-1}, while standard deviation was constant at 5 cm·s^{-1}. The corresponding increase of total swimming costs with a standard deviation of flow of 8 cm·s^{-1} was 52.9%. On average, total swimming costs of a 10-g fish increased by 31.9% ($\bar{u}$ = 18 cm·s^{-1}) and by 25.0% ($\bar{u}$ = 23 cm·s^{-1}) as the standard deviation of the flow velocity increased from 5 to 8 cm·s^{-1}.

Swimming costs model

Statistical analyses indicated that body mass ($F_{[1,83]}$ = 447.16, $p < 0.001$), water temperature ($F_{[2,83]}$ = 17.55, $p < 0.001$), mean flow velocity ($F_{[1,83]}$ = 650.62, $p < 0.001$), and standard deviation of flow velocity ($F_{[1,83]}$ = 196.05, $p < 0.001$) had a significant effect on total swimming costs. No interaction term of the three-way ANOVA was significant ($0.10 < p < 0.99$), indicating that the direction of the effect of body mass, water temperature, mean flow velocity, and standard deviation of flow velocity on the total swimming costs was similar among the different combinations of experimental conditions. Body mass, water temperature, and mean and standard deviation of flow velocity explained a statistically significant proportion of the variations of total swimming costs ($F_{[4,91]}$ = 337.37, R^2 = 0.93, $p < 0.001$) (Table 3). Mean flow velocity and body mass explained respectively 46% and 31% of the variations of total swimming costs, while standard deviation of flow velocity explained 14% of this variation. Water temperature explained 2% of the observed variations of total swimming costs. Total swimming costs could not be related to turbulence intensity. In contrast, a model combining body mass, water temperature, and turbulent kinetic energy explained 49% of the variation in total swimming costs ($F_{[3,92]}$ = 29.41, $p < 0.001$). The most influential variable in this model was the body mass, which explained 31% of the variance of total swimming costs. Turbulent kinetic energy and water temperature explained respectively 16% and 3% of the variations of total swimming costs.

Table 2. Temperature, flow condition (selected combination of mean flow velocity ($\bar{u}$) and standard deviation of flow velocity (u_{SD})), range of body mass (M) of fish used in the respirometry experiments, and total swimming costs (C_R) measured in the corresponding turbulence flow condition.

Temperature (°C)	$\bar{u}$ (cm·s^{-1})	u_{SD} (cm·s^{-1})	M (g wet mass)	C_R (mg O_2·h^{-1})
10	18	5	5.3–16.4	1.5–3.2
	18	8	5.6–16.3	1.7–4.1
	23	5	5.4–17.6	2.2–5.5
	23	8	6.4–15.0	3.5–7.1
15	18	5	5.6–15.5	1.6–3.5
	18	8	5.2–15.0	2.0–4.3
	23	5	4.9–16.0	2.7–6.0
	23	8	5.1–15.0	3.7–8.0
	40	10	4.3–14.0	5.0–14.9
20	18	5	5.2–15.2	1.7–3.9
	18	8	5.9–16.1	2.4–5.1
	23	5	5.9–16.1	2.7–6.2
	23	8	5.9–16.8	3.6–8.2

Note: Number of experiments (n) equalled 8 for each combination of water temperature and flow condition.

Data included in our second grouping of experiments (G2) confirmed the effects of body mass on the total swimming costs. The observations performed at higher mean flow velocities indicated that body mass ($F_{[1,34]}$ = 285.87, $p < 0.001$), mean flow velocity ($F_{[1,34]}$ = 294.27, $p < 0.001$), and standard deviation of flow velocity ($F_{[1,34]}$ = 83.46, $p < 0.001$) significantly affected total swimming costs. The interaction term between mean and standard deviation of flow velocity was not significant (p = 0.71), indicating that the direction of the effect of two variables on the total swimming costs was similar among the different experimental conditions. Multiple regression analyses based on G2 allowed us to develop a three-variable model ($F_{[3,36]}$ = 146.30, R^2 = 0.92, $p < 0.001$) where body mass, mean flow velocity, and standard deviation of flow velocity contributed respectively to 16%, 61%, and 15% of the variation in total swimming costs. We again observed no correlation between the turbulence intensity and the total swimming costs. However, total swimming costs increased with body mass and turbulent kinetic energy, resulting in a two-variable model ($F_{[2,37]}$ = 53.46, R^2 = 0.74, $p < 0.001$) with body mass contributing 16% and turbulent kinetic energy 58% of the variation in total swimming costs.

Discussion

Our analyses demonstrated that total swimming costs of JAS swimming in turbulent flow increased with body mass, water temperature, mean flow velocity, standard deviation of flow velocity, and turbulent kinetic energy. The exponent of

© 2005 NRC Canada

Fig. 2. Total swimming costs of juvenile Atlantic salmon (*Salmo salar*) at four different flow conditions: (*a*) $\bar{u}$ = 18 cm·s^{-1} and u_{SD} = 5 cm·s^{-1}, (*b*) $\bar{u}$ = 18 cm·s^{-1} and u_{SD} = 8 cm·s^{-1}, (*c*) $\bar{u}$ = 23 cm·s^{-1} and u_{SD} = 5 cm·s^{-1}, and (*d*) $\bar{u}$ = 23 cm·s^{-1} and u_{SD} = 8 cm·s^{-1} at 10 °C (triangles), 15 °C (open circles), and 20 °C (solid circles). Values are means ± SE (n = 12). Regression lines of the log linear relationship between body mass and total swimming costs are presented.

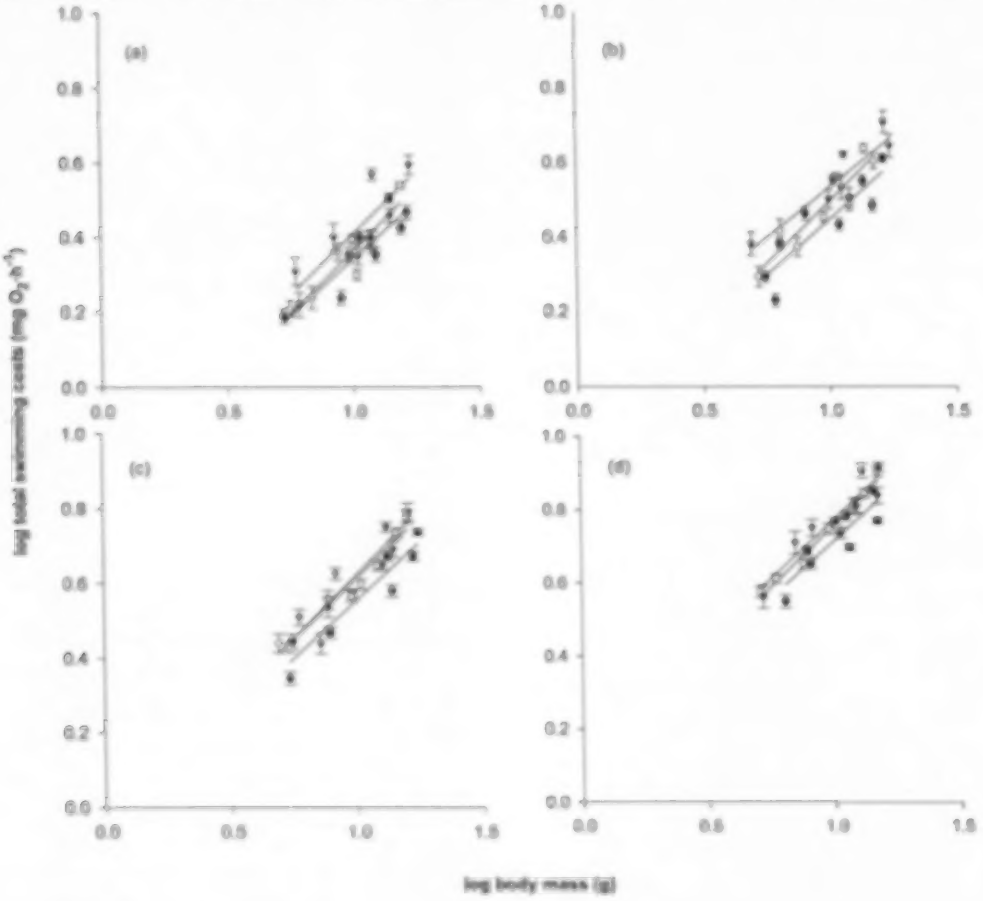

body mass (0.62–0.79 depending on the model) was similar to those of models developed for forced-swimming models, indicating that the slope of the increase of metabolic rates of fish was similar to that found in other swimming costs models. Our analyses suggest that water temperature explained a significant proportion of the variations in the metabolic rates. A 10 °C increase in water temperature increased total respiration rates by 12%–18%. It has long been recognized that fish swimming costs increase with swimming velocity (Beamish 1978; Boisclair and Tang 1993; Tang et al. 2000). Our study confirmed this situation but also indicated that descriptors of flow turbulence explain a significant fraction of total swimming costs. The energetic costs of swimming at a given mean flow velocity increased by 21%–31% as the standard deviation of the flow velocity increased from 5 to 8 cm·s^{-1}. Among the three descriptors of flow turbulence that we examined, standard deviation of flow velocity and turbulent kinetic energy significantly contributed to the predictive power of the models developed. In contrast, turbulence intensity never explained a significant fraction of the variation of the total swimming costs. Standard deviation of flow velocity explained from 14% (with G1) to 15% (with G2) of the variations of total swimming costs compared with 16% (with G1) to 58% (with G2) for turbulent kinetic energy. Hence, turbulent kinetic energy appears to be a more powerful predictor of total swimming costs than standard deviation of low flow velocity alone. However, the combination of mean flow velocity and standard deviation of flow velocity explained a higher fraction of the variations of total swimming costs (from 60% to 76%) than turbulent kinetic energy. This suggests that the model using mean and standard deviation of flow velocity may have the highest predictive power.

Comparison between observed swimming costs and predictions by forced-swimming models

Most studies that estimate the cost of swimming for stream-dwelling fish use respiration models based on experimental designs that minimize flow heterogeneity (Brett 1964; Beamish 1978). Our findings suggest that flow turbulence significantly increases fish swimming costs and consequently that the use of such forced-swimming models may

© 2005 NRC Canada

Fig. 3. Total swimming costs of juvenile Atlantic salmon (*Salmo salar*) under low (triangles), medium (circles), and high (squares) flow velocities at water temperatures of (*a*) 10 °C, (*b*) 15 °C, and (*c*) 20 °C. The open symbols represent the low turbulence condition and the solid symbols represent the medium and the high turbulence conditions. Values are means ± SE (n = 12 for the low and medium flow velocities and n = 6 for the high flow velocity). Regression lines of the log linear relationship between body mass and total swimming costs are presented.

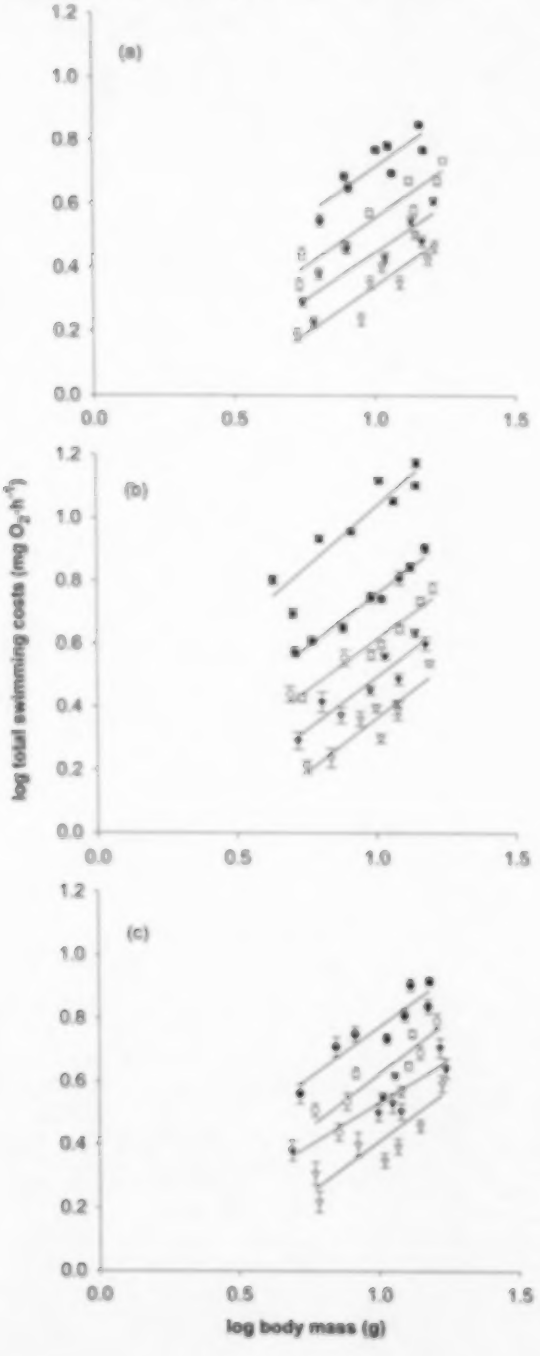

underestimate actual swimming costs. This situation can be illustrated by comparing the predictions of our turbulence swimming model with predictions of a classical forced-swimming model proposed by Boisclair and Tang (1993). However, this forced-swimming model predicts the net swimming costs of fish. In contrast, our observations and models focused on total swimming costs (standard metabolic rate plus net swimming costs). This strategy was used in the absence of a standard metabolic rate model for JAS compromising the entire body mass and water temperature ranges used in our study. Consequently, to perform the comparison between the models, we reanalysed the data set used by Boisclair and Tang (1993) and developed a new forced-swimming model predicting total swimming costs. The forced-swimming model we obtained is

$$\log_{10} \mathrm{FTSC} = 0.96 \log_{10} M + 0.23 \log_{10} \bar{u} + 0.67 \log_{10} T - 1.85 \quad (3)$$

where FTSC is the forced total swimming costs (milligrams of oxygen per hour) under minimized flow heterogeneity, M is the fish body mass (grams wet), T is the water temperature (degrees Celsius), and $\bar{u}$ is the mean flow velocity (centimetres per second). All variables were significant; however, body mass explained most (79%) of the variation in the total swimming costs ($F_{[3,114]}$ = 162.35, R^2 = 0.81, $p < 0.0001$). The model predicted that total swimming costs of a 10-g fish swimming in minimized flow heterogeneity at a water temperature of 15 °C and a swimming speed of 18 and 23 cm·s^{-1} should be 1.50 and 1.58 mg O_2·h^{-1}, respectively. Under low-turbulence conditions, the total swimming costs that we estimated for 10-g JAS at 15 °C were 2.0 to 2.7 times higher than predicted by the forced-swimming model (Fig. 4). The differences were more pronounced under medium-turbulence conditions, ranging from 3.0- to 3.6-fold. Under high-turbulence conditions, we observed a further increase in the difference between our estimation and prediction of the forced-swimming model. The estimated total swimming costs were 14.0 times higher than predicted by the forced-swimming model. However, it is important to note that this comparison should only be taken as an indication because we extrapolate the prediction of the forced-swimming model to a twofold higher flow velocity than the model was originally developed to (maximal flow velocity 20 cm·s^{-1}).

The increase in the actual total swimming costs under turbulent conditions above those predicted by the forced-swimming model is consistent with the hypothesis that unsteady swimming movements, such as active accelerations and decelerations and changes in speed, are energetically more costly than steady swimming movements at constant speed and direction (Webb 1983; Boisclair and Tang 1993; Kramer and McLaughlin 2001). In turbulent flow, fish have to adjust to the fluctuations in velocity and direction of flow by constantly moving their fins to maintain their position. These movements substantially increase the energetic costs of unsteady swimming above those of steady swimming for the same average swimming speed (Tang et al. 2000; Enders and Herrmann 2003).

The experimental flow conditions used in our experiments are within the range of mean flow velocities (5–40 cm·s^{-1}) (DeGraaf and Bain 1986; Guay et al. 2000) and of standard deviations of flow velocity (4–14 cm·s^{-1}) JAS experience at

© 2005 NRC Canada

Table 3. Four multiple regression models to estimate the total swimming costs (C_R; mg $O_2 \cdot h^{-1}$) in turbulent flow for juvenile Atlantic salmon (*Salmo salar*) using water temperature (T), body mass (M), mean flow velocity ($\bar{u}$), and turbulent kinetic energy (TKE) as explanatory variables.

	Contribution of variable					Model statistics		
Turbulent swimming model	T (°C)	M (g wet mass)	$\bar{u}$ (cm·s^{-1})	u_{SD} (cm)	TKE (g·cm^{-1}·s^{-2})	n	R^2	p
$\log C_R = 0.23 \log T + 0.64 \log M + 2.43 \log \bar{u} + 0.67 \log u_{SD} - 4.06$	0.02	0.31	0.46	0.14	0.16	96	0.93	<0.001
$\log C_R = 0.23 \log T + 0.62 \log M + 0.44 \log \mathrm{TKE} - 1.21$	0.03	0.31				96	0.49	<0.001
At 18 °C								
$\log C_R = 0.79 \log M + 1.47 \log \bar{u} + 0.47 \log u_{SD} - 2.45$		0.16	0.61	0.15		40	0.92	<0.001
$\log C_R = 0.66 \log M + 0.68 \log \mathrm{TKE} - 1.44$		0.16			0.58	40	0.74	<0.001

Fig 4. Ratios of the total swimming costs in turbulent and forced swimming for different fish body mass and flow conditions at (*a*) 10 °C and (*b*) 20 °C. Light and dark lines represent the flow conditions with mean flow velocity $\bar{u}$ of 18 cm·s^{-1} and 23 cm·s^{-1}, respectively. Broken lines indicate low turbulence condition u_{SD} of 5 cm·s^{-1}, and solid lines indicate medium turbulence conditions of 8 cm·s^{-1}.

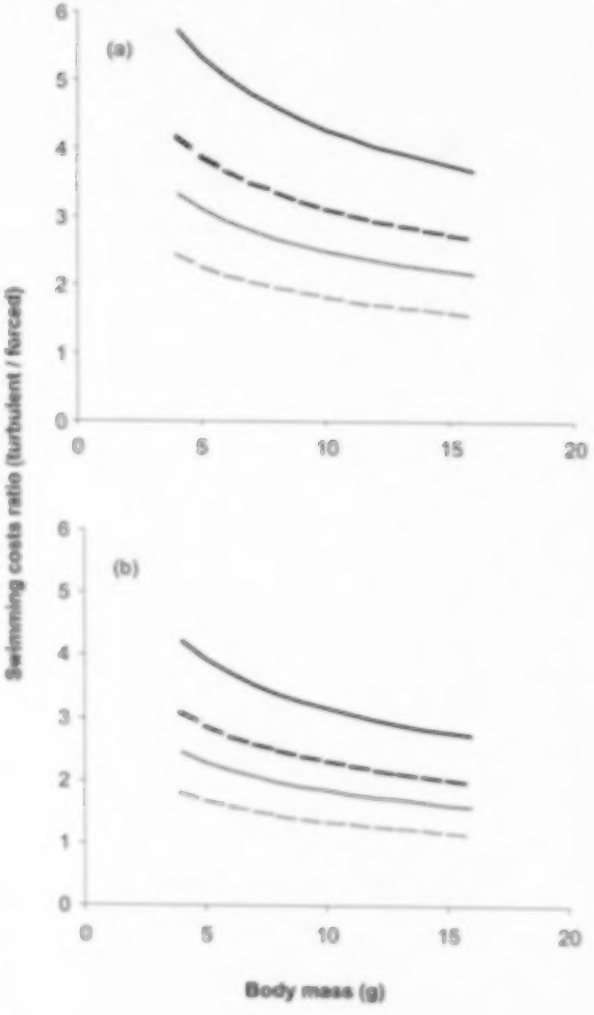

their station-holding position in nature. At their station-holding position, JAS also experience intense flow velocity fluctuations often referred to as large-scale flow structures. These large-scale flow structures are intermittent fluids of high velocity divided by fluids of low velocity. We simulated these large-scale flow structures in our respirometer. The examination of the velocity time series allowed us to identify from two to five low-speed flow events per minute and five high-speed flow events per minute. The mean duration of the flow events was 1.0 s (SD = 0.24 s). However, in their natural environment, JAS are also exposed to a variety of spatial flow structures such as vortices, which are generated by the roughness of the riverbed. Protruding obstacles like the

© 2005 NRC Canada

"home rocks" of JAS used as station-holding positions during active foraging cause the formation of vortex shedding motions at the lee side of obstacles. Liao et al. (2003) demonstrated in a laboratory study that adult rainbow trout might profit from the energy of such vortex shedding. Fish changed their swimming patterns to slalom between the vortices resulting in a reduction of the axial muscle activity. Similarly, it has been suggested that adult sockeye salmon (*Oncorhynchus nerka*) exploit recirculation zones during upriver spawning migration to minimize the energy expenditures (Hinch and Rand 1998; Standen et al. 2002). It is also known that schooling fish profit from the vortices generated by the leading fish. Sea bass (*Dicentrarchus labrax*) swimming at speed of 15–32 $cm \cdot s^{-1}$ in front of the fish school had a 9%–14% higher tail beat frequency than the fish swimming in the rear (Herskin and Steffensen 1998). This behavior resulted in a decrease of the total swimming costs of 9%–23%. The studies demonstrate that under stable vortex shedding, fish may use the energy of these vortices to minimize their energy expenditure of swimming. However, in their natural flow environments, vortex shedding is quasi-periodic phenomena and therefore less regular than simulated in laboratory studies (Roy et al. 1999). This means that under natural flow conditions, fish experience vortex shedding that is less predictable than under laboratory conditions. Therefore, it may be more difficult for fish in natural flow environments to benefit from vortex shedding than demonstrated in laboratory studies.

The applicability of the turbulent swimming model to field situations depends on the ability of our experimental design to reflect natural conditions found in rivers and streams and on the validity of the assumptions that we used to estimate fish swimming costs. First, the model is based on the assumption that the experimental conditions allow fish to swim in a way that may mimic their swimming in the field. Therefore, we tried in swimming experiments to simulate natural flow conditions choosing mean and standard deviation of flow velocities as well as pulses of high- and low-speed flow velocities as observed under natural conditions. However, it is well understood that our results do not cover the complete range of flow conditions that JAS may encounter in natural environments.

Second, the model assumes that, within the range of the duration of the experiments performed, the length of an experiment (hours) has no effect on the validity of the respiration rates obtained. The swimming experiments may be particularly susceptible to this assumption because the experiments required that fish swim continuously for hours at steady swimming speeds, which may not correspond to the natural behavior of JAS. The approach also assumes that, if fish continue to swim for the complete duration of an experiment, and if the metabolic rates do not significantly increase or decrease through time, fish are not fatigued and that their metabolic rates adequately represent swimming costs under the experimental conditions. As such, when developing swimming costs models, combinations of swimming intensity and duration of the experiments are selected to avoid fatigue. In our experiments, the metabolic rate was independent of time, indicating that time spent swimming had no effect on the models developed within the swimming durations used in our study.

Third, the model assumes that swimming costs are adequately estimated by measuring oxygen consumption by fish. This assumption also presumes that the energy required to swim comes mostly from the aerobic metabolism. If anaerobic metabolism contributes to the swimming costs, the potential exists for oxygen consumption rates to underestimate actual swimming costs. The anaerobic metabolism could theoretically interfere with estimates of fish swimming costs obtained by measuring oxygen consumption by fish. The interference caused by anaerobic metabolism is circumvented by modulating the experimental flow velocities and the duration of the experiments to minimize the expression of anaerobic metabolism.

Fourth, the model is based on the assumption that the 2-day deprivation period permitted, on one hand, the exclusion of any increased oxygen consumption rates due to digestion and, on the other hand, did not affect the swimming performance of the fish due to depletion of muscle metabolites (Beamish 1964).

Fifth, we assume that body size rather than fish age influences the swimming performance of fish. The fish that we used for the respirometry experiments were all from the same cohort (age 1+ at the beginning of the experimental period and age 2+ at the end). However, no data are available to determine to what extent fish age actually influences the swimming performance.

The models of total swimming costs in turbulent flow that we developed may be applied to estimate the energy expenditures that JAS would experience in situations where they swim in turbulent flow. These situations may include foraging attempts in the water column to capture drifting food particles or migrations between different habitats (e.g., changes between summer and winter habitat). The models may also be applied to nonterritorial individuals that inhabit the spaces between territories (Martel 1996). The foraging strategy of nonterritorial individuals differs from the commonly described station-holding behavior of JAS. The nonterritorial fish may minimize their energy expenditure related to territorial defense, but they may do so at the expense of increased swimming costs due to exposure to turbulent flow. It is anticipated that in situations where territorial JAS use home rocks in their typical sit-and-wait position near the substrate, no increase in the metabolic costs due to activity occurs (Facey and Grossman 1990). Similarly, in situations where JAS seek shelter in the interstices of the riverbed substrate, especially during low water temperature, no increase in the swimming costs are anticipated (Cunjak 1988; Bremset 2000).

This study showed that bioenergetics models aiming to estimate the energetic costs of habitat utilization by stream-dwelling fish in turbulent environments may require both a description of the behavior of the fish in relation to turbulence and swimming costs models in which the effects of the flow turbulence are explicitly represented. The comprehension of the effects of turbulence on swimming costs may also be relevant to models developed for habitat restoration and management and to the design of migratory fish passages (Odeh et al. 2002; Guiny et al. 2003). We conclude that turbulent swimming models using the mean and standard deviation of flow velocity or turbulent kinetic energy may provide estimates of the cost of habitat utilization for

© 2005 NRC Canada

stream-dwelling fish that are more accurate than the commonly used forced-swimming models.

Acknowledgements

We thank the Pisciculture de Tadoussac for providing us the juvenile Atlantic salmon, Jean-Pierre Martin and Guillaume Guénard for their help in constructing the turbulence-creating transformer, and Judith Bouchard and Sébastien Dupuis for their help in fish husbandry and during the respirometry experiments. Normand Bergeron graciously provided the acoustic Doppler velocimeter. Funding for this study was provided by an individual grant from the Natural Sciences and Engineering Research Council of Canada and by Fonds pour les Chercheurs et l'Aide à la Recherche (FCAR-Équipe) to D. Boisclair. E.C. Enders was supported by scholarships from the Fondation Joseph-Arthur Paulhus, the Faculté des Études Supérieures (Université de Montréal), and the Groupe de Recherche Interuniversitaire en Limnologie (GRIL, FCAR-Centre).

References

Beamish F.W.H. 1964. Respiration of fishes with special emphasis on standard oxygen consumption. II. Influence of weight and temperature on respiration of several species. Can. J. Zool. **42**: 177–188.

Beamish, F.W.H. 1978. Swimming capacity. *In* Fish physiology — locomotion. *Edited by* W.S. Hoar and J.R. Randall. Academic Press, New York. pp. 101–187.

Boisclair, D., and Leggett, W.C. 1989. The importance of activity in bioenergetics models applied to actively foraging fishes. Can. J. Fish. Aquat. Sci. **46**: 1859–1867.

Boisclair, D., and Tang, M. 1993. Empirical analysis of the influence of swimming pattern on the net energetic cost of swimming in fishes. J. Fish Biol. **42**: 169–183.

Bremset, G. 2000. Seasonal and diel changes in behaviour, microhabitat use and preferences by young pool-dwelling Atlantic salmon, *Salmo salar*, and brown trout, *Salmo trutta*. Environ. Biol. Fishes, **59**: 163–179.

Brett, J.R. 1964. The respiratory metabolism and swimming performance of young sockeye salmon. J. Fish. Res. Board Can. **21**: 1183–1226.

Brett, J.R., and Groves, D.D. 1979. Physiological energetics. *In* Fish physiology — bioenergetics and growth. *Edited by* W.S. Hoar, J.R. Randall, and J.R. Brett. Academic Press, New York. pp. 279–352.

Cunjak, R.J. 1988. Behaviour and microhabitat of young Atlantic salmon (*Salmo salar*) during winter. Can. J. Fish. Aquat. Sci. **45**: 2156–2160.

Cunjak, R.A., and Therrien, J. 1998. Inter-stage survival of wild juvenile Atlantic salmon, *Salmo salar* L. Fish. Manag. Ecol. **5**: 209–223.

Cutts, C.J., Metcalfe, N.B., and Taylor, A.C. 1998. Aggression and growth depression in juvenile Atlantic salmon — the consequences of individual variation in standard metabolic rate. J. Fish Biol. **52**: 1026–1037.

DeGraaf, D.A., and Bain, L.H. 1986. Habitat use by and preferences of juvenile Atlantic salmon in two Newfoundland rivers. Trans. Am. Fish. Soc. **115**: 671–681.

Enders, E.C., and Herrmann, J.P. 2003. Energetic costs of spontaneous activity in horse mackerel quantified by a computerized imaging analysis. Arch. Fish. Mar. Res. **50**: 205–219.

Enders, E.C., Boisclair, D., and Roy, A.G. 2003. The effect of turbulence on the cost of swimming for juvenile Atlantic salmon (*Salmo salar*). Can. J. Fish. Aquat. Sci. **60**: 1149–1160.

Enders, E.C., Buffin-Bélanger, T., Boisclair, D., and Roy, A.G. 2005. The feeding behaviour of juvenile Atlantic salmon in relation to turbulent flow. J. Fish Biol. **66**: 242–253.

Facey, D.E., and Grossman, G.D. 1990. The metabolic cost of maintaining position for four North American stream fishes: effects of season and velocity. Physiol. Zool. **63**: 757–776.

Fausch, K.D. 1984. Profitable stream positions for salmonids: relating specific growth rate to net energy gain. Can. J. Zool. **62**: 441–451.

Guay, J.C., Boisclair, D., Rioux, D., Leclerc, M., Lapointe, M., and Legendre, P. 2000. Development and validation of numerical habitat models for juveniles of Atlantic salmon (*Salmo salar*). Can. J. Fish. Aquat. Sci. **57**: 2065–2075.

Guiny, E., Armstrong, J.D., and Ervine, D.A. 2003. Preferences of mature male brown trout and Atlantic salmon parr for orifice and weir fish pass entrances matched for peak velocities and turbulence. Ecol. Freshw. Fish, **12**: 190–195.

Hansen, M.J., Boisclair, D., Brandt, S.B., Hewett, S.W., Kitchell, J.F., Lucas, M.C., and Ney, J.J. 1993. Applications of bioenergetics models to fish ecology and management — where do we go from here? Trans. Am. Fish. Soc. **122**: 1019–1030.

Herskin, J., and Steffensen, J.F. 1998. Energy savings in sea bass swimming in a school — measurements of tail beat frequency and oxygen consumption at different swimming speeds. J. Fish Biol. **53**: 366–376.

Hill, J., and Grossman, G.D. 1993. An energetic model of microhabitat use for rainbow trout and rosyside dace. Ecology, **74**: 685–698.

Hinch, S.G., and Rand, P.S. 1998. Swim speeds and energy use of upriver-migrating sockeye salmon (*Oncorhynchus nerka*) — role of local environment and fish characteristics. Can. J. Fish. Aquat. Sci. **55**: 1821–1831.

Hutchings, J.A., and Jones, M.E.B. 1998. Life history variation and growth rate thresholds for maturity in Atlantic salmon, *Salmo salar*. Can. J. Fish. Aquat. Sci. **55**: 22–47.

Kalleberg, H. 1958. Observations in a stream tank of territoriality and competition in juvenile Atlantic salmon and trout (*Salmo salar* L. and *S. trutta* L.). Fish. Board Swed. Inst. Freshw. Res. Drottingholm Rep. **39**: 55–98.

Kramer, D.L., and McLaughlin, R.L. 2001. The behavioral ecology of intermittent locomotion. Am. Zool. **41**: 137–153.

Liao, J.C., Beal, D.N., Lauder, G.V., and Triantafyllou, M.S. 2003. Fish exploiting vortices decrease muscle activity. Science (Wash., D.C.), **302**: 1566–1569.

Martel, G. 1996. Growth rate and influence of predation risk on territoriality in juvenile coho salmon (*Oncorhynchus kisutch*). Can. J. Fish. Aquat. Sci. **53**: 660–669.

Morgan, I.J., McCarthy, I.D., and Metcalfe, N.B. 2000. Life-history strategies and protein metabolism in overwintering juvenile Atlantic salmon: growth is enhanced in early migrants through lower protein turnover. J. Fish Biol. **56**: 637–647.

Morgan, I.J., McCarthy, I.D., and Metcalfe, N.B. 2002. The influence of life-history strategy on lipid metabolism in overwintering juvenile Atlantic salmon. J. Fish Biol. **60**: 674–686.

Ney, J.F. 1993. Bioenergetics modelling today: growing pains on the cutting edge. Trans. Am. Fish. Soc. **122**: 736–748.

Nislow, K.H., Folt, C.L., and Parrish, D.L. 2000. Spatially explicit bioenergetic analysis of habitat quality for age-0 Atlantic salmon. Trans. Am. Fish. Soc. **129**: 1067–1081.

Odeh, M., Noreika, J.F., Haro, A., Maynard, A., Castro-Santos, T., and Cada, G.F. 2002. Evaluation of the effects of turbulence on

© 2005 NRC Canada

the behavior of migratory fish. Final report 2002. Report to Bonneville Power Administration, Contract No. 00000022, Project No. 200005700 (BPA Report DOE/BP-00000022-1). Available at www.efw.bpa.gov/Publications/D00000022-1.pdf.

Pavlov, D.S., Lupandin, A.I., and Skorobogatov, M.A. 2000. The effects of flow turbulence on the behavior and distribution of fish. J. Ichthyol. **40**: S232–S261.

Roy, A.G., and Buffin-Bélanger, T. 2001. Advances in the study of turbulent flow structures in gravel-bed rivers. *In* Gravel-bed river. V. *Edited by* M.P. Mosley. New Zealand Hydrological Society, Christchurch, New Zealand. pp. 375–397.

Roy, A.G., Biron, P.M., Buffin-Bélanger, T., and Levasseur, M. 1999. Combined visual and quantitative techniques in the study of natural turbulent flows. Water Resour. Res. **35**: 871–877.

Roy, A.G., Buffin-Bélanger, T., Lamarre, H., and Kirkbride, A.D. 2004. Size, shape and dynamics of large-scale turbulent flow structures in a gravel-bed river. Water Resour. Res. **500**: 1–27.

Standen, E.M., Hinch, S.G., Healey, M.C., and Farrell, A.P. 2002. Energetic costs of migration through the Fraser River Canyon, British Columbia, in adult pink (*Oncorhyncus gorbuscha*) and sockeye (*Oncorhynchus nerka*) salmon as assessed by EMG telemetry. Can. J. Fish. Aquat. Sci. **59**: 1809–1818.

Tang, M., Boisclair, D., Menard, C., and Downing, J.A. 2000. Influence of body weight, swimming characteristics, and water temperature on the cost of swimming in brook trout (*Salvelinus fontinalis*). Can. J. Fish. Aquat. Sci. **57**: 1482–1488.

Webb, P.W. 1983. Speed, acceleration and manoeuvrability of two teleost fishes. J. Exp. Biol. **102**: 115–122.

© 2005 NRC Canada

Invertebrate resting stages in residual ballast sediment of transoceanic ships

Sarah A. Bailey, Ian C. Duggan, Philip T. Jenkins, and Hugh J. MacIsaac

Abstract: Ballast water has been the primary vector of nonindigenous species (NIS) to the Laurentian Great Lakes over the past 45 years. Although ballast water exchange regulations were implemented in 1993 to reduce propagule loads, new NIS continue to be discovered. A possible explanation for this trend is the importance of alternative vectors, such as residual ballast of ships claiming "no ballast on board". We investigate resting stages of invertebrates in residual ballast sediments of transoceanic ships as a possible vector of NIS to the Great Lakes. To model the introduction effort potentially associated with this vector, we collected sediment samples from 39 ships entering the Great Lakes and measured the density, viability, and species richness of resting stages contained therein. Viable resting stages of NIS were found in 32% of ships, at a mean density of 3.0×10^5·ship^{-1}. Temperature, salinity, and removal of eggs from sediment during incubation had a significant impact on total abundance and species richness of hatched taxa. A total of 21 NIS were identified, consisting exclusively of rotifers and cladocerans. Salinity of residual ballast water and geographic region of ballast uptake were predictive variables for profiling invasion risk due to ships, although explained variability was low.

Résumé : L'eau de ballastage a été le vecteur principal d'introduction des espèces non indigènes (NIS) dans les Grands Lacs laurentiens au cours des 45 dernières années. Bien que des règlements concernant l'échange des eaux de ballastage en vigueur depuis 1993 visent à réduire les charges de propagules, de nouvelles NIS continuent d'être découvertes. Une explication possible de cette tendance est l'importance des vecteurs secondaires, tels que l'eau résiduelle de ballastage dans les navires qu'on déclare avoir les ballasts vides. Nous avons étudié les stades de repos d'invertébrés dans les sédiments des eaux résiduelles des ballasts de navires transocéaniques comme vecteurs possibles des NIS vers les Grands Lacs. Afin de faire un modèle du potentiel d'introduction associé à ce vecteur, nous avons récolté des sédiments dans 39 navires à leur arrivée dans les Grands Lacs et nous avons mesuré la densité, la viabilité et la richesse spécifique des stades de repos présents. Nous avons trouvé des stades de repos viables de NIS dans 32 % des navires, à une densité moyenne de $3,0 \times 10^5$·navire^{-1}. La température, la salinité et la récolte des oeufs dans les sédiments durant l'incubation ont un impact significatif sur l'abondance totale et la richesse spécifique des taxons éclos. Nous avons identifié 21 NIS en tout, toutes des rotifères et des cladocères. La salinité de l'eau résiduelle de ballastage et la provenance géographique de l'eau sont des variables prédictives pour évaluer le risque d'invasion présenté par le navire, bien que la variabilité qu'elles expliquent soit faible.

[Traduit par la Rédaction]

Introduction

The introduction of nonindigenous species (NIS) beyond their native ranges is a major threat to global biodiversity, particularly for lake ecosystems (Brönmark and Hansson 2002; Rahel 2002). Because economic and ecological costs associated with NIS are significant (e.g., Pimentel et al. 2000; Colautti et al. 2005), predicting and preventing invasions is an increasingly important global priority (Kolar and Lodge 2001). Predicting invasion success requires knowledge of all of the stages inherent in the invasion process, including uptake, transportation, release, and establishment (Kolar and Lodge 2001; Sakai et al. 2001). The starting point, and arguably the most important aspect of an invasion, is the introduction effort or propagule pressure associated with transfer of NIS to new areas (Kolar and Lodge 2001; Duncan et al. 2003; Colautti and MacIsaac 2004).

Vectors associated with transoceanic shipping (e.g., ballast water, hull fouling) are recognized as the largest source of aquatic NIS introductions globally (e.g., Ruiz et al. 2000; Leppäkoski et al. 2002; Lewis et al. 2003), and account for 67% of the species introduced to the Laurentian Great Lakes

Received 21 June 2004. Accepted 31 December 2004. Published on the NRC Research Press Web site at http://cjfas.nrc.ca on 26 May 2005.
J18190

S.A. Bailey,[1] I.C. Duggan,[2] and H.J. MacIsaac. Great Lakes Institute for Environmental Research, University of Windsor, Windsor, ON N9B 3P4, Canada.
P.T. Jenkins. P.T. Jenkins & Associates Ltd., Marine Consulting & Management Services, Fonthill, ON L0S 1E1, Canada.

[1]Corresponding author (e-mail: sarahbailey@canada.com).
[2]Present address: Centre for Biodiversity and Ecology Research, Department of Biological Sciences, University of Waikato, Hamilton, New Zealand.

 doi: 10.1139/F05-024 © 2005 NRC Canada

since 1959 (Grigorovich et al. 2003). Changes in the type of NIS associated with shipping have occurred concomitantly with a transformation in the nature of ships' ballast. Initial invaders of the Great Lakes were predominantly plants, transported as seeds in solid ballast; this pattern shifted during the 20th century to dominance by algae and invertebrates carried by liquid ballast (Ricciardi and MacIsaac 2000; Colautti et al. 2003). A number of invertebrate species that inhabit the sediment–water interface have been reported since 1988 (Holeck et al. 2004), possibly reflecting another shift as the relative importance of ships claiming "no ballast on board" (NOBOB) status increased after ballast water exchange regulations were introduced (Colautti et al. 2003).

NOBOB ships are exempt from current ballast water exchange legislation because their ballast tanks are considered empty. However, NOBOB ships carry an average of 60 t of residual water and sediments while operating on the Great Lakes (Bailey et al. 2003). NOBOB ships could pose a risk of introduction of NIS to the Great Lakes because they theoretically carry more live freshwater individuals and participate in a greater number of inoculation events than do ballasted vessels (MacIsaac et al. 2002; Colautti et al. 2003). Thus, dormant resting stages in residual sediments are a potentially important contributor to the number of propagules carried by NOBOB ships (Bailey et al. 2003); however, this mechanism has not been thoroughly quantified.

Dormant resting stages are produced by many invertebrates, particularly freshwater taxa, and occur in various forms at different life-history stages (e.g., diapausing eggs, dormant buds, quiescent juveniles, and anhydrobiotic adults; for a review see Cáceres 1997). While distributions of many rotifer and cladoceran taxa capable of producing resting stages have been considered cosmopolitan, owing to widespread passive dispersal, recent work has shown a greater prevalence of endemism between continents (Dodson and Frey 2001; Wallace and Snell 2001). As transfer of resting stages in relocated sediments has been previously implicated as a vector for zooplankton introductions (Schrimpf and Steinberg 1982; Koste and Shiel 1989; Hairston et al. 1999), and considering that over one hundred million tonnes are being transported internationally by ships annually (Endresen et al. 2003; assuming that sediment constitutes <10% of ballast water), ballast sediments have emerged as a potentially important source of NIS.

We carried out a preliminary study of diapausing eggs in ballast sediments of ships trading on the Great Lakes, involving an examination of the viability of eggs from a few dominant species from nine ships (Bailey et al. 2003). Studies of ballast sediments in ships in other trade areas have also been limited, focusing primarily on marine phytoplankton (e.g., Hallegraeff and Bolch 1992; Kelly 1993; Hamer et al. 2000). In this study we test the hypothesis that NOBOB ships are transport vectors of NIS to the Great Lakes. We sampled transoceanic ships entering the system during a 2-year period to quantitatively characterize the density, viability, and species richness of dormant propagules carried in residual ballast sediments. We use these results to construct a heuristic model of the propagule pressure associated with sediments of NOBOB ships, and to predict the number of NIS carried by NOBOB ships to the Great Lakes annually. Finally, we test the hypothesis that ballast-history parameters can be used to predict which ships present a "high risk" of causing new invasions.

Materials and methods

Thirty-nine transoceanic ships of NOBOB status were boarded for collection of residual sediments from 69 ballast tanks between December 2000 and December 2002 inclusive. This sample size represents approximately 16% of the annual "multiport" NOBOB traffic in the Great Lakes (i.e., NOBOB ships that fill and empty ballast tanks within the Great Lakes). Collection methods are described in detail in Bailey et al. (2003). Salinity of residual ballast water, if any was present, was measured at the time of sediment collection, using an optical refractometer. Information regarding ships' ballast histories and other physical parameters was recorded at the time of sampling (see Analysis of ballast history). Four ships were sampled twice during the sampling period, with each independent trip into the Great Lakes considered a unique ship sample, since new ballast had been held in the tanks between sampling periods.

We calculated Sorensen's coefficient of similarity (Krebs 1999), based on presence/absence of species in each sample, for pairs of tanks within and between ships to analyze both the spatial and the temporal variation in community composition. Sorensen's coefficient typically ranges from 0 to 1, with higher values indicating greater similarity of samples. First, to determine whether tanks from the same ships were biologically more similar than randomly drawn pairs of tanks from different ships, we contrasted Sorensen's coefficients for all pairs of tanks within ships ($n = 17$) against those for 1000 randomly drawn pairs of tanks between ships using a Mann–Whitney U test (SYSTAT® version 8.0; SPSS Inc. 1998). Secondly, to confirm that the four ships sampled on two occasions should be treated as independent samples, we contrasted Sorensen's coefficients for all pairs of tanks on ships sampled repeatedly ($n = 10$) against those for the same 1000 randomly drawn pairs of tanks between ships, using a Mann–Whitney U test. Only 1 of the 10 pairs of tanks was a true temporally replicated sample, with the same tank sampled at both time periods. The other "pairs" were independent tanks that had each been sampled once, with one tank sampled during the first visit and a different tank sampled on the second visit. Since the spatial analysis determined that tanks within ships at a single time point are more similar than random pairs, we included these "pairs" as replicates for investigation of temporal trends. Species lists generated from maximum-diversity experiments conducted in 0‰ medium at 20 °C (described below) for 47 tanks on 29 ships were used to calculate all Sorensen's coefficients.

Resting stage density counts

After thorough mixing, four 40-g sediment subsamples (wet weight) were taken from each ballast-tank sample and preserved in 95% ethanol. Resting stages were enumerated under a dissecting microscope after separation from coarse sediment using the colloidal silica Ludox® HS 40 (Burgess 2001). Average density calculated from the four subsamples was subsequently converted to density of resting stages per tonne of sediment.

© 2005 NRC Canada

Hatching experiments

Unprocessed sediments were stored in plastic containers in the dark at 4 °C for at least 4 weeks to allow a refractory period before hatching experiments commenced (see Grice and Marcus 1981; Schwartz and Hebert 1987). After this time, sediments were stirred manually and 40-g subsamples were removed in four 10-g allotments. Synthetic pond water of 0‰ salinity (Hebert and Crease 1980) or serial dilutions (8‰, 16‰, or 32‰) of filtered natural seawater were used as hatching media. Natural seawater for these experiments was collected from a ship loaded with ocean-water ballast, filtered through a 2.5-µm Whatman paper filter, and diluted using the same synthetic pond water. All experiments were conducted using a cycle of 16 h light : 8 h dark. We conducted two types of experiments: maximum diversity and whole sediment.

Maximum-diversity experiments were designed to promote maximum hatching abundance of the dormant taxa in the sediment community to assess species richness and abundance across ships. Resting stages were separated from sediments collected from five tanks (four ships) — selected for high density of resting stages — using a sugar flotation method (Bailey et al. 2003). Briefly, four 40-g subsamples of each tank sediment were processed through a 45 µm mesh sieve to remove fine sediment before being washed into centrifuge tubes using a 1:1 (w/v) mixture of sucrose and water. After centrifugation for 5 min at 2700*g* (~7.7 $m \cdot s^{-2}$), the supernatant was decanted and rinsed thoroughly with water through 45 µm mesh. The supernatant from each subsample was subsequently transferred to a 9-cm^2 petri dish containing 40 mL of sterile medium. Four replicates were incubated in each of four treatments: 0‰ and 8‰ media at each of 10 and 20 °C. Dishes were checked for emergence every 24 h for the first 10 days and every 48 h for the subsequent 10 days. All hatched individuals were immediately removed for enumeration and identification. Controls containing blank growth medium were kept in each treatment group to monitor for introduction of organisms from the environment. Sediments from an additional two tanks were incubated only in 0‰ medium at 20 °C for 10 days. Variation in total abundance and species richness of hatched organisms between salinity and temperature treatments was analyzed using two-way multivariate analysis of variance (MANOVA) (SYSTAT® version 8.0; SPSS Inc. 1998). For consistency, the two 10-day experiments were excluded from analyses. If a significant multivariate effect was observed, univariate analysis of variance (ANOVA) was performed to discern the effect of salinity and temperature on each dependent variable. Both total abundance and species richness were transformed to improve normality before analysis. As these experiments were extremely labour-intensive, an unreplicated 40-g sediment sample was prepared in the same way and incubated in 0‰ medium at 20 °C for 20 days, for all remaining sediments (50 tanks from 28 ships). In this manner, we could collect information on richness and abundance of common species from a broad array of ships with reduced overall effort.

Whole-sediment experiments were designed to give a more realistic estimate of hatching abundance and species richness in situ. The protocol used was modified from that of May (1986) and Duggan et al. (2002). Four 40-g subsamples were removed from each of 19 tank sediments (16 ships) and placed in 500-mL glass vessels. One hundred and fifty millilitres of 0‰ medium was added to each vessel before incubation at 20 °C. Vessels were swirled by hand to mix the sediment with the medium. Vessels were examined for emergence of invertebrates every 48 h for 20 days by carefully decanting the medium through a 45-µm mesh screen. All material retained on the mesh was washed into a counting tray for enumeration and identification. Growth medium was immediately returned to each vessel. Vessels were examined at time 0 to ensure that any active copepods present in the sediment would not be mistaken later for those awakening from quiescent stages; one taxon in one experiment was disregarded for this reason. Controls containing autoclaved sediment were kept in each treatment group to monitor for introduction of organisms from the environment.

Three additional salinity treatments, 8‰, 16‰, and 32‰, were added for a subset of the whole-sediment experiments (10 tanks from eight ships) to determine whether brackish- or salt-water taxa were also present in the sediment egg bank. Variation in total abundance and species richness of organisms hatched between salinity treatments was analyzed using one-way MANOVA. Both total abundance and species richness were transformed to improve normality before analysis. Sediments analyzed for 20 days in both the replicated maximum-diversity and whole-sediment experiments in 0‰ medium at 20 °C were analyzed by one-way MANOVA to determine if total abundance and species richness of hatched organisms differed according to the experimental method used ($n = 5$). Again, all significant MANOVA results were subsequently investigated using ANOVA and Bonferroni post-hoc tests were used to determine differences between the four salinity levels on each dependent variable.

For all experiments conducted in the laboratory, hatched individuals were removed to separate vials and raised to maturity, when possible, to aid in identification. Taxa were identified using standard taxonomic keys. No individuals were recovered from control vials at any time. All waste generated during the experiments was autoclaved prior to disposal to minimize the possibility of environmental contamination.

Analysis of ballast history

We recorded ballast-history information, obtained from each ship's crew, to determine whether risk identified from hatching trials was related to each ship's activities. Information collected included total ballast capacity, previous dates and locations of ballast uptake, and prevalence of salt-water exchange or tank flushing. As some ships did not have records beyond the last change of crew, management, and (or) ownership, we could only obtain an adequate set of records for the two most recent ports of ballast uptake. Locations of ballast uptake were assigned to one of seven broad geographic regions: "Baltic Sea", "Great Lakes basin" (including the St. Lawrence Seaway), "Mediterranean and Black Seas", "North Sea", "northwest Pacific Ocean", "west-central Atlantic Ocean", and "other". In addition, we used current and historical records of tank residuals obtained from ships' crews, as well as personal observations made while inside ballast tanks, to estimate the amount of residual sediment aboard each ship.

© 2005 NRC Canada

Most tanks on the same ship have identical ballast histories, thus we chose to average data for these tanks to avoid pseudoreplication problems. However, we excluded data collected from six tanks, each from a different ship, because the salinity of the residual ballast water in those tanks could not be explained by the ballast history provided by the crew. Averaging tanks for this truncated data set was further justified by separate paired t tests of residual-water salinity and resting-stage density, each of which showed no significant difference between paired tanks within ships. Stepwise multiple regression was used to determine if any of the continuous ballast history variables (i.e., residual-water salinity, total ballast capacity, volume of residual sediment, and month of last ballast uptake) were important predictor variables of resting-stage density or total abundance of hatched invertebrates. Subsequently, analysis of covariance was used to investigate the relationships between both egg density and total abundance hatched and previous regions of ballast uptake. Again, only total abundances of hatched invertebrates in 0‰ medium at 20 °C during maximum-diversity experiments were used for analysis, as this was our most comprehensive data set. Dependent and independent variables were transformed when necessary to improve normality prior to analysis.

Estimation of propagule pressure

We calculated the number of viable dormant propagules, π_φ carried by any ship as

$$(1) \qquad \pi_\varphi = \delta\varphi\tau$$

where δ is the density of resting stages per tonne of sediment for that vessel, φ is the proportion of resting stages that are viable, and τ is the amount of sediment in tonnes aboard the vessel. We calculated propagule pressure for the 34 ships analyzed in the maximum-diversity experiments above, using parameter values generated in 0‰ medium at 20 °C. To deduce the number of viable NIS propagules carried, π_ν, we added a term, v, to indicate the proportion of viable propagules that are considered nonindigenous to the receiving area:

$$(2) \qquad \pi_\nu = \delta\varphi\tau\nu$$

where v is the product of the number of nonindigenous individuals divided by the total number of individuals. The method of maximum likelihood coupled with parametric bootstrapping techniques (Efron and Tibshirani 1998) was used to estimate the mean and confidence limits for the number of resting stages of NIS carried by NOBOB ships (X), when present, using a log-likelihood function for an exponential distribution (eq. 3), after removal of one outlier point (see Discussion):

$$(3) \qquad l(\omega|X) = \sum_i^n (\ln\omega - \omega x_i)$$

where $\omega = 3.39064 \times 10^{-6}$ is the estimate when eq. 3 is maximized.

To determine the total number of species associated with NOBOB ships deballasting in the Great Lakes annually, we conducted a Monte Carlo simulation of the cumulative number of non-redundant species (i.e., not identified from a previously selected ship) as a function of the number of ships sampled, using data generated from both maximum-diversity and whole-sediment experiments. We randomly selected samples of incremental size, from 1 to 36 ships, without replacement. This procedure was repeated for 500 bootstrap iterations, with the average and standard error of the cumulative number of non-redundant species calculated. A species–area curve was fitted as an asymptotic (i.e., hyperbolic) curve to the average of the iterations using STATISTICA® version 5.5 (StatSoft Inc. 2000) after preliminary inspection of the data. We used least-squares loss functions and Hooke–Jeeves/quasi-Newton root-solving methods (Hooke and Jeeves 1961) to build the nonlinear model describing the number of non-redundant species as

$$(4) \qquad y = \frac{\alpha\beta x^\theta}{1 + \beta x^\theta}$$

where γ is the mean cumulative number of non-redundant species, x is the number of ships sampled, and α, β, and θ are estimated parameters. Species–area curves were developed separately for species considered indigenous and nonindigenous to the Great Lakes. Although most concern currently centres on the latter group, it is possible that in the case of some species in the former group, intraspecific genetic invasions may occur. Finally, we extrapolated the species–area curves to 250 ships, which is typical of the number of multiport NOBOB ships deballasting in the Great Lakes in any given year (Colautti et al. 2003).

Results

The amount of residual ballast sediment ranged from <1 to 65 t per ship, with an average of 14 t. Spatial variation in community composition in tanks within ships was significantly lower than that in tanks between ships, with mean Sorensen's coefficients of 0.35 and 0.25, respectively (Mann-Whitney U test, $p < 0.05$; Fig. 1). In contrast, ships sampled on two occasions showed significant temporal variation in community composition, as Sorensen's coefficients for tanks on repeatedly sampled ships were not significantly different from those of 1000 randomly selected pairs of tanks between ships (Mann–Whitney U test, $p > 0.05$; see Fig. 1).

The density of invertebrate resting stages in ship sediments had a lognormal distribution, ranging from 4.0×10^4 to 9.1×10^7 resting stages·t^{-1} (median and mean values of 7.2×10^5·t^{-1} and 3.6×10^6·t^{-1}, respectively). Taxonomic identifications, based upon resting-stage morphology, were made for 12 groups in the sediments (see Table 1). Clearly, total species richness was underestimated, as many resting stages could not be differentiated beyond genus, while other, smaller taxa (e.g., Dicranophoridae) may have been overlooked. Diapausing eggs of rotifers, particularly *Brachionus* species, dominated (77.9%) resting-stage abundance. This pattern was influenced by one ship with an extremely high density of diapausing eggs of *Brachionus* spp. (65.3% of resting-stage abundance for all ships), although the general pattern was the same even if that ship was excluded.

Sufficient quantities of sediment for laboratory experiments were lacking for three ships, limiting assessments to

© 2005 NRC Canada

Fig. 1. Sorensen's coefficients of similarity (mean ± standard error) for tanks within ships (n = 17), tanks on ships sampled repeatedly (n = 10), and tanks between ships (n = 1000). Between-ship pairs were selected randomly from a possible 47 tanks on 29 ships.

Table 1. Percent occurrence and abundance of resting stages collected from 39 ships by taxon, arranged phylogenetically.

	Percent occurrence	Percent abundance
Rotifera	**100**	**77.9**
Asplanchna spp.	66.7	1.0
Brachionus spp.	97.4	76.2
Conochilus spp.	5.1	<1
Filinia spp.	48.2	<1
Synchaeta spp.	5.1	<1
Bryozoa	**61.5**	**<1**
Anomopoda	**76.9**	**9.3**
Bosmina spp.	51.3	<1
Chydoridae	5.1	<1
Daphnia spp.	46.2	7.9
Moina spp.	25.6	<1
Ctenopoda	**2.6**	**<1**
Diaphanosoma spp.	2.6	<1
Copepoda	**76.9**	**2.6**
Indeterminate	**100**	**9.8**

Note: Values in boldface type are total values by taxon.

Table 2. Species hatched from diapausing eggs in residual ballast sediment that are considered nonindigenous to the Great Lakes.

	Occurrence[a]	Abundance[b]	Habitat match?[c]
Daphnia magna[d]	4	6	Yes
Filinia passa[d]	4	3.5	Yes
Brachionus leydigi[d]	4	3	Yes
Filinia cornuta[d]	3	3	Yes
Asplanchna girodi[d]	2	1	Yes
Cephalodella stenroi[d]	1	4.75	Yes
Bosmina maritima[e]	1	2	Yes
Diaphanosoma orghidani	1	1.25	Yes
Brachionus forficula	1	1	Yes
Brachionus nilsoni[d]	1	1	Yes
Conochilus coenobasis[d]	1	0.5	Yes
Diaphanosoma mongolianum	1	0.5	Yes
Cephalodella cf. *stenroni*	1	0.3	Yes
Alona rustica	1	0.25	Yes
Brachionus bennini[d]	1	0.25	Yes
Brachionus diversicornis	1	0.25	Yes
Diaphanosoma sarsi	1	0.25	Yes
Hexarthra intermedia[d]	1	0.25	Yes
Moina affinis[f]	1	na	Yes
Synchaeta baltica	1	2.75	No
Synchaeta bacillifera	1	2.25	No
Evadne nordmanni[g]	1	0.5	No
Pleopis polyphemoides[g]	1	na	No

Note: Species are listed in order of decreasing risk, according to propagule pressure and suitability of habitat.

[a]The number of ships from which the species was collected (out of a possible 35).

[b]The cumulative mean number of individuals that emerged from 40-g sediment samples from all ships on which that species was found (na, not applicable).

[c]Species hatched in 0‰ medium during laboratory experiments were considered a match for the habitat in the Great Lakes.

[d]Species with a broad geographic distribution.

[e]Species already established in the Great Lakes.

[f]From Bailey et al. (2003).

[g]S. Bailey, unpublished data.

© 2005 NRC Canada

Fig. 2. Box plots of (*a*) total abundance and (*b*) species richness of organisms hatched from residual sediments of five ballast tanks during the replicated maximum-diversity experiments, according to salinity and temperature. Note the difference in scale for each y axis.

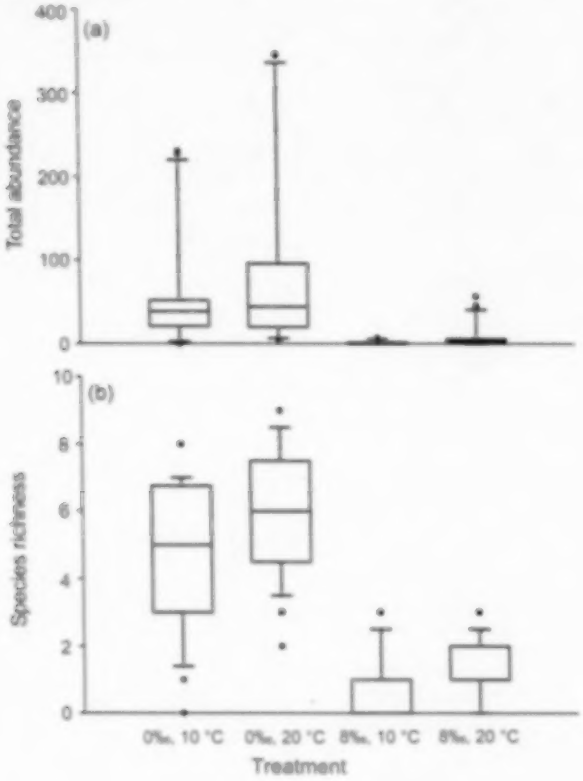

Fig. 3. Box plots of (*a*) total abundance and (*b*) species richness of organisms hatched from residual sediments of eight ballast tanks during the whole-sediment experiments. In all treatments, organisms were incubated at 20 °C. Note the difference in scale for each y axis.

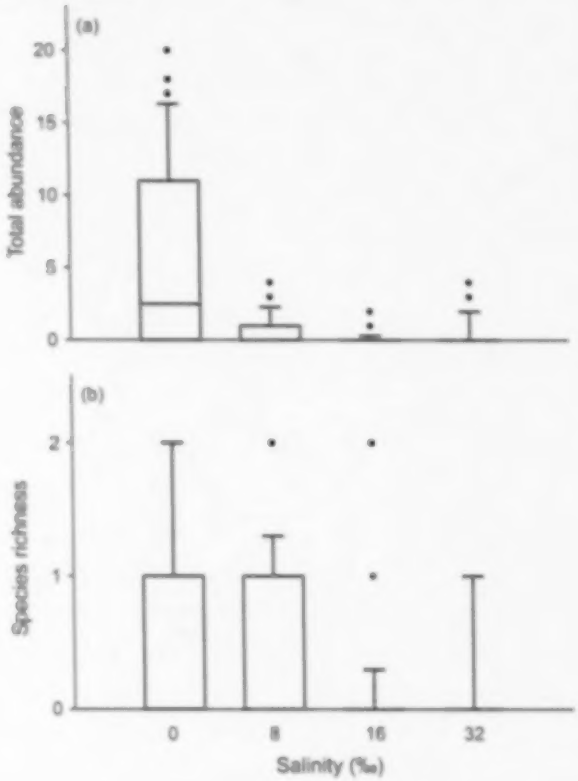

density of resting stages. For the remaining 36 ships, we hatched 76 distinct taxa. Twenty-one NIS were identified, consisting of 14 rotifers and 7 cladocerans (Table 2). One NIS identified in this study, *Bosmina maritima*, has already become established in the Great Lakes. Both the total abundance and the frequency of occurrence of NIS were low compared with species considered native to the Great Lakes (see Appendix A).

In the maximum-diversity experiments, 59 taxa were hatched in the replicated trials, although this number may be conservative, owing to the presence of unidentifiable juvenile invertebrates. Species richness ranged from 0 to 20 taxa per sediment, with a median value of 3. Thirteen additional unique taxa, of 45 in total, were identified from the 50 unreplicated maximum-diversity trials. All taxa were hatched from true diapausing stages; no quiescent copepodids were recovered by this method. The rotifer *Synchaeta bacillifera* and the cladoceran *Evadne nordmanni* were the only organisms that hatched exclusively in brackish water. Rotifers were the most species-rich group, comprising 75% of all species hatched. Cladocerans were the second richest taxon, representing 23% of hatched species. Copepod nauplii were hatched from 14 sediments, though they could not be identified to the species level and were considered one taxon in consequence. Of the organisms hatched, the 0‰, 20 °C treatment group had both the highest abundance and greatest species richness, followed by the 0‰, 10 °C treatment group (Fig. 2). Both total abundance and species richness were significantly affected by experimental temperature and salinity (MANOVA, $p < 0.01$; Table 3). Univariate analyses indicated that higher salinity and lower temperature each suppressed total abundance and species richness of hatched taxa independently, and that there was no interaction effect for salinity × temperature on either variable (ANOVA, $p < 0.05$; Table 3).

In the whole-sediment experiments, 21 taxa hatched, although for six sediments, no animals emerged under any treatment regime. Three taxa, *Acanthocyclops robustus*, *Nitocra lacustris*, and an unidentified juvenile cyclopoid, were found as quiescent copepodids. All remaining taxa were hatched from diapausing eggs. Species richness ranged from 0 to 13 taxa per sediment, with a median value of 2. The rotifers *Synchaeta baltica* and an unidentified *Synchaeta* species and copepod nauplii were the only taxa that hatched exclusively in salt water. Rotifers and copepods were the most species-rich groups, comprising 76% and 14% of all species hatched from whole sediments, respectively. Copepod nauplii hatched from six sediments, and were again

© 2005 NRC Canada

Table 3. Results of two-way multivariate analysis of variance addressing the effect of experimental temperature and salinity treatment on total abundance and species richness of the invertebrates hatched during the maximum-diversity experiments.

Variable	Sum of squares	df	Mean square	*F*	*p*
Salinity					
Univariate *F* tests					
Total abundance	26.30	1	26.30	92.50	<0.001
Error	21.32	75	0.28		
Species richness	5.07	1	5.07	125.89	<0.001
Error	3.02	75	0.04		
Multivariate test (Wilks' λ = 0.36)		2,74		64.54	<0.001
Temperature					
Univariate *F* tests					
Total abundance	1.76	1	1.76	6.20	0.015
Error	21.32	75	0.28		
Species richness	0.45	1	0.45	11.23	0.001
Error	3.02	75	0.04		
Multivariate test (Wilks' λ = 0.87)		2,74		5.55	<0.01
Interaction					
Univariate *F* tests					
Total abundance	0.33	1	0.33	1.18	0.28
Error	21.32	75	0.28		
Species richness	0.002	1	0.002	0.06	0.82
Error	3.02	75	0.04		
Multivariate test (Wilks' λ = 0.98)		2,74		0.89	0.42

Table 4. Results of multivariate analysis of variance addressing the effect of experimental salinity treatment on total abundance and species richness of the invertebrates hatched during the whole-sediment experiments.

Variable	Sum of squares	df	Mean square	*F*	*p*
Univariate *F* tests					
Total abundance	3.20	3	1.07	21.29	<0.001
Error	6.22	124	0.05		
Species richness	2.81	3	0.94	13.00	<0.001
Error	8.94	124	0.07		
Multivariate test (Wilks' λ = 0.58)		6,244		12.63	<0.001

considered a single taxon. One cladoceran, *Daphnia magna*, hatched from ephippial eggs. The experimental salinity treatment had a significant influence on total abundance and species richness of hatched invertebrates (MANOVA, $p < 0.001$; Table 4). Univariate analyses further revealed that increased salinity suppressed both total abundance and species richness (ANOVA, $p < 0.001$; Table 4). However, pairwise contrasts revealed that total abundance was significantly greater at 0‰ than for all other treatments (Bonferroni post-hoc test, $p < 0.001$), while species richness did not differ between the 0‰ and 8‰ treatments (Bonferroni post-hoc test, $p > 0.05$; see Fig. 3). Burial in sediment significantly decreased both total abundance and species richness of hatched taxa, with 0%–43% of individuals hatched from isolated resting stages also emerging from buried resting stages (MANOVA, $p < 0.001$; Table 5; Fig. 4). Again this effect was significant for both total abundance and species richness independently (ANOVA, $p < 0.001$; Table 5).

Of the geographic regions where the most recent site of ballast uptake was located, the two dominant ones were the North Sea (n = 14) and west-central Atlantic Ocean (n = 8). The Great Lakes basin was the most frequent penultimate source of ballast (n = 14). Since the total abundance of hatched individuals was significantly related to the density of resting stages (linear regression, $r^2 = 0.49$, $p < 0.001$; Fig. 5), relationships to ballast-history variables are nearly identical and we only present results of the analysis of resting-stage density. Resting-stage density was weakly related to the salinity of residual ballast water (stepwise multiple regression, $r^2 = 0.195$, $p = 0.013$). All other continuous ballast history variables were found to be unimportant in relation to resting-stage density ($p > 0.05$). Furthermore, analysis of previous regions of ballast uptake showed that only the interaction between the most recent and penultimate sources of ballast was a significant determinant of resting-stage density after residual-water salinity was held as a covariate (analysis of covariance, $p < 0.05$).

Incorporation of experimental values for resting-stage density and viability and sediment tonnage into our propagule-pressure model (eq. 1) revealed that the distribution of the number of viable resting stages per ship is right-skewed (mean and median numbers 9.8×10^6 and 1.4×10^6, respectively; Fig. 6). Resting stages recovered from sediments of six ships (17.5%) could not be induced to hatch in the labo-

© 2005 NRC Canada

Table 5. Results of multivariate analysis of variance addressing the effect of experimental method on total abundance and species richness of the invertebrates hatched.

Variable	Sum of squares	df	Mean square	F	p
Univariate F tests					
Total abundance	6.22	1	6.22	29.10	<0.001
Error	8.97	42	0.21		
Species richness	15.07	1	15.07	128.40	<0.001
Error	4.93	42	0.12		
Multivariate test (Wilks' λ = 0.23)		2,41		69.71	<0.001

Note: Maximum-diversity (isolated resting stages) and whole-sediment (buried resting stages) experiments are described in detail in Methods.

Fig. 4. (*a*) Total abundance and (*b*) species richness (mean ± standard error) of organisms hatched from residual sediments from five ballast tanks in whole-sediment (buried) and maximum-diversity (isolated) experiments. All replicates were incubated in 0‰ growth medium at 20 °C. Note the difference in scale for each *y* axis.

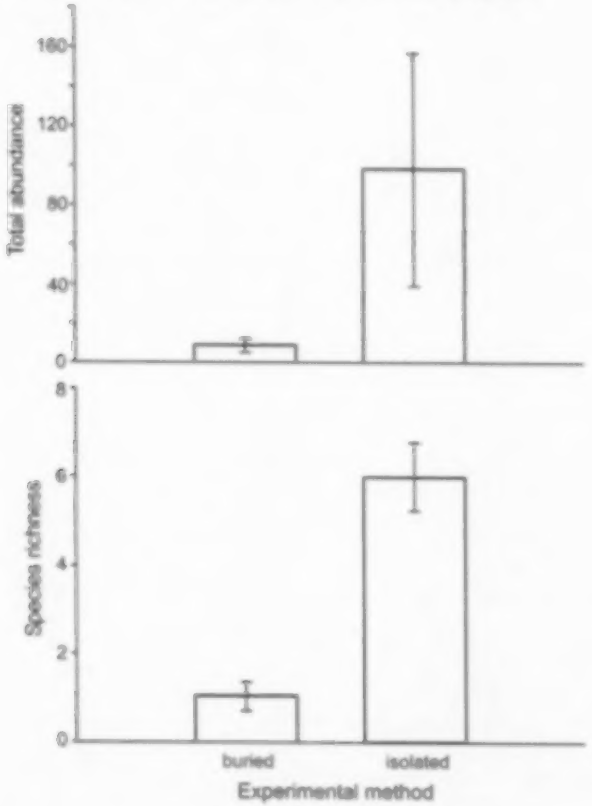

ratory under any conditions, and were apparently nonviable. Thirty-two percent of ships sampled carried viable resting stages of NIS, at a mean density of 3.0×10^5, estimated from a fitted exponential distribution (95% confidence interval: 1.3×10^5 to 4.9×10^5; Fig. 6). The nonlinear model generated to predict the number of non-redundant species transported in residual sediments fit the data robustly (r^2 = 0.99). From species–area curves we predict that up to 150 invertebrate species, including 52 NIS, are transported as resting stages to the Great Lakes each year (Fig. 7).

Fig. 5. Scatterplot of total abundance hatched versus density of resting stages. Both variables were log-transformed prior to analysis. The regression line is $y = 0.89x + 1.22$.

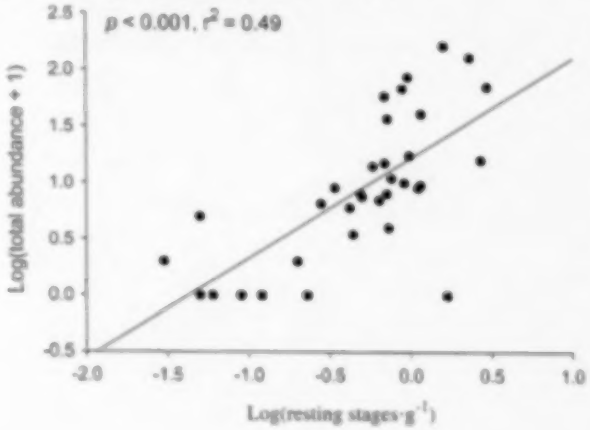

Discussion

Propagule pressure is emerging as an important factor in the prediction of invasion success in both aquatic and terrestrial environments (e.g., Grevstad 1999; Forsyth and Duncan 2001; Drake and Lodge 2004). The propagule-pressure hypothesis states that invasion success is directly related to introduction effort. Our results indicate that the average NOBOB ship entering the Great Lakes carries about 9.8×10^6 viable, dormant propagules in residual sediment, one order of magnitude more than the number of live freshwater propagules estimated to be carried in residual ballast water (MacIsaac et al. 2002). In previous studies of ballast-water taxa, the proportion of propagules that are nonindigenous to the receiving area has not been described; we suggest that the actual risk posed by resting stages is much lower than the above numbers indicate, as only ~2.5% of viable resting stages are NIS (i.e., 2.2×10^5). However, considering that approximately 250 NOBOB ships engage in multiport activities on the Great Lakes each year (Colautti et al. 2003), the expected number of ships entering the system carrying dormant resting stages of NIS is 81 (standard deviation = 7.4), or 2.4×10^7 resting stages of NIS per year. Furthermore, this study recorded one extreme event, a single ship carrying 4.5×10^6 resting stages, which was excluded when calculating the population mean to allow for application of maximum-

© 2005 NRC Canada

Fig. 6. Numbers of viable resting stages transported in sediments of 34 ships designated "no ballast on board" (NOBOB). Solid bars denote egg-density distribution for all taxa; open bars represent only those species considered non-indigenous to the Great Lakes.

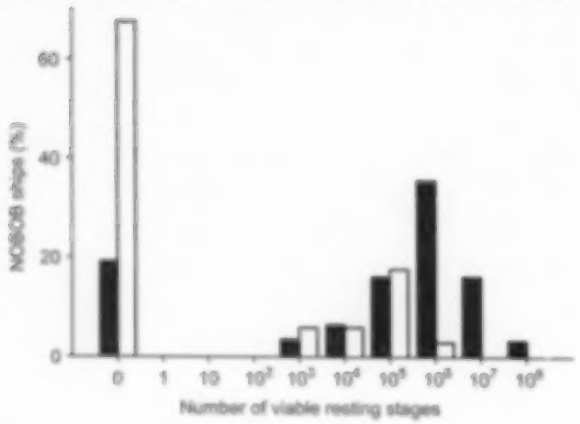

Fig. 7. Monte Carlo simulations of the cumulative number (mean ± standard error) of non-redundant native (●) and non-indigenous (○) species by number of ships sampled. Results were bootstrapped 500 times.

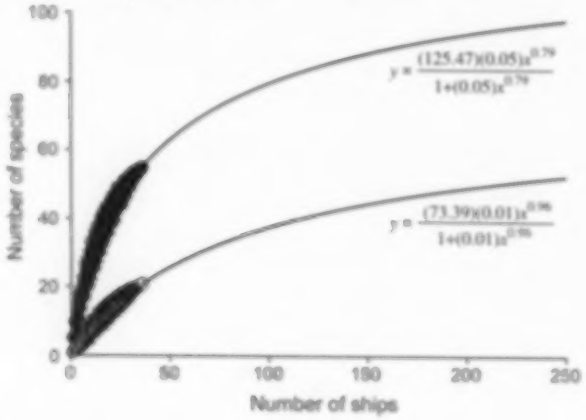

likelihood estimation. Rare events can be very important in biological invasions (e.g., Lewis 1997), so even though we did not use this value in our propagule-pressure calculations, its biological significance should not be overlooked. In a management context, identification of the very small number of vessels transporting large egg banks should be a priority.

Our Monte Carlo simulation indicates that resting stages of 150 species are likely transported to the Great Lakes each year in NOBOB sediments, and of these 52 are NIS. To date, 23 NIS have been recorded from residual ballast sediments. Four of these taxa (17%) are brackish-/salt-water species (*E. nordmanni*, *Pleopis polyphemoides*, *S. bacillifera*, and *S. baltica*) that probably would not survive if introduced to the Great Lakes. One freshwater species, *B. maritima*, is already established in the Great Lakes, possibly owing to transfer in freshwater ballast (De Melo and Hebert 1994). The remaining 18 taxa consist exclusively of rotifers (67%) and cladocerans (33%), and all appear capable of surviving abiotic conditions in the Great Lakes. According to the propagule-pressure hypothesis, *D. magna* should have the greatest opportunity to invade the Great Lakes considering that it had the highest frequency and abundance of propagules of NIS. This species has not been recorded in the Great Lakes to date despite having a broad global distribution. Its large body size may predispose it to size-selective predation by planktivorous fishes (Boersma et al. 1999), reducing its likelihood of successful establishment even if introduced to the lakes in large inocula. Interestingly, the next five highest risk NIS (*Brachionus leydigi*, *Filinia passa*, *Filinia cornuta*, *Asplanchna girodi*, and *Cephalodella sterea*), and indeed over half the list of NIS, also possess broad global distributions, yet none have been reported from the Great Lakes. The remaining species (~25%) are almost entirely restricted to the Palaearctic and Oriental biogeographic regions, possibly reflecting current trade patterns of NOBOB ships. To date, no NIS of rotifers have been recorded from the Great Lakes, although Gray et al. (2005) recorded one species from Lake Erie whose status remains uncertain. Our hatching studies suggest that rotifers should present the predominant invasion risk to the Great Lakes. Alternatively, the lack of reported invasions by this group may indicate that resting stages contained in residual sediments are a weak or emerging vector. It is not clear whether copepods also represent an invasion threat via NOBOB ships, as we were unable to ascertain the species of any of the naupliar stages that hatched from diapausing eggs contained in ballast sediments.

In total, we identified 76 distinct taxa from resting stages in residual sediment, with nearly the entire assemblage representing planktonic freshwater species, particularly rotifers (e.g., *Brachionus* spp., *Keratella* spp., *Polyarthra* spp.). This may be an indication that resting stages are deposited directly into ballast tanks by reproductive females drawn in with ballast water rather than being brought in with disturbed sediments. In addition, rotifers of the genus *Brachionus* were the most common and abundant species in this study. This could be because ballast was taken in areas — such as the lower Rhine River — where *Brachionus* species dominate the planktonic community (van Dijk and van Zanten 1995). However, the predominantly freshwater *Brachionus* species are minor components of other ballast-loading regions, such as the Baltic Sea (Viitasalo et al. 1995; M. Simm and A. Põllumäe, Estonian Marine Institute, Viljandi mnt. 18B, 11216 Tallinn, personal communication), and presumably also of coastal areas with high salinity. Thus, the ubiquitous occurrence of these species may be due to enhanced survivability within ballast tanks associated with a broad salinity tolerance (see Bailey et al. 2004). Although 73% of species encountered during this study are considered native to the Great Lakes and do not appear to represent an invasion risk, there is potential for cryptic invasions through genetic introgression if novel genotypes are introduced from ports in other parts of the world (e.g., Saltonstall 2002; Turon et al. 2003). Furthermore, the possibility exists that some Nearctic species (e.g., *Daphnia retrocurva*, *Brachionus havanaënsis*, and *Trichocerca multicrinis*) could be transferred from the Great Lakes to trading partners overseas.

It is important to note that our measure of propagule pressure is an estimate of the number of dormant individuals

© 2005 NRC Canada

transported by NOBOB vessels, rather than the number released into the system. Furthermore, heavily compacted ballast sediments may offer little opportunity for direct expulsion of resting stages from ballast tanks. Therefore, the potential for introduction of dormant NIS in residual sediments is greatest if resting stages are stimulated to hatch inside the ballast tanks of multiport NOBOB ships, prior to ballast discharge elsewhere on the Great Lakes (Bailey et al. 2003). Our measures of viability and species richness may not reflect actual hatch rates inside ballast tanks of operational ships, as all of these experiments were conducted in the laboratory under conditions designed to induce hatching. It is to be expected that a large proportion of resting stages will not hatch within ballast tanks because they do not receive the requisite cues for termination of diapause. Although ballast tanks are typically dark, hatching success should not be greatly impacted, as previous work has demonstrated that light is not always an essential cue for hatching (Bailey et al. 2003). Instead, the greatest impediment to hatching may come from burial. For example, fewer than 50% of resting stages hatched during our laboratory experiments when buried in sediment 2 cm thick, compared with an average of 20% of those isolated from sediment. Thus, the propagule pressure estimated in this study should be considered a maximum value, with the number of propagules available for introduction from resting stages being at least one order of magnitude lower than that being transported (i.e., ~4.2×10^5 resting stages of NIS).

Even if only a small number of resting stages receive hatching cues, it is theoretically possible that these individuals could develop a substantial population within ballast tanks before ballast discharge occurs (see Bailey et al. 2003). All rotifers and cladocerans in this study are capable of parthenogenetic reproduction and all have short, multivoltine life cycles, both of which facilitate rapid population growth during warm summer months. Both hatch rate and subsequent population growth rate are affected by temperature (Ruttner-Kolisko 1974; Allan 1976). Thus, season could also influence the invasion risk posed by vessels, all else being equal. In terms of the multiport NOBOB ship on the Great Lakes, we expect that the invasion risk would be greatest during late summer, when temperatures are highest.

Can risk be related to ballast history?

Our results suggest that the biological composition of tank contents varies through time, as Sorensen's coefficients for repeated ship samples were only marginally higher than that for pairs of tanks from different ships. Ballast-history information may be useful for determining differences in community composition. Although resting-stage density was significantly related to the salinity of residual ballast water, it could only explain ~20% of the variability and thus would not be a particularly informative tool for making management decisions; high salinities may simply reflect a low occurrence of freshwater taxa in the region of ballast uptake. However, there may be some predictive value in performing a risk analysis of ballast source regions. Although we could not deduce which geographic regions pose a "high risk" statistically, the significance of the interaction between previous areas of ballast uptake may be an indicator that sediment is retained in ballast tanks from numerous ballast events. In terms of risk of NIS introduction to the Great Lakes, ships loading ballast at ports in the Mediterranean and Black seas, northwest Pacific and west-central Atlantic oceans, and regions classified as "other" appear to pose a minimal risk because these areas are predominantly saline. By contrast, ships loading ballast in the Baltic Sea or North Sea may pose a relatively higher risk, owing to the occurrence of freshwater ports in these regions. In our study, 7 of the 12 ships carrying NIS had last loaded ballast at ports in the North Sea, while 3 did so in the Baltic Sea, supporting the hypothesis that these two areas are important donors of NIS to the Great Lakes (Ricciardi and MacIsaac 2000; MacIsaac et al. 2001; Holeck et al. 2004).

While we have described the propagule supply of resting stages associated with NOBOB ships in the transportation stage, measurement error associated with any parameters in the propagule-pressure model could have significant consequences, and caution must be used in interpreting these data. Furthermore, we can make only preliminary estimations of the subsequent success of NIS carried as resting stages at the introduction and establishment stages of the invasion process. Ongoing in-situ studies should help further refine the risks associated with release of propagules from NOBOB vessels by assessing hatch rates of invertebrate resting stages from ballast sediments under operational conditions.

Acknowledgements

We thank D. Gray, C. Rixon, and C. van Overdijk for field and laboratory support, and C. Jerde, J. Muirhead, G. Paterson, Dr. A. Potapov, and Dr. M. Weis for assistance with data analysis. The Shipping Federation of Canada, ship agents, masters, officers, and crew were very cooperative throughout sample collection. Financial support from an Industrial Postgraduate Scholarship from the Natural Sciences and Engineering Research Council of Canada in partnership with the Shipping Federation of Canada, an Ontario Graduate Scholarship to S.A.B., and an Invasive Species Research Chair from the Department of Fisheries and Oceans to H.J.M. is gratefully acknowledged. This work was conducted under the multi-institutional Great Lakes NOBOB Project funded by the Great Lakes Protection Fund, the National Oceanic and Atmospheric Administration (NOAA), the US Environmental Protection Agency, and the U.S. Coast Guard. The project was co-managed by the Cooperative Institute of Limnology and Ecosystems Research and the NOAA Great Lakes Environmental Research Laboratory and sponsored under cooperative agreement NA17RJ1225 from the NOAA Office of Oceanic and Atmospheric Research.

References

Allan, J.D. 1976. Life history patterns in zooplankton. Am. Nat. **110**: 165–180.

Bailey, S.A., Duggan, I.C., van Overdijk, C.D.A., Jenkins, P.T., and MacIsaac, H.J. 2003. Viability of invertebrate diapausing eggs collected from residual ballast sediment. Limnol. Oceanogr. **48**: 1701–1710.

© 2005 NRC Canada

Bailey, S.A., Duggan, I.C., van Overdijk, C.D.A., Jenkens, T.H., Reid, D.F., and MacIsaac, H.J. 2004. Salinity tolerance of diapausing eggs of freshwater zooplankton. Freshw. Biol. **49**: 286–295.

Boersma, M., De Meester, L., and Spaak, P. 1999. Environmental stress and local adaptation in *Daphnia magna*. Limnol. Oceanogr. **44**: 393–402.

Brönmark, C., and Hansson, L. 2002. Environmental issues in lakes and ponds: current state and perspectives. Environ. Conserv. **29**: 290–306.

Burgess, R. 2001. An improved protocol for separating meiofauna from sediments using colloidal silica sols. Mar. Ecol. Prog. Ser. **214**: 161–165.

Cáceres, C.E. 1997. Dormancy in invertebrates. Invertebr. Biol. **116**: 371–383.

Colautti, R.I., and MacIsaac, H.J. 2004. A neutral terminology for defining invasive species. Divers. Distrib. **10**:135–141.

Colautti, R.I., Niimi, A.J., van Overdijk, C.D.A., Mills, E.L., Holeck, K., and MacIsaac, H.J. 2003. Spatial and temporal analysis of transoceanic shipping vectors to the Great Lakes. *In* Invasive species: vectors and management strategies. *Edited by* G.M. Ruiz and J.T. Carlton. Island Press, Washington, D.C. pp. 227–246.

Colautti, R.I., Bailey, S.A., van Overdijk, C.D.A. Amundsen, K., and MacIsaac, H.J. 2005. Characterised and projected costs of nonindigenous species in Canada. Biol. Invasions, **7**(6). In press.

De Melo, R., and Hebert, P.D.N. 1994. A taxonomic reevaluation of North American Bosminidae. Can. J. Zool. **72**: 1808–1825.

Dodson, S.I., and Frey, D.G. 2001. Cladocera and other Branchiopoda. *In* Ecology and classification of North American freshwater invertebrates. 2nd ed. *Edited by* J.H. Thorp and A.P. Covich. Academic Press, San Diego. pp. 850–914.

Drake, J.M., and Lodge, D.M. 2004. Global hot spots of biological invasions: evaluating options for ballast-water management. Proc. R. Soc. Lond. B Biol. Sci. **271**: 575–580.

Duggan, I.C., Green, J.D., and Shiel, R.J. 2002. Rotifer resting egg densities in lakes of different trophic state, and their assessment using emergence and egg counts. Arch. Hydrobiol. **153**: 409–420.

Duncan, R.P., Blackburn, T.M., and Sol, D. 2003. The ecology of bird introductions. Annu. Rev. Ecol. Syst. **34**: 71–98.

Efron, B., and Tibshirani, R.J. 1998. An introduction to the bootstrap. Monographs on statistics and applied probability No. 57. Chapman and Hall / CRC Press, Boca Raton, Fla.

Endresen, Ø., Sørgård, E., Behrens, H.L., and Anderson, A.B. 2003. How much ballast? Ballast Water News, **14**: 6–7.

Forsyth, D.M., and Duncan, R.P. 2001. Propagule size and the relative success of exotic ungulate and bird introductions to New Zealand. Am. Nat. **157**: 583–595.

Gray, D.K., Bailey, S.A., Duggan, I.C., and MacIsaac, H.J. 2005. Viability of invertebrate diapausing eggs exposed to saltwater: implications for Great Lakes' ship ballast management. Biol. Invasions, **7**: 531–539.

Grevstad, F.S. 1999. Experimental invasions using biological control introductions: the influence of release size on the chance of population establishment. Biol. Invasions, **1**: 313–323.

Grice, G.D., and Marcus, N.H. 1981. Dormant eggs of marine copepods. Oceanogr. Mar. Biol. Annu. Rev. **19**: 125–140.

Grigorovich, I.A., Colautti, R.I., Mills, E.L., Holeck, K., Ballert, A.G., and MacIsaac, H.J. 2003. Ballast-mediated animal introductions in the Laurentian Great Lakes: retrospective and prospective analyses. Can. J. Fish. Aquat. Sci. **60**: 740–756.

Hairston, N.G., Jr., Perry, L.J., Bohonak, A.J., Fellows, M.Q., Kearns, C.M., and Engstrom, D.R. 1999. Population biology of a failed invasion: paleolimnology of *Daphnia exilis* in upstate New York. Limnol. Oceanogr. **44**: 447–486.

Hallegraeff, G.M., and Bolch, C.J. 1992. Transport of diatom and dinoflagellate resting spores in ships' ballast water: implications for plankton biogeography and aquaculture. J. Plankton Res. **14**: 1067–1084.

Hamer, J.P., McCollin, T.A., and Lucas, I.A.N. 2000. Dinoflagellate cysts in ballast tank sediments: between tank variability. Mar. Pollut. Bull. **40**: 731–733.

Hebert, P.D.N., and Crease, T.J. 1980. Clonal coexistence in *Daphnia pulex* (Leydig): another planktonic paradox. Science (Wash., D.C.), **207**: 1363–1365.

Holeck, K.R., Mills, E.L., MacIsaac, H.J., Dochoda, M.R., Colautti, R.I., and Ricciardi, A. 2004. Bridging troubled waters: biological invasions, transoceanic shipping, and the Laurentian Great Lakes. Bioscience, **54**: 919–929.

Hooke, R., and Jeeves, T.A. 1961. "Direct search" solution of numerical and statistical problems. J. Assoc. Comput. Mach. **8**: 212–229.

Kelly, J.M. 1993. Ballast water and sediments as mechanisms for unwanted species introductions into Washington State. J. Shellfish Res. **12**: 405–410.

Kolar, C.S., and Lodge, D.M. 2001. Progress in invasion biology: predicting invaders. Trends Ecol. Evol. **16**: 199–204.

Koste, W., and Shiel, R.J. 1989. Rotifera from Australian inland waters, 3. Euchlanidae, Mytilinidae, and Trichotriidae (Rotifera: Monogononta). Trans. R. Soc. S. Aust. **113**: 85–114.

Krebs, C.J. 1999. Ecological methodology. 2nd ed. Addison–Wesley Educational Publishers, Inc., Menlo Park, Calif.

Leppäkoski, E., Gollasch, S., Gruszka, P., Ojaveer, H., Olenin, S., and Panov, V. 2002. The Baltic — a sea of invaders. Can. J. Fish. Aquat. Sci. **59**: 1175–1188.

Lewis, M. 1997. Variability, patchiness, and jump dispersal in the spread of an invading population. *In* Spatial ecology: the role of space in population dynamics and interspecific interactions. Princeton University Press, Princeton, N.J. pp. 46–69.

Lewis, P.N., Hewitt, C.L., Riddle, M., and McMinn, A. 2003. Marine introduction in the Southern Ocean: an unrecognised hazard to biodiversity. Mar. Pollut. Bull. **46**: 213–223.

MacIsaac, H.J, Grigorovich, I.A., and Ricciardi, A. 2001. Reassessment of species invasion concepts: the Great Lakes basin as a model. Biol. Invasions, **3**: 405–416.

MacIsaac, H.J., Robbins, T.C., and Lewis, M.A. 2002. Modeling ships' ballast water as invasion threats to the Great Lakes. Can. J. Fish. Aquat. Sci. **59**: 1245–1256.

May, L. 1986. Rotifer sampling — a complete species list from one visit? Hydrobiologia, **134**: 117–120.

Pimentel, D., Lach, L., Zuniga, R., and Morrison, D. 2000. Environmental and economic costs of nonindigenous species in the United States. Bioscience, **50**: 53–65.

Rahel, F.J. 2002. Homogenization of freshwater faunas. Annu. Rev. Ecol. Syst. **33**: 291–315.

Ricciardi, A., and MacIsaac, H.J. 2000. Recent mass invasion of the North American Great Lakes by Ponto-Caspian species. Trends. Ecol. Evol. **15**: 62–65.

Ruiz, G.M., Fofonoff, P.W., Carlton, J.T., Wonham, M.J., and Hines, A.H. 2000. Invasion of coastal marine communities in North America: apparent patterns, processes and biases. Annu. Rev. Ecol. Syst. **31**: 481–531.

Ruttner-Kolisko, A. 1974. Plankton rotifers, biology and taxonomy. Die Binnengewässer (Suppl.), **26**: 1–146.

Sakai, A.K., Allendorf, F.W., Holt, J.S., Lodge, D.M., Molofsky, J., With, K.A., et al. 2001. The population biology of invasive species. Annu. Rev. Ecol. Syst. **32**: 305–332.

© 2005 NRC Canada

Saltonstall, K. 2002. Cryptic invasion by a non-native genotype of the common reed, *Phragmites australis*, into North America. Proc. Natl. Acad. Sci. U.S.A. **99**: 2445–2449.
Schrimpf, A., and Steinberg, C. 1982. Further recordings of the newly observed cladoceran *Daphnia parvula*, new record in southern Germany. Arch. Hydrobiol. **94**: 372–381.
Schwartz, S.S., and Hebert, P.D.N. 1987. Methods for the activation of the resting eggs of *Daphnia*. Freshw. Biol. **17**: 373–379.
SPSS Inc. 1998. SYSTAT®. Version 8.0 [computer program]. SPSS Inc., Chicago.
StatSoft Inc. 2000. STATISTICA®. Version 5.5 [computer program]. StatSoft Inc., Tulsa, Okla.
Turon, X., Tarjuelo, I., Duran, S., and Pascual, M. 2003. Characterising invasion processes with genetic data: an Atlantic clade of *Clavelina lepadiformis* (Ascidiacea) introduced into Mediterranean harbours. Hydrobiologia, **503**: 29–35.
van Dijk, G.M., and van Zanten, B. 1995. Seasonal changes in zooplankton abundance in the lower Rhine during 1987–1991. Hydrobiologia, **304**: 29–38.
Viitasalo, M., Vuorinen, I., and Saesmaa, S. 1995. Mesozooplankton dynamics in the northern Baltic Sea: implications of variations in hydrogeography and climate. J. Plankton Res. **17**: 1857–1878.
Wallace, R.L., and Snell, T.W. 2001. Phylum Rotifera. *In* Ecology and classification of North American freshwater invertebrates. 2nd ed. *Edited by* J.H. Thorp and A.P. Covich. Academic Press, San Diego, Calif. pp. 195–254.

Appendix A.

Table A1. List of invertebrate taxa hatched from resting stages during this study, arranged taxonomically.

			Experiment type[c]	
	Occurrence[a]	Abundance[b]	Maximum diversity	Whole sediment
Gastrotricha				
Chaetonotidae, unidentified	1	3	×	
Rotifera				
Ascomorpha ecaudis	1	0.25	×	
Ascomorpha saltans	1	0.25	×	
Ascomorpha sp.	1	1	×	
Asplanchna brightwelli	4	0.25–1 (0.75)	×	×
Asplanchna girodi	2	0.5 (0.5)	×	×
Asplanchna priodonta	3	1–11.5 (3)	×	×
Brachionus angularis	21	0.25–21.8 (4)	×	×
Brachionus bennini	1	0.25	×	
Brachionus budapestinensis	15	0.75–341.5 (3)	×	×
Brachionus calyciflorus	25	0.63–77.77 (3)	×	×
Brachionus caudatus	2	0.5–2 (1.25)	×	
Brachionus diversicornis	1	0.25	×	
Brachionus forficula	1	1	×	
Brachionus havanaënsis	2	1 (1)	×	
Brachionus leydigi	4	0.25–1 (0.78)	×	×
Brachionus nilsoni	1	1	×	
Brachionus quadridentatus	4	0.5–12.25 (1.25)	×	×
Brachionus urceolaris	9	0.25–78 (1)	×	×
Cephalodella catellina	2	0.25 (0.25)	×	
Cephalodella forficula	1	0.25	×	
Cephalodella cf. *stenroosi*	1	0.3		×
Cephalodella stevea	1	4.75	×	
Cephalodella cf. *theodora*	1	0.25	×	
Cephalodella sp.	1	1	×	
Conochilus coenobasis	1	0.5	×	
Conochilus dossuarius	1	1	×	
Conochilus hippocrepis	2	1 (1)	×	
Conochilus cf. *natans*	1	0.25	×	
Conochilus unicornis	1	0.8		×
Dicranophoridae, unidentified	1	83	×	
Euchlanis cf. *dilatata*	2	0.25–1 (0.63)	×	
Filinia brachiata	1	0.25	×	
Filinia cornuta	3	0.5–1 (0.5)	×	
Filinia longiseta	6	0.25–4 (1)	×	
Filinia passa	4	0.25–1 (0.75)	×	

© 2005 NRC Canada

Table A1 (*continued*).

	Occurrence[a]	Abundance[b]	Experiment type[c]	
			Maximum diversity	Whole sediment
Filinia terminalis	5	0.38–2.5 (1)	×	
Flosculariidae, unidentified	1	0.25	×	
Hexarthra intermedia	1	0.25	×	
Hexarthra mira	3	0.25–1 (1)	×	
Keratella cochlearis	3	0.25–1 (1)	×	
Keratella quadrata	5	0.25–4 (0.5)	×	×
Keratella tropica	1	2	×	
Keratella sp.	1	1	×	
Lacinularia sp.	1	0.25	×	
Lecane closterocerca	2	0.3–0.5 (0.4)	×	×
Lecane flexilis	1	0.25	×	
Lindia truncata	1	0.5	×	
Ploesoma truncatum	3	0.25–2 (2)	×	
Polyarthra dolichoptera	9	0.5–5 (1)	×	
Polyarthra vulgaris	6	0.25–21 (2)	×	
Polyarthra spp.	2	0.25–1 (0.63)	×	
Pompholyx sulcata	4	0.25–7 (3.5)	×	
Synchaeta bacillifera	1	2.25	×	
Synchaeta baltica	1	2.75		×
Synchaeta kitina	1	0.25	×	
Synchaeta oblonga	1	0.25	×	
Synchaeta stylata	4	0.25–1 (0.28)	×	×
Synchaeta tremula	2	1–3.5 (1)	×	×
Synchaeta sp.	1	0.25		×
Trichocerca multicrinis	1	39	×	
Trichocerca pusilla	7	1–17.63 (1.25)	×	
Trichocerca rattus	1	1	×	
Trichocerca similis	1	0.25	×	
Monogonont, unidentified	2	1 (1)	×	
Bryozoa				
Plumatella casmiana	2	0.25–1 (0.63)	×	
Plumatella sp.	1	0.25	×	
Anomopoda				
Alona rectangula	1	0.5	×	
Alona rustica	1	0.25	×	
Bosmina liederi	3	1–6 (1)	×	
Bosmina maritima	1	2	×	
Bosmina spp.	2	1 (1)	×	
Ceriodaphnia quadrangula	1	0.25	×	
Ceriodaphnia sp.	2	1 (1)	×	
Daphnia longiremis	2	1 (1)	×	
Daphnia magna	4	0.5–2 (1)	×	×
Daphnia retrocurva	1	2	×	
Disparalona leei	1	0.25	×	
Moina micrura	2	1–47.88 (24.44)	×	
Moina sp.	1	1	×	
Ctenopoda				
Diaphanosoma birgei	2	0.75–6 (3.38)	×	
Diaphanosoma brachyurum	1	0.25	×	
Diaphanosoma mongolianum	1	0.5	×	
Diaphanosoma orghidani	1	1.25	×	
Diaphanosoma sarsi	1	0.25	×	
Diaphanosoma spp.	6	1 (1)	×	
Onychopoda				
Evadne nordmanni	1	0.5	×	

© 2005 NRC Canada

Table A1 *(concluded).*

	Occurrence[a]	Abundance[b]	Experiment type[c]	
			Maximum diversity	Whole sediment
Copepoda				
Acanthocyclops robustus	1	0.8		×
Cyclopoida, unidentified	3	0.25–1.25 (0.25)		×
Nitocra lacustris	1	1		×
Copepod nauplii, unidentified	14	0.25–20 (3)	×	×

[a]The number of ships on which the species was collected, of a possible 35.
[b]The range of numbers of individuals emerging from 40 g of sediment for all ships, with the median number in parentheses.
[c]The taxa present in maximum-diversity (isolated from sediment) and whole-sediment (buried in sediment) trials. All were able to hatch in 0‰ medium, except *S. bacillifera*, *Synchaeta* sp., and *E. nordmanni*, which hatched exclusively in 8‰, and *S. baltica*, which hatched exclusively in 32‰.

© 2005 NRC Canada

Intergenerational valuation of fisheries resources can justify long-term conservation: a case study in Atlantic cod (*Gadus morhua*)

C.H. Ainsworth and U.R. Sumaila

Abstract: Where the conventional model of discounting advocates aggressive harvest policies, intergenerational discounting could have been used to render the historic gross overfishing of Atlantic cod (*Gadus morhua*) economically unappealing compared with a more conservative long-term strategy. Under these discounting approaches, we compare the historic harvest trend from 1985 (and projected postcollapse earnings) with theoretical optimal harvest profiles determined by an ecosystem model. The optimal scenarios generate less initial harvest than the historic profile but maintain the resource and provide greater yields over the long term. At a discount rate equal to market interest, we demonstrate that it was more economic under conventional valuation to harvest the cod stock to collapse than it would have been to sustain the population. However, under intergenerational valuation, the sustainable optimal scenarios outperform the actual harvest profile. Application of conventional discounting by fishing consortiums may be partly to blame for depletion, yet management fell short of even that ideal.

Résumé : Alors que le modèle traditionnel d'escomptage prône des politiques agressives de récolte, l'escomptage intergénérationnel aurait pu servir à rendre la surpêche grossière de la morue franche (*Gadus morhua*) du passé moins intéressante économiquement qu'une stratégie à long terme plus conservatrice. À l'aide de ces approches d'escomptage, nous comparons les tendances de la récolte réelle depuis 1985 (et les revenus projetés après l'effondrement) avec les profils théoriques optimaux de récolte déterminés par un modèle écosystémique. Les scénarios optimaux permettent une récolte initiale moins importante que le profil réel, mais ils conservent la ressource et fournissent de meilleurs rendements à long terme. À un taux d'escompte égal à l'intérêt du marché, nous démontrons qu'il était plus rentable économiquement d'après l'évaluation conventionnelle de récolter le stock de morues jusqu'à l'épuisement que de maintenir la population. Cependant, dans une évaluation intergénérationnelle, les scénarios durables optimaux ont une meilleure performance que le profil réel de récolte. L'utilisation de l'escomptage conventionnel par les consortiums de pêche peut être en partie responsable de l'épuisement de la ressource, mais leur gestion n'a même pas atteint cet idéal-là.

[Traduit par la Rédaction]

Introduction

In cost–benefit analysis (CBA), standard discounting is often unable to sanction long-term environmental policies that fulfill the frequently stated mandate to provide for the needs of future generations (e.g., Department of Fisheries and Oceans (DFO) 2001; Environment Canada 2002). Scaling down the value of future benefits exponentially through time ensures that immediate costs will outweigh far-off benefits at any practicable level of discounting so that only myopic policies can result (Clark 1973; Sumaila 2004). In valuing the stream of benefits from a fisheries resource, use of conventional discounting may lead to early profit taking at the expense of sustained productive potential. Evidence of this type of "front-loading" of fisheries benefits is clear in the harvest record of northern Atlantic cod (*Gadus morhua*) in the years before the 1992 collapse.

In a departure from what he called the "standard economic argument for overexploitation", Clark (1973) proposed that depletion of the Grand Banks demersal fisheries could be blamed on the discounting practices of fishing consortiums rather than open competition among impoverished fishermen. If true, then a CBA of the harvest record would find depletion justified over a more conservative harvest strategy at a discount rate equal to the market interest rate.

Among other factors, the discount rate used in CBA reflects investors' time preference for early consumption and delayed payment and reflects uncertainties associated with the investment (Brennan 1997). In this respect, discounting is used to model human behavior; it provides an analytical basis for our value-based decisions. Yet, a CBA of education by Ainsworth and Sumaila (2003) demonstrates that conventional discounting does not wholly capture human tendency. If an alternative investment were to promise a greater return than a person's increased earning potential through education, we would expect children to be rarely educated to the highest levels. However, parents and society chose to do so. People, perhaps unwittingly, apply some form of intergenerational valuation where assured benefit to one's children carries significant value in the present. For long-term

Received 9 January 2004. Accepted 21 October 2004. Published on the NRC Research Press Web site at http://cjfas.nrc.ca on 26 May 2005.
J17909

C.H. Ainsworth[1] and U.R. Sumaila. Fisheries Centre, The University of British Columbia, 2259 Lower Mall, Vancouver, BC V6T 1Z4, Canada.

[1]Corresponding author (e-mail: c.ainsworth@fisheries.ubc.ca).

 doi: 10.1139/f05-010 © 2005 NRC Canada

environmental conservation to work economically, similar intergenerational consideration may be required.

A very low discount rate has been suggested as a means to protect the environment (Hasselmann et al. 1997; United Nations Framework Convention on Climate Change 1997), although others have cautioned against this (Fisher and Krutilla 2002; Goulder and Stavins 2002). Recently, alternatives to standard discounting have been proposed that limit discounting of future benefits (e.g., Heal 1998; Nielsen 2001; Weitzman 2001). A method by Sumaila and Walters (2005) (available at http://www.fisheries.ubc.ca/publications/reports/fcrr.php) allows us to separate the discount rates that we use to value benefits to ourselves (i.e., standard discount rate, δ) and benefits destined for future generations (δ_{fg}). Their approach is applied here.

We test the ability of three intergenerational discount rates to preserve the cod resource from a precollapse perspective: one that is less than, one that is equal to, and one that is greater than the standard discount rate (equivalent to the market interest rate). A CBA of education by Ainsworth and Sumaila (2003) informs us as to what may be considered an upper and lower estimate of δ_{fg} that society may be willing to apply to value benefits destined for future generations. The lower limit discount rate is set approximately equal to the internal rate of return (IRR) needed to make a Ph.D. education financially worthwhile; the upper limit corresponds to the IRR needed to make a grade 10 education worthwhile. By finding the effective discount rate that parents and society use to value a child's education, we account for a variety of nonmonetary benefits that may be considered by those investors. Similar benefits, we argue, could also apply to resource conservation where future generations are the recipients of today's investment.

Comparing conventional and intergenerational discounting approaches, we perform CBAs on five cod harvest profiles: the actual historic trend since 1985 followed by projected postcollapse earnings, the conventional optimum estimated using an ecosystem model, and three intergenerational optima maximizing net present value (NPV), when $\delta > \delta_{fg}$, $\delta = \delta_{fg}$, and $\delta < \delta_{fg}$. Although optimal scenarios generate less immediate benefit than the historic pattern, they maintain higher resource abundance at equilibrium and so permit greater sustained yields over time.

Methods

Model parameterization

The Ecopath with Ecosim model used for this evaluation is based on Heymans (2003) (Ecopath with Ecosim: Polovina 1984; Christensen and Pauly 1992; Walters et al. 1997). It represents the Grand Banks marine ecosystem off Newfoundland as it appeared in 1985, prior to the 1992 northern cod collapse (Canadian DFO statistical areas 2J3KLNO). Minor modifications to the diet matrix and basic parameters were made in the static Ecopath base model to improve dynamic predictions, particularly concerning cod. When driven by historic fishing mortalities, the sum of squares between the predicted and observed biomass trends were reduced slightly for the ecosystem overall (~2% based on residuals from 17 species groups) and much more for cod alone (~50%) (see Heymans (2003) for data sources regarding fishing mortality and biomass time series).

Fig. 1. Stability analysis of a dynamic ecosystem model showing mean variance of biomass change per species group over a 16-year simulation. There is a nonlinear increase in the directional responsiveness of biomass change with increasing predator–prey vulnerabilities (Ecosim's primary user-controlled variable). Solid bars show simulations optimized for intergenerational benefit ($\delta = \delta_{fg}$ (standard discount rate equals rates destined for future generations)); open bars show conventional discounting optima ($\delta = 10\%$). A global vulnerability setting of 0.3 for all species groups should provide a stable dynamic response, although perhaps conservative in magnitude; model dynamics become less stable when vulnerabilities exceed 0.5. Model adapted from Heymans (2003); stability analysis after Okey and Wright (2004).

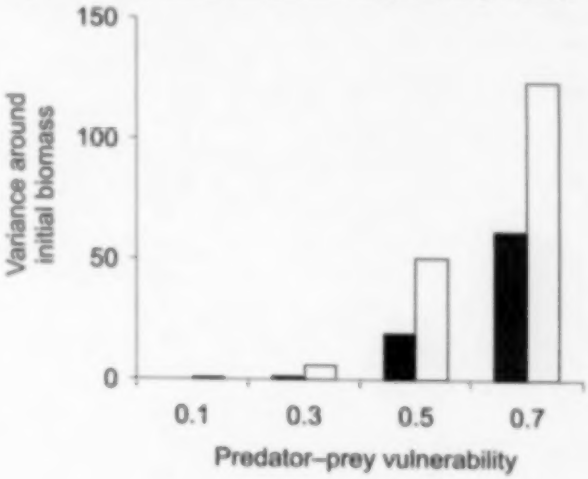

In the dynamic model Ecosim, the primary user-controlled variable for each species group is the predator–prey vulnerability setting. It describes the rate of flux between vulnerable and invulnerable prey pools (cf. foraging arena theory: Walters and Juanes 1993; Walters and Martell 2004). A vulnerability of 0 indicates bottom-up control (donor driven) and a vulnerability of 1 indicates top-down control (Lotka–Volterra). Our Ecosim model was parameterized using a global setting of 0.3 for all functional groups to emulate mixed trophic control. This intermediate value (default in Ecosim) has been well established by convention and is used often where better estimates are lacking. Following the methodology of Okey and Wright (2004), a stability analysis confirms that this value results in reasonably stable and conservative ecosystem dynamics (Fig. 1).

Determining optimal harvest patterns

The optimal fishing mortalities (F) per gear type that would maximize cod value over a 16-year harvest simulation were determined using the policy search routine in Ecosim (Christensen and Walters 2004).

To have the fisheries optimization routine return a harvest strategy geared for maximum cod catch, we restricted the search criterion to an economic optimization and cod were assigned a high price compared with other target groups in the model. This configuration causes the search routine to

© 2005 NRC Canada

increase the cod fishery at the expense of other sectors. The procedure does not merely regulate cod biomass to achieve maximum sustainable yield, it will tailor the entire ecosystem to augment cod production, redefining maximum sustainable yield at an inflated level. Through selective fishing, predators and competitors of cod are eliminated, while other species groups are preserved only in so much as they may support a large cod population.

The fishing mortalities per gear type maximizing NPV under conventional and intergenerational discounting approaches were identified by the optimization and applied to a 16-year dynamic simulation using the 1985 model as a starting point. End-state catch equilibrium was maintained for another 24 years, totaling 40 years (consisting of two generations of an assumed 20 years each).

Valuation of the harvest profile

Conventional discounting

Under conventional discounting, the flow of fishery benefits is summarized in the NPV term using

$$\text{(1)} \qquad \text{NPV} = \sum_{t=0}^{T} (d^t \cdot \text{NB}_t)$$

where NB is net benefit accruing in year t, and d is discount factor given by

$$\text{(2)} \qquad d = \frac{1}{(1+\delta)}$$

where δ is discount rate.

Intergenerational discounting

Under the intergenerational discounting approach of Sumaila and Walters (2005), the NPV term considers the value of benefits received by the current generation (calculated at a standard discount rate) plus the value of benefits received by an annual influx of 1/(generation time) new stakeholders. These participants bring with them a renewed perspective on future earnings, partially resetting the discounting clock. The equation requires a standard annual discount factor (d) and a discount factor to evaluate benefits destined for future generations (d_{δ_g}) such that

$$\text{(3)} \qquad \text{NPV} = \begin{cases} \displaystyle\sum_{t=1}^{T} \text{NB}_t \left[d^t + \frac{d_{\delta_g} \cdot d^{t-1}}{G} \left(\frac{1-\Delta^t}{1-\Delta} \right) \right] & \text{if } \delta \neq \delta_g \\ \displaystyle\sum_{t=0}^{T} \frac{\text{NB}_t}{(1+\delta)^t} \left(1 + \frac{t}{G} \right) & \text{otherwise} \end{cases}$$

where $\Delta = d_{\delta_g}/d$ and where G is generation time (assumed here to be 20 years).

Calculating fisheries profits

The policy search routine maximizes NPV of future earnings. If we apply a large discount rate, the optimal fishing mortalities are high and the population is aggressively harvested. Landings increase under high discount rates to the point where future productivity is finally compromised. However, since greater harvests leave less standing stock biomass, which in turn increases harvesting cost, we introduce the following linear cost–abundance relationship to capture this effect:

$$\text{(4)} \qquad \text{NB}_t = \text{GB}_t \left\{ 1 - C \left[1 + \left(\frac{B_{\delta>\delta_g} - B_t}{B_{\delta>\delta_g}} \right) \right] \right\}$$

where GB is gross benefit (i.e., landed value) in year t, C is the base cost of fishing (assumed 60% of landed value based on DFO 1994), $B_{\delta>\delta_g}$ is the equilibrium biomass resulting from our optimum solution when $\delta > \delta_g$ ($\delta_g = 5\%$), and B is biomass in year t. Net benefit is therefore standardized so that costs equal 60% of gross benefit at the stock density left by our most conservative strategy, with cost of fishing increasing linearly as standing biomass is reduced from this level.

Fig. 2. Real price of Atlantic cod based on the entire harvest from the Atlantic Canada. Trend line (broken) shows linear price projection used in the analysis based on data from 1972 to 1992. The price increase after 1992 (open circles) may have been influenced by the cod collapse, whereas optimal solutions would have averted the collapse. Data based on DFO Department of Statistical Services, Ottawa, Ontario.

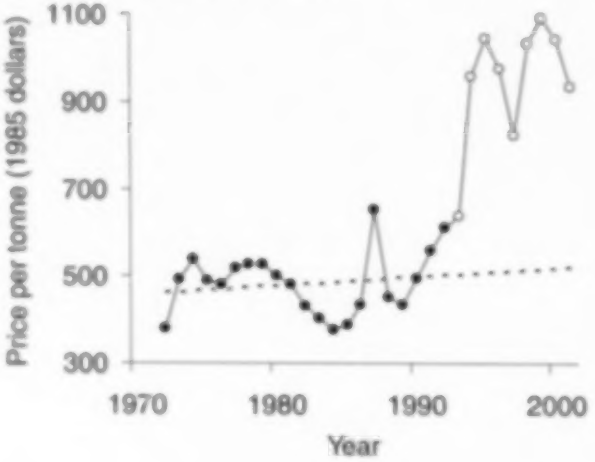

For all projections, we have assumed a steadily increasing price for cod that reflects the trend from 1972 to 1992 (Fig. 2) based on historical value and landings data obtained from the DFO Department of Statistical Services, Ottawa, Ontario (available at http://www.dfo-mpo.gc.ca/communic/statistics/commercial/landings/historical/seafisheries_e.htm). Trend is adjusted for inflation using the Bank of Canada consumer price index. We did not consider prices after 1992 in calculating the trend, since the collapse of the cod fishery may have contributed to the jump in price after that year, whereas optimal solutions would have averted the collapse. We find this assumption reasonable for our purpose, even though it is worth noting that price formation and determination is a broad area of research activity and that prices are determined by various variables. For instance, prices are determined by many variables, such as the income level of consumers, the availability of substitutes, the specific market in which the fish is sold, etc.

© 2005 NRC Canada

Table 1. Effect of discount rate on educational attainment (from Ainsworth and Sumaila 2003, reproduced with permission of Fish. Cent. Res. Rep. No. 11(3), p. 29, © 2003 The Fisheries Centre, The University of British Columbia).

Educational level	Years of education	δ where education is worthwhile (IRR in %)	Discounted constant 1981 dollars ($\times 10^3$)		
			Cost	Benefit	NPV
High school dropout	10	15.0	22.2	42.0	19.9
High school diploma	12	10.3	25.1	28.5	3.4
Trade school diploma	13	11.4	27.5	36.3	8.7
College diploma	14	8.6	29.8	26.8	−3.0
Bachelors degree	16	7.5	33.6	25.0	−8.6
Masters degree	18	7.4	36.9	26.5	−10.4
Ph.D. degree	22	6.3	41.8	24.6	−17.3

Note: δ, standard discount rate; IRR, internal rate of return; NPV, net present value based on alternate rate of return from bank interest (δ = 9.3%).

Selection of discount rate

For all analyses in this paper, the conventional discount rate used to represent the rate of return for an alternate investment (δ = 10%) approximately corresponds to the average annual rate of return for Bank of Canada long-term (10+ years) marketable bonds from 1981 to 2001, which was 9.3% (Bank of Canada, Department of Monetary and Financial Analysis). Since the early 1980s saw anomalously high interest rates (e.g., 15.2% in 1981), we have instead used the average rate during this 20-year period to inform our choice.

The intergenerational rates chosen for this evaluation were 5%, 10%, and 15% (for cases $\delta > \delta_{ig}$, $\delta = \delta_{ig}$, and $\delta < \delta_{ig}$, respectively). These represent discount rates that society may be willing to apply to value benefits received by future generations. The specific values are based on the CBA of education by Ainsworth and Sumaila (2003); the rates approximately correspond to the IRR required to make education financially worthwhile in British Columbia to the Ph.D. level (when $\delta < \delta_{ig}$) and the grade 10 level (when $\delta > \delta_{ig}$) (Table 1).

In their CBA of education, Ainsworth and Sumaila (2003) have disregarded nonmonetary benefits. However, even if we were to increase the benefit of education by 50% to approximate those considerations, the IRR required to make a Ph.D. worthwhile would be only 8.6%, still less than the alternative rate of return. Further, we likewise ignore other incidental benefits in the following analysis of the Atlantic cod fishery (e.g., increased ecotourism and other enterprises that may accompany high cod abundance). Ultimately, however, we argue that commercial considerations center foremost when deciding fishing policy.

Results

Optimal policies

Harvest profiles optimized under intergenerational valuation return more conservative exploitation rates than those optimized under conventional valuation ($F = 0.172 \cdot \text{year}^{-1}$ ($\delta > \delta_{ig}$), $F = 0.202 \cdot \text{year}^{-1}$ ($\delta = \delta_{ig}$), $F = 0.229 \cdot \text{year}^{-1}$ ($\delta < \delta_{ig}$), and $F = 0.415 \cdot \text{year}^{-1}$ (conventional)), so intergenerational policies maintain a greater standing stock abundance. We compare the stock biomass profiles optimized under these valuation schemes with the real-world trend (Fig. 3). A Monte Carlo procedure was used to vary basic Ecopath parameters for biomass, consumption, and production ($n = 20$, CV = 0.2); error bars show the effect of parameter uncertainty on the model's biomass estimates. The real-world time series data are taken from virtual population analysis stock assessment (Ahrens 1999); the 1985 (baseline) model estimate is based on Heymans (2003). The difference in end-state biomass between the conventional optimum and the intergenerational optimum may be blamed on the application of conventional discounting (A in Fig. 3). If we can assume that fishing consortiums operate at a discount rate equal to the market interest rate, then the difference in end-state biomass between the real-world profile and the conventional optimum may be blamed on ineffective management and (or) environmental factors (B in Fig. 3).

We then show end-state biomass (year 16) of all harvest simulations in Fig. 4. Intergenerational solutions preserve the resource better than the conventional solution and far better than the real-world harvest profile. Not shown, the real-world biomass estimate in 2000 is 0.116 $\text{t} \cdot \text{km}^{-2}$ based on Ahrens (1999).

Comparing end-state catch rates between optimal solutions (Fig. 5), we see a curve analogous to a surplus production plot. At the lowest intergenerational discount rate ($\delta > \delta_{ig}$, $\delta_{ig} = 5\%$), the conservative optimal harvest plan does not fully capitalize on available production. The maximum long-term harvest rate is reached by the intermediate intergenerational solution ($\delta = \delta_{ig}$, $\delta_{ig} = 10\%$). At greater exploitation rates, such as those advocated by the most aggressive intergenerational solution ($\delta < \delta_{ig}$, $\delta_{ig} = 15\%$) and the conventional solution ($\delta = 10\%$), the standing stock is depleted to the point where productivity is compromised. Not shown, the actual end-state cod catch (0.013 $\text{t} \cdot \text{km}^{-2}$) is based on 2000 landings and estimated unreported discards from unpublished DFO and Northwest Atlantic Fisheries Organization records (Watson et al. 2000).

Economic results

The NPV of harvest profiles based on the real-world cod data set and optimal solutions is shown under conventional and intergenerational valuation (Fig. 6). Under intergenerational valuation, the conservative strategies are worth more than the depletory real-world harvest profile. However, under

© 2005 NRC Canada

Fig. 3. Atlantic cod biomass profiles from virtual population analysis time series (solid line), intergenerational optimum ($\delta = \delta_{fg}$ (standard discount rate equals rates destined for future generations)) (open circles), and conventional optimum ($\delta = 10\%$) (solid circles). Difference between end biomasses: A represents depletion that may be blamed on the application of conventional discounting; B represents depletion that may be blamed on environment factors or ineffective management. Error bars show ±1 SD around the mean from a Monte Carlo procedure varying basic Ecopath parameters (biomass, production, and consumption) for all species groups ($n = 20$, CV = 0.2). Model adapted from Heymans (2003); virtual population analysis from Ahrens (1999).

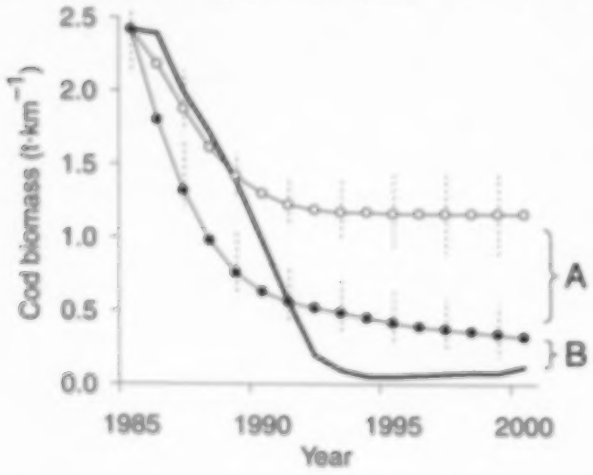

Fig. 4. Optimal end-state biomasses after 16 years of harvest under various discounting methods. Under harvest profiles optimized for net present value, the conventional discounting method (conv.) leaves a small standing biomass at $\delta = 10\%$ (right). Intergenerational optima ($\delta > \delta_{fg}$, $\delta = \delta_{fg}$, and $\delta < \delta_{fg}$) leave larger standing biomasses, especially at low intergenerational discount rates (left) ($\delta_{fg} = 5\%$, 10%, and 15%, respectively). Real-world biomass in 2001 is 0.116 t·km^{-2} (not shown). δ, standard discount rate; δ_{fg}, rates destined for future generations.

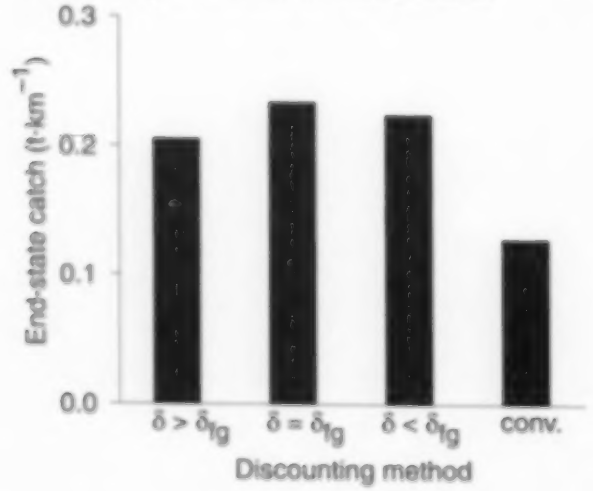

Fig. 5. Optimal end-state catches after 16 years of harvest under various discounting methods. Under harvest profiles optimized for net present value, the conventional discounting method (conv.) depletes the system early, leaving only small catches by end time (right), while intergenerational optima ($\delta > \delta_{fg}$, $\delta = \delta_{fg}$, and $\delta < \delta_{fg}$) maintain larger harvests to simulation's end ($\delta_{fg} = 5\%$, 10%, and 15% respectively). Real-world catch in 2001 is 0.013 t·km^{-2} (not shown). δ, standard discount rate; δ_{fg}, rates destined for future generations.

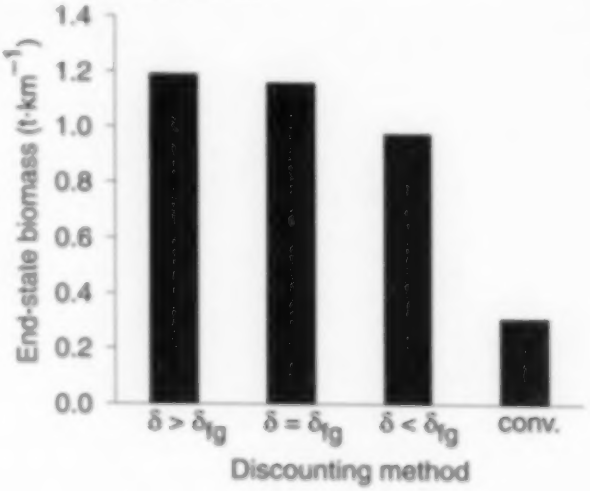

Fig. 6. Annual net present value of a 40-year harvest profile based on a real-world data set (solid bars) and optimum solutions (open bars) under four discounting methods. Under intergenerational discounting, the conservative optimal solutions outperform the depletory real-world harvest profile. However, under conventional valuation (conv.), early benefits make the real-world pillage more valuable than an optimal (long-term) solution. δ, standard discount rate; δ_{fg}, rates destined for future generations; NPV, net present value based on alternate rate of return from bank interest ($\delta = 10\%$).

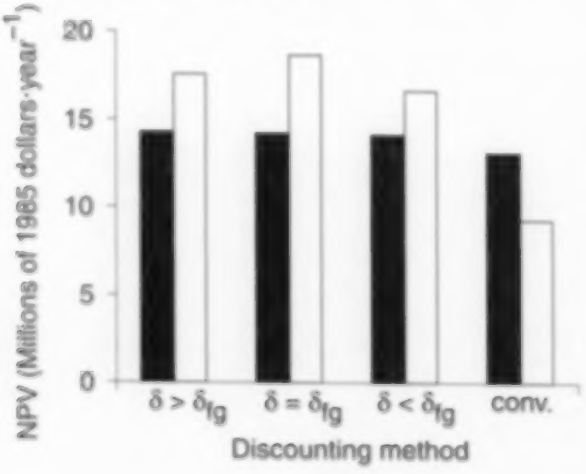

© 2005 NRC Canada

Fig. 7. Generational share of catch after 40 years for three harvest profiles. Solid bars show catch taken by the first generation; open bars show catch taken by the second generation (generation time = 20 years). The harvest profile optimized under intergenerational discounting (IG) ($\delta = \delta_{fg}$, $\delta_{fg} = 10\%$; δ is the standard discount rate, and δ_{fg} is the rate destined for future generations) leaves almost an even split to each generation, while the conventional discounting optimum (conv.) ($\delta = 10\%$) and the real-world harvest profile (actual) grant most catch to the first generation. Actual harvest profile includes projected catch to 2025 at current levels.

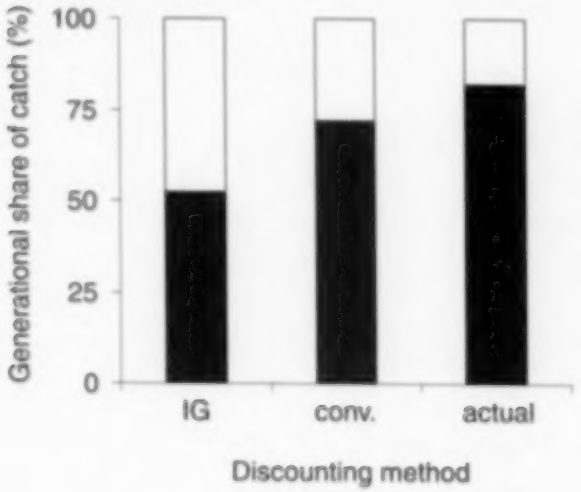

Fig. 8. Sensitivity analysis showing the effect of discount rate on the optimal end-state biomass for conventional (solid circles) and intergenerational ($\delta = \delta_{fg}$; (standard discount rate equals rates destined for future generations)) (open circles) discounting procedures. Large discount rates leave less standing biomass in the ecosystem, but the intergenerational solution maintains the stock at higher levels than the conventional solution. The conventional solution advocates stock collapse at discount rates greater than $\delta = 15\%$.

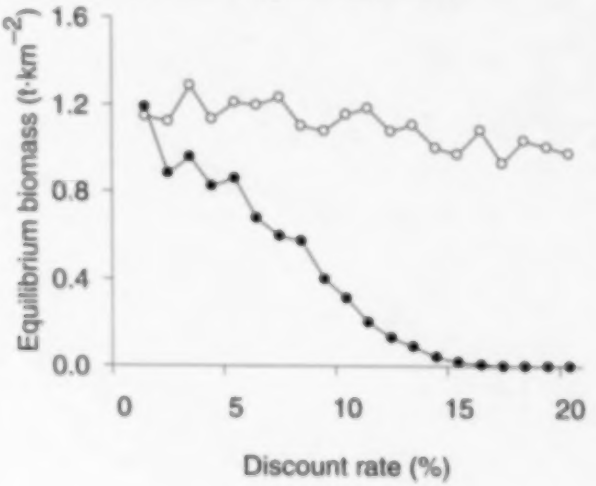

conventional valuation, the real-world pillage outperforms the more conservative optimal plan. NB: all optimizations use a fixed exploitation rate throughout the 16-year harvest simulation, providing a long-term (equilibrium level) optimal solution.

The share of catch enjoyed by the first and second generations under intergenerational and conventional discounting models (generation time = 20 years) is compared with the real-world harvest profile, including projected catches until 2025 at current levels (Fig. 7). Benefit to the second generation carries considerable weight under intergenerational valuation, so a higher catch rate is maintained into the future.

Sensitivity analysis

The relationship between the discount rate and the equilibrium biomass for conventional and intergenerational valuation ($\delta = \delta_{fg}$) is shown in Fig. 8. At all levels of discounting, intergenerational optima leave a larger biomass at end-state than conventional optima.

Discussion

Impatience of the individual is fundamental to cost–benefit decisions at all levels. It is an ingrained human attribute that allows us to instinctively, even subconsciously, account for uncertainty, lost opportunity costs, and other considerations relevant in resource acquisition. The economist's practice of discounting merely emulates this tendency, providing a quantitative and analytical guide for us to make our value-based judgments. Yet under the conventional model of discounting, it may be impossible to conserve a fisheries resource like Atlantic cod or implement an environmental protection scheme whose benefits may be years or decades in the coming.

Using education as an example of an existing and well-established multigenerational enterprise, parents and society seemingly disregard conventional financial wisdom and educate their children with little promise of return, except the confidence that they have equipped them with the tools needed to prosper. If that confidence carries value in the present, then this new form of intergenerational discounting provides a more accurate model of human valuation. It can be used to justify long-term environmental protection when investors are separated in time from recipients. As conventional discounting emulates an instinctive human behavior, so too may intergenerational discounting emulate our willingness to support future generations.

As management agendas turn toward long-term environmental conservation, proactively or in response to fishery failures, we will need to change the way we value the stream of benefits derived from our living resources. Like a ratcheting effect, it is easier to degrade the system than it is to restore it. By protecting the resource for our children's inheritance, we will preserve the option for them to harvest traditional target species rather than only the opportunist species that succeed a fishery collapse.

Acknowledgements

The authors thank C. Walters and V. Christensen at The University of British Columbia Fisheries Centre for their

© 2005 NRC Canada

advice and correspondence regarding Ecopath with Ecosim and the policy search; also, thank you to J. Heymans at The University of British Columbia Fisheries Centre for her assistance with the Newfoundland model and interpreting its predictions. U.R. Sumaila acknowledges the support of the Sea Around Us Project, Pew Charitable Trusts, and Oceana.

References

Ahrens, R. 1999. Heritable risk sensitive foraging in juvenile fish: potential implications for the dynamics of harvested populations. M.Sc. thesis, Department of Zoology, The University of British Columbia, Vancouver, B.C.

Ainsworth, C.H., and Sumaila, U.R. 2003. Intergenerational discounting and the conservation of fisheries resources: a case study in Canadian Atlantic cod. *In* Three essays on the economics of fishing. *Edited by* U.R. Sumaila. Fish. Centre Res. Rep. No. 11(3). pp. 26–32.

Brennan, T.J. 1997. Discounting the future: economics and ethics. *In* The RFF reader in environmental and resource management. *Edited by* W.E. Oates. Resources for the Future, Washington, D.C.

Christensen, V., and Pauly, D. 1992. ECOPATH II — a software for balancing steady-state models and calculating network characteristics. Ecol. Model. **61**: 169–185.

Christensen, V., and Walters, C.J. 2004. Trade-offs in ecosystem-scale optimization of fisheries management policies. Bull. Mar. Sci. **74**: 549–562.

Clark, C.W. 1973. The economics of overexploitation. Science (Wash., D.C.), **181**: 630–634.

DFO. 1994. Report on fishing vessel performance Scotia–Fundy fisheries — Maritimes region. Economic and Commercial Analysis Report No. 152. Available from Fisheries and Oceans Canada, Communications Branch, 200 Kent Street, 13th floor, Station 13228, Ottawa, ON K1A 0E6 (e-mail: info@dfo-mpo.gc.ca).

DFO. 2001. Sustainable development strategy 2001–2003. Cat. No. Fs23-329/2001E-IN. Available from http://www.dfo-mpo.gc.ca/sds-sdd/contents_e.htm [accessed January 2003; updated February 2001].

Environment Canada. 2002. Report on plans and priorities of Environment Canada. Cat. No. Bt31–2/2003-III-16. Available from http://www.tbs-sct.gc.ca/est-pre/20022003/vrEC_e.pdf [accessed January 2003; updated February 2002].

Fisher, A.C., and Krutilla, J.V. 2002. Resource conservation, environmental preservation, and the rate of discount. Q. J. Econ. **89**: 358–370.

Goulder, L.H., and Stavins, R.N. 2002. Discounting: an eye on the future. How economists' controversial practice of discounting really affects the evaluation of environmental policies. Nature (Lond.), **419**: 673–674.

Hasselmann, K., Hasselmann, S., Giering, R., Ocana, V., and Storch, H.V. 1997. Sensitivity study of optimal CO_2 emission paths using a simplified structural integrated assessment model (SIAM). Clim. Change, **37**: 335–343.

Heal, G.M. 1998. Valuing the future: economic theory and sustainability. Columbia University Press, New York.

Heymans, J.J. (*Editor*). 2003. A revised model for Newfoundland and southern Labrador (2J3KLNO) for the time period 1985–1987. *In* Ecosystem models of Newfoundland and southeastern Labrador. Additional information and analyses for 'Back to the Future'. Fish. Centre Res. Rep. No. 11(5). pp. 40–61.

Nielsen, U. 2001. Hyperbolic discounting and sustainable development. Department of Economics and Natural Resources, Royal Veterinary and Agricultural University, Copenhagen, Denmark. Available from http://www.flec.kvl.dk/kok/ore-seminar/hyperbsustdev.pdf [accessed January 2003; updated June 2001].

Okey, T.A., and Wright, B.A. 2004. Toward ecosystem-based extraction policies for Prince William Sound, Alaska: integrating conflicting objectives and rebuilding pinnipeds. Bull. Mar. Sci. **74**: 727–747.

Polovina, J.J. 1984. Models of a coral reef ecosystem I: the Ecopath model and its application to French frigate shoals. Coral Reefs, **3**: 1–11.

Sumaila, U.R. 2004. Intergenerational cost benefit analysis and marine ecosystem restoration. Fish and Fisheries, **5**: 329–343.

Sumaila, U.R., and Walters, C.J. 2005. Intergenerational discounting: a new intuitive approach. Ecol. Econ. **52**: 135–142.

United Nations Framework Convention on Climate Change. 1997. Kyoto protocol to the United Nations Framework Convention on Climate Change, Document FCCC/CP/1997;7/Add1. Available from http://unfccc.int/2860.php [accessed January 2003].

Walters, C.J., and Juanes, F. 1993. Recruitment limitation as a consequence of natural selection for use of restricted feeding habitats and predation risk taking by juvenile fishes. Can. J. Fish. Aquat. Sci. **50**: 2058–2070.

Walters, C.J., and Martell, S.J. 2004. Harvest management for aquatic ecosystems. Princeton University Press, Princeton, N.J.

Walters, C.J., Christensen, V., and Pauly, D. 1997. Structuring dynamic models of exploited ecosystems from trophic mass-balance assessments. Rev. Fish Biol. Fish. **7**: 139–172.

Watson, R., Guénette, S., Fanning, P., and Pitcher, T.J. 2000. The basis for change: part I — reconstructing fisheries catch and effort data. *In* Methods for assessing the impact of fisheries on marine ecosystems of the North Atlantic. *Edited by* D. Pauly and T.J. Pitcher. Fish. Centre Res. Rep. No. 8(2). pp. 23–39.

Weitzman, M.L. 2001. Gamma discounting. Am. Econ. Rev. **91**: 260–272.

© 2005 NRC Canada

Community interactions affecting the relative abundances of native and invasive amphipods in the St. Lawrence River

M.E. Palmer and Anthony Ricciardi

Abstract: The Eurasian amphipod *Echinogammarus ischnus* is reportedly replacing the common native amphipod *Gammarus fasciatus* in the Great Lakes – St. Lawrence River system. A potential mechanism for this replacement is competition mediated by resident species. Other Eurasian invaders, dreissenid mussels (*Dreissena polymorpha* and *Dreissena bugensis*), dominate rocky substrates throughout the system and might be promoting the rapid expansion of *E. ischnus* by providing habitat and refugia from predation. Using an in-situ predator-exclusion experiment, we tested the hypothesis that *E. ischnus* is better able than *G. fasciatus* to use *Dreissena* spp. colonies as refugia and thus is less susceptible to predators in the St. Lawrence River. Co-occurring *E. ischnus* and *G. fasciatus* showed similar increases in density in the presence of *Dreissena* spp., in spite of *E. ischnus* having evolutionary experience with *Dreissena* spp. Predators reduced the density of both amphipod species, but *E. ischnus* was more susceptible to predation on dreissenid substrates, which suggests that predation mediates the coexistence of *G. fasciatus* and *E. ischnus* in the river.

Résumé : L'amphipode eurasiatique *Echinogammarus ischnus* est, rapporte-t-on, en train de remplacer l'amphipode indigène commun *Gammarus fasciatus* dans le système des Grands Lacs et du Saint-Laurent. Un mécanisme possible de cette substitution est une compétition par l'intermédiaire des espèces résidantes. D'autres envahisseurs eurasiatiques, les bivalves dreissénidés (*Dreissena polymorpha* et *Dreissena bugensis*), dominent les substrats rocheux dans tout le système et peuvent peut-être favoriser l'expansion rapide d'*E. ischnus* en fournissant un habitat et des refuges contre la prédation. À l'aide d'une expérience in situ d'exclusion des prédateurs, nous avons éprouvé l'hypothèse selon laquelle, dans le Saint-Laurent, *E. ischnus* est plus habile que *G. fasciatus* à utiliser les colonies de *Dreissena* spp. comme refuges et il est moins vulnérable aux prédateurs. Les *E. ischnus* et les *G. fasciatus* en cohabitation montrent les mêmes accroissements de densité en présence de *Dreissena* spp., bien qu'*E. ischnus* ait une expérience de cohabitation avec *Dreissena* spp. au cours de son évolution. Les prédateurs réduisent la densité des deux espèces, mais *E. ischnus* est plus vulnérable à la prédation sur les substrats de dreissenidés, ce qui laisse croire que la prédation explique la coexistence de *G. fasciatus* et d'*E. ischnus* dans le fleuve.

[Traduit par la Rédaction]

Introduction

The impact of an introduced exotic species can vary across communities, causing the extirpation of native species at some sites while coexisting with the same species at others (MacNeil et al. 1999, 2001). One explanation for this variance, apart from the influence of abiotic variables, is that the composition of the recipient community determines the effects of a species' introduction (Ricciardi 2003; Ricciardi and Atkinson 2004). The impact of an introduced species is reduced in communities where its abundance is limited by predators (Robinson and Wellborne 1988; Arnott and Vanni 1993), which may promote its coexistence with native species (Celik et al. 2002). Moreover, differential susceptibility to predators may lead to the dominance of one competing species over another (DiDonato and Lodge 1993).

Conversely, some resident species, including previous invaders, can facilitate the establishment and population growth of an introduced species, thereby enhancing its impact within the community (Castellanos et al. 1994; Simberloff and Von Holle 1999; Ricciardi 2005). Facilitative interactions between introduced species appear to be at least as common as antagonistic interactions (Simberloff and Von Holle 1999; Ricciardi 2001). The introduction of an "ecosystem engineer" (Crooks 2002) can increase the frequencies of both direct and indirect facilitative interactions, as has been observed in the Laurentian Great Lakes following the introduction of two Eurasian molluscs, the zebra mussel,

Received 31 March 2004. Accepted 4 December 2004. Published on the NRC Research Press Web site at http://cjfas.nrc.ca on 27 May 2005.
J18057

M.E. Palmer. Department of Biology and Redpath Museum, McGill University, Montréal, QC H3A 2K6, Canada.
Anthony Ricciardi.[1] School of Environment and Redpath Museum, McGill University, Montréal, QC H3A 2K6, Canada.

[1]Corresponding author (email: tony.ricciardi@mcgill.ca).

 doi: 10.1139/F05-012 © 2005 NRC Canada

Dreissena polymorpha, and the quagga mussel, *Dreissena bugensis* (Ricciardi 2001; hereinafter referred to collectively as *Dreissena*). The proliferation of these macrofouling bivalves has altered substrate quality (by the formation of aggregated mussel colonies) and increased water clarity and sedimentation (by their filtration activities) throughout the system (Vanderploeg et al. 2002). *Dreissena* may have facilitated the invasion of other Eurasian species by providing an abundant food source for the round goby, *Neogobius melanostomus*, increased grazing area and refugia for the faucet snail, *Bithynia tentaculata*, and increased light availability for exotic macrophytes such as watermilfoil, *Myriophyllum spicatum*, and curly pondweed, *Potamogeton crispus* (Ricciardi and MacIsaac 2000; Ricciardi 2001; Vanderploeg et al. 2002).

Dreissena might also be promoting the expansion of the Eurasian amphipod crustacean *Echinogammarus ischnus*, a species native to large rivers in the Black and Caspian seas basin (Jażdżewski 1980). *Echinogammarus ischnus* was discovered in North America in the Detroit River in 1995 (Witt et al. 1997) and by 2002 it had spread to all of the Great Lakes (Dermott et al. 1998; Nalepa et al. 2001; Grigorovich et al. 2003) and as far downstream in the St. Lawrence River as Québec City (Vanderploeg et al. 2002; M.E. Palmer and A. Ricciardi, unpublished data). Throughout much of this invaded range, *E. ischnus* appears to be replacing a taxonomically and morphologically similar species, the native North American amphipod *Gammarus fasciatus* (Dermott et al. 1998; Stewart et al. 1999; Nalepa et al. 2001). This replacement seems to be particularly prevalent on *Dreissena*-covered substrates (Dermott et al. 1998).

Formed by clumped mussels attached to solid substrate, dreissenid colonies are structurally complex, with a greater surface area and more interstitial spaces than typical bare substrate (Ricciardi et al. 1997). Gammarid amphipods show increased abundance as a result of this enhanced microhabitat complexity (Ricciardi et al. 1997; González and Downing 1999; Ricciardi 2003), which provides small invertebrates with refugia from large predators (Diehl 1992). To a large predator, an amphipod in an interstitial space is less visually apparent and difficult to reach (Ryer 1988). The Great Lakes – St. Lawrence River system contains many predators of amphipods, including yellow perch, *Perca flavescens*, which commonly use *G. fasciatus* as a prey item (Harnois et al. 1992; Pothoven et al. 2000). *Echinogammarus ischnus* occurs naturally in dreissenid colonies in its native range and may be adapted to living in mussel beds (Köhn and Waterstraat 1990). Therefore, *E. ischnus* may be better able than *G. fasciatus* (which has no evolutionary experience with *Dreissena*) to use *Dreissena* colonies as both habitat and refugia from predators. Because mussel colonies are patchy and limited in size, amphipods might compete for interstitial spaces. A weaker ability to use interstitial spaces may render *G. fasciatus* more exposed to predation, and thus disadvantaged in competition with *E. ischnus*.

In this study we use a predator-exclusion experiment to investigate whether *Dreissena* is facilitating the replacement of native amphipods by *E. ischnus*. Specifically, we test the hypotheses that (*i*) *E. ischnus* shows a stronger positive response to *Dreissena* than does *G. fasciatus*, and (*ii*) *E. ischnus* and *G. fasciatus* have differential susceptibilities to large predators (fish and crayfish) in the presence of *Dreissena*.

Methods

Experimental protocol

Experiments were carried out at Pointe-du-Moulin, Île Pérrot, Quebec, which is located within a fluvial lake (Lac St-Louis) on the St. Lawrence River (73°51′01″W, 45°22′0.5″N). Pointe-du-Moulin is a public park where human activities are prohibited near the shore. It is a shallow-water (<3-m depth) site with a substrate of bedrock and a few scattered boulders, and its bottom is covered with abundant patches of *Dreissena* and macrophyte (*Vallisneria americana*) beds. Potential amphipod predators commonly found at the site include yellow perch, rock bass (*Ambloplites rupestris*), smallmouth bass (*Micropterus dolomieu*), American eel (*Anguilla rostrata*), and crayfish (*Orconectes* spp.) (M.E. Palmer, personal observations). The experiment was carried out over 2 years: September–October 2002, July–August 2003, and September–October 2003.

Experimental treatments consisted of a combination of predator-exclusion cages and artificial substrates (cement bricks 19 cm × 9 cm × 5.7 cm) covered with *Dreissena* shells. In 2002, six treatment combinations were used. Reference treatments were uncaged bare bricks and bricks with their top face fully covered with a monolayer of *Dreissena* shells. Experimental treatments consisted of bare bricks and *Dreissena*-covered bricks enclosed by a stainless-steel cage. An additional set of treatment bricks was placed in predator-accessible open cages to control for cage effects. Upon analysis it was determined that the open cages introduced additional variables affecting amphipod abundance and did not provide a direct control for cage effects. Thus, open-cage controls were replaced with low-density (half-covered) *Dreissena* cover bricks in 2003. Ten replicates of each treatment combination (uncaged, open-caged, and caged zero-density (ZD), low-density (LD), and high-density (HD) *Dreissena* cover) were used, resulting in a total sample size of 60 per experimental period and a statistical power of 83% (Eckblad 1991), based on a preliminary survey in August 2002.

Prior to use, all bricks were soaked in St. Lawrence River water for 7 days. Dreissenid mussels (average length 27 mm, standard deviation (SD) 4.3 mm) were collected at the site from a depth of 1–3 m by SCUBA. Mussels were boiled and rinsed to remove all tissue as well as any attached invertebrates. Following a drying period of at least 3 days for both bricks and shells, bricks designated LD and HD were covered with a layer of empty shells. Nontoxic aquarium silicone was used to attach the shells to the upper surface of the bricks (~9.5 cm × 4.5 cm for LD bricks and 19 cm × 9 cm for HD bricks). Mussels were glued at their base so that shell valves remained closed, and they were placed adjoining each other so as to resemble a natural, clumped colony. The average number of mussels per brick was 25 (±5) for LD bricks and 47 (±15) for HD bricks; the former had mussels placed either in the middle or at one end of the brick (determined randomly), leaving the rest of the top face of the brick uncovered.

Cages (29 cm × 20 cm × 19 cm) were constructed of stainless-steel wire (mesh size 1.25 cm) and their sides were connected with plastic cable ties. Predator-access cages (20 cm × 19 cm) had one open side. Bricks were placed centrally in the cages. Bricks were placed at depths of 1.5–2 m;

© 2005 NRC Canada

Table 1. Multivariate analysis of variance for amphipod species in 2002 and 2003.

	Wilks' λ	*F*	df	*p*[a]
2002				
Dreissena	0.1769	120.99	2,52	**<0.0001**
Cage	0.8156	2.79	4,104	**0.0301**
Dreissena × cage	0.8536	2.14	4,104	0.0809
2003				
Season	0.4701	58.05	2,103	**<0.0001**
Dreissena	0.1874	67.46	4,206	**<0.0001**
Cage	0.7840	14.19	2,103	**<0.0001**
Season × *Dreissena*	0.6838	10.78	4,206	**<0.0001**
Season × cage	0.9503	2.69	2,103	0.0724
Dreissena × cage	0.6915	10.43	4,206	**<0.0001**
Season × *Dreissena* × cage	0.9526	1.26	4,206	0.2851

[a]Values in boldface type are significant.

placement and orientation were random except that all bricks were separated by at least 2 m. After 5 weeks, all bricks were collected and placed in labeled plastic bags (doubled to prevent leaks) while under water. Cages were cut open under water and the bricks were removed and transferred into bags with as little disturbance as possible to prevent the escape of amphipods. Bagged bricks were transported back to the laboratory within 2–4 h. Amphipods were collected by filtering the water contained in each bag through a 500 µm mesh sieve and removing all invertebrates from the brick with forceps, as well as by rinsing each brick with water passed through another 500 µm mesh sieve. Amphipods were then preserved in 70% ethanol. A Hund–Wetzlar SM33 stereoscope was used to identify the species of each amphipod using standard morphological features (Witt et al. 1997).

Statistical analysis

The relationship between mean (m) and variance (s^2) for total amphipod density across treatments ($s^2 = 0.38m^{1.46}$; $r^2 = 0.92$, $p < 0.001$) indicated that a fourth-root transformation was required for stabilizing variances (Downing 1979). Multivariate analysis of variance (MANOVA) tests were performed to determine whether amphipod species density varied among treatments in 2002 and 2003. Analysis of variance (ANOVA) tests were then used to identify treatment differences for individual species. *Echinogammarus ischnus* and *G. fasciatus* densities in 2002 were examined using two-fixed-factor (*Dreissena* and cage type) ANOVAs. The 2003 densities were evaluated using three-fixed-factor (season, *Dreissena*, and cage type) ANOVAs. Individual density differences for *E. ischnus* in 2002 and 2003 were detected using the Tukey–Kramer multiple-comparison procedure for factors with significant interactions. The same procedure was used for *G. fasciatus* in 2003, while the Tukey–Kramer multiple comparison for factors without interactions was applied to the 2002 data.

For 2003 data, the strength of the interaction between amphipods and *Dreissena* on uncaged and caged bricks was determined by simple linear regression. The relationships were then compared using analysis of covariance (ANCOVA).

ANCOVA was also used to compare the relationship between *E. ischnus* density and *G. fasciatus* density as a function of time. As both amphipod densities were subject to measurement error and dimensionless after fourth-root transformation, major axis (model II) regression (Sokal and Rohlf 1995) was used to examine the linear relationship between

Fig. 1. Densities (mean + standard error) of (*a*) *Echinogammarus ischnus* and (*b*) *Gammarus fasciatus* on bricks with zero-density (ZD) and high-density (HD) *Dreissena* cover in September–October 2002. Open bars represent uncaged reference bricks (n = 10), hatched bars represent open-cage bricks (n = 9), and solid bars represent caged bricks (n = 10). Different letters above the bars indicate statistical differences (α = 0.05).

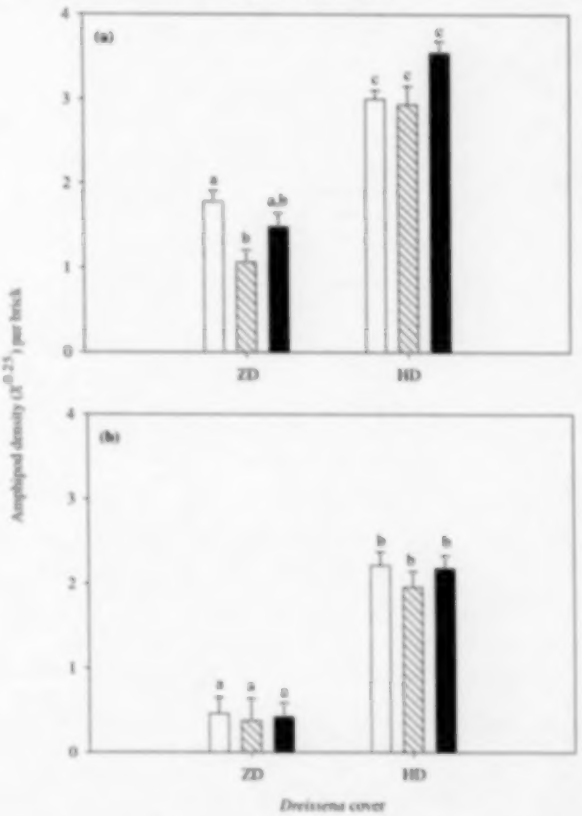

© 2005 NRC Canada

Table 2. Analysis of variance for amphipod species in 2002 and 2003.

	MS	*F* test	*df*	*p*[a]
Echinogammarus ischnus, 2002				
Model	9.48	40.21	5	**<0.0001**
Dreissena	43.37	183.94	1	**<0.0001**
Cage	1.39	5.88	2	**0.0049**
Dreissena × cage	0.95	4.04	2	**0.0232**
Error	0.24		53	
Gammarus fasciatus, 2002				
Model	8.58	23.79	5	**<0.0001**
Dreissena	42.51	117.84	1	**<0.0001**
Cage	0.16	0.43	2	0.651
Dreissena × cage	0.05	0.14	2	0.873
Error	0.36		53	
Echinogammarus ischnus, 2003				
Model	8.65	31.19	11	**<0.0001**
Season	26.56	95.79	1	**<0.0001**
Dreissena	25.00	90.15	2	**<0.0001**
Cage	0.59	2.13	1	0.1474
Season × *Dreissena*	2.84	10.25	2	**<0.0001**
Season × cage	1.31	4.73	1	**0.0320**
Dreissena × cage	6.41	23.11	2	**<0.0001**
Season × *Dreissena* × cage	0.27	0.98	2	0.3791
Error	0.28		104	
Gammarus fasciatus, 2003				
Model	10.49	37.43	11	**<0.0001**
Season	2.02	7.22	1	**0.0084**
Dreissena	47.33	168.87	2	**<0.0001**
Cage	7.97	28.45	1	**<0.0001**
Season × *Dreissena*	4.92	17.54	2	**<0.0001**
Season × cage	0.43	1.54	1	0.2169
Dreissena × cage	0.37	1.33	2	0.2699
Season × *Dreissena* × cage	0.37	1.31	2	0.2732
Error	0.28		104	

[a]Values in boldface type are significant.

E. ischnus and *G. fasciatus*. This was done separately for the 2002, July–August 2003, and September–October 2003 data. All statistical procedures were performed using the SAS statistical package version 8 (SAS Institute Inc. 1999).

Results

All bricks were recollected in 2002. However, a single ZD brick that was found outside its open cage was not included in our statistical analyses. In August 2003, 1 uncaged HD brick was lost. In October 2003, 1 LD and 2 HD caged bricks were lost. These losses were due to poor visibility. At all times of collection, bricks and cages had very low levels of fouling (<10%).

In 2002, multivariate analysis indicated that *Dreissena* and cage type affected amphipod densities ($p < 0.0001$ and 0.0301, respectively; Table 1). *Echinogammarus ischnus* was the dominant amphipod over all treatment combinations (Fig. 1) and 79% of its variance was explained by *Dreissena*, cage type, and their interaction (Table 2). *Echinogammarus ischnus* density was 2.2 times greater on HD bricks than on ZD bricks and was reduced on ZD bricks in open cages compared with uncaged bricks (adjusted $p = 0.027$). *Gammarus fasciatus* density was 5 times higher on HD bricks than on LD bricks and was not affected by predation (Table 2; Fig. 1*b*). Over 69% of its variance was explained by *Dreissena*, cage type, and their interaction.

In 2003, MANOVA indicated that one or more amphipod species was affected by season, *Dreissena*, and cage type ($p < 0.0001$; Table 1). Individual ANOVA found that the combined variables of season, *Dreissena*, cage type, and their interactions explained 77% of variation in *E. ischnus* density (Table 2). *Echinogammarus ischnus* density was 2.1 times higher in September–October than in July–August and increased by a factor of 2.7 and 4 on LD and HD bricks, respectively, compared with ZD bricks. Predation reduced *E. ischnus* density on LD and HD bricks in July–August ($p = 0.007$ and 0.023, respectively). Cage treatments had a negative effect on *E. ischnus* density on ZD bricks. This trend was significant in September–October ($p = 0.027$) but nonsignificant in July–August ($p = 0.084$; Fig. 2*a*).

Gammarus fasciatus was the dominant amphipod in 2003 (Fig. 2). Season, *Dreissena*, cage type, and their interactions explained 80% of the variation in *G. fasciatus* density (Table 2). *Gammarus fasciatus* was 1.1 times more abundant in July–August than in September–October. Densities on LD

© 2005 NRC Canada

Fig. 2. Densities (mean + standard error) of (*a*) *Echinogammarus ischnus* and (*b*) *Gammarus fasciatus* for two seasons in 2003. An asterisk indicates a significant difference between uncaged and caged bricks within *Dreissena*-cover densities (zero density (ZD), low density (LD), and high density (HD)) and seasons ($p \leq 0.05$).

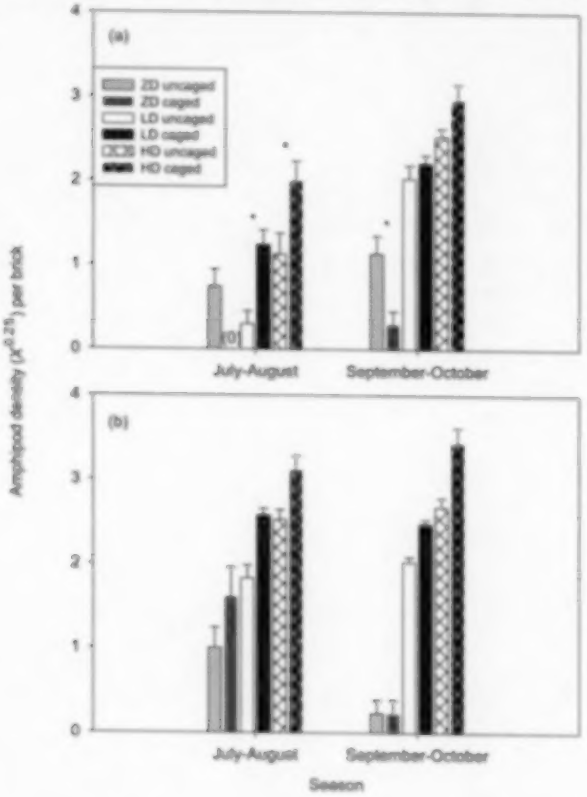

Fig. 3. Densities (mean ± standard error) of (*a*) *Echinogammarus ischnus* and (*b*) *Gammarus fasciatus* on bricks with zero-density (ZD), low-density (LD), and high-density (HD) *Dreissena* cover in 2003. Open circles represent uncaged bricks ($n = 59$) and solid circles represent caged bricks ($n = 57$). For both species, amphipod density increased with density of *Dreissena* cover in both caged and uncaged treatments (analysis of variance, $p < 0.0001$, except for the *E. ischnus* uncaged treatment, where $p = 0.002$). Predation weakened the relationship between *E. ischnus* and *Dreissena* (analysis of covariance, $p = 0.0004$) but did not affect the relationship between *G. fasciatus* and *Dreissena* ($p = 0.569$).

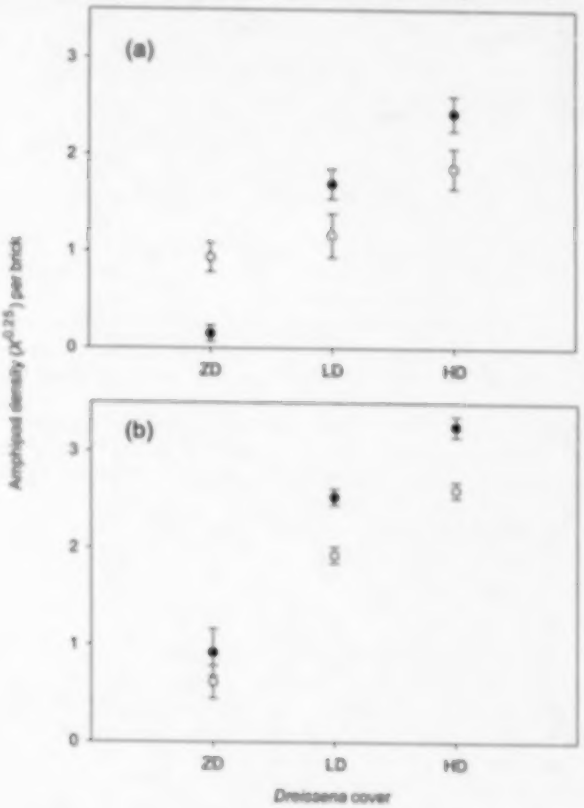

and HD bricks were 2.9 and 3.8 times higher, respectively, than on ZD bricks. *Gammarus fasciatus* was negatively affected by predation, but differences on *Dreissena*-covered bricks were not significant ($p > 0.05$; Fig. 2*b*). Predation weakened the relationship between *E. ischnus* and *Dreissena* (ANCOVA, $p = 0.0004$; Fig. 3*a*), but had no effect on the relationship between *G. fasciatus* and *Dreissena* ($p = 0.569$; Fig. 3*b*).

The relationship between *E. ischnus* and *G. fasciatus* varied among the three experimental periods (ANCOVA, $p < 0.0001$), but was consistently positive, with both species exhibiting high density on the same experimental substrates (model II regression results: 2002 (Fig. 4), $r^2 = 0.59$, $p < 0.0001$; July–August 2003 (Fig. 5*a*), $r^2 = 0.25$, $p < 0.0001$; September–October 2003 (Fig. 5*b*), $r^2 = 0.76$, $p < 0.0001$). These relationships remained significant when zero values were removed.

Discussion

Although both the invasive amphipod *E. ischnus* and the native *G. fasciatus* were present on experimental substrates in 2002, *E. ischnus* was numerically dominant. In the following year, *G. fasciatus* outnumbered *E. ischnus*. These findings contrast with those in the Great Lakes, where *E. ischnus* has progressively become the dominant amphipod at numerous sites (Van Overdijk et al. 2003), often within a year of detection (Dermott et al. 1998). Given that *E. ischnus* has been present in the St. Lawrence River near Montreal since at least 1998 (A. Ricciardi, unpublished data) and specimens collected in 2002 contained reproductive individuals (indicated by the presence of eggs) and three size classes (M.E. Palmer, unpublished data), the species had likely been established at Pointe-du-Moulin for at least a year prior to this experiment; *E. ischnus* reproduces twice per year (Köhn and Waterstraat 1990) and the most recent date of establishment that could produce three size classes was early summer 2001. Unfortunately, past *G. fasciatus* densities at the site are not known and so comparisons of density before and after invasion cannot be made.

© 2005 NRC Canada

Fig. 4. Relationship between *Echinogammarus ischnus* and *Gammarus fasciatus* densities in September–October 2002 (major axis model II regression: $y = 0.6225x - 0.1633$, $r^2 = 0.59$, $p < 0.0001$, $n = 59$). When zeros are removed, $y = 0.6832x + 0.0083$, $r^2 = 0.52$, $p < 0.0001$, $n = 39$.

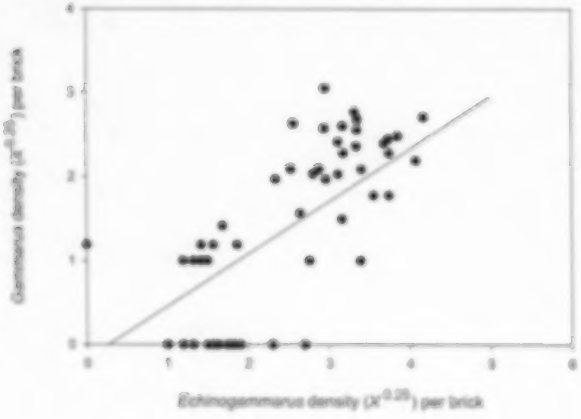

Because results of short-term experiments may not be representative of natural community responses, it is conceivable that amphipod densities did not have sufficient time to equilibrate during our experiment and thus were not representative of the surrounding community. However, Stewart et al. (1998*c*) concluded that a colonization period of 37 days was long enough for non-mussel macroinvertebrate densities on experimental live *Dreissena* substrates to equal those on surrounding substrates, which suggests that the time frame of our experiment was sufficient to permit amphipod densities to reach equilibrium.

Effect of *Dreissena*

Total amphipod density was enhanced in the presence of *Dreissena*, consistent with previous findings (Ricciardi et al. 1997; Stewart et al. 1998*b*; Van Overdijk et al. 2003). Surprisingly, *G. fasciatus* showed a similar (in 2003) or more rapid increase (in 2002) in density than did *E. ischnus* on *Dreissena*-covered bricks. These results do not support the hypothesis of greater (coevolved) interaction strength between *E. ischnus* and *Dreissena* (Ricciardi and MacIsaac 2000).

Gammarus fasciatus is a substrate generalist and can use a broad range of microhabitats (Dermott et al. 1998), an ability that apparently allows it to thrive within dreissenid colonies. In fact, after *Dreissena* became established in the Great Lakes – St. Lawrence River system, *G. fasciatus* increased in abundance at many sites and was often the dominant non-dreissenid invertebrate present (Stewart and Haynes 1994; Wisenden and Bailey 1995; Ricciardi et al. 1997).

The greater enhancement of *G. fasciatus* in the presence of *Dreissena* may be a result of differing colonization abilities of the two amphipod species. *Gammarus fasciatus* has a higher fecundity and shorter generation time than *E. ischnus* (Dermott et al. 1998). During our experiments, *G. fasciatus* was also more abundant on surrounding natural substrates (M.E. Palmer and A. Ricciardi, unpublished data), perhaps giving it first access to the added experimental substrate.

Fig. 5. Relationship between *Echinogammarus ischnus* and *Gammarus fasciatus* densities in 2003: (*a*) July–August (major axis model II regression: $y = 2.1131x + 0.2082$, $r^2 = 0.25$, $p < 0.0001$, $n = 59$); (*b*) September–October ($y = 1.0553x - 0.1359$, $r^2 = 0.76$, $p < 0.0001$, $n = 57$). Note the difference in *x*-axis scales in *a* and *b*. When zeros are removed, $y = 1.6048x + 0.0082$, $r^2 = 0.28$, $p = 0.0015$, $n = 33$, in *a*, and $y = 1.0827x - 0.0156$, $r^2 = 0.63$, $p < 0.0001$, $n = 40$, in *b*.

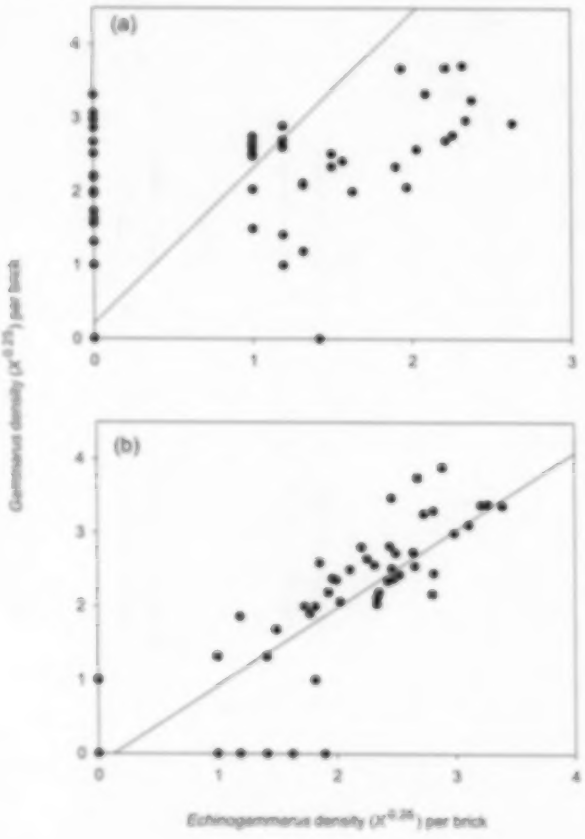

However, the proportion of total amphipod density made up by *E. ischnus* was higher on experimental substrates than on natural *Dreissena* and *V. americana* substrates in 2003 (30% and 15%, respectively; M.E. Palmer and A. Ricciardi, unpublished data), which indicates that *E. ischnus* was able to rapidly colonize experimental bricks despite an apparent disadvantage in the size of its local source population. Alternatively, our use of dead *Dreissena* shells, which accumulate less organic matter (i.e., detritus and pseudofeces) than living mussels (Stewart et al. 1998*c*), may have affected amphipod colonization if *E. ischnus* and *G. fasciatus* differ in their foraging ability and resource use. Nevertheless, even when *E. ischnus* was more prevalent on experimental substrates (in 2002), *G. fasciatus* still produced a greater increase in density in the presence of *Dreissena*.

Amphipod densities may have been too low for space competition to occur within the experimental *Dreissena* colonies. High *Dreissena* abundance might reduce competition by adding an abundant resource over which the two amphi-

© 2005 NRC Canada

pod species can segregate. Positive responses by both species to the same extrinsic factors might account for the positive relationship between *E. ischnus* and *G. fasciatus*. Van Overdijk et al. (2003) also found that the two species were positively correlated on experimental scales. Perhaps *E. ischnus* has a competitive advantage when amphipod densities increase and resources become limited, which might be the case for littoral sites in Lake Erie and Lake Ontario, where it dominates amphipod communities (Dermott et al. 1998).

Effect of predation

Predator-access cages

The open-cage treatment was omitted from the 2003 experiments because it was a poor control for cage effects. *Echinogammarus ischnus* density was reduced on bricks in open cages, possibly because the cage structure attracted small fish and crayfish by allowing them to feed while being protected against larger predators; in Lake Erie, Stewart et al. (1999) observed that some predator species were attracted to open cages. *Gammarus fasciatus* did not show this pattern, which implies that *E. ischnus* is more susceptible to small predators — particularly when it is present at higher densities.

Predator-exclusion cages

Amphipod density was apparently reduced by predation. However, predation effects on *G. fasciatus* in the presence of *Dreissena* were not significant, whereas predation reduced *E. ischnus* density on *Dreissena*-covered bricks in July–August. *Echinogammarus ischnus* is more active than *G. fasciatus* (Van Overdijk et al. 2003) and uses its uropods and antennae to move across *Dreissena* shells (Dermott et al. 1998), while *G. fasciatus* tends to burrow into interstitial spaces amongst mussels, where silty detritus accumulates (M.E. Palmer, personal observations). It would be worthwhile to test whether these respective behaviors render *E. ischnus* more susceptible to predation on *Dreissena*-covered substrates, especially as our use of dead shells may have resulted in unusually high levels of *E. ischnus* foraging activity that cause it to be more conspicuous to predators. Predation effects also vary seasonally and were not significant for *E. ischnus* on *Dreissena*-covered bricks in September–October for either year. The reduction in *E. ischnus* density on caged ZD bricks in 2003 suggests that cage structure has a negative effect on *E. ischnus*, perhaps because of impeded water flow. This implies that the positive response of *E. ischnus* to predator exclusion on *Dreissena*-covered bricks is underestimated.

Our findings do not support the hypothesis that predation is mediating the replacement of *G. fasciatus* by *E. ischnus* on *Dreissena*-covered substrate. Rather, predation appears to be contributing to the coexistence of the two species, as large predators had a greater negative effect on *E. ischnus*, preventing it from becoming competitively dominant. Additional support for this conclusion is given by Stewart et al. (1998*a*, 1999), who found that when the species occurred separately, the presence of large predators did not affect *G. fasciatus* biomass but coincided with a decline in *E. ischnus* biomass.

The replacement of *G. fasciatus* by *E. ischnus* that is observed in the Great Lakes has not yet occurred in the upper St. Lawrence River, even though *E. ischnus* has been present since the late 1990s. We suggest that the species replacement reported for the lower Great Lakes is not a result of *E. ischnus* being better able than *G. fasciatus* to use dreissenid colonies as habitat and refugia. The dominance of one species over the other might be determined by differential environmental preferences (M.E. Palmer and A. Ricciardi, unpublished data) as well as direct interactions between the two species. Dermott et al. (1998) found that when *E. ischnus* was present, the number of immature *G. fasciatus* was reduced, possibly as a result of intraguild predation (cf. Dick and Platvoet 1996). Small-scale experiments are needed to examine the interactions of *E. ischnus* and *G. fasciatus* to determine precisely their direct impacts on each other.

Acknowledgements

We thank Dr. Krzysztof Jażdżewski for confirming our initial *E. ischnus* identifications, and we are grateful to L. Jones, A. Jokela, and S. Atkinson for their field assistance. Several graduate students in the Biology Department of McGill University provided valuable comments on an early draft of the manuscript. This research is supported by a grant from the Natural Sciences and Engineering Research Council of Canada to A.R.

References

Arnott, S.E., and Vanni, M.J. 1993. Zooplankton assemblages in fishless bog lakes: influence of biotic and abiotic factors. Ecology, **74**: 2361–2380.

Castellanos, E.M., Figueroa, M.E., and Davy, A.J. 1994. Nucleation and facilitation in saltmarsh succession: interactions between *Spartina maritima* and *Arthrocnemum perenne*. J. Ecol. **82**: 239–248.

Celik, K., Schlinder, J.E., Foris, W.J., and Knight, J.C. 2002. Predator-mediated coexistence of exotic and native crustaceans in a freshwater lake? Biol. Invasions, **4**: 451–455.

Crooks, J.A. 2002. Characterizing ecosystem-level consequences of biological invasions: the role of ecosystem engineers. Oikos, **97**: 153–166.

Dermott, R., Witt, J., Um, Y.M., and Gonzalez, M. 1998. Distribution of the Ponto-Caspian amphipod *Echinogammarus ischnus* in the Great Lakes and replacement of native *Gammarus fasciatus*. J. Gt. Lakes Res. **24**: 442–452.

Dick, J.T.A., and Platvoet, D. 1996. Intraguild predation and species exclusions in amphipods: the interaction of behaviour, physiology and environment. Freshw. Biol. **36**: 375–383.

DiDonato, G.T., and Lodge, D.M. 1993. Species replacements among *Orconectes* crayfishes in Wisconsin lakes: the role of predation by fish. Can. J. Fish. Aquat. Sci. **50**: 1484–1488.

Diehl, S. 1992. Fish predation and benthic community structure: the role of omnivory and habitat complexity. Ecology, **73**: 1646–1661.

Downing, J.A. 1979. Aggregation, transformation, and the design of benthos sampling programs. J. Fish. Res. Board Can. **36**: 1454–1463.

Eckblad, J.W. 1991. How many samples should be taken? BioScience, **41**: 346–348.

González, M.J., and Downing, A. 1999. Mechanisms underlying amphipod responses to zebra mussel (*Dreissena polymorpha*) in-

© 2005 NRC Canada

vasion and implications for fish–amphipod interactions. Can. J. Fish. Aquat. Sci. **56**: 679–685.

Grigorovich, I.A., Gray, D.K., Duggan, I.C., Colautti, R.I., and MacIsaac, H.J. 2003. Lake Superior: an invasion coldspot? Hydrobiologia, **499**: 191–210.

Harmois, E., Couture, R., and Magnan, P. 1992. Variation saisonnière dans la repartition des resources alimentaires entre cinq espèces de poissons en fonction de la disponibilité des proies. Can. J. Zool. **70**: 769–803.

Jażdżewski, K. 1980. Range extensions of some gammaridean species in European inland waters caused by human activity. Crustaceana, **6**(Suppl.): 84–107.

Köhn, J., and Waterstraat, A. 1990. The amphipod fauna of Lake Kummerow (Mecklenberg, German Democratic Republic) with reference to *Echinogammarus ischnus* Stebbing, 1899. Crustaceana, **58**: 74–82.

MacNeil, C., Elwood, R.W., and Dick, J.T.A. 1999. Differential microdistributions and interspecific interactions in coexisting *Gammarus* and *Crangonyx* amphipods. Ecography, **22**: 415–423.

MacNeil, C., Dick, J.T.A., Elwood, R.W., and Montgomery, W.I. 2001. Coexistence among native and introduced freshwater amphipods (Crustacea): habitat utilization patterns in littoral habitats. Arch. Hydrobiol. **151**: 591–607.

Nalepa, T.F., Schloesser, D.W., Pothoven, S.A., Hondorp, D.W., Fanslow, D.L., Tuchman, M.L., and Fleischer, G.W. 2001. First finding of the amphipod *Echinogammarus ischnus* and the mussel *Dreissena bugensis* in Lake Michigan. J. Gt. Lakes Res. **27**: 384–391.

Pothoven, S.A., Nalepa, T.F., and Brandt, S.B. 2000. Age-0 and age-1 yellow perch diet in southeastern Lake Michigan. J. Gt. Lakes Res. **26**: 235–239.

Ricciardi, A. 2001. Facilitative interactions among aquatic invaders: is an "invasional meltdown" occurring in the Great Lakes? Can. J. Fish. Aquat. Sci. **58**: 2513–2525.

Ricciardi, A. 2003. Predicting the impacts of an introduced species from its invasion history: an empirical approach applied to zebra mussel invasions. Freshw. Biol. **48**: 972–981.

Ricciardi, A. 2005. Facilitation and synergistic interactions among introduced aquatic species. *In* Invasive alien species: a new synthesis. *Edited by* H.A. Mooney, R.N. Mack, J. McNeely, L.E. Neville, P.J. Schei, and J.K. Waage. Island Press, Washington, D.C. In press.

Ricciardi, A., and Atkinson, S.K. 2004. Distinctiveness magnifies the impact of biological invaders in aquatic ecosystems. Ecol. Lett. **7**: 781–784.

Ricciardi, A., and MacIsaac, H.J. 2000. Recent mass invasion of the North American Great Lakes by Ponto-Caspian species. Trends Ecol. Evol. **15**: 62–65.

Ricciardi, A., Whoriskey, F.G., and Rasmussen, J.B. 1997. The role of the zebra mussel (*Dreissena polymorpha*) in structuring macroinvertebrate communities on hard substrata. Can. J. Fish. Aquat. Sci. **54**: 2596–2608.

Robinson, J.V., and Wellborn, G.A. 1988. Ecological resistance to the invasion of a freshwater clam, *Corbicula fluminea*: fish predation effects. Oecologia, **77**: 445–452.

Ryer, C.H. 1988. Pipefish foraging: effects of fish size, prey size, and altered habitat complexity. Mar. Ecol. Prog. Ser. **48**: 37–45.

SAS Institute Inc. 1999. SAS/STAT user's guide, release 8 ed. SAS Institute Inc., Cary, N.C.

Simberloff, D., and Von Holle, B. 1999. Positive interactions of nonindigenous species: invasional meltdown? Biol. Invasions, **1**: 21–32.

Sokal, R.R., and Rohlf, F.J. 1995. Biometry. 3rd ed. W.H. Freeman and Co., New York.

Stewart, T.W., and Haynes, J.M. 1994. Benthic macroinvertebrate communities of southwestern Lake Ontario following invasion of *Dreissena*. J. Gt. Lakes Res. **20**: 479–493.

Stewart, T.W., Miner, J.G., and Lowe, R.L. 1998*a*. An experimental analysis of crayfish (*Orconectes rusticus*) effects on a *Dreissena*-dominated benthic macroinvertebrate community in western Lake Erie. Can. J. Fish. Aquat. Sci. **55**: 1043–1050.

Stewart, T.W., Miner, J.G., and Lowe, R.L. 1998*b*. Macroinvertebrate communities on hard substrates in western Lake Erie: structuring effects of *Dreissena*. J. Gt. Lakes Res. **24**: 868–879.

Stewart, T.W., Miner, J.G., and Lowe, R.L. 1998*c*. Quantifying mechanisms for zebra mussel effects on benthic invertebrates: organic matter production and shell-generating habitat. J. N. Am. Benthol. Soc. **17**: 81–94.

Stewart, T.W., Miner, J.G., and Lowe, R.L. 1999. A field experiment to determine *Dreissena* and predator effects on zoobenthos in a nearshore, rocky habitat of western Lake Erie. J. N. Am. Benthol. Soc. **18**: 488–498.

Wisendon, P.A., and Bailey, R.C. 1995. Development of macroinvertebrate community structure associated with zebra mussel (*Dreissena polymorpha*) colonization of artificial substrates. Can. J. Zool. **73**: 1438–1443.

Witt, J.D.S., Hebert, P.D.N., and Morton, W.B. 1997. *Echinogammarus ischnus*: another crustacean invader in the Laurentian Great Lakes basin. Can. J. Fish. Aquat. Sci. **54**: 264–268.

Vanderploeg, H.A., Nalepa, T.F., Jude, D.J., Mills, E.L., Holeck, K.T., Liebig, J.R., Grigorovich, I.A., and Ojaveer, H. 2002. Dispersal and emerging ecological impacts of Ponto-Caspian species in the Laurentian Great Lakes. Can. J. Fish. Aquat. Sci. **59**: 1209–1228.

Van Overdijk, C., Grigorovich, I.A., Mabee, T., Ray, W.J., Ciborowski, J.J.H., and MacIsaac, H.J. 2003. Microhabitat selection by the invasive amphipod *Echinogammarus ischnus* and native *Gammarus fasciatus* in laboratory experiments and in Lake Erie. Freshw. Biol. **48**: 567–578.

© 2005 NRC Canada

Flexible diet and trophic position of dreissenid mussels as inferred from stable isotopes of carbon and nitrogen

David W. Garton, Christopher D. Payne, and Joseph P. Montoya

Abstract: In this study, the trophic position and food-web impacts of invading zebra mussels (*Dreissena polymorpha*) were investigated by sampling mussels, seston (= phytoplankton), macrophytes, zooplankton, and surficial sediment in two small inland lakes (1999–2002) and similarly in western Lake Erie (1999 only). Tissues from quagga mussels (*Dreissena bugensis*) from Lake Erie were also analyzed. Stable-isotope ratios ($^{15}N/^{14}N$ and $^{13}C/^{12}C$) were used to identify likely food sources and estimate relative trophic position. For Lake Erie, stable-isotope ratios indicated no diet differences between the two mussel species. For all lakes, zooplankton $\delta^{13}C$ was indicative of phytoplanktivory. The ^{13}C stable isotope ratios indicated that seston comprised ~50% of food sources for mussels in Lake Erie, but 73%–97% and 52%–100% of the diet of mussel populations in Lake Wawasee and Clark Lake, respectively. Stable nitrogen isotope ratios placed zooplankton at trophic levels equal to or higher than those of mussels in seven of eight comparisons. *Dreissena polymorpha* and *D. bugensis* are able to exploit suspended detritus as a significant energy source, as well as compete directly with zooplankton for seston as a food source and with each other in areas of sympatry.

Résumé : Nous avons étudié la position trophique et les impacts sur le réseau alimentaire des moules zébrées (*Dreissena polymorpha*) envahissantes en échantillonnant les moules, le seston (= phytoplancton), les macrophytes, le zooplancton et les sédiments de surface dans deux petits lacs continentaux (1999–2002) et aussi dans la région occidentale du lac Érié (seulement en 1999). Nous avons aussi analysé des tissus de *D. bugensis* (moule quagga) du lac Érié. Les rapports des isotopes stables $^{15}N/^{14}N$ et $^{13}C/^{12}C$ ont servi à identifier les sources probables de nourriture et à déterminer la position trophique moyenne. Au lac Érié, les rapports d'isotopes stables n'indiquent pas de différence dans les régimes alimentaires des deux espèces de moules. Dans tous les lacs, le $\delta^{13}C$ du zooplancton indique que celui-ci se nourrit de phytoplancton. Les rapports d'isotopes stables de ^{13}C montrent que le seston représente ~50 % des sources de nourriture des moules au lac Érié, mais respectivement 73–97 % et 52–100 % de celles des populations de moules des lacs Wawasee et Clark. Dans sept de huit comparaisons, les rapports d'isotopes stables de N placent le zooplancton au même niveau trophique que les moules ou à un niveau supérieur. Les moules *D. polymorpha* et *D. bugensis* sont donc capables d'utiliser le détritus en suspension comme source significative d'énergie; elles sont en compétition directe avec le zooplancton pour l'exploitation du seston comme source d'alimentation et sont en compétition l'une avec l'autre dans les zones de sympatrie.

[Traduit par la Rédaction]

Introduction

The introduction of dreissenid mussels (zebra mussel, *Dreissena polymorpha*, and quagga mussel, *Dreissena bugensis*) into North America in the late 1980s has resulted in significant changes in aquatic ecosystems (reviewed by MacIsaac 1996). In particular, *D. polymorpha* has spread widely and is now common throughout the Great Lakes, major river systems (St. Lawrence, Mississippi, Ohio, Tennessee, and Hudson rivers), and hundreds of smaller inland lakes and watersheds (Johnson and Carlton 1996). In the absence of significant control through natural predators, pathogens, or parasites, the explosive growth of *D. polymorpha* populations results in very high densities (>10 000 individuals·m^{-2}), often carpeting all suitable substrates in many invaded lakes and rivers (Mackie and Schloesser 1996). In contrast, *D. bugensis* is currently distributed throughout Lake Erie, Lake Ontario, and the St. Lawrence River, and recently Lake Michigan, but has not spread widely beyond the Great Lakes basin. There is a weak ecological separation between the two species, with *D. bugensis* replacing *D. polymorpha* in deeper, cooler water

Received 22 September 2003. Accepted 16 September 2004. Published on the NRC Research Press Web site at http://cjfas.nrc.ca on 27 May 2005.
J17754

D.W. Garton,[1] C.D. Payne,[2] and J.P. Montoya. School of Biology, Georgia Institute of Technology, 310 Ferst Drive, Atlanta, GA 30332, USA.

[1]Corresponding author (e-mail: david.garton@biology.gatech.edu).
[2]Present address: Earth and Ocean Sciences Department, University of British Columbia, 6339 Stores Road, Vancouver, BC V6T 1Z4, Canada.

 doi: 10.1139/F05-025 © 2005 NRC Canada

(Mills et al. 1993*a*); however, the two species do occur in sympatry in high abundance in shallow-water habitats (Berkman et al. 2000).

Dreissenid mussels are efficient filter-feeders, with both high clearance rates and high particle-retention efficiencies, that are capable of ingesting particles as small as bacterioplankton (Frischer et al. 2000). Increased water transparency and declines in phytoplankton abundance have followed the invasion of *D. polymorpha*, with concomitant decreases in zooplankton biomass and productivity as a consequence of direct competition for food sources (MacIsaac et al. 1992). For the western basin of Lake Erie, mathematical models and mussel physiological energy budgets agree in estimating that as much as 50% or more of annual phytoplankton production is consumed by benthic *D. polymorpha* populations (Madenjian 1995; Stoeckmann and Garton 1997). However, in spite of over a decade of intense grazing pressure on phytoplankton, populations of dreissenid mussels are continuing to expand at a very high rate (~1000 km^2·$year^{-1}$; Haltuch et al. 2000). This observation implies that alternative sources of organic matter are contributing to the sustained growth of mussel populations in Lake Erie.

Although well adapted to filter phytoplankton, dreissenid mussels can also consume bacteria and small organic particles efficiently (Frischer et al. 2000). Laboratory studies have demonstrated that mussels can feed on bacteria and suspended detritus, but the contribution of these resources to the energetics of natural populations has yet to be quantified. A significant potential source of carbon for mussel populations is the detritus resulting from bacterial colonization and degradation of macrophyte biomass. Macrophyte abundance often increases markedly in response to the increased water clarity resulting from mussel invasions (Sellinger and Quinn 2001). Although both *D. polymorpha* and *D. bugensis* occur in habitats where suspended detritus is available, and perhaps relatively abundant (Madon et al. 1998; Schneider et al. 1998), the actual contribution of detritus to the diets of dreissenid mussel remains unknown.

The ^{13}C content of a consumer corresponds to the ^{13}C content of its food, typically within 1 part per mil (‰) (DeNiro and Epstein 1978). Preferential excretion of ^{14}N via metabolic pathways leads to an enrichment of ^{15}N of approximately 3‰–4‰ per trophic level (DeNiro and Epstein 1981). Studies combining analysis of stable isotopes of carbon and nitrogen have proved useful in determining sources of dietary carbon and the trophic position of species within aquatic food webs (e.g., Vander Zanden and Rasmussen 1999; Vander Zanden et al. 2000). However, caution should be applied to interpreting the results of stable-isotope content, as tissue-specific stable-isotope ratios can vary within an organism, as well as lag changes in stable-isotope content of food sources as they vary over the season (e.g., Lorrain et al. (2002) and Vizzini and Mazzola (2003), respectively). Although stable carbon and nitrogen isotope contents respond to various environmental influences, they reflect food-web linkages reasonably well.

Quantifying impacts of invading organisms on the trophic dynamics of the invaded system is often limited by a lack of appropriate pre-invasion data. Hence, most estimates of the ecosystem-level impacts of *D. polymorpha* are derived from studies of mussel energetics (e.g., Stoeckmann and Garton 1997), ecological models (e.g., Madenjian 1995), and direct measurements of population responses of community members (e.g., phytoplankton, zooplankton, and fishes; Idrisi et al. 2001) to the dreissenid mussels. In this study we applied stable carbon and nitrogen isotope analyses of food webs in one large and two small midwestern lakes colonized by *D. bugensis* and *D. polymorpha* to determine (*i*) the relative contribution of phytoplankton- and macrophyte-derived carbon to dreissenid diets, (*ii*) whether or not *D. polymorpha* and *D. bugensis* partition energy resources within zones of sympatry, (*iii*) the extent of diet overlap between planktonic (zooplankton) grazers and benthic grazers (e.g., *D. polymorpha* and *D. bugensis*), and (*iv*) the trophic position of dreissenid mussels within invaded lake ecosystems.

Methods and materials

Study lakes

Three lakes were sampled during this study. Samples were collected from western Lake Erie at Ohio State University's F.T. Stone Laboratory on Gibraltar Island (41°38′N, 82°50′W). *Dreissena polymorpha* were first detected at this site in October 1988, within 4 months of the first identification of this species in North America (Lake St. Clair; Hebert et al. 1989). *Dreissena bugensis* also occurs in western Lake Erie, and the combined density of both species frequently exceeds 10 000 individuals·m^{-2}, with *D. polymorpha* accounting for 75% or more of the dreissenid community (Berkman et al. 2000). Western Lake Erie was sampled once during this study, in the fall of 1999.

Lake Wawasee is located in Kosciusko County, northern Indiana (41°20′N, 85°45′W). *Dreissena polymorpha* were first detected here in 1991 and within 4 years occupied all shallow-water habitats <10 m in depth, growing attached to macrophytes as well as to natural and artificial hard substrates. Peak mussel densities exceeded 70 000 individuals·m^{-2}, with an average of 11 350 individuals·m^{-2} in depths <7 m (Garton and Johnson 2000). Site 1 of Garton and Johnson (2000), located on the south shore of Lake Wawasee, was sampled early each fall (late September – early October) during this study (1999–2002).

Clark Lake is located in Jackson County, south-central Michigan (42°08′N, 84°10′W). *Dreissena polymorpha* were first reported in 1994. In contrast to Lakes Erie and Wawasee, mussel population growth was modest, with a peak mussel density of 6264 individuals·m^{-2} and an average density of 3678 individuals·m^{-2} within macrophyte beds, the major mussel habitat in this lake (D.W. Garton and L.E. Johnson, unpublished data). A site located on the north shore of Clark Lake was sampled early each fall in 1999–2002.

Dreissena bugensis was not observed in either Lake Wawasee or Clark Lake during the period 1994–2002. In all three lakes, dreissenid mussels are the dominant benthic macroinvertebrate.

Sample collection and handling

Organic carbon within these study lakes was assumed to be derived from two sources of primary production, phytoplankton and macrophytes. As filter-feeders, *D. polymorpha*

© 2005 NRC Canada

have direct access to suspended organic particles (live and dead phytoplankton, bacteria, fecal pellets, resuspended sediment, referred to collectively as seston in this paper, and with a stable carbon isotope ratio dominated by the contribution from phytoplankton). Organic carbon derived from macrophyte primary production becomes available to mussels only through a detritus pathway involving fungal and bacterial degradation of plant material into sufficiently small particles accumulating within the sediment, or perhaps as dissolved organic carbon (Roditi 2000). The stable carbon isotope content of living plants was used to identify the contribution of macrophyte primary production to mussel diets through the detritus pathway. Resuspended sediment detritus particles include organic carbon from both seston and macrophyte sources, and hence were not considered a distinct dietary source in the models discussed in the Results.

Replicate samples of seston (suspended live and dead phytoplankton) were collected by filtering raw surface-water (upper ~10 cm) samples through precombusted GF/F filters under gentle vacuum. The filters were air-dried at 60 °C and stored over desiccant until analysis. Water samples were filtered until the filter clogged, and the volume filtered was recorded. Seston and zooplankton samples were collected 100–250 m offshore (water depth >10 m) from the sites used for benthic sampling, which avoided any contamination of these samples by resuspended sediment.

Zooplankton was collected by means of 4-m vertical hauls of a 64-μm mesh plankton net. Concentrated zooplankton removed from the sample bucket was resuspended in approximately 500 mL of lake water. Using a stereomicroscope, live zooplankters were picked and placed on precombusted filters and then dried at 60 °C for stable-isotope analysis. A minimum of 50 live zooplankters representing the dominant cladocerans and copepods present at the time of collection were placed on each filter.

Mussels, sediment, and submerged macrophytes were collected from ~4 m depth in each lake using SCUBA. Within these inland lakes, few mussels or macrophytes occur below 5 m depth, thus samples collected at 4 m depth correspond to mussels, macrophytes, and sediment occurring in close proximity to each other (D.W. Garton and L.E. Johnson, personal observation). Clark Lake and Lake Wawasee stratify thermally briefly each summer, but western Lake Erie rarely stratifies; study lakes were not thermally stratified at the time of sample collections. Mussels were gently removed from their substrates and taken live to the laboratory. During the first year of the study, mussel tissues, representing gills, mantle, and viscera (gonad plus digestive gland), were analyzed separately to determine if isotope-turnover rates were uniform among tissues (tissue-specific analyses were not conducted in later years, as whole-body stable-isotope ratios were very similar to those of the viscera, the largest body component; see Results). Likewise, the influence of size (age) on the stable-isotope content of mussels collected in 2001 from Lake Wawassee and Clark Lake was also tested. Mussel tissues were dried at 60 °C and ground to a fine powder, which was subsampled for isotopic analysis. Approximately 0.5 mg of dry ground tissue was used for each stable-isotope analysis.

Surficial sediment (~upper 1 cm) was collected by hand, scooping unconsolidated material into small plastic bags. Rooted macrophytes were present at each sampling site, and care was taken to exclude visible plant fragments and roots from the sediment sample at the time of collection. Sediments were dried (60 °C), then treated with dilute HCl to remove carbonates, and approximately 3–5 mg was used for each stable-isotope analysis.

Macrophytes growing in each area of the sampling site were hand-collected. Upright, actively growing sections of plants were selected. In the field each plant species was placed in a separate plastic bag and later air-dried at 60 °C. Dried plant material was ground, then treated with dilute HCl to remove carbonates, and approximately 0.5–2.0 mg was used for stable-isotope analysis.

Stable carbon and nitrogen isotope analysis

Seston and zooplankton samples on filters were placed directly in tin capsules and pelletized for continuous-flow isotope-ratio mass spectrometry. Subsamples of ground mussel tissues were weighed using an electrobalance, then placed in tin capsules for pelletization. All natural abundance measurements were made by continuous-flow isotope-ratio mass spectrometry using a Micromass Optima interfaced to a Carlo Erba NC 2500 elemental analyzer for on-line combustion and purification of sample nitrogen and carbon.

All isotope abundances are expressed as $\delta^{15}N$ or $\delta^{13}C$ values relative to atmospheric nitrogen and Pee Dee Belemnite carbonate standard, respectively. Each analytical run included a size series of elemental (acetanilide) and isotopic (peptone) standards, which provided a check on the stability of the instrument and allowed us to remove the contribution of any analytical blank to our isotope measurements. In almost all cases, the nitrogen blank was trivially small relative to the samples run and a blank correction was unnecessary. In contrast, we routinely encountered a measurable carbon blank. We conservatively estimate that the overall analytical precision of our isotope measurements is better than ±0.3‰ for ^{15}N and better than ±0.2‰ for ^{13}C.

Statistical analysis

Differences in stable-isotope content of mussel tissues were tested using analysis of variance (ANOVA). Within each lake and for each year separately, ANOVA was used to test for differences among stable-isotope contents of whole mussels, seston, zooplankton, sediment, and the various plant species, as well as to estimate pooled variances for determining 95% confidence intervals of the means presented in the figures. Simple correlation was used to test the relationship between mussel size and stable-isotope ratio ($\delta^{13}C$ and $\delta^{15}N$, expressed relative to isotope standards (‰)). All statistical analyses and calculation of simple descriptive statistics (sample means and standard deviations presented in each table) were made using MINITAB® release 12 (Minitab Inc. 1998).

The appropriateness of applying ANOVA to stable carbon and nitrogen isotope content data was confirmed by examining standardized residuals (uniform pattern with fitted values), and the result of Bartlett's tests for homogeneous variance among tissues was not significant. When the two species were compared, homogeneity of variance was not confirmed. The stable carbon isotope content of the viscera of *D. polymorpha* had an extremely small range (only

© 2005 NRC Canada

Table 1. Stable-isotope ratios (mean and SD) for ^{15}N and ^{13}C from samples collected in western Lake Erie in early fall 1999; sources (A) were analyzed separately from tissue samples (B).

	$\delta^{15}N$ (‰)			$\delta^{13}C$ (‰)		
	Mean	SD	*n*	Mean	SD	*n*
(A) Sources						
Seston	6.69a	1.47	4	−23.87a	0.30	4
Zooplankton	17.52b	2.07	2	−23.59a	0.76	2
Sediment	4.09c	1.09	3	−22.02a	1.01	3
Vallisnaria sp.	8.10ad	0.07	2	−10.48b	0.10	2
Dreissena bugensis	8.89d	0.31	5	−17.65c	0.63	5
Dreissena polymorpha	8.79d	0.29	4	−17.39c	1.31	4
(B) Tissue samples						
D. bugensis						
Gill	10.22a	0.19	3	−17.62a	1.33	3
Mantle	9.18b	0.20	3	−18.38a	1.19	3
Viscera*	8.48c	0.31	3	−16.73a	2.43	3
D. polymorpha						
Gill	10.04a	0.06	3	−16.73a	0.05	3
Mantle	9.25b	1.10	3	−19.04b	1.60	3
Viscera*	8.46c	0.18	3	−16.58a	0.28	3

Note: SD is the standard deviation of the sample mean. Values followed by the same letter are not significantly different (Tukey's significant-difference test).

*Includes the digestive gland and gonad.

Fig. 1. Stable-isotope ratios for ^{15}N and ^{13}C in samples collected from western Lake Erie in fall 1999. Vertical and horizontal bars represent 95% confidence intervals about the mean, calculated using a pooled estimate of the standard deviation from analysis of variance.

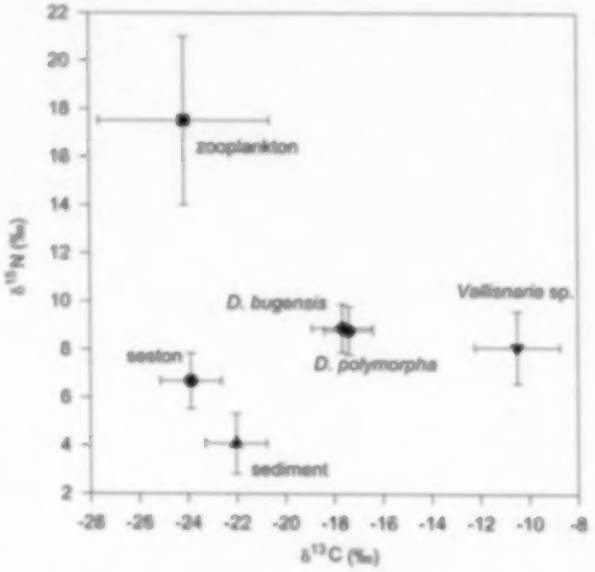

0.08‰ among three samples) and hence very low variance. As an alternative to the ANOVA approach, applying a nonparametric Kruskall–Wallis test yielded the same results for species and tissue effects on stable carbon and nitrogen isotope content. As sample sizes for all species and tissue combinations were small ($n = 3$ for each), a power analysis was performed for the effect of tissue on stable carbon and nitrogen isotope content. For stable nitrogen isotope content with $n = 6$ and sigma (from mean square error) = 0.24, power was 1.000, hence this analysis was a reasonable test for tissue effects. However, as a result of greater variance (sigma = 1.96) the power for the stable carbon isotope content analysis was only 0.33. Thus, a larger sample size (total $n = 17$, greater than the nine samples in this study) would be required to confirm that differences among tissue means for stable carbon isotope content were indeed not significant.

Results

Lake Erie

Stable-isotope ratios of samples collected from western Lake Erie (1999) varied significantly among sources (^{15}N content: $F_{[5,18]} = 60.0$, $p < 0.0001$; ^{13}C content: $F_{[5,18]} = 73.8$, $p < 0.0001$) (Table 1; Fig. 1). The whole-body $\delta^{13}C$ and $\delta^{15}N$ values for the two species of mussels were identical (the ANOVA result was not significant for both isotopes, $p < 0.850$ and $p < 0.852$, respectively), indicating that these two species occupy the same trophic level and consume the same diet (Fig. 1). This was also reflected in specific tissue stable-isotope ratios, which are identical for the two species (Table 1). Tissue $\delta^{15}N$ values varied significantly, with gills > mantle > viscera for both species (ANOVA, $F_{2,12} = 17.52$, $p < 0.001$), but tissue $\delta^{13}C$ values did not vary significantly among tissues (ANOVA, $p < 0.064$).

Stable carbon isotope ratios were similar for seston and zooplankton samples, −23.87‰ and −23.59‰, respectively, with sediment approximately 2‰ heavier (Table 1; Fig. 1). In contrast, *Vallisnaria* sp. samples were about 12‰ heavier (at −10.48‰; Table 1). Zooplankton ^{15}N ratios were highly enriched relative to seston (~10‰), whereas mussel tissues were enriched approximately 2‰ relative to seston and 1‰ relative to *Vallisnaria* sp. (Table 1). Stable carbon and nitrogen isotope ratios for macrophyte and sediment samples were dissimilar from each other and from those for seston (Table 1; Fig. 1). The shallow waters adjacent to the sampling site in Put-in-Bay, Ohio, were dominated by a near-100% forest of *Vallisnaria americana*.

Lake Wawasee

Results of stable-isotope analyses for samples collected from Lake Wawasee (1999–2002) revealed significant differences among sources for stable nitrogen and carbon isotope ratios (^{15}N: 2000, $F_{[5,11]} = 317.8$, $p < 0.0001$; 2001, $F_{[7,16]} = 103.1$, $p < 0.0001$; 2002, $F_{[6,31]} = 121.5$, $p < 0.0001$; ^{13}C: 2000, $F_{[5,12]} = 88.5$, $p < 0.0001$; 2001, $F_{[7,16]} = 429.6$, $p < 0.0001$; 2002, $F_{[6,22]} = 62.0$, $p < 0.0001$) (Table 2; Fig. 2). In contrast to Lake Erie samples, $\delta^{13}C$ values for mussel tissues lie much closer to those for seston than to those for macrophyte samples: within 1‰–4‰ of seston values but with a >10‰ difference from the overall average for macrophytes (Table 2). Consistently across all 3 years, zooplankton $\delta^{13}C$ values are similar to seston $\delta^{13}C$ values, within 1‰ for each year (Table 2). As was observed in Lake Erie samples, $\delta^{13}C$ for sediment samples is approximately 2‰–3‰ heavier than for seston samples (−25‰ to −26‰).

© 2005 NRC Canada

Table 2. Stable-isotope ratios for ^{15}N and ^{13}C (mean and SD) for samples collected from Lake Wawasee, Indiana, in early fall of 1999–2002.

		$\delta^{15}N$ (‰)			$\delta^{13}C$ (‰)		
Year	Source	Mean	SD	n	Mean	SD	n
1999	*D. polymorpha*	10.54	0.42	4	–28.47	0.73	4
2000	Seston	6.20a	0.44	3	–29.41a	0.84	4
	Zooplankton	12.42b	0.34	3	–28.96a	0.52	3
	Sediment	3.16c	0.31	2	–25.08b	0.57	2
	Chara sp.	5.61a	0.46	2	–13.68c	0.04	2
	Myriophyllum sp.	10.19d	0.04	2	–14.95c	0.04	2
	D. polymorpha	9.55d	0.14	5	–25.26b	1.78	5
2001	Seston	5.86a	0.54	2	–28.15a	0.35	2
	Zooplankton	9.99b	0.35	2	–28.63a	0.35	2
	Sediment	5.73a	0.18	2	–26.06b	0.68	2
	Chara sp.	5.82a	0.37	2	–14.33c	0.09	2
	Myriophyllum sp.	7.07c	0.12	2	–14.24c	0.06	2
	Potamogeton sp.	9.10b	0.13	2	–19.54d	0.14	2
	Ceratophyllum sp.	7.29c	0.44	2	–18.93d	0.12	2
	D. polymorpha	10.69b	0.42	10	–27.84a	0.58	10
2002	Seston	4.06a	0.87	2	–31.01a	0.15	2
	Zooplankton	6.91b	0.51	4	–30.99a	0.72	4
	Sediment	5.29a	0.51	9	–25.56b	0.23	3
	Potamogeton sp.	1.70c	0.50	4	–15.73cd	1.12	3
	Chara sp.	7.27b	0.33	4	–11.01d	0.97	4
	Myriophyllum sp.	4.81a	0.29	5	–16.09c	0.03	3
	D. polymorpha	9.87d	0.13	10	–28.46ab	0.90	10
	Average for all plants (2000–2002)	6.54			–15.12		

Note: SD is the standard deviation of the sample mean. Within each year, values followed by the same letter are not significantly different (Tukey's significant-difference test).

Macrophyte $\delta^{13}C$ values range from –14‰ to –20‰, but all are greater than seston and sediment $\delta^{13}C$ values.

Stable-isotope ratios displayed evidence of annual variation. The $\delta^{15}N$ values were greater for zooplankton than for *D. polymorpha* in samples collected in 2000 but not in 2001 or 2002. Stable nitrogen isotope values for *D. polymorpha* collected in 2000 indicated a lower trophic level than zooplankton; this pattern was reversed for 2001 samples (Fig. 2). The ^{15}N enrichment for zooplankton and mussel samples varied between 3‰ and 6‰ relative to seston throughout the sampling period (Table 2). Species-specific $\delta^{13}C$ values for macrophytes were consistent across years, but $\delta^{15}N$ values varied by up to 7‰.

Clark Lake

Results of stable-isotope analysis for samples collected from Clark Lake (1999–2002) show significant variation in stable nitrogen and carbon isotope ratio among sources (^{15}N: 2000, $F_{[6,12]} = 184.0$, $p < 0.0001$; 2001, $F_{[8,18]} = 146.9$, $p < 0.0001$; 2002, $F_{[3,29]} = 58.0$, $p < 0.0001$; ^{13}C: 2000, $F_{[6,12]} = 65.6$, $p < 0.0001$; 2001, $F_{[8,18]} = 201.9$, $p < 0.0001$; 2002, $F_{[8,22]} = 180.0$, $p < 0.0001$) (Table 3; Fig. 3). As with samples from Lake Wawasee, stable carbon isotope ratios for *D. polymorpha* fall much closer to seston than to macrophytes (with the exception of *Ceratophyllum* sp.; see Discussion), within 1‰–6‰ compared with 7‰–12‰, respectively (Table 3). In 2000, zooplankton $\delta^{13}C$ was similar to seston $\delta^{13}C$ (–30.51‰ and –30.18‰, respectively), but in 2001 and 2002, zooplankton $\delta^{13}C$ was 1.5‰–2.5‰ lighter than seston $\delta^{13}C$ (Table 3). Mussel-tissue $\delta^{13}C$ values followed the same interannual pattern as zooplankton values: for 2001 and 2002, $\delta^{13}C$ was 1‰–2.5‰ lighter than for seston samples (Table 3). *Ceratophyllum* sp. $\delta^{13}C$ was lighter than for other species of macrophytes, within 2‰–3‰ of mussels, sediment, and seston in 2000 and 2002 and very similar to seston and sediment in 2001 (Fig. 3). The 3‰–4‰ greater $\delta^{15}N$ values indicate a higher trophic position for zooplankton than for *D. polymorpha* for each year, with mussel ^{15}N enriched 1‰–4‰ relative to seston (Table 3). As in Lake Wawasee, $\delta^{13}C$ values for macrophyte species varied widely (approximately –13‰ to –26‰), reflecting a macrophyte community more diverse than in the other two lakes.

Mussel length – stable isotope relationship

There was a significant positive correlation between shell length and $\delta^{15}N$ for *D. polymorpha* collected from Clark Lake in fall 2001 ($r = 0.860$, $p < 0.001$, $n = 10$), but no relationship for Lake Wawasee mussels ($r = -0.058$, $p < 0.873$, $n = 10$). For both lakes, $\delta^{13}C$ was not significantly related to shell length (Clark Lake, $r = -0.497$, $p < 0.144$; Lake Wawasee, $r = -0.192$ and $p < 0.595$; $n = 10$ for both).

Estimates of dietary contributions of carbon

The contribution of seston and macrophytes to the diet of dreissenid mussels was estimated assuming a simple mass-

© 2005 NRC Canada

Fig. 2. Stable-isotope ratios for ^{15}N and ^{13}C in samples collected annually from Lake Wawasee in (*a*) 2000, (*b*) 2001, and (*c*) 2002. Vertical and horizontal bars represent 95% confidence intervals about the mean, calculated using a pooled estimate of the standard deviation from analysis of variance (*Cerato*, *Ceratophyllum* sp.; *Myrio*, *Myriophyllum* sp.; *Potamo*, *Potamogeton* sp.).

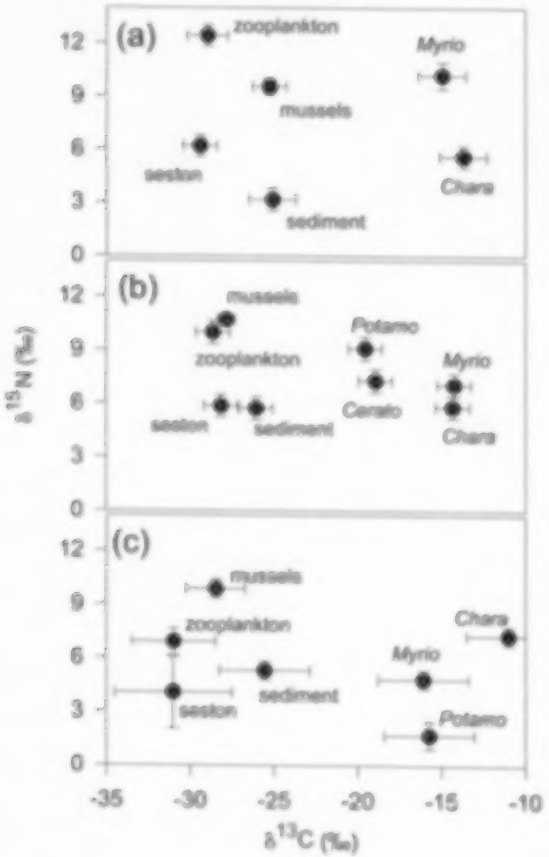

balance model with two compartments, seston and macrophytes, as ultimate sources of dietary carbon. For a nearshore habitat in western Lake Erie, assuming that seston ($\delta^{13}C = -23.87‰$) and detritus, derived from *Vallisneria* sp. ($\delta^{13}C = -10.48‰$), are the principal sources of carbon implies that seston constitutes 53% and suspended detritus 47% of the diets of dreissenid mussels in western Lake Erie.

The same calculations performed for each year separately reveal annual variation in the contribution of seston to mussel diets in the inland lakes. For Lake Wawasee, seston-derived carbon contributed an estimated 73%, 97%, and 85% of mussel diets in 2000, 2001, and 2002, respectively. In contrast, for Clark Lake, the seston contribution to mussel diets fluctuated, from 52% for 2000 to >100% for 2001 and 2002. The $\delta^{13}C$ measured for seston collected in 2001 and 2002 in Clark Lake was heavier than both zooplankton and *D. polymorpha* tissues. This may reflect different time courses for turnover within these carbon pools, with $\delta^{13}C$ of zooplankton and zebra mussels lagging changes in the seston (see Discussion).

Discussion

The major components of primary production within the aquatic food webs in each of the three study lakes were isotopically distinct, permitting identification of putative dietary sources in dreissenid mussels. Based on stable-isotope content, sympatric populations of *D. polymorpha* and *D. bugensis* in Lake Erie occupy apparently identical niches, and do not rely as much upon seston-derived carbon as a food source as *D. polymorpha* populations in Lake Wawasee and Clark Lake. The high degree of similarity between mussel-tissue and seston $\delta^{13}C$ values confirms that in the latter two lakes, *D. polymorpha* relies much more heavily on seston as an energy source (ranging from 73% to 97% and from 52% to 100% for Lake Wawasee and Clark Lake, respectively) than in Lake Erie (53%). Stable nitrogen isotope ratios of mussel tissues relative to dietary sources also vary across the three study lakes. The apparent trophic position of *D. polymorpha* and *D. bugensis*, as indicated by their $\delta^{15}N$ values relative to those of zooplankton and seston, is lower in Lake Erie than in Lake Wawasee or Clark Lake, perhaps reflecting their greater reliance on non-seston food sources.

Broad inferences concerning diet composition must be qualified by those factors known to influence the dynamics of stable isotopes of carbon and nitrogen within aquatic food webs. Estimates of the relative contributions of different dietary sources of carbon based on stable-isotope ratios are sensitive to seasonal variation of pCO_2, species composition of the diet, growth rate of organisms, and time courses for these changes to propagate through trophic levels (Zohary et al. 1994; Leggett et al. 1999; Vizzini and Mazzola 2003). Stable carbon isotope ratios in seston fluctuate up to 3.5‰ between seasons, with changes in higher trophic levels lagging changes in lower trophic levels (Vizzini and Mazzola 2003). Similarly, temporal and among-lake variability in $\delta^{13}C$ and $\delta^{15}N$ values has been described for zooplankton taxa (Gu et al. 1999; Matthews and Mazumder 2003). In this study, samples were collected annually in the fall, thus the magnitude of seasonal changes in stable-isotope ratios cannot be assessed. An indication of the magnitude of seasonal changes in isotope ratios is provided by a separate study in which stable carbon and nitrogen isotope ratios were determined for food-web compartments in Clark Lake during the summer of 2001 (A. Wilson, School of Biology, Georgia Institute of Technology, Atlanta, unpublished data). The $\delta^{13}C$ values for Clark Lake seston were 1.5‰ lighter in the summer than in the fall; likewise, zooplankton and mussel-tissue samples were also isotopically lighter than those collected 3 months later as part of this study. The lighter isotope ratios of zooplankton and *D. polymorpha* observed in Clark Lake in 2001 and 2002 are thus interpreted as lagging modest seasonal changes in seston $\delta^{13}C$.

Stable isotopes of carbon and nitrogen are subject to fractionation by bacterial processes during the decomposition of macrophytes, as well as by seston settling onto the sediment surface. Macrophyte-derived carbon becomes accessible to filter-feeding mussels via the formation of organic detritus

© 2005 NRC Canada

Table 3. Stable-isotope ratios for ^{15}N and ^{13}C (mean and SD) for samples collected from Clark Lake, Michigan, in early fall of 1999–2002.

Year	Source	$\delta^{15}N$ (‰)			$\delta^{13}C$ (‰)		
		Mean	SD	n	Mean	SD	n
1999	*D. polymorpha*	4.30	0.28	4	–29.12	0.39	4
2000	Seston	2.51a	0.59	2	–30.18a	0.28	4
	Zooplankton	6.65b	0.60	3	–30.51a	0.37	3
	Sediment	1.41ac	0.25	3	–26.72b	0.45	3
	Ceratophyllum sp.	1.16c	0.26	2	–24.17b	0.19	2
	Vallisnaria sp.	4.66d	0.04	2	–16.32c	0.10	2
	Potamogeton sp.	–3.96e	0.11	2	–14.05c	0.09	2
	D. polymorpha	3.84d	0.34	5	–24.37b	1.99	5
2001	Seston	0.33a	0.70	2	–27.46a	0.39	2
	Zooplankton	9.62b	0.80	2	–30.01b	0.35	2
	Sediment	1.59a	0.46	2	–26.66a	0.75	2
	Ceratophyllum sp.	0.00ac	0.37	2	–26.65a	0.16	2
	Vallisnaria sp.	0.94a	0.21	2	–17.57c	0.02	2
	Potamogeton sp. 1	–5.00d	0.06	2	–14.64d	0.01	2
	Chara sp.	–1.90c	1.10	2	–16.13cd	0.06	2
	Nitella sp.	5.09e	0.35	2	–22.03e	0.06	2
	D. polymorpha	4.98e	0.51	10	–30.18b	0.94	10
2002	Seston	0.50ab	2.29	2	–28.57a	0.24	2
	Zooplankton	6.27c	1.14	2	–30.20a	0.11	2
	Sediment	1.88ad	0.38	8	–28.03a	0.16	2
	Ceratophyllum sp.	–1.98b	0.11	4	–23.61b	0.38	4
	Myriophyllum sp.	2.05d	0.21	4	–14.65c	1.10	4
	Vallisnaria sp.	1.86ad	0.05	5	–14.65c	0.37	5
	Potamogeton sp. 1	–5.00e	0.28	4	–14.42c	0.78	3
	Potamogeton sp. 2	1.26ad	0.18	4	–12.59c	0.37	4
	D. polymorpha	2.94d	0.29	5	–29.09a	0.23	5
	Average for all plants (2000–2002)	0.05			–17.85		

Note: SD is the standard deviation of the sample mean. Within each year, values followed by the same letter are not significantly different (Tukey's significant-difference test).

as the plants decompose, and suspension of these particles in the water column. Certain groups of bacteria, e.g., methanogens, can create isotopically light particulate organic carbon (up to –60‰) (Grey et al. 2004). However, all sediment samples were collected at 4 m depth, in the epilimnion, and $\delta^{13}C$ values for sediment samples in these three study lakes were consistently lighter than those for macrophytes but never isotopically lighter than those for seston samples (although at times they were very similar). Hence, calculations used for estimating the contribution of macrophyte-derived carbon this study have assumed no significant fractionation of ^{13}C by bacteria.

Similar to the temporal variation in $\delta^{13}C$ values, $\delta^{15}N$ baseline values for certain taxa (e.g., zooplankton) also varied among lakes (e.g., Matthews and Mazumder 2003). This likely reflects spatial as well as temporal variation of ^{15}N inputs as a function of watershed dynamics, surface versus subsurface water sources, and anthropogenic inputs of nitrogen. Thus, for this study, inferences regarding trophic position of mussels have been made relative to internal ^{15}N baseline values within each lake. Additionally, any differences in turnover rates of nitrogen pools within zooplankton and mussels would lead to apparent differences in trophic level, but quantifying this effect would require additional study of the dynamics of ^{15}N turnover within mussels relative to zooplankton.

The mass-balance models described in Results assume that annual carbon production rates for macrophytes, and their subsequent contributions to suspended detritus accessible to filtering mussels, are equal. A negligible contribution of carbon via primary production on the sediment surface relative to macrophytes and plankton is also assumed, thus simplifying these calculations to identify putative carbon sources. Biomass and carbon fixation among macrophyte species are expected to vary, thus influencing estimates of detrital contributions to mussel diets, as $\delta^{13}C$ of macrophytes is likewise species-dependent. However, the sensitivity of the mass-balance model to variation in $\delta^{13}C$ among macrophytes can be assessed by arbitrarily weighting the contribution of macrophyte species to annual carbon production. For Lake Wawassee, if it is assumed that the two isotopically lighter species (*Potamogeton* sp. and *Ceratophyllum* sp.) collectively fix three times the carbon of the two "heavier" species (*Chara* sp. and *Myriophyllum* sp.) (weighting factors 0.375, 0.375, 0.125, and 0.125, respectively), then the contribution of seston carbon to mussel diets declines only slightly, from 84% to 81%. The same analysis applied to data from Clark Lake, where two species of

© 2005 NRC Canada

Fig. 3. Stable-isotope ratios for ^{15}N and ^{13}C in samples collected annually from Clark Lake in (*a*) 2000, (*b*) 2001, and (*c*) 2002. Vertical and horizontal bars represent 95% confidence intervals about the mean, calculated using a pooled estimate of the standard deviation from analysis of variance (*Cerato*, *Ceratophyllum* sp.; *Myrio*, *Myriophyllum* sp.; *Potamo* 1, *Potamogeton* sp. 1; *Potamo* 2, *Potamogeton* sp. 2; *Val*, *Vallisneria* sp.).

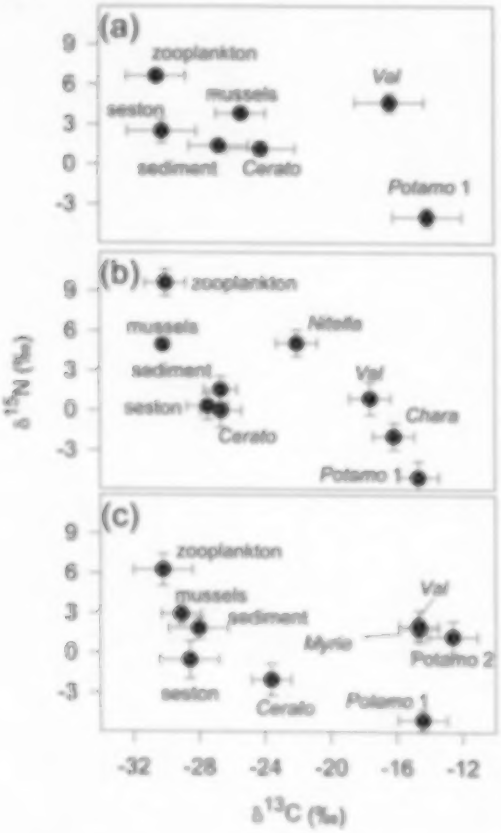

macrophytes have $\delta^{13}C$ values similar to that of seston (weighting factors 0.375 for both *Ceratophyllum* sp. and *Nitella* sp. and 0.05 for each of the remaining five plant species), reduces the contribution of seston to mussel diets from 92% to 84%. Thus, increasing the contribution of macrophyte species with carbon-isotope ratios more similar to that of seston does not significantly alter the interpretation that mussels in these two lakes rely heavily on seston as a food source.

Intra- and Inter-specific competition

The presence of a second dreissenid species in the North American Great Lakes was first noted in 1991 (May and Marsden 1992), and subsequently this species was confirmed to be *D. bugensis* (Spidle et al. 1994). From surveys in Lakes Erie and Ontario it was determined that *D. bugensis* replaced *D. polymorpha* as water depth increased, implying that physiological differences may be responsible for an ecological separation between the two species (Mills et al. 1993*a*). However, in many shallow-water habitats of Lakes Erie and Ontario, *D. bugensis* are much more numerous than *D. polymorpha* (Department of Fisheries and Oceans Canada 2000). Larvae of *D. bugensis* have been shown to mature and settle at a larger size than larvae of *D. polymorpha* (Martel et al. 2001), which may provide a competitive edge, and the range of *D. bugensis* has been expanding at the expense of *D. polymorpha* in the Ukraine (Mills et al. 1996) and western Lake Erie (Stoeckmann 2003). The results of this study confirm that these two species have nearly identical diets, and hence in areas of sympatry will experience strong, direct competition for resources.

The identical $\delta^{13}C$ values confirm that zooplankters (composed of cladocerans and copepods) were obligate consumers of seston (phytoplankton). These results agree with the $\delta^{13}C$ relationship between zooplankton and seston reported by Mitchell et al. (1996) for Oneida Lake in New York State. The consistency of the zooplankton–seston relationship provides a benchmark for interpreting $\delta^{13}C$ values for mussel tissues. In the case of Lake Erie, it is clear that seston is not as important in the diets of dreissenid mussels as in other inland lakes (Mitchell et al. 1996; this study), and thus for smaller lake systems, direct competition occurs between mussels and zooplankton for planktonic primary production.

In this study there was a very large difference in $\delta^{15}N$ values between zooplankton and seston (>10‰) in Lake Erie, much greater than the usual range of 3‰–4‰ per trophic level (DeNiro and Epstein 1981; Cabana and Rasmussen 1994). Likewise, the difference in trophic $\delta^{15}N$ between zooplankton and seston was larger than expected in Lake Wawasee and Clark Lake, averaging 4.41‰ and 6.73‰, respectively. These differences were much greater than those reported between *Daphnia* sp. and seston in Oneida Lake (~2‰), a lake also invaded by *D. polymorpha* (Mitchell et al. 1996). Higher than expected $\delta^{15}N$ values have been observed for zooplankton under nutritional stress, requiring greater turnover rates of intracellular pools of nitrogen, thus enriching tissue $\delta^{15}N$ (Adams and Sterner 2000). Without additional information on seasonal patterns of carbon- and nitrogen-isotope ratios, coupled with measures of food quantity and quality, it is not possible to determine likely causes of the exceptionally large trophic differences in $\delta^{15}N$ observed between zooplankton and seston in western Lake Erie.

Occupation of different microhabitats may also have a significant influence on the diets of dreissenid mussels. In western Lake Erie, nearly all mussels live attached directly to the benthos, occupying both hard and soft substrates (Berkman et al. 2000). In smaller inland lakes (e.g., Lake Wawasee and Clark Lake), macrophytes are the primary substrate colonized by mussels, which allows direct access to seston in the water column as well as possibly reducing access to suspended detritus. Although western Lake Erie is a very large (~5000 km^2) and shallow (average depth 8 m) basin, the water column is not completely mixed, thus restricting access of benthic mussels to seston and creating a chlorophyll *a*-depleted zone 2 m above the bottom (Ackerman et al. 2001). Perhaps reflecting differences in microhabitats, the data in this study show that Lake Erie mussels are more reliant on macrophyte-derived detritus as a

© 2005 NRC Canada

dietary source than mussels associated with macrophyte beds in the smaller inland lakes.

Within-mussel variation in stable-isotope ratios

Tissue-specific $\delta^{15}N$ ratios did not differ significantly between *D. bugensis* and *D. polymorpha*, but among-tissue differences in $\delta^{15}N$ ratios were significant, with gills > mantle > viscera. These differences likely reflect metabolic turnover rates of intracellular pools of nitrogen, as $\delta^{15}N$ increases with turnover rate (Adams and Sterner 2000). For mussels, the metabolically active tissues are the gills, which generate continuous water flow for feeding and gas exchange, and the mantle, which is responsible for shell secretion. The viscera comprise mainly the digestive gland and gonad. The reproductive cycle drives the metabolic activity of the gonad, and for dreissenid mussels reproduction peaks in early summer and the gonad is much reduced during the fall (Haag and Garton 1992), the period when samples were collected for this study. As the major portion of soft-tissue mass in mussels is the viscera, whole-body $\delta^{15}N$ values were similar to those for the viscera.

A size-specific relationship was detected for $\delta^{15}N$ ratios in Clark Lake mussels but not in mussels collected from Lake Wawasee. As age increases with size, this relationship may reflect annual differences in the $\delta^{15}N$ ratios of inorganic nitrogen sources utilized by seston. Between 2000 and 2001 there was a greater decline of the $\delta^{15}N$ ratios for seston in Clark Lake (from 2.51‰ to 0.33‰) than in Lake Wawasee (from 6.20‰ to 5.86‰), thus younger (smaller) *D. polymorpha* in Clark Lake would have lower $\delta^{15}N$ ratios than older (larger) mussels. In contrast to $\delta^{15}N$ ratios, no significant differences in $\delta^{13}C$ ratios were detected among tissues or associated with mussel age/size.

Implications for food-web dynamics in western Lake Erie

The potential impact of filter feeding by *D. polymorpha* and *D. bugensis* in diverting energy from pelagic to benthic food webs has attracted considerable attention, especially in the highly productive western basin of Lake Erie. It has been difficult to quantify total consumption by mussels, owing to the dynamic and seasonally variable rates of mussel-community grazing combined with a lack of comprehensive estimates of total primary production across the 5000-km^2 basin. Total consumption by mussels has been estimated indirectly using energetic models (e.g., Madenjian 1995) and direct measurements of growth, metabolic rate, and reproductive output (e.g., Stoeckmann and Garton 1997). The two approaches have yielded similar results, and these imply that existing mussel populations require energy equivalent to 12%–60% (reflecting the lower to upper limits of estimates of mussel-population density) of total annual primary production in western Lake Erie (Stoeckmann and Garton 1997). However, stable-isotope analysis in this study has revealed that in western Lake Erie only about one-half of dreissenid mussel diets is actually composed of phytoplankton. Initial concern regarding the potential collapse of pelagic-based food webs in Lake Erie has proved to be unfounded, principally because access of benthic mussels to suspended phytoplankton is limited. However, by exploiting alternative food sources, mussel populations have apparently not been limited in their growth and stability by the lack of full access to phytoplankton, as they are continuing to expand (Haltuch et al. 2000). As a result, productive pelagic and benthic communities currently co-exist in western Lake Erie, which represents a fundamental change from the ecosystem dominated by pelagic production that existed prior to the invasion by dreissenid mussels.

Stable isotopes have been used to demonstrate the impact of an invader on the diet and trophic position of native species (e.g., Vander Zanden and Rasmussen 1999; Vander Zanden et al. 1999, 2000). Changes in trophic position and sources of dietary carbon have been identified in lake trout (*Salvelinus namaycush*) following invasion by smallmouth bass (*Micropterus dolomieu*) in Canadian lakes (Vander Zanden et al. 1999). For this study, data are lacking regarding pre-invasion trophic dynamics (as indicated by stable isotopes) for these lakes. However, $\delta^{15}N$ and $\delta^{13}C$ ratios allow the impact of invasive mussels on food-web dynamics to be assessed, and provide a benchmark for comparison with lake systems not yet invaded. As expected, stable-isotope ratios reveal direct competition between mussels and zooplankton for seston, particularly within the two smaller study lakes. The significance of detritus in the diets of *D. bugensis* and *D. polymorpha* in Lake Erie reflects the flexibility and filtration efficiency of these two species, previously suggested only by laboratory studies (Frischer et al. 2000) but now confirmed as an important autecological feature contributing to the spectacular success of these invading organisms. This study further demonstrates the potential for stable-isotope ratios of carbon and nitrogen for studying the impact of invasive species on aquatic ecosystems, which has become a serious issue for North America during the past two decades (Mills et al. 1993*b*).

Acknowledgments

Mr. John Hageman and the staff of Ohio State University's F.T. Stone Laboratory kindly assisted in the collection of samples from western Lake Erie. The Wawasee Property Owners' Association, Wawasee Area Conservation Foundation, and Griffith's Wawasee Marina have provided continued support for our work on Lake Wawasee. Mr. John Kopplin and Mr. Vic Morrow kindly assisted in the collection of samples from Clark Lake. We thank Dr. Ladd Johnson, Laval University, Quebec, for assistance during the collection of samples from all three study lakes, and Mr. Alan Wilson, Georgia Institute of Technology, for sharing portions of his unpublished data for Clark Lake.

References

Ackerman, J.D., Loewen, M.R., and Hamblin, P.F. 2001. Benthic–pelagic coupling over a zebra mussel reef in western Lake Erie. Limnol. Oceanogr. **46**: 892–904.

Adams, T.S., and Sterner, R.W. 2000. The effect of dietary nitrogen content on trophic level ^{15}N enrichment. Limnol. Oceanogr. **45**: 601–607.

Berkman, P.A., Garton, D.W., Haltuch, M.A., Kennedy, G.W., and Febo, L.R. 2000. Habitat shift in invading species: zebra and quagga mussel population characteristics on shallow soft substrates. Biol. Invasions, **2**: 1–6.

© 2005 NRC Canada

Cabana, G., and Rasmussen, J.B. 1994. Modelling food chain structure and contaminant bioaccumulation using stable nitrogen isotopes. Nature (Lond.), **372**: 255–257.

DeNiro, M.J., and Epstein, S. 1978. Influence of diet on the distribution of carbon isotopes in animals. Geochem. Cosmochim. Acta, **42**: 495–506.

DeNiro, M.J., and Epstein, S. 1981. Influence of diet on the distribution of nitrogen isotopes in animals. Geochem. Cosmochim. Acta, **45**: 341–353.

Department of Fisheries and Oceans Canada. 2000. Zebra (*Dreissena polymorpha*) and quagga mussel (*Dreissena bugensis*) distribution and density in Lake Erie 1992–1998. Can. Tech. Rep. Fish. Aquat. Sci. No. 2304.

Fischer, M.E., Nierzwicki-Bauer, S.A., Parsons, R.H., Vathanodorn, K., and Waitkus, K.R. 2000. Interactions between zebra mussels (*Dreissena polymorpha*) and microbial communities. Can. J. Fish. Aquat. Sci. **57**: 591–599.

Garton, D.W., and Johnson, L.E. 2000. Variation in growth rates of the zebra mussel, *Dreissena polymorpha*, within Lake Wawasee. Freshw. Biol. **45**: 443–451.

Grey, J., Kelly, A., and Jones, R. 2004. High intraspecific variability in carbon and nitrogen stable isotope ratios of lake chironomid larvae. Limnol. Oceanogr. **49**: 239–244.

Gu, B., Alexander, V., and Schell, D. 1999. Seasonal and interannual variability of plankton carbon isotope ratios in a subarctic lake. Freshw. Biol. **42**: 417–426.

Haag, W.R., and Garton, D.W. 1992. Synchronous spawning in a recently established population of the zebra mussel, *Dreissena polymorpha*, in western Lake Erie, USA. Hydrobiologia, **234**: 103–110.

Haltuch, M.A., Berkman, P.A., and Garton, D.W. 2000. Geographic information system (GIS) analysis of ecosystem invasion: exotic mussels in Lake Erie. Limnol. Oceanogr. **45**: 1778–1787.

Hebert, P.D.N., Muncaster, B.W., and Mackie, G.L. 1989. Ecological and genetic studies on *Dreissena polymorpha* (Pallas): a new mollusc in the Great Lakes. Can. J. Fish. Aquat. Sci. **46**: 1587–1591.

Idrisi, N., Mills, E.L., Rudstam, L.G., and Stewart, D.J. 2001. Impact of zebra mussels (*Dreissena polymorpha*) on the pelagic lower trophic levels of Oneida Lake, New York. Can. J. Fish. Aquat. Sci. **58**: 1430–1441.

Johnson, L.E., and Carlton, J. 1996. Post-establishment spread in large-scale invasions: dispersal mechanisms of the zebra mussel, *Dreissena polymorpha*. Ecology, **77**: 1686–1690.

Leggett, M.F., Servos, M.R., Hesslein, R., Johansson, O., Millard, E.S., and Dixon, D.G. 1999. Biogeochemical influences on the carbon isotope signatures of Lake Ontario biota. Can. J. Fish. Aquat. Sci. **56**: 2211–2218.

Lorrain, A., Paulet, Y.-M., Chauvaud, L., Savoye, N., Donval, A., and Saout, C. 2002. Differential $\delta^{13}C$ and $\delta^{15}N$ signatures among scallop tissues: implications for ecology and physiology. J. Exp. Mar. Biol. Ecol. **275**: 47–61.

MacIsaac, H.J. 1996. Potential biotic and abiotic impacts of zebra mussels on the inland waters of North America. Am. Zool. **36**: 339–363.

MacIsaac, H.J., Sprules, W.G., Johansson, O.E., and Leach, J.H. 1992. Filtering impacts of larval and sessile zebra mussels (*Dreissena polymorpha*) in western Lake Erie. Oecologia, **92**: 30–39.

Mackie, G.L., and Schloesser, D.W. 1996. Comparative biology of zebra mussels in Europe and North America: an overview. Am. Zool. **36**: 244–258.

Madenjian, C.P. 1995. Removal of algae by the zebra mussel (*Dreissena polymorpha*) population in western Lake Erie: a bioenergetics approach. Can. J. Fish. Aquat. Sci. **52**: 381–390.

Madon, S.P., Schneider, D.W., Stoeckel, J.A., and Sparks, R.A. 1998. Effects of inorganic sediment and food concentrations on energetic processes of the zebra mussel, *Dreissena polymorpha*: implications for growth in turbid rivers. Can. J. Fish. Aquat. Sci. **55**: 401–413.

Martel, A.L., Baldwin, B.S., Dermott,R.M., and Lutz, R.A. 2001. Species and epilimnion/hypolimnion-related differences in size at larval settlement and metamorphosis in *Dreissena* (Bivalvia). Limnol. Oceanogr. **46**: 707–713.

Matthews, B., and Mazumder, A. 2003. Compositional and interlake variability of zooplankton affect baseline stable isotope signatures. Limnol. Oceangr. **48**: 1977–1987.

May, B., and Marsden, J.E. 1992. Genetic identification and implications of another invasive species of dreissenid mussel in the Great Lakes. Can. J. Fish. Aquat. Sci. **49**: 1501–1506.

Mills, E.L., Dermott, R.M., Roseman, E.F., Dustin, D., Mellina, E., Conn, D.B., and Spidle, A. 1993*a*. Colonization, ecology, and population structure of the quagga mussel in the lower Great Lakes. Can. J. Fish. Aquat. Sci. **50**: 2305–2314.

Mills, E.L., Leach, J.H., Carlton, J.T., and Secor, C.L. 1993*b*. Exotic species in the Great Lakes: a history of biotic crises and anthropogenic introductions. J. Gt. Lakes Res. **19**: 1–54.

Mills, E.L., Rosenberg, G., Spidle, A.P., Ludyanskiy, M., Pligin, Y., and May, B. 1996. A review of the biology and ecology of the quagga mussel (*Dreissena bugensis*), a second species of freshwater dreissenid introduced to North America. Am. Zool. **36**: 271–286.

Minitab Inc. 1998. MINITAB® Release 12 [computer program]. Minitab Inc., State College, Pa.

Mitchell, M.J., Mills, E.L., Idrisi, N., and Michener, R. 1996. Stable isotopes of nitrogen and carbon in an aquatic food web recently invaded by *Dreissena polymorpha* (Pallas). Can. J. Fish. Aquat. Sci. **53**: 1445–1450.

Roditi, H.A., Fisher, N.S., and Sanudo-Wilhelmy, S.A. 2000. Uptake of dissolved organic carbon and trace elements by zebra mussels. Nature (Lond.), **407**: 78–80.

Schneider, D.W., Madon, S.P., Stoeckel, J.A., and Sparks, R.E. 1998. Seston quality controls zebra mussel (*Dreissena polymorpha*) energetics in turbid rivers. Oecologia, **117**: 331–341.

Sellinger, C.E., and Quinn, F.H. 2001. Assessment of impacts of increased weed growth on Detroit River flows. NOAA Tech. Mem. ERL GLERL 119.

Spidle, A., Marsden, J.E., and May, B. 1994. Identification of the Great Lakes quagga mussel as *Dreissena bugensis* from the Dneipr River, Ukraine, on the basis of allozyme variation. Can. J. Fish. Aquat. Sci. **51**: 1485–1489.

Stoeckmann, A. 2003. Physiological energetics of Lake Erie dreissenid mussels: a basis for the displacement of *Dreissena polymorpha* by *Dreissena bugensis*. Can. J. Fish. Aquat. Sci. **60**: 126–134.

Stoeckmann, A., and Garton, D.W. 1997. A seasonal energy budget for zebra mussels (*Dreissena polymorpha*) in western Lake Erie. Can. J. Fish. Aquat. Sci. **54**: 2743–2751.

Vander Zanden, M.J., and Rasmussen, J.B. 1999. Primary consumer $\delta^{15}N$ and $\delta^{13}C$ and the trophic position of aquatic consumers. Ecology, **80**: 1395–1404.

Vander Zanden, M.J., Casselman, J.M., and Rasmussen, J.B. 1999. Stable isotope evidence for food web consequences of species invasions in lakes. Nature (Lond.), **401**: 467–469.

Vander Zanden, M.J., Shuter, B.J., Lester, N.P., and Rasmussen, J.B. 2000. Within- and among-population variation in the trophic posi-

© 2005 NRC Canada

tion of a pelagic predator, lake trout (*Salvelinus namaycush*). Can. J. Fish. Aquat. Sci. **57**: 725–731.

Vizzini, S., and Mazzola, A. 2003. Seasonal variations in the stable carbon and nitrogen isotope ratios ($^{13}C/^{12}C$ and $^{15}N/^{14}N$) of primary producers and consumers in a western Mediterranean coastal lagoon. Mar. Biol. (Berl.), **142**: 1009–1018.

Zohary, T., Erez, J., Gophen, M., Berman-Frank, I., and Stiller, M. 1994. Seasonality of stable carbon isotopes within the pelagic food web of Lake Kinneret. Limnol. Oceanogr. **39**: 1030–1043.

© 2005 NRC Canada

Inferring the depth distribution of catchability for pelagic fishes and correcting for variations in the depth of longline fishing gear

Peter Ward and Ransom A. Myers

Abstract: We introduce a new method that uses generalized linear mixed models to infer the depth distribution of pelagic fishes. It uses existing data from research surveys and observers on commercial vessels to estimate changes in catchability when longline fishing gear is lengthened to access deeper water. We infer the depth distribution of catchability for 37 fish species that are caught on pelagic longlines in the Pacific Ocean. We show how the estimates of catchability can be used to correct abundance indices for variations in longline depth. Our method facilitates the inclusion of data from early surveys in the time series of commercial catch rates used to estimate abundance. It also resolves inconsistencies in the time series caused by a rapid switch to deep longlining in the 1970s. The catchability distribution does not always match depth preferences derived from tracking studies. Therefore, depth preferences from tracking studies should not be used to correct abundance indices without additional information on feeding behavior.

Résumé : Nous présentons une nouvelle méthode qui utilise des modèles linéaires généralisés mixtes pour estimer la répartition des poissons pélagiques en fonction de la profondeur. La méthode exploite les données existantes d'inventaires scientifiques et d'observations faites sur les navires commerciaux afin d'estimer les changements de capturabilité qui se produisent lorsqu'on allonge les palangres pour pêcher en eau plus profonde. Nous estimons la répartition de la capturabilité en fonction de la profondeur chez 37 espèces de poissons récoltés à la palangre pélagique dans le Pacifique. Nous démontrons comment les estimations de capturabilité peuvent servir à corriger les indices d'abondance en fonction des variations de la profondeur des palangres. Notre méthode facilite l'inclusion de données d'inventaires plus anciens dans la série chronologique de taux de capture commerciaux utilisée pour estimer l'abondance. Elle permet aussi de résoudre les irrégularités dans la série chronologique causées par un passage rapide à la pêche à la palangre en profondeur durant les années 1970. La répartition de la capturabilité ne correspond pas toujours aux préférences de profondeur déterminées par les études qui traquent les poissons; il ne faut donc pas utiliser les préférences de profondeurs obtenues de ces études pour corriger les indices d'abondance s'il n'existe pas de renseignements supplémentaires sur le comportement alimentaire.

[Traduit par la Rédaction]

Introduction

Recent analyses indicate that the state of the world's pelagic fish stocks is much worse than previously believed. Most species of pelagic shark in the northwest Atlantic are now declining by about 10%·year^{-1} (Baum et al. 2003). Ward and Myers (2005) found that the biomass of large sharks, tunas, and billfishes has fallen to one tenth of the level when pelagic longline fishing commenced in the tropical Pacific Ocean. Globally, the abundance of many large marine predators is now less than 10% of the pre-exploitation level (Myers and Worm 2003).

The new perspective on the status of pelagic fishes is directly linked to the recovery of historical data from longline surveys and commercial operations. However, critics have challenged conclusions based on those data, pointing to uncertainties in using longline catch rates as indices of abundance. Longline fishing effort must be corrected or "standardized" for variations in fishing practices and oceanographic conditions if abundance indices for early years are to be comparable with indices from recent years. The timing of longlining operations in relation to peak feeding periods is an example of a historical change in fishing practices. Ward et al. (2004) found that changes in the timing of longlining operations, which now have hooks available during dusk as well as dawn, have resulted in the overestimation of abundance for many species in recent years.

Another important historical change in longlining operations is the depth range of the gear (Fig. 1), which is the topic of this article. Two methods have been used to account for changes in the depth distribution of longline hooks. One

Received 26 June 2004. Accepted 31 December 2004. Published on the NRC Research Press Web site at http://cjfas.nrc.ca on 31 May 2005.
J18197

P. Ward[1,2] and R.A. Myers. Department of Biology, Dalhousie University, Halifax, NS B3H 4J1, Canada.

[1]Corresponding author (e-mail: peter.ward@brs.gov.au).
[2]Present address: Fisheries and Marine Sciences, Bureau of Rural Sciences, G.P.O. Box 858, Canberra ACT 2601, Australia.

 doi: 10.1139/F05-021 © 2005 NRC Canada

Fig. 1. Configuration of (*a*) a regular longline with six hooks between floats, like the longlines deployed by the US Pacific Oceanic Fisheries Investigations survey and (*b*) a deep longline with 28 hooks between floats, like those deployed by Hawaii-based longliners to catch bigeye tuna. Many longliners began using deep longlines in the tropical Pacific Ocean after 1974 and in the tropical Atlantic Ocean after 1979.

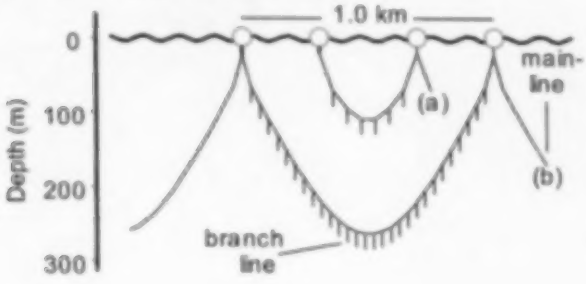

method is to use generalized linear models to relate catches to longline depth and other explanatory variables. In most longline fisheries, however, a switch to deep gear was so rapid in the mid-1970s that there is inadequate temporal overlap to allow comparison of the performance of regular and deep gear (Suzuki et al. 1977). Takeuchi (2001) concluded that it was not possible to make reliable inferences about changes in abundance from historical longline catch and effort data.

The second method of correcting abundance indices for longline depth is to model the species' preferred habitat. Oceanographic information (e.g., thermocline depth) is combined with information from tracking studies (e.g., Musyl et al. 2003) to estimate the species' depth distribution in time and area strata (e.g., Hinton and Nakano1996; Bigelow et al. 2002). The habitat-based model is then combined with the inferred depth distribution of longline hooks to adjust the fishing effort for the species' availability in each time–area stratum.

The previous methods required the estimation of an additional parameter for each longlining operation included in the analysis. Consequently, estimates become increasingly biased as the sample size increases (Kiefer and Wolfowitz 1956). The generalized linear models used the proportions of catch at depth. However, the local abundance and gear configuration vary among longlining operations, causing further biases in the interpretation of the depth distribution derived from catch proportions. This article describes a new method that uses data from individual longline hooks to estimate relative catchability at depth. The lack of an adequate statistical framework has previously precluded the use of individual hook data to derive statistically valid estimates of the depth distribution of catchability.

We use generalized linear mixed effect models (Wolfinger and O'Connell 1993), which have considerable advantages for estimating catchability at depth: (*i*) they allow for nonlinear relationships between independent variables and the dependent variable (mean catch), (*ii*) a variety of error distributions (e.g., Poisson) can be modeled, and (*iii*) they allow local abundance to be a random variable, providing statistically consistent estimates with improved accuracy (Robinson 1991).

Variations in fishing gear and oceanographic conditions affect catchability, the part of a stock that is caught by a defined unit of fishing effort. The catchability coefficient q relates catch C to the species' local abundance N and the amount of fishing effort E:

$$(1) \qquad C = qEN$$

A reliable estimate of catchability is therefore necessary to estimate abundance from catch and effort data (Murphy 1960). Catches are the product of catchability, local abundance, and fishing effort. For longline gear, fishing effort is often measured as the number of longline hooks available at each depth. Our approach is to first estimate the depth distribution of catchability independent of availability. We then take availability into account by adjusting the number of hooks at each depth by the estimated catchability.

Materials and methods

Data

We analyzed data collected by scientists involved in a research survey and by observers on commercial vessels using pelagic longlines. The data included gear dimensions for each longlining operation, which we used to estimate the maximum settled depth of each hook deployed. The scientists and observers also reported a unique identifier, a sequential number, for each longline hook. Combined with the gear dimensions, the individual hook data were used to estimate the depth at which each animal was caught.

We combined three data sets. The US Pacific Oceanic Fisheries Investigations conducted 1157 longlining operations in an area of the Pacific Ocean bounded by 175°E–115°W and 12°S–44°N during 1950–1958 (Fig. 2). Survey longliners used fishing gear and techniques adopted from Japan (Murphy and Shomura 1972). They typically deployed longlines at dawn each day and retrieved in the afternoon. They usually attached six hooks between each pair of floats, amounting to about 240 hooks in each daily longlining operation. The maximum settled depth of the hooks ranged from 18 to 103 m (unless otherwise indicated, all hook depths were estimated from the catenary formula reduced by 25% for the effects of currents). The survey longliners occasionally deployed longlines at night and deep longlines with up to 21 hooks between floats (18–144 m). They mostly used sardines (*Sardinella* spp.) as bait but also experimented with saury (*Scomberesox* spp.), squids (*Illex* spp.), and various other baits.

The second data set was from US National Marine Fisheries Service observers placed on commercial longliners in the Pacific Ocean during 1994–2002. The data consisted of 8037 daily longlining operations in an area bounded by 5°N–40°N and 174°E–134°W. The longliners targeted broadbill swordfish (*Xiphias gladius*) or tunas, specifically bigeye tuna (*Thunnus obesus*) and yellowfin tuna (*Thunnus albacares*), for domestic fresh-fish markets. To catch tunas in tropical waters, they deployed deep longlines with sardines as bait during the day with about 28 hooks between floats (40–230 m). To catch swordfish in temperate waters,

© 2005 NRC Canada

Fig. 2. Geographical ranges of data sets used to derive the depth distribution of catchability for each species. The data were collected by longline surveys under the US Pacific Oceanic Fisheries Investigations and compiled by the Secretariat of the Pacific Community from observers on commercial longliners operating in the western Pacific and by observers placed on Hawaii-based longliners by the US National Marine Fisheries Service. The Hawaii longliners targeted swordfish in the North Pacific or bigeye tuna in the tropical Pacific Ocean.

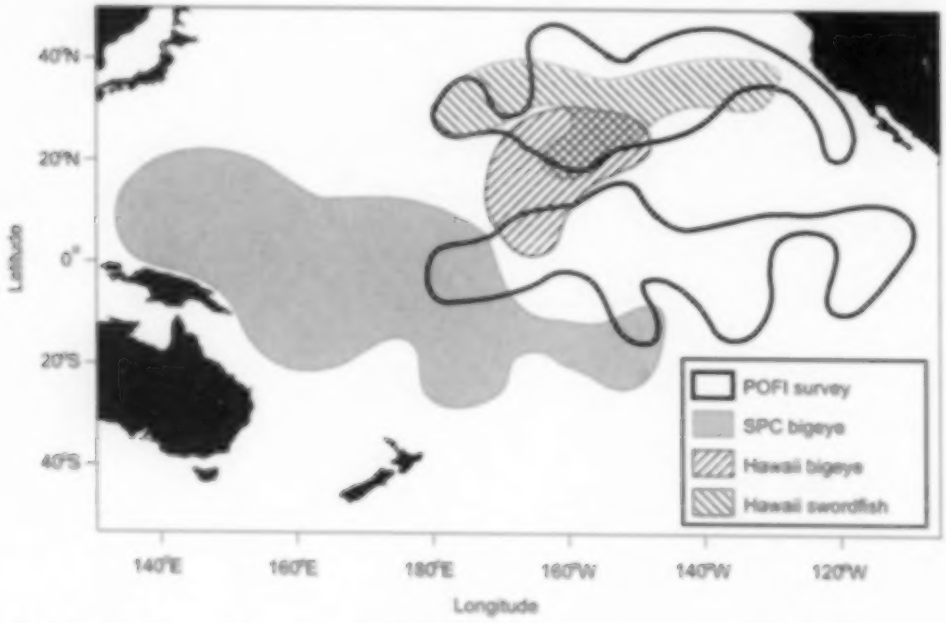

they deployed shallower longlines (39–121 m) with shortfin squid (*Illex illecebrosus*) as bait at night.

The Secretariat of the Pacific Community assembled the third data set from data collected by observers placed on commercial longliners during 1992–2002. The data consisted of 1813 longlining operations in an area of the Pacific Ocean bounded by 27°S–12°N and 138°E–172°W. Most of the longliners targeted bigeye tuna during the day with deep longlines consisting of about 30 hooks between floats (33–267 m). They used saury, sardines, or squids as bait.

The longliners used similar fishing gear, e.g., comparable hook sizes and wire leaders to connect hooks to branch lines. The longliners monitored by US National Marine Fisheries Service and Secretariat of the Pacific Community observers deployed monofilament-nylon branch lines, whereas the survey longliners used rope gear. The next section describes the random effects model that are used to account for variations in local abundance and catches among longlining operations. It was included to reduce the effects on catchability of variations in bait and fishing gear among longline operations.

Observers and survey scientists identified the species and recorded the hook number for each animal caught. Occasionally, they did not identify animals to the species level, so that species were combined into species groups. For brevity, we use the term species group to refer to individual species as well as species groups. The US National Marine Fisheries Service observers did not record the hook number for species groups other than tunas, billfishes, and sharks.

We assumed that the mainline formed a catenary curve between each pair of floats and estimated the depth of each hook by applying the formula presented by Suzuki et al. (1977) to longline dimensions reported for each operation. We assumed that the shape of the catenary curve (and therefore the corresponding depth of hooks) did not systematically vary along each longline or during each longline operation. Observed depths and predicted depths are known to vary, with ocean currents and wind having the most important influence on hook depth. Bigelow et al. (2002) estimated that hook numbers 3 and 10 of longline gear with 13 hooks between floats shoaled by about 20% when subjected to a current velocity of 0.4 $m \cdot s^{-1}$. To represent shoaling of longlines in our study area, we reduced all depths predicted by the catenary formula by 25%. The data were then binned into 40-m depth categories ranging from 0–40 to 480–520 m.

We estimated catchability distributions separately for day and night operations. Most day operations commenced at dawn (the median deployment time was 0705 (local) with 50% beginning between 0520 and 0747). Night operations often started at dusk (median time of 1817 with 50% between 1711 and 1930). We analyzed a total of 3155 night operations (13 679 animals) and 7852 day operations (32 046 animals) (Table 1).

Models

We used generalized linear mixed effect models (Wolfinger and O'Connell 1993) to estimate parameters that describe the shape of the depth distribution of catchability of each species group. The catch of each species group in longlining operation i at depth D was assumed to follow an overdispersed Poisson distribution with a mean of $\mu_{i,D}$. The assumption of a Poisson distribution is reasonable because

© 2005 NRC Canada

Table 1. Common and scientific names of each species or species group analyzed and the number of animals modeled for day and for night longlining operations.

Common name	Scientific name	No. modeled	
		Day	Night
Tunas and tuna-like species			
Albacore tuna	*Thunnus alalunga*	2777	1267
Bigeye tuna	*Thunnus obesus*	2980	1819
Skipjack tuna	*Katsuwonus pelamis*	2771	241
Wahoo	*Acanthocybium solandri*	528	122
Yellowfin tuna	*Thunnus albacares*	3131	1417
Billfishes			
Black marlin	*Makaira indica*	225	98
Blue marlin	*Makaira nigricans*	1902	593
Broadbill swordfish	*Xiphias gladius*	1277	2332
Sailfish	*Istiophorus platypterus*	402	148
Shortbill spearfish	*Tetrapturus angustirostris*	2477	269
Striped marlin	*Tetrapturus audax*	2726	743
Other teleosts			
Barracudas[a]	*Sphyraena* spp.	240	0[b]
Escolar	*Lepidocybium flavobrunneum*	266	107
Great barracuda	*Sphyraena barracuda*	102	0[b]
Lancetfishes[a]	*Alepisaurus* spp.	358	0[b]
Longnosed lancetfish	*Alepisaurus borealis*	46	0[b]
Mahi mahi	*Coryphaena hippurus*	349	157
Oilfish	*Ruvettus pretiosus*	254	96
Opah	*Lampris guttatus*	197	0[b]
Pomfrets[a]	Family Bramidae	179	35
Shortnosed lancetfish	*Alepisaurus brevirostris*	53	7
Sickle pomfret	*Taractichthys steindachneri*	20	0[b]
Snake mackerel	*Gempylus serpens*	102	113
Sharks and rays			
Bigeye thresher shark	*Alopias superciliosus*	956	139
Blue shark	*Prionace glauca*	3050	2444
Common thresher shark	*Alopias vulpinus*	30	0[b]
Crocodile shark	*Pseudocarcharias kamoharai*	384	84
Dusky shark	*Carcharhinus obscurus*	54	0[b]
Grey reef shark	*Carcharhinus amblyrhynchos*	25	0[b]
Long-finned mako shark	*Isurus paucus*	153	0[b]
Oceanic whitetip shark	*Carcharhinus longimanus*	1910	494
Pelagic stingray	*Dasyatis violacea*	356	204
Short-finned mako shark	*Isurus oxyrinchus*	665	388
Silky shark	*Carcharhinus falciformis*	1019	362
Silver-tip shark	*Carcharhinus albimarginatus*	29	0[b]
Tiger shark	*Galeocerdo cuvier*	34	0[b]
Whip stingray	*Dasyatis akajei*	19	0[b]

[a]Occasionally, observers did not identify animals to the species level. Consequently, we modeled data for species groups (e.g., barracudas (*Sphyraena* spp.)) separately to data for identified species (e.g., great barracuda (*Sphyraena barracuda*)).
[b]Insufficient numbers caught to allow reliable parameter estimation.

only a small proportion of the hooks are occupied by a species group, e.g., the mean percentage of hooks occupied by one of the most abundant species, yellowfin tuna, was 1.7% ± 4.1% SD.

For each species group, the model predicts the mean catch $\mu_{i,D}$ using a log link:

$$(2) \qquad \log(\mu_{i,D}) = \lambda_i + \gamma_1 D + \gamma_2 D^2 + \gamma_3 D^3 + \log(H_{i,D})$$

where λ_i and γ_j are parameters estimated for each species group and the offset $H_{i,D}$ is the number of hooks H deployed at depth D of longlining operation i. Our method includes a random effects model that accounts for variations in the local abundance of each species. We assumed that the log abundance of the species group, when it is encountered, followed the random effects distribution, which we assumed to be a normal distribution,

$$\lambda_i \sim N(\mu, \sigma^2)$$

The regression coefficients γ_j in eq. 2 describe how catchability changes with depth (μ represents catch, H is

© 2005 NRC Canada

fishing effort, and the γ_j parameters represent catchability in eq. 1). For each species group, we sequentially tested increasingly complex functional forms of eq. 2 to find the most appropriate model. We initially fitted eq. 2 with $\gamma_1 = \gamma_2 = \gamma_3 = 0$ and then tested the model in which we estimated γ_1 while constraining the quadratic and cubic parameters to zero. We sequentially added other γ_j parameters until the increase in the fit of the model was not significant as judged by a likelihood ratio test. The cubic model adequately described most of the variation in depth; including additional terms had very little effect on parameter estimates.

We then used parameter estimates, denoted by the "hat" symbol, from eq. 2 to estimate the catchability of each species group as a function of hook depth D (metres):

$$f(D) = \exp(\alpha + \hat{\gamma}_1 D + \hat{\gamma}_2 D^2 + \hat{\gamma}_3 D^3)$$

where α is chosen such that the mean of $f(D)$ equals one over the depth range considered. We refer to these standardized $f(D)$ as the depth distribution of catchability or simply the catchability distribution.

Correcting abundance indices for depth effects

To correct abundance indices for variations in longline depth, we can apply our estimates to data where gear dimensions are known for each operation. They can also be used to correct indices for changes in catchability when only the proportion of gear configurations is known. In almost all cases, the longline configuration is identical between floats and symmetrical. Therefore, the number of depths k that needs to be considered for each gear configuration is half the number of hooks between floats. We then estimated q_g, which is the average catchability of the species group for gear configuration g:

$$q_g = \sum_k f(D_k) p_g(D_k)$$

where $p_g(D_k)$ is the proportion of hooks at depth D_k. For each year, the catchability averaged over all gear configurations is

$$\overline{q}_y = \sum_g P_{y,g} q_g$$

where $P_{y,g}$ is the proportion of longlining operations using gear configuration g in year y. For each species group, we standardized the average catchability $\overline{q}_y$ by dividing it by its value in the first year of the time series.

We illustrate the effect of the depth correction by applying it to a time series of annual catch rates for Japan's longline fleet operating in the southern Atlantic Ocean. Estimation of the average annual catchability used the depth distribution of catchability combined with changes in gear configurations reported by Suzuki et al. (1977) and Uozumi and Nakano (1996). For each year, we divided the species' catch rate by our estimate of its average catchability for all gear configurations $\overline{q}_y$. We then standardized the estimate by dividing it by the average catchability in 1975 (the first year of the time series).

Results and discussion

Precision of depth estimates

The application of our estimates of the depth distribution of catchability should not be affected by uncertainty over the depths of longline hooks estimated by the catenary formula. It is true that observed depths (obtained using depth sensors) and predicted depths often differ. The weight of the longline causes a gradual shortening in the distance between floats during the operation. Consequently, longline hooks may sink to deeper depths than those predicted by the catenary formula. At the same time, wind and current sheer may cause hooks to rise towards the surface or "shoal" (Hanamoto 1987; Mizuno et al. 1999). However, we contacted several observers and longline fishers who pointed out that commercial fishers adjust their fishing practices to maximize the availability of longline hooks to target species, such as deep-dwelling bigeye tuna. Since the 1980s, many longliners have used Doppler current profilers to monitor the velocity and direction of subsurface currents. Most fishers minimize shoaling by deploying their longline in the same direction as prevailing currents. Furthermore, the predicted depth distributions of the hooks are surrogates for their true, but unknown, depth distributions. Our approach does not require accurate depth estimates because exactly the same methods and corrections that we used to estimate depth for our models can be applied to the longline data that are being corrected. By contrast, the depth estimates from tracking studies that are used in habitat-based models are not calibrated against longline depth.

Various factors may influence the depth distribution of catchability derived from observer data, e.g., spatial and seasonal variations in wind, currents and thermal structure and differences in fishing practices and gear among fleets. Our presentation of one night and one day distribution for each species should not preclude further investigation of the importance of those influences on depth distributions.

Ecological groups

We derived reliable estimates of the depth distribution of catchability for 37 species groups over a depth range of 18–512 m for day operations (Fig. 3) and for 24 species groups over 28–504 m for night operations (Fig. 4) (Appendix A provides parameter estimates for each species). The species groups show considerable variability in the distribution of catchability. The distributions indicate at least three distinct ecological groups, which should be considered separately in ecosystem models: epipelagic species that feed in surface waters (<200 m) during the day, wide-ranging pelagic species whose catchability does not vary over the observed depth range, and mesopelagic species that feed at intermediate and deep depths (>200 m) by day and then range more widely at night. Few species groups show high catchability at intermediate depths (200–400 m).

Swordfish, blue shark (*Prionace glauca*), and yellowfin tuna are members of the wide-ranging pelagic group. Their daytime catchability shows only minor variations over the observed depth range (Fig. 3). Tracking studies indicate that they range throughout the epi- and meso-pelagic zones (e.g., Carey and Robison 1981; Carey and Scharold 1990; Holland et al. 1990*a*).

© 2005 NRC Canada

Fig. 3. Estimates of the depth distribution of catchability $f(D)$ (thick line) with the 95% prediction intervals (thin lines) for day longlining operations. The mean catchability has been set to 1 to facilitate comparison between species and species groups.

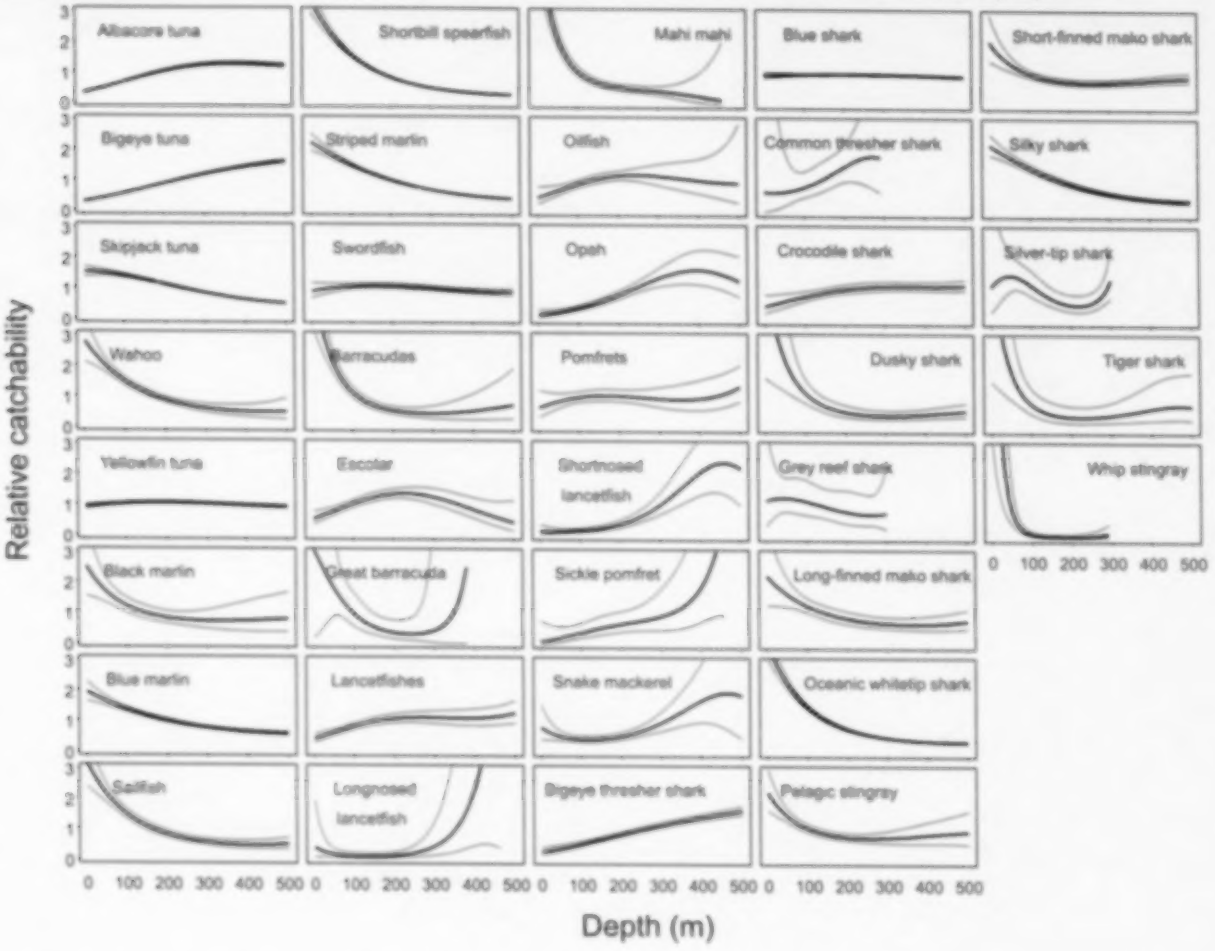

The epipelagic group includes oceanic whitetip shark (*Carcharhinus longimanus*), dusky shark (*Carcharhinus obscurus*), skipjack tuna (*Katsuwonus pelamis*), mahi mahi (*Coryphaena hippurus*), wahoo (*Acanthocybium solandri*), and all billfishes except swordfish. They were most often caught in surface waters above the thermocline (about 140 m in the tropical Pacific Ocean) during the day (Fig. 3). However, some were also caught on deep hooks. This is probably because animals may be caught when "deep" hooks pass through surface waters during longline deployment and retrieval (Boggs 1992).

Diel variation

Comparisons of catchability for day and night operations (Figs. 3 and 4) reveal patterns of diel variation among the mesopelagic species that probably represent vertical migration. The catchability of bigeye tuna, for example, increases with depth during the day, whereas it shows a much more uniform distribution at night. Our interpretation is that visibility is critical to the vertical distribution of large predators like bigeye tuna in the open ocean. They have several physiological adaptations, such as large eyes, that provide acute vision and allow them to hunt at low light levels (Pereira 1996). They feed below the sunlit zone during the day where they can avoid detection by their prey. At night, they range more widely because the ocean is almost uniformly dark. The distributions of other large predators indicate patterns of vertical migration that are similar to that of bigeye tuna, e.g., albacore tuna (*Thunnus alalunga*), escolar (*Lepidocybium flavobrunneum*), and bigeye thresher shark (*Alopias superciliosus*).

Visibility is also critical for predator avoidance by small species, such as snake mackerel (*Gempylus serpens*), which are the prey of large tunas, billfishes, and sharks (Kitchell et al. 1999; Rosas-Alayola et al. 2002). These small species concentrate at deep depths, below the sunlit zone during the day, where they can avoid their predators. At night, they venture into surface waters. Several epipelagic species show the opposite pattern, concentrating in surface waters during the day and then ranging more widely at night, e.g., shortbill spearfish (*Tetrapturus angustirostris*) and striped marlin (*Tetrapturus audax*).

© 2005 NRC Canada

Fig. 4. Estimates of the depth distribution of catchability $f(D)$ (thick line) with the 95% prediction intervals (thin lines) for night longlining operations. The mean catchability has been set to 1.

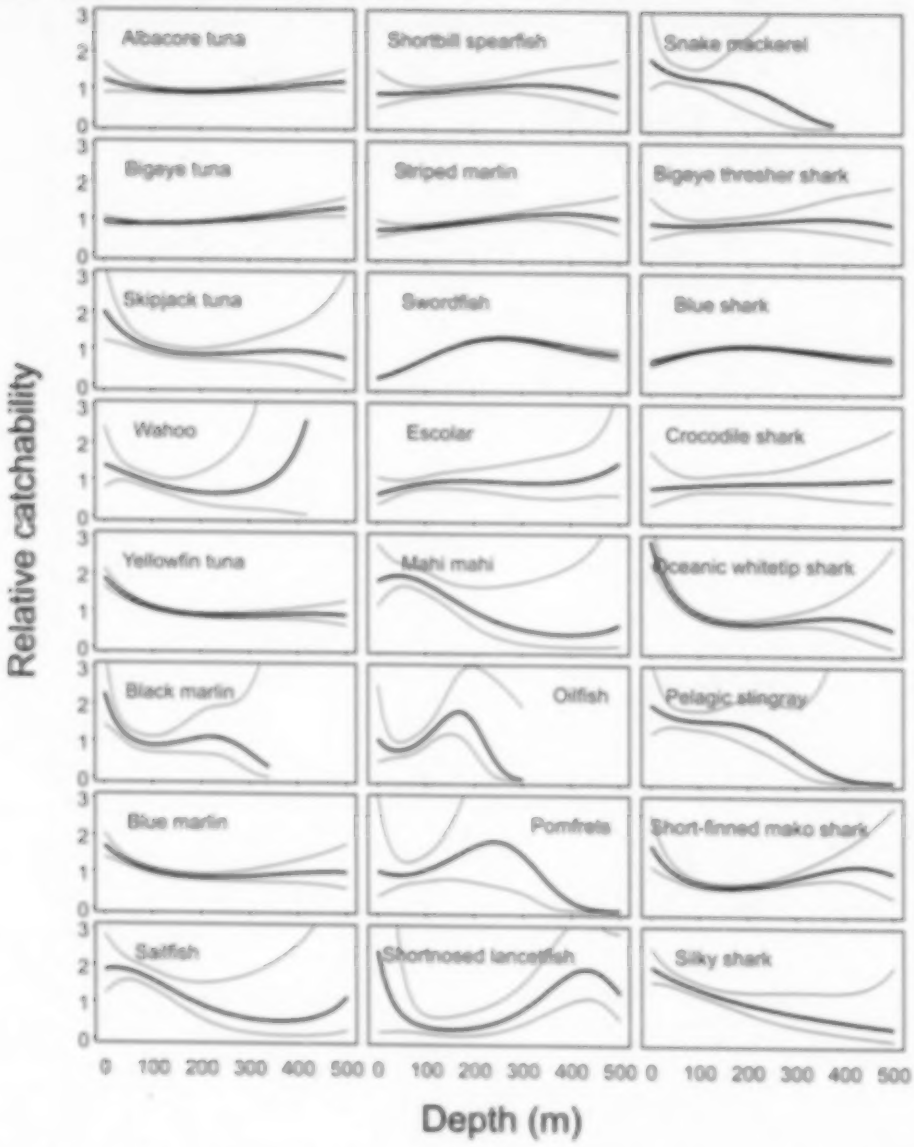

The depth distribution of catchability does not change markedly between day and night for several species, e.g., skipjack tuna, mahi mahi, and sailfish (*Istiophorus platypterus*). These epipelagic species are most abundant in surface waters. Hook-timer experiments (e.g., Boggs 1992) confirm that they are often caught in surface waters, particularly during longline deployment and retrieval. Night longlining operations caught fewer species groups than day operations, and the night depth distributions for several epipelagic species are poorly estimated compared with the estimates of their daytime distributions. This is partly due to differences in sample sizes (we analyzed 3155 night operations compared with 7852 day operations). The poor estimates of night distributions might also be related to diel variations in feeding activity. Stomach content analyses indicate reduced feeding activity among many epipelagic species at night. Analyses of the stomach contents of sailfish by Rosas-Alayola et al. (2002), for example, show that this species feeds mainly in surface waters during the day.

Comparison with tracking studies

For several species groups, the depth preferences derived from acoustic telemetry in the open ocean can be compared with the catchability distributions that we derived from longline data. The tracking studies are mostly limited to large, commercially important species of tunas and billfishes and several shark species (Table 2). Each study involved small numbers fitted with acoustic transmitters and tracked for

© 2005 NRC Canada

Table 2. Details of tracking data used to estimate the proportion of time spent at each depth.

Species	Device	No. of animals	Time at liberty	Location	Reference
Bigeye tuna	Archival tags	4	9–76 days	Southwestern Hawaii	Musyl et al. 2003
Yellowfin tuna	Ultrasonic transmitters	11	5 h – 6 days	Hawaii	Holland et al. 1990*a*
Blue marlin	Ultrasonic transmitters	5	24–42 h	Hawaii	Holland et al. 1990*b*
Black marlin	Ultrasonic transmitters	4	18–24 h	Northeastern Australia	Pepperell and Davis 1999

Fig. 5. Estimates of the depth distribution of catchability $f(D)$ of longline-caught fishes (thick line) compared with the percentage of time at each depth for tracked animals (histograms) for day and night periods: (*a*, *b*) bigeye tuna, (*c*, *d*) yellowfin tuna, (*e*, *f*) blue marlin, and (*g*, *h*) black marlin. Where available, standard errors (vertical lines) are shown for the mean percentage of time at depth. Thin lines are 95% prediction intervals for catchability.

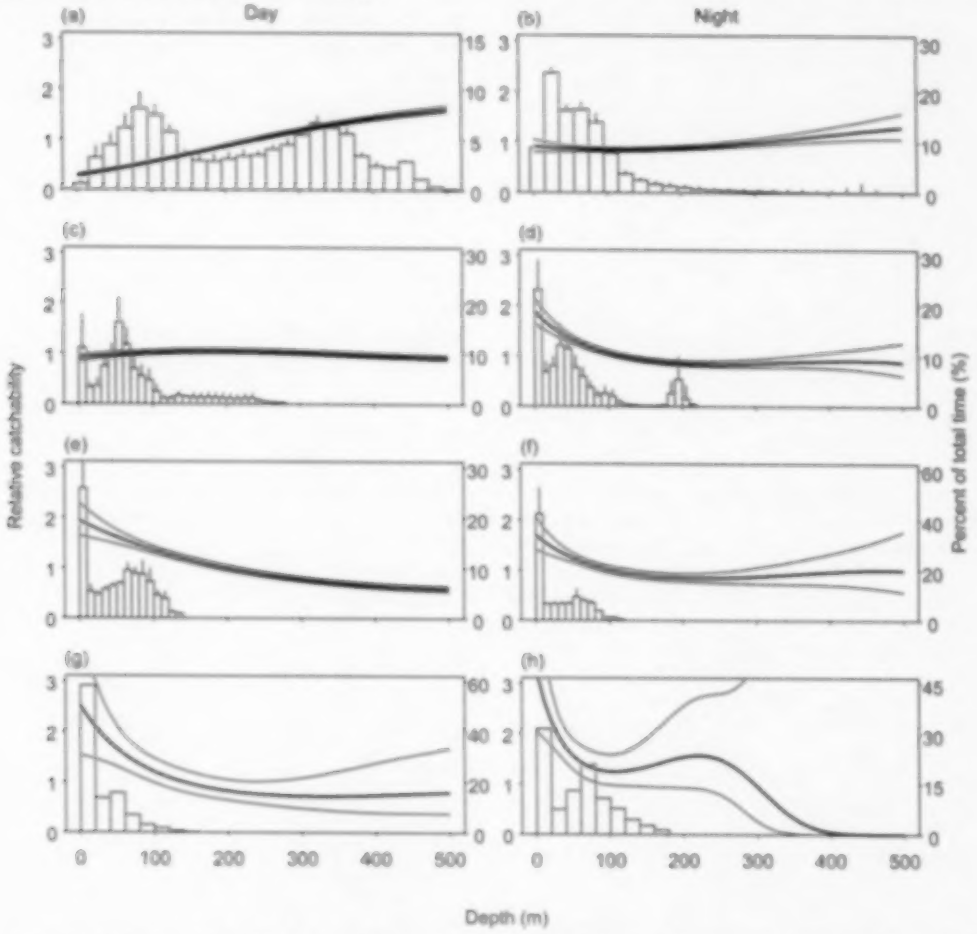

several days. Recent studies using archival tags (e.g., Musyl et al. 2003) have allowed the depth preferences of animals to be estimated over longer periods, thereby providing a more complete understanding of their behavior.

Our estimates of catchability distributions from longlining operations provide a good match to the tracking data in several cases (Fig. 5). For example, tagged black marlin (*Makaira indica*) spent most of the day in surface waters, which matches the catchability distribution (Fig. 5*g*). For bigeye tuna, however, the tracking data show patterns different from the catchability distribution (Figs. 5*a* and 5*b*). The inconsistencies between catchability distributions and depth preferences may be due to the small numbers of animals tracked or differences in behavior and oceanographic conditions between our broad study area and the areas where the animals were tracked. Eight of the yellowfin tuna tracked by Holland et al. (1990*a*) (Fig. 5*c*), for example, were associated with fish-aggregating devices. Those animals were found to behave quite differently from yellowfin tuna in the open ocean.

The inconsistencies between the depth distribution of catchability and depth preferences derived from tracking studies might also reflect a mismatch between the estimated

© 2005 NRC Canada

depth of longline hooks and tracking depths or differential vulnerability to longline fishing gear. It is quite possible for a species to be abundant at depths where they have a reduced vulnerability to the gear. For example, bigeye tuna might be present in surface waters during the day but not caught on longline hooks there because they are not feeding or cannot detect the baits. This is not of concern because we intend the estimates of catchability to be used to correct abundance indices derived from longline data. However, the mismatch between catches on longline hooks and the species' depth preference is a flaw in habitat-based models that are solely based on tracking data. Tracking data show an animal's depth preference, which may not always match the species' vulnerability to longline fishing gear. From an analysis of simulated data for blue marlin (*Makaira nigricans*), Goodyear (2003) concluded that the propensity of the species to take longline baits and the actual depth profile of the fishing gear strongly influenced habitat-based model estimates of abundance. The development of statistical habitat-based models, which fit observed catches (Hinton and Maunder 2003), may help to correct for differences between depth preferences and vulnerability.

An alternative to our approach is to use hook-timers that record the time and depth when each animal was caught (e.g., Boggs 1992). However, a very large number of hook-timer experiments are required to derive reliable estimates of depth preference. For example, Matsumoto et al. (2001) analyzed over 300 longlining operations, each deploying 10–163 hook-timers. However, that number of experiments was not large enough to obtain reliable estimates of depth preference.

Environmental constraints on depth distribution

The tracking studies show that environmental conditions set broad limits to the vertical distribution of each species. Those limits will also apply to the depth distribution of catchability. For example, Brill et al. (1993) concluded that sharp gradients in water temperature between the mixed layer and deeper waters represented a barrier to vertical migrations of striped marlin near Hawaii. Other conditions, such as oxygen concentration, are also known to limit the vertical distribution of pelagic fishes (Hanamoto 1987). The efficacy of those thresholds will vary seasonally, spatially, among species, and with body size (Dagorn et al. 2000). Caution is required in applying our estimates of catchability distributions to regions outside the study area. For example, the shallow thermocline in the tropical eastern Pacific Ocean results in very low catch rates of striped marlin on longline hooks below about 100 m (Matsumoto and Miyabe 2002). By contrast, our estimates indicate an average level of catchability for striped marlin below 100 m (Figs. 3 and 4).

Further work is required to determine whether our estimates can be applied to other regions. Several organizations hold hook-level data that we could not access, e.g., data collected by British observers on longliners in the Indian Ocean and surveys by Japan's National Research Institute of Far Seas Fisheries. Such data sets should be used to test the hypothesis that the shape of a species' catchability distribution does not vary among regions or seasons but is compressed or extended by local conditions that limit the species' depth range. Data were not available to model the effects of body size on the depth distribution of each species, but we expect further work to show that larger animals generally have a wider depth range.

Correcting longline catch rates

There are two ways that our estimates of the depth distribution of catchability can be used to improve estimates of abundance. First, correction factors can be applied to operation-level data where gear dimensions and the number of hooks between floats are known for each operation. Such data exist for a large number of longline surveys conducted before commercial fishing commenced (e.g., Wathne 1959) and for more recent research cruises and monitoring programs. Ward and Myers (2005) illustrated how the correction factors can adjust abundance indices derived from longline surveys in the 1950s and commercial operations in the 1990s.

The second application of our estimates is to correct abundance indices for changes in depth when only the proportion of gear configurations is known. Japan's longliners rapidly switched from regular longlining (<120 m) to deep longlining (deepest hooks ranging beyond 120 m) in the Atlantic Ocean in the late 1970s (Fig. 6*a*). The introduction of deep longlining had virtually no effect on the catchability of yellowfin tuna and swordfish (Figs. 6*b* and 6*c*). Catchability declined for marlins and sailfish but increased by 60% for bigeye tuna and by 40% for albacore tuna. While these changes warrant their inclusion in assessment models, they are less than those estimated by the early nonstatistical habitat-based models (e.g., Hinton and Nakano 1996).

The application of our depth correction to annual catch rates of longliners in the southern Atlantic Ocean illustrates how variations in gear configurations can affect estimates of abundance. We have previously advised caution in applying our estimates of catchability to regions outside the study area; this application to the southern Atlantic Ocean is only intended to illustrate how the estimates can be used. The use of longline catch rates as indices of abundance is also subject to debate (R.A. Myers and A.M. Edwards, unpublished data). The introduction of deep longlines resulted in the overestimation of bigeye tuna abundance but had a relatively small effect on abundance indices for other species (Fig. 7). In absolute terms, the effect is small on estimates of blue marlin, sailfish, and albacore tuna because of the significant decline in the abundance of those species well before the switch to deep longlining (Myers and Worm 2003). Furthermore, deep hooks take about 30 min to move through shallow and intermediate depths during longline deployment and retrieval. Consequently, catches are smeared over a range of depths (Boggs 1992).

The effects of the increased depth range on catchability indicate that the 90% decline in the abundance of tunas and billfishes reported by Myers and Worm (2003) would be an underestimate. This is because the animal community has been modified so that most of the biomass is now concentrated in swordfish, bigeye tuna, and yellowfin tuna, which declined less dramatically than other species. The catchability of target species has not changed or it has increased. Although the catchability of marlins and sailfish has declined,

© 2005 NRC Canada

Fig. 6. Historical variations in gear configurations and catchability. (*a*) Number of hooks between floats deployed by Japan's longline fleet in the tropical Atlantic Ocean (modified from Yokawa and Uozumi (2001)). Hooks between floats is a rough indicator of longline depth range (for these operations, six hooks between floats produces a depth range of about 50–150 m compared with 50–300 m for a configuration with 14 hooks between floats). (*b*) Estimated change in average catchability over all gear configurations $\overline{q}_t$ used by the tropical Atlantic fleet relative to the 1975 gear configuration. (*c*) Change in the depth distribution of catchability q_g relative to the gear configuration with three hooks between floats for six species taken by the tropical Atlantic fleet.

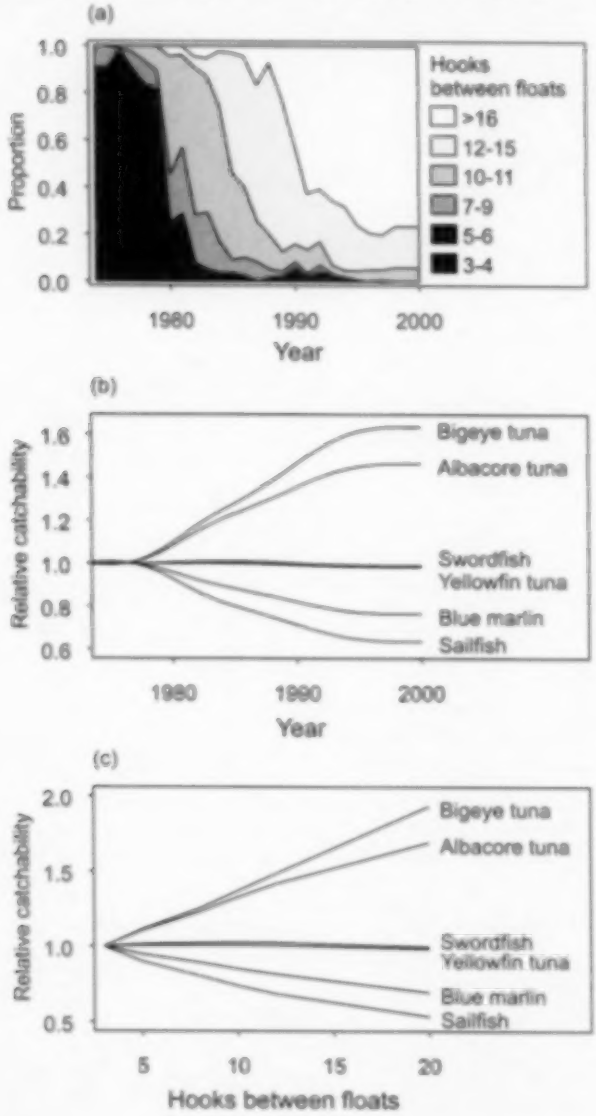

Fig. 7. Abundance indices of four species in the southern Atlantic Ocean (modified from Myers and Worm (2003)) with (solid line) and without (broken line) the depth correction from Fig. 6c. Species are as follows: (*a*) albacore tuna, (*b*) bigeye tuna, (*c*) blue marlin, and (*d*) sailfish.

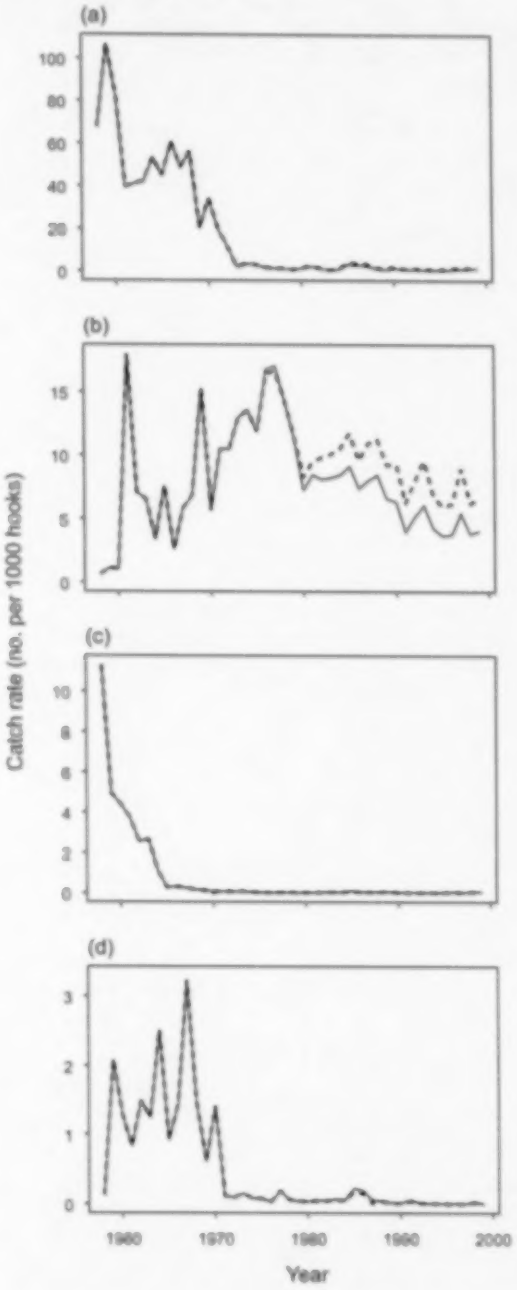

they now constitute only a small part of the pelagic fish community available to longline fishing gear.

In summary, we have demonstrated a method where abundance indices derived from longline catch rates can be corrected for historical variations in the depth range of the fishing gear. The method is relatively simple to apply and uses existing data that previously lacked the appropriate statistical framework for analysis. It can be applied to bycatch spe-

© 2005 NRC Canada

cies that have not been the subject of tracking studies and it accommodates early data where only approximate gear characteristics are known and detailed oceanographic data are not available. Our method also eliminates the confounding in other statistical methods caused by the rapid switch to deep longline gear in the 1970s. Thus, we reject the claim by Takeuchi (2001) that abundance indices cannot be corrected for historical changes in the depth of longline hooks.

Longliners have maintained catch rates of target species by improving the efficiency of their fishing gear (Stone and Dixon 2001), increasing soak time, ensuring that hooks are available at peak feeding periods (Ward et al. 2004), and by extending the geographical limits of fishing grounds (Myers and Worm 2003). In the 1970s, they also began to exploit a much greater depth range. Our analyses show that deep longlining has resulted in the underestimation of the abundance of several epipelagic species (e.g., sailfish). However, it has resulted in the overestimation of the abundance of several pelagic species, including target species like bigeye tuna. Those large predators not only support valuable fishing industries, they have unique ecological roles, influencing the diversity and abundance of lower trophic levels.

Acknowledgments

The work is part of a larger project on pelagic longlining that was initiated and sponsored by the Pew Charitable Trusts. We also thank the Pelagic Fisheries Research Program, the Natural Sciences and Engineering Research Council of Canada, and the Future of Marine Animal Populations project of the Sloan Foundation Census of Marine Life for financial support. Tim Davis, Brent Miyamoto, Mike Musyl, Tom Swenarton, and Peter Williams provided data and information on the fisheries. Wade Blanchard and Darren Swan provided technical advice. Two reviewers provided comments on the manuscript.

References

Baum, J.K., Myers, R.A., Kehler, D.G., Worm, B., Harley, S.J., and Doherty, P.A. 2003. Collapse and conservation of shark populations in the northwest Atlantic. Science (Wash., D.C.), **299**: 389–392.

Bigelow, K.A., Hampton, J., and Miyabe, N. 2002. Application of a habitat-based model to estimate effective longline fishing effort and relative abundance of Pacific bigeye tuna (*Thunnus obesus*). Fish. Oceanogr. **11**: 143–155.

Boggs, C.H. 1992. Depth, capture time, and hooked longevity of longline-caught pelagic fish: timing bites of fish with chips. Fish. Bull. **90**: 642–658.

Brill, R.W., Holts, D.B., Chang, R., Sullivan, S., Dewar, H., and Carey, F.G. 1993. Vertical and horizontal movements of striped marlin (*Tetrapturus audax*) near the Hawaiian Islands, determined by ultrasonic telemetry, with simultaneous measurement of oceanic currents. Mar. Biol. **117**: 567–574.

Carey, F.G., and Robison, B.H. 1981. Daily patterns in the daily activity patterns of swordfish, *Xiphias gladius*, observed by acoustic telemetry. Fish. Bull. **79**: 277–291.

Carey, F.G., and Scharold, J. 1990. Movements of blue sharks (*Prionace glauca*) in depth and course. Mar. Biol. **106**: 329–342.

Dagorn, L., Bach, P., and Josse, E. 2000. Movement patterns of large bigeye tuna (*Thunnus obesus*) in the open ocean, determined using ultrasonic telemetry. Mar. Biol. **136**: 361–371.

Goodyear, C.P. 2003. Tests of the robustness of habitat-standardized abundance indices using simulated blue marlin catch-effort data. Mar. Freshw. Res. **54**: 369–381.

Hanamoto, E. 1987. Effect of oceanographic environment on bigeye tuna distribution. Bull. Jpn. Soc. Fish. Oceanogr. **51**: 203–216.

Hinton, M.G., and Maunder, M.N. 2003. Methods for standardizing cpue and how to select among them. ICCAT Coll. Vol. Sci. Pap. SCRS/2003/034.

Hinton, M.G., and Nakano, H. 1996. Standardizing catch and effort statistics using physiological, ecological, or behavioural constraints and environmental data, with an application to blue marlin (*Makaira nigricans*) catch and effort data from the Japanese longline fisheries in the Pacific. Inter-Am. Trop. Tuna Comm. Bull. **21**: 169–200.

Holland, K., Brill, R., and Chang, R. 1990*a*. Horizontal and vertical movements of yellowfin and bigeye tuna associated with fish aggregating devices. Fish. Bull. **88**: 493–507.

Holland, K., Brill, R., and Chang, R. 1990*b*. Horizontal and vertical movements of Pacific blue marlin captured and released using sportfishing gear. Fish. Bull. **88**: 397–402.

Kiefer, J., and Wolfowitz, J. 1956. Consistency of the maximum likelihood estimator in the presence of infinitely many incidental parameters. Ann. Math. Stat. **27**: 887–906.

Kitchell, J.F., Boggs, C., He, P., and Walters, C.J. 1999. Keystone predators in the central Pacific. *In* Ecosystem approaches for fisheries management. *Edited by* J.N. Ianelli. University of Alaska Sea Grant, Fairbanks, Alaska. pp. 665–684.

Matsumoto, T., and Miyabe, H.S.N. 2002. Report of observer program for Japanese tuna longline fishery in the Atlantic Ocean from September 2001 to March 2002. Tech. Rep. SCRS/02/140, ICCAT Coll. Vol. Sci. Pap.

Matsumoto, T., Uosumi, Y., Uosaki, K., and Okazaki, M. 2001. Preliminary review of billfish hooking depth measured by small bathythermograph systems attached to longline gear. *In* Report of the Fourth ICCAT Billfish Workshop, Miami, Fla., 18–28 July 2000). International Commission for the Conservation of Atlantic Tunas, Madrid. pp. 337–344.

Mizuno, K., Okazaki, M., Nakano, H., and Okamura, H. 1999. Estimating the underwater shape of tuna longlines with microbathythermographs. Inter-Am. Trop. Tuna Comm. Spec. Rep. No. 21.

Murphy, G.I. 1960. Estimating abundance from longline catches. J. Fish. Res. Board Can. **17**: 33–40.

Murphy, G.I., and Shomura, R.S. 1972. Pre-exploitation abundance of tunas in the equatorial central Pacific. Fish. Bull. **70**: 875–913.

Musyl, M.K., Brill, R.W., Boggs, C.H., Curran, D.S., Kazama, T.K., and Seki, M.P. 2003. Vertical movements of bigeye tuna (*Thunnus obesus*) associated with islands, buoys, and seamounts near the main Hawaiian Islands from archival tagging data. Fish. Oceanogr. **12**: 152–169.

Myers, R.A., and Worm, B. 2003. Rapid worldwide depletion of predatory fish communities. Nature (Lond.), **423**: 281–283.

Pepperell, J., and Davis, T. 1999. Post-release behaviour of black marlin, *Makaira indica*, caught off the Great Barrier Reef with sportfishing gear. Mar. Biol. **135**: 369–380.

Pereira, J.G. 1996. Bigeye tuna: access to deep waters. *In* First World Meeting on Bigeye Tuna, 11–15 November 1996. *Edited by* R.B. Deriso, W.H. Bayliff, and N.J. Webb. Inter-American Tropical Tuna Commission, La Jolla, Calif. pp. 243–249.

Robinson, G.K. 1991. That BLUP is a good thing: the estimation of random effects. Stat. Sci. **6**: 15–51.

Rosas-Alayola, J., Hernandez-Herrera, A., Galvan-Magana, F., Abitia-Cardenas, L., and Muhlia-Melo, A.F. 2002. Diet composition of

© 2005 NRC Canada

sailfish (*Istiophorus platypterus*) from the southern Gulf of California, Mexico. Fish. Res. (Amst.), **57**: 185–195.

Stone, H.H., and Dixon, L.K. 2001. A comparison of catches of swordfish, *Xiphias gladius*, and other pelagic species from Canadian longline gear with alternating monofilament and multifilament nylon gangions. Fish. Bull. **99**: 210–216.

Suzuki, Z., Warashina, Y., and Kishidam, M. 1977. The comparison of catches by regular and deep tuna longline gears in the western and central equatorial Pacific. Bull. Far Seas Fish. Res. Lab. **15**: 51–89.

Takeuchi, Y. 2001. Is historically available hooks-per-basket information enough to standardize actual hooks-per-basket effects on cpue? Preliminary simulation approach. ICCAT Coll. Vol. Sci. Pap. **53**: 356–364.

Uozumi, Y., and Nakano, H. 1996. A historical review of Japanese longline fishery and billfish catches in the Atlantic Ocean. *In* Collective volume of scientific papers. Report of the second ICCAT Billfish Workshop. International Commission for the Conservation of Atlantic Tunas, Madrid. pp. 233–243.

Ward, P., and Myers, R.A. 2005. Shifts in open-ocean fish communities coinciding with the commencement of commercial fishing. Ecology, **86**(4): 835–847.

Ward, P., Myers, R.A., and Blanchard, W. 2004. Fish lost at sea: the effect of soak time and timing on pelagic longline catches. Fish. Bull. **102**: 179–195.

Wathne, F. 1959. Summary report of exploratory longline fishing for tuna in Gulf of Mexico and Caribbean Sea, 1954–1957. Commer. Fish. Rev. **21**: 1–26.

Wolfinger, R., and O'Connell, M. 1993. Generalized linear mixed models: a pseudo-likelihood approach. J. Stat. Comput. Sim. **48**: 233–243.

Yokawa, K., and Uozumi, Y. 2001. Analysis of operation pattern of Japanese longliners in the tropical Atlantic Ocean and their blue marlin catch. ICCAT Coll. Vol. Sci. Pap. **53**: 318–336.

Appendix A. Estimates of depth distribution parameters derived from pelagic longline data.

We used generalized linear mixed effect models with a Poisson distribution to model the mean catch μ of each species or species group in longline operation i at depth D. The model predicted the mean catch using a log link:

$$\log(\mu_{i,D}) = \lambda_i + \gamma_1 D + \gamma_2 D^2 + \gamma_3 D^3 + \log(H_{i,D})$$

where the "offset" $H_{i,D}$ is the number of hooks deployed at depth D in longline operation i, and λ_i is the random effects distribution for the species in operation i (we assumed that the log abundance of the species encountered by each operation follows a normal distribution). The regression coefficients γ_j describe how the species' catchability varies with depth. For each species, we used the GLIMMIX macro in SAS (version 8.0) to fit the models separately to day (Table A1) and night longlining operations (Table A2). We also investigated the alternative assumption of extrabinomial variation, which gave results very similar to those of the Poisson distribution. We report only the Poisson results because they are simpler to interpret.

Table A1. Parameter estimates and the number of each species or species group modeled for day longlining operations (standard errors of each estimate are in parentheses).

		Parameter			
Common name	No. modeled	λ	γ_1	γ_2	γ_3
Tunas and tuna-like species					
Albacore tuna	2777	−6.47 (0.04)	9.44 (0.43)	−20.34 (1.39)	13.81 (1.34)
Bigeye tuna	2980	−6.44 (0.05)	7.83 (0.48)	−12.25 (1.45)	7.20 (1.33)
Skipjack tuna	2771	−5.38 (0.06)	−0.09 (0.63)	−9.69 (2.12)	10.97 (2.10)
Wahoo	528	−5.68 (0.14)	−6.88 (2.51)	4.46 (12.34)	4.95 (15.94)
Yellowfin tuna	3131	−5.48 (0.04)	1.73 (0.39)	−6.05 (1.35)	5.32 (1.37)
Billfishes					
Black marlin	225	−6.06 (0.25)	−9.48 (4.28)	22.77 (19.67)	−16.81 (23.33)
Blue marlin	1902	−5.81 (0.08)	−3.77 (1.06)	1.83 (3.78)	1.86 (3.89)
Sailfish	402	−5.81 (0.14)	148.00 (2.22)	8.61 (9.28)	2.61 (10.43)
Shortbill spearfish	2477	−4.79 (0.07)	−7.95 (0.84)	4.31 (2.97)	3.34 (3.03)
Striped marlin	2726	−5.11 (0.06)	−3.82 (0.77)	−2.30 (2.62)	6.29 (2.61)
Swordfish	1277	−6.94 (0.14)	2.74 (1.61)	−11.45 (5.38)	11.84 (5.24)
Other teleosts					
Barracudas	240	−5.45 (0.20)	−19.17 (3.87)	47.12 (19.04)	−32.90 (23.27)
Escolar	266	−6.71 (0.19)	8.72 (3.24)	−21.67 (16.64)	6.73 (24.41)
Great barracuda	102	−4.91 (1.44)	−8.86 (33.83)	−45.90 (232.52)	178.29
Lancetfishes	358	−6.20 (0.15)	9.50 (2.22)	−30.57 (9.56)	31.86 (11.61)
Longnosed lancetfish	46	−6.27 (0.81)	−20.84 (16.97)	93.31 (92.41)	−74.91 (136.92)
Mahi mahi	349	−4.41 (0.18)	−25.17 (4.32)	86.37 (29.58)	−108.34 (58.60)
Oilfish	254	−7.72 (0.30)	9.58 (4.95)	−29.23 (24.06)	25.94 (32.87)
Opah	197	−8.24 (0.33)	8.81 (4.78)	−0.74 (20.18)	−17.56 (24.37)

© 2005 NRC Canada

Table A1 (*concluded*).

Common name	No. modeled	Parameter			
		λ	γ_1	γ_2	γ_3
Pomfrets	179	−6.95 (0.31)	6.69 (4.92)	−29.87 (21.93)	38.71 (26.09)
Shortnosed lancetfish	53	−7.41 (0.45)	−2.93 (6.33)	51.76 (27.49)	−70.62 (35.01)
Sickle pomfret	20	−8.87 (1.08)	20.50 (17.01)	−73.37 (79.15)	102.60 (106.75)
Snake mackerel	102	−6.34 (0.33)	−11.78 (6.06)	63.10 (30.00)	−72.36 (42.00)
Sharks and rays					
Bigeye thresher shark	956	−8.08 (0.21)	7.88 (1.98)	−12.95 (5.69)	8.52 (4.98)
Blue shark	3050	−5.43 (0.05)	0.35 (0.52)	−0.77 (1.68)	−0.16 (1.62)
Common thresher shark	30	−7.67 (1.52)	−2.40 (27.45)	59.64 (149.25)	−135.85 (247.22)
Crocodile shark	384	−7.79 (0.30)	7.17 (3.18)	−18.88 (9.83)	16.39 (9.14)
Dusky shark	54	−4.55 (0.57)	−19.05 (7.22)	47.48 (25.06)	−35.91 (25.48)
Grey reef shark	25	−6.51 (0.56)	3.43 (16.68)	−46.59 (130.00)	101.53 (283.53)
Long-finned mako shark	153	−6.00 (0.29)	−6.66 (4.00)	9.83 (14.42)	−1.46 (14.66)
Oceanic whitetip shark	1910	−4.92 (0.07)	−9.85 (0.97)	11.61 (3.48)	−2.09 (3.56)
Pelagic stingray	356	−5.85 (0.15)	−9.97 (2.65)	28.78 (12.82)	−24.50 (16.14)
Short-finned mako shark	665	−6.14 (0.18)	−9.11 (2.33)	26.32 (8.22)	−22.57 (8.45)
Silky shark	1019	−5.17 (0.08)	−3.56 (1.00)	−4.43 (3.76)	9.90 (4.02)
Silver-tip shark	29	−6.34 (0.66)	12.75 (15.51)	−162.55 (105.60)	407.47 (211.62)
Tiger shark	34	−5.03 (0.69)	−27.92 (10.81)	91.35 (43.29)	−87.35 (49.00)
Whip stingray	19	−2.69 (0.86)	−75.92 (15.42)	298.97 (64.83)	−322.17 (76.22)

Table A2. Parameter estimates and the number of each species or species group modeled for night longlining operations (standard errors of each estimate are in parentheses).

Common name	Number modeled	Parameter			
		λ	γ_1	γ_2	γ_3
Tunas and tuna-like species					
Albacore tuna	1267	−4.92 (0.17)	−3.99 (2.17)	14.44 (8.43)	−13.26 (9.83)
Bigeye tuna	1819	−5.53 (0.07)	−1.50 (1.00)	8.32 (4.10)	−7.84 (4.76)
Skipjack tuna	241	−5.63 (0.26)	−10.47 (4.74)	39.32 (24.12)	−44.72 (34.83)
Wahoo	122	−6.12 (0.29)	−3.83 (8.24)	−12.18 (64.44)	59.35 (128.00)
Yellowfin tuna	1417	−5.00 (0.07)	−7.97 (1.14)	25.43 (5.58)	−25.02 (7.89)
Billfishes					
Black marlin	98	−5.57 (0.24)	−21.65 (8.46)	151.63 (77.45)	−310.27 (189.09)
Blue marlin	593	−5.70 (0.10)	−7.35 (1.91)	24.06 (9.64)	−22.96 (13.05)
Sailfish	148	−6.19 (0.21)	1.58 (5.16)	−39.99 (34.39)	69.81 (47.04)
Shortbill spearfish	269	−6.56 (0.29)	−0.08 (4.34)	8.10 (18.86)	−16.20 (23.66)
Striped marlin	743	−6.35 (0.16)	0.88 (2.37)	6.05 (10.39)	−12.54 (13.72)
Swordfish	2332	−6.22 (0.07)	16.38 (0.95)	−47.07 (3.54)	39.58 (3.87)
Other teleosts					
Escolar	107	−6.55 (0.28)	6.57 (5.19)	−28.51 (26.10)	37.79 (35.79)
Mahi mahi	157	−6.09 (0.23)	3.88 (5.65)	−48.80 (37.60)	74.12 (51.85)
Oilfish	96	−6.25 (0.43)	−17.73 (14.76)	268.21 (144.36)	−854.80 (410.20)
Pomfrets	35	−6.58 (0.54)	−5.46 (13.57)	75.28 (99.03)	−177.15 (195.89)
Shortnosed lancetfish	7	−4.76 (1.18)	−32.04 (17.98)	145.64 (69.78)	−168.07 (79.16)
Snake mackerel	113	−5.99 (0.29)	−6.92 (9.85)	48.80 (95.07)	−133.89 (243.15)
Sharks and rays					
Bigeye thresher shark	139	−6.58 (0.29)	−1.20 (4.43)	10.49 (18.75)	−16.13 (22.29)
Blue shark	2444	−5.00 (0.07)	5.79 (0.84)	−19.62 (3.15)	17.38 (3.34)
Crocodile shark	84	−6.55 (0.40)	1.44 (5.97)	−4.02 (24.39)	4.66 (27.48)
Oceanic whitetip shark	494	−4.97 (0.11)	−17.14 (2.39)	66.41 (14.78)	−77.27 (26.39)
Pelagic stingray	204	−6.00 (0.24)	−5.54 (6.86)	43.57 (56.22)	−119.38 (127.20)
Short-finned mako shark	388	−5.74 (0.20)	−13.66 (3.31)	58.33 (16.64)	−66.17 (24.42)
Silky shark	362	−4.99 (0.12)	−3.90 (2.71)	3.82 (19.07)	−5.10 (30.97)

© 2005 NRC Canada

Alternative life-history patterns of estuarine fish: barium in otoliths elucidates freshwater residency

Travis S. Elsdon and Bronwyn M. Gillanders

Abstract: Elemental concentrations in fish otoliths (earstones) can reconstruct environmental histories of fish if predictable relationships between the environment and elemental incorporation are established. We assessed whether freshwater occupancy of black bream (*Acanthopagrus butcheri*) can be inferred from otolith barium concentrations (Ba was standardized to calcium (Ca) and expressed as a ratio, Ba:Ca). Otolith Ba:Ca of fish was correlated with ambient Ba:Ca. Using the natural relationships of increasing ambient and otolith Ba:Ca with decreasing salinity, fish from fresh- and salt-water environments were distinguishable. Fish caught in fresh water had approximately double the otolith Ba:Ca of those from salt-water estuaries, for both summer and winter collections. Fish with otolith Ba:Ca ≤5 μmol·mol^{-1} were classified as resident in salt water, and those with ≥6 μmol·mol^{-1} as resident in fresh water. Transects of Ba:Ca across fish otoliths classified fish to fresh- or salt-water environments. Fish were identified as having migratory patterns typical of residents, migrants with irregular patterns of diadromy, or migrants with cyclic patterns of anadromomy. Multiple migratory behaviours occurred in fish from the same estuary, indicating far more complex migratory behaviours than were previously known. The application of otolith Ba:Ca to infer freshwater occupancy of fish has rarely been studied, yet may provide more accurate classifications of estuarine environments than strontium (Sr) isotopes and otolith Sr:Ca.

Résumé : Les concentrations d'éléments chimiques dans les otolithes des poissons permettent de reconstituer leur histoire environnementale, lorsqu'on réussit à établir des relations de prédiction entre l'environnement et l'incorporation des éléments. Nous avons vérifié si les concentrations de barium (Ba:Ca) dans les otolithes permettent de déterminer les séjours de « brèmes noires » (*Acanthopagrus butcheri*). Les concentrations de Ba:Ca des otolithes de poissons sont en corrélation avec les concentrations de Ba:Ca du milieu ambiant. À l'aide de la relation naturelle de l'accroissement de Ba:Ca dans les otolithes et le milieu en fonction inverse de la salinité, il est possible de distinguer les poissons des environnements d'eau douce et ceux d'eau salée. Les poissons capturés en eau douce possèdent des concentrations de Ba:Ca dans leurs otolithes approximativement deux fois plus élevées que les poissons provenant des estuaires d'eau salée, tant dans les récoltes d'été que d'hiver. Les poissons ayant des concentrations de Ba:Ca ≤5 μmol·mol^{-1} sont classifiés comme résidants d'eau salée et ceux qui en ont ≥6 μmol·mol^{-1} comme résidants d'eau douce. Des transects des concentrations de Ba:Ca en travers des otolithes permettent d'assigner les poissons aux environnements d'eaux douce et salée. Les poissons ont pu être ainsi classifiés comme possédant des patrons migratoires typiques de résidants, de migrateurs avec des patrons irréguliers de diadromie et de migrateurs avec des patrons cycliques d'anadromie. Divers comportements migratoires existent chez les poissons d'un même estuaire, ce qui indique que les comportements de migration sont beaucoup plus complexes qu'on le croyait jusqu'à maintenant. L'utilisation des concentrations Ba:Ca des otolithes pour identifier une résidence en eau douce reste encore peu étudiée, mais elle peut fournir des classications plus précises des environnements estuariens que l'utilisation des concentrations de Sr:Ca ou celle des isotopes de strontium.

[Traduit par la Rédaction]

Introduction

Determining movements and migrations of fish between environments is crucial, especially if we are to understand life-history characteristics of species. In complex environments, such as estuaries, movements are affected by multiple factors, including flow dynamics and population abundances (Hughes 1999; Yako et al. 2002). In these environments, conventional tags (e.g., dart tags) have little application, owing to low tag returns. Although advanced methods of fish tagging, such as acoustic and radio tags, can be used to determine movements of fish entering and exiting rivers and streams (e.g., Comeau et al. 2002), their application is limited by expense and to tracking fish over short periods of

Received 2 August 2004. Accepted 31 December 2004. Published on the NRC Research Press Web site at http://cjfas.nrc.ca on 27 May 2005.
J18248

T.S. Elsdon[1,2] and B.M. Gillanders. Southern Seas Ecology Laboratories, Darling Building DP-418, School of Earth and Environmental Science, The University of Adelaide, South Australia 5005, Australia.

[1]Corresponding author (e-mail: travis.elsdon@adelaide.edu.au).
[2]Present address: SUNY – College of Environmental Science and Forestry, 241 Illick Hall, 1 Forestry Drive, Syracuse, NY 13210, USA.

 doi: 10.1139/F05-029 © 2005 NRC Canada

their life history (fish can not be tagged as larvae or juveniles). However, natural tags within the fish, such as the elements present within otoliths (earbones), are ideally suited to answering ecological questions regarding life histories of fish (Elsdon and Gillanders 2003*a*), because all fish are essentially already tagged.

The ability of otoliths to act as natural tags is reliant on elements, such as barium (Ba) and strontium (Sr), being incorporated into their calcium carbonate matrix ($CaCO_3$) through either substitution (e.g., $BaCO_3$ or $SrCO_3$) or binding within the lattice matrix (for an overview see Nielson and Christoffersen 1982). Ba and Sr concentrations in otoliths are influenced by the environmental variables of temperature, salinity, and ambient elemental concentrations (e.g., Elsdon and Gillanders 2002, 2003*b*; Martin et al. 2004), with little influence from dietary uptake of elements (Farrell and Campana 1996; Milton and Chenery 2001). When predictable relationships between environmental variables and otolith chemistry are found (e.g., Tzeng 1996; Bath et al. 2000; Elsdon and Gillanders 2003*b*), elemental concentrations within otoliths provide a means for determining the environmental history of fish. Determining relationships between otolith Sr:Ca (i.e., Sr standardized to Ca and expressed as a ratio) and salinity, such as that for eels (*Anguilla* sp.), allows for reconstructions of freshwater occupation by individuals (e.g., Jessop et al. 2002; Tzeng et al. 2002). Consequently, life-history characteristics of eels, which were thought to be simple, are now understood to be complex, with migratory patterns varying between environments that differ in salinity. Despite the use of the otolith Sr:Ca to investigate environmental histories of fish, the application of otolith Ba:Ca to answer similar questions has not been examined.

Ambient Ba:Ca positively influences Ba:Ca in fish otoliths and scales (Bath et al. 2000; Wells et al. 2000; Elsdon and Gillanders 2003*b*). Although ambient temperature and salinity can affect otolith chemistry (e.g., Secor et al. 1995; Bath et al. 2000; Elsdon and Gillanders 2002) and influence the effect of ambient Ba:Ca on otolith Ba:Ca (Bath et al. 2000; Elsdon and Gillanders 2004), their effects on otolith chemistry are minimal compared with the influence of ambient Ba:Ca (Bath et al. 2000; Elsdon and Gillanders 2004). Therefore, otolith Ba:Ca provides a means to determine environmental histories of fish in environments where large differences in ambient ratios occur.

Determining environmental histories of fish on the basis of otolith Ba:Ca can take advantage of the natural bioavailability and distribution of Ba in water. Ba in freshwater is weakly complex, existing as 99% free Ba compared with 86% free Ba in salt water (free from compound binding, such as in BaCl, $BaSO_4$, or $BaCO_3$) (Turner et al. 1981); hence, Ba has a greater bioavailability to fish in freshwater than in salt-water environments. In addition, Ba is closely bound to fluvial sediments, such as fluvial runoff within estuaries (as opposed to resuspended sediments) (Li and Chan 1979; Coffey et al. 1997), and concentrations are high within upwelling waters (Lea et al. 1989), resulting in freshwater estuaries often receiving large inputs of sediment from land runoff. Although ambient Ba concentrations vary among and within freshwater locations (e.g., Guay and Falkner 1998), primarily because of differences in geology, the delivery of fluvial runoff, and changes in flow-related Ba release from fluvial sediments, salt-water (35‰) and freshwater locations are distinguishable from each other. Applications for reconstructing environmental histories of Ba can be found in the coral literature (e.g., Lea et al. 1989; McCulloch et al. 2003). McCulloch et al. (2003) used the greater bioavailability and concentration of Ba in fresh water to document peaks in coastal coral Ba concentration: peaks were related to changed flood regimes associated with European settlement in Australia. Similar applications using fish otoliths for determining environmental histories should be possible, such as determining the proportion of time fish spend in freshwater environments.

The aims of the current study were to assess if otolith Ba:Ca relates to salinity, and, if so, determine whether this relationship can be used to reconstruct environmental histories of fish. Specifically, field-collected black bream (*Acanthopagrus butcheri*) were used to test two hypotheses: (1) otolith Ba:Ca in wild black bream can be related to ambient Ba:Ca, and (2) otolith Ba:Ca in wild black bream were higher in freshwater locations than in salt-water locations. Data used to test these hypotheses were then used to assess the freshwater occupancy of black bream. As with otolith Sr:Ca, it is assumed that fish inhabited environments long enough to incorporate elements at ambient concentrations.

Materials and methods

Sampling design

Black bream were collected in the austral summer (defined as November and December) and winter (defined as May and June) from temperate estuaries. Ten estuaries were sampled in summer and 7 in winter. At each estuary, 8–10 fish were obtained by line and baited hook. The outside edge (representing the last 30 µm of growth) of otoliths from these fish was analysed to relate ambient Ba:Ca to otolith Ba:Ca. Concurrently with fish collections, salinity was recorded and water samples were collected for analysis of ambient Ba:Ca ($n = 3$ for both at each location); replicate readings and samples were separated by at least 5 m. Water samples for analysis of Ba:Ca were collected in 70-mL acid-washed polypropylene sample jars following the methods of Elsdon and Gillanders (2002).

Based on estuarine salinity characteristics, fish from two freshwater and two salt-water locations in each season were chosen for further analysis of otolith Ba:Ca (see Fig. 1). Freshwater locations (South West River and Glenelg River in summer and Ewens Ponds and Glenelg River in winter) ranged in salinity from 0.32 ± 0.00‰ (Ewens Ponds) to 4.14 ± 0.45‰ (Glenelg River in summer; mean ± standard error of the mean (SE)). Fish caught in these estuaries were typically 3–4 km upstream from salt water; in Ewens Ponds this represents the source of fresh water from groundwater. Salt-water estuaries (Port Adelaide and Onkaparinga River) ranged in salinity from 25.93 ± 1.09‰ (Onkaparinga in summer) to 37.57 ± 0.53‰ (Port Adelaide in winter). All estuaries were freely connected to salt-water environments.

Otolith preparation and analysis

The standard length of each fish was recorded prior to dissection, which included otoliths being dissected out, washed

© 2005 NRC Canada

Fig. 1. Map showing the sampling locations along the coastline of southern Australia. Circles represent locations of fish and water sampling; shaded circles (labelled by name) indicate locations where life histories of black bream (*Acanthopagrus butcheri*) were reconstructed, based on transects of otolith Ba:Ca ratios.

and cleaned in deionized water, and allowed to air-dry in microcentrifuge tubes. One otolith from each fish was embedded in EpoFix® resin (Struers, Denmark) that was spiked with 40 ppm indium (In) to allow for discrimination between the otolith and resin upon analysis. Otoliths were sectioned transversely through the focus (centre section) using a low-speed diamond saw lubricated with deionized water. Sections were approximately 300 µm thick and were polished to 200 µm using 30- and 9-µm lapping film. Polished sections were fixed to glass slides with EpoFix® resin; slides were then sonicated in deionized water and allowed to air-dry. Sectioned otoliths were digitally photographed after analysis of elements using a compound microscope and image-analysis software to determine the position of annuli, which were then matched to elemental concentrations along transects.

The concentrations of Ba and Ca in otolith samples were determined using a Merchantek LUV 266 Q-switched Nd:YAG UV laser microprobe with an ablation spot size of 30 µm. The laser ablation station was connected to a Finnigan MAT Element high-resolution inductively coupled plasma mass spectrometer (HR-ICP-MS) with operating conditions similar to those reported in Elsdon and Gillanders (2002). Ablations occurred inside a sealed chamber, with the sample gases extracted to the HR-ICP-MS via a smoothing manifold. The chamber was purged for 20 s after each ablation to remove background gas from previous ablations (Lahaye et al. 1997). Elements within the chamber were measured before each ablation (for 25 s) to allow for background correction of samples. Otoliths were analysed in several sampling sessions with two reference standards, which allowed for comparison among sampling sessions. Blank ablations measured the chamber gases in the absence of any sample before and after each sampling session, and were used to determine the detection limits of the machine. A reference standard (National Institute of Standards and Technology, NIST 612) was analysed after every 10 otolith ablations to correct for machine drift (Ludden et al. 1995). Ba and Ca concentrations in otoliths were corrected using a fish otolith standard (a 32 mm diameter pressed powdered disk of finely ground otolith, similar to that described for coral by Fallon et al. 1999), which was analysed at the beginning and end of each sampling session. Analytical accuracies determined from the NIST concentrations and averaged across all samples were 100% for Ca^{44} and 106% for Ba^{138}. Detection limits determined from black ablations were <0.0006 µmol·mol^{-1} for Ca and <0.0001 µmol·mol^{-1} for Ba.

All otoliths were analysed using spot analysis on the outside edge (outermost 30 µm of otolith growth). Detailed otolith analysis of Ba:Ca in fish from four fresh- and saltwater estuaries was done using transect analysis that consisted of continually moving the laser during ablations at ap-

© 2005 NRC Canada

Fig. 2. Plots of otolith versus ambient Ba:Ca from summer (*a*) and winter (*c*) field collections and of otolith Ba:Ca versus salinity from summer (*b*) and winter (*d*) field collections. Data points are displayed as the mean ± standard error of the mean. Equations characterizing relationships are presented, with r^2 values.

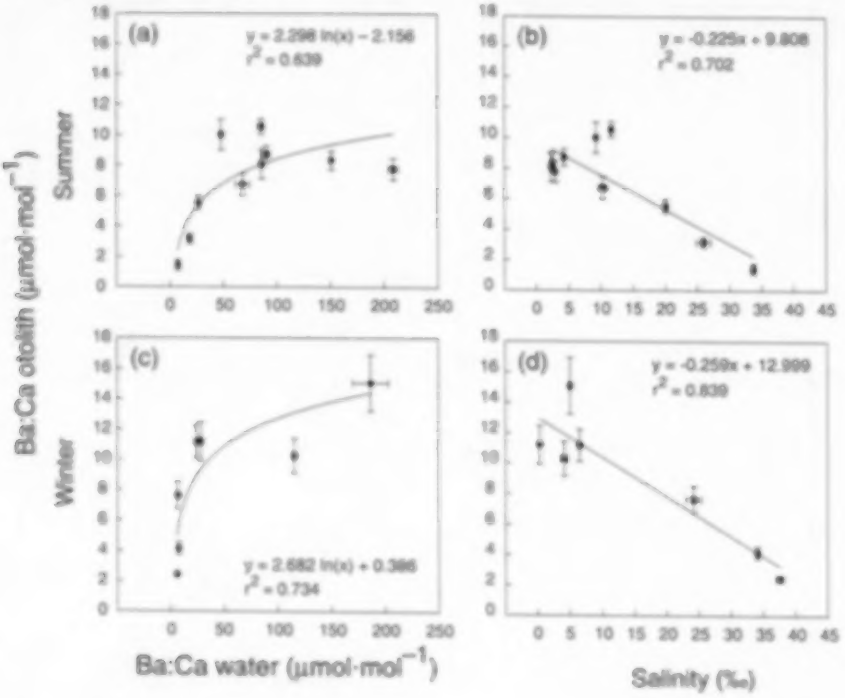

proximately 1.3 µm·s^{-1} across the otolith surface, which resulted in a continuous transect of data across the otolith (Sinclair et al. 1998; Fallon et al. 2002). Otoliths were analysed from the centre (core region) to the outside edge; standard materials were similarly ablated for a total of 100 µm.

Data reduction for spot analyses were done on spreadsheets and consisted of smoothing, background subtracting, standardizing to NIST 612, normalizing to Ca (internal standard for ablation yield), and correcting to the fish standard (for detailed methods see Elsdon and Gillanders 2002). Data reduction from transects of Ba:Ca across individual otoliths was also done on spreadsheets. Transect data are noisy and require filtering to determine trends. To reduce noise along transects, a 9-point running mean and 9-point running median were applied (Sinclair et al. 1998). The results of both smoothing processes were transects that displayed little noise. Ba concentrations were corrected to both the NIST 612 and the fish standards. Ba concentrations from both spot and transect analyses were standardized to Ca (e.g., Ba:Ca), as Ba is likely to substitute for Ca (Campana 1999).

Water-sample preparation and analysis

One-third of each sample (25 mL) was filtered using a 0.45-µm filter and acidified with 500 µL of high-grade nitric acid. Samples were further diluted (1:10 sample : deionized water) before analysis.

Water samples were analysed using a Perkin Elmer 3000 dual view inductively coupled plasma atomic emission spectrometer (DV ICP-AES) for Ca^{44} and a Perkin Elmer Elan 6000 dynamic reaction cell inductively coupled plasma mass spectrometer (DRC ICP-MS) for Ba^{138} to maximize detection limits. Internal standards of In (5 ppb) and lutetium (2 ppb) were used to correct for drift of the ICP-MS and ICP-AES, respectively. Detection limits calculated from blank samples were <5.0 µg·L^{-1} for Ca and <1.0 µg·L^{-1} for Ba, all sample values being above detection limits. The analytical accuracies averaged across all samples were 101% for Ca and 99% for Ba. Ba was standardized to Ca and expressed as a ratio (Ba:Ca).

Results

Relationship between otolith and environmental variables

Ba:Ca at the outermost edge of black bream otoliths represented the ratio at the time of capture. Otolith Ba:Ca in all locations in summer and winter was strongly correlated with the ambient Ba:Ca (Figs. 2*a*, 2*c*). Similarly, otolith Ba:Ca was negatively correlated with salinity in summer and winter (Figs. 2*b*, 2*d*). Equations describing the relationship between otolith and ambient Ba:Ca and between otolith Ba:Ca and salinity differed in slope between summer and winter field collections. This influence was due to fish having high otolith Ba:Ca in winter. However, the direction of these relationships remained consistent between seasons.

© 2005 NRC Canada

Fig. 3. Otolith Ba:Ca ratios in fresh- and salt-water locations in summer and winter field collections. Data are displayed as the mean ± standard error of the mean. Numbers below the *x* axis denote locations.

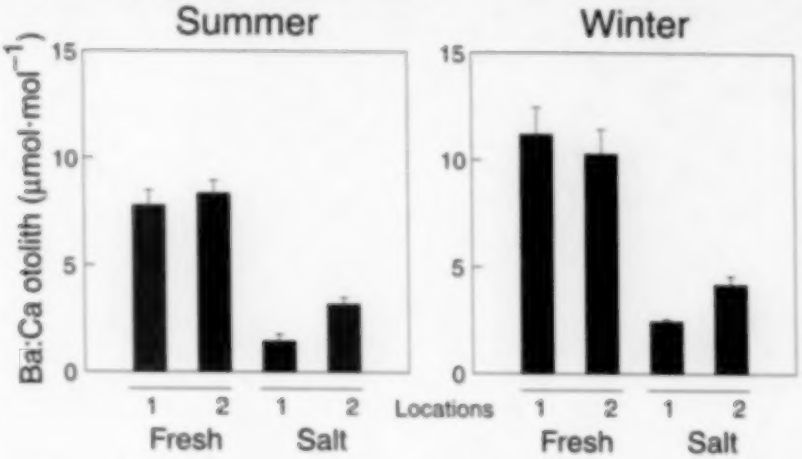

Fish from two freshwater and two salt-water estuaries were chosen in each season to compare otolith Ba:Ca statistically. In both seasons, the otolith Ba:Ca was greater in the freshwater locations than in the salt-water locations (Fig. 3; Table 1). However, the magnitude of the difference between environments differed with season. Fish from the freshwater locations of South West River and Glenelg River (summer) had otolith Ba:Ca ranging from 7.79 ± 0.71 to 8.35 ± 0.61 μmol·mol^{-1} (mean ± SE), whilst fish from Glenelg River and Ewens Ponds (winter) had values ranging from 10.28 ± 1.15 to 11.20 ± 2.36 μmol·mol^{-1} (mean ± SE). These differences may represent higher freshwater inflow in winter than in summer. In contrast to this, otolith Ba:Ca in the salt-water locations Port Adelaide and Onkaparinga River were stable irrespective of season and ranged from 1.43 ± 0.33 to 2.44 ± 0.10 μmol·mol^{-1} and 3.18 ± 0.32 to 4.17 ± 0.40 μmol·mol^{-1}, respectively.

Table 1. Analysis of variance comparing Ba:Ca ratios in otoliths between fish from fresh- and salt-water locations.

Source of variation	df	Mean square	*F*	*P*
Summer				
Salinity	1	265.5671	39.33	*
Location (salinity)	2	6.7516	3.15	ns
Residual	28	2.1432		
Winter				
Salinity	1	441.8260	57.25	*
Location (salinity)	2	7.7175	1.26	ns
Residual	28	6.1450		

Note: Cochran's *C* test was used to test homogeneity of variance. All tests were nonsignificant; ns, $P > 0.05$; *, $P < 0.05$.

Environmental histories

Transects of otolith Ba:Ca revealed different trends between freshwater- and salt-water-caught fish (Fig. 4). Fish from the freshwater locations South West River and Glenelg River (summer) and Ewens Ponds and Glenelg River (winter) showed periods of high otolith Ba:Ca interspersed with periods of lower ratios (Figs. 4*a*, 4*b*, 4*e*, 4*f*); peaks and troughs in Ba:Ca often showed no relationship to the position of annuli. Plots of data from fish collected in the salt-water locations Port Adelaide and Onkaparinga River (summer and winter) appear flat and ratios are low (Figs. 4*c*, 4*d*, 4*g*, 4*h*), which is vastly different from plots for fish collected in freshwater locations; otolith Ba:Ca showed no trends with position of annuli.

Transect analysis allowed small portions of fish otoliths to be classified to fresh- or salt-water residency. Differences in otolith Ba:Ca between fresh and salt water (Fig. 3) were used to classify fish to different environments, where ratios ≤5 μmol·mol^{-1} represented otolith growth incorporated during salt-water occupancy and concentrations ratios ≥6 μmol·mol^{-1} represented otolith growth incorporated during freshwater occupancy. Ba:Ca ratios between 5 and 6 μmol·mol^{-1} were not classified to either environment and remained unassigned, as they may represent transitional stages between environments, or occupation of brackish waters of uncertain origin. The portion of time that otolith Ba:Ca represented freshwater growth was calculated as a percentage of the total otolith Ba:Ca transect.

Life-history movements of black bream from freshwater locations showed that they spent large periods of time in freshwater environments (between 62.63 ± 6.12 and 95.3 ± 3.12% (mean ± SE); Table 2). Although some individuals spent 100% of their time in fresh water, the majority of fish had at least one environmental change (fresh to salt water or vice versa). Two fish from Glenelg River in summer had five and six environmental changes; these fish were identical in size (160.5 ± 0.50 mm (mean ± SE)) to others that made considerably fewer changes (164.67 ± 8.07 mm).

Patterns of environmental change inferred from otolith Ba:Ca were largely irregular; fish either remained resident or moved unpredictably between environments (for an example of environmental patterns see Figs. 5*a* and 5*b*). Indeed, only four fish, two each from the South West and Glenelg rivers (all of which were caught in summer), showed cyclic and predictable changes in environment, which coincided with

© 2005 NRC Canada

Fig. 4. Representative transects of otolith Ba:Ca from individual fish from freshwater locations during summer (*a* and *b*) and winter (*e* and *f*) and salt-water locations during summer (*c* and *d*) and winter (*g* and *h*). Transects are plotted such that a distance of 0 μm represents the otolith core and greater distances along the transect represent increasing proximity to the otolith edge. Plots have unequal *x* axes, as fish with otoliths of different sizes were analysed. Arrows on each transect indicate the position of annuli. The collection location, with standard length, of the fish are displayed within each plot (SWR, South West River; EP, Ewens Ponds; GR, Glenelg River; PA, Port Adelaide; OR, Onkaparinga River).

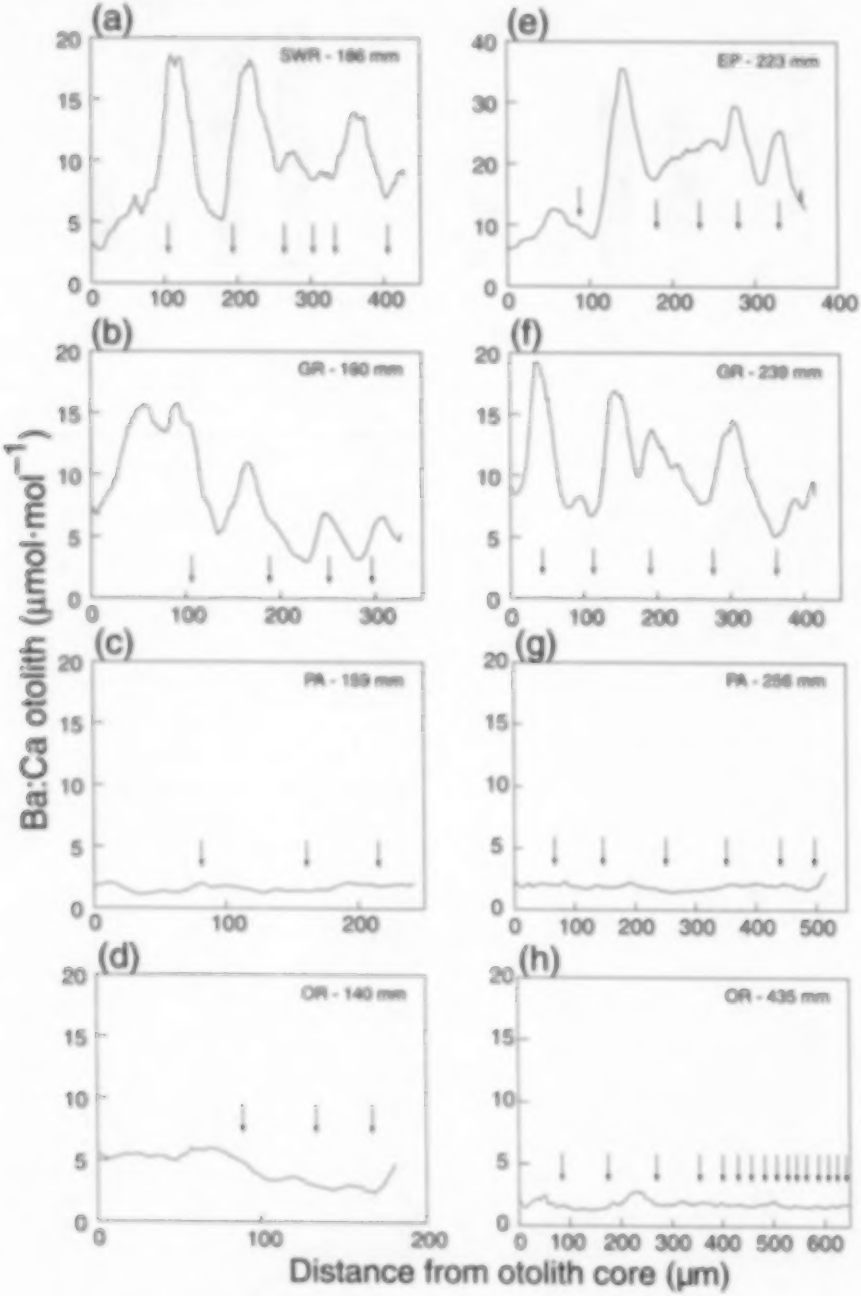

annulus position (e.g., Fig. 5*c*). Conversely, black bream caught in the salt-water location Port Adelaide did not enter freshwater environments, this pattern being consistent between seasons (Table 2). The majority of fish from the Onkaparinga River only changed environments once; one fish had three changes in environment in winter. One fish

© 2005 NRC Canada

Table 2. Fish life-history patterns in summer and winter in fresh- and salt-water locations.

Environment and season	Location[a]	Salinity (‰)[b]	Time spent in fresh water (%)[b]	No. of environmental changes[c]	Environmental pattern[d]	No. of fish	Standard length[b]
Fresh water							
Summer	SWR	2.48±0.06	91.66±0.89	2–3	C	2	193.50±7.50
			90.74±4.62	0–3	I/INP	6	176.50±11.98
	GR	2.94±0.01	62.63±6.12	5–6	C	2	160.50±0.50
			93.62±4.34	0–4	I/INP	6	164.67±8.07
Winter	EP	0.36±0.00	95.38±3.12	0–2	I	8	216.50±4.39
	GR	4.14±0.45	92.71±5.18	0–4	I/INP	8	220.90±9.32
Salt water							
Summer	PA	33.70±0.20	0.00±0.00	0	NP	8	236.89±4.58
	OR	25.93±1.09	82.16±7.99	0–1	I/INP	8	190.00±19.89
Winter	PA	37.57±0.53	0.00±0.00	0	NP	8	187.30±29.41
	OR	34.07±0.23	55.08±11.78	0–3	I/INP	8	184.67±31.38

[a]SWR, South West River; GR, Glenelg River; EP, Ewens Ponds; PA, Port Adelaide; OR, Onkaparinga River.
[b]Values are given as the mean ± standard error of the mean.
[c]Given as a range.
[d]C, cyclic; I, irregular pattern; NP, no pattern.

was considerably larger than the other seven (standard length 435 mm), hence the large variation in standard length for this site. Of those fish that changed environments only once, all were in salt water for the later stage of their life, which corresponded to the time they were captured.

Discussion

Otolith Ba:Ca as an environmental indicator

Otolith Ba:Ca increased with increasing ambient Ba:Ca. Although the relationships between otolith and ambient Ba:Ca differed in magnitude between laboratory-reared fish (Elsdon and Gillanders 2003*b*) and field-collected fish (this study), the direction of the relationship was consistent with trends seen in other fish species (e.g., Bath et al. 2000; Martin et al. 2004). Processes that affect the uptake and incorporation of Ba into otoliths include physiological and environmental variables, such as growth, temperature, salinity, and ambient chemistry (e.g., Kalish 1989; Sadovy and Severin 1994; Elsdon and Gillanders 2004). In addition, Elsdon and Gillanders (2003*b*) have shown that the period of time fish are exposed to differences in ambient chemistry can affect the incorporation of Sr:Ca in otoliths. Thus, several mechanisms that affect elemental incorporation may account for the discrepancy between the field results we present and findings from laboratory experiments. Nevertheless, the predictable differences in otolith Ba:Ca in black bream collected from environments differing in salinity, combined with the results of several laboratory experiments that have examined the influence of ambient chemistry on otolith chemistry in the same species (Elsdon and Gillanders 2002, 2003*b*, 2004), make otolith Ba:Ca an ideal tool for reconstructing environmental histories of fish.

Classifying environmental histories of fish to either fresh- or salt-water environments relies on ambient Ba:Ca being higher in freshwater locations than in salt-water locations. Although ambient Ba:Ca differed between summer and winter collections, ratios remained constantly higher in fresh water. Seasonal differences in otolith and ambient Ba:Ca may represent higher land runoff during winter in South Australia, which results in higher flow rates and increased bioavailability of Ba to fish (Coffey et al. 1997). This model is supported by Li and Chan (1979), who found high Ba concentrations in fluvial particles, such as suspended sediments and clays, both of which are abundant in land runoff. Therefore, the natural increase in Ba with decreasing salinity provides a means to determine environmental histories of fish, as fish incorporated greater Ba:Ca ratios in their otoliths while living in freshwater estuaries.

Predictions concerning fish environmental histories rely on the stability (temporal and spatial) of ambient Ba:Ca within estuaries. Although temporal variability in elemental concentrations occurs within estuaries (Hatje et al. 2003), we deliberately sampled the relatively stable environments of Port Adelaide and the Onkaparinga River. Both of these estuaries were salt-water-dominated, with limited freshwater inputs over the winter months (salinity 31.38 ± 0.55‰ in Port Adelaide and 30.36 ± 0.54‰ in the Onkaparinga River (mean ± SE; n = 16)). Similarly, the freshwater environments of Ewens Ponds, South West River, and Glenelg River were either permanently spring-fed or have high freshwater flow that maintained low salinity. Importantly, all sampled estuaries were open to salt-water environments, thus allowing free movement of fish between adjacent environments. The stability of salinity in the locations sampled is likely to contribute to the successful classification of environmental histories of fish. We stress, therefore, that the application of this technique was tested in an ideal situation and may not be justified for all estuaries, nor for all species of fish where experimental data cannot support field correlations.

Environmental histories derived from otolith Ba:Ca

Identifying environmental histories of fish, particularly migrations of individuals between fresh- and salt-water environments, has previously been done using Sr:Ca and Sr isotopes (^{87}Sr:^{86}Sr) in otoliths (e.g., Kennedy et al. 2000; Tsukamoto and Arai 2001). Reconstructions commonly use the predictable relationship between salinity and otolith Sr concentration (even though salinity influences ambient Sr) to infer environmental histories; however, this relationship does

© 2005 NRC Canada

Fig. 5. Representative transects of otolith Ba:Ca ratios characteristic of a resident fish (*a*), a fish with irregular patterns of movement between fresh- and salt-water environments (*b*), and a fish with cyclic patterns of movement between fresh- and salt-water environments (*c*). Transects are plotted such that a distance of 0 μm represents the otolith core and greater distances along the transect represent increasing proximity to the otolith edge. Plots have unequal *x* axes, as fish with otoliths of different sizes were analysed. The collection location, with standard length, of the fish are as follows: (*a*) PA, Port Adelaide, 256 mm; (*b*) SWR, South West River, 186 mm; (*c*) GR, Glenelg River, 161 mm. Arrows on each transect indicate the position of annuli.

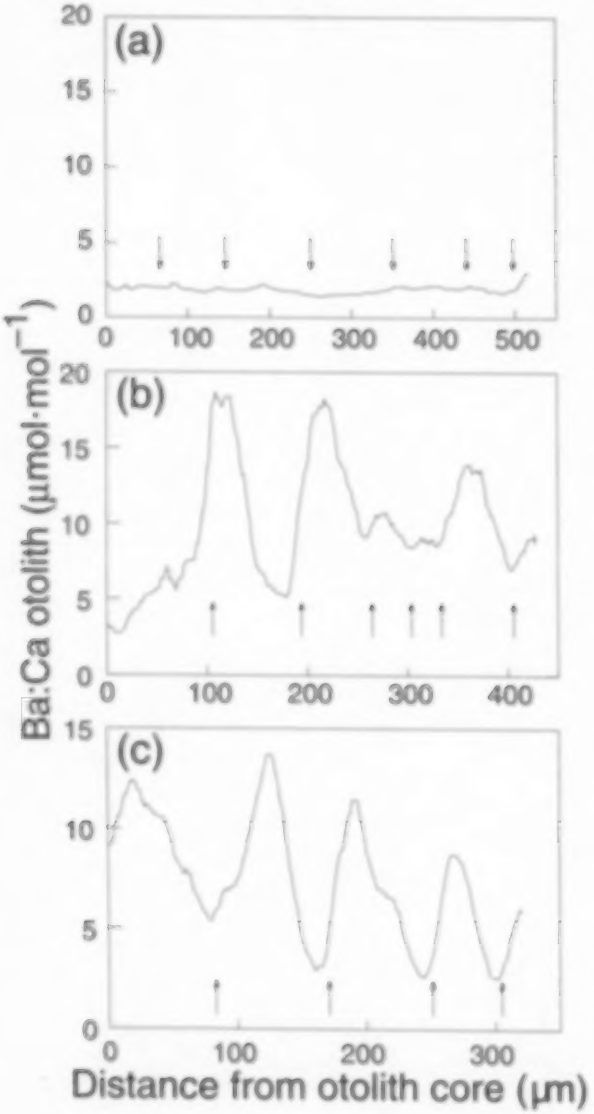

not exist in all rivers and estuaries (Kraus and Secor 2004) and is dependent largely on the geology of the surrounding rock. In addition, in species, such as black bream, where salinity has a reduced effect on otolith Sr:Ca compared with temperature and ambient chemistry (Elsdon and Gillanders 2004), or in estuaries where Sr gradients are minimal, the application of Sr to determine environmental histories of individual fish is limited. Likewise, although Sr isotopes are ideally suited to determining differences in freshwater streams, their application is limited to low-salinity environments (Kennedy et al. 2002; Milton and Chenery 2003), and may not be suited to brackish water estuaries. However, the ability of Ba:Ca in otoliths to discriminate between environments appears promising, with large detectable differences in ratios occurring between freshwater and salt-water environments.

Ontogeny has little influence on otolith Ba:Ca in black bream at different life-history stages (T.S. Elsdon and B.M. Gillanders, unpublished data); thus, interpretations of environmental histories need not be limited to particular ontogenetic stages. Accordingly, we have classified environmental histories of black bream across entire otoliths, representing the entire life history of individual fish. Two distinct trends in otolith Ba:Ca were found: (1) when no changes in Ba:Ca occurred across otoliths, fish were classified as resident in fresh water (high Ba:Ca) or salt-water environments (low Ba:Ca), and (2) when otolith Ba:Ca changed across otoliths, fish were classified as migratory. For the majority of migratory fish, movements were irregular and typical of diadromous migrations between fresh and salt water (McDowall 1988). However, a few fish displayed cyclic and predictable patterns of movement between environments with respect to position of annuli, these patterns being characteristic of anadromous migrations. The classifications of diadromous and anadromous migrations in black bream were similar to those made for eel (*Anguilla* sp.), zander (*Sander lucioperca*), and common bream (*Abramis brama*) (Tzeng et al. 1997; Kafemann et al. 2000; Jessop et al. 2002).

Differences in the regularity of environmental changes in black bream, in which irregular and cyclic patterns of movement occur, represent contrasting migrations of individual fish. Fish caught in the Glenelg River during summer provide an excellent example of individuals with different migratory patterns in the one estuary. Of the fish caught in the Glenelg River, six displayed no pattern (freshwater fish) or irregular patterns of movement between environments with respect to position of annuli, spending an average of 93% of their lives in fresh water. However, two fish displayed cyclic changes, with low otolith Ba:Ca coinciding with the formation of annuli; these fish spent 63% of their lives in fresh water. Fish exhibiting cyclic changes most likely represent those that undertake anadromous migrations, with annual movements from salt-water to freshwater environments. Thus, within a single population of black bream, individual fish showed resident, diadromous, and anadromous migratory patterns. Although we did not account for differences in otolith growth rate within and among years (owing to availability of adequate numbers of fish), determining the relative portions of otolith growth that occur during different seasons and months may enhance interpretation. Nevertheless, gaining an understanding of such detailed migrations from relatively few fish would be impossible using conventional tagging techniques (for a review of techniques see Gillanders et al. 2003). Indeed, multiple migratory patterns within the same population of eels have been found using otolith Sr:Ca

© 2005 NRC Canada

(Tzeng and Tsai 1994; Tsukamoto and Arai 2001; Kotake et al. 2003). Thus, our study concurs with others in demonstrating the usefulness of otolith chemistry for resolving the environmental histories and migrations of fish.

Information on the movement and environmental histories of black bream is limited, and is reliant on tagging and catch per unit effort data. To date, this information has been used to identify a mixture of environmental histories of black bream, ranging from permanent freshwater occupancy to intermittent use of coastal habitats (seagrass and rocky reef), the nature of the environment (i.e., closed or intermittently open estuaries) being thought to determine movement patterns of individuals (for a review see Norriss et al. (2002) and references therein). The otolith Ba:Ca ratios of black bream that we present suggest that movements between estuarine and coastal waters are frequent and often unpredictable. Therefore, the hypothesis that black bream movements are primarily controlled by the nature of the environment is questionable. The co-occurrence of multiple movement strategies of similar-sized fish in estuaries suggests that migratory patterns of black bream are dynamic and several migratory cues may operate independently on individual fish.

In conclusion, we have highlighted the application of fish otolith Ba:Ca to determine the environmental histories of individuals of an estuarine species. Discriminating between environments is possible because of the positive relationship between ambient and otolith Ba:Ca and the natural negative relationship between ambient Ba:Ca and salinity. Classifications of migratory patterns of fish were consistent with diadromous and anadromous migrations. We stress that our observations and interpretations do not imply that Ba:Ca ratios in otoliths can be related to salinity changes in all estuaries, or to all species; laboratory experiments testing the influence of environmental variables on otolith chemistry are needed to validate the use of such tools. However, we believe that the use of Ba:Ca in fish otoliths to infer environmental histories is under-used in studies examining otolith chemistry, and too much emphasis is placed on the use of Sr:Ca to answer similar ecological questions.

Acknowledgements

This research was supported by an Australian Postgraduate Award and an Australian Federation of University Women bursary to T.S.E and an Australian Research Council Queen Elizabeth II Fellowship to B.M.G. Funding was provided by a Mark Mitchell grant, a Fisheries Society of the British Isles grant, and an Onkaparinga Catchment Water Management Board grant to T.S.E.

References

Bath, G.E., Thorrold, S.R., Jones, C.M., Campana, S.E., McLaren, J.W., and Lam, J.W.H. 2000. Strontium and barium uptake in aragonitic otoliths of marine fish. Geochim. Cosmochim. Acta, **64**: 1705–1714.

Campana, S.E. 1999. Chemistry and composition of fish otoliths: pathways, mechanisms and applications. Mar. Ecol. Prog. Ser. **188**: 263–297.

Coffey, M., Dehairs, F., Collette, O., Luther, G., Church, T., and Jickells, T. 1997. The behaviour of dissolved barium in estuaries. Estuar. Coast. Shelf Sci. **45**: 113–121.

Comeau, L.A., Campana, S.E., and Guastonguay, M. 2002. Automated monitoring of a large-scale cod (*Gadus morhua*) migration in the open sea. Can. J. Fish. Aquat. Sci. **59**: 1845–1850.

Elsdon, T.S., and Gillanders, B.M. 2002. Interactive effects of temperature and salinity on otolith chemistry: challenges for determining environmental histories of fish. Can. J. Fish. Aquat. Sci. **59**: 1796–1808.

Elsdon, T.S., and Gillanders, B.M. 2003*a*. Reconstructing migratory patterns of fish based on environmental influences on otolith chemistry. Rev. Fish Biol. Fish. **13**: 219–235.

Elsdon, T.S., and Gillanders, B.M. 2003*b*. Relationship between water and otolith elemental concentrations in juvenile black bream *Acanthopagrus butcheri*. Mar. Ecol. Prog. Ser. **260**: 263–272.

Elsdon, T.S., and Gillanders, B.M. 2004. Fish otolith chemistry influenced by exposure to multiple environmental variables. J. Exp. Mar. Biol. Ecol. **313**: 269–284.

Fallon, S.J., McCulloch, M.T., van Woesik, R., and Sinclair, D.J. 1999. Corals at their latitudinal limits: laser ablation trace element systematics in *Porites* from Shirigai Bay, Japan. Earth Planet. Sci. Lett. **172**: 221–238.

Fallon, S., White, J., and McCulloch, M. 2002. *Porites* corals as recorders of mining and environmental impacts: Misima Island, Papua New Guinea. Geochim. Cosmochim. Acta, **66**: 45–62.

Farrell, J., and Campana, S.E. 1996. Regulation of calcium and strontium deposition on the otoliths of juvenile tilapia, *Oreochromis niloticus*. Comp. Biochem. Physiol. **115**: 103–109.

Gillanders, B.M., Able, K.W., Brown, J.A., Eggleston, D.B., and Sheridan, P.F. 2003. Evidence of connectivity between juvenile and adult habitats for mobile marine fauna: an important component of nurseries. Mar. Ecol. Prog. Ser. **247**: 281–295.

Guay, C.K., and Falkner, K.K. 1998. A survey of dissolved barium in the estuaries of major Arctic rivers and adjacent seas. Cont. Shelf Res. **18**: 859–882.

Hatje, V., Apte, S.C., Hales, L.T., and Birch, G.F. 2003. Dissolved trace metal distributions in Port Jackson estuary (Sydney Harbour), Australia. Mar. Pollut. Bull. **46**: 719–730.

Hughes, N.F. 1999. Population processes responsible for larger-fish-upstream distribution patterns of Arctic grayling (*Thymallus arcticus*) in interior Alaskan runoff rivers. Can. J. Fish. Aquat. Sci. **56**: 2292–2299.

Jessop, B.M., Shiao, J.C., Iizuka, Y., and Tzeng, W.N. 2002. Migratory behaviour and habitat use by American eel *Anguilla rostrata* as revealed by otolith microchemistry. Mar. Ecol. Prog. Ser. **233**: 217–229.

Kafemann, R., Adlerstein, S., and Neukamm, R. 2000. Variation in otolith strontium and calcium ratios as an indicator of life-history strategies of freshwater fish species within a brackish water system. Fish. Res. (Amst.), **46**: 313–325.

Kalish, J.M. 1989. Otolith microchemistry: validation of the effects of physiology, age and environment on otolith composition. J. Exp. Mar. Biol. Ecol. **132**: 151–178.

Kennedy, B.P., Blum, J.D., Folt, C.L., and Nislow, K.H. 2000. Using natural strontium isotopic signatures as fish markers: methodology and application. Can. J. Fish. Aquat. Sci. **57**: 2280–2292.

Kennedy, B.P., Klaue, A., Blum, J.D., Folt, C.L., and Nislow, K.H. 2002. Reconstructing the lives of fish using Sr isotopes in otoliths. Fish. Bull. **59**: 925–929.

Kotake, A., Arai, T., Ozawa, T., Nojima, S., Miller, M.J., and Tsukamoto, K. 2003. Variation in migratory history of Japanese

© 2005 NRC Canada

eels, *Anguilla japonica*, collected in coastal waters of the Amakusa Islands, Japan, inferred from otolith Sr/Ca ratios. Mar. Biol. (Berl.), **142**: 849–854.

Kraus, R.T., and Secor, D.H. 2004. Incorporation of strontium into otoliths of an estuarine fish. J. Exp. Mar. Biol. Ecol. **302**: 85–106.

Lahaye, Y., Lambert, D., and Walters, S. 1997. Ultraviolet laser sampling and high resolution inductively coupled plasma-mass spectrometry of NIST and BCR-2G glass reference materials. Geostand. Newsl. **21**: 205–214.

Lea, D.W., Shen, G.T., and Boyle, E.A. 1989. Coralline barium records temporal variability in equatorial Pacific upwelling. Nature (Lond.), **340**: 373–376.

Li, Y.H., and Chan, L.H. 1979. Desorption of Ba and ^{226}Ra from riverborne sediments in the Hudson estuary. Earth Planet. Sci. Lett. **43**: 343–350.

Ludden, J.N., Feng, R., Gauthier, G., Stix, J., Shi, L., Francis, D., Machado, N., and Wu, G. 1995. Applications of LAM-ICP-MS analysis to minerals. Can. Mineral. **33**: 419–434.

Martin, G., B., Thorrold, S.R., and Jones, C.M. 2004. Temperature and salinity effects on strontium incorporation in otoliths of larval spot (*Leiostomus xanthurus*). Can. J. Fish. Aquat. Sci. **61**: 34–42.

McCulloch, M., Fallon, S.J., Wyndham, T., Hendy, E., Lough, J., and Barnes, D. 2003. Coral record of increased sediment flux to the inner Great Barrier Reef since European settlement. Nature (Lond.), **421**: 727–730.

McDowall, R.M. 1988. Diadromy of fish: migrations between freshwater and saltwater environments. Cambridge University Press, Cambridge.

Milton, D.A., and Chenery, S.R. 2001. Sources and uptake of trace metals in otoliths of juvenile barramundi (*Lates calcarifer*). J. Exp. Mar. Biol. Ecol. **264**: 47–65.

Milton, D.A., and Chenery, S.R. 2003. Movement patterns of the tropical shad hilsa (*Tenualosa ilisha*) inferred from transects of $^{87}Sr/^{86}Sr$ isotope ratios in their otoliths. Can. J. Fish. Aquat. Sci. **60**: 1376–1385.

Nielson, A.E., and Christoffersen, J. 1982. The mechanisms of crystal growth and dissolution. *In* Biological mineralization and demineralization. *Edited by* G.H. Nancollas. Springer-Verlag, New York. pp. 37–77.

Norriss, J.V., Tregonning, J.E., Lenanton, R.C.J., and Sarre, G.A. 2002. Biological synopsis of the black bream, *Acanthopagrus butcheri* (Munro) (Teleostei: Sparidae), in Western Australia with reference to information from other southern states. *Edited by* J.V. Norriss, J.E. Tregonning, R.C.J. Lenanton, and G.A. Sarre. Department of Fisheries, Government of Western Australia, Perth.

Sadovy, Y., and Severin, K.P. 1994. Elemental patterns in red hind (*Epinephelus guttatus*) otoliths from Bermuda and Puerto-Rico reflect growth rate, not temperature. Can. J. Fish. Aquat. Sci. **51**: 133–141.

Secor, D.H., Henderson-Arzapalo, A., and Piccoli, P.M. 1995. Can otolith microchemistry chart patterns of migration and habitat utilization in anadromous fishes? J. Exp. Mar. Biol. Ecol. **192**: 15–33.

Sinclair, D.J., Kinsley, L.P.J., and McCulloch, M.T. 1998. High resolution analysis of trace elements in corals by laser ablation ICP-MS. Geochim. Cosmochim. Acta, **62**: 1889–1901.

Tsukamoto, K., and Arai, T. 2001. Facultative catadromy of the eel *Anguilla japonica* between freshwater and seawater habitats. Mar. Ecol. Prog. Ser. **220**: 265–276.

Turner, D.R., Whitfield, M., and Dickson, A.G. 1981. The equilibrium speciation of dissolved components in freshwater and seawater at 25 °C and 1 atm pressure. Geochim. Cosmochim. Acta, **45**: 855–881.

Tzeng, W.N. 1996. Effects of salinity and ontogenetic movements on strontium:calcium ratios in the otoliths of the Japanese eel, *Anguilla japonica* Temminck and Schlegel. J. Exp. Mar. Biol. Ecol. **199**: 111–122.

Tzeng, W.N., and Tsai, Y.C. 1994. Changes in otolith microchemistry of the Japanese eel, *Anguilla japonica*, during its migration from the ocean to the rivers of Taiwan. J. Fish Biol. **45**: 671–683.

Tzeng, W.N., Severin, K.P., and Wickström, H. 1997. Use of otolith microchemistry to investigate the environmental history of European eel *Anguilla anguilla*. Mar. Ecol. Prog. Ser. **149**: 73–81.

Tzeng, W.N., Shiao, J.C., and Iizuka, Y. 2002. Use of otolith Sr:Ca ratios to study the riverine migration behaviours of Japanese eel *Anguilla japonica*. Mar. Ecol. Prog. Ser. **245**: 213–221.

Wells, B.K., Bath, G.E., Thorrold, S.R., and Jones, C.M. 2000. Incorporation of strontium, cadmium, and barium in juvenile spot (*Leiostomus xanthurus*) scales reflects water chemistry. Can. J. Fish. Aquat. Sci. **57**: 2122–2129.

Yako, L.A., Mather, M.E., and Juanes, F. 2002. Mechanisms for migration of anadromous herring: an ecological basis for effective conservation. Ecol. Appl. **12**: 521–534.

© 2005 NRC Canada

Spawning behaviour and success of mature male Atlantic salmon (*Salmo salar*) parr of farmed and wild origin

Laura K. Weir, Jeffrey A. Hutchings, Ian A. Fleming, and Sigurd Einum

Abstract: We examined genetic differences in the reproduction of an alternative maturation phenotype in Atlantic salmon (*Salmo salar*) by comparing the spawning behaviour and success among farmed, first-generation hybrid, and wild mature male parr raised in similar environments. Parr competed for spawning opportunities in the presence of either wild or farmed large males. There were no consistent differences among groups in aggression; however, there were differences in spawning participation with respect to large male origin and among parr types. There was a strong negative temporal effect on mature male parr spawning participation that differed by parr type; wild and farmed parr were most likely to participate in early spawnings, with hybrids being the most likely to participate in late spawnings. Overall, parr were also less likely to participate in spawnings involving large farmed males. Variance in reproductive success was higher among parr than among large males. Our results are consistent with the hypothesis that there are genetically based behavioural differences among mature male parr of farmed and wild origin that may potentially lead to differences in reproductive success.

Résumé : Nous avons examiné les différences génétiques lors de la reproduction d'un phénotype mature de rechange du saumon atlantique (*Salmo salar*) en comparant le comportement de fraye et le succès de la fraye chez des tacons mâles matures hybrides de première génération de pisciculture et des tacons mâles matures sauvages élevés dans des conditions similaires. Les tacons font compétition pour obtenir des occasions de frayer en présence de mâles de grande taille provenant soit du milieu naturel, soit de pisciculture. Il n'y a pas de différences soutenues dans l'agression entre les groupes; il y a cependant des différences dans la participation à la fraye, en fonction de l'origine des grands mâles et des types de tacons. Il y a un fort effet temporel négatif sur la participation des tacons mâles matures à la fraye qui varie en fonction du type de tacon; les tacons du milieu naturel et de pisciculture sont plus susceptibles de participer à des frayes hâtives, alors que les hybrides le sont pour les frayes tardives. En général, les tacons sont moins susceptibles de participer à des frayes qui impliquent de grands mâles de pisciculture. La variance dans le succès de la reproduction est plus élevée chez les tacons que chez les grands mâles. Nos résultats s'accordent avec l'hypothèse qui veut qu'il y ait des différences de comportement génétiquement déterminées chez les tacons matures provenant du milieu naturel et de pisciculture qui mènent potentiellement à des différences de succès reproductif.

[Traduit par la Rédaction]

Introduction

Mating systems, being highly diverse among fishes, frequently involve alternative reproductive strategies (Taborsky 2001). These strategies are thought to be maintained in populations along some sort of evolutionarily stable continuum, resulting in approximately equal average fitness among individuals adopting either strategy at equilibrium (Gross 1985; Hutchings and Myers 1994). Among fish species, Atlantic salmon (*Salmo salar*) males express one of the most extreme size differences among alternative reproductive morphs (Hutchings and Myers 1994; Fleming 1996). This life history variability results in two distinct male maturation phenotypes: anadromous males and mature male parr (Jones 1959). Both phenotypes spend juvenile stages in fresh water; the former mature at a large size (~50–100 cm) following migration and feeding at sea, whereas the latter mature in fresh water at a considerably smaller size (~7–15 cm), whereafter they may or may not migrate to sea.

During the reproductive season, mature male parr sneak spawnings by darting under the female and attempting to fertilize eggs while anadromous males are releasing sperm (Jones 1959). For mature male parr, interactions with large fish can be injurious or fatal (sea trout (*Salmo trutta*): Bohlin

Received 6 April 2004. Accepted 7 September 2004. Published on the NRC Research Press Web site at http://cjfas.nrc.ca on 31 May 2005.
J18062

L.K. Weir[1] and J.A. Hutchings. Department of Biology, Life Sciences Centre, Dalhousie University, Halifax, NS B3H 4J1, Canada.
I.A. Fleming. Ocean Sciences Centre, Memorial University of Newfoundland, St. John's, NL A1A 1T3, Canada.
S. Einum. Norwegian Institute for Nature Research, Tungasletta, 2 N-7485, Trondheim, Norway.

[1]Corresponding author (e-mail: lweir@dal.ca).

 doi: 10.1139/F05-032 © 2005 NRC Canada

1975; Atlantic salmon: Hutchings and Myers 1987; brown trout (*S. trutta*): Broberg et al. 2000). It is generally held that mature male parr establish dominance hierarchies behind females (Jones 1959; Myers and Hutchings 1987) and that parr closest to females at the time of spawning realize the highest fertilization success (Jones 1959). However, to our knowledge, there has been no empirical study of mature male parr behaviour immediately prior to the release of sperm.

In contrast with the paucity of behavioural information about mature male parr during spawning, several studies have assessed their relative reproductive success (e.g., Hutchings and Myers 1988; Jordan and Youngson 1992; Thomaz et al. 1997). In some cases, this has led to estimates of the contribution of mature male parr to the genetic variability and effective population size of natural salmon populations (L'Abée-Lund 1989; Jones and Hutchings 2001, 2002). Such genetic contributions by parr may be important in maintaining the genetic variability, or reducing its rate of decline, as the size of the anadromous population declines, a demographic imbalance now common throughout much of the species' range (Parrish et al. 1998).

Among several potential threats to the persistence of salmon populations are concerns about the impact of escaped farmed fish on the genetic structure and demography of wild populations (Hindar et al. 1991; Hutchings 1991). Considering the high potential for genetic contribution from mature male parr during spawning, they might represent a primary means of introgression of foreign genes from escaped farmed fish into wild populations. In a controlled experiment, Garant et al. (2003) found that mature male parr of farmed origin were extremely successful in fertilizing eggs when competing with their wild counterparts. They suggested that behavioural differences, such as increased aggression among farmed juveniles, provided one potential explanation for the observed success of farmed parr.

We document behavioural interactions and quantify fertilization success of mature male parr of wild, hybrid, and farmed origin in competition with either wild or farmed large males in a simulated natural environment. Specifically, we compare and contrast mortality, wounding, aggression, spawning participation, and fertilization success among mature male parr of different genetic origin raised under similar hatchery conditions.

Materials and methods

Experimental groups and treatments

The experiment was conducted at the Norwegian Institute for Nature Research field station in Ims, Norway, from 6 November to 14 December 2001 in four 47-m^2 outdoor spawning arenas (Fleming 1996). Wild parr originated from the Imsa River; farmed parr originated from a Norwegian aquaculture strain called AquaGen. Hybrids were first-generation crosses of Imsa and AquaGen individuals. All parr were raised from eggs at the hatchery under similar environmental conditions. Prior to the experiment, all farmed and hybrid fish were sampled from separate stock tanks, of which 50 of 3000 AquaGen and 60 of 2270 Imsa × AquaGen parr were mature males. Imsa parr were sampled from a separate tank until approximately 100 mature males had been collected.

Mature males were distributed among the four arenas such that each contained 30 parr with equal numbers of Imsa, Imsa × AquaGen hybrids, and AquaGen individuals. Mature male parr were marked with a 5-mm white plastic bead in one of three locations, at the back of the dorsal fin on the right side of the fish, at the front of the dorsal fin on the left side of the fish, or at the front of the dorsal fin on the right side of the fish, to identify Imsa, hybrid, or AquaGen individuals, respectively. Large fish were from two different environments. Imsa wild fish were caught in a fish trap during their autumn migration; AquaGen fish were raised at the field station. Twenty-four Imsa females and 24 AquaGen females were placed in the arenas, six of each type in each arena. Two arenas each held 12 Imsa large males, while the other two arenas each held 12 AquaGen large males. Henceforth, we refer to the arenas containing only Imsa anadromous males as Imsa 1 and Imsa 2 and those with only AquaGen large males as AquaGen 1 and AquaGen 2. Anadromous fish were marked with 3.5-cm tags for individual identification. Prior to tagging, weight (grams) and fork length (centimetres) were recorded for all fish. Fin tissue samples were obtained and preserved in 95% ethanol for genetic analysis of parentage.

All mortalities were removed from the arenas and frozen for measurement at the end of the experiment. Parr recovered during and at the end of the experiment were photographed and examined for wounds. We classified the parr as wounded if the marks on their bodies included gashes that were characteristic of anadromous fish lingual and mandibular teeth (Hutchings and Myers 1987).

Behavioural observations

Parr and anadromous fish activity in each arena was monitored for 16 h daily from an observation tower. Each day, four 5-min periods of live observations of aggressive interactions among mature male parr and between anadromous fish and mature male parr were recorded at least 3 h apart. During these observation periods, we recorded the origin of the mature male parr initiating and receiving aggression. When anadromous fish were involved in interactions, their identity was recorded. Aggressive behaviours among parr consisted mainly of chases, whereby one individual swims rapidly toward another causing the latter to change direction, charges, which differ from chases in that the receiver of aggression does not flee, and bites. Anadromous fish were observed either chasing or biting mature male parr.

In addition to live observations, we videotaped behaviour at most nests from the time when a female had started digging until a few minutes after the time of egg release (t). We took 5-min samples of parr aggression beginning at $t - 10$ min and ending at $t - 5$ min. During these videotape sampling periods, we identified to group the initiator and receiver of each aggressive behaviour, noted whether the aggressor or receiver left the nest following a chase or bite, quantified the number of mature male parr of different origin present at the nest, and recorded the identity of anadromous fish present when the attack occurred. Maximum and minimum number of parr at the nest and the length of time the

© 2005 NRC Canada

female was present during the 5-min sample were also recorded. Encounters occurred when two or more parr were at the nest at a given time. One minute prior to spawning and at the time of spawning, we recorded the number of mature male parr of each origin and the identity and number of anadromous males present at the nest.

Genetic analyses

All egg nests in each arena (n_{nests} = 165, n_{eggs} = 50 745) were recovered between 25 February and 28 February 2002. Based on the range in spawning dates and the water temperatures in the arenas during winter, eggs were between approximately 140 and 330 degree-days old at the beginning of the excavation period and were at the "eyed" stage. Eyed and noneyed eggs were sorted and counted, and eggs containing live embryos were preserved in 95% ethanol for parentage analysis and transported to Dalhousie University, Halifax, Nova Scotia.

DNA was extracted from fin tissue using Qiagen DNeasy™ tissue extraction kits (Qiagen Inc., Mississauga, Ontario). Eggs were dissected and embryo heads were removed and placed in 100 µL of eyeball buffer (10 mmol Tris·L^{-1}, 50 mmol KCl·L^{-1}, 0.5% Tween 20) with 2 mg proteinase K·mL^{-1}. Samples were digested overnight at 55 °C and vortexed prior to denaturing the proteinase K at 95 °C for 15 min. We froze the samples at –20 °C after centrifuging at 2000 r·min^{-1} (1 r = 2π·rad) or 20000*g* for 2 min. Individuals were genotyped at five microsatellite loci: Ssa197 (O'Reilly et al. 1996), SSsp2213, SSsp2215, SSsp2216, and SSsp2210 (Paterson et al. 2004). One primer of each set was labelled with fluorescein or hexachlorofluorescein at the 5′ end. Polymerase chain reactions were carried out in 10-µL total volumes consisting of 2.0 µL of template DNA, 3.5 µL of double-distilled water, 1.0 µL of 10× *Taq* DNA polymerase buffer, 1.5 µL of 15 mmol $MgCl_2$·L^{-1}, 1.0 µL of 2 mmol dNTP·L^{-1}, 0.5 µL of 10 mmol forward primer·L^{-1}, 0.5 µL of 10 mmol reverse primer·L^{-1}, and 0.5 U (1 U ≈16.67 nkat) of *Taq* DNA polymerase. Polymerase chain reaction profiles for all loci were designed as follows: denaturation at 95 °C for 3 min followed by 35 cycles of 30 s at 95 °C, 30 s at 58 °C, 30 s at 72 °C, and a final extension for 30 min at 72 °C. Samples were run on 6% acrylamide gels and visualized using an FMBIO scanner (Hitachi Software Engineering America Ltd., Mirai Bio Division, Alameda, California). Individuals were genotyped against standard samples with known sizes, and each individual was rescored three times. All potential parents were amplified twice and genotyped four times.

Statistical analyses

Differences in body weight, length, and body condition among arenas and parr of different origin were tested using factorial ANOVAs with arena and origin entered as main factors. We used χ^2 tests to investigate differences in the numbers of recaptured and wounded parr of different origin among the four arenas. Aggressive behaviour initiated by mature male parr and large fish was analysed using χ^2 contingency tests or Fisher's exact tests for both live observations and aggression at nests prior to spawning, excluding instances when parr of a given origin were not present during the interactions. The number of nests attended by mature male parr of different origin was also analysed using χ^2 tests, with the expected values being equal for parr of different origin. To examine the effects of anadromous male and parr origin on the number of parr participating in spawnings, we constructed generalized linear models (GLMs) using S-Plus 6.1, specifying Poisson error and the log link function. Significance for all tests was set at $\alpha = 0.05$.

Offspring were assigned parents based on the maximum likelihood procedures of PAPA 1.1 (Duchesne et al. 2002). Video footage was used to corroborate ambiguous parentage assignments. As the focus of the genetic analysis was to determine group success among mature male parr, we verified through exclusion that offspring assigned to more than one most likely father of the same origin had no other potential fathers of different origin. Offspring that were not unambiguously assigned to fathers of only one origin were excluded from the analysis. As genotyping errors are not uncommon, analyses were carried out specifying an error rate across loci of 0.01 and an error distribution among alleles of 5 (Duchesne et al. 2002). Exclusion probabilities for potential parents were calculated using CERVUS 2.0 (Marshall et al. 1998). We used χ^2 tests to determine differences in fertilization success among groups and nonlinear regression analyses to examine changes in fertilization success of the different groups over the course of the spawning season.

Results

Body size and mortality

There were no size differences in parr among the arenas (ANOVA: length, $F_{[3,108]} = 0.035$, $P = 0.99$; weight, $F_{[3,108]} = 0.014$, $P = 0.99$; condition (grams per cubic centimetre × 100), $F_{[3,108]} = 0.12$, $P = 0.95$) (Table 1) or among the parr of different origin (ANOVA: length, $F_{[2,108]} = 0.11$, $P = 0.90$; weight, $F_{[2,108]} = 0.391$, $P = 0.68$; condition, $F_{[2,108]} = 3.08$, $P = 0.05$). In addition, there were no arena by parr type interactions affecting body size (ANOVA: length, $F_{[6,108]} = 0.026$, $P > 0.99$; weight, $F_{[6,108]} = 0.052$, $P = 0.99$; condition, $F_{[6,108]} = 0.84$, $P = 0.44$). The number of parr recovered at the end of the experiment did not differ among arenas (χ^2 test: $\chi^2 = 0.836$, df = 6, $P = 0.99$) (Table 1), nor were there differences in the incidence of wounding with respect to arena and parr origin (χ^2 test: $\chi^2 = 6.27$, df = 6, $P = 0.39$). One Imsa parr, one Imsa × AquaGen parr, and one AquaGen parr were found in the stomachs of three different Imsa females.

Aggressive interactions

Aggressive interactions against parr initiated by anadromous fish differed between sexes and among arenas. Attacks by males and females differed among arenas (Fisher's exact test: $P = 0.0002$) such that large males in Imsa 1 and AquaGen 1 were observed attacking mature male parr more often than females, whereas the opposite was true in AquaGen 2. However, there was no tendency for large fish in the different arenas to attack mature male parr of a given origin more frequently (Fisher's exact test: $P = 0.50$).

Similarly, parr–parr aggression differed among arenas. Total mature male parr aggression tended to be higher in are-

© 2005 NRC Canada

Table 1. Length (cm), weight (g), and condition ($g \cdot cm^{-3} \times 100$) of parr ($n = 10$ per type) at the beginning of the experiment, number of parr recaptured from each arena at the end of the experiment, and number of wounded parr of Imsa, Imsa × AquaGen, and AquaGen origin in each of the four experimental arenas.

Variable	Imsa 1	Imsa 2	AquaGen 1	AquaGen 2
Imsa				
Length	11.62±0.37	11.63±0.41	11.67±0.46	11.73±0.36
Weight	20.21±2.16	19.86±2.21	20.28±2.30	20.39±1.85
Condition	1.24±0.02	1.21±0.02	1.22±0.02	1.23±0.02
Recaptures	9	9	8	9
Wounded	5	4	5	5
Imsa × AquaGen				
Length	11.76±0.46	11.73±0.35	11.72±0.33	11.73±0.34
Weight	21.49±2.68	21.58±1.91	20.98±1.66	20.64±1.66
Condition	1.25±0.02	1.30±0.03	1.27±0.02	1.25±0.03
Recaptures	9	8	10	10
Wounded	3	2	3	6
AquaGen				
Length	11.77±0.47	11.87±0.46	11.66±0.50	11.91±0.47
Weight	21.19±2.29	21.61±2.60	21.01±2.35	22.32±2.77
Condition	1.24±0.03	1.23±0.03	1.28±0.04	1.25±0.02
Recaptures	8	9	6	8
Wounded	0	5	3	3

Table 2. Total nests sampled from videotape recordings (n), total nests with encounters and aggression, and the number of nests at which parr of a given origin initiated aggression.

	n	Encounters	Aggression	Imsa	Imsa × AquaGen	AquaGen
Imsa 1	22	14	10	2 (8)	3 (8)	8 (9)
Imsa 2	27	12	6	5 (6)	1 (4)	2 (4)
AquaGen 1	37	14	9	5 (8)	3 (9)	1 (8)
AquaGen 2	43	17	14	5 (8)	7 (12)	6 (8)

Note: Data in parentheses indicate the number of samples during which parr of a particular origin were observed at the nest. The number of nests with aggression is lower than the sum total of the number of nests at which parr of a given origin was aggressive because parr of different origin may have initiated aggression at the same nest.

nas with Imsa anadromous males and differed among arenas (χ^2 test: $\chi^2 = 11.09$, df = 3, $P = 0.01$). The number of aggressive interactions initiated by mature male parr of different origin varied among arenas (χ^2 test: $\chi^2 = 17.32$, df = 6, $P < 0.01$); AquaGen parr were most aggressive in the presence of Imsa large males in the Imsa 1 arena and Imsa parr were most aggressive in AquaGen 1. The number of aggressive interactions received did not differ among parr of different origins or among arenas (χ^2 test: $\chi^2 = 8.41$, df = 6, $P = 0.21$).

Video footage of parr behaviour at nests 5 min prior to spawning was available for 22, 27, 37, and 43 nests in Imsa 1, Imsa 2, AquaGen 1, and AquaGen 2, respectively (Table 2). There were no differences in the number of encounters among the four arenas (χ^2 test: $\chi^2 = 4.36$, df = 2, $P = 0.22$). Encounters resulted in aggression in 71%, 50%, 64%, and 82% of cases in Imsa 1, Imsa 2, AquaGen 1, and AquaGen 2, respectively, and did not differ significantly among arenas (Fisher's exact test: $P = 0.89$). Similar to the live observations, the number of nests at which parr of a given origin were aggressive varied among arenas (Table 2), and differences in aggression with respect to parr origin were found only in Imsa 1 (Fisher's exact test: $P = 0.02$) in which AquaGen parr attacked more frequently than Imsa or Imsa × AquaGen individuals.

Mature male parr spawning participation

To determine whether mature male parr origin affected positioning near the female before egg release, we recorded the group identity of the individual closest to the female 1 min prior to spawning and found some differences among arenas with respect to the origin of the parr closest to the female. In the Imsa 1, Imsa 2, and AquaGen 2 arenas, there were no differences among groups in proximity to the female, including only cases where two or more types of parr were present (Fisher's exact test: Imsa 1, $P = 0.51$; Imsa 2, $P = 0.16$; AquaGen 2, $P > 0.9$) (Table 3). However, in AquaGen 1, Imsa parr attained a closer position to females than other types of parr (Fisher's exact test: $P < 0.01$).

Overall, parr participated in 68%, 70%, 68%, and 73% of observed spawning events in Imsa 1, Imsa 2, AquaGen 1, and AquaGen 2 arenas, respectively (Table 3), and there were differences in parr attendance at spawnings within arenas. Parr of each origin were equally likely to be present at spawnings attended by at least one parr in arenas with Imsa anadromous males (χ^2 test: Imsa 1, $\chi^2 = 3.91$, df = 2, $P =$

© 2005 NRC Canada

Table 3. Total number of videotaped spawnings analysed, total number of spawnings with parr, number of spawnings at which parr of a given origin were closest to the female 1 min prior to spawning, and number of spawnings attended by parr of different origin in the four arenas.

	Total no.	No. with parr	Origin	No. closest	No. of spawnings attended
Imsa 1	25	17	Imsa	4 (3)	15 (9)
			Imsa × AquaGen	4 (4)	10 (8)
			AquaGen	7 (4)	13 (11)
Imsa 2	27	19	Imsa	10 (4)	17 (9)
			Imsa × AquaGen	5 (5)	12 (9)
			AquaGen	1 (1)	14 (10)
AquaGen 1	40	27	Imsa	11 (5)	14 (5)
			Imsa × AquaGen	13 (2)	23 (6)
			AquaGen	2 (0)	7 (6)
AquaGen 2	44	32	Imsa	5 (3)	15 (8)
			Imsa × AquaGen	19 (4)	27 (9)
			AquaGen	3 (3)	18 (8)

Note: The number of spawnings for which these data were obtained differs slightly from those in Table 2 because some spawning events did not contain adequate footage prior to female egg release for aggression data to be collected. For the same reason, the closest parr 1 min prior to spawning was not attainable for all nests sampled. Figures in parentheses exclude cases where parr of a single origin only were observed and thus refer to the number of nests at which parr of two or three different origins were present.

0.14; Imsa 2, $\chi^2 = 3.60$, df = 2, $P = 0.17$) (Table 3). However, there were differences among the three parr types in arenas with AquaGen large males (χ^2 test: AquaGen 1, $\chi^2 = 19.85$, df = 2, $P < 0.001$; AquaGen 2, $\chi^2 = 10.40$, df = 2, $P < 0.01$) (Table 3), where hybrid parr consistently attended more nests than Imsa or AquaGen parr.

To control for arena differences in number of spawnings, we analysed the number of parr of different origin at nests with respect to spawning number using only the first 25 spawnings in each arena. Spawnings were numbered sequentially from 1 to 25 from the first observed spawning and occurred over a period lasting between 20 and 22 days. Overall spawning attendance differed between arenas containing Imsa or AquaGen large males (GLM: $F_{[1,94]} = 13.45$, $P < 0.001$) (Fig. 1). Interestingly, there was a strong temporal decline in parr spawning, as indicated by a highly significant negative effect of spawning number on the total number of parr attending spawnings (GLM: $F_{[1,94]} = 60.13$, $P < 0.001$).

There was a three-way interaction among spawning number, parr origin, and large male origin (GLM: $F_{[2,279]} = 3.35$, $P = 0.036$) (Fig. 2) on the number of parr attending spawning events. To examine differences among parr of different origin, we removed the effect of large male origin by analysing the AquaGen and Imsa treatments separately. In arenas containing AquaGen large males, there was also an interaction between parr origin and spawning number on parr attending spawnings (GLM: $F_{[2,141]} = 6.16$, $P < 0.01$), where more hybrids participated in spawning later in the experiment. In arenas with Imsa large males, more Imsa and AquaGen than Imsa × AquaGen individuals were involved in spawnings (GLM: $F_{[2,140]} = 4.84$, $P < 0.01$), and the number of parr of every origin per spawning decreased with increasing spawning number (GLM: $F_{[1,140]} = 94.61$, $P < 0.001$).

Genetic analysis

Embryo survival was extremely poor, with very few surviving in Imsa 1 and AquaGen 1; only a few nests from Imsa 2 and AquaGen 2 could be analysed for parentage assignment. Nests were analysed if more than 20 embryos survived, and in all but two cases, the number of eggs analysed per nest was greater than 90. In these two cases, be-

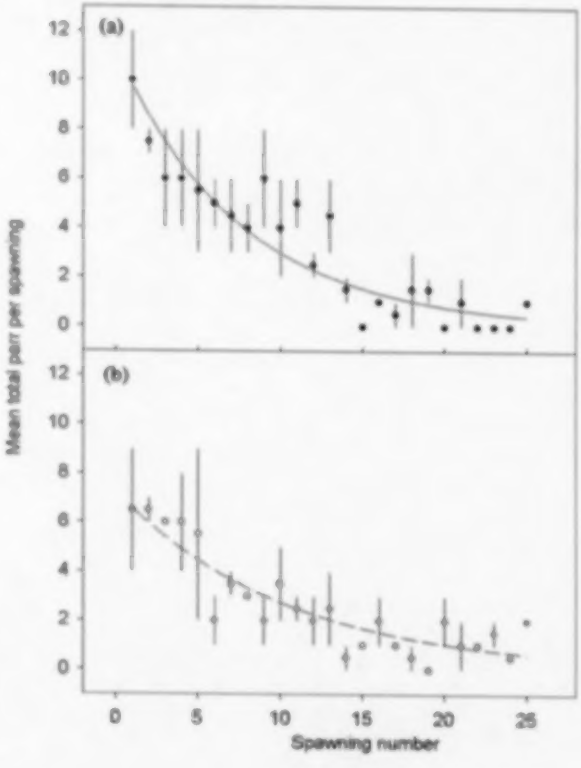

Fig. 1. Mean ± SE of the total number of mature male parr attending per spawning for the first 25 spawnings in arenas with (*a*) Imsa or (*b*) AquaGen large males.

© 2005 NRC Canada

Fig. 2. Mean number of Imsa, Imsa × AquaGen, and AquaGen mature male parr per spawning for the first 25 spawnings in arenas with (*a*) Imsa or (*b*) AquaGen large males.

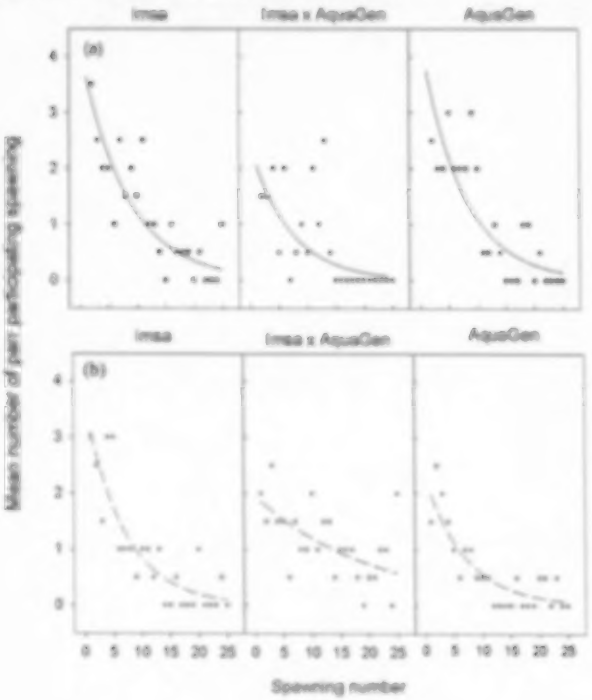

Fig. 3. (*a*) Proportion of total fertilization success among males and (*b*) CV ($s/\bar{x} \times 100$) (%) of group fertilization success in arenas with Imsa (solid circles) or AquaGen (open circles) large males.

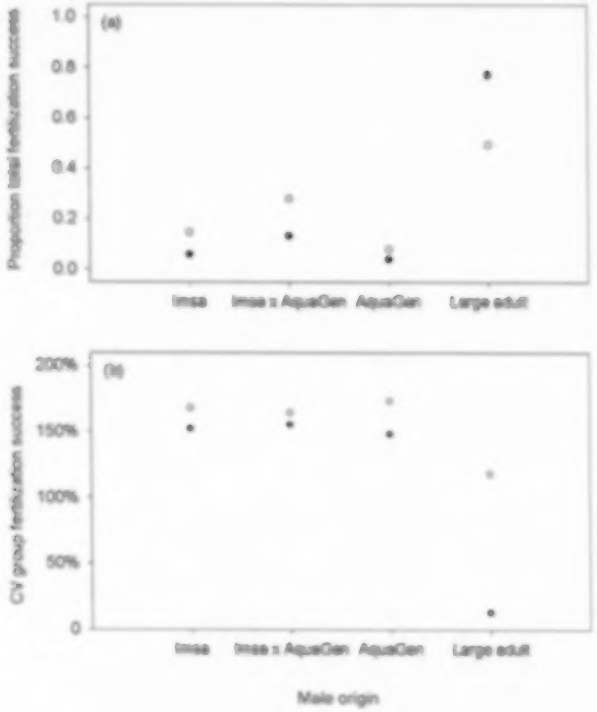

havioural observations confirmed that only large fish were present at the nest and thus obtained 100% fertilization success. Five nests and a total of 816 embryos were genotyped from Imsa 2 and three nests for a total of 415 embryos were genotyped from AquaGen 2. Of these, 757 and 387 offspring could be unambiguously assigned to mothers and fathers of a given origin in Imsa 2 and AquaGen 2, respectively. Overall exclusion probability among possible parents was 0.998 in both Imsa 2 and AquaGen 2 and there were no deviations from Hardy–Weinberg equilibrium among potential parents.

In light of the poor embryo survival in the experiment, our estimates of fertilization success are based on overall success within either Imsa 2 or AquaGen 2. There were differences between the arenas with respect to the proportion of eggs sired by males of different origin (Fig. 3*a*). Imsa large males in Imsa 2 were assigned 77% of the offspring, while Imsa, Imsa × AquaGen, and AquaGen mature male parr fathered 6%, 13%, and 4% of offspring, respectively. In contrast, 15%, 28%, and 8% of offspring were fathered by Imsa, Imsa × AquaGen, and AquaGen parr in AquaGen 2, respectively, with the remaining 49% assigned to AquaGen large males. Although the proportion of eggs fertilized by mature male parr of different origin differed between arenas, the rank order of fertilization success remained the same; Imsa × AquaGen had the highest fertilization success followed by Imsa and AquaGen parr. Overall, mature male parr fertilized a higher proportion of eggs in the presence of AquaGen large males. More interestingly, there was a large range in individual fertilization success of the different parr groups among nests (Imsa 2: Imsa, 0%–12%; Imsa × AquaGen, 0%–16%; AquaGen, 0%–6%; AquaGen 2: Imsa, 0%–42%; Imsa × AquaGen, 0%–100%; AquaGen, 0%–23%). In Imsa 2, variance in fertilization success was an order of magnitude higher within groups of mature male parr (CV = $(s/\bar{x}) \times 100\%$; CV: Imsa, 152; Imsa × AquaGen, 155; AquaGen, 148) than large Imsa males (CV = 13) (Fig. 3*b*). In contrast, the high variation in fertilization success per nest among AquaGen large males in AquaGen 2 (CV = 118) was closer to that expressed within groups of mature male parr (CV: Imsa, 168; Imsa × AquaGen, 164; AquaGen, 173).

Discussion

Our findings provide insight into the spawning behaviour and fertilization success of mature male parr of different genetic origin. We document differences in behaviour among mature male parr of different genetic origin and a strong negative temporal effect on spawning participation. Our results also indicate a high variance in fertilization success among mature male parr and that parr of farmed origin can successfully fertilize eggs in competition with wild parr. We found no consistent differences in either aggression or proximity to females prior to spawning among mature male parr of different genetic origin. By contrast, there were some notable differences in spawning participation among the three parr types. Interestingly, although the number of hybrids participating per spawning event tended to be lower than ei-

© 2005 NRC Canada

ther of the pure crosses, their participation persisted over a longer period of time in the presence of AquaGen large males. Prolonged participation by hybrid parr could have been attributable to high female activity in the arenas containing AquaGen large males (Weir 2003). Mature male Atlantic salmon parr show a hormonal response and increased milt production when exposed to the sound of female digging (Moore and Waring 1999), and male salmonids are known to respond behaviourally (Takeuchi et al. 1987) and hormonally (Rouger and Liley 1993) to spawning females. Thus, higher levels of female nesting activity in the arenas containing AquaGen males may have triggered participation by mature male parr for a longer period of time than in the arenas containing less active females. The lower number of hybrids participating early in the spawning season, when Imsa and AquaGen parr were present at high numbers, may have enabled them to partake in spawning for a longer period of time.

The similarity in spawning participation between Imsa and AquaGen male parr was unexpected based on previous comparisons of either hatchery and wild or farmed and wild juveniles: one group is usually reported to outperform the other. However, this similarity in behaviour may also signify similarities in the mode of competition among farmed and wild mature male parr during spawning. There may be many reasons why the documented differences in aggression did not result in parallel trends in spawning participation, and one likely explanation may be that mature male parr use scramble rather than interference competition during spawning. Parr spawning participation occurred mainly at the beginning of the experiment, when parr were associated near spawning females in groups. Large numbers of competitors are often associated with low individual aggression, as the defence of a resource against many competitors may not be economical (Brown 1964; Warner and Hoffman 1980; Grant et al. 2000). Although spawning in larger numbers may negatively affect individual parr reproductive success, the early participation by parr may have allowed them to avoid prolonged interactions with large fish, given that attacks from large fish can result in parr mortality (Hutchings and Myers 1987; Broberg et al. 2000; present study).

Indirect evidence of a reduction in parr participation over time has been reported in some experiments estimating fertilization success of mature male parr (Hutchings and Myers 1988; Thomaz et al. 1997). Given that our experiment was a closed system in which parr were not free to leave or enter the spawning grounds, we cannot conclusively infer that there is a negative temporal effect of parr participation under natural conditions. However, based on the sole study of parr migration to spawning grounds, evidence suggests that mature male parr migrate to natural spawning grounds at the beginning of the spawning season and that the likelihood of new parr arriving on the spawning grounds diminishes rapidly over time (Hutchings 1986) (Fig. 4).

Our behavioural data suggest that Imsa and AquaGen male parr spawning participation decreased over time, as did their fertilization success. Conversely, Imsa × AquaGen parr had the highest fertilization success among groups of mature male parr, and this success may be partly attributable to the fact that they tended to participate in spawning later in the experiment, when competition among parr was lower. Consequently, hybrid parr fertilized more eggs as participation by Imsa and AquaGen parr decreased, particularly in the presence of AquaGen large males. The relatively high mature male parr success in competition with AquaGen large males can probably be attributed to less frequent sperm release during spawning by farmed large males (Weir et al. 2004) and to our observation that mature male parr spawning success was significantly higher in the presence of farmed than wild large males. Although we cannot draw firm conclusions regarding relative fertilization success among parr of different origin owing to unfortunately small sample sizes, they do corroborate the results of our behavioural data and allow for some extrapolation of those results to sources of potential differences in fertilization success. The ranks in parr fertilization success were consistent between the two arenas, with hybrids consistently fertilizing more eggs than wild and farmed parr. Furthermore, an interesting and robust result is the high variance in parr fertilization success, a finding consistent with previous studies (Jones and Hutchings 2001, 2002).

Fig. 4. Average number of mature male parr moving out of Wings (solid circles) or Bluehill (shaded circles) Pond into streams in the autumn of 1982 in the Wings Brook system, Bonavista Bay, Newfoundland. Spawning usually occurs in late October – early November in the system. Data are from J.A. Hutchings (unpublished data).

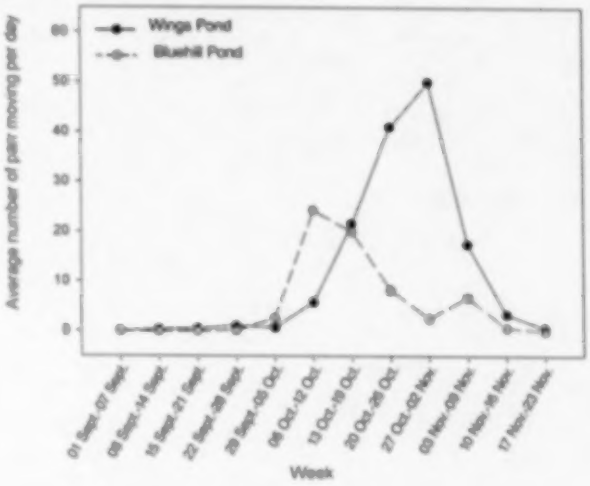

We conclude that behavioural differences among mature male parr of different genetic origin can result in differences in reproductive success. Moreover, parr of farmed origin can adequately compete with wild parr and succeed in fertilizing eggs. Thus, in addition to making them a potential source of introgression of farmed genes into wild populations, parr of farmed origin may increase the intergenerational rate at which such introgression occurs, given that they mature earlier than their large counterparts.

Acknowledgements

We thank Dag Karlsen and Roar Lund and the staff at Norwegian Institute for Nature Research for their support throughout this project and for assistance with the experi-

© 2005 NRC Canada

ments. Matthew Jones, Roxanne Bower, and Blair Adams provided advice for the genetic analyses. Paul Bentzen, Andrew Horn, Felicity Huntingford, Ransom Myers, and two anonymous referees provided helpful comments on an earlier version of the manuscript. This research was funded by an AquaNet Network Centres of Excellence grant to J.A.H. and I.A.F., grants from the Norwegian Research Council and the Norwegian Directorate for Nature Management to I.A.F. and S.E., a Natural Sciences and Engineering Research Council of Canada research grant to J.A.H., and a Natural Sciences and Engineering Research Council of Canada postgraduate scholarship to L.K.W.

References

Bohlin, T. 1975. A note on the aggressive behavior of large male sea trout towards "precocious" males during spawning. Inst. Freshw. Res. Drottingholm Rep. **54**: 118.

Broberg, M.M., Nielsen, E.E., and Dieperink, C. 2000. Incidence of physical injury of mature male parr in a natural population of brown trout. J. Fish Biol. **57**: 1610–1612.

Brown, J.L. 1964. The evolution of diversity in avian mating systems. Wilson Bull. **76**: 160–169.

Duchesne, P., Godbout, M-H., and Bernatchez, L. 2002. PAPA (package for the analysis of parental allocation): a computer program for simulated and real parental allocation. Mol. Ecol. Notes, **2**: 191–193.

Fleming, I.A. 1996. Reproductive strategies of Atlantic salmon: ecology and evolution. Rev. Fish Biol. Fish. **6**: 379–416.

Garant, D., Fleming, I.A., Einum, S., and Bernatchez, L. 2003. Alternative male reproductive tactics speed genetic introgression of escaped, cultured organisms into wild populations: experimental evidence from Atlantic salmon. Ecol. Lett. **6**: 541–549.

Grant, J.W.A., Gadboury, C.L., and Levitt, H.L. 2000. Competitor-to-resource ratio, a general formulation of operational sex ratio, as a predictor of competitive aggression in Japanese medaka (Pisces: Oryziidae). Behav. Ecol. **11**: 670–675.

Gross, M.R. 1985. Disruptive selection for alternative life histories in salmon. Nature (Lond.), **313**: 47–48.

Hindar, K., Ryman, N., and Utter, F. 1991. Genetic effects of cultured fish on natural fish populations. Can. J. Fish. Aquat. Sci. **48**: 945–957.

Hutchings, J.A. 1986. Lakeward migrations by juvenile Atlantic salmon, *Salmo salar*. Can. J. Fish. Aquat. Sci. **43**: 732–741.

Hutchings, J.A. 1991. The threat of extinction to native populations experiencing spawning intrusions by cultured Atlantic salmon. Aquaculture, **98**: 119–132.

Hutchings, J.A., and Myers, R.A. 1987. Escalation of an asymmetric contest: mortality resulting from mate competition in Atlantic salmon, *Salmo salar*. Can. J. Zool. **65**: 766–768.

Hutchings, J.A., and Myers, R.A. 1988. Mating success of alternative maturation phenotypes in male Atlantic salmon, *Salmo salar*. Oecologia, **75**: 169–174.

Hutchings, J.A., and Myers, R.A. 1994. The evolution of alternative mating strategies in variable environments. Evol. Ecol. **8**: 256–268.

Jones, J.W. 1959. The salmon. Collins, London, UK.

Jones, M.W., and Hutchings, J.A. 2001. The influence of male parr body size and mate competition on fertilization success and effective population size in Atlantic salmon. Heredity, **86**: 675–684.

Jones, M.W., and Hutchings, J.A. 2002. Individual variation in Atlantic salmon fertilization success: implications for effective population size. Ecol. Appl. **12**: 184–193.

Jordan, W.C., and Youngson, A.F. 1992. The use of genetic marking to assess the reproductive success of mature male Atlantic salmon parr (*Salmo salar* L.) under natural spawning conditions. J. Fish Biol. **41**: 613–618.

L'Abée-Lund, J.H. 1989. Significance of mature male parr in a small population of Atlantic salmon (*Salmo salar*). Can. J. Fish. Aquat. Sci. **46**: 928–931.

Marshall, T.C., Slate, J., Kruuk, L.E.B., and Pemberton, J.M. 1998. Statistical confidence for likelihood-based paternity inference in natural populations. Mol. Ecol. **7**: 639–655.

Moore, A., and Waring, C.P. 1999. Reproductive priming in mature male Atlantic salmon parr exposed to the sound of redd cutting. J. Fish Biol. **55**: 884–887.

Myers, R.A., and Hutchings, J.A. 1987. Mating of anadromous Atlantic salmon, *Salmo salar* L., with mature male parr. J. Fish Biol. **31**: 143–146.

O'Reilly, P.T., Hamilton, L.C., McConnell, S.K., and Wright, J.M. 1996. Rapid analysis of genetic variation in Atlantic salmon (*Salmo salar*) by PCR multiplexing of dinucleotide and tetranucleotide microsatellites. Can. J. Fish. Aquat. Sci. **53**: 2292–2298.

Parrish, D.L., Behnke, R.J., Gephard, S.R., McCormick, S.D., and Reeves, G.H. 1998. Why aren't there more Atlantic salmon (*Salmo salar*)? Can. J. Fish. Aquat. Sci. **55**(Suppl. 1): 281–287.

Paterson, S., Piertney, B., Knox, D., Gilbey, J., and Verspoor, E. 2004. Characterization and PCR multiplexing of novel highly variable tetranucleotide Atlantic salmon (*Salmo salar* L.) markers. Mol. Ecol. **4**: 160–162.

Rouger, Y., and Liley, N.R. 1993. Effect of social environment on plasma hormone and availability of milt in spawning male rainbow trout (*Oncorhynchus mykiss* Walbaum). Can. J. Zool. **71**: 280–285.

Taborsky, M. 2001. The evolution of bourgeois, parasitic and cooperative reproductive behaviors in fishes. J. Hered. **92**: 100–110.

Takeuchi, H., Takei, K., Satou, M., Matsushima, T., Okumoto, N., and Ueda, K. 1987. Visual cues as key stimuli for courtship behaviour in the male himé salmon (landlocked red salmon, *Oncorhynchus nerka*). Anim. Behav. **35**: 936–939.

Thomaz, D., Beall, E., and Burke, T. 1997. Alternative reproductive tactics in Atlantic salmon: factors affecting mature male parr success. Proc. R. Soc. Lond. B Biol. Sci. **264**: 219–226.

Warner, R.R., and Hoffman, S.G. 1980. Population density and the economics of territorial defense in a coral reef fish. Ecology, **61**: 772–780.

Weir, L.K. 2003. The influence of artificial selection on the spawning behaviour and reproductive success of male Atlantic salmon, *Salmo salar*. M.Sc. thesis, Dalhousie University, Halifax, N.S.

Weir, L.K., Hutchings, J.A., Fleming, I.A., and Einum, S. 2004. Dominance relationships and behavioural correlates of individual spawning success in farmed and wild male Atlantic salmon, *Salmo salar*. J. Anim. Ecol. **73**: 1069–1079.

© 2005 NRC Canada

Evidence for biomagnification of rubidium in freshwater and marine food webs

Linda M. Campbell, Aaron T. Fisk, Xiaowa Wang, Günter Köck, and Derek C.G. Muir

Abstract: Rubidium (Rb), a rarely studied alkali metal, may be an essential ultra-trace element for humans and other organisms. However, very little information exists in regard to the concentrations and distribution of Rb in freshwater and marine food webs. We measured Rb concentrations in freshwater fish from Lake Erie and two Arctic lakes (Lake Hazen and Resolute Lake) and in seabirds, ringed seals, and invertebrates from the marine Northwater Polynya in Baffin Bay. The alkali analogues of Rb, cesium (Cs), and potassium (K) were also analysed in a subset of fish from Lakes Erie and Hazen. Rb and Cs concentrations and Cs:K ratios in the sampled biota are significantly regressed against $\delta^{15}N$ values, indicating biomagnification through the food web in diverse ecosystems. However, there is no relationship between K concentrations and $\delta^{15}N$ values, indicating a lack of biomagnification and the presence of homeostatistic mechanisms for this essential trace element. Rb must be included with mercury and Cs as metals that consistently biomagnify in diverse food webs and should be considered in multi-element biomagnification studies.

Résumé : Le rubidium (Rb) est un métal alcalin rarement étudié qui peut être un élément en « ultra-trace » essentiel pour les humains et les autres organismes. Il existe, cependant, très peu de données sur ses concentrations et sa répartition dans les chaînes alimentaires aquatiques et marines. Nous avons mesuré les concentrations de Rb dans des poissons d'eau douce du lac Érié et de deux lacs arctiques (Hazen et Resolute), ainsi que dans des oiseaux marins, des phoques annelés et des invertébrés dans la polynie des eaux du nord de la baie de Baffin. Nous avons aussi analysé les analogues alcalins du rubidium, le césium (Cs) et le potassium (K), dans un sous-ensemble de poissons des lacs Érié et Hazen. Il y a une relation significative entre les concentrations de Rb et de Cs et le rapport Cs:K dans les organismes échantillonnés, d'une part, et $\delta^{15}N$, d'autre part, ce qui indique qu'il se produit une biomagnification dans le réseau alimentaire des divers écosystèmes. Il n'y a pas, cependant, de relation entre les valeurs de K et de $\delta^{15}N$, ce qui indique l'absence de biomagnification pour cet élément en trace essentiel et la présence de mécanismes homéostatiques. Il faut ajouter le Rb à Hg et Cs dans la liste des métaux qui subissent systématiquement une biomagnification dans les réseaux alimentaires et en tenir compte dans les études de biomagnification qui considèrent plusieurs éléments chimiques.

[Traduit par la Rédaction]

Introduction

Trophic transfer of metals in food webs has been a cause for concern for decades, especially as mercury (Hg), methylmercury, and cesium (Cs) have been demonstrated to exhibit biomagnification potential in freshwater and marine ecosystems worldwide and can provoke toxicity responses (Rowan and Rasmussen 1994; Mason et al. 1995). Very few elements, such as selenium and even zinc (Zn), are also known to biomagnify in certain ecosystems (i.e., Quinn et al. 2003), but many elements, such as copper (Cu) or iron (Fe), do not biomagnify in food webs, owing to either homeostatistic mechanisms or biochemical aspects that prevent trophic accumulation (Wang 2002). However, many other elements in the periodic table, including rubidium (Rb), have not yet been assessed for biomagnification potential in food webs.

Rb is a rarely studied but abundant alkali metal located between potassium (K) and Cs in the periodic table. Rb is associated with K and Cs minerals worldwide, including mica and alkali-feldspar minerals in soils (Jones 1992) and illite clays (Perel'man 1965), granite (Heier and Billings 1970), and granitic pegmatites, especially pollucite and lepidolite ores (Cerny et al. 2003). Like Cs, Rb is a K^+ analogue and can compete with K^+ for enzymatic sites in fish and other organisms (Peters et al. 1999; Tipsmark and Madsen 2001). The importance of Rb as an ultra trace essential element to humans and other biota has been the subject of conjecture, based on a study that demonstrated poor health

Received 24 February 2004. Accepted 22 October 2004. Published on the NRC Research Press Web site at http://cjfas.nrc.ca on 31 May 2005.
J18004

L.M. Campbell,[1,2] X. Wang, and D.C.G. Muir. National Water Research Institute, Environment Canada, 867 Lakeshore Road, Burlington, ON L7R 4A6, Canada.
A.T. Fisk. Warnell School of Forest Resources, University of Georgia, Athens, GA 30602-2152, USA.
G. Köck. Austrian Academy of Sciences, Dr. Ignaz Seipel-Platz 2, A-1010 Vienna, Austria.

[1]Corresponding author (e-mail: campbelm@biology.queensu.ca).
[2]Present address: School of Environmental Studies, Queen's University, Kingston, ON K7L 3N6, Canada.

 doi: 10.1139/f05-027 © 2005 NRC Canada

of goats fed low-Rb (<0.28 mg·kg^{-1}·day^{-1}) diets relative to those fed high-Rb diets (>1 mg·kg^{-1}·day^{-1}) (Nielsen 1998). Some cyanobacterial species can grow in Rb media in absence of K^+, albeit more slowly than those grown in K^+-sufficient media (Richie 1997). "Safe" concentrations are not known, although experimental toxic responses linked with elevated Rb have been observed in mammals fed low-K high-Rb diets, which are linked to physiological interference with K^+ and sodium (Na^+) (Kosla et al. 2002). Toxic responses have also been described in cultured oysters (*Crassostera gigas*), with elevated Rb concentrations linked to ionic modification and tissue disorganization (Salaün and Truchet 1996)

Transfer of Rb between predator and prey has been documented (Johnson and Reeves 1995; Nyholm and Tyler 2000) and Rb has been used as a tracer in insect dispersal studies, since emerging insects will retain the Rb signature from pre-emergent exposure (Johnson and Reeves 1995; Payne and Dunley 2002). Hypothetically, biomagnification involves the co-uptake of Rb and Cs, which have smaller cation radii than K^+, via active transport H^+ and K^+ membrane channels in primary producers and the subsequent transfer and accumulation of Rb and Cs up the food chain (Rowan and Rasmussen 1994). Even so, consistent biomagnification of Rb across food webs has not yet been demonstrated. Stable nitrogen (N) isotopes have been used as a trophic-position indicator and to estimate the biomagnification potential of contaminants and metals in diverse ecosystems (e.g., Kidd 1998). The ratio of ^{15}N to ^{14}N (in biological tissues relative to air), which is expressed as delta-^{15}N ($\delta^{15}N$), in tissue typically increases consistently by 3.4‰–3.6‰ with each trophic transfer because ^{15}N is retained from the food resource relative to ^{14}N. Since concentrations of biomagnifying contaminants and metals also increase with trophic position, there will be a significant relationship between the biomagnifying compound with increasing $\delta^{15}N$ values in biota, therefore linear-regression slopes can be used to predict metal and contaminant behaviour within food webs.

The objective of this study was to compare Rb concentrations and biomagnification in freshwater and marine food webs spanning over 30° latitude. The littoral northeastern Lake Erie ecosystem in Long Point Bay (42°47′N, 80°11′W) includes a number of fish species, including smallmouth bass, *Micropterus dolomieu*, and the round goby, *Neogobius melanostomus*, a Ponto-Caspian invader. Lake Hazen, the largest lake above the Arctic Circle (Quttinirpaaq National Park, Ellesmere Island, 81°40′N, 73°0′W), and Resolute Lake (Quasuittuq, Cornwallis Island, 74°43′N, 94°58′W) both contain non-anadromous Arctic char, *Salvelinus alpinus*, which span a wide trophic gradient from omnivory to piscivory. The Northwater (NOW) Polynya in Baffin Bay (77°N, 75°W, 50 000 km^2) is a large permanent opening in the sea ice that supports large numbers of Arctic cod, *Boreogadus saida*, marine birds, mammals, and invertebrates. This study represents the first time that comparative evidence for biomagnification of Rb and Cs (based on stable N isotopes) in freshwater and marine food webs has been presented.

Methods

Arctic char were collected from Lake Hazen in 2003 and Resolute Lake in 2001 using gill nets (Köck et al. 2004). Various littoral fish species were collected from Lake Erie in 2002 using overnight gill-netting. Physiochemical parameters of these freshwater lakes are listed in Table 1. From the marine NOW Polynya in 1998, seal samples were obtained from Inuit hunters and birds were collected by shotgun, zooplankton with vertical tows of 1 m diameter 250 µm mesh net, and Arctic cod by hand-held nets (Fisk et al. 2001).

All analyses of Rb and other elements were conducted using inductively coupled plasma-sector field mass spectrometry at low resolution (NLET Method 02-2704/5) at the National Water Research Institute, Burlington, Ontario (National Laboratory for Environmental Testing 2003). To ascertain relationships with Cs and K, subsamples from Lakes Erie and Hazen were processed using the same method but including standards for determining Cs and K concentrations. The dried Lake Erie fish samples were converted to wet weight, assuming 80% water content, which is a standard assumption in the literature. The Arctic samples were not dried. Approximately 25%–30% of an analytical run was dedicated to various quality control samples, including certified reference materials from the National Research Council of Canada (DORM-2, DOLT-2 and TORT-2) and duplicates. No certified values were available for Rb; however, values for 11 elements in DORM-2 (dogfish muscle) averaged within 12.7% of certified values.

Stable-isotope values were analysed using continuous-flow isotope-ratio mass spectrometer technology (L.M. Campbell and D.C.G. Muir). The ratios of stable N isotopes were measured against N_2 in ambient air, and delta notation (δ) is used to indicate the parts per thousand (‰) differences in the isotopic ratio of the sample from the reference standard. Standard deviations for the analytical standards and replicate samples inserted in every run were ±0.3‰ for $\delta^{15}N$.

Relationships of Rb, Cs, and K with $\delta^{15}N$ and with each other were determined by simple linear regressions in SYSTAT® version 10 (Systat Software Inc. 2000). Prior to regressing, metals were log^{10}-transformed to ensure normality of distribution. Plots of residuals versus predicted values were examined to ensure homoscedasticity. To compare Rb concentrations in Arctic char from Lakes Hazen and Resolute, an independent-samples t test was utilized, with normality and homogeneity of variances assessed first (i.e., Shapiro–Wilk test).

Results

Fish from Lake Erie, especially higher trophic level omnivores and piscivores such as freshwater drum (*Aplodinotus grunniens*) and smallmouth bass, usually had higher mean Rb concentrations relative to other fishes and biota from the Arctic (Fig. 1; Table 2). Arctic char from Lake Hazen have significantly higher Rb concentrations than those from Resolute Lake (Table 2; t test, $t = 3.467$, df = 35, $p \leq 0.001$). Significant regressions of log[Rb] with $\delta^{15}N$ values are observed in all systems sampled (Fig. 1), with slopes ranging from 0.064 to 0.081 (Table 3). Log[Cs] is also significantly regressed with $\delta^{15}N$ values in Lakes Erie and Hazen, with slopes of 0.112 and 0.140, respectively (Table 3). Log[K] did not show significant relationships with $\delta^{15}N$ values in Lake Erie or Lake Hazen (Table 3).

© 2005 NRC Canada

Table 1. Physiochemical parameters (average ± standard deviation) of the sampled freshwater lakes.

	Lake Hazen (1990–1998)[a]	Resolute Lake (1997–2002)	Lake Erie (Aug. 2001)[b]
Area (km^2)	541.8	1192	25 655
pH	8.40±0.01	8.28±0.18[c]	8.23±0.1
Conductivity ($\mu S \cdot cm^{-1}$)	149±10	252.7±32.6[c]	271.7±0.6
Alkalinity ($\mu equiv. \cdot L^{-1}$)	1085±487		9367±577
Chlorophyll *a* ($\mu g L^{-1}$)		<0.1[d]	1.0±0.0
SO_4 ($mg \cdot L^{-1}$)	7.2±4.4	20.3[d]	22±0.0
Total dissolved N ($\mu g \cdot L^{-1}$)	102±76	0.09[d]	267±23
Total dissolved P ($\mu g \cdot L^{-1}$)	2.9±3.2	0.012[d]	4.0±0.0
Dissolved inorganic C ($\mu g \cdot L^{-1}$)	1380±163		21.7±0.2
Dissolved organic C ($\mu g \cdot L^{-1}$)	69±51		1.8±0.0
Na ($mg \cdot L^{-1}$)	0.61±0.06	10.9±1.5[c]	9.46±0.04
K ($mg \cdot L^{-1}$)	0.51±0.06	0.9±0.1[c]	1.44±0.04
Mg ($mg \cdot L^{-1}$)	2.9±0.3	5.9±0.9[c]	8.45±0.02
Ca ($mg \cdot L^{-1}$)	25.2±2.5	26.8±3.8[c]	32.5±0.87
Zn ($mg \cdot L^{-1}$)	0.005±0.003	0.01±0.01[c]	1.2±0.4
Cu ($mg \cdot L^{-1}$)	0.007±0.003	0.03±0.04[c]	1.8±0.06
Ni ($mg \cdot L^{-1}$)	0.013±0.007		0.6±0.1
Fe ($mg \cdot L^{-1}$)	0.040±0.076	0.02±0.02[c]	7.3±0.56
Ba ($\mu g \cdot L^{-1}$)	14.17±1.17		22.3±0.6
Sr ($\mu g \cdot L^{-1}$)	128±13		157.0±3.5
Cd ($\mu g \cdot L^{-1}$)		0.025±0.019[e]	nd[f]
Pb ($\mu g \cdot L^{-1}$)		0.022±0.003[e]	nd[e] – 0.01

[a]From Babaluk et al. (1999).
[b]Integrated photic-zone samples ($n = 3$) collected near Peacock Point (42°46'30", 79°58'57"). Unpublished data from T. Howell, Ontario Ministry of Environment and Energy, 125 Resources Road, Etobicoke, ON M9P 3V6, Canada.
[c]From Köck et al. (2004).
[d]Unpublished data from D.C.G. Muir and X. Wang, National Water Research Institute, Environment Canada, 867 Lakeshore Road, Burlington, ON L7R-4A6, Canada.
[e]Not detected.

Arctic char from Lake Hazen tend to have higher K and Cs concentrations than most fish species from Lake Erie, which is the opposite of the trend for Rb (Table 2). Rb concentrations in fish from both lakes are significantly regressed with Cs and K concentrations (Table 3). However, relationships for Cs and K concentrations are dissimilar, showing significance for fish from Lake Erie but not for those from Lake Hazen (Table 3). Although K concentration was not significantly regressed with $\delta^{15}N$ values for fish in Lake Erie, there may be a slight trophic-level-related increase in K concentration, based on significant relationships of K with Cs and Rb concentrations for fish in Lake Erie.

Discussion

Most biological Rb and Cs kinetics studies make use of radionuclides (Richie 1997; Peters et al. 1999). For example, ^{86}Rb, ^{137}Cs, and ^{134}Cs are frequently used as proxy tracers of K-linked transport (Tipsmark and Madsen 2001; Leggett et al. 2003). While different isotopes of an element can have varying biochemical properties (as handily illustrated by the use of $\delta^{15}N$ in this study), total Rb and Cs kinetics, including both stable (^{133}Cs, ^{85}Rb) and radioactive isotopes, can be approximated by those radionuclide studies. Based on those studies and our results, important factors likely affecting Rb bioavailability and concentration in freshwater and marine ecosystems are (*i*) sources and ambient concentrations of Rb in water and sediment, (*ii*) ambient K^+ concentrations, (*iii*) ambient pH and temperature, and (*iv*) trophic position.

Possible anthropogenic sources of Rb and Cs include coal-burning. Rb in coals and fly ash is related with Cs and K and can be a significant source in local environments (Ward et al. 1999; Seredin 2003). The large coal-fired Nanticoke Generating Station on Lake Erie is near Long Point Bay and may partially explain the elevated Rb concentrations in the Lake Erie fish (although not the low Cs concentrations relative to Lake Hazen Arctic char). However, a trace-element study in western Lake Erie in 1984 did not show elevated Rb concentrations in adult yellow perch, *Perca flavescens* (mean 3 $\mu g \cdot g^{-1}$ wet weight) caught near an Ohio power plant in comparison with those from a reference site several kilometres away (Hatcher et al. 1992). Rb concentrations in the Ohio yellow perch are similar to those found for the same species in this study, suggesting consistent Rb uptake by fish over time and space in Lake Erie. The most likely sources of Rb in lakes include Rb-rich geological features (Heier and Billings 1970) and Rb minerals in soil (Jones 1992). For example, drinking water derived from areas with increased Rb mineralization will have correspondingly high aqueous Rb concentrations (Anke and Angelow 1995). The type of mineralization and the proportions of Cs, Rb, and K found in lake catchments are probably important factors determining baseline aquatic alkali concentrations and elemental ratios in freshwater ecosystems.

© 2005 NRC Canada

Fig. 1. Regressions of Rb concentrations in biota versus their $\delta^{15}N$ values for freshwater (*a*) and marine (*b*) sites. To simplify the plots, data points for various species sampled from Lake Erie (broken line) and the North Water Polynya are shown as the mean ± standard deviation, while data for Arctic char from Resolute Lake (dotted line) and Lake Hazen (solid line) are shown individually. Regression lines for all sites are based on individual data, not the mean values.

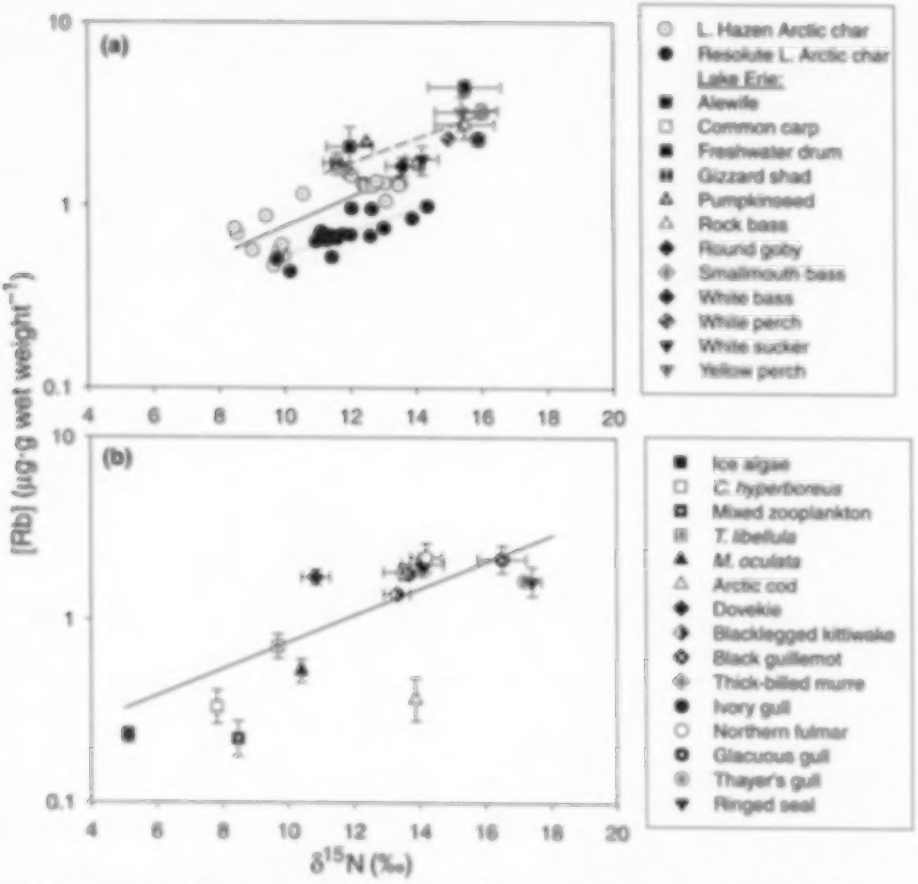

Even so, studies have shown that Rb concentrations in terrestrial plants are only weakly related to Rb concentrations in surrounding soil because the pH, K^+ content, and even Na^+ content of soil have a more significant impact on Rb and Cs bioavailability to plants and subsequently to animals (Drobner and Tyler 1998; Nyholm and Tyler 2000). Furthermore, increasing K^+ concentrations in ambient water and sediment are linked to reduced ^{137}Cs bioaccumulation in fish and invertebrates (Rowan and Rasmussen 1994). As a result, marine fish tend to have lower Cs concentrations relative to fish from soft-water lakes (Rowan and Rasmussen 1994). This trend is reflected in marine Arctic cod, which had lower Rb concentrations (0.3–0.5 $\mu g \cdot g^{-1}$) relative to all the freshwater fish (0.7–4.5 $\mu g \cdot g^{-1}$). Even the piscivorous seabirds and seals from the marine NOW Polynya had Rb concentrations (0.2–1.7 $\mu g \cdot g^{-1}$) lower than or similar to those of omnivorous fish from Lake Erie (1.7–4.5 $\mu g \cdot g^{-1}$). In addition, comparing individuals of the same species from two different lakes can provide additional insights into Rb biogeochemistry. For example, Arctic char from Lake Hazen had significantly higher Rb concentrations and a higher log[Rb]: $\delta^{15}N$ slope than those from Resolute Lake. Lake Hazen has lower ionic water concentrations (K = 0.5 $mg \cdot L^{-1}$, Na = 0.6 $mg \cdot L^{-1}$, and conductivity = 149 $\mu S \cdot mm^{-1}$) than Resolute Lake (0.9 $mg \cdot L^{-1}$, 10.9 $mg \cdot L^{-1}$, and 253 $\mu S \cdot mm^{-1}$, respectively). Increased uptake and biomagnification of Rb by Arctic char may result when ambient K and other ionic concentrations are low (Peters et al. 1999), suggesting that Rb concentration in fish is dependent not only upon the amount of ambient Rb but also upon the ratios of Rb to other alkali metals in the environment.

Another important factor is temperature, as ^{137}Cs and ^{86}Rb uptake in fish is temperature-dependent, and more rapid depuration of these radionuclides will occur with increase in temperature (Peters et al. 1999). Lake Erie is the warmest site in this study, and Long Point Bay water has higher K (1.4 $mg \cdot L^{-1}$) and Na (9.5 $mg \cdot L^{-1}$) concentrations and conductivity (272 $\mu S \cdot mm^{-1}$) relative to the northern lakes. This would seem to suggest that both Rb and Cs concentrations should be lowest in fish from Lake Erie, while K concentrations should be higher. However, the Lake Erie fish tend to contain higher Rb and lower Cs and K concentrations than other freshwater fish. These contrary results, the opposite of what one would expect from the literature on plants and Cs,

© 2005 NRC Canada

Table 2. Sampling sites and species sampled, with the number of samples analysed (N), $\delta^{15}N$ (‰), and mean Rb and Cs ($\mu g \cdot g^{-1}$ wet weight) and K ($mg \cdot g^{-1}$ wet weight) concentrations.

Site	Common name	Scientific name	N	$\delta^{15}N$	Rb	Total length (cm)	N^a	Cs	K
Long Point Bay, Lake Erie	Alewife	*Alosa pseudoharengus*	4	12.0±0.7	2.1±0.6	14.4±0.6	—	—	—
	Common carp	*Cyprinus carpio*	1	14.1	1.7	—	1	0.006	2.9
	Freshwater drum	*Aplodinotus grunniens*	5	15.5±1.1	4.5±0.4	38.0±4.4	5	0.016±0.003	3.6±0.2
	Gizzard shad	*Dorosoma cepedianum*	7	11.6±0.4	1.7±0.2	24.4±11.5	1	0.004±0.002	3.1±01.8
	Pumpkinseed	*Lepomis gibbosus*	1	12.5	2.2	—	—	—	—
	Rock bass	*Ambloplites rupestris*	6	15.5±0.9	2.8±0.5	187.2±47.3	4	0.006±0.003	3.3±0.2
	Round goby	*Neogobius melanostomus*	6	13.6±0.5	1.7±0.2	12.1±4.1	—	—	—
	Smallmouth bass	*Micropterus dolomieu*	15	16.0±0.5	3.3±0.3	319.5±86.8	5	0.014±0.0004	4.1±0.2
	White bass	*Morone chrysops*	4	15.9±0.2	2.3±0.2	177.3±11.9	4	0.007±0.001	3.4±0.5
	White perch	*Morone americana*	2	14.8–15.2	2.3–2.4	228–237	2	0.006–0.007	3.3–3.6
	White sucker	*Catostomus commersoni*	3	14.2±0.5	1.8±0.3	30.3±3.4	3	0.006±0.002	3.9±0.5
	Yellow perch	*Perca flavescens*	11	15.4±0.8	3.3±0.7	213.5±46.9	7	0.008±0.004	3.4±0.2
Lake Hazen	Arctic char	*Salvelinus alpinus*	20	11.3±1.8	1.0±0.4	44.7±11.1	20	0.21±0.16	4.3±0.4
Resolute Lake	Arctic char	*Salvelinus alpinus*	17	11.8±1.2	0.7±0.2	39.3±2.9			
NOW Polynya	Ice algae		3	5.1±0.1	0.2±0.02				
	Calanid copepod	*Calanus hyperboreus*	3	7.8±0.01	0.3±0.1				
	Mixed zooplankton		4	8.5±0.1	0.2±0.1				
	Ice amphipod	*Themisto libellula*	3	9.7±0.1	0.7±0.1				
	Mysid	*Mysis oculata*	3	10.4±0.1	0.5±0.1				
	Arctic cod	*Boreogadus saida*	3	14.1±0.2	0.4±0.1				
	Dovekie	*Alle alle*	10	10.9±0.4	1.7±0.2				
	Blacklegged kittiwake	*Rissa tridactyla*	10	13.3±0.4	1.4±0.1				
	Black guillemot	*Cepphus grylle*	10	13.7±0.1	1.7±0.2				
	Thick-billed murre	*Uria lomvia*	10	13.5±0.6	1.7±0.2				
	Ivory gull	*Pagophilia eburnea*	5	14.1±0.6	2.0±0.3				
	Northern fulmar	*Fulmarus glacialis*	10	14.2±0.5	2.2±0.4				
	Glacuous gull	*Larus hyperboreus*	10	16.5±0.7	2.2±0.4				
	Thayer's gull	*Larus thayeri*	1	17.2	1.7				
	Ringed seal	*Pusa hispida*	9	17.4±0.3	1.7±0.3				

Note: Values are given as the mean ± standard deviation.
[a]Because subsets of Lake Erie and Lake Hazen samples were analysed for Cs and K, the numbers analysed are different from the original totals analysed for $\delta^{15}N$ and Rb, hence the second N column.

© 2005 NRC Canada

Table 3. Linear-regression equations for relationships between Rb, Cs, and K concentrations and $\delta^{15}N$ for biota from Lake Erie, Lake Hazen, Resolute Lake, and the NOW Polynya.

Regression	Site	N^a	Slope	Intercept	R^2_{adj}	p
Log[Rb] vs. $\delta^{15}N$	Erie	65	0.067	–0.575	0.470	<0.001
	Resolute	17	0.064	–0.920	0.603	<0.001
	Hazen	20	0.081	–0.926	0.655	<0.001
	NOW	94	0.073	–0.851	0.501	<0.001
Log[Cs] vs. $\delta^{15}N$	Erie	32	0.112	–3.796	0.283	0.001
	Hazen	20	0.140	–2.367	0.660	<0.001
Log[K] vs. $\delta^{15}N$	Erie	32	0.012	3.366	0.051	0.113
	Hazen	20	0.009	3.531	0.093	0.103
Log([Cs]:[K]) vs. $\delta^{15}N$	Erie	32	0.100	–4.162	0.261	0.002
	Hazen	20	0.131	–2.897	0.554	<0.001
Log[Rb] vs. log[Cs]	Erie	32	0.457	1.385	0.597	<0.001
	Hazen	20	0.320	0.238	0.266	0.012
Log[Rb] vs. log[K]	Erie	32	1.015	–3.175	0.115	0.044
	Hazen	20	2.428	–8.831	0.306	0.007
Log[Cs] vs. log[K]	Erie	32	2.233	–10.021	0.212	0.003
	Hazen	20	–0.260	0.156	0.000	0.980

[a]The number of samples included in each regression.

indicate that the biogeochemistry and bioavailability of alkali metals in aquatic environments require more research.

Peters et al. (1999) pointed out that the biological half-lives of ^{86}Rb (9–181 days) are shorter than those of K and Cs radionuclides (37–600 days) in various fish species. This explains the lower biomagnification potential of Rb, as indicated by its lower log[Rb]:$\delta^{15}N$ slope relative to Cs, because Rb is more rapidly depurated than Cs from freshwater biota. Within fish species, no correlations or weakly significant correlations were found for Rb with size (p = 0.069–0.888), suggesting that biomagnification of Rb is significant within a food-web context, but not necessarily within species. More exploration is needed to determine whether fish species that experience large dietary shifts with size show a corresponding significant relationship of Rb concentration with size. For example, a radiocesium food-web study showed that while Cs will biomagnify through various food webs, there were still variable patterns in Cs biomagnification within fish species, which were attributed to consumption rates (Rowan et al. 1998). Furthermore, the slope values for log[Rb] and log[Cs] are lower than those seen for log[Hg] versus $\delta^{15}N$ regressions (0.2–0.3) for aquatic food webs worldwide, as summarized in Campbell et al. (2003). In other words, Rb and Cs do not biomagnify as rapidly as ubiquitous methylmercury, which forms stable protein complexes. However, the consistent biomagnification of Rb and Cs in food webs indicates that these alkali metals should be considered along with Hg and organic contaminants when studying biomagnifying compounds in food webs.

Prior to the widespread use of cost-effective $\delta^{15}N$ measurements as a trophic-level indicator in the early 1990s, Cs:K ratios were used as a numerical surrogate for trophic position in food-web studies (Mearns et al. 1981), and were even successfully applied to biomagnification research in California marine ecosystems (Young et al. 1980). The increase in Cs:K ratio with trophic level has been estimated to be 2.4–2.5 (Mearns et al. 1981), while the increase in $\delta^{15}N$ value of biota with trophic level has been traditionally assumed to be 3.4‰–3.6‰ (Minagawa and Wada 1984). Based on these hypothetical trophic values, the slope of the log([Cs]:[K]) versus $\delta^{15}N$ regression should be 0.106–0.117. The slopes for this regression for Lakes Erie and Hazen are 0.100 and 0.131, respectively, and interestingly, the mean value of these two slopes is 0.116, quite close to the maximum hypothetical slope. Although unknown variability will influence trophic-level-related changes in Cs:K ratios and $\delta^{15}N$ values, further investigation of alkali-metal trophodynamics and biogeochemistry may provide an additional tool for food-web analyses.

Acknowledgements

Staff at the Canadian National Laboratories for Environmental Testing at the National Water Research Institute prepared and analysed the biotic samples. The Lake Erie fish samples were obtained and processed for a separate study in collaboration with Dr. Robert E. Hecky and Reagan Johnston, Department of Biology, University of Waterloo, and Dixie Greenwood, Lake Erie Management Unit, Ontario Ministry of Natural Resources, Port Dover. Arctic sampling was undertaken with the assistance of National Water Research Institute Research Support Services, Parks Canada, at Quttinirpaaq National Park, the Polar Continental Shelf Project at Resolute Lake (Nunavut), and the captains and crew of the Coast Guard vessel *Pierre Radisson*. The Lake Resolute sampling was carried out within the framework of the International Geosphere–Biosphere Programme (Austrian Academy of Sciences). Dr. Todd Howell, Ontario Ministry of Environment, Toronto, provided the physiochemical data for Lake Erie in Table 1. Funding included, in part, a Postdoctoral Fellows Award from the Natural Sciences and Engineering Research Council of Canada to Linda Campbell, Northern Ecosystem Initiative funds to Aaron Fisk, Austrian Academy of Sciences (IGBP Research Program) funding to Günter Köck, and Environment Canada Great Lakes 20/20

© 2005 NRC Canada

and Northern Contaminants Program (Indian and Northern Affairs Canada) funding to Derek Muir.

References

Anke, M., and Angelow, L. 1995. Rubidium in the food chain. Frescenius' J. Anal. Chem. **352**: 236–239.

Babaluk, J.A., Heuring, L.G., Reist, J.D., and Billeck, B.N. 1999. Selected chemical analyses of water from lakes in Ellesmere Island National Park Reserve, Northwest Territories. Can. Data Rep. Fish. Aquat. Sci. No. 1050.

Campbell, L.M., Hecky, R.E., Nyaundi, J., Muggide, R., and Dixon, D.G. 2003. Distribution and food-web transfer of mercury in Napoleon and Winam Gulfs, Lake Victoria, East Africa. J. Gt. Lakes Res. **29**(Suppl. 2): 267–282.

Cerny, P., Chapman, R., Teertstra, D.K., and Novák, M. 2003. Rubidium- and cesium-dominant micas in granitic pegmatites. Am. Minerol. **88**: 1832–1835.

Drobner, U., and Tyler, G. 1998. Conditions controlling relative uptake of potassium and rubidium by plants from soils. Plant Soil, **201**: 285–293.

Fisk, A.T., Hobson, K.A., and Norstrom, R.J. 2001. Influence of chemical and biological factors on trophic transfer of persistent organic pollutants in the Northwater Polynya marine food web. Environ. Sci. Technol. **35**: 732–738.

Hatcher, C.O., Ogawa, R.E., Poe, T.P., and French, J.R.P. 1992. Trace elements in lake sediment, macrozoobenthos, and fish near a coal ash disposal basin. Freshw. Ecol. **7**: 257–269.

Heier, K.S., and Billings, G.K. 1970. Rubidium. *In* Handbook of geochemistry. *Edited by* K.H. Wedepohl. Springer-Verlag, Berlin and Heidelberg. pp. 37-C-1 to 37-N-1.

Johnson, P.C., and Reeves, R.M. 1995. Incorportion of the biological marker rubidium in gypsy moth (Lepidoptera: Lymantriidae) and its transfer to the predator *Carabus nemoralis* (Coleoptera: Carabidae). Environ. Entomol. **24**: 46–51.

Jones, R.L. 1992. Extractable rubidium in surface horizons of Illinois soils. Soil Sci. Soc. Am. J. **56**: 1453–1454.

Kidd, K.A. 1998. Use of stable isotope ratios in freshwater and marine biomagnification studies. *In* Environmental toxicology. *Edited by* J. Rose. Gordon and Breach Science Publishers, Amsterdam. pp. 357–376.

Köck, G., Babaluk, J., Berger, B., Bright, D., Doblander, C., Flannigan, M., et al. 2004. Fish from sensitive ecosystems as bioindicators of global climate change — High-Arctic 1997–2003. *Edited by* G. Köck. Veroeff. Univ. Innsbruck No. 245 (ISBN-3-901249-68-0).

Kosla, T., Skibniewska, E., Debski, B., and Urbanska-Slomka, G. 2002. Rubidium in the trophic chain soil–plants–animals. Trace Elem. Electrolytes, **4**: 171–176.

Leggett, R.W., Williams, L.R., Melo, D.R., and Lipsztein, J.L. 2003. A physiologically based biokinetic model for cesium in the human body. Sci. Total Environ. **317**: 235–255.

Mason, R.P., Reinfelder, J.R., and Morel, F.M.M. 1995. Bioaccumulation of mercury and methylmercury. Water Air Soil Pollut. **80**: 915–921.

Mearns, A.J., Olson, R.J., Young, D.R., and Schafer, H.A. 1981. Trophic structure and the cesium–potassium ratio in pelagic ecosystems. Calif. Coop. Ocean. Fish. Investig. Rep. No. 22. pp. 99–110 (also available at http://calcofi.org [accessed 16/05/2005]).

Minagawa, M., and Wada, E. 1984. Stepwise enrichment of ^{15}N along food chains: further evidence and the relation between $\delta^{15}N$ and animal age. Geochim. Cosmochim. Acta, **48**: 1135–1140.

National Laboratory for Environmental Testing. 2003. NLET schedule of services. National Water Research Institute, Environment Canada, Burlington, Ont.

Nielsen, F.H. 1998. Ultratrace elements in nutrition: current knowledge and speculation. J. Trace Elem. Exp. Med. **11**: 251–274.

Nyholm, N.E.I., and Tyler, G. 2000. Rubidium content of plants, fungi and animals closely reflects potassium and acidity conditions of forest soils. For. Ecol. Manag. **134**: 89–96.

Payne, J.C., and Dunley, J.E. 2002. Use of an elemental marker, rubidium, to study dispersal of aquatic insects. J. North Am. Benthol. Soc. **21**: 715–727.

Perel'man, F.M. 1965. Rubidium and caesium. [Translated from Russian by R.G.P. Towndrow.] The Macmillan Co., New York.

Peters, E.L., Schultz, I.R., and Newman, M.C. 1999. Rubidium and cesium kinetics and tissue distributions in channel catfish (*Ictalurus punctatus*). Ecotoxicology, **8**: 287–300.

Quinn, M.R., Feng, X., Folt, C.L., and Chamberlain, C.P. 2003. Analyzing trophic transfer of metals in stream food webs using nitrogen isotopes. Sci. Total Environ. **317**: 73–89.

Richie, R.J. 1997. Rubidium transport in the cyanobacterium *Synechococcus* R-2 (*Anacystis nidulans*, *S. leopoliensis*) PCC 7942. Plant Cell Environ. **20**: 907–918.

Rowan, D.J., and Rasmussen, J.B. 1994. Bioaccumulation of radiocesium by fish: the influence of physicochemical factors and trophic structure. Can. J. Fish. Aquat. Sci. **51**: 2388–2410.

Rowan, D.J., Chant, L.A., and Rasmussen, J.B. 1998. The fate of radiocesium in freshwater communities — Why is biomagnification variable both within and between species? J. Environ. Radioact. **40**: 15–36.

Salaün, M.-L., and Truchet, M. 1996. Étude, par émission ionique secondaire, de l'accumulation du rubidium dans les tissus mous de l'huître *Crassostrea gigas* (Mollusque, Lamellibranche). Cah. Biol. Mar. **37**: 329–340.

Seredin, V.V. 2003. Anomalous concentrations of trace elements in the spetsugli germanium deposit (Pavlovka Brown coal deposit, southern Primorye): Communication 2. Rubidium and cesium. Lithol. Miner. Resour. **38**: 233–241.

Systat Software Inc. 2000. SYSTAT®. Version 10 [computer program]. Systat Software Inc., Point Richmond, Calif.

Tipsmark, C.K., and Madsen, S.S. 2001. Rapid modulation of Na^+/K^+-ATPase activity in osmoregulatory tissues of a salmonid fish. J. Exp. Biol. **204**: 701–709.

Wang, W.-X. 2002. Interactions of trace metals and different marine food chains. Mar. Ecol. Prog. Ser. **243**: 295–309.

Ward, C.R., Spears, D.A., Booth, C.A., Staton, I., and Gurba, L.W. 1999. Mineral matter and trace elements in coals of the Gunnedah Basin, New South Wales, Australia. Int. J. Coal Geol. **40**: 281–308.

Younge, D.R., Mearns, A.J., Jan, T.-K., Heesen, T.C., Moore, M.D., Eganhouse, R.P., et al. 1980. Trophic structure and pollutant concentrations in marine ecosystems of southern California. Calif. Coop. Ocean. Fish. Investig. Rep. No. 21. pp. 197–206 (also found at http:// www.calcofi.org [accessed 16/05/2005]).

© 2005 NRC Canada

Stream acidification and mortality of brook trout (*Salvelinus fontinalis*) in response to timber harvest in Catskill Mountain watersheds, New York, USA

Barry P. Baldigo, Peter S. Murdoch, and Douglas A. Burns

Abstract: Effects of clear-cut and timber-stand improvement (TSI) harvests on water chemistry and mortality of caged brook trout (*Salvelinus fontinalis*) were evaluated in a study of three Catskill Mountain streams, 1994–2000. Harvests removed 73% of tree basal area (BA) from a clearcut subbasin, 5% BA from a TSI subbasin, and 14% BA at a site below the confluence of both streams. A fourth nonharvested site served as a control. Water quality and trout mortality were affected only in the clearcut stream. Acidity and concentrations of nitrate and inorganic monomeric aluminum (Al_{im}) increased sharply during high flows after the first growing season (fall 1997). Acid–Al_{im} episodes were severe during this period and decreased steadily in magnitude and duration thereafter. All trout at this site died within 7 days during spring 1998 and 85% died during spring 1999. Only background mortality was observed in other years at this site and at the other three sites during all tests. The absence of mortality in TSI watersheds indicates that limited harvests should not harm brook trout populations in acid-sensitive streams. Effects of tree harvests on fish communities are of concern, however, because many stream-dwelling species are more sensitive to acidified waters than brook trout.

Résumé : Nous avons étudié en 1994–2000 les effets de la coupe à blanc et des opérations d'amélioration forestière (TSI, « timber-stand improvement ») sur la chimie de l'eau et la mortalité d'ombles de fontaine (*Salvelinus fontinalis*) encagés dans trois cours d'eau des Catskills. Les coupes forestières ont retiré 73 % de la surface terrière (BA) des arbres dans un sous-bassin soumis à la coupe à blanc, 5 % de BA dans un sous-bassin TSI et 14 % de BA dans un site situé en aval de la confluence des deux cours d'eau. Un quatrième site sans coupe a servi de témoin. La qualité de l'eau et la mortalité des ombles n'ont été affectées que dans le cours d'eau du bassin soumis à la coupe à blanc. L'acidité et les concentrations de nitrates et d'aluminium inorganique monomère (Al_{im}) ont augmenté rapidement durant les périodes de crue après la première saison de croissance (automne 1997). Les épisodes d'acidité–Al_{im} ont été intenses durant cette période pour ensuite diminuer en force et en importance par après. Tous les ombles de ce site sont morts en sept jours au printemps 1998 et 85 % sont morts au printemps 1999. Les autres années, à ce site, il n'y avait qu'une mortalité de base, comme c'était le cas aux autres trois sites durant tous les tests. L'absence de mortalité dans les bassins versants TSI indique que des coupes restreintes ne devraient pas nuire aux populations d'ombles de fontaine dans les cours d'eau sensibles à l'acidité. Les effets de la coupe des arbres sur les communautés de poissons restent préoccupants, car beaucoup d'espèces lotiques de poissons sont plus sensibles aux eaux acidifiées que ne l'est l'omble de fontaine.

[Traduit par la Rédaction]

Introduction

Stream acidification, caused by acid deposition, was first documented in New York State during the 1970s (Colquhoun et al. 1981). The adverse effects of acid deposition on water quality, fish survival, and fish populations were reported in other parts of the northeast but were most acute in lakes of the Adirondack Mountains of northern New York (Haines and Baker 1986; Baker and Gallagher 1990; Baker et al. 1993). The only large river in the Catskill Mountains of southeastern New York with moderately to severely acidified reaches was the Neversink River (Colquhoun et al. 1981). Recent studies in the Neversink have documented brook trout (*Salvelinus fontinalis*) mortality in response to episodic and chronic stream acidification (Van Sickle et al. 1996; Baldigo and Murdoch 1997) and the spatial extent of negative effects on fish communities (Baldigo and Lawrence 2000).

A variety of forest harvest practices have also been shown to affect the chemical quality of soil and stream waters in the northeastern United States (Likens et al. 1970; Dahlgren and Driscoll 1994; Burns et al. 1997), but the effects of tree harvesting on fish survival (or mortality) and resident fish populations in acid-sensitive streams have not been well documented. Forest harvests can alter the rates of biogeochemical processes in soils and affect the chemistry of soil, ground, and surface waters for a few years to several

Received 18 February 2004. Accepted 9 October 2004. Published on the NRC Research Press Web site at http://cjfas.nrc.ca on 31 May 2005.
J17974

B.P. Baldigo,[1] P.S. Murdoch, and D.A. Burns. US Geological Survey, 425 Jordan Road, Troy, NY 12180, USA.

[1]Corresponding author (e-mail: bbaldigo@usgs.gov).

 doi: 10.1139/F05-022 © 2005 NRC Canada

decades (Likens et al. 1970; Swank and Waide 1988; Dahlgren and Driscoll 1994). Clear-cutting has been found to increase the rates of nitrate (NO_3^-) leaching from soils through increased N mineralization and nitrification and (or) decreased N uptake by vegetation, which can increase surface water concentrations of NO_3^- by more than an order of magnitude (Likens et al. 1970; Vitousek 1981; Burns et al. 1997). Characterizing the effects of forest harvest on stream water quality is problematic owing to the complexity of the N cycle, which responds simultaneously to cyclic or random variations in atmospheric deposition of nitrous oxides, soil freezing, air temperature, and defoliation of vegetation by insects (Mitchell et al. 1996; Murdoch et al. 1998).

The N cycle in the Catskill Mountain region is especially sensitive to disturbance because high rates of atmospheric N deposition (about 10–12 $kg \cdot ha^{-1} \cdot year^{-1}$) have induced a condition of N saturation whereby N retention and utilization capacity of the vegetation and microbial communities are exceeded, yielding net N surpluses and elevated concentrations of NO_3^- in shallow soil and surface waters (Murdoch and Stoddard 1992, 1993). Increased NO_3^- concentrations can increase acidity (lower pH), which in turn can increase the concentrations of total monomeric aluminum (Al_m) and inorganic monomeric aluminum (Al_{im}) in surface waters (Driscoll 1985). A decrease in stream pH to below 5.5 can cause concentrations of Al_{im} to exceed levels that are acutely toxic to brook trout and many other fish species (Baker et al. 1990; Baker and Christensen 1991; Baldigo and Murdoch 1997).

In 1992, the New York City Department of Environmental Protection and the US Geological Survey began a 7-year forest harvest study (Burns et al. 1997) to document the effects of clear-cut and timber-stand improvement (TSI) forest harvest practices on soil nitrification and N mineralization rates, soil- and surface-water chemistry, and brook trout mortality. Tree harvests were conducted in two adjacent subbasins of one headwater stream and chemistry and trout mortality were monitored at both streams, at a third site just below their confluence, and at a fourth site in an adjacent undisturbed (reference) subbasin. The clear-cut harvest (winter of 1996–1997) decreased tree basal area (BA) in that subbasin by 73%, and the partial TSI harvest (winter of 1995–1996 and fall of 1996) decreased tree BA in the adjacent subbasin by 5%. The result was a 14% decrease in tree BA in the combined watershed of the third site located at the confluence of the other two streams. The study investigated hypotheses that (*i*) decreased uptake of N, and the attendant increase in rates of nitrification and N mineralization, would produce significant increases in NO_3^- concentrations in the soil and stream waters of harvested watersheds, (*ii*) increased soil acidity would increase Al_m mobilization and increase Al_{im} concentrations in streams of harvested watersheds, and (*iii*) concentrations of Al_{im} in both streams would exceed levels that are acutely toxic to brook trout after the trees were harvested. This paper summarizes the water quality changes observed at streams within clear-cut, partially harvested (TSI), and reference watersheds and associated effects on brook trout mortality in each stream during 30-day exposures in the spring of each year from 1995 to 2000.

Materials and methods

Study area

The study was conducted in small watersheds draining into the West Branch Neversink River in the Catskill Mountains, southeastern New York (Fig. 1). Three of the four monitoring sites are in the Shelter Creek basin: the Dry Creek clearcut site (dc57), which is a tributary to Shelter Creek with a drainage area of 24 ha, the upper Shelter Creek TSI site (sc40) with a drainage area of 109 ha, and the lower Shelter Creek confluence site (sc20), immediately downstream of where Dry Creek joins Shelter Creek, with a drainage area of 161 ha. The reference stream site (cl25) is in an adjacent basin to the southwest (Fig. 1) and has a drainage area of 48 ha. Elevations at the monitoring stations range from about 650 to 880 m.

The Catskill Mountains consist of an uplifted plateau of Devonian sedimentary rock that has been eroded and dissected by streams and then overlain by till of varying thickness from the most recent glaciation of North America about 1000 years ago (Rich 1934; Buttner 1977). The soil is an Inceptisol and classified in the Arnot–Oquaga–Lackawana series (Tornes 1979) as a bouldery silt loam with shallow organic horizons (1.5–8 cm).

The principal land cover in the study area is mainly mixed-hardwood forest dominated by American beech (*Fagus grandifolia*), sugar maple (*Acer saccharum*), and yellow birch (*Betula alleghaniensis*). Small stands of eastern hemlock (*Tsuga canadensis*) also occupy parts of the lower reference stream basin and upper Shelter Creek subbasin, but only a few isolated hemlock trees are evident in the Dry Creek subbasin.

The climate in the study area is classified as humid continental, with cold winters and moderately warm summers. The mean annual temperature at the Slide Mountain weather station (about 5 km east of the study area, 808 m elevation) was 4.6 °C from 1961 to 1990 (National Oceanic and Atmospheric Administration 1990); mean annual precipitation at the same station was 134 cm from 1984 through 2001 (http://nadp.sws.uiuc.edu/sites/siteinfo.asp?net=NTN&id=NY68, accessed 1 December 2002). About 20%–25% of precipitation falls as snow. Precipitation amounts are fairly uniformly distributed throughout the year, but 32% of the Neversink River annual runoff (0.97 m) normally occurs during the snowmelt period of March and April and 28% of the annual runoff occurs during the summer months of May–September (Firda et al. 1995).

Timber harvests

Two timber harvests were completed between December 1995 and March 1997. During each harvest, slash (tree branches and tops) was left on the ground and some branches were arranged perpendicular to temporary skidding roads to form a "corduroy" surface and helped minimize physical disturbance of the forest floor. About 23% of the upper Shelter Creek subbasin (upstream of sc40) was partially cut for the TSI harvest between December 1995 and November 1996. The rest of the watershed is mostly within a New York State Wilderness Area where logging is prohibited. About 22% of tree BA was removed during the TSI

© 2005 NRC Canada

Fig. 1. Location of tree harvests and surface-water monitoring sites in Shelter Creek, Dry Creek, and Reference Creek subbasins in the Neversink River basin, New York. Tree harvest areas are denoted by crosshatching (clearcut) or stippling (timber-stand improvement), drainage-basin boundaries by broken lines, and stream sites by circles.

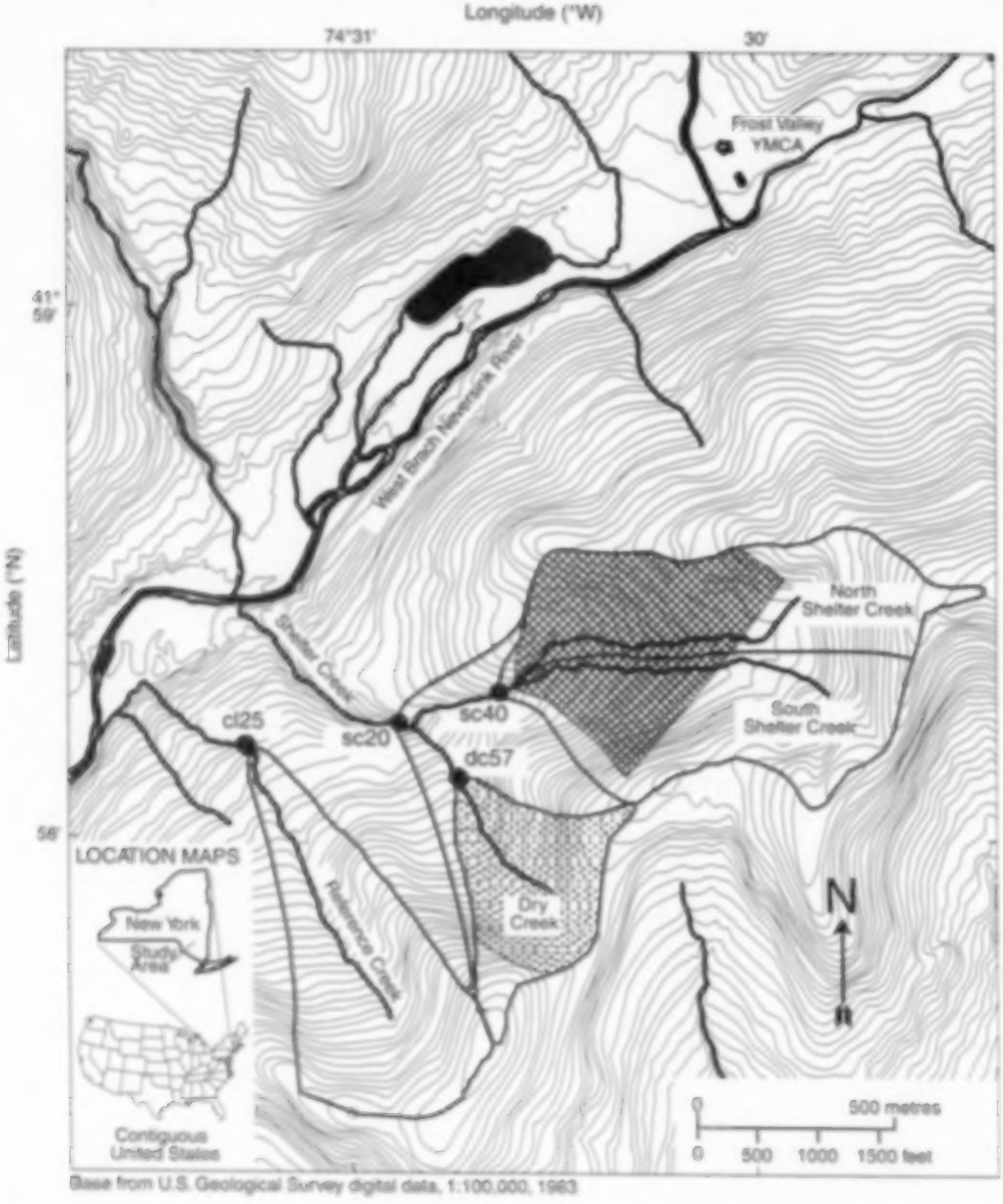

harvest, which resulted in a 5% decrease in tree BA in the upper Shelter Creek watershed upstream of sc40 (Fig. 1). About 75% of the Dry Creek watershed (upstream of dc57) was clear-cut from December 1996 through March 1997. The southwestern (upper) part of the Dry Creek subbasin is designated as wilderness and therefore was not harvested. The clear-cut removed about 97% of the trees in the harvested part of the Dry Creek subbasin and decreased tree BA in the watershed upstream from dc57 by about 73%. The harvests in both the Dry Creek and upper Shelter Creek subbasins decreased tree BA in the watershed upstream from sc20 by about 14%. The upper Shelter Creek and Dry Creek subbasins had respective similar tree BA (27 and 29 $m^2 \cdot ha^{-1}$), total tree biomass (216 and 232 $Mg \cdot ha^{-1}$), and understory biomass (2.3 and 3.0 $Mg \cdot ha^{-1}$) before the harvests. Total tree BA (36 $m^2 \cdot ha^{-1}$) and biomass (295 $Mg \cdot ha^{-1}$) in the reference

© 2005 NRC Canada

watershed were greater than and understory biomass (3.1 Mg·ha^{-1}) was comparable with levels in the two harvested subbasins.

Stream stage and discharge

Stream stage at the three Shelter Creek sites (sc40, sc20, and dc57) was measured every 15 min with a submersible pressure transducer and recorded with an electronic data logger during the study period. Discharge was measured biweekly at all four sites in accordance with standard US Geological Survey methods (Rantz 1983). The data were used to generate stage-to-discharge relation curves (discharge rating) and continuous 15-min (and hourly) discharge records for the three Shelter Creek sites (sc40, sc20, and dc57). Fifteen-minute stage data were not logged at the reference site (cl25); therefore, biweekly discharge measurements made at cl25 and sc20 on the same dates were used to generate a model that predicts flow at cl25 from the flow at sc20. The flow model and continuous flow records from sc20 were used to estimate hourly discharge data for the reference site (cl25).

Stream chemistry

Stream water samples were collected by hand weekly or biweekly at all four stream sites from April 1993 through September 2000 for chemical analyses. The samples were collected in 500-mL polyethylene bottles and stored on ice until they could be returned to the US Geological Survey laboratory in Troy, New York. In addition, electronic data loggers were linked to stream-stage sensors only at the three Shelter Creek sites (sc40, sc20, and dc57) and were programmed to activate automated samplers to collect water samples at specified increments of rising and falling stage during storms. Storm water samples were usually returned to the laboratory within 48 h and stored at 4 °C until preparation for analyses.

Most water samples were aliquoted within 2 or 7 days, depending on whether they were hand-grab or storm water samples, and analyzed for pH, acid-neutralizing capacity (ANC), sulfate (SO_4^{2-}), NO_3^-, ammonium (NH_4^+), chloride (Cl^-), calcium (Ca^{2+}), magnesium (Mg^{2+}), sodium (Na^+), silica (SiO_2), potassium (K^+), dissolved organic carbon (DOC), total aluminum (Al_t), Al_{im}, organic monomeric aluminum (Al_{om}), and Al_{in} at the US Geological Survey laboratory by standard methods (Lawrence et al. 1995). Data quality objectives for precision and accuracy for all analyses were 10% (coefficient of variation), and these objectives were generally met for more than 95% of the quality assurance samples (Lincoln et al. 1996).

Estimates of continuous (hourly) Al_{in} and pH data at the clearcut site and median, minimum, and maximum values for biologically important constituents at each site were assessed for each 30-day exposure period. Continuous Al_{in} and pH records at dc57 were estimated for respective exposure periods from hourly discharge data and the relationships between constituent concentrations and log-transformed discharge values. The discharge–Al_{in} relationships were significant but weak in 1997 (R^2 = 0.13) and 1995 (R^2 = 0.32) when Al_{in} concentrations stayed low. The relationships were stronger in 1996 (R^2 = 0.78), 1998 (R^2 = 0.80), 1999 (R^2 = 0.55), and 2000 (R^2 = 0.76) when Al_{in} concentrations varied more widely with stream flows. The discharge–pH relationships were stronger than discharge–Al_{in} relationships and followed similar trends; R^2 was 0.38 in 1997 and 0.52 in 1995 and ranged from 0.67 to 0.91 during the other four years. Continuous Al_{in} and pH records were not generated for the other sites where annual differences were minor and trout mortality was low or nonexistent.

Toxicity tests

Young-of-the-year brook trout (age 0+) from the New York State Department of Environmental Conservation hatchery in Rome, New York, were exposed (in cages) to stream waters at all four sites for 30-day periods during each spring from 1995 through 2000 in accordance with techniques described by Johnson et al. (1987) and Baldigo and Murdoch (1997). The exposure periods were 4 April through 5 May 1995, 2 April through 3 May 1996, 10 April through 11 May 1997, 3 April through 4 May 1998, 3 April through 3 May 1999, and 31 March through 1 May 2000. Each year, brook trout were transported from Rome to the West Branch Neversink River and placed into a large holding chamber to acclimate to local conditions for 24 h. The next day, 20 trout were placed into sixteen 4-L plastic, screen-sided jars (five trout per jar) and then transported to exposure cages at each study site (four jars and 20 trout per site). Trout were not fed during the exposure periods and mortality was checked and recorded every 2–4 days. Total length of caged trout ranged from 35 to 51 mm and averaged 43.5 mm; individual weights averaged 1.2 g. Trout lengths and weights did not differ significantly ($p \leq 0.05$) among streams or test periods.

Results and discussion

Stream stage and discharge

Daily discharge records for the four study streams, 1994–2000 (Figs. 2–5), show seasonal cycles typical of headwater streams, with the highest flows in late winter or early spring and the lowest flows in late summer or early fall. Flows at the four sites were relatively stable during all 30-day fish exposure periods, except in 1996 when two storms increased discharge at all sites by at least an order of magnitude above base flows (Fig. 6). Over the 6-year study, mean annual discharge values were 0.0046 m^3·s^{-1} at dc57, 0.0346 m^3·s^{-1} at sc40, 0.0576 m^3·s^{-1} at sc20, and 0.0178 m^3·s^{-1} at c125. Discharge at sites dc57 and sc40 in the two harvested watersheds, on average, represented 8% and 60% of the total flow at the confluence site (sc20). Because of their semiperennial nature, steep channel slopes, and vertical barriers, resident fish communities in the four streams were limited. Although not surveyed, fish were not apparent at dc57 and sc40 and only a small number of brook trout were observed at sc20 and cl25 prior to this investigation.

Stream chemistry

Prior to tree harvests, water chemistry at all four sites was typical of acid-sensitive headwater streams in the Catskill region (Figs. 2–5). ANC levels were generally <50 μequiv.·L^{-1} and occasionally negative during high flows. All four streams experienced at least one event with pH <5.0. There-

© 2005 NRC Canada

Fig. 2. Daily discharge, acid-neutralizing capacity (ANC), pH, and concentrations of SO_4^{2-}, NO_3^-, Ca^{2+}, and inorganic monomeric aluminum (Al_{im}) for water samples from the clearcut site (dc57) in the Neversink River basin, New York, 1994–2000. The clear-cut harvest period is denoted by light stippling and the 30-day brook trout (*Salvelinus fontinalis*) exposure periods are indicated by heavy stippling.

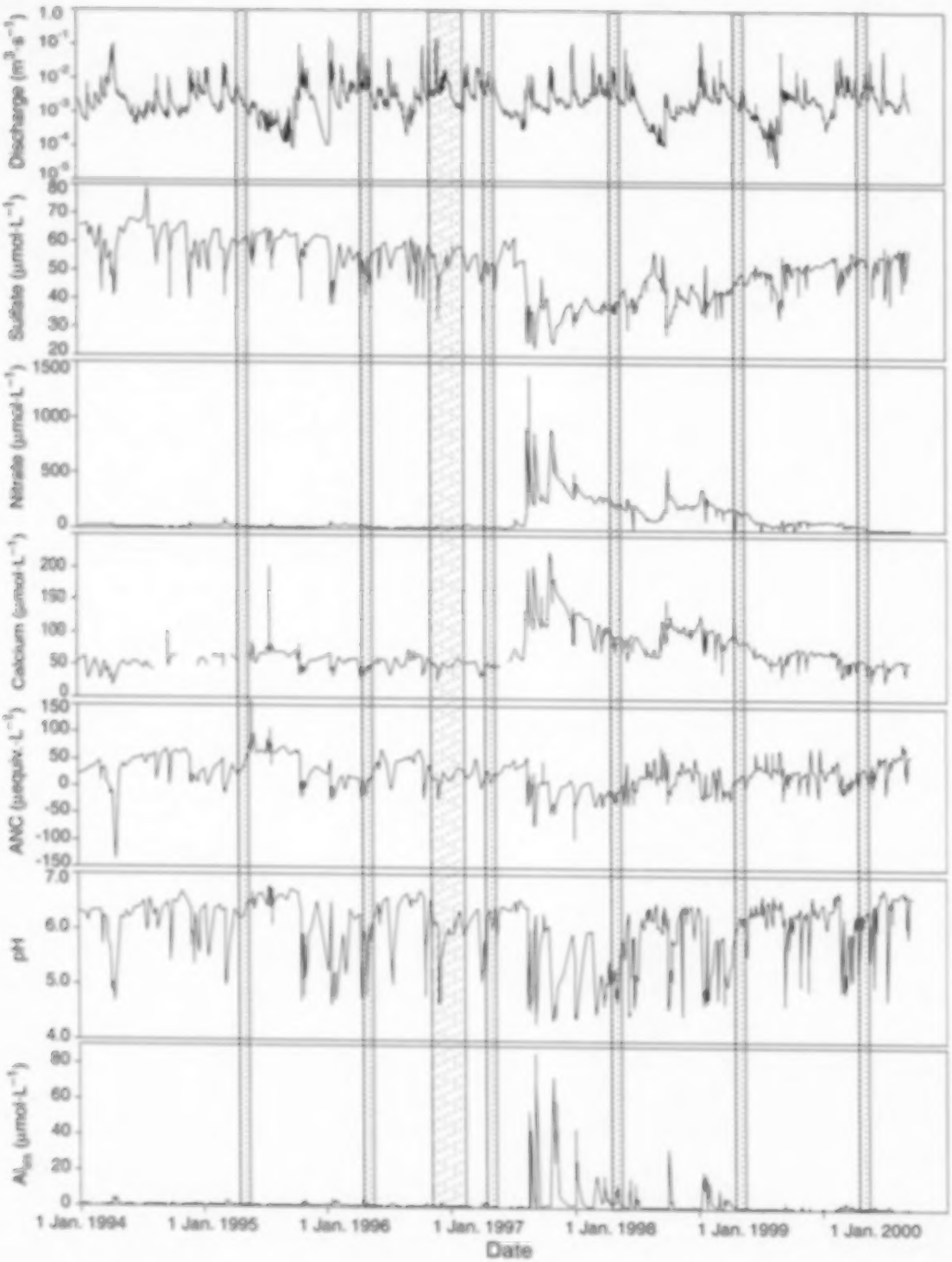

© 2005 NRC Canada

Fig. 3. Daily discharge, acid-neutralizing capacity (ANC), pH, and concentrations of SO_4^{2-}, NO_3^-, Ca^{2+}, and inorganic monomeric aluminum (Al_m) for water samples from the confluence site (sc20) in the Neversink River basin, New York, 1994–2000. The harvest periods in the Shelter Creek and Dry Creek subbasins are denoted by light stippling and the 30-day brook trout (*Salvelinus fontinalis*) exposure periods are indicated by heavy stippling.

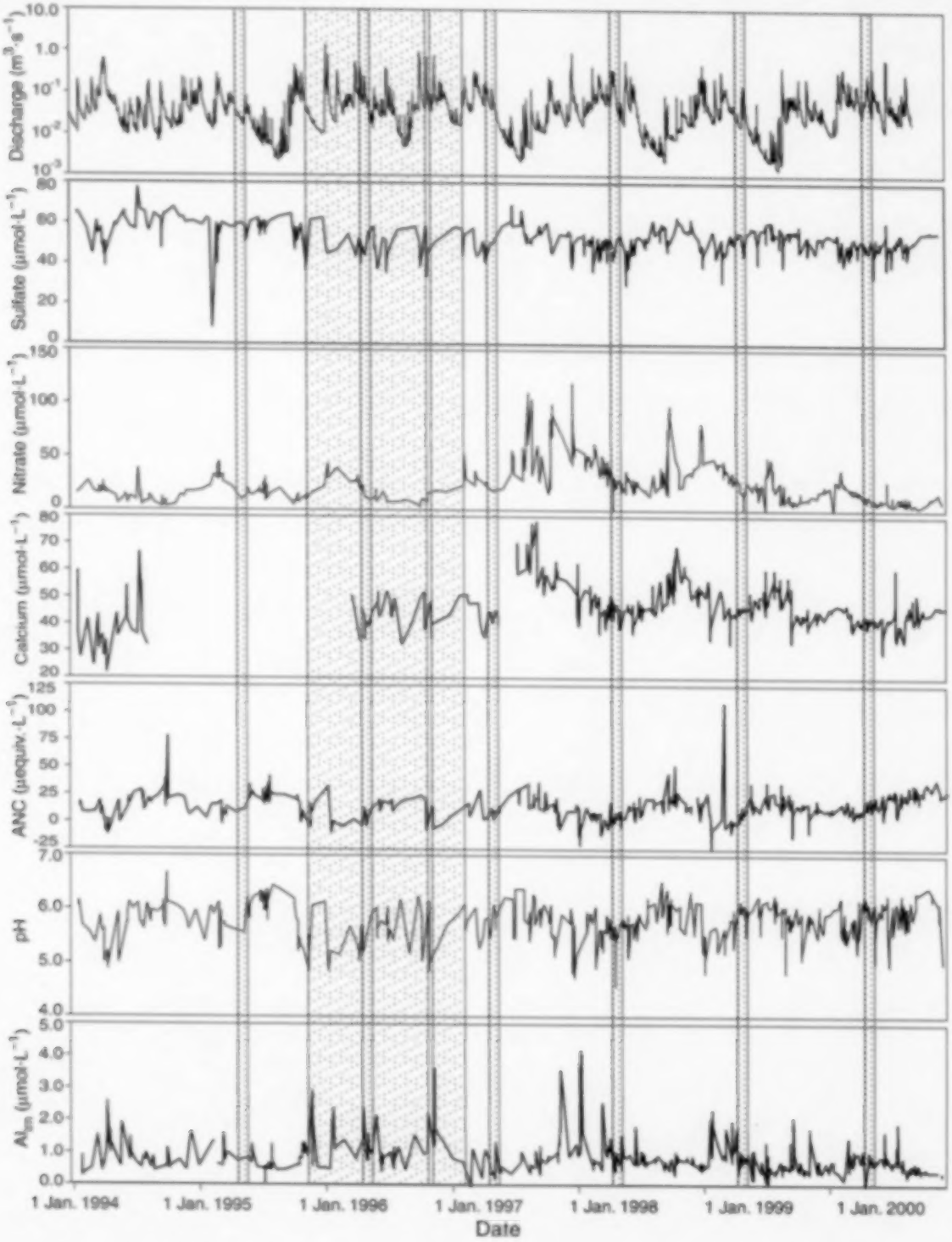

© 2005 NRC Canada

Fig. 4. Daily discharge, acid-neutralizing capacity (ANC), pH, and concentrations of SO_4^{2-}, NO_3^-, Ca^{2+}, and inorganic monomeric aluminum (Al_{im}) for water samples from the timber-stand improvement (TSI) site (sc40) in the Neversink River basin, New York, 1994–2000. The TSI harvest period is denoted by light stippling and the 30-day brook trout (*Salvelinus fontinalis*) exposure periods are indicated by heavy stippling.

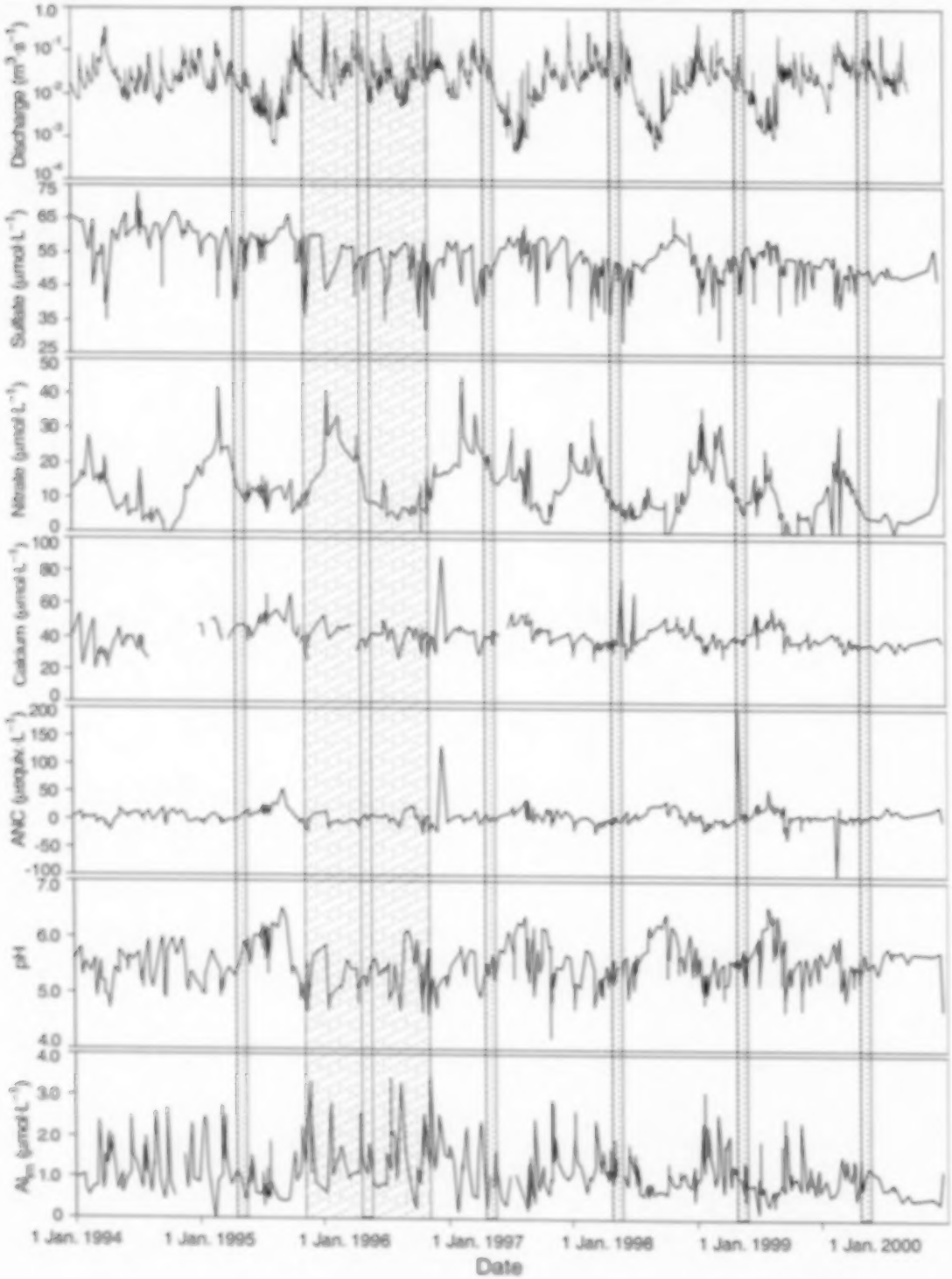

© 2005 NRC Canada

Fig. 5. Daily discharge, acid-neutralizing capacity (ANC), pH, and concentrations of SO_4^{2-}, NO_3^-, Ca^{2+}, and inorganic monomeric aluminum (Al_m) for water samples from the reference site (cl25) in the Neversink River basin, New York, 1994–2000. The 30-day brook trout (*Salvelinus fontinalis*) exposure periods are indicated by heavy stippling.

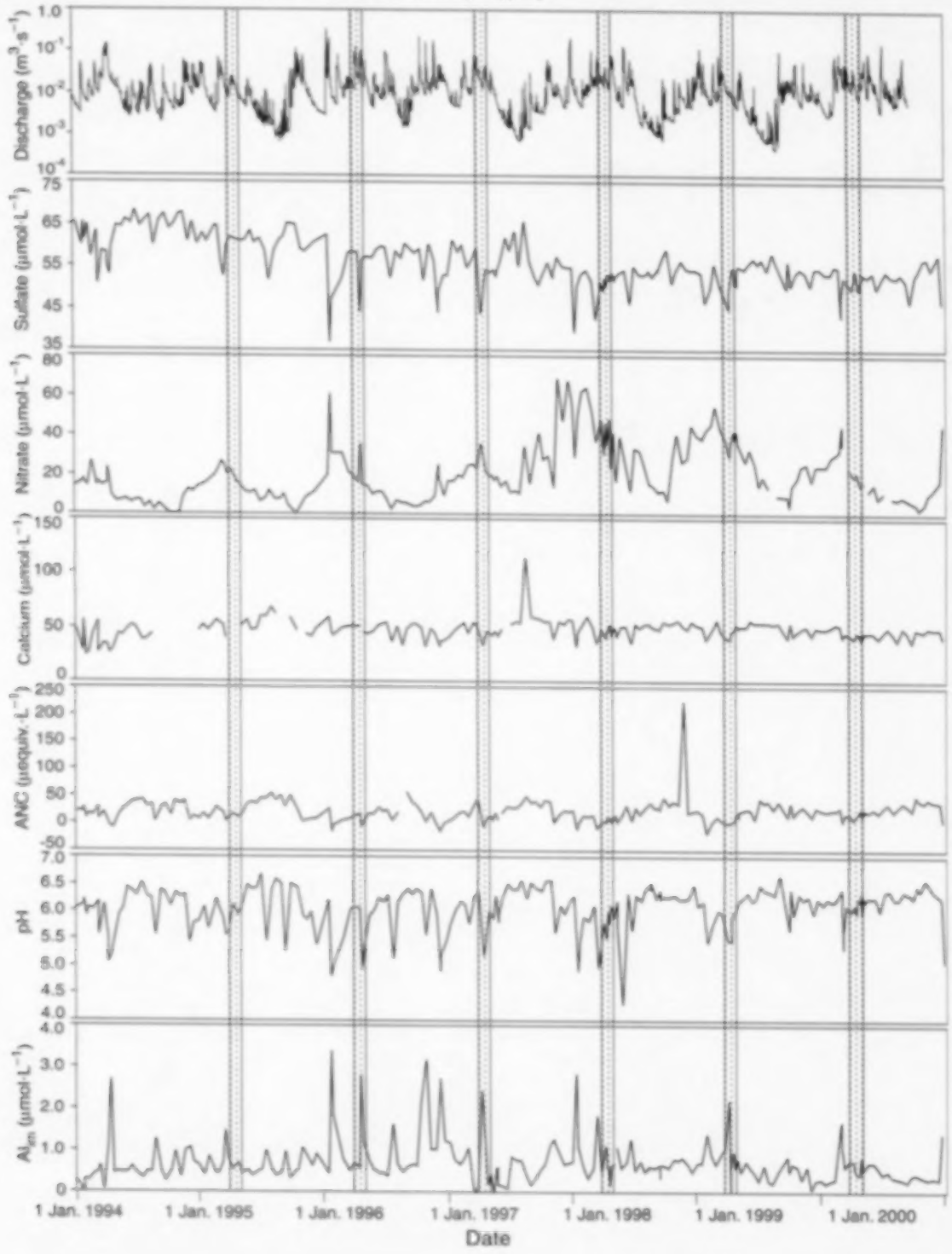

© 2005 NRC Canada

Fig. 6. Hourly discharge at (*a*) dc57, (*b*) sc20, (*c*) sc40, and (*d*) cl25 during 30-day toxicity tests, spring 1995 (light dotted line), 1996 (medium dashed line), 1997 (light dash-dotted line), 1998 (thick solid line), 1999 (thick dash-dotted line), and 2000 (thick dashed line).

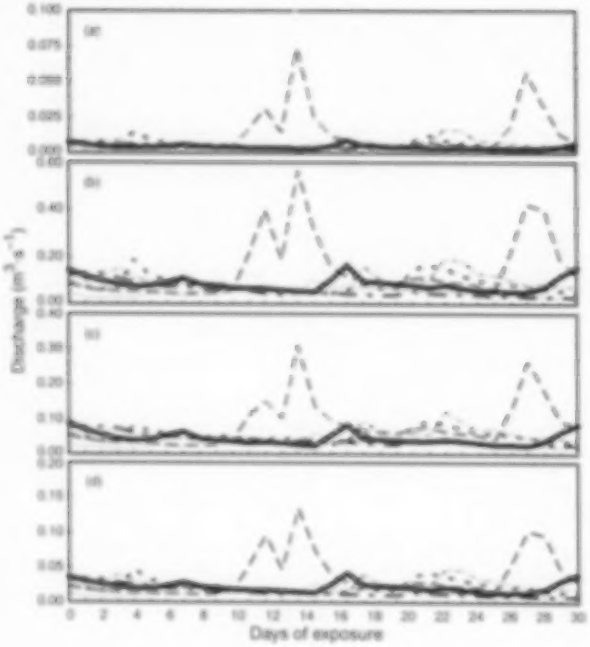

fore, all four streams would be classified as susceptible to acidification and episodically acidic.

Over the 6-year study, NO_3^- concentrations in the reference stream (cl25) showed no long-term trend, but SO_4^{2-} concentrations decreased from a median of 60.9 μmol·L^{-1} in 1994 to 52.4 μmol·L^{-1} in 2000 (Table 1; Fig. 5). Similar long-term SO_4^{2-} declines occurred at dc57 (Table 1) and at sc20 and sc40 (not shown) prior to tree harvests. Several studies also reported SO_4^{2-} declines during the 1980s and 1990s in acidified streams and lakes in eastern North America and Europe (Stoddard et al. 1999; Martin et al. 2000; Driscoll et al. 2003). The decline in the northeastern United States has been associated with decreasing rates of atmospheric SO_4^{2-} deposition in response to decreased S emissions from power-generating facilities as mandated by the Clean Air Act Amendments of 1990 (Lynch et al. 2000; Butler et al. 2001; Stoddard et al. 2003).

Distinct negative effects of tree harvests on water chemistry were evident only at Dry Creek (dc57) in the clearcut subbasin, especially as compared with stable chemistry at cl25 (Table 1; Figs. 2 and 5). Tree harvest occurred during winter 1996–1997, but changes in stream chemistry at dc57 were not obvious until late summer and fall 1997 and corresponded mainly to increasing stream discharge following the first summer growing season. NO_3^- concentrations increased 10-fold from a median of 25.8 μmol·L^{-1} to a median of 259.9 μmol·L^{-1} (peak of 1390.5 μmol·L^{-1}) in 1997 (Table 1). Concentrations of Al_{im} also increased from medians of 0.53 and 1.01 μmol·L^{-1} in 1995 and 1996 to a median of 1.81 μmol·L^{-1} in 1998 (Table 1). Al_{im} concentrations increased dramatically during high-flow (storm) events in fall 1997 and spring 1998, reaching a peak of 1390.5 μmol·L^{-1} (Table 1; Fig. 2). While pH ranged as low as 4.65 during high-flow events prior to clear-cutting, pH dropped to 4.32 and 4.42 during several storm events in the first fall (1997) and spring (1998) after tree harvests (Table 1). A twofold increase in stream water concentrations of Ca^{2+} (increased from 48.8 μmol·L^{-1} in 1996 to 111.5 μmol·L^{-1} in 1997) also occurred following tree removal; this increase may have helped prevent larger decreases in pH and ANC than those observed. The observed departures from normal water quality continued through 1999 and much of 2000, but with gradually declining severity.

Decreases in pH and ANC in the clearcut stream post-harvest were related mainly to increased NO_3^- concentrations, not to SO_4^{2-} concentrations. SO_4^{2-} levels decreased from an average of 50–60 μmol·L^{-1} before and during harvest (1995–1996) to less than 40 μmol·L^{-1} in late 1997. Results from a concurrent study in these subbasins (Welsh et al. 2004) suggest that the decreases in stream water SO_4^{2-} concentrations induced by the clear-cut were possibly caused by increased soil acidification and SO_4^{2-} adsorption. SO_4^{2-} concentrations at the clearcut site, like NO_3^- and Ca^{2+}, returned to near-preharvest levels by late 2000.

In contrast with the marked changes in stream chemistry at dc57, water quality at the TSI site (sc40) did not change following tree harvests, and chemistry at the site below the confluence of Dry Creek and Shelter Creek (sc20) only deviated slightly from normal. The TSI harvest in the upper Shelter Creek subbasin had no discernable effect on surface-water chemistry at sc40 over the long term (Fig. 4) or during the 30-day test periods (Table 2). The lack of water quality changes at the TSI site (sc40) and the major changes in water quality at the clearcut site (dc57) after tree harvests suggest that small changes in water quality at the confluence site (sc20; Fig. 3) were due entirely to the clear-cut harvest in the Dry Creek subbasin. NO_3^- and Ca^{2+} concentrations increased moderately at the confluence site during fall 1997 (NO_3^- and Ca^{2+} peaked at about 110 and 80 μmol·L^{-1}, respectively), but pH, ANC, and Al_{im} levels changed little compared with prior years (Fig. 3).

Except for the long-term SO_4^{2-} decline noted earlier, concentrations of most constituents at the reference site (cl25) were relatively stable during base flows and fluctuated normally during high flows from 1994 through 2000 (Table 1; Fig. 5). Concentrations of NO_3^- increased moderately during late 1997, 1998, and 1999 ostensibly because deep soil waters "leaked" from the clearcut watershed across surface-elevation or topographic boundaries into the drainage of the reference stream. The extremely low pH (4.31) observed from one water sample collected at cl25 during the spring of 1998 (Table 1; Fig. 5) does not correspond to a high-flow event and thus may be a missidentified sample. The lack of substantial chemical changes at the reference site (Table 1) and at both TSI sites indicates that other regional trends had little or no effect on the chemistry of waters at the clearcut site during the period of study.

Brook trout mortality

Mortality of caged brook trout before and after the harvests was generally nil or low at all sites except the clearcut

© 2005 NRC Canada

Table 1. Annual median, minimum, and maximum values for selected chemical constituents measured from all routine and storm event samples collected at the clearcut site (dc57) and reference site (cl25), 1995–2000.

	ANC (μequiv·L^{-1})	Ca^{2+} (μmol·L^{-1})	DOC (μmol·L^{-1})	pH	NO_3^- (μmol·L^{-1})	Al_{om} (μmol·L^{-1})	SO_4^{2-} (μmol·L^{-1})	Al_{im} (μmol·L^{-1})	Al_m (μmol·L^{-1})	Al_t (μmol·L^{-1})
Clearcut site: dc57										
1995, n = 86										
Median	59.9	67.9	184.1	6.43	21.0	0.39	57.8	0.53	0.87	11.29
Range	–20.2–160.2	37.1–202.6	33.1–780.7	4.72–6.77	6.6–83.1	0–2.71	39.6–64.9	0.21–3.59	0.33–5.54	4.92–38.24
1996, n = 75										
Median	13.3	48.8	175.7	5.86	25.8	1.02	49.4	1.01	2.05	11.06
Range	–27.0–70.1	26.5–74.3	59.2–486.2	4.65–6.71	4.5–77.8	0.09–3.70	32.7–61.9	0–5.09	0.52–6.81	5.38–48.10
1997, n = 68										
Median	11.5	111.5	115.1	5.91	259.9	1.06	38.9	1.07	1.76	35.76
Range	–71.0–56.4	34.2–226.9	37.1–421.5	4.32–6.56	17.2–1390.5	0–4.57	22.8–62.1	0–86.38	0.18–88.44	0.66–99.94
1998, n = 122										
Median	2.8	93.8	110.5	5.51	227.2	0.10	38.7	1.81	2.08	6.88
Range	–95.6–76.6	61.5–153.4	41.1–426.9	4.42–6.50	84.2–570.3	0–3.04	27.9–57.0	0.03–43.97	0–45.85	0.04–61.53
1999, n = 119										
Median	20.5	70.6	105.0	6.08	89.3	0.23	46.4	0.74	1.10	4.06
Range	–23.0–75.3	35.5–130.6	29.9–682.2	4.66–6.67	0–380.9	0–4.03	33.6–55.5	0–20.89	0–21.25	0.73–31.41
2000, n = 104										
Median	26.8	54.8	139.0	6.27	37.9	0.00	52.6	0.66	0.40	2.49
Range	–9.7–85.4	29.3–76.6	55.0–566.1	4.77–6.78	0–87.2	0–2.63	38.5–58.9	0.07–3.65	0–4.81	0.63–12.75
Reference site: cl25										
1995, n = 25										
Median	26.0	51.8	146.6	6.07	11.1	0.42	60.9	0.55	1.09	4.98
Range	2.5–54.7	40.6–668.1	56.3–681.2	5.26–6.67	0–26.4	0–1.19	51.5–65.0	0.33–1.50	0.32–2.30	3.60–9.40
1996, n = 27										
Median	11.6	48.8	129.3	6.03	11.0	0.69	57.0	0.76	1.53	8.26
Range	–16.0–57.2	32.3–58.7	66.4–400.3	4.80–6.41	2.5–61.0	0.23–3.12	36.8–62.4	0.39–3.38	0.67–6.50	3.96–13.68
1997, n = 31										
Median	20.9	50.7	129.4	6.18	19.4	0.23	54.8	0.66	1.13	2.43
Range	–5.4–49.1	33.4–114.3	75.4–534.0	5.17–6.57	10.7–68.8	0–2.17	43.7–65.9	0–2.46	0.21–4.58	0.97–8.12
1998, n = 37										
Median	16.8	50.2	130.8	6.19	29.6	–0.01	53.2	0.65	0.65	2.11
Range	–9.9–224.1	32.7–59.9	80.8–356.8	4.31–6.51	6.6–64.0	0–2.22	39.4–59.1	0.15–2.85	0.13–5.07	0.96–44.61
1999, n = 32										
Median	17.1	49.9	116.7	6.19	28.9	0.21	53.6	0.64	0.71	2.22
Range	–17.0–44.0	39.1–57.0	86.7–328.7	5.42–6.65	3.7–55.0	0–1.27	44.9–58.2	0–2.20	0.02–2.46	1.34–4.25
2000, n = 35										
Median	22.8	45.0	121.7	6.22	16.0	–0.18	52.4	0.44	0.29	1.64
Range	3.3–49.6	36.8–52.7	86.7–176.6	5.09–6.56	2.6–45.2	0–1.14	42.9–57.8	0.21–1.70	0–2.08	0.76–6.71

Note: ANC, acid-neutralizing capacity; DOC, dissolved organic carbon; Al_{om}, organic monomeric aluminum; Al_{im}, inorganic monomeric aluminum; Al_m, total monomeric aluminum; Al_t, total dissolved aluminum; n, the number of samples analyzed.

© 2005 NRC Canada

Table 2. Estimated median, minimum, and maximum values for selected chemical constituents measured at the four sites during 30-day brook trout (*Salvelinus fontinalis*) exposure periods each year from 1995 to 2000.

	ANC (μequiv·L^{-1})	Ca^{2+} (μmol·L^{-1})	DOC (μmol·L^{-1})	pH	NO_3^- (μmol·L^{-1})	Al_{om} (μmol·L^{-1})	SO_4^{2-} (μmol·L^{-1})	Al_{im} (μmol·L^{-1})	Al_m (μmol·L^{-1})	Al_i (μmol·L^{-1})
Clearcut site: dc57										
1995, n = 4										
Median	27.1	61.8	72.5	6.23	28.5	0.05	59.5	0.54	0.59	4.92
Range	10.8–39.6	58.2–65.3	33.1–96.7	5.69–6.36	19.9–34.6	0–0.52	55.7–61.2	0.48–1.49	0.43–2.01	4.92–4.92
1996, n = 14										
Median	–13	36.2	218.6	4.87	37.3	1.39	44.6	2.94	4.79	10.14
Range	–21.7–15.7	30.7–59.5	59.2–302.6	4.76–6.28	23.2–47.2	0.28–2.08	41.6–56.7	0.55–5.09	0.83–6.81	7.45–20.2
1997, n = 7										
Median	11.3	47.5	138.9	6.05	23.3	1.53	49.3	0.59	1.82	5.73
Range	–2.1–31.2	34.2–54.9	82.7–207.4	5.08–6.39	19.1–31.4	1.11–1.89	45.7–53.8	0.01–3.90	0.85–5.72	2.54–8.91
1998, n = 15										
Median	–12.8	100.5	90.6	5.03	263.0	0.26	38.0	4.48	4.61	9.30
Range	–29.5-(-)2.8	79.5–110.7	64.7–181.8	4.64–5.47	220.0–296.3	0–1.11	35.6–40.1	2.02–13.89	2.04–14.84	4.80–21.4
1999, n = 11										
Median	3.9	93.6	68.9	5.69	187.9	0	44.1	1.37	1.16	3.90
Range	–21.3–16.7	77.0–122.7	55.3–106.5	5.00–6.21	180.0–203.3	0–0.13	42.3–46.6	0.77–5.92	0.65–5.94	2.23–10.9
2000, n = 17										
Median	15.7	56.8	104.3	6.02	54.0	0	53.7	0.82	0.39	2.29
Range	1.9–33.7	43.5–61.8	87.3–205.8	5.14–6.38	38.3–59.9	0–0.23	51.3–57.0	0.43–2.55	–0.06–2.78	1.20–10.9
Confluence site: sc20										
1995, n = 3										
Median	12.23	na	136.4	5.63	21.7	0.65	59.9	0.83	1.44	4.84
Range	8.4–13.60	na	133.4–154.3	5.55–5.70	9.7–26.3	0.61–0.70	57.8–60.1	0.75–0.99	1.40–1.69	4.80–5.56
1996, n = 9										
Median	2.10	42.8	292.1	5.47	23.1	1.67	49.6	1.08	2.75	na
Range	–4.7–13.2	34.1–50.4	126.0–444.4	5.03–5.72	17.3–33.2	0.79–2.76	39.5–54.3	0.75–2.43	1.61–4.69	na
1997, n = 7										
Median	6.80	42.9	235.5	5.82	24.2	2.30	45.6	0.39	3.18	5.96
Range	1.70–12.9	35.0–45.2	118.0–410.6	5.28–6.10	18.9–29.2	1.40–3.41	40.7–51.5	0.17–1.33	1.79–4.74	na
1998, n = 18										
Median	5.10	45.7	211.4	5.67	36.9	0.52	49.1	0.99	1.67	4.73
Range	–3.3–18.4	41.6–50.8	128.9–386.5	5.21–5.90	22.0–52.0	0.36–1.84	41.0–53.3	0.41–1.54	0.91–2.85	2.35–17.4
1999, n = 14										
Median	8.06	45.1	125.3	5.79	29.1	0.30	51.0	0.88	1.19	3.30
Range	–0.83–14.3	42.7–46.9	110.7–187.0	5.29–6.00	25.7–37.1	0.11–0.71	44.7–55.0	0.30–1.78	0.87–2.04	1.92–4.84
2000, n = 12										
Median	11.19	41.1	150.0	5.83	16.3	0.08	50.3	0.78	0.78	3.18
Range	7.67–23.55	38.6–43.5	124.1–365.6	5.20–6.17	13.5–20.8	0–1.47	43.4–52.9	–0.04–1.08	0.52–2.33	2.38–7.67

© 2005 NRC Canada

Table 2 *(concluded).*

	ANC (μequiv.·L^{-1})	Ca^{2+} (μmol·L^{-1})	DOC (μmol·L^{-1})	pH	NO_3^- (μmol·L^{-1})	Al_{om} (μmol·L^{-1})	SO_4^{2-} (μmol·L^{-1})	Al_{im} (μmol·L^{-1})	Al_m (μmol·L^{-1})	Al_t (μmol·L^{-1})
TSI site: sc40										
1995, n = 4										
Median	1.2	45.9	136.9	5.47	15.9	0.85	57.8	0.88	1.68	5.56
Range	−2.5–11.9	39.1–47.5	110.7–179.7	5.30–5.91	10.5–24.8	0.59–1.02	40.9–62.6	0.46–1.14	1.19–2.10	5.15–6.44
1996, n = 8										
Median	−4.9	34.6	242.7	5.15	22.5	1.5	50.7	1.48	2.97	8.23
Range	−13.5–8.4	31.2–47.2	105.2–326.7	4.82–5.42	13.8–28.3	0.72–2.58	42.1–56.9	1.06–2.58	1.78–5.16	4.20–10.3
1997, n = 7										
Median	0.9	39.9	244.1	5.40	21.6	2.61	46.9	0.88	3.60	5.92
Range	−7.3–8.8	28.7–40.9	129.9–412.8	4.93–5.70	18.0–25.3	1.56–3.70	39.4–51.5	0.26–2.37	1.62–5.44	3.48–8.35
1998, n = 17										
Median	−2.9	35.5	209.1	5.30	13.0	0.85	48.5	1.28	2.09	5.63
Range	−10–3.5	32.3–37.9	20.7–566.5	4.92–5.62	6.8–22.0	0.42–3.18	37.8–54.0	0.83–1.96	1.41–4.75	3.30–12.5
1999, n = 9										
Median	−0.3	38.2	140.1	5.54	13.8	0.54	50.5	1.16	1.61	3.83
Range	−8.7–218.1	35.0–40.1	126.5–183.4	5.20–5.65	9.5–17.3	0.28–0.82	46.0–54.6	0.82–2.05	1.39–2.76	2.69–7.53
2000, n = 19										
Median	4.0	35.5	174.2	5.44	11.6	0.30	49.0	1.08	1.35	4.04
Range	−4.3–12.5	32.4–37.2	139.3–366.0	5.14–5.62	7.7–15.1	0–1.48	43.3–52.1	0.48–1.45	0.83–2.83	2.53–7.78
Reference site: cl25										
1995, n = 4										
Median	17.0	54.6	103.3	6.13	15.0	0.29	61.1	0.54	0.89	na
Range	10.1–34.4	52.5–56.6	56.3–107.2	5.94–6.46	11.1–21.9	0.22–0.78	60.9–61.9	0.46–0.70	0.70–1.34	na
1996, n = 5										
Median	11.6	47.6	96.9	5.91	16.2	0.50	57.1	0.73	1.20	11.02
Range	−6.5–17.2	43.5–51.0	80.6–252.9	4.93–6.07	14.1–35.5	0.29–1.84	43.8–58.4	0.57–2.83	0.86–4.67	na
1997, n = 5										
Median	10.9	44.3	113.7	5.91	19.5	1.38	53.8	0.35	1.75	8.12
Range	−5.4–20.0	33.4–46.0	102.5–173.8	5.17–6.29	17.1–35.9	1.22–2.17	43.7–54.1	−0.22–2.46	1.57–4.58	na
1998, n = 8										
Median	10.0	48.2	130.1	5.97	37.9	0.29	52.0	0.65	0.88	2.51
Range	2.5–14.1	40.9–53.0	93.4–187.7	5.50–6.19	23.4–48.5	0.12–0.64	49.2–53.3	0.15–1.13	0.72–1.58	1.80–4.03
1999, n = 9										
Median	12.5	49.3	104.9	6.12	36.1	0.04	51.4	0.69	0.69	2.22
Range	0.4–21.4	39.1–52.4	96.3–158.2	5.46–6.22	28.9–41.8	0–0.30	44.9–54.9	0–2.20	0.06–2.27	1.34–3.58
2000, n = 9										
Median	15.8	42.4	121.7	6.16	16.7	0	51.7	0.60	0.42	2.05
Range	8.0–26.7	38.7–45.0	107.1–153.0	5.95–6.33	14.2–20.9	0–0.03	49.5–54.0	0.42–0.83	0.14–0.77	1.56–3.24

Note: ANC, acid-neutralizing capacity; DOC, dissolved organic carbon; Al_{om}, organic monomeric aluminum; Al_{im}, inorganic monomeric aluminum; Al_m, total monomeric aluminum; Al_t, total dissolved aluminum; n, the number of samples analyzed; na, not applicable; TSI, timber-stand improvement.

© 2005 NRC Canada

Fig. 7. Brook trout (*Salvelinus fontinalis*) mortality observed during 30-day exposures at (*a*) dc57, (*b*) sc20, (*c*) sc40, and (*d*) cl25 during toxicity tests, spring 1995 (light dotted line), 1996 (medium dashed line), 1997 (light dash-dotted line), 1998 (thick solid line), 1999 (thick dash-dotted line), and 2000 (thick dashed line).

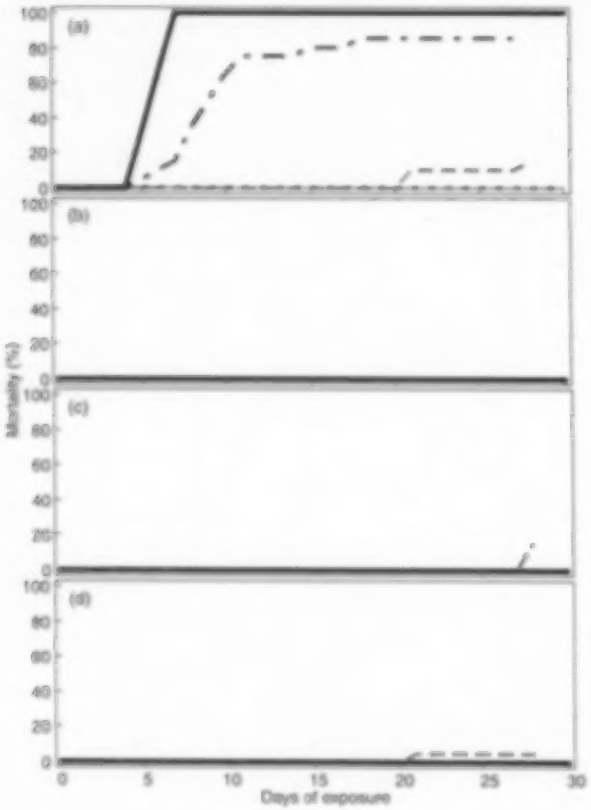

site (dc57) in 1998 and 1999 (Fig. 7). Trout mortality at dc57 ranged from 0% to 15% before the clear-cut (spring 1995 and 1996) and during the first exposure period after the clear-cut (spring 1997). All (100%) caged brook trout died during the first 7 days of the spring 1998 test at dc57 and 85% died during 30 days of exposure in spring 1999. None (0%) died during the 30-day exposure in 2000. Bioassays were not conducted during fall high-flow periods at any site; however, chemistry data from dc57 (Fig. 2) strongly indicate that water toxicity and trout mortality rates in fall 1997 would have been greater than those observed during spring 1998. No precise tree harvest threshold for trout mortality could be defined from our results, but the 14% reduction in tree BA at the TSI site (sc40) caused no mortality, while the 73% reduction in tree BA produced 100% mortality at the clearcut site (dc57).

Increased trout mortality in acidified streams of the northeastern United States is generally induced by elevated Al_{im} concentrations or some combination of acid and Al_{im} toxicity (Baker et al. 1990; Baker and Christensen 1991). Previous studies of episodic acidification and toxicity in New York and Pennsylvania streams determined that mean or median Al_{im} or Al_i concentration, or a combined duration and Al_{im} concentration factor, consistently explained the greatest amount of variability in mortality of native brook trout (Gagen et al. 1993; Simonin et al. 1993; Baldigo and Murdoch 1997). Acid–Al_{im} episodes in the Neversink River basin were found to cause significant mortality in native brook trout when Al_{im} levels exceeded 0.200 mg·L^{-1} (7.4 μmol·L^{-1}) for 2 or more days and that several constituents, including pH, DOC, Ca^{2+}, and Cl^-, were also significantly correlated with brook trout mortality (Baldigo and Murdoch 1997). A concurrent study in several acidic streams of Pennsylvania found that ionoregulation of native brook trout failed, and mortality occurred, when Al_i concentrations reached 0.2–0.3 mg·L^{-1} (7.4–11.1 μmol·L^{-1}) and exposure durations were longer than 1.5 days; more than 90% of Al_i was typically in the reactive inorganic form (Gagen and Sharpe 1987*a*, 1987*b*). A third concurrent investigation in four streams of the western Adirondack Mountains of New York found that an Al_{im} concentration of 0.1 mg·L^{-1} (3.7 μmol·L^{-1}) was the threshold for mortality of native brook trout during acid–Al_{im} episodes (Simonin et al. 1993). Other field and laboratory studies documented significant mortality of native and hatchery-raised brook trout when concentrations of Al_{im} and (or) Al_i exceed either 0.200 or 0.300 mg·L^{-1} under low Ca (<2.0 mg·L^{-1}), DOC (<2.0 mg·L^{-1}), and pH (4.4–5.2) conditions (Baker et al. 1990; Van Sickle et al. 1996). These findings demonstrate that Al_{im} can be acutely toxic to juvenile brook trout in waters of the northeastern United States when concentrations reach 3.7–7.4 μmol·L^{-1}.

Fig. 8. Estimated hourly (*a*) pH and (*b*) inorganic monomeric aluminum (Al_{im}) concentrations at dc57 during 30-day brook trout (*Salvelinus fontinalis*) exposure periods, spring 1995 (light dotted line), 1996 (medium dashed line), 1997 (light dash-dotted line), 1998 (thick solid line), 1999 (thin solid line), and 2000 (thick dashed line).

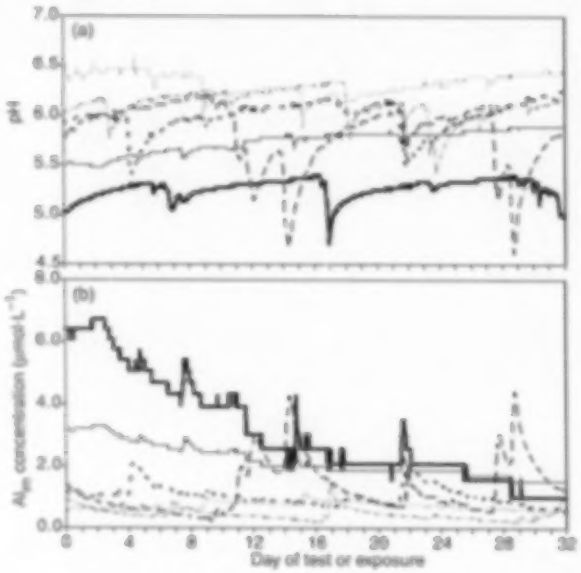

© 2005 NRC Canada

Estimates of continuous (hourly) pH and Al_{im} data (Fig. 8) and from samples collected during the 30-day exposure periods each year (Table 2) at dc57 confirm that the clear-cut affects water chemistry and indicate that the toxic Al_{im} threshold may be somewhat lower for hatchery brook trout used in the present investigation than for native brook trout used in other studies. Although estimated Al_{im} records are somewhat subdued, they depict concentrations well above 3.7 $\mu mol \cdot L^{-1}$ during the first 7 days during the 1998 tests where all trout died, levels near 3.7 $\mu mol \cdot L^{-1}$ for several days in 1999 where 85% died, and short excursions in excess of 3.7 $\mu mol \cdot L^{-1}$ in 1996 where 15% died (Fig. 8*b*). Few or no trout died during the tests done in 1995, 1997, and 2000 where Al_{im} concentrations did not exceed 3.0 $\mu mol \cdot L^{-1}$. Data from samples collected during test periods show that Al_{im} concentrations at the clearcut site did not surpass 3.9 $\mu mol \cdot L^{-1}$ during exposure periods in 1995, 1997, and 2000 but reached a maximum of 13.9 $\mu mol \cdot L^{-1}$ during the 1998 test, 5.9 $\mu mol \cdot L^{-1}$ during the 1999 test, and 3.9 $\mu mol \cdot L^{-1}$ during the 1996 test (Table 2). Thus, the high rates of mortality during the springs of 1998 and 1999 could be attributable to Al_{im} concentrations that exceeded brook trout thresholds for survival that range near 3.7 $\mu mol \cdot L^{-1}$. The death of all brook trout at the clearcut site during the first 7 days of the 1998 test was attributed to persistent acute toxicity, possibly intensified by a storm flow that occurred shortly before the test began. Maximum concentrations of Al_{im} at the other three sites did not exceed 2.9 $\mu mol \cdot L^{-1}$ during any 30-day test period or at the clearcut site during 1995 and 2000 (Table 2). The low level of trout mortality (15%) at the clearcut site (dc57) during 1996 was possibly related to two or three consecutive high flows that produced strong acidification (minimum pH 4.8) along with the highest Al_{im} concentration (5.09 $\mu mol \cdot L^{-1}$) observed at any of the sites before tree harvests. Thus, stream water concentrations of Al_{im} may have approached and surpassed thresholds toxic to brook trout. The low levels of brook trout mortality during spring 1996 at the TSI (15%) and reference (5%) sites, however, do not appear to be related to high Al_{im} concentrations.

The increase in Al_{im} concentration and mortality of brook trout at the clearcut site after the harvest appear to have been caused by decreases in N uptake by vegetation and increased nitrification, NO_3^-, and acidity in soil and surface waters throughout affected parts of the subbasin (Burns and Murdoch 2005). These changes, in turn, can increase mineral-Al solubility in affected soils and consequently elevate Al_{im} concentrations in receiving streams. An analysis of Catskill stream chemistry data through a simple chemistry equilibrium model, ALCHEMI (Schecher and Driscoll 1987), indicates that Al concentrations are consistent with control by an aluminum hydroxide solid phase similar to gibbsite, $Al(OH)_3$. Water pH controls the dissolution of the aluminum hydroxide solid and, therefore, Al speciation and Al_{im} concentrations (Driscoll 1985). Dissolution of gibbsite and the aluminum hydroxide solid increases at pH levels above and below 6.0; thus, decreases in water pH below 6.0 typically cause the concentration of inorganic Al species to increase (Driscoll 1985). The high rates of brook trout mortality in waters of the clearcut watershed, therefore, can be attributed to sequential alterations in normal hydrogeochemical processes that occurred as a result of tree harvest. The low rates of trout mortality at the TSI (sc40) and confluence (sc20) sites after removal of 5% and 14% of tree biomass in their respective subbasins indicate that these levels of biomass removal were not sufficient to strongly affect Al_{im} mobilization and produce water toxicity.

Brook trout are relatively tolerant of acidic conditions compared with many other stream-dwelling fish species (Baker and Christensen 1991). Several studies in New York and Pennsylvania streams have demonstrated that slimy sculpin (*Cottus cognatus*), mottled sculpin (*Cottus bairdi*), and blacknose dace (*Rhinichthys atratulus*), species that coinhabit small streams with brook trout, almost always experienced higher levels of mortality than juvenile brook trout when exposed to toxic acid–Al_{im} conditions during in situ bioassays (Johnson et al. 1987; Gagen et al. 1993; Simonin et al. 1993). This is corroborated by fish species distributions throughout the upper Neversink River basin (Baldigo and Lawrence 2001). These authors found that no fish species occurred in the most toxic headwater reaches and brook trout alone extended farthest into headwater reaches with very low pH and high Al_{im} concentrations; additional fish species accrued in community assemblages farther downstream as pH increased and Al_{im} decreased. The sequence of community additions could be predicted from species acid–Al_{im} tolerance levels derived from in situ bioassays: slimy sculpin were the next most tolerant species and added first followed by brown trout (*Salmo trutta*), longnose dace (*Rhinichthys cataractae*), blacknose dace, and Atlantic salmon (*Salmo salar*) (Baldigo and Lawrence 2001). Although no other fish species were observed in the Shelter Creek study reaches, the acutely toxic conditions after the clear-cut in Dry Creek would probably have killed all other resident fish species if any had been present. Thus, the brook trout mortality reported herein may underestimate the potential implications of acidification induced by the clearcut for other fish species. The likelihood that local clear-cutting harvests across other parts of eastern North America could adversely affect resident fish species and fish communities cannot be determined from our results, but may be substantial, considering the tolerance of brook trout to Al_{im} and acidity and the extent of tree harvests within high-elevation watersheds containing small headwater streams.

In summary, the combined effects of clear-cut harvest and acid deposition on water quality of small streams in the Catskill Mountain region can produce severe stream acidification and conditions that are acutely toxic to juvenile brook trout. Clear-cutting may not be the universal logging practice in the region, but our results indicate that it nevertheless can adversely affect the chemistry of circumneutral and acidified streams in the Catskill region. Partial or TSI harvests in subbasins with few acid-sensitive streams would probably not adversely affect surface-water chemistry or harm resident brook trout populations if the harvests were limited to the extent and intensity applied in this study. Populations of other acid-sensitive fish species and of entire aquatic ecosystems are more susceptible than brook trout to the effects of episodic acidification and thus to any practice that could increase the magnitude, duration, or frequency of acid–Al_{im} episodes in poorly buffered streams. Therefore, decisions as to the type, extent, and intensity of timber harvests in some watersheds may warrant consideration of the status of soil

© 2005 NRC Canada

acidity, the susceptibility of stream waters to acidification, and the sensitivity of resident biota to acid–Al_{in} episodes. The forest harvest thresholds that adversely affect survival of brook trout and other fish species in acidified streams of the Catskill Mountain region and other parts of eastern North America remain to be defined through additional research.

Acknowledgments

The authors thank Deborah Horan-Ross, Tricia Lincoln, Thomas Suleski, and Alton Anderson of the US Geological Survey for technical support; Steve Smith, Anne Gallagher, and Anne Finch of the US Geological Survey for technical and editorial reviews of the manuscript; and the Frost Valley YMCA for access to streams on their property. This research was cooperatively funded by the New York City Department of Environmental Protection and the US Geological Survey.

References

Baker, J.P., and Christensen, S.W. 1991. Effects of acidification on biological communities in aquatic ecosystems. *In* Acidic deposition and aquatic ecosystems. *Edited by* D.F. Charles. Springer-Verlag New York Inc., New York. pp. 83–106.

Baker, J.P., and Gallagher, J. 1990. Fish communities in Adirondack lakes. *In* Adirondack lakes survey: an interpretive analysis of fish communities and water chemistry, 1984–87. *Edited by* J.P.B.A.S.A. Gherini. Adirondack Lakes Survey Corporation, Ray Brook, N.Y. pp. 3.1–3.150.

Baker, J.P., Bernard, D.P., Christensen, S.W., Sale, M.J., Freda, J., Heltcher, K., Marmorek, D., Rowe, L., Scanlon, P., Suter, G., Warren-Hicks, W., and Welbourn, P. (*Editors*). 1990. Biological effects of changes in surface water acid-base chemistry. NAPAP Rep. No. 13. National Acid Precipitation Assessment Program, Oak Ridge, Tenn.

Baker, J.P., Warren-Hicks, W., Gallagher, J., and Christensen, S.W. 1993. Fish population losses from Adirondack lakes: the role of surface water acidity and acidification. Water Resour. Res. **29**: 861–874.

Baldigo, B.P., and Lawrence, G.B. 2000. Composition of fish communities in relation to stream acidification and habitat in the Neversink River, New York. Trans. Am. Fish. Soc. **129**: 60–76.

Baldigo, B.P., and Lawrence, G.B. 2001. Effects of stream acidification and habitat on fish populations of a North American river. Aquat. Sci. **63**: 196–222.

Baldigo, B.P., and Murdoch, P.S. 1997. Effect of stream acidification and inorganic aluminum on mortality of brook trout (*Salvelinus fontinalis*) in the Catskill Mountains, New York. Can. J. Fish. Aquat. Sci. **54**: 603–615.

Burns, D.A., and Murdoch, P.S. 2005. Effects of a clearcut on the net rates of nitrification and N mineralization in a northern hardwood forest, Catskill Mountains, New York, USA. Biogeochemistry. In press.

Burns, D.A., Karouna, N.K., and Murdoch, P.S. 1997. Effects of forest harvesting on nitrogen-cycling processes in headwaters of the Neversink River of New York. US Geological Survey, Troy, N.Y. FS-243-96.

Butler, T.J., Likens, G.E., and Stunder, B.J.B. 2001. Regional-scale impacts of Phase I of the Clean Air Act Amendments in the USA: the relation between emissions and concentrations, both wet and dry. Atmos. Environ. **35**: 1015–1028.

Buttner, P.J.R. 1977. Physical stratigraphy, sedimentology, and environmental geology of the Upper Devonian stream deposits of the Catskill Mountains of eastern New York State. *In* Guidebook to field excursions. *Edited by* P.C. Wilson. 49th Annual Meeting, New York State Geological Association, Trip A-7. New York State Geological Association, Syracuse, N.Y. pp. 1–29.

Colquhoun, J.R., Symula, J., Pfeiffer, M., and Feuer, J. 1981. Preliminary report of stream sampling for acidification studies — 1980. New York State Department of Environmental Conservation, Albany, N.Y.

Dahlgren, R.A., and Driscoll, C.T. 1994. The effects of whole-tree clear-cutting on soil processes at the Hubbard Brook Experimental Forest, New Hampshire, USA. Plant Soil, **158**: 239–262.

Driscoll, C.T. 1985. Aluminum in acidic surface waters: chemistry, transport, and effects. Environ. Health Perspect. **63**: 93–104.

Driscoll, C.T., Driscoll, K.M., Roy, K.M., and Mitchell, M.J. 2003. Chemical response of lakes in the Adirondack region of New York to declines in acidic deposition. Environ. Sci. Technol. **37**: 2036–2042.

Firda, G.D., Lumia, R., Murray, P.M., and Freeman, W.O. 1995. Water resources data, New York, water year 1994. US Geological Survey, Albany, N.Y. Annual USGS-WRD-NY-94-1.

Gagen, C.J., and Sharpe, W.E. 1987*a*. Net sodium loss and mortality of three salmonid species exposed to a stream acidified by atmospheric deposition. Bull. Environ. Contam. Toxicol. **39**: 7–14.

Gagen, C.J., and Sharpe, W.E. 1987*b*. Influence of acid runoff episodes on survival and net sodium balance of brook trout (*Salvelinus fontinalis*) confined in a mountain stream. *In* ecophysiology of acid stress in aquatic organisms. *Edited by* H. Witters and O. Vanderborght. Societe Royale Zoologique de Belgique, Antwerp, Belgium. pp. 219–230.

Gagen, C.J., Sharpe, W.E., and Carline, R.F. 1993. Mortality of brook trout, mottled sculpins, and slimy sculpins during acidic episodes. Trans. Am. Fish. Soc. **122**: 616–628.

Haines, T.A., and Baker, J.P. 1986. Evidence of fish population responses to acidification in the eastern United States. Water Air Soil Pollut. **31**: 605–629.

Johnson, D.W., Simonin, H.A., Colquhoun, J.R., and Flack, F.M. 1987. In situ toxicity tests of fishes in acid waters. Biogeochemistry, **3**: 181–208.

Lawrence, G.B., Lincoln, T., Horan-Ross, D.A., Olson, M.L., and Waldron, L.A. 1995. Analytical methods of the U.S. Geological Survey's New York District water-analysis laboratory. Open-File 95-416. US Geological Survey, Troy, N.Y.

Likens, G.E., Bormann, F.H., Johnson, N.M., Fisher, D.W., and Pierce, R.S. 1970. Effects of forest cutting and herbicide treatment on nutrient budgets in the Hubbard Brook watershed-ecosystem. Ecol. Monogr. **40**: 23–47.

Lincoln, T.A., Horan-Ross, D.A., Olson, M.L., and Lawrence, G.B. 1996. Quality-assurance data for routine water analyses by the US Geological Survey Laboratory in Troy, New York, May 1991 – June 1993. DOI/US Geological Survey WRD, Troy, N.Y. Open-File Rep. 96-167.

Lynch, J.A., Bowersox, V.C., and Grimm, J.W. 2000. Changes in sulfate deposition in eastern USA following implementation of Phase I of Title IV of the Clean Air Act Amendments of 1990. Atmos. Environ. **34**: 1665–1680.

Martin, C.W., Driscoll, C.T., and Fahey, T.J. 2000. Changes in streamwater chemistry after 20 years from forested watersheds in New Hampshire, USA. Can. J. For. Res. **30**: 1206–1213.

Mitchell, M.J., Driscoll, C.T., Kahl, J.S., Likens, G.E., Murdoch, P.S., and Pardo, L.H. 1996. Climatic control of nitrate loss from

© 2005 NRC Canada

forested watersheds in the northeast United States. Environ. Sci. Technol. **30**: 2609–2612.

Murdoch, P.S., and Stoddard, J.L. 1992. The role of nitrate in the acidification of streams in the Catskill Mountains of New York. Water Resour. Res. **28**:2707–2720.

Murdoch, P.S., and Stoddard, J.L. 1993. Chemical characteristics and temporal trends in eight streams of the Catskill Mountains, New York. Water Air Soil Pollut. **67**: 367–395.

Murdoch, P.S., Burns, D.A., and Lawrence, G.B. 1998. Relation of climate change to the acidification of surface waters by nitrogen deposition. Environ. Sci. Technol. **32**: 1642–1647.

National Oceanic and Atmospheric Administration. 1990. NOAA National Climate Data Center, 1961–90 climatological data — annual summary New York. Annual various, National Oceanographic and Atmospheric Administration, National Climatic Data Center, Asheville, N.C.

Rantz, S.E. 1983. Measurement and computation of streamflow. Vol. 1. Measurement of stage and discharge. Water Supply Pap. 2175. US Geological Survey, Albany, N.Y.

Rich, J.L. 1934. Glacial geology of the Catskills. New York State Mus. Bull. 299.

Schecher, W.D., and Driscoll, C.T. 1987. An evaluation of uncertainty associated with aluminum equilibrium calculations. Water Resour. Res. **23**: 525–534.

Simonin, H.A., Kretser, W.A., Bath, D.W., Olson, M., and Gallagher, J. 1993. In situ bioassays of brook trout (*Salvelinus fontinalis*) and blacknose dace (*Rhinichthys atratulus*) in Adirondack streams affected by episodic acidification. Can. J. Fish. Aquat. Sci. **50**: 902–912.

Stoddard, J.L., Jefferies, D.S., Lukewille, A., Clair, T.A., Dillon, P.J., Driscoll, C.T., Forsius, M., Johannessen, M., Kahl, J.S., Kellogg, J.H., Kemp, A., Mannio, J., Monteith, D.T., Murdoch, P.S., Patrick, S., Rebsdorf, A., Skjelkvale, B.L., Stainton, M.P., Traaen, T., van Dam, H., Webster, K.E., Wieting, J., and Wilander, A. 1999. Regional trends in aquatic recovery from acidification in North America and Europe. Nature (Lond.), **401**: 575–578.

Stoddard, J.L., Kahl, J.S., Deviney, F.A., DeWalle, D.R., Driscoll, C.T., Herlihy, A.T., Kellogg, J.H., Murdoch, P.S., Webb, J.R., and Webster, K.E. 2003. Response of surface water chemistry to the Clean Air Act Amendments of 1990. US Environmental Protection Agency, Research Triangle Park, N.C. EPA 620/R-03/001.

Swank, W.T., and Waide, J.B. 1988. Characterization of baseline precipitation and stream chemistry and nutrient budgets for control watersheds. Forest hydrology and ecology at Coweeta. Ecol. Stud. **66**: 57–79.

Tornes, L.A. 1979. Soil survey of Ulster County, New York. US Department of Agriculture, Soil Conservation Service, Washington, D.C.

Van Sickle, J., Baker, J.P., Simonin, H.A., Baldigo, B.P., Kretser, W.A., and Sharpe, W.E. 1996. Episodic acidification of small streams in the northeastern United States: fish mortality in field bioassays. Ecol. Appl. **6**: 408–421.

Vitousek, P.M. 1981. Clear-cutting and the nitrogen cycle. Ecol. Bull. (Stockholm), **33**: 631–642.

Welsh, D.L., Burns, D.A., and Murdoch, P.S. 2004. Processes affecting the response of sulfate concentrations to clearcutting in a northern hardwood forest, Catskill Mountains, New York, USA. Biogeochemistry, **68**: 337–354.

© 2005 NRC Canada

Relating plaice (*Pleuronectes platessa*) recruitment to deteriorating habitat quality: effects of macroalgal blooms in coastal nursery grounds

Leif Pihl, Johan Modin, and Håkan Wennhage

Abstract: Concentration of juveniles of marine fishes in nurseries may act as a bottleneck during the life cycle, where quantity and quality of nurseries determine population size. Macroalgal blooms have become a common phenomenon in eutrophic shallow waters worldwide, and matforming algae may now cover many essential nursery habitats. In this investigation, the aim was to assess the quantitative effect of algal mats on the recruitment of plaice (*Pleuronectes platessa*) from nurseries in the Swedish Skagerrak archipelago. A model was constructed using data on nursery size, settling density, and mortality of plaice combined with data on algal distribution. Recruitment of 0-group plaice from nurseries could be reduced by 30%–40% due to algae. The largest negative effect occurred during high settlement, reducing the important influence of strong year classes on stock size. The model predicted a reduction of juveniles due to algae of 45–46 × 10^5 individuals at high settlement. This amounts to 68% of the output at medium settlement and equals the amount of plaice produced during 5 years of low settlement. Up to 75% of the total reduction could occur in one quarter of the study area. With limiting resources, management actions should not be generally applied but rather be concentrated to optimize the cost-benefit of measures taken.

Résumé : La concentration des jeunes poissons marins dans les nurseries peut agir comme un goulet dans les cycles biologiques au point où la qualité et la quantité des nurseries déterminent la taille des populations. Les proliférations de macro-algues sont devenues courantes dans les eaux eutrophes peu profondes à l'échelle globale et les tapis d'algues peuvent maintenant couvrir plusieurs habitats essentiels dans les nurseries. L'objectif de notre étude est d'évaluer les effets quantitatifs des tapis d'algues sur le recrutement de la plie (*Pleuronectes platessa*) dans des nurseries de l'archipel suédois de Skaggerrak. Notre modèle incorpore des données sur la taille des nurseries, le taux de colonisation et la mortalité de la plie et les combine à des données sur la répartition des algues. La présence d'algues dans les nurseries peut réduire de 30–40 % le recrutement des plies d'âge 0. L'effet négatif le plus significatif se produit lors des périodes de forte colonisation des plies, ce qui réduit l'influence considérable des cohortes annuelles fortes sur la taille des stocks. Le modèle prédit une réduction de 45–46 × 10^5 jeunes plies à cause des algues lors de colonisations importantes. Cela représente 68 % de la production lors de colonisations moyennes et l ensemble des plies produites pendant cinq ans de colonisations faibles. Jusqu'à 75 % de la réduction pourrait se produire dans un quart de la zone d'étude. Étant donné les ressources limitées, les actions d'aménagement ne devraient pas être appliquées de façon générale, mais plutôt être concentrées de manière à optimiser les coûts et les bénéfices des gestes posés.

[Traduit par la Rédaction]

Introduction

The importance of habitat-related fisheries management for the long-term conservation of aquatic resources has recently received increasing attention. It has been recognized that marine fish species commonly are dependent on a number of different habitats during their life cycle, sometimes referred to as "essential fish habitats" in the literature (e.g., Stoner et al. 2001). The degradation and loss of any of these essential fish habitats, including habitat fragmentation, may accordingly pose a threat to the sustainability and productivity of marine fish populations (Peterson 2003). Many marine fish species utilize shallow coastal areas during the early juvenile stage, and these nursery grounds commonly only make up a small fraction of the species' entire spatial distribution. The dependency on nursery grounds varies among fish species, but there is indirect evidence that the size of some fish populations using coastal nurseries is related to the geographical extension (quantity) of the nursery grounds. It is known, for example, that for different populations of flatfish, there is a close relationship between recruitment and the spatial extent of the nursery grounds (Rijnsdorp et al. 1992). Degradation or alteration of these nursery grounds, affecting habitat quality, may therefore have profound effects on the recruitment and persistence of the fish populations. Further, it has been noted that variability in recruitment is related to the extent to which fish species are

Received 4 March 2004. Accepted 15 November 2004. Published on the NRC Research Press Web site at http://cjfas.nrc.ca on 31 May 2005.
J18011

L. Pihl,[1] J. Modin, and H. Wennhage. Department of Marine Ecology, Göteborg University, Kristineberg Marine Research Station, 450 34 Fiskebäckskil, Sweden.

[1]Corresponding author (e-mail: l.pihl@kmf.gu.se).

 doi: 10.1139/F05-023 © 2005 NRC Canada

Table 1. Cover of algal mats (% of sediment surface) and sizes and densities of plaice (*Pleuronectes platessa*) in experimental and field investigations.

	Algal cover (%)	Plaice size class (mm)	Density (individuals·m^{-2})		Reduction in plaice density (%)	Reference
			Algae	No algae		
Experimental	50	11–15	2.60	6.40	60	Wennhage and Pihl 1994
	80	11–15	1.80	7.20	75	Wennhage and Pihl 1994
	70	16–26	0.16	0.84	81	Wennhage and Pihl 1994
	70	26–52	0.50	0.50	0	Wennhage and Pihl 1994
Field	50	16–38	0.10	0.94	89	Pihl and van der Veer 1992
	80	17–34	1.20	17.00	93	Wennhage 1999
	40	14–36	0.10	0.48	79	Svenson and Pihl 2001

Note: Reduction in plaice density is calculated as the difference in density between vegetation-free and vegetation-covered sediment.

concentrated during the juvenile stage, suggesting that density-dependent processes act in the nursery grounds (Beverton 1995). Changes in habitat quality would therefore be predicted to modify such processes, e.g., through changes in food supply and refuge from predators. Thus, both the quantity and the quality of coastal nursery grounds may be of great importance for the population size and the persistence of these fish populations.

The propagation of North Sea plaice (*Pleuronectes platessa*) occurs on offshore spawning grounds in the North Sea and the Skagerrak–Kattegat area where pelagic eggs are released (Harding et al. 1978; Nielsen et al. 1998). After hatching, larvae are transported to the coastal zone by residual and wind-driven surface currents (Creutzberg et al. 1978; Pihl 1990), where they metamorphose into juvenile fish and settle on shallow (<4 m) soft bottoms during spring (van der Veer et al. 1990). The initial settlement density of plaice in a nursery is suggested to be directly related to larval supply, and variations in larval supply are therefore a major factor for the development of strong and weak year classes (van der Veer 1986; Wennhage and Pihl 2001). The first benthic stage is 11–16 mm in length (Riley 1966), and the fish grow about five times in length during their first summer, remaining stationary in shallow waters. The concentration of early juvenile plaice in defined nursery areas is considered to be a bottleneck during the recruitment to the adult stock (Beverton 1984, 1995; van der Veer 1986). Thus, the process of recruitment of plaice includes both a phase of larval input and settlement in potential coastal nurseries and a benthic juvenile phase where several factors (e.g., food availability, predation pressure, sediment structure, and water chemistry) related to habitat quality of the nursery grounds are important (Gibson 1994).

On the Swedish Skagerrak coast, plaice larvae settle during April and May on soft sediment bottoms within a water depth of less than 1 m, and the juvenile fish are stationary within this depth range until August (Pihl and Rosenberg 1982; Modin and Pihl 1994). Shallow soft-bottom areas occur in a heterogeneous pattern of embayments and open beaches in the archipelago, interrupted by rocky shores and deeper water. Historically, such areas were free of vegetation, with the exception of small patches of seagrass (*Zostera marina*) or brown algae (*Fucus* spp.) (Pihl 1986).

Over the last decades, increasing loads of nutrients have been discharged into the Skagerrak area. The input of nitrogen has been estimated to be about three times higher today then before 1950 (Rosenberg et al. 1990). One of the consequences of this enrichment to coastal waters is an increasing occurrence of filamentous green algae. Monitoring of vegetation in 10 shallow soft-bottom bays on the Swedish west coast has shown that the mean cover of filamentous algae increased from less than 3% between 1976 and 1978 to around 40% in the years 1992–1994 (Pihl et al. 1995). Green macroalgae, dominated by the genera *Cladophora* and *Enteromorpha*, start to grow in shallow bays during May and can develop into mats covering the sediment within a few weeks (Pihl et al. 1996). Algal cover may vary between bays and regions along the coast, but during summer (June–August), algal mats could cover half of the total surface area of shallow (0–1 m) soft-sediment bottoms (Pihl et al. 1999), areas that are potential nursery grounds for flatfish like plaice. The effects of such algal mats on the benthic and epibenthic community in the area have recently been investigated in several experimental and field studies (e.g., Isaksson et al. 1994; Norkko and Bonsdorff 1996; Österling and Pihl 2001).

Studies in the laboratory have shown that larvae and early benthic stages of plaice actively select a sediment substratum free of vegetation and that abundances are considerably reduced in experimental plots with sediment partly covered by algae (Table 1) (Wennhage and Pihl 1994). Other experiments have shown that metamorphosing larvae and juvenile plaice experience a significant reduction in survival and growth during short-term exposure to algal mats (Larson 1997). In field investigations, where abundance of plaice has been compared between vegetated and nonvegetated areas during the summer, the population density of plaice was observed to be reduced drastically in areas partly covered with algae (Table 1) (Pihl and van der Veer 1992; Wennhage 1999; Svenson and Pihl 2001). In the closely related European flounder (*Platichthys flesus*), the change in habitat complexity following the proliferation of algae was suggested to lower the foraging efficiency of the juveniles (Carl 2003). Thus, algal mats seem to have a strong influence on the behaviour, distribution, growth, and mortality of early juvenile stages of plaice and thereby drastically decrease the habitat quality of flatfish nurseries. Given that nursery grounds may act as a bottleneck in the life history of plaice, conservation of the nursery grounds should be of high priority to fisheries managers.

Environmental and fisheries management of coastal nursery grounds can be made more effective by including predictive models reflecting different management options. The

© 2005 NRC Canada

data available for these often elaborate models are, however, commonly limited in terms of the spatial and temporal scales over which the different patterns and processes have been studied. Field studies are commonly small scale, whereas management actions have to be implemented over much larger scales (see Ellis et al. 2000). Ecological theory has recognized that environmental impacts and ecological processes studied over small scales may not translate to predict patterns over larger spatial and temporal scales relevant to management (Wiens 1989; Levin 1992).

In this paper, we make use of comprehensive data sets on plaice density, mortality, and behaviour and information about the distribution of green macroalgae in coastal fish nurseries to predict the effects of matforming macroalgae on plaice recruitment. More specifically, the aim was to assess the quantitative effect of algal mats on the output of 0-group plaice from shallow nursery grounds at a regional level and for the entire Swedish Skagerrak archipelago. For this purpose, a numerical model was constructed using extensive data sets available at the spatial and temporal scales relevant for management to estimate the reduction in the output of 0-group juvenile plaice from shallow nursery grounds. The data used included distribution of nursery grounds, settlement densities of plaice, natural mortality of plaice, and cover of filamentous green algae in nursery grounds. The density of plaice was monitored in bays with and without green macroalgae during the course of a summer to verify assumptions of the model.

Materials and methods

Distribution of nursery grounds

On the Swedish Skagerrak coast, nursery grounds for plaice consist of shallow (0–1 m) embayments with a soft bottom substratum. Such embayments typically have a size of 2–20 ha and are separated from each other by rocky habitats and by deeper soft bottoms. Sediment structure varies from sand to sandy silt to silt, with an organic matter content of the sediment typically between 1% and 2% (Pihl 1986). An inventory of the Swedish Skagerrak coast, using aerial photography and sea charts, suggested that the total potential nursery area for plaice in the archipelago could be separated into 742 bays with a average size for each bay of approximately 9 ha (Pihl et al. 1999), resulting in a total area of 6700 ha. Further, the investigated area in the archipelago has been divided into four coastal regions based on a separation between drainage basins. Each region has an extension of about 50 km along the Skagerrak coast (Fig. 1), and the number of bays and the size of the nurseries are equally distributed between the four coastal regions (Table 2).

Settlement densities of plaice

Settlement densities of plaice were compared between 32 nursery grounds in the four coastal regions along the Swedish Skagerrak coast in 1998 (Pihl et al. 2000). The hierarchical sampling design of the study revealed that the spatial variation in settlement densities between nurseries was at the same level on different scales from 1 to 50 km, but higher variation was found on a larger interregional scale (Pihl et al. 2000). Thus, the local variation within a region of the archipelago appears to be random and unpredictable, and it could be assumed that the different nurseries in a region have equal potential for larval supply and settlement. Therefore, the average settlement densities within regions were used to characterize the supply of larvae to each of the four coastal regions.

Fig. 1. Map of the investigated area on the Swedish Skagerrak coast with the division in four regions indicated.

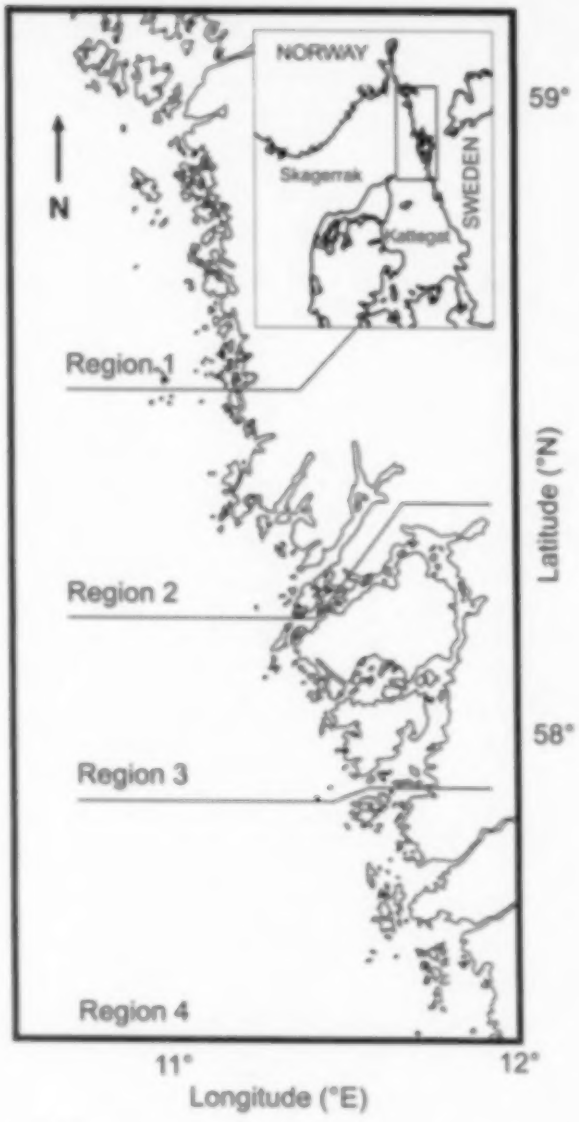

To get input data for the model on the initial densities of plaice in the nursery grounds, we also need information on the temporal variation. For one of the regions in this investigation (Region 2), such long-term data sets are available from two previous studies, where one nursery has been sampled over a 23-year period (L. Pihl, personal communication) and where four nurseries were sampled over a period of 5 years (Wennhage and Pihl 2001). Data from these two studies were used to estimate the average densities for plaice during low, medium, and high settlement.

© 2005 NRC Canada

Table 2. Input data for the model simulations arranged by three plaice (*Pleuronectes platessa*) recruitment scenarios.

Scenario	Region	Size of nursery area (10^4 m^2)	Mean algal cover (%)	Settlement densities of plaice (individuals·m^{-2})	Total number of settlers (individuals × 10^6)
High recruitment	1	1701	60	22.3	379.3
	2	1179	27	7.1	83.7
	3	2187	30	5.5	120.3
	4	1811	29	2.3	41.7
Medium recruitment	1	1701	60	6.9	117.4
	2	1179	27	2.2	25.9
	3	2187	30	1.7	37.2
	4	1811	29	0.71	12.9
Low recruitment	1	1701	60	0.69	11.7
	2	1179	27	0.22	2.6
	3	2187	30	0.17	3.7
	4	1811	29	0.07	1.3

Note: Regions defined in Fig. 1.

Natural mortality

The natural mortality of juvenile plaice in nurseries on the Swedish west coast has been investigated in several studies (van der Veer et al. 1990; Modin and Pihl 1994; Pihl et al. 2000) and has also been compared with that in other nursery areas in European waters (Beverton and Iles 1992). Information from Pihl et al. (2000) is used in the model in this study to describe mortality rates during the summer (June–August) at low, medium, and high initial settlement densities.

Distribution of algal mats

Occurrence and cover of filamentous green algal mats (genera *Cladophora* and *Enteromorpha*) were investigated by means of aerial photography in the four coastal regions of the study area during 1994–1996 (Pihl et al. 1999). Surveys were carried out in July and August each year and on each occasion, 125–285 randomly selected bays were sampled. Between 23 and 88 bays were photographed within each region each time. Photographs of each location were projected onto a digitizing table (Jandel Opaque Tablet) and the mean percent cover of filamentous algae was calculated for each region (Sigma Scan software). The average percent cover of algal mats over the sampling period (3 years, six occasions) was used in the model to describe the cover of vegetation in nurseries within each region.

The model

Postmetamorphic plaice in areas covered by algal mats can be expected to either stay among algae or to move to nonvegetated areas. These options were explored using a behavioural model to illustrate effects of algal mats on the survival of plaice in nurseries. The model assumes that mortality is exponential and consists of a density-independent and a density-dependent fraction. The two options (*i*) stay and (*ii*) move were contrasted. In the stay option, plaice that settled within vegetated areas would perish, while the remaining plaice in nonvegetated areas would be exposed to density-dependent and density-independent mortality. This scenario implies that the initial numbers of plaice are reduced relative to the area of the algal mats. The number of survivors after time t, N_t, was calculated as

$$N_t = O[N_0 - (N_0V)]e^{(-Mt)}$$

where O is the size of nursery area (square metres), N_0 is the settlement density (individuals per square metre), V is the proportional vegetation cover, and $e^{(-Mt)}$ is the proportional survival of individuals in nonvegetated areas; M is the density-dependent and density-independent mortality expressed as a function of settlement density N_0 (Pihl et al. 2000):

$$M = 0.008 + 0.0008N_0$$

In the move option, all plaice in areas with algal mats would move actively out of the vegetated areas and join plaice that settled in nonvegetated areas. Consequently, local density and density-dependent mortality would increase in nonvegetated areas:

$$N_t = ON_0e^{-M_c t}$$

where M_c is the total density-dependent and density-independent mortality expressed as a function of the concentration of plaice, $N_0/(1 - V)$, in nonalgae areas:

$$M_c = 0.008 + 0.0008[N_0/(1 - V)]$$

Both options in the model predict that the number of survivors will decrease with an increased proportion of vegetated areas. The stay option will result in a maximum of survivors at intermediate settlement densities, although this effect will be leveled out at high algal cover (Fig. 2*a*). The move option implies that the maximum number of survivors will be reached at progressively lower settlement densities with increasing cover of algae (Fig. 2*b*). The model was used to assess the spatial effect of algal mats on the survival of plaice during 90 days from the time of settlement until the time for emigration to deeper waters. Three scenarios were envisaged: low, medium, and high settlement of postmetamorphosed plaice. Input data to realize the model were derived from studies mentioned above (Table 2). The survival, expressed as number of survivors, within each of the four coastal regions of the investigated area was estimated for a base line option (without algae) and for two model options with algae (stay and move). The total number of settlers was calculated by multiplying mean settlement densities by the area of nursery grounds within each coastal region. Data on plaice density are shown in Table 2 for the three scenarios (high, medium, and low larval settlement) and the average

© 2005 NRC Canada

Fig. 2. Behavioural model: effects of percentage algal cover on survivors by density of plaice (*Pleuronectes platessa*) settlers assuming (*a*) a nonmigratory behaviour (stay option) or (*b*) a migratory behaviour (move option).

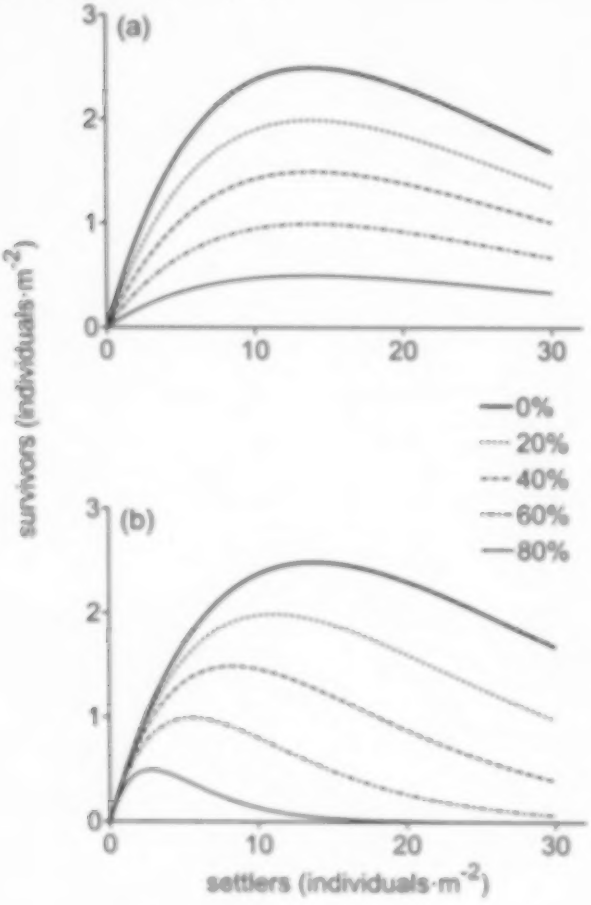

mean cover of filamentous algae within each coastal region used in the model.

Verification of the model

In 1998, six nursery grounds in Region 1 were sampled for plaice independently from the survey including 32 bays preformed that year. From previous monitoring in the area (L. Pihl, personal observation), algal mats were predicted to develop in three of the bays, whereas three bays should be free of vegetation. Region 1 was selected because of the high densities of juvenile plaice and high cover of algae in this region. Sampling was preformed shortly after plaice settlement and was repeated at approximately days 60 and 90 after settlement. Mat-forming filamentous macroalgae proliferated in two of the bays after plaice had settled (approximately day 30) and the other four bays remained unvegetated during the course of the summer. The two vegetated bays remained covered (70%–80%) with filamentous macroalgae beyond the last sampling in August. Plaice abundance was estimated quantitatively from 10 randomly allocated samples taken with a 1-m^2 drop-trap in each bay (methods in Pihl and Rosenberg (1982) and Modin and Pihl (1994)).

Results

Settlement densities of plaice

Densities of newly settled plaice varied from 0.2 to 74 individuals·m^{-2} among nursery bays, with an overall mean of 9.0 individuals·m^{-2}. Mean settlement densities in the four geographical regions were estimated at 22.3, 7.1, 5.5, and 2.3 individuals·m^{-2}, respectively (see Appendix A), with a gradual increase in density from the south (Region 4) to the north (Region 1). This pattern was confirmed in a similar study in the same area during 1999–2002, each year including 16 bays (H. Wennhage, unpublished data). The long-term data sets observed from Region 2 indicate that densities in 1998 were among the highest recorded (see Appendix A). Therefore, data from 1998 were used in the model to characterize high larval supply and settlement in nurseries in the four coastal regions. The two studies in Region 2 on temporal variation in plaice density showed that initial settling density fluctuated between 0.2 and 10.0 individuals·m^{-2} in the study with the longest duration (23 years) and between 0.4 and 6.1 individuals·m^{-2} in the other study (5 years). In the latter study, variations among the four locations were small. The average density of plaice in the two time series was calculated to be 2.2 and 2.0 individuals·m^{-2}, respectively (see Appendix A), and the value 2.2 individuals·m^{-2} from the longest time-series was used in the model to represent medium settlement density in Region 2. The lowest recorded density observed from the two time series (0.2 individual·m^{-2}) was used to characterize low settlement densities in Region 2. The proportional differences between regions, observed during the high settlement in 1998, was used to calculate medium and low settlement densities in Regions 1, 3, and 4. Calculated settlement densities in the four regions during the three scenarios are provided in Table 2.

Distribution of algal mats

The cover of filamentous green algae in nursery grounds was similar during the 3 years of investigation but differed among regions. On all six sampling occasions, algal mats had the largest distribution in Region 1 where on average, 60% of the total nursery area was covered by vegetation (Table 2). The average vegetation cover was approximately 30% in the other three regions. During the 3 years of investigation, mats of filamentous algae were estimated to cover between 30% and 50% of the total area of potential nursery grounds in the coastal zone of the Swedish Skagerrak.

Model results

The model simulated three scenarios: low, medium, and high settlement of juvenile plaice. The highest numbers of settlers were in the northern region (Region 1) for all scenarios, whereas the lowest numbers occurred in Region 4 (Table 2). The simulations showed that higher settlement densities generally resulted in a larger number of survivors at the end of the three summer months (Tables 2 and 3). When settlement was assumed to be low or medium, the base option (with no algae) predicted that the number of survivors was

© 2005 NRC Canada

Table 3. Predicted number of surviving plaice (*Pleuronectes platessa*) juveniles after 90 days per scenario and region for all options and the predicted additional reduction of survivors due to algal mats assuming migratory behaviour (move option) or nonmigratory behaviour (stay option).

			Move option		Stay option	
Scenario	Region	Base option, survivors (individuals × 10^6)	Survivors (individuals × 10^6)	Reduction (%)	Survivors (individuals × 10^6)	Reduction (%)
High recruitment	1	37.07	3.42	–91	14.92	–60
	2	24.44	20.17	–17	17.77	–27
	3	39.4	33.36	–15	27.74	–30
	4	17.18	16.03	–7	12.12	–29
	All	118.09	72.98	–38	72.55	–39
Medium recruitment	1	34.76	16.62	–52	13.99	–60
	2	10.78	10.15	–6	7.83	–27
	3	16.01	15.21	–5	11.27	–30
	4	5.95	5.82	–2	4.19	–30
	All	67.5	47.8	–29	37.28	–45
Low recruitment	1	5.44	5.05	–7	2.19	–60
	2	1.24	1.24	–1	0.9	–28
	3	1.79	1.78	–1	1.26	–30
	4	0.61	0.61	–1	0.43	–30
	All	9.08	8.68	–4	4.78	–47

Note: Regions defined in Fig. 1.

larger in the north (Region 1) compared with the south (Region 4). However, as the number of settlers increased, the proportional survival decreased in the base option due to density-dependent mortality, and during the scenario of high settlement densities, the largest number of survivors was observed in Region 3 (Table 3). The base option, i.e., no vegetation in the simulations, resulted in the largest numbers of survivors by all scenarios and regions, and occurrence of algal mats always resulted in lower survival. The additional reduction in survival, due to algae in the study area, was largest during the stay option and increased from 39% to 47% with decreasing settlement density (Table 3). During the move option, however, the highest reduction (38%) occurred during high settlement and decreased to 4% at low settlement density. At a regional scale, the simulations showed that migratory behaviour due to algal mats (move option) yielded a larger number of survivors in all but one case compared with a nonmigratory behaviour (stay option). High settlement in Region 1 resulted in fewer survivors for the migratory compared with nonmigratory behaviour (Table 3). As a consequence, during the high settlement scenario, the overall reduction of juvenile plaice in the whole investigated area was similar for the move and stay options (Table 3). The reduction of surviving plaice in the presence of algal mats compared with the base option was larger in the north (Region 1) than in the south (Region 4) (Table 3). Further, the model predicted that a migratory behaviour resulted in a higher proportional reduction of plaice with increasing settlement density, whereas the proportional reduction with a nonmigratory behaviour was not related to settlement densities. Therefore, when settlement was assumed to be large, the number of survivors in Region 1 was comparable with or lower than that in the other regions (Table 3). This was caused by the combined effect of density-dependent mortality and high algal cover in Region 1.

Verification of the model

Measured settlement densities were high and similar (8–19 individuals·m^{-2}) in May and June in the six nursery grounds investigated (Fig. 3). In the four bays with bare sand habitat, plaice densities were reduced to 3–5 individuals·m^{-2} at the end of the summer. However, in the two vegetated habitats, the density of plaice was below the detection level in August.

Discussion

Assumptions of the model

The data used to model the influence of macroalgae on the recruitment of plaice were derived from collections over large geographical areas and comprised long-term data series. We acknowledge that the data lack detailed information on the ecological processes in plaice nursery grounds, but by using this simple and robust model, general predictions can be made at the spatial and temporal scales relevant to management. The density-dependent mortality function used in the model was based on empirical data relating mortality to settlement densities in the field. Experimental data using the major predator *Crangon crangon* on newly settled plaice confirms that at least one predator has the capacity to regulate plaice abundance (Wennhage 2002). The numerical model presented two options. Under the first option, plaice juveniles were stationary and the algal-induced mortality over a 90-day period was 100% in areas covered with algae. Consequently, the quantity of nursery area is reduced by the area being covered by algae, whereas other areas are unaffected by the presence of algae. The field observations showed that plaice densities are below the detection level in August (approximately day 90) in areas that had been covered by algae during the summer. Under the assumption of plaice being stationary, it therefore seems reasonable to use 100% mortality among algae for the 90-day period.

© 2005 NRC Canada

Fig. 3. Density of 0-group plaice (*Pleuronectes platessa*) in six shallow bays within Region 1 in 1998. All bays were free of vegetation in May and early June. Four of the bays (open circles) remained vegetation free through the summer, but two bays (solid circles) were 70%–80% covered by filamentous green algae from mid-June through August.

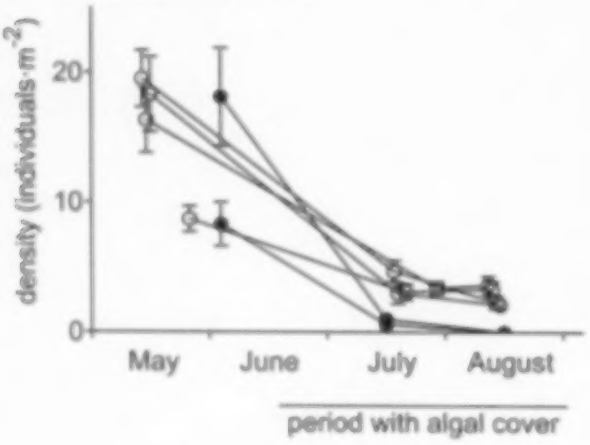

Under the second option, areas becoming covered with algae were instantly subjected to a 100% emigration of plaice. In each region, the settlement density in unvegetated areas would therefore increase in relation to the proportion of nursery area being covered by algae. Plaice were, however, not allowed to migrate among regions and the regions would therefore respond independently to the variation in algal cover and plaice settlement density. One important feature of the second option is that the relative importance of pre- and post-settlement regulation in plaice numbers affects the outcome. If larval supply were in excess in a nursery ground, the migration of plaice from the vegetated part would have no positive effects on the recruitment from the bay. The model used even suggests that the output of plaice from a nursery ground peaks at a settlement density of approximately 14 individuals·m^{-2} and is reduced at higher densities of plaice. Immigration of plaice from the area with algae would therefore be expected to have a negative effect on the output of plaice from the unvegetated part when there is a high natural density of plaice. Conversely, at low settlement densities, the immigration of plaice from areas with algae would only lead to a minor increase in density-dependent mortality and the recruitment from the whole nursery ground would almost remain unchanged despite the reduction in nursery ground surface area.

Comparison between options

The field observations showed that plaice disappeared in bays being covered by algae. This pattern could be caused by either emigration or mortality and both options find some support in the literature. Experimental studies have shown that juvenile plaice prefer bare sediment over filamentous algae, selecting the preferred habitat over small spatial scales (Wennhage and Pihl 1994), but have also demonstrated that the combined effects of hypoxia and exudates from algae may lead to plaice mortality (Larson 1997). Most likely, the two processes interact at different spatial scales to give the patterns observed in the field.

In the present study, regions were used as the spatial scale at which the model operated. The spatial resolution of the model was primarily set by the resolution of available data linking plaice abundance and algae cover. Given that the presence of filamentous algae can cause adverse conditions that may lead to mortality, plaice could be envisaged to make full use of their ability to migrate away from vegetated areas. In addition, plaice would undoubtedly be expected to be able to migrate faster than the rate at which algae proliferate. Wennhage and Pihl (1994) showed that juvenile plaice prefer open sand to algae and exhibit this habitat preference at the scale of bays. Soon after settlement, plaice are known to develop a tidally related migration pattern in tidal areas (Burrows et al. 1994) and a diurnal migration pattern in nontidal areas (Gibson et al. 1998). The examples of habitat selection and cyclic migration patterns given above strongly suggest that plaice can migrate within nursery grounds (i.e., bays). Other studies indicate that plaice are confined to their bay of settlement during the first summer (Pihl and Rosenberg 1982; Modin and Pihl 1994) and are absent from samples in deeper waters (Pihl 1989). The existing information consequently suggests that the second option would be most likely within bays.

The data used to establish the cover of algae in the four regions (Pihl et al. 1999) showed that only 7.9% of the bays had an algal cover exceeding 95% of the available nursery area. Plaice would generally have the opportunity to exercise their ability to migrate into bare sediment parts within bays. The first option could therefore be expected to be a poor representation of the mechanism causing algal induced mortality of plaice, except at higher algal cover where a larger proportion of bays would become completely covered with algae. The second option mimics the migration suggested to occur in the field, but at a regional scale instead of a bay scale. It will under- or overestimate the algal-induced mortality occurring at the bay scale depending on algal cover and settlement density of plaice but should give a reasonable average at the regional level.

Interactions between output of juvenile plaice and algal growth

Our model suggested that a considerable reduction could occur in the output of juvenile plaice from nursery grounds as a consequence of algal mats covering the sediment. However, the two options presented in the model gave somewhat contrasting results. During the scenario with low settlement densities of plaice, only a marginal effect (4% reduction) was predicted if the juvenile fish moved out of the vegetated parts, whereas almost half (47%) of the output was lost if they stayed among the algae. In the scenario with a medium larval supply to nurseries, the reduction in the output of juveniles increased to 29% when fish could move out of the vegetation and was similar (45%) under the option that fish stayed. During high settlement densities, the two options in the model predicted almost the same result, a reduction with 38% and 39% during the move option and stay option, respectively. It is most likely that both processes occur in nature, but laboratory experiments and field data mainly

© 2005 NRC Canada

supported the move option. If the juvenile plaice arrive to the nursery grounds before algal mats develop, the fish may be able to migrate out of the growing vegetation, but if algal mats already exist when the larvae are recruiting to the nurseries, larvae may be captured by the algae (Olafsson 1988) and the stay option may be of greater importance. However, with any combination of the two options, effects of algal mats on recruitment is likely to be less during years with low densities in nurseries. At medium and high larval settlement, reduction in the output of juvenile plaice from nurseries will increase and may reach 30%–40%. Thus, it can be concluded that the effect on recruitment will increase with increasing larval supply, and algal mats in the nurseries will severely reduce strong year classes. Our model predicts that the reduction in the output of juveniles due to algae will be 45×10^6 – 46×10^6 individuals at high settlement. Such a reduction amounts to 68% of the output at medium settlement and equals the amount of juvenile plaice produced during 5 years of low settlement.

It has since long been shown that year-class strength determines the size of the subsequent spawning stock (Hjort 1914). This truism is apparent in present-day fisheries where fish stocks have been overfished to the extent that the fisheries depend on a few younger age classes in the stock. A recent example is the Atlantic cod (*Gadus morhua*) fisheries in the North Sea, which are sustained only due to incoming year classes (International Council for the Exploration of the Sea 2002). Another example is the dramatic increase in cod biomass in the Baltic Sea during the mid-1980s, which was mainly caused by extremely large year classes in 1976, 1979, and 1980 (Cardinale and Arrhenius 2000). Although the variation in year-class strength of plaice stocks in the Skagerrak and Kattegat has been low during the last 20 years, occasional large year classes have contributed to temporary increases in adult biomass on the order of 100%–150% compared with the long-term average (International Council for the Exploration of the Sea 2002). It is obvious that strong year classes are important for the plaice fishery and will result in higher landings during several consecutive years. Therefore, a dampening of strong years classes as a consequence of decreasing habitat quality in nursery grounds when sediment becomes covered by algal mats will have an overall negative impact on the fishery.

Algal mats have also been reported to occur on the Danish coast of the Skagerrak–Kattegat since the early 1980s (Nielsen and Bagge 1985; Bagge and Nielsen 1988). Thus, a larger part of potential nursery grounds in the Skagerrak–Kattegat area is subjected to overgrowth of algal mats. Nursery areas can act as bottlenecks in fish species' life cycle. This is especially true for species like plaice, where early benthic stages are highly habitat specific and concentrate in restricted areas in a relatively short time (Beverton 1995). Further, as the stock size and extension of nursery areas of flatfish are suggested to be positively related (Rijnsdorp et al. 1992), the reduction in available nursery areas due to cover of algal mats will consequently impact the development of the stock. If the situation with algal mats prevails, it is most likely that the recruitment to the adult stock and the potential for fishery will be reduced to a lower level.

Management

Problems with eutrophication are seen in many coastal systems around the world. Blooms of toxic phytoplankton, proliferation of opportunistic macroalgae, and hypoxia in the bottom water are common, especially in enclosed and stratified coastal water receiving freshwater discharges (Baden et al. 1990). Measures are needed to reduce nutrient load to the coastal zone to prevent deterioration of the essential habitats for fish. Our study showed that algae were not evenly distributed along the coast, and settlement densities of plaice also exhibited a spatial variation. The northern region of the coast had larger areas covered by algal mats, and it was also in the northern region that the highest densities of newly settled plaice occurred. Consequently, in the northern region, the largest reduction in recruitment was seen, and from a management perspective, efforts to reduced algal mats should be concentrated to this region to achieve the highest cost-benefit effect. Thus, our model, by providing important information about the spatial and temporal variation in the recruitment of plaice and distribution of macroalgae, helps to focus the necessary measures on areas where the best result will be expected.

The model suggested that the adverse effects of macroalgal mats would be most pronounced during years with high larval supply. For species like plaice, where early benthic stages are highly habitat specific and concentrated in restricted areas, nursery areas can act as a bottleneck in the life cycle. It is obvious that strong year classes are important for the plaice fishery and will result in higher landings during several consecutive years. There is also a general concern that the slow recovery of overexploited fish stocks could be due to anthropogenically induced changes in the ecosystems. Macroalgal blooms would be expected to slow down the buildup of stock size when fishing pressure is released by preventing the formation of strong year classes. The status and conservation of plaice nursery grounds should therefore be included in risk assessments made to obtain a sustainable management of plaice stocks.

Acknowledgements

We thank Alf Norkko for giving valuable comments on this manuscript. Financial support for this study was supplied by the Swedish Research Council for Environment, Agriculture Sciences, and Spatial Planning, the Swedish Environmental Protection Agency, and the Water Quality Association of the Bohus Coast, Sweden, which is kindly acknowledged.

References

Baden, S.P., Loo, L.-O., Pihl, L., and Rosenberg, R. 1990. Effects of eutrophication on benthic communities including fish: Swedish west coast. Ambio, **19**: 113–122.

Bagge, O., and Nielsen, E. 1988. The change in abundance and growth of plaice and dab in subdivision 23, 1962–1985. ICES Bal/No. 27.

Beverton, R.J.H. 1984. Dynamics of single species. Group report. *In* Exploitation of marine communities. Dahlem Konferenzen. *Edited by* R.M. May. Springer-Verlag, Berlin. pp. 13–58.

Beverton, R.J.H. 1995. Spatial limitation of population size: the concentration hypothesis. Neth. J. Sea Res. **34**: 1–6.

© 2005 NRC Canada

Beverton, R.J.H., and Iles, T.C. 1992. Mortality rates of 0-group plaice (*Pleuronectes platessa* L.), dab (*Limanda limanda* L.) and turbot (*Scophthalmus maximus* L.) in European waters. II. Comparison of mortality rates and construction of life tables for 0-group plaice. Neth. J. Sea Res. **29**: 49–59.

Burrows, M.T., Gibson, R.N., Robb, L., and Comely, C.A. 1994. Temporal patterns of movement in juvenile flatfish and their predators: underwater television observations. J. Exp. Mar. Biol. Ecol. **177**: 251–268.

Cardinale, M., and Arrhenius, F. 2000. The influence of stock structure and environmental conditions on the recruitment process of Baltic cod estimated using a generalized additive model. Can. J. Fish. Aquat. Sci. **57**: 2402–2409.

Carl, J.D. 2003. Assessment of habitat quality for juvenile flounder (*Platichthys flesus* L.). Ph.D. thesis, University of Aarhus, Denmark.

Creutzberg, F., Eltink, A.T.G.W., and van Noort, G.J. 1978. The migration of plaice larvae *Pleuronectes platessa* into the western Wadden Sea. *In* Physiology and behaviour of marine organisms. *Edited by* D.S. McLusky and A.J. Berry. Pergamon Press, Oxford, England. pp. 243–251.

Ellis, J.I., Norkko, A., and Thrush, S.F. 2000. Broad-scale disturbance of intertidal and shallow sublittoral soft-sediment habitats: effects on the benthic macrofauna. J. Aquat. Ecosyst. Stress Recovery, **7**: 57–74.

Gibson, R.N. 1994. Impact of habitat quality and quantity on the recruitment of juvenile flatfishes. Neth. J. Sea Res. **32**: 191–206.

Gibson, R.N., Pihl, L., Burrows, M.T., Modin, J., Wennhage, H., and Nickell, L.A. 1998. Diel movements of juvenile plaice (*Pleuronectes platessa*) in relation to predators, competitors, food availability and abiotic factors on a microtidal nursery ground. Mar. Ecol. Prog. Ser. **165**: 145–159.

Harding, D., Nichols, J.H., and Tungate, D.S. 1978. The spawning of plaice (*Pleuronectes platessa* L.) in the southern North Sea and English Channel. Rapp. P.-V. Reun. Cons. Int. Explor. Mer, **172**: 102–113.

Hjort, J. 1914. Fluctuation in the great fisheries of northern Europe, reviewed in the light of biological research. Rapp. P.-V. Reun. Cons. Perm. Int. Explor. Mer, **20**: 1–228.

International Council for the Exploration of the Sea. 2002. Report of the ICES Advisory Committee on Fishery Management, 2002. ICES Coop. Res. Rep. 255.

Isaksson, I., Pihl, L., and van Montfrans, J. 1994. Eutrophication-related changes in macrovegetation and foraging of young cod (*Gadus morhua* L.): a mesocosm experiment. J. Exp. Mar. Biol. Ecol. **177**: 203–217.

Larson, F. 1997. Survival and growth of plaice (*Pleuronectes platessa*) larvae and juveniles in mats of *Enteromorpha* sp. The effects of algal exudates and nocturnal hypoxia. M.S. thesis, Department of Marine Ecology, Göteborg University, Fiskebäckskil, Sweden.

Levin, S.A. 1992. The problem of pattern and scale in ecology. Ecology, **73**: 1943–1967.

Modin, J., and Pihl, L. 1994. Differences in growth and mortality of juvenile plaice, *Pleuronectes platessa* L., following normal and extremely high settlement. Neth. J. Sea Res. **32**: 331–341.

Nielsen, E., and Bagge, O. 1985. Preliminary investigations on 0-group plaice surveys in the Kattegat in the period 1950–1984. ICES G:19. Dem. Fish Com.

Nielsen, E., Bagge, O., and MacKenzie, B.R. 1998. Wind-induced transport of plaice (*Pleuronectes platessa*) early life history stages in the Skagerrak–Kattegat. J. Sea. Res. **39**: 11–28.

Norkko, A., and Bonsdorff, E. 1996. Population response of coastal zoobenthos to stress induced by drifting algal mats. Mar. Ecol. Prog. Ser. **140**: 141–151.

Olafsson, E.B. 1988. Inhibition of larval settlement to soft bottom benthic community by drifting algal mats — an experimental test. Mar. Biol. **97**: 571–574.

Österling, M., and Pihl, L. 2001. Effects of filamentous green algal mats on benthic macrofaunal functional feeding groups. J. Exp. Mar. Biol. Ecol. **263**: 159–183.

Peterson, M.S. 2003. A conceptual view of environment–habitat–production linkages in tidal river estuaries. Rev. Fish. Sci. **11**: 291–313.

Pihl, L. 1986. Exposure, vegetation and sediment as primary factors for mobile epibenthic faunal community structure and production in shallow marine soft bottom areas. Neth. J. Sea Res. **20**: 75–83.

Pihl, L. 1989. Abundance, biomass and production of juvenile flatfish in southeastern Kattegat. Neth. J. Sea Res. **24**: 69–81.

Pihl, L. 1990. Year-class strength regulation in plaice (*Pleuronectes platessa* L.) on the Swedish west coast. Hydrobiologia, **195**: 79–88.

Pihl, L., and Rosenberg, R. 1982. Production, abundance and biomass of mobile epibenthic marine fauna in shallow waters, western Sweden. J. Exp. Mar. Biol. Ecol. **57**: 273–301.

Pihl, L., and van der Veer, H.W. 1992. Importance of exposure and habitat structure for the population density of 0-group plaice, *Pleuronectes platessa* L., in coastal nursery areas. Neth. J. Sea Res. **29**: 145–152.

Pihl, L., Isaksson, I., Wennhage, H., and Moksnes, P-O. 1995. Recent increase of filamentous algae in shallow Swedish bays: effects on the community structure of epibenthic fauna and fish. Neth. J. Aquat. Ecol. **29**: 349–358.

Pihl, L., Magnusson, G., Isaksson, I., and Wallentinus, I. 1996. Distribution and growth dynamic of ephemeral macroalgae in shallow bays on the Swedish west coast. J. Sea Res. **35**: 169–180.

Pihl, L., Svensson, A., Moksnes, P-O., and Wennhage, H. 1999. Distribution of green algal mats throughout shallow soft bottoms of the Swedish archipelago in relation to nutrient loads and wave exposure. J. Sea Res. **41**: 281–294.

Pihl, L., Modin, J., and Wennhage, H. 2000. Spatial distribution patterns of newly settled plaice (*Pleuronectes platessa* L.) along the Swedish Skagerrak archipelago. J. Sea Res. **44**: 65–80.

Rijnsdorp, A.D., Beek, F.A., Flatman, S., Millner, R.M., Riley, J.D., Giret, M., and De Clerck, R. 1992. Recruitment of sole stocks, *Solea solea* (L.), in the Northeast Atlantic. Neth. J. Sea Res. **29**: 173–192.

Riley, J.D. 1966. Marine fish culture in Britain: VII. Plaice (*Pleuronectes platessa* L.) post-larval feeding on *Artemia salina* L. nauplii and the effects of varying feeding levels. J. Cons. Perm. Int. Explor. Mer, **30**: 204–221.

Rosenberg, R., Elmgren, R., Fleischer, S., Jonsson, P., Persson, G., and Dahlin, H. 1990. Marine eutrophication case studies in Sweden. Ambio, **19**: 102–108.

Stoner, A.W., Manderson, J.P., and Pessutti, J.P. 2001. Spatially explicit analysis of estuarine habitat for juvenile winter flounder: combining generalized additive models and geographic information systems. Mar. Ecol. Prog. Ser. **213**: 253–271.

Svenson, A., and Pihl, L. 2001. Biological investigations in shallow soft bottom bays: effects of filamentous algae and removal of algae. EU-Life Algae (Life 96 ENV/s/380) Rapp. 2001:44.

van der Veer, H.W. 1986. Immigration, settlement and density-dependent mortality of a larval and early post-larval 0-group plaice (*Pleuronectes platessa*) population in the western Wadden Sea. Mar. Ecol. Prog. Ser. **29**: 223–236.

van der Veer, H.W., Pihl, L., and Bergman, M.J.N. 1990. Recruitment mechanisms in North Sea plaice, *Pleuronectes platessa*. Mar. Ecol. Prog. Ser. **64**: 1–12.

© 2005 NRC Canada

Wennhage, H. 1999. Recruitment processes in the flatfish *Pleuronectes platessa* (L.): larval supply, habitat selection and predator–prey interactions at settlement. Ph.D. thesis, Department of Marine Ecology, Göteborg University, Fiskebäckskil, Sweden.

Wennhage, H. 2002. Vulnerability of newly settled plaice *Pleuronectes platessa* (L.) to predation: effects of habitat structure and predator functional response. J. Exp. Mar. Biol. Ecol. **269**: 129–145.

Wennhage, H., and Pihl, L. 1994. Substratum selection by juvenile plaice (*Pleuronectes platessa* L.): impact of benthic microalgae and filamentous macroalgae. Neth. J. Sea Res. **32**: 343–351.

Wennhage, H., and Pihl, L. 2001. Settlement patterns of newly settled plaice (*Pleuronectes platessa*) in a non-tidal Swedish fjord in relation to larval supply and benthic predators. Mar. Biol. **139**: 877–889.

Wiens, J.A. 1989. Spatial scaling in ecology. Funct. Ecol. **3**: 385–397.

Appendix A

Table A1. Basic data used in the model.

A		B		C		D	
	Vegetation cover (%)		Settlement density (individuals·m^{-2})		Settlement density (individuals·m^{-2})		Settlement density (individuals·m^{-2})
Region 1		Region 1	1.7	1977	0.60	Bay N1	
July 1994	73		11.8	1978	1.30	1994	0.00
August 1994	49		27.9	1979	2.40	1995	0.50
July 1995	54		16.3	1980	0.30	1996	0.93
August 1995	64		18.7	1981	0.80	1997	0.53
July 1996	61		19.3	1982	2.70	1998	2.00
August 1996	62		74.3	1983	2.40		
Mean (SD)	60.3 (8.1)		8.4	1984	0.50	Bay N2	
		Mean (SD)	22.3 (22.4)	1985	2.50	1994	0.27
Region 2				1986	3.80	1995	0.27
July 1994	22	Region 2	1	1987	1.60	1996	0.53
August 1994	16		4.1	1988	0.20	1997	0.80
July 1995	26		2.3	1989	3.20	1998	2.36
August 1995	41		2.3	1990	1.10		
July 1996	33		12.7	1991	1.10	Bay S1	
August 1996	24		16.6	1992	10.60	1994	0.67
Mean (SD)	27.0 (8.8)		12.2	1993	0.40	1995	3.40
			5.7	1994	0.40	1996	1.07
Region 3		Mean (SD)	7.1 (5.9)	1995	1.40	1997	1.20
July 1994	34			1996	2.00	1998	12.00
August 1994	15	Region 3	0.2	1997	0.80		
July 1995	16		0.3	1998	8.70	Bay S2	
August 1995	57		3.9	1999	3.70	1994	0.40
July 1996	37		0.4			1995	1.40
August 1996	23		10.7	Mean (SD)	2.2 (2.6)	1996	2.00
Mean (SD)	30.3 (15.9)		4.9			1997	0.80
			13			1998	8.67
Region 4			9.9				
July 1994	41	Mean (SD)	5.5 (5.2)			Mean (SD)	2.0 (3.0)
August 1994	24						
July 1995	23	Region 4	1.2				
August 1995	28		4.1				
July 1996	31		1.7				
August 1996	30		1.5				
Mean (SD)	29.4 (6.4)		2.7				
			1.7				
			3.9				
			1.6				
		Mean (SD)	2.3 (1.1)				

Note: A, observed in shallow nurseries in Regions 1–4 during sampling in July and August 1994–1996 (from Pihl et al 1999); B, sampled in Regions 1–4 (eight bays per region in 1998) (from Pihl et al. 2000); C, one bay in Region 2 during 23 consecutive years (L. Pihl, personal communication); D, four bays in Region 2 sampled over 5 years (Wennhage and Pihl 2001).

© 2005 NRC Canada

PERSPECTIVE / PERSPECTIVE

Are marine protected areas a red herring or fisheries panacea?[1]

Michel J. Kaiser

Abstract: Chronic failures in marine fisheries management have led some to suggest that marine protected areas (MPAs) are the solution to achieve sustainable fisheries. While such systems work for certain habitat-specific and nonmobile species, their utility for highly mobile stocks is questionable. Often the debate among proponents and critics of MPAs is confused by a lack of appreciation of the goals and objectives of such systems. The current consideration of MPAs as the basis of future fisheries management is a symptom of, and not the singular solution to, the problem of inappropriate implementation of fishing effort controls. The latter will provide greater overall conservation benefits if properly applied. Any future use of MPAs as an effective tool to achieve sustainable fisheries management in temperate systems should be treated as a large-scale, rigorously designed experiment to ensure that the outcome of using MPAs is interpreted correctly and not discredited for false reasons.

Résumé : Les échecs répétés qui se produisent dans l'aménagement des pêches marines ont incité certains à avancer que les zones de protection marine (MPA) sont la solution pour l'obtention de pêches durables. Bien que ces systèmes fonctionnent pour certaines espèces sédentaires à habitat bien défini, leur utilité chez les stocks très mobiles peut être mise en doute. Les débats entre les partisans et les critiques des MPA sont souvent obscurcis parce que les buts et les objectifs de ces systèmes sont mal compris. L'évaluation des MPA comme bases d'un aménagement des pêches futures est un symptôme de l'application inadéquate des contrôles des efforts de pêche, plutôt que la solution parfaite au problème. Lorsqu'ils sont bien exercés, ces contrôles sont, dans l'ensemble, plus bénéfiques pour la conservation. Toute utilisation future des MPA comme outil efficace pour mettre en place un aménagement durable des pêches dans les systèmes tempérés devrait être vue comme une expérience à grande échelle et à planification rigoureuse, afin de s'assurer que les résultats de l'utilisation des MPA soient interprétés correctement et ne soient pas discrédités pour les mauvaises raisons.

[Traduit par la Rédaction]

Marine protected areas (MPAs) have been heralded as the saviour of global fisheries by some conservationists, fishers, and managers and are seen as the solution to the perceived failures of current management methods. The potential benefits of excluding fishing activity from parts of the sea is an easy concept for nonspecialists to grasp, making MPAs an alluring alternative to the complex array of current management tools (Roberts et al. 2001; Gell and Roberts 2003). Here, I argue that while MPAs can and have been used with success in certain locations for particular species (Gell and Roberts 2003; Roberts et al. 2005), they are not the cure-all that some purport, and the scientific evidence chosen to support such conclusions on occasion has been drawn from those studies that demonstrate a positive outcome of MPA implementation (Halpern 2003; Zeller and Russ 2004). Needless to say, it may be equally important to understand better those circumstances when the use of MPAs has not been successful, as such instances provide useful metadata. In areas where highly mobile species are the target of the fishery, assessment of the full potential of MPAs as management tools are confounded by factors such as previous and concurrent fishing history, changes in size-at-age, community structure, genetic bottlenecks, stock collapse, and Allee effects (Frank et al. 2000; Willis et al. 2003*a*). Furthermore, the successful implementation of MPAs requires a cross-disciplinary approach that is far more complex than the biological conservation goals originally envisaged (Agardy et al. 2003; Ray 2004).

Much of the confusion surrounding the use of MPAs has stemmed from their intended objectives. The purpose of MPAs to conserve habitat and biodiversity of nontarget species is not necessarily consistent with the maintenance of sustainable fish stocks, although it is clear that in some cases these two goals can be met to some degree by the implemen-

Received 10 May 2004. Accepted 31 December 2004. Published on the NRC Research Press Web site at http://cjfas.nrc.ca on 31 May 2005.
J18127

M.J. Kaiser.[2,3] Marine Policy Center, Woods Hole Oceanographic Institute, Woods Hole, MA02543, USA.

[1]Contribution No. 11271 of the Marine Policy Center, Woods Hole Oceanographic Institute.
[2]Corresponding author (e-mail: michel.kaiser@bangor.ac.uk).
[3]Present address: School of Ocean Sciences, University of Wales-Bangor, Menai Bridge, Anglesey, LL59 5AB, UK.

 doi: 10.1139/F05-056 © 2005 NRC Canada

tation of an MPA. The scientific community is split regarding the efficacy of the unilateral use of MPAs to achieve sustainable exploitation of fish and shellfish stocks (Steele and Hoagland 2003, 2004; Zeller and Russ 2004). The appropriate and rigorous use of fishing effort controls that consider natural, long-term fluctuations in fish populations should achieve sustainable management. However, advocates of MPAs counter that the current severe decline in fish stocks has eliminated the potential for population increase even under favourable environmental conditions (Zeller and Russ 2004).

The wider ecosystem effects of fishing are cited as being incompatible with the aim of sustainable harvesting (Gell and Roberts 2003). Harvesting of fish from the seabed and the collateral damage that occurs from this has been compared with the clear-cutting of forests to catch deer (Watling and Norse 1998). These viewpoints typically lead to the conclusion that the only way to achieve sustainable use of fisheries is to exclude fishing activities from "large" areas of the ocean (Watling and Norse 1998). However, the implementation of appropriate MPAs is fraught with ecological, economic, and social problems that tend to be overlooked (Agardy et al. 2003). Although some of these problems are shared with current effort control systems (Hilborn et al. 2004), MPAs have a greater potential to exclude access by some fishers according to their geographic location. Worse still, MPAs have the potential to displace current fishing activities and thereby cause wider ecological damage to previously undisturbed and perhaps unknown, critical seabed habitats (i.e., essential fish habitat). However, there are circumstances when the benefits of using spatial effort control measures will offset some of the negative ecological effects of the displacement of fishing activities to alternative areas. Such examples would include the use of temporary closed areas to prevent fishing on spawning aggregations, on nursery areas, or at migration bottlenecks.

Most reviews of the ecological effects of MPAs draw on case studies in which fish biomass increased within areas from which fishing was excluded (Roberts et al. 2001; Gell and Roberts 2003; Halpern 2003). In general, these case studies focused on habitat-specific systems (e.g., coral or rock reefs) that are relatively small in scale (<500 km^2; Halpern 2003). These systems are easier to protect from the effects of fishing, as the target species usually remain in close proximity to a well-delineated habitat (Russ and Alcala 1996; Willis et al. 2003*b*). Fishers that prosecute these systems usually live within kilometres of the specific habitat and depend upon it for a considerable proportion of their diet or income (Jennings et al. 1996; Blyth et al. 2002). Hence, their motivation to participate in MPAs is much greater compared with those who fish across areas of tens of thousands of square kilometres and who compete against fishers with whom they have little or no social contact.

A recent meta-analysis of MPAs reported general, positive biological effects that were most usually expressed as an increase in biomass within the reserve of both target and nontarget species (Halpern 2003). Interestingly, no relationship was found between the spatial extent of the MPA and the magnitude of the change in biomass or abundance of the protected target species' population (Halpern 2003). While it might be tempting to conclude that an MPA of any size would provide conservation benefits, even if only at a local scale, this holds true for only the majority of studies on which this meta-analysis was based: coral or temperate rock reefs. These conclusions are not valid for many of the commercially important, temperate fish species that are widespread across a variety of habitats, exhibit entirely different behaviours between sea basins, and may move considerable distances within a year (Metcalfe and Arnold 1997; Horwood et al. 1998; Horwood 2000). For these species, the critical and most demanding issue relating to the design of appropriate MPAs is the scale of the area required to achieve effective protection and stock enhancement of highly mobile fish stocks. Recent estimates indicate that a mean area equivalent to approximately 32% (range 10%–65%) of the area available for fishing would require protection (Gell and Roberts 2003). Note that these figures are once again based largely on studies of fish species with strong habitat-specific associations. However, for wide-ranging species such as Atlantic cod (*Gadus morhua*), calculations indicate that excluding fishing from an area as large as 25% of the North Sea would have a negligible effect on their spawning stock biomass (Horwood 2000). Given the multispecies nature of most temperate fisheries, the different MPA requirements of each species would add yet another layer of management complexity.

What would the composite map of species-specific MPAs look like and could they be implemented? These important questions are yet to be addressed; indeed, little if any consideration is given to the likely social and economic consequences for the inevitably reduced number of fishers in the system. With fishing excluded from large areas of the sea, a negotiated placement of MPAs to take into account useable fishing grounds that are accessible to all remaining participants would seem hopeful at best. In regions of the world where total control of exclusive economic zones is exercised out to 200 nautical miles, the placement of MPAs can be imposed through legislation. However, such simple solutions are not likely to be found in more complex systems, such as Europe, where multiple nations share access to the same resources. Even if such systems can be implemented, fishers can expect to wait decades before signs of stock recovery for certain stocks occur (Hutchings 2000; Steele and Beet 2003). Steele and Beet (2003) make the telling observation that the initial stages of MPA implementation would be doubly painful as fishers are deprived access to traditional fishing grounds and forced into less favourable fishing areas. This is further compounded by the added reductions in fishing effort (Zeller and Russ 2004). Furthermore, in the initial stages after MPA implementation, benthic production in the newly protected areas is likely to be low as it enters a phase of recovery once fishing disturbance has been removed, while those areas newly affected by displaced demersal effort will experience a severe decline in production varying according to habitat type (Jennings et al. 2001; Dinmore et al. 2003; J. Hiddink, School of Ocean Sciences, University of Wales-Bangor, Menai Bridge, Anglesey LL59 5AB, UK, unpublished data).

Given the unknown social and variable predicted economic consequences of a switch to management based on MPAs (Sanchiro and Wilen 2001), one has to ask what is supposedly wrong with current fishery management tech-

© 2005 NRC Canada

Fig. 1. The relative fishing effort (sightings of fishing vessels per 100 h of overflight time) by bottom-fishing fleets in the Irish Sea, UK (inset box) that target sea scallops (*Pecten maximus*), demersal fishes, and *Nephrops norvegicus* (a type of burrowing crustacean). Data are from enforcement agency direct observations from light aircraft that overfly these areas on a regular basis. For each vessel sighting, the position, name, type, and activity of each vessel are noted. The data extend back to 1985 and have been aggregated into 5-year bins for ease of comparison and are expressed as sightings per unit effort of overflight (SPUE) (*a*) 1985–1989, (*b*) 1990–1994, (*c*) 1995–1999.

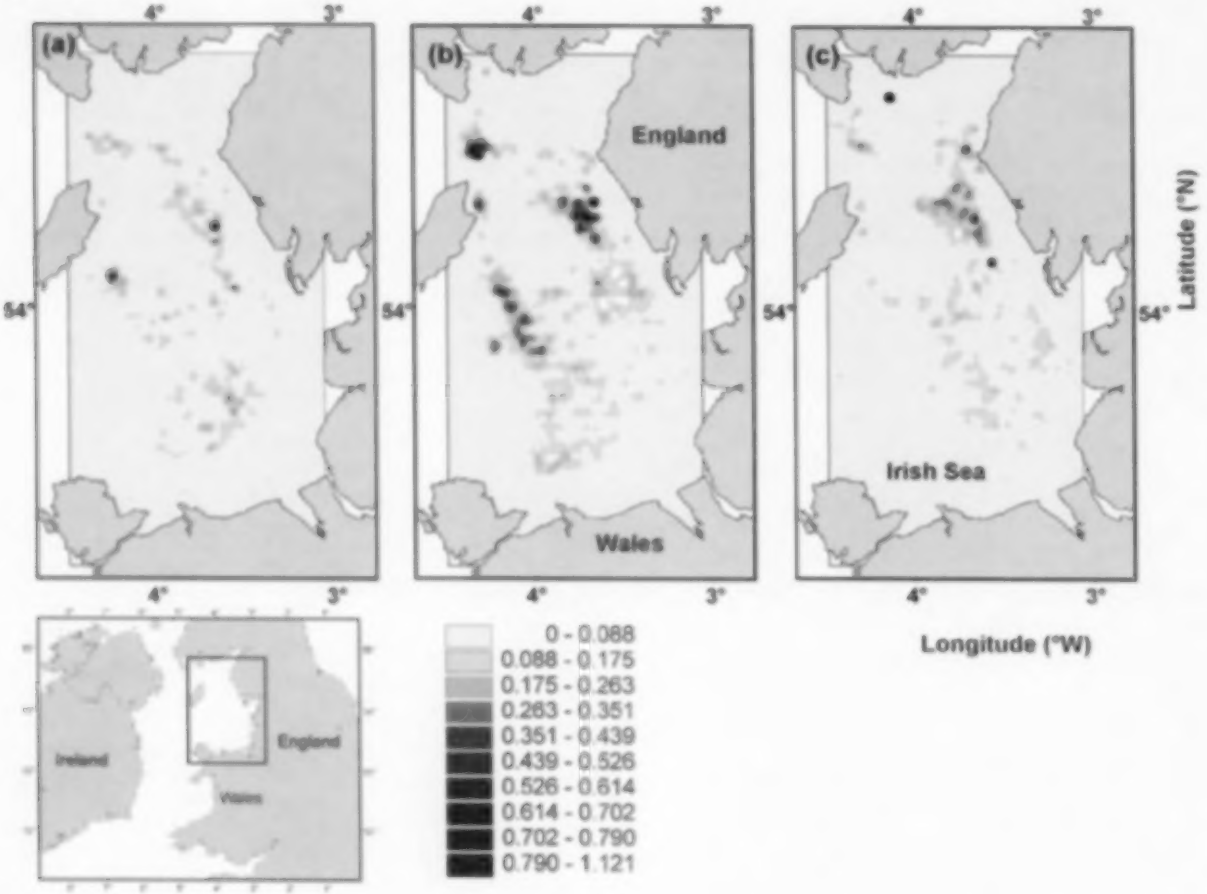

niques? I would argue that for many temperate species there is nothing fundamentally wrong with either the methodology of stock assessment or the available effort controls (e.g., days at sea) used in conjunction with catch controls, such as total allowable catches and individual transferable quotas. Indeed, when fishing effort control has been implemented effectively, fisheries have been managed successfully (e.g., the Western Australian rock lobster (*Palinurus cygnus*), New Zealand hoki (*Macruronus novaezealandiae*), Alaska salmon (*Oncorhynchus* spp.), and the Thames herring (*Clupea harengus*) fisheries, all of which have achieved Marine Stewardship Council certification as sustainable fisheries).

So why have other fisheries failed so dismally? Current fisheries management depends on annual forecasts of recruitment and catches that incorporate significant uncertainty. The political need to appease a desperate fishing industry has tended to push management decisions towards, and often beyond, the upper confidence limits for future allowable catches (Hutchings and Myers 1995). Such behaviour is not surprising given the typical short life-span of the average government, for whom the shadow of the future does not apply (Hart 1998). Do proponents of MPAs believe that scientific debate and uncertainty over the precise size, position, and configuration of MPAs will not provide the very same pathway to politically compromised management? If we ultimately move to a management system that is underpinned by a system of MPAs, we will still have to set a figure of how much and where. As soon as such figures are set, they will be vulnerable to erosion by a system of political negotiation. Given the effort that will be required to implement these systems, there is likely to be considerable resistance to alter their configuration should we decide at some point in the future that management objectives or large-scale environmental changes dictate their reconfiguration.

Furthermore, it is often stated that we require a portfolio of both MPAs and effort reduction to achieve sustainable use

© 2005 NRC Canada

of fish stocks (Zeller and Russ 2004). If the latter is a prerequisite for the successful implementation of the former, the prognosis does not look too promising. If fishers are displaced by the imposition of an MPA from favoured fishing grounds into areas where catch rates of legal-sized target species are lower, the use of quota management is likely to result in a considerable increase in bycatch as fishers work harder (spend more time fishing at sea) to land the same quota. If the use of MPAs is to be successful, we first need to achieve effective fishing effort control. The failure or success of the use of an MPA as a fishery management tool (note the use of an MPA to protect specific habitat is excluded in this context) is inextricably linked to effective fishing effort control in the surrounding waters. As a result, there is a real risk that inadequately designed MPAs instigated without effective parallel effort control will be perceived by the industry and the wider public as failures and their utility discredited.

So far, our focus has been directed almost entirely on the fish and their biology. We have sought to control the activities of a predator, mankind, without devoting an equal effort to understanding the dynamics of a predator that operates in a system with imperfect knowledge about the distribution of the prey and the habitat in which they hunt them. Fishers sample the fish population and record their reward rate in space and time (Gillis and Peterman 1998). Nets are towed over areas of the seabed about which knowledge is known at a coarse scale. Charts with seabed features are not based on metre-accurate remote sensing as is possible on the land, but on sample points located tens or even hundreds of kilometres apart. What lies in between is uncertain. Even using echo-sounders, the instantaneous knowledge relayed to the wheelhouse of a fishing vessel provides information of only a few metres of the seabed directly beneath the hull and tells one nothing about the 20 m of seabed on either side that are about to be swept by the following fishing net. Thus every new exploratory tow using a bottom-towed fishing gear is potentially hazardous.

When fish stocks are healthy, fishers are most likely to repeatedly return to locations that they know from past experience to yield economically rewarding catches with a minimum risk to gear and vessel safety and avoid excessive competition with other fishers (Gillis and Peterman 1998; Holland and Sutinen 2000; Jin et al. 2002). As stocks decline and more fishing effort is required to maintain the same catch, fishers are forced to explore new areas where knowledge of the seabed and catch is uncertain. Evidence for this behaviour comes from vessel-monitoring systems and direct observations that demonstrate that fishing effort is highly aggregated and is only homogeneous at a scale of 1 km^2 (Rijnsdorp et al. 1998). It is clear that large areas of the seabed remain unfished, while other areas receive intensive fishing activity (Fig. 1). As fishing effort rises to compensate for falling landings, previously unfished grounds begin to become the focus of attention. However, as effort falls, fishers largely return to their favoured localities (Fig. 2). Indeed, the proportion of seabed affected by fishing is highly predictable in line with fluctuations in total effort (Fig. 2). Faced with declining stocks and unrestricted fishing effort under a quota management system, fishers have the incentive to explore new grounds, thereby increasing their

Fig. 2. (*a*) Landings ($\times 10^4$ tonnes) for International Council for the Exploration of the Sea (ICES) statistical area VIIa aggregated over three time periods, broken down into bottom-dwelling fish (solid bars), scallops (*Pecten maximus*, open bars) and *Nephrops norvegicus* (gray bars), which represent the target of the three main fleets that operate in these waters (data taken from Fishstat v. 2.3). While landings of scallops and *Nephrops* remained relatively constant across the three time periods, landings of fish (a proxy for fishing effort) declined concomitant with a contraction of areas of the sea affected by fishing effort in the third time period (1995–1999). (*b*) The change in the distribution of different intensities of overflight sightings is expressed as percent area of seabed for the 10 different categories of vessel sightings (1 = 0.000–0.088; 10 = 0.79–1.121 sightings per unit effort (SPUE)). 1995–1999, ●; 1990–1994, ■; 1985–1989, □. (*c*) A plot of the difference in the change in distribution of sightings from the first to the second time period and from the second to the third time period. This strongly linear relationship indicates the predictability of the allocation of fishing effort in response to overall effort.

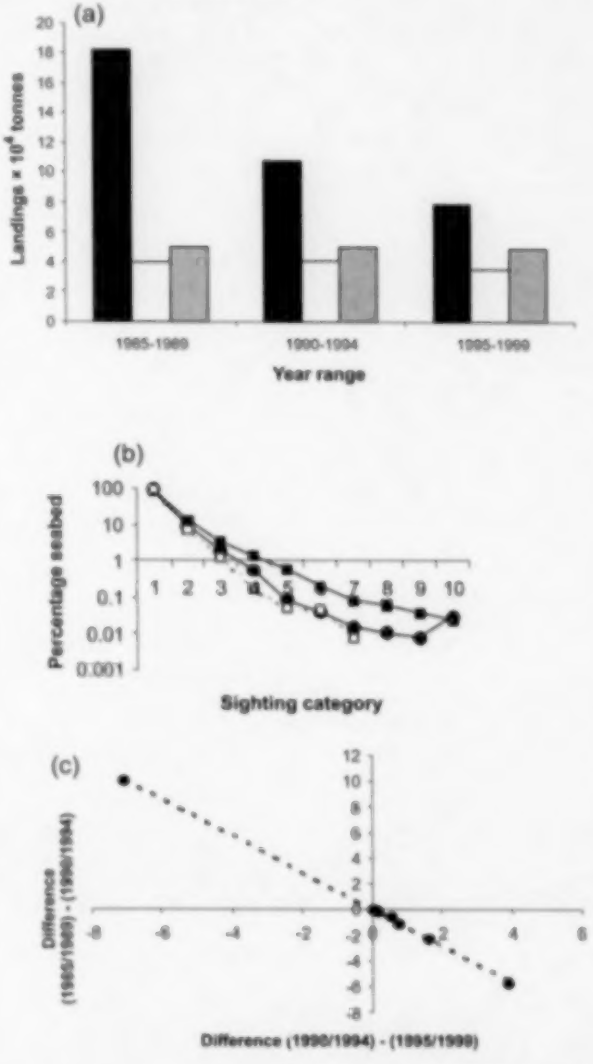

© 2005 NRC Canada

portfolio of knowledge and making it more likely that these grounds will be adversely affected in the future (Fig. 2*b*).

The aggregative behaviour of fishers has important ecological consequences, since the first few passages of bottom-fishing gear across the seabed cause the biggest reduction in seabed community production and thereafter remains in a relatively constant condition of reduced benthic production (Jennings et al. 2001). It is important to appreciate that some fishers repeatedly fish the same tows several (or more) times per year on an annual basis. This aggregative behaviour occurs even over areas that have the same environmental conditions and hence the same potential benthic production in the absence of fishing (J. Hiddink, School of Ocean Sciences, University of Wales-Bangor, Menai Bridge, Anglesey LL59 5AB, UK, unpublished data). Thus restricting bottom-fishing activities to confined areas of the seabed minimizes the spatial extent of the negative effects on seabed community production, which is a status that is already achieved as a result of fishers' behaviour and without the imposition of MPAs (Fig. 1). The imposition of MPAs without due consideration for fishers' behavioural responses may cause more damage than the status quo as evidenced by the recent "cod box" in the North Sea, which forced fishers to reallocate their effort to areas of the seabed where previously fishing boats had not been recorded (Dinmore et al. 2003).

The use of MPAs clearly has beneficial effects for very habitat-specific fish species associated with coral and temperate rock reefs, and they are the only tool that can effectively protect sensitive habitats such as beds of ancient calcareous algae and deep water corals (Willis et al. 2003*b*). In temperate waters, where the majority of the seabed is characterized by sediments and aggregates, sedentary species such as sea scallops and fish that have restricted movements are the most likely candidates to benefit from the exclusion of fishing activities (Horwood et al. 1998; Murawski et al. 2000). However, the scale of MPAs required to ensure sustainable fisheries of wide-ranging, long-lived species, such as cod and plaice, may be both impractical and equally prone to the same political horse-trading that has neutered many current management systems. New evidence suggests that in the worst case scenario, the ill-considered use of MPAs will displace fishing activity and thereby could result in additional damage to the marine environment before recolonization occurs in the newly protected area (Dinmore et al. 2003), whereas the proper implementation of fishing effort reduction still has the potential to out-perform the use of MPAs in terms of increasing spawning stock biomass (Steele and Beet 2003). As stocks recover and catch efficiency increases, the necessity to fish for prolonged periods and in marginal areas of the seabed should diminish. These beneficial effects of stock recovery can easily be undone by allowing the industry to expand uncontrolled, thereby exacerbating the "ratchet effect". In temperate systems, MPAs are not the singular solution to sustainable fisheries and are perhaps more a symptom of chronic failures to apply scientific advice (Hall 1999). Uncompromised management of fishing effort would simultaneously solve many of the wider negative, ecological, and socio-economic effects of overfishing.

If we are to advocate MPAs as a fundamental tool that can help to achieve sustainable use of marine resources, it is imperative that the uncertainty regarding the outcome of such a management system is made clear to all stakeholders and that it is dependent upon adequate regulation and uncompromised implementation. In effect, any such shift towards the use of MPAs as part of our management tool portfolio should be tested using a rigorously designed, experimental management regime, the performance of which is tested in a scientifically objective manner and reviewed on a regular basis.

Acknowledgments

The author acknowledges financial support from the Marine Policy Center, Woods Hole Oceanographic Institute, and is grateful for the input of John Steele, Porter Hoagland, Di Jin, Nancy Shackell, and two anonymous referees. The views expressed in this article are those of the author alone and in no way reflect the views of affiliated institutions.

References

Agardy, T., Bridgewater, P., Crosby, M.P., Day, J., Dayton, P.K., Kenchington, R., Laffoley, D., McConney, P., Murray, P.A., Parks, J.E., and Peau, L.2003. Dangerous targets? Unresolved issues and ideological clashes around marine protected areas. Aquat. Conserv. Mar. Freshw. Ecosyst. **13**: 353–367.

Blyth, R.E., Kaiser, M.J., Edwards-Jones, G., and Hart, P.J.B. 2002. Voluntary management in an inshore fishery has conservation benefits. Environ. Conserv. **29**: 493–508.

Dinmore, T.A., Duplisea, D.E., Rackham, B.D., Maxwell, D.L., and Jennings, S. 2003. Impact of a large-scale area closure on patterns of fishing disturbance and the consequences for benthic communities. ICES J. Mar. Sci. **60**: 371–380.

Frank, K.T., Shackell, N.L., and Simon, J.E. 2000. An evaluation of the Emerald/Western Bank juvenile haddock closed areas. ICES J. Mar. Sci. **57**: 1023–1034.

Gell, F.R., and Roberts, C.M. 2003. Benefits beyond boundaries: the fishery effects of marine reserves. Trends Ecol. Evol. **18**: 448–455.

Gillis, D.M., and Peterman, R.M. 1998. Implications of interference among fishing vessels and the ideal free distribution to the interpretation of CPUE. Can. J. Fish. Aquat. Sci. **55**: 37–46.

Hall, S.J. 1999. The effects of fishing on marine ecosystems and communities. Blackwell Science, Oxford.

Halpern, B.S. 2003. The impact of marine reserves: Do reserves work and does reserve size matter? Ecol. Appl. **13**: S117–S137.

Hart, P.J.B. 1998. Enlarging the shadow of the future: avoiding conflict and conserving fish off south Devon, U.K. *Edited by* T.J. Pitcher, P.J.B. Hart, and D. Pauly. Reinventing Fisheries Management, Kluwer, Dordrecht.

Hilborn, R., Stokes, T.K., Maguire, J.-J., Smith, A., Botsford, L.W., Mangel, M., Orensanz, J., Parma, A., Rice, J., Bell, J.D., Cochrane, K.L., Garcia, S., Hall, S.J., Kirkwood, G.P., Sainsbury, J.C., Stefansson, G., and Walters, C.J. 2004. When can marine reserves improve fisheries management? Ocean Coast. Manag. **47**: 197–205.

Holland, D.S., and Sutinen, J.G. 2000. Location choice in New England trawl fisheries: old habits die hard. Landsc. Ecol. **76**: 133–149.

Horwood, J.W. 2000. No-take zones: a management context. *Edited by* M.J. Kaiser and S.J. de Groot. The effects of fishing on non-target species and habitats: biological, social and economic issues. Blackwell Science, Oxford.

© 2005 NRC Canada

Horwood, J.W., Nichols, J.H., and Milligan, S. 1998. Evaluation of closed areas for fish stock conservation. J. Appl. Ecol. **35**: 893–903.

Hutchings, J.A. 2000. Collapse and recovery of marine fishes. Nature (London), **406**: 882–885.

Hutchings, J.A., and Myers, R.A. 1995. The North Atlantic Fisheries: successes, failures, and challenges. *Edited by* R. Amason and L. Felt. Institute of Island Studies, Charlottetown, P.E.I., Canada. pp. 38–93.

Jennings, S., Marshall, S.S., and Polunin, N.V.C. 1996. Seychelles' marine protected areas: comparative structure and status of reef fish communities. Biol. Conserv. **75**: 201–209.

Jennings, S., Dinmore, T.A., Duplisea, D.E., Warr, K.J., and Lancaster, J.E. 2001. Trawling disturbance can modify benthic production processes. J. Anim. Ecol. **70**: 459–475.

Jin, D., Kite-Powell, H.L., Thunberg, E., Solow, A.R., and Talley, W.K. 2002. A model of fishing vessel accident probability. J. Saf. Res. **33**: 497–510.

Metcalfe, J.D., and Arnold, G.P. 1997. Tracking fish with electronic tags. Nature (London), **387**: 665–666.

Murawski, S.A., Brown, R., Lai, H.-L., Rago, P.J., and Hendrickson, L. 2000. Large-scale closed areas as a fishery-management tool in temperate marine systems: the Georges Bank experiment. Bull. Mar. Sci. **66**: 775–798.

Ray, G.C. 2004. Reconsidering "dangerous targets" for marine protected areas. Aquat. Conserv. Mar. Freshw. Ecosyst. **14**: 211–215.

Rijnsdorp, A.D., Buijs, A.M., Storbeck, F., and Visser, E. 1998. Micro-scale distribution of beam trawl effort in the southern North Sea between 1993 and 1996 in relation to the trawling frequency of the sea bed and the impact on benthic organisms. ICES J. Mar. Sci. **55**: 403–419.

Roberts, C.M., Bohnsack, J.A., Gell, F.R., Hawkins, J., and Goodridge, R. 2001. Marine reserves enhance adjacent fisheries. Science (Washington, D.C.), **294**: 1920–1923.

Roberts, C.M., Hawkins, J.P., and Gell, F.R. 2005. The role of marine reserves in achieving sustainable fisheries. Philos. Trans. R. Soc. Lond. B Biol. Sci., **360**: 123–132

Russ, G., and Alcala, A. 1996. Marine reserves-rates and patterns of recovery and decline of large predatory fish. Ecol. Appl. **6**: 947–961.

Sanchiro, J.N., and Wilen, J. E. 2001. A bioeconomics model of marine reserve creation. J. Environ. Econ. Manag. **42**: 257–276.

Steele, D.H., and Beet, A.R. 2003. Marine protected areas in "nonlinear" ecosystems. Proc. R. Soc. Lond. B Biol. Sci. **270**(Suppl.): S230–S233.

Steele, J.H., and Hoagland, P. 2003. Are fisheries "sustainable"? Fish. Res. **64**: 1–3.

Steele, J.H., and Hoagland, P. 2004. Are fisheries "sustainable"? A counterpoint to Steele and Hoagland: a reply. Fish. Res. **67**: 247–248.

Watling, L., and Norse, E.A. 1998. Disturbance of the seabed by mobile fishing gear: a comparison to forest clearcutting. Conserv. Biol. **12**: 1180–1197.

Willis, T.J., Millar, R.B., Babcock, R.C., and Tolimieri, N. 2003*a*. Burdens of evidence and the benefits of marine reserves: putting Descartes before des horse? Environ. Conserv. **30**: 97–103.

Willis, T.J., Millar, R.B., and Babcock, R.C. 2003*b*. Protection of exploited fishes in temperate regions: high density and biomass of snapper *Pagurus auratus* (Sparidae) in northern New Zealand marine reserves. J. Appl. Ecol. **40**: 214–227.

Zeller, D., and Russ, G.R. 2004. Are fisheries "sustainable"? A counterpoint to Steele and Hoagland. Fish. Res. **67**: 241–245.

© 2005 NRC Canada

NRC Biography Series
Collection de biographies des Presses du CNRC

Gerhard Herzberg: An Illustrious Life in Science

By / Par Boris Stoicheff

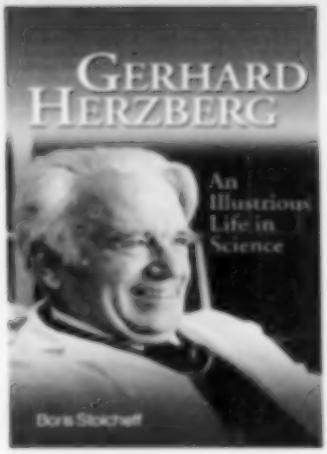

NRC Press Biography Series No.1 /
Collection de biographies des Presses du CNRC nº 1

468 Pages 2002
Hardcover / Édition reliée
ISBN 0-660-18757-4; ISSN 1701-1833
NRC / CNRC 44462
$49.95 CAN. Other countries $49.95 US /
49,95 $CAN. À l'étranger $49.95 US
Canadian customers add GST (7%) /
Clients du Canada, ajoutez la TPS (7 %)

George J. Klein: The Great Inventor

By / Par Richard I. Bourgeois-Doyle

NRC Press Biography Series No. 2 /
Collection de biographies des Presses du CNRC nº 2

289 Pages 2004
Hardcover / Édition reliée
ISBN 0-660-19322-1; ISSN 1701-1833
NRC / CNRC 46323
$49.95 CAN. Other countries $49.95 US /
49,95 $CAN. À l'étranger $49.95 US /
Canadian customers add GST (7%) /
Clients du Canada, ajoutez la TPS (7 %)

Orders may be submitted by mail or fax to:
Les commandes peuvent être soumises par courrier ou par télécopieur à :

Order Office / Bureau des commandes

NRC Research Press / Presses scientifique du CNRC
National Research Council / Conseil national de recherches
Ottawa, ON K1A 0R6, Canada
Telephone / Téléphone : (613) 990-2254
Fax / Télécopieur : (613) 952-7656
E-mail / Courriel : pubs@nrc-cnrc.gc.ca
Website / Site web : http://pubs.nrc-cnrc.gc.ca

PLEASE PRINT/LETTRES MOULÉES

☐ Payment enclosed / Paiement inclus ☐ Charge to/ Imputer à ☐ Visa ☐ MasterCard

Account no./N° de compte Expiry date/Date d'expiration

Name/Nom

Signature

Address/Adresse

City/Ville Province

Postal code/Code postal Country/Pays

Telephone/Téléphone Fax/Télécopieur

E-mail/Courriel

Prepayment required unless order is accompanied by a purchase order number. Cheques or money orders should be made payable to : "Receiver General for Canada, Credit NRC". All sales are final.
Les commandes doivent être payées d'avance à moins qu'elles ne soient accompagnées d'un numéro de bon de commande. Les chèques ou mandats doivent être libellés au « Receveur général du Canada, crédit du CNRC ». Toutes les ventes sont finales.

Fisheries and Aquatic Sciences
Sciences halieutiques et aquatiques

Photographic Atlas of Fish Otoliths of the Northwest Atlantic Ocean
By / Par Stephen E. Campana

$54.95 CAN. Other countries $54.95 US
54,95 $CAN. À l'étranger 54,95 $US
Softcover / Édition brochée
(*Can. Spec. Publ. Fish. Aquat. Sci. / Publ. spéc. can. sci. halieut. aquat. 133*)
284 pages ISBN 0-660-19108-3 ISSN 0706-6481 NRC / CNRC 46328

Salmonine Introductions to the Laurentian Great Lakes:
An Historical Review and Evaluation of Ecological Effects
By / Par Stephen S. Crawford

$42.95 CAN. Other countries $42.95 US
42,95 $CAN. À l'étranger 42,95 $US
Softcover / Édition brochée
(*Can. Spec. Publ. Fish. Aquat. Sci. / Publ. spéc. can. sci. halieut. aquat. 132*)
215 pages ISBN 0-660-17639-4 ISSN 0706-6481 NRC / CNRC 42734

Marine Protected Areas and Fisheries Closures in British Columbia
By Glen S. Jamieson and Joanne Lessard

$69.95 CAN. Other countries $69.95 US
69,95 $CAN. À l'étranger 69,95 $US
Softcover / Édition brochée
(Can. Spec. Publ. Fish. Aquat. Sci. / Publ. spéc. can. sci. halieut. aquat. 131)
414 pages ISBN 0-660-17788-9 ISSN 0706-6481 NRC / CNRC 42846

Workshop on Rebuilding Abalone Stocks in British Columbia
By / Par Alan Campbell

$42.95 CAN. Other countries $42.95 US
42,95 $CAN. À l'étranger 42,95 $US
Softcover / Édition brochée
(*Can. Spec. Publ. Fish. Aquat. Sci. / Publ. spéc. can. sci. halieut. aquat. 130*)
158 pages ISBN 0-660-18292-0 ISSN 0706-6481 NRC / CNRC 42841

To order any of the above titles / Commandez n'importe quel titre ci-dessus à :

Telephone / Téléphone : (613) 990-2254
Fax / Télécopieur : (613) 952-7656
E-mail / Courriel : pubs@nrc-cnrc.gc.ca
Web site / Site web : http://pubs.nrc-cnrc.gc.ca

Order Office / Bureau des commandes
NRC Research Press / Presses scientifique du CNRC
National Research Council / Conseil national de recherches
Ottawa, ON K1A 0R6, Canada

Canadian customers add GST (7%). Prepayment required unless order is accompanied by a purchase order number. Cheques or money orders should be made payable to : "Receiver General for Canada, Credit NRC". For all orders outside Canada, rates are in U.S. Dollars. All sales are final.
Clients du Canada, ajoutez la TPS (7 %). Les commandes doivent être payées d'avance à moins qu'elles ne soient accompagnées d'un numéro de bon de commande. Les chèques ou mandats doivent être libellés au « Receveur général du Canada, crédit du CNRC ».
Pour les commandes hors-Canada, les tarifs sont en dollars américains. Toutes les ventes sont finales.

Sea Buckthorn (*Hippophae rhamnoides L.*): Production and Utilization

By T.S.C. Li and T.H.J. Beveridge

137 Pages 2003
Softcover
ISBN 0-660-19007-9
NRC 46317
$44.95 CAN. Other countries $44.95 US
Canadian customers add GST (7%)

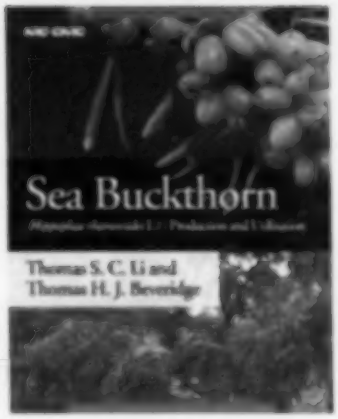

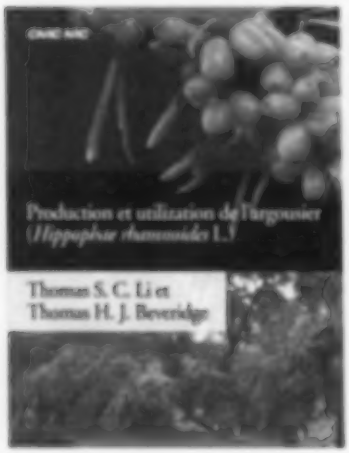

Production et utilisation de l'argousier *(Hippophae rhamnoides L.)*

Par T.S.C. Li et T.H.J. Beveridge

140 Pages 2004
Édition brochée
ISBN 0-660-96931-9
CNRC 46841
44,95 $CAN. À l'étranger 44,95 $US
Clients du Canada, ajoutez la TPS (7 %)

Orders may be submitted by mail or fax to:
Les commandes peuvent être soumises par courrier ou par télécopieur à :

Order Office / Bureau des commandes

NRC Research Press / Presses scientifique du CNRC
National Research Council / Conseil national de recherches
Ottawa, ON K1A 0R6, Canada
Telephone / Téléphone : (613) 990-2254
Fax / Télécopieur : (613) 952-7656
E-mail / Courriel : pubs@nrc-cnrc.gc.ca
Website / Site web : http://pubs.nrc-cnrc.gc.ca

PLEASE PRINT/LETTRES MOULÉES

☐ Payment enclosed / Paiement inclus ☐ Charge to/ Imputer à ☐ Visa ☐ MasterCard

Account no./N° de compte | Expiry date/Date d'expiration

Name/Nom

Signature

Address/Adresse

City/Ville | Province

Postal code/Code postal | Country/Pays

Telephone/Téléphone | Fax/Télécopieur

E-mail/Courriel

Prepayment required unless order is accompanied by a purchase order number. Cheques or money orders should be made payable to : "Receiver General for Canada, Credit NRC". All sales are final.
Les commandes doivent être payées d'avance à moins qu'elles ne soient accompagnées d'un numéro de bon de commande. Les chèques ou mandats doivent être libellés au « Receveur général du Canada, crédit du CNRC ». Toutes les ventes sont finales.

Eva C. Enders, Daniel Boisclair, and André G. Roy	**1079–1089**	A model of total swimming costs in turbulent flow for juvenile Atlantic salmon (*Salmo salar*)
Sarah A. Bailey, Ian C. Duggan, Philip T. Jenkins, and Hugh J. MacIsaac	**1090–1103**	Invertebrate resting stages in residual ballast sediment of transoceanic ships
C.H. Ainsworth and U.R. Sumaila	**1104–1110**	Intergenerational valuation of fisheries resources can justify long-term conservation: a case study in Atlantic cod (*Gadus morhua*)
M.E. Palmer and Anthony Ricciardi	**1111–1118**	Community interactions affecting the relative abundances of native and invasive amphipods in the St. Lawrence River
David W. Garton, Christopher D. Payne, and Joseph P. Montoya	**1119–1129**	Flexible diet and trophic position of dreissenid mussels as inferred from stable isotopes of carbon and nitrogen
Peter Ward and Ransom A. Myers	**1130–1142**	Inferring the depth distribution of catchability for pelagic fishes and correcting for variations in the depth of longline fishing gear
Travis S. Elsdon and Bronwyn M. Gillanders	**1143–1152**	Alternative life-history patterns of estuarine fish: barium in otoliths elucidates freshwater residency
Laura K. Weir, Jeffrey A. Hutchings, Ian A. Fleming, and Sigurd Einum	**1153–1160**	Spawning behaviour and success of mature male Atlantic salmon (*Salmo salar*) parr of farmed and wild origin
Linda M. Campbell, Aaron T. Fisk, Xiaowa Wang, Günter Köck, and Derek C.G. Muir	**1161–1167**	Evidence for biomagnification of rubidium in freshwater and marine food webs
Barry P. Baldigo, Peter S. Murdoch, and Douglas A. Burns	**1168–1183**	Stream acidification and mortality of brook trout (*Salvelinus fontinalis*) in response to timber harvest in Catskill Mountain watersheds, New York, USA
Leif Pihl, Johan Modin, and Håkan Wennhage	**1184–1193**	Relating plaice (*Pleuronectes platessa*) recruitment to deteriorating habitat quality: effects of macroalgal blooms in coastal nursery grounds
	PERSPECTIVE	PERSPECTIVE
Michel J. Kaiser	**1194–1199**	Are marine protected areas a red herring or fisheries panacea?

National Research Council Canada
Ottawa, Canada K1A 0R6

Conseil national de recherches Canada
Ottawa, Canada K1A 0R6

Postage paid at Ottawa
Publications mail
Registration No. 40062591

Port payé à Ottawa
Poste-publication
Enregistrement n° 40062591

USPS periodical postage paid at Champlain, NY 12919, USA

Canadian Journal of Fisheries and Aquatic Sciences

Volume 62, Number 5, May 2005

Journal canadien des sciences halieutiques et aquatiques

Volume 62, numéro 5, mai 2005

RAPID COMMUNICATION		COMMUNICATION RAPIDE
Mark D. Scheuerell, Phillip S. Levin, Richard W. Zabel, John G. Williams, and Beth L. Sanderson	**961–964**	A new perspective on the importance of marine-derived nutrients to threatened stocks of Pacific salmon (*Oncorhynchus* spp.)
ARTICLES		ARTICLES
John W. Watson, Sheryan P. Epperly, Arvind K. Shah, and Daniel G. Foster	**965–981**	Fishing methods to reduce sea turtle mortality associated with pelagic longlines
A. Gravel, P.G.C. Campbell, and A. Hontela	**982–990**	Disruption of the hypothalamo-pituitary-interrenal axis in 1+ yellow perch (*Perca flavescens*) chronically exposed to metals in the environment
Michael A. Turner, David B. Huebert, David L. Findlay, Leonard L. Hendzel, Wolfgang A. Jansen, R.A. (Drew) Bodaly, Llwellyn M. Armstrong, and Susan E.M. Kasian	**991–1003**	Divergent impacts of experimental lake-level drawdown on planktonic and benthic plant communities in a boreal forest lake
Mark V. Trevorrow	**1004–1018**	The use of moored inverted echo sounders for monitoring meso-zooplankton and fish near the ocean surface
F.C. Wu, R.B. Mills, Y.R. Cai, R.D. Evans, and P.J. Dillon	**1019–1027**	Photodegradation-induced changes in dissolved organic matter in acidic waters
Russell B. Millar and Wayne S. Stewart	**1028–1036**	Automatic calculation of the sensitivity of Bayesian fisheries models to informative priors
A. Folkvord	**1037–1052**	Comparison of size-at-age of larval Atlantic cod (*Gadus morhua*) from different populations based on size- and temperature-dependent growth models
John M. Drake	**1053–1059**	Risk analysis for species introductions: forecasting population growth of Eurasian ruffe (*Gymnocephalus cernuus*)
Kevin R. Piner, Owen S. Hamel, Jennifer L. Menkel, John R. Wallace, and Charles E. Hutchinson	**1060–1066**	Age validation of canary rockfish (*Sebastes pinniger*) from off the Oregon coast (USA) using the bomb radiocarbon method
Biplob Das, Rolf D. Vinebrooke, Arturo Sanchez-Azofeifa, Benoit Rivard, and Alexander P. Wolfe	**1067–1078**	Inferring sedimentary chlorophyll concentrations with reflectance spectroscopy: a novel approach to reconstructing historical changes in the trophic status of mountain lakes

Continued on inside back cover / Suite au verso

Canada

Printed in Canada by / Imprimé au Canada par
NRC Reprographic Services / Service de reprographie CNRC
Page production by / Mise en page par
NRC Research Press / Presses scientifiques du CNRC

0706-652X(200505)62:5;1-3